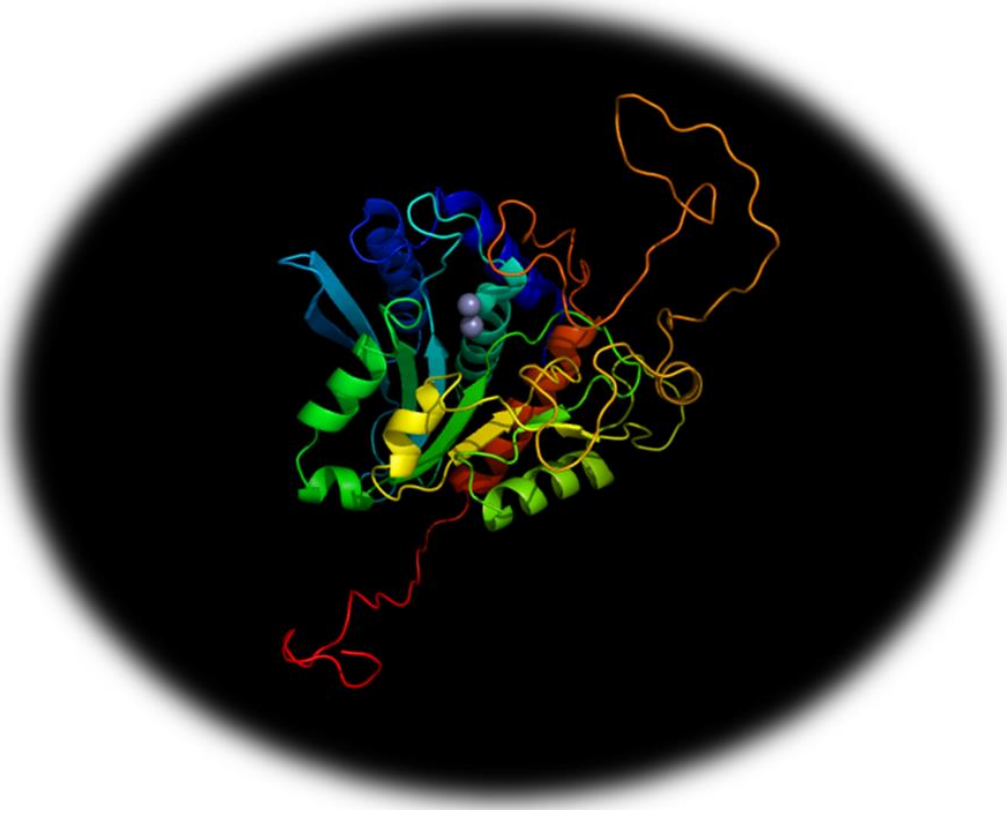
Surviving and Thriving in the Cystic Fibrosis Lung:

Contribution of an Arginine Specific Aminopeptidase to Sustained Infection by *Pseudomonas aeruginosa*

Daniella Lucy Spencer BSc, September 2018



Thesis submitted to the University of Nottingham for the degree of Doctor of Philosophy

Declaration

Unless otherwise acknowledged, the work presented in this thesis is my own. No part has been submitted for a different degree at The University of Nottingham or any other establishment of learning.

Daniella Spencer, September 2018

Abstract

Pseudomonas aeruginosa is a prominent pathogen within the Cystic Fibrosis (CF) community which can survive the challenges posed by the immune system and antibiotic treatment in patient lungs. *P. aeruginosa* is such a success in this environment for numerous reasons that including (i) a multifactorial virulence strategy, (ii) capacity to form biofilms, and (iii) the ability to thrive under low oxygen conditions. *P. aeruginosa* possesses an Arginine specific Autotransporter Aminopeptidase (AaaA). The arginine that AaaA releases from the N-terminal of proteins/peptides is used by *P. aeruginosa* as a nitrogen and energy source, which is hypothesized to confer a fitness advantage in oxygen limited environments. To further understand the relevance of AaaA to chronic *P. aeruginosa* CF airway infections, this work investigated whether *aaaA*: (i) is controlled by regulators relevant to the CF environment; (ii) is present and active in CF isolates; (iii) can be purified for the purpose of inhibitor development, and (iv) plays a role in biofilm formation. A panel of CF isolates showed the presence of a highly conserved *aaaA* gene with some SNPs outside the active site. The levels of AaaA activity in these strains differed, but did not correlate with any particular phenotypic trait. Comparison of *aaaA* promoter sequences from GenBank revealed a 169 bp promoter deletion in some *P. aeruginosa* strains including the Liverpool epidemic strain (LES). AaaA activity responded positively to a reduced oxygen concentration in the environment, and in line with this, activation of *aaaA* was found to be under the potential control of several transcription factors including ArgR, NarX/NarL plus the alternative sigma factor RpoN and AaaA itself. A qRT-PCR assay was developed for further testing of *aaaA* expression under low oxygen tensions. A recombinant protein was created to facilitate further studies including crystallisation and inhibitor screening. Finally, *aaaA* was found to be involved in biofilm development depending on the strain background and environmental conditions. This data supports the idea of a subtle, but important, role for AaaA in the chronic persistence of CF lung *P. aeruginosa* infections.

Acknowledgments

It has been a long and rocky journey to get to the point of submission and I could not have done it without the help of some special people. I would like to mention everyone, but I think I might need another thesis to fit you all in. You know who you are! Thank you.

I have to start with the funding bodies which have made this project possible. The MRC, University of Nottingham and Roche Biosciences have all contributed to the resources available to carry out this research.

I want to personally thank my supervisors Kim, Alan and Miguel. I never was without avenues to try: Miguel never failed to produce fountains of ideas and more than the average amount of enthusiasm. Alan helped me to keep my work in context and think about the bigger picture, while always being very supportive. Kim has guided me through the maze that has been AaaA and the world of research in general, as well as spending a great deal of quality time with my thesis for which I am very grateful.

To the members of *Pseudomonas* and gram-negative groups, thank you for your technical expertise, for listening to my dilemmas and for your helpful tips & suggestions. My particular thanks includes, but is not exclusive of, Jeni, Matt, Manual, Freya, Phil, Simon, Esteban, Noreen and Hazel. Two people who have gone beyond the usual degree of helpfulness and have been true sources of inspiration are Diana Palenzuela and Mahmoud Ashawesh.

I have shared the AaaA experience with a number of masters, undergraduate and work experience students. I want to thank them for their enthusiasm and contribution as well as wishing them the best for the future.

To my friends in the lab and outside, thank you for keeping me sane (or, at least, limiting the damage). To draw some parallels with Tolkein, it has felt like the end of the PhD experience has been the one place I didn't want to get any closer to, while being the one place I have been trying to reach. For the times when I was really lost and thought I wouldn't make it, you made all the difference. Some special mentions from UoN are Osman and Hazel for all the laughter; Alex for the moral support and for always surprising me with general knowledge facts; Paolo, Victoria and Rickesh for good food and great company; members of B50, C69, C75 and C81 for the conversations and for finding the funny side in difficult times. Also to Louisa, Hristina and Becky; Briony; Rowan; Jill and Whizzey; you've all been wonderful!

I have the best family who have been incredibly supportive. Especial thanks to my granny Sheila, my nanny Mickey, and my auntie Sue, who sent me regular care packages.

The greatest thanks are for my parents Janet and John Spencer, who are the reason I made it this far and could not have been more supportive in every way possible. I have FINALLY finished! This thesis is for them.





Also to our cat Alfie, who did nothing apart from remind me it was snack time.

Contents

Declaration 1

Abstract 2

Acknowledgments 3

Figures 11

Tables 19

Abbreviations 20

1 Chapter 1: Introduction 22

1.1 Pseudomonas aeruginosa 22

1.1.1 Metabolism 23

1.1.2 Virulence 36

1.1.3 *P. aeruginosa* as a biofilm forming bacterium 41

1.1.4 Regulation 51

1.2 Cystic Fibrosis 55

1.1.4 Cause and Pathogenesis of Cystic Fibrosis 55

1.1.5 Altered microbiota of the CF respiratory system and how this is linked to the susceptibility of these patients for contracting lung infection 57

1.1.6 *P. aeruginosa* as a CF pathogen 63

1.1.7 *P. aeruginosa* as a clinically important pathogen outside of the CF airway . 66

1.3 Autotransporter Proteins 67

1.1.8 Secretion systems in *P. aeruginosa* 67

1.1.9 The Type V Secretion System 71

1.3.3 Type V secretion systems in *P. aeruginosa* 75

1.3.4 The arginine specific aminopeptidase autotransporter of *P. aeruginosa* (AaaA) 76

1.4 Conclusion 79

1.5 Aims 79

2 Chapter 2: Materials and Methods 81

2.1 General Chemicals 81

2.2 Bacterial Strain Storage and Growth Conditions 81

2.2.1 Microaerobic growth 81

2.3 Optical density ($OD_{600\ nm}$) 81

2.4 Transfer of genetic material into bacteria 82
2.4.1 Conjugation 82
2.4.2 Transformation 82
2.5 DNA manipulation 83
2.5.1 PCR 84
2.5.2 Cloning 84
2.5.3 Tables relevant to nucleic acid manipulation 85
2.6 RNA 87
2.6.1 RNA extraction 87
2.6.2 RNA conversion to cDNA 88
2.6.3 RT-qPCR endogenous reference screening 88
2.6.4 Primer efficiency testing 88
2.6.5 qRT-PCR for gene expression in different growth conditions 89
2.7 P-nitroanilide degradation assay 89
2.7.1 Inhibitor Assays 90
2.7.2 Specialised conditions 90
2.8 Tecan assay to measure gene expression using the miniCTX-*lux* transcriptional reporter 91
2.8.1 Specialised Media 91
2.8.2 Changes to assay to investigate CF specific conditions 93
2.9 Phenotypic Assays 95
2.9.1 Motility 95
2.9.2 Pyocyanin 96
2.9.3 Elastase 96
2.10 Biofilm 97
2.10.1 Microscopy 97
2.10.2 8-well chamber slide assay (microchambers) 98
2.10.3 Bioflux 98
2.10.4 Congo red colony biofilm assay 98
2.10.5 Floating biofilm assay in ASM 99
2.10.6 *ex vivo* pig lung model 99
2.10.7 Murine *P. aeruginosa* respiratory infection model (Liverpool University) 100
2.11 Statistical analysis 101

2.12 Strain and Plasmid Tables 101

3 Chapter 3: Regulation of AaaA and development of a qRT-PCR assay for the improved investigation of gene expression in response to internal regulators and extracellular factors 106

3.1 Introduction.....106

3.1.1 Background 106

3.1.2 Chapter aims 117

3.2 Results.....117

3.2.1 Promoter analysis of *aaaA* suggests the existence of a complex regulatory network 117

3.2.2 STRING database analysis places aaaA between diverse gene networks ..133

3.2.3 DNA curvature analysis of the promoter for MvaT/MvaU binding reveals region overlapping the putative RpoN site 137

3.2.4 The negative regulation problem and significance of oxygen 139

3.2.5 RpoN may not repress *aaaA* expression consistently 140

3.2.6 Development of a qRT-PCR assay to complement miniCTX-*lux* data 143

3.3 Discussion 163

3.3.1 Promoter analysis 163

3.3.2 The association of *aaaA* with other genes: STRING database findings.....168

3.3.3 In line with previous data, *PaaaA* activation is reduced in the PAO1 WT, but this cannot be explained by RpoN mediated repression 168

3.3.4 qRT-PCR development.....169

3.3.5 Final conclusions 172

4 Chapter 4: The Relationship of AaaA with Cystic Fibrosis.....173

4.1 Introduction.....173

4.1.1 Background 174

4.1.2 A note on media choice and naming.....179

4.2 Results.....180

4.2.1 Characterisation of Cystic Fibrosis isolates 180

4.2.2 The role of AaaA in cystic fibrosis isolates 206

4.2.3 Investigation of conditions relevant to the Cystic Fibrosis airway: PAO1 and PAO1 *ΔaaaA* strains.....226

4.2.4 Investigation of conditions relevant to the Cystic Fibrosis airway in the CF isolates 247

4.2.5 CF isolate trait comparison and relationship to AaaA 257
4.3 Discussion 262
4.3.1 Phenotypic characteristics of CF isolates 262
4.3.2 AaaA in CF isolates.....270
4.3.3 CF lung conditions effect on AaaA 274
4.3.4 Correlation of traits and final conclusions.....282
5 Chapter 5: Purification and Characterisation of AaaA 285
5.1 Introduction.....285
5.1.1 Background 285
5.2 Results.....288
5.2.1 Truncating AaaA for purification, structural analysis and inhibitor screening: version 1 289
5.2.2 Production of a second truncated version of AaaA (AaaAt2) to improve solubility and ease of purification 302
5.2.3 Engineering AaaAt3 309
5.3 Discussion 317
5.3.1 Inclusion body formation: what are they, how do they form and how can they be dealt with 317
5.3.2 Taking AaaAt3 further 324
5.3.3 Conclusion 325
6 Chapter 6: impact of AaaA on biofilm formation and virulence 326
6.1 Introduction.....326
6.1.1 Background 326
6.1.2 Aims 328
6.2 Results.....328
6.2.1 Biofilms grown in 10% LB media using 8 well chamber slides show no difference between PAO1 and PAO1 *ΔaaaA* strains.....328
6.2.2 Nitrogen limited media optimisation and comparison to artificial sputum media 330
6.2.3 Biofilms using the minimal media cocktail in 8 well chamber slides do not differ between PAO1 and PAO1 *ΔaaaA* strains 342
6.2.4 A LESB65 *ΔaaaA* strain was constructed which showed an activity phenotype similar to PAO1 *ΔaaaA* 344

6.2.5 PAO1 and PAO1 *ΔaaaA* do not differ when grown in aerobic ASM in a Bioflux system ……347

6.2.6 LESB65 biofilms differ structurally from PAO1 and the LESB65 *ΔaaaA* biofilms are thinner than the WT 352

6.2.7 Investigation of arginine and tripeptide on PAO1 biofilms using the Bioflux model showed biofilm production in the *ΔaaaA* mutant was impaired when arginine was absent 354

6.2.8 PAO1 and PAO1 *ΔaaaA* biofilms do not differ when grown in either aerobic or microaerobic conditions in ASM using the microchamber model 359

6.2.9 Making an IPTG independent complemented PA01 *ΔaaaA* strain 365

6.2.10 Cloning 365

6.2.11 Comparison of the inducible strains show all to have activity greater than PAO1 *ΔaaaA* in LB 371

6.2.12 A complementation disparity could be due to alternatively reading ORFs .373

6.2.13 Floating ASM tube biofilms show a difference between PAO1 and PAO1 *ΔaaaA* strains 378

6.2.14 AaaA could compensate for phenazine mediated redox dependent systems in low oxygen areas of biofilm 380

6.2.15 The PAO1 *ΔaaaA* CFU count is higher than PAO1 from biofilms grown in an *ex vivo* pig lung model 385

6.2.16 A chronic murine infection model with PAO1 and PAO1 *ΔaaaA* showed mixed findings (Liverpool data) 389

6.3 Discussion 391

6.3.1 Biofilm assays: what they have revealed about AaaA 391

6.3.2 Development of minimal media for AaaA assays and the effect of amino acids on *aaaA* expression 395

6.3.3 The complementation phenomenon.....399

6.3.4 Conclusion 401

7 Chapter 7: Final Conclusion and Future Directions 402

7.1 Introduction.....402

7.2 Discussion 402

7.2.1 The AaaA functional domain is highly conserved between *P. aeruginosa* CF isolates and the population can be divided into two types of *aaaA* upstream region ……402

7.2.2 Phenotypic traits associated with a more virulent cell state were reduced or absent in CF isolates, and no difference was observed between PAO1 and PAO1 *ΔaaaA* strains ……404

7.2.3 The expression and activity of AaaA in CF relevant conditions was most affected by oxygen and arginine presence 404

7.2.4 Regulation of *aaaA* is complex and analysis of its promoter reveals the potential for a highly intricate multilayer regulation 406

7.2.5 A recombinant version of AaaA is suitable for further purification and crystallisation 408

7.2.6 Abnormally high expression of *aaaA* may be problematic for cell viability, and weaken *P. aeruginosa's* ability to form biofilm.....409

7.2.7 The dependence of *P. aeruginosa* on AaaA for biofilm formation applies to particular conditions and strain backgrounds 409

7.3 Summary 412

7.4 The End 413

Appendices 414

1.1 Appendix A: minimal media cocktail validation 414

References 417

Figures

Figure 1.1.1: *P. aeruginosa* phylogenetic tree.. 23
Figure 1.1.2: The arginine succinyltransferase (AST) pathway.. 26
Figure 1.1.3: The arginine dehydrogenase (ADH, or ATA) pathway..... 27
Figure 1.1.4: The ADC pathway. 28
Figure 1.1.5: The D-arginine dehydrogenase pathway. 29
Figure 1.1.6: The arginine anabolic pathways.. 30
Figure 1.1.7: The denitrification pathway in *P. aeruginosa*..... 31
Figure 1.1.8: A detailed outline of each step in the *P. aeruginosa* denitrification pathway. 33
Figure 1.1.9: A simplified diagram of pyruvate fermentation in *P. aeruginosa*. 34
Figure 1.1.10: The arginine deiminase (ADI) pathway 35
Figure 1.1.11: The stages of biofilm development. 45
Figure 1.1.12: The balance of c-di-GMP promotes a biofilm or planktonic existence. 46
Figure 1.1.13: Biofilm regulation in *P. aeruginosa*.. 47
Figure 1.1.14: Two potential modes of initial colonisation of the CF airway by *P. aeruginosa*. 49
Figure 1.1.15: How RpoN can mediate gene repression (Figure adapted from Schaerer *et al* 2015). 53
Figure 1.2.1: An overview of the symptoms experienced by Cystic Fibrosis patients. 56
Figure 1.2.2: The structure of the CFTR receptor and the 6 classes of mutations..... 57
Figure 1.2.3: *P. aeruginosa* as a successful CF airway pathogen: a summary diagram.. .. 66
Figure 1.3.1: The structure of a typical autotransporter protein. 72
Figure 1.3.2: Overview of the autotransporter mechanism of secretion.. 73
Figure 1.3.3: Models for how autotransporter proteins cross the outer membrane..... 75
Figure 1.3.4: Predicted catalytic residues and active site pocket of AaaA, from Luckett *et al* 2012 (showing parts A-C). 77
Figure 2.5.1: Ligation equation used in cloning work.. 85
Figure 3.1.1: Summary of the 4 L-arginine catabolic pathways in *P. aeruginosa* and their regulatory influences.. 108
Figure 3.1.2: Model of relationship between arginine, arginine catabolic pathways, and AaaA. 110
Figure 3.1.3: How oxygen and nitrogen availability could influence *aaaA* expression through the regulators ANR, NarXL and ArgR.....111
Figure 3.1.4: RpoN could inhibit *aaaA* directly or indirectly. 114
Figure 3.1.5: Autoregulation of *aaaA* could be mediated at different stages. 116
Figure 3.2.1: The *aaaA* gene is encoded on the negative strand and transcription factors which also read in this direction will be indicated. 118
Figure 3.2.2: A putative binding site for RpoN was found in the *aaaA* 500 bp UPS region. 123

Figure 3.2.3: A putative ArgR binding site was identified in the 500 bp UPS *aaaA* upstream region.. 124
Figure 3.2.4: Putative NarL binding sites were identified in the *aaaA* 500 bp UPS region. 125
Figure 3.2.5: Two putative IHF binding sites were identified in the 500 bp *aaaA* upstream region. 126
Figure 3.2.6: A putative NtrC binding site was identified in the 500 bp *aaaA* UPS region. 128
Figure 3.2.7: A putative ArcA binding site was identified in the 500 bp *aaaA* UPS region. 129
Figure 3.2.8: A putative RhlR binding site was identified in the 500 bp *aaaA* UPS region. 131
Figure 3.2.9: Putative FleQ binding sites were identified in the 500 bp *aaaA* UPS region.133
Figure 3.2.10: Output from the STRING database on 21-05-2018 shows the connections known about *aaaA* (here *PA0328*).. 134
Figure 3.2.11: Output from the STRING database on 21-05-2018 shows the connections known about *PA0329*.....136
Figure 3.2.12: Curvature prediction and GC content of the *aaaA* 500 bp upstream region shows at least 7 peaks of curvature. 138
Figure 3.2.13: Activation of the *aaaA* promoter is higher in the PAO1 *ΔaaaA* strain than the WT. 140
Figure 3.2.14: GEO expression data presented on the *Pseudomonas* genome database shows that *aaaA* expression increases in the *rpoN* mutant strains of PAO1.. 142
Figure 3.2.15: RpoN does not reduce P*aaaA* activation, opposing expectation, while the complemented strain shows increased promoter activation in *PaaaA* and *Pkan*.....142
Figure 3.2.16: From the different categories of qRT-PCR, the relative, comparative C_T method is used here.....144
Figure 3.2.17: Sampling points representative of lag, exponential, and early stationary phase were selected along growth curves of PAO1 and PAO1 *ΔaaaA* strains in aerobic LB, aerobic ASM, microaerobic LB and microaerobic ASM.....147
Figure 3.2.19: Reference gene selection using the online tool RefFinder shows *16S* to be the most stable in the conditions tested. 150
Figure 3.2.20: Design and choosing of qRT-PCR primers for *aaaA* amplification by the NCBI BLAST Primer design tool.. 152
Figure 3.2.21: Design and selection of qRT-PCR primers for *PA0329* amplification by the NCBI BLAST Primer design tool. 153
Figure 3.2.22: Optimised primer efficiencies for primer pairs aaaA_7 and PA0329_1 show efficiencies close to 90% for aaaA_7 and close to 100% for PA0329_1. 155
Figure 3.2.23 Fold change of *aaaA* and *PA0329* expression in different conditions at exponential and early stationary phase, show no significant differences in *aaaA* expression and a significant increase in *PA0329* expression in the PAO1 *ΔaaaA* microaerobic samples 153

Figure 3.2.24: Differences in gene expression between growth phases in PAO1 and PAO1 *ΔaaaA* backgrounds is mostly insignificant. 161
Figure 3.2.25: Fold change of *PA0329* expression from *aaaA* expression in exponential and early stationary phase samples in the PAO1 strain show generally higher expression in *PA0329* but this is only significant in microaerobic and aerobic LB stationary phase samples. 162
Figure 3.3.1: Potential mechanism of RpoN mediated control of *PaaaA* activation. 167
Figure 4.1.1: *P. aeruginosa* clinical isolates from Cystic Fibrosis patient sputum. 174
Figure 4.1.2: Three CF isolates exhibited mucoid phenotypes or failed to generate defined colonies: CF 326, CF 393 and CF 030. 174
Figure 4.1.3: Where does the nitric oxide (NO) go? 179
Figure 4.2.1: All CF isolates differed to PA01 at some point during the growth curve in aerated, LB media. 182
Figure 4.2.2: All CF isolates differed to PA01 at some point during the growth curve in aerated, artificial sputum media. 184
Figure 4.2.3: All CF isolates differed to PA01 at some point during the growth curve in microaerobic, LB media.. 186
Figure 4.2.4: All CF isolates differed to PA01 at some point during the growth curve in microaerobic, ASM media. 188
Figure 4.2.5: CF isolates differ from PAO1 in their capacity to swarm. 189
Figure 4.2.6 CF isolates differ from PAO1 in their capacity to swim. 190
Figure 4.2.7 CF isolates differ from PAO1 in their capacity to twitch.. 191
Figure 4.2.8: Elastase activity is low in the CF isolates in comparison to PAO1. 192
Figure 4.2.9: The majority of CF isolates do not produce detectable pyocyanin when grown in LB, aerobically. 193
Figure 4.2.10: Congo red colony biofilms produced by CF isolates on days 1-4 show variation in colour, shape, size and rugosity.. 196
Figure 4.2.11 Congo red colony biofilms produced by CF isolates on days 5-6 show variation in colour, shape, size and rugosity. 197
Figure 4.2.12: Only CF 393 showed a clumping phenotype in the floating biofilm assay. 199
Figure 4.2.13: The PAO1 WT shows a clumping phenotype in the floating biofilm assay. 199
Figure 4.2.14: PAO1 grown in a Bioflux system in ASM media produces a biofilm which is highly clustered.. 202
Figure 4.2.15: CF 326 grown in a Bioflux system in ASM media produces a biofilm which has more evenly spaced, smaller microcolonies than PAO1. 203
Figure 4.2.16: CF 983 grown in a Bioflux system in ASM media produces a biofilm which has more evenly spaced, smaller microcolonies and more red (dead) areas than PAO1. .204
Figure 4.2.17: CF 393 grown in a Bioflux system in ASM media produces a biofilm which shows the beginning of large microcolonies forming similar to PAO1. 205
Figure 4.2.18: The *aaaA* gene is present in *P. aeruginosa* isolated from a range of CF patients. 207

Figure 4.2.19: The *aaaA* gene is present in multiple *P. aeruginosa* strains isolated from a single CF patient (from Darch *et al* 2015). 207
Figure 4.2.20: AaaA passenger domain mutations in CF isolates do not overlap with active site residues indicating that this is conserved. 210
Figure 4.2.21: Common mutation pattern 1. 211
Figure 4.2.22: Common mutation pattern 2 (A and B) and 3 (C and D). 211
Figure 4.2.23: Mutation patterns in CF 393 (A) and CF 484 (B).. 212
Figure 4.2.24: Mutations unique to individual isolates in the AaaA passenger domain. ...214
Figure 4.2.25: Some strains of *P. aeruginosa* have a deletion of 169bp at the beginning of the intergenic region between *PA0329* and *aaaA*. 216
Figure 4.2.27: Most of the CF isolates have the deletion identified in Fig 3.31, and a sequence with good homology to LESB65. 224
Figure 4.2.28: Single nucleotide changes to the upstream region of *aaaA* shared by the CF isolates intersect with some identified putative regulatory sites. 225
Figure 4.2.29: Construction of strains to measure *aaaA* expression using the miniCTX-*lux* reporter. 227
Figure 4.2.30: Metabolic hierarchy of *P. aeruginosa.* 228
Figure 4.2.31: In LB media, activation of the *aaaA* promoter is not reduced by addition of KNO_3. 229
Figure 4.2.32: In LB media, activation of the *aaaA* promoter is not reduced by addition of NH_4Cl. 230
Figure 4.2.33: In LB media, activation of the *aaaA* promoter is increased in higher NaCl concentrations in the PAO1 *ΔaaaA* mutant but not the PAO1 WT strain. 232
Figure 4.2.34: In LB media, pH values between 5.8 and 6.8 do not affect the activation of *PaaaA.* 234
Figure 4.2.35: The miniCTX-*lux* reporter driven by a constitutive promoter (*Pkan*) produces less bioluminescence when oxygen is limited. 236
Figure 4.2.36 The AaaA activity assay measures hydrolysis of L-arginine coupled to the dye P-nitroanilide and can be used to test activity of cell-associated enzyme as the bacteria are not growing and the background non-specific activity is low. 237
Figure 4.2.37: PAO1 and the PAO1 *ΔaaaA* mutant have lower AaaA activities in ASM compared to in LB media when cells are grown aerobically. 238
Figure 4.2.38: In microaerobic conditions, AaaA activity differs between LB and ASM at all time points above 0 in PAO1 *ΔaaaA* but not PAO1. 240
Figure 4.2.39: AaaA activity is different in ASM and substantially increases when the oxygen concentration is lower in PAO1 and PAO1 *ΔaaaA* strains. 242
Figure 4.2.40 Addition of exogenous KNO_3 and NH_3Cl does not affect AaaA activity in LB media. 244
Figure 4.2.41: NaCl concentration does not affect AaaA activity in LB media in the range tested. 246
Figure 4.2.42: AaaA activity is higher at pH 6.8 and pH 7.2 than pH 5.8 and pH 6.2. 247

Figure 4.2.43: In aerobic LB media, CF isolates exhibit variation in *PaaaA* activation, while the *Pkan* promoter does not consistently drive luminescence. 249
Figure 4.2.44: All CF isolates exhibit more than the baseline AaaA activity when grown aerobically in LB. 250
Figure 4.2.45: The activation of *PaaaA* is different in CF isolates grown in ASM compared to LB, however the kanamycin promoter did not drive comparable levels of bioluminescence in ASM and LB when integrated into CF isolates grown in aerobically. 252
Figure 4.2.46 : CF isolates show a general increase in *PaaaA* activation in KNO_3 enriched media, while AaaA activity is affected differently depending on the CF isolate. 254
Figure 4.2.47: In most CF isolates less *PaaaA* activation is observed in high NaCl LB, while a lower AaaA activity correlates with a low concentration of NaCl. 256
Figure 4.3.1: Formulae used in nitrogen percentage calculations. 264
Figure 4.3.2: The redox cycling capabilities of phenazines allow ATP generation from glucose and pyruvate in anaerobic conditions but this is not required for functioning of the ADI pathway. 267
Figure 4.3.3: Microaerobic conditions stimulate AaaA activity when its substrate is present. 276
Figure 4.3.4: Hypothesis of the effect NarXL has on *aaaA* transcription. 277
Figure 4.3.5: AaaA activity could be influenced by the relative expression and changes to the open reading frame (ORF). 279
Figure 5.1.1: Structure of AaaA based on protein sequence comparison with SGAP highlighting active site residues. 288
Figure 5.2.1: Truncation of AaaA to facilitate protein purification. 291
Figure 5.2.2: AaaAt1 is overproduced at the slightly higher than expected size of 50 kDa. 294
Figure 5.2.3*:* AaaAt1 produced from *E.coli* BL21 *pET21a::aaaAt1* was less active than full length (FL) AaaA. 296
Figure 5.2.4: Process of AaaAt1 purification. 298
Figure 5.2.5: Dialysed AaaAt1 is active and sensitive to inhibition by ion chelators. 300
Figure 5.2.6: Gel filtration chromatography shows AaaAt1 to be aggregating (data kindly provided by Dr Simon Caulton). 302
Figure 5.2.7: Truncation of AaaA to facilitate protein purification, version 2 303
Figure 5.2.8: Cloning *aaaAt2*. 305
Figure 5.2.9: AaaAt2 is insoluble and overproduction kills the producing cells. 307
Figure 5.2.10: Lysis is necessary for activity of AaaAt2. 308
Figure 5.2.11: Induction is better at 22°C for AaaAt2. 308
Figure 5.2.12: AaaAt3 engineering. 310
Figure 5.2.13: Cloning process of AaaAt3. 312
Figure 5.2.14: A small amount of AaaAt3 is soluble. 314
Figure 5.2.15: Induction at 37°C yields more AaaAt3 activity than at 22°C with 0.3 mM IPTG 315
Figure 5.2.16: The soluble fraction of AaaAt3 is active. 316

Figure 5.3.1: How inclusion bodies of AaaAt1 could form in *E.coli* BL21.....319
Figure 5.3.2: How to deal with inclusion bodies summary. 321
Figure 5.3.3: The first truncation left hydrophobic residues exposed which could have compromised protein solubility.. 323
Figure 5.3.4: Solubilisation and Purification of AaaAt3 by use of the 'salting-out' method 325
Figure 6.2.1: No difference in biofilm formation was found between PAO1, PAO1 *ΔaaaA* and PAO1 *ΔaaaA* miniCTX*::aaaA* strains grown in aerated, LB using the microchamber system. 329
Figure 6.2.2: Growth of *P. aeruginosa* is supported by arginine and succinate. 332
Figure 6.2.3: Growth of *P. aeruginosa* is supported by tripeptide and succinate. 333
Figure 6.2.4: Growth of *P. aeruginosa* is supported by KNO_3 and succinate. 334
Figure 6.2.5: Comparison between MMP + 20 mM succinate media supplemented with KNO_3, arginine or tripeptide shows that arginine and tripeptide activate both *PaaaA* and *Pkan* more than KNO_3, while arginine significantly increases *PaaaA* compared to tripeptide. 335
Figure 6.2.6: Minimal media cocktail containing non-nitrogen containing R-group amino acids supports growth, while *PaaaA* remains more activated in PAO1 than PAO1 *ΔaaaA*. 337
Figure 6.2.7: Addition of different amino acids and KNO_3 to the minimal media cocktail influence *PaaaA* activation (part 1).....340
Figure 6.2.8: Addition of different amino acids and KNO_3 to the minimal media cocktail influence *PaaaA* activation (part 2).....341
Figure 6.2.9: No difference in biofilm formation was found between PAO1 and PAO1 *ΔaaaA* strains grown in aerated, minimal media cocktail using the microchamber system, but PAO1 *ΔaaaA* miniCTX*::aaaA* produced less biofilm. 343
Figure 6.2.10: Strategy for the deletion of *aaaA* in LESB65. 345
Figure 6.2.11: Activity of AaaA in LESB65 and LESB65 ΔaaaA strains grown in LB media is significantly different. 346
Figure 6.2.12: The activity of AaaA in LESB65 and PAO1 backgrounds did not differ significantly between ASM and LB. PAO1, PAO1 *ΔaaaA,* LESB65 and LESB65 *ΔaaaA* were grown in LB or ASM until exponential phase. 347
Figure 6.2.13: PAO1 forms a clumpy biofilm which is not affected by the deletion of *aaaA* in a Bioflux system.....349
Figure 6.2.14: Showing all images taken across the Bioflux channel for the PAO1 biofilms. 350
Figure 6.2.15: Showing all images taken across the Bioflux channel for the PAO1 *ΔaaaA* biofilms. 351
Figure 6.2.16: LESB65 forms biofilm that is reduced in thickness upon deletion of *aaaA* in a Bioflux system.. 353
Figure 6.2.17: PAO1 and PAO1 *ΔaaaA* in normal ASM produce biofilms similar to each other when grown in the Bioflux system for 15 hours, 37°C aerobically 355

Figure 6.2.18: PAO1 and PAO1 *ΔaaaA* in ASM 2x arginine produced biofilms showing greater dispersal from the clusters and did not show a repeatable difference between the strains when grown in the Bioflux system for 15 hours, 37°C aerobically. 356
Figure 6.2.19: PAO1 and PAO1 *ΔaaaA* in ASM + 10 mM tripeptide produced biofilms which were similar in both strains when grown in the Bioflux system for 15 hours, 37°C aerobically. 357
Figure 6.2.20: PAO1 and PAO1 *ΔaaaA* in ASM without arginine created a difference in biofilm formation between the WT and mutant strains when grown in the Bioflux system for 15 hours, 37°C aerobically.....358
Figure 6.2.21: PAO1 and PAO1 *ΔaaaA* in ASM without arginine + tripeptide may have created a difference in biofilm formation between the WT and mutant strains when grown in the Bioflux system for 15 hours, 37°C aerobically, but as the biofilms are not healthy in the second repeat this would need to be determined by further investigation. 359
Figure 6.2.22: : PAO1 T7-gfp biofilms grown in aerobic ASM in 8 well chamber slides for 48 hours show a flat, thin patchy biofilm. 361
Figure 6.2.23: PAO1 *ΔaaaA* T7-gfp biofilms grown in aerobic ASM in 8 well chamber slides for 48 hours show a flat, thin patchy biofilm. 362
Figure 6.2.24: PAO1 T7-gfp biofilms grown in microaerobic ASM in 8 well chamber slides for 48 hours show a flat, thin patchy biofilm. 363
Figure 6.2.25: PAO1 *ΔaaaA* T7-gfp biofilms grown in microaerobic ASM in 8 well chamber slides for 48 hours show a flat, thin patchy biofilm. 364
Figure 6.2.26: Construction of *miniCTX::araC::aaaA*. 366
Figure 6.2.27: Activity of AaaA in PAO1 and PAO1 *ΔaaaA* conjugated with miniCTX:*:araC::aaaA* in LB is not significantly different when the inducer is present. 367
Figure 6.2.28: Comparison of arabinose concentrations to test induction efficacy of the miniCTX::*araC::aaaA* construct in PAO1 and PAO1 *ΔaaaA* backgrounds shows that 0.2% arabinose is best for differentiation between induced and uninduced strains. 369
Figure 6.2.29: Comparison of AaaA activity in succinate and glucose supplemented ASM shows there is increased activity in glucose media in the PAO1 *ΔaaaA* miniCTX::*araC::aaaA* strain. 371
Figure 6.2.30: Comparison of AaaA activity in different complementation strains in LB shows all inducible strains are significantly more active than the PAO1 *ΔaaaA* strain.. ...372
Figure 6.2.31: Comparison of AaaA activity in different complementation strains in ASM shows IPTG induction to be less effective in differentiating induced and uninduced strains. 373
Figure 6.2.32: Regardless of arabinose induction PAO1 *ΔaaaA* miniCTX*::araC::aaaA* forms less biofilm than both PAO1 and PAO1 *ΔaaaA* strains.....375
Figure 6.2.33: Investigation of alternative ORFs within *aaaA*. 377
Figure 6.2.34: Clumping is observed in PAO1 but not PAO1 *ΔaaaA* in ASM. 379
Figure 6.2.35: Clumping is observed in the PAO1 *ΔaaaA* miniCTX::*araC::aaaA* strains grown in ASM. 379

Figure 6.2.36: Clumping is observed in the PAO1 *ΔaaaA pME6032::aaaA* strain grown in ASM. 380
Figure 6.2.37: Clumping is not observed in LESB65 or LESB65 *ΔaaaA* in ASM.....382
Figure 6.2.39: *aaaA* and *phz* could work in parallel to support *P. aeruginosa* growth in biofilms. 383
Figure 6.2.40: *aaaA* and *phz* could work in parallel to support *P. aeruginosa* growth in biofilms. 384
Figure 6.2.41: PA14 *ΔphzΔaaaA* shows a wrinkly phenotype that is indicative of increased oxygen reliance. 385
Figure 6.2.42: Bronchiole sections used as a scaffold for biofilm growth.....386
Figure 6.2.43: CFU count from homogenised EVPL bronchiole tissue after 24 hours of growth shows increased growth of PAO1 *ΔaaaA* compared to PAO1. 387
Figure 6.2.44: *Ex vivo* pig lung bronchiole tissue sections infected with PAO1, PAO1 *ΔaaaA* or PAO1 *ΔaaaA* miniCTX*::aaaA* strains show a similar amount of bacterial invasion and tissue damage, which is not apparent in the mock-infected control. 388
Figure 6.2.45: No significant difference in CFU count was found between PAO1 and PAO1 *ΔaaaA* strains in a 5 day mouse model. 390
Figure 6.2.46: AaaA may be involved in facilitating chronic infection. 390
Figure 6.2.47: No significant difference between PAO1 and PAO1 *ΔaaaA* strains was found in the four pro-inflammatory indicators tested. 390
Figure 6.3.1: Association between nitrogen availability, glutamine, histidine and *aaaA.* Based on Janssen *et al* (1982).....397
Figure 6.3.2: Ammonium and ammonia are produced in the asparagine metabolic pathway. Image taken from the PseudoCyc database. 399
Figure 7.2.1: Simple model for how AaaA could support the metabolism of *P. aeruginosa* in a biofilm. Figure adapted from Toyofuku *et al* (2012). 412
Figure 1.1.1: Comparison between KNO_3 and NH_4Cl nitrate sources with the investigation of the effect of different salts on growth & expression. 415
Figure 1.1.2: Showing the activation of the *PaaaA* and *Pkan* promoters in PAO1 and PAO1 *ΔaaaA* strains in the optimised combined solution named minimal media cocktail.....416

Tables

Table 1.1.1: The aerobic oxidases possessed by *P. aeruginosa*. 24
Table 1.1.2: Predominant virulence factors of *P. aeruginosa*. 40
Table 1.2.1: Microbial life discovered in the CF respiratory tract.....63
Table 1.1.3: Sigma factors in *P. aeruginosa*..... 51
Table 1.3.1: Secretion systems in gram-negative bacteria. 70
Table 2.5.1: Amplification conditions used in this work. 85
Table 2.5.2: Table of Primers. 87
Table 2.6.1: Temperature cycling used in qRT-PCR assays. 89
Table 2.8.1: Composition of ASM used in this thesis based on the protocol by Palmer *et al* (2007)..... 92
Table 2.8.2: Minimal media cocktail composition. 93
Table 2.8.3: NaCl concentrations used in the NaCl comparison experiment. 94
Table 2.8.4: Ratio of Na_2HPO_4 and NaH_2PO_4 for a 0.1 M 100 ml stock solution at different pHs. 95
Table 2.9.1: Media for motility assays. 96
Table 2.9.2: Elastin-Congo red solution preparation. 97
Table 2.12.1: Bacterial strains used in this study. 104
Table 2.12.2 plasmids used in this study.....105
Table 3.2.1: Identified Sigma Factors using the tool Virtual Footprint (Prodoric). 119
Table 3.2.2: Identified Transcription Factors using the tool Virtual Footprint (Prodoric). .121
Table 3.2.3: Curvature peak location in the *aaaA* UPS in relation to putative sites of transcription or sigma factors. 139
Table 3.2.4: RNA yield and quality from extraction process after DNA digestion. 149
Table 3.2.5: Optimised qRT-PCR conditions for the detection of *aaaA* and *PA0329* transcripts. 154
Table 3.2.6: qRT-PCR terms used in the following section. 157
Table 4.2.1: Identities of the sequences belonging to group 1 or group 2.....223
Table 4.2.2: Summary of results.....261
Table 5.2.1: Basic properties of the AaaA protein. 289
Table 5.2.2: Basic properties of the truncated versions of AaaA protein. 293
Table 6.2.1: Summary of amino acid addition effect on the activation of *PaaaA* or *Pkan*.. 339

Abbreviations

°C	degrees Celcius
% (v/v)	percentage volume per volume
% (w/v)	percentage weight per volume
AaaA	arginine specific amino peptidase autotransporter of *P. aeruginosa*
ADC	arginine decarboxylase pathway
ADI	arginine deiminase pathway
Ap	ampicillin
ASM	artificial sputum media (Palmer et al 2007)
AST	arginine succyl-transferase pathway
AT	autotransporter
AUC	area under the curve
bp	base pair
CCR	carbon catabolite repression
CF	cystic fibrosis
CFU	colony forming unit
c-di-GMP	bis-(3',5') cyclic di guanylase
DNA	deoxyribonucleic acid
dNTP	deoxynucleoside triphosphate
dyn	dyne
eDNA	extracellular DNA
EPS	extracellular polysaccharide
g	grams
GFP	green fluorescent protein
Gm	gentamycin
h	hour
IPTG	isopropyl-1-thio-(B-D-galactopyranoside)
H_2O	water
Kb	kilobase
kDa	kilodalton
KNO_3	potassium nitrate
LB	lysogeny broth
LES	Liverpool epidemic strain
µg	microgram
µL	microlitre
µM	micromolar
M	molar
MOPS	3-(N-morpholino) propane sulfonic acid
mA	milliampere
mg	milligram
min	minute
mL	millilitre
MMP	minimal medium P
NH_4Cl	ammonium chloride
nm	Nano molar
OD	optical density
O/N	overnight
ORF	open reading frame
PCR	polymerase chain reaction
PBS	phosphate buffered saline
PBST	phosphate buffered saline 0.1%(v/v) Tween 20
PGD	*Pseudomonas* genome database
PQS	*Pseudomonas* quinolones signal
PIA	*Pseudomonas* isolation agar
PI	Propidium iodide
QS	quorum sensing
RLU	relative luminescence units

RNA	ribonucleic acid
Rpm	revolutions per minute
SDS	sodium dodecyl sulphate
SDS-PAGE	sodium dodecyl sulphate
SGAP	*Streptomyces griseus* aminopeptidase
TAE	Tris acetate EDTA buffer
Tc	tetracycline
TCS	two component system
TF	transcription factor
TT1S	type one secretion system
TT2S	type two secretion system
TT3S	type three secretion system
TT4S	type four secretion system
TT5S	type five secretion system
TT5S	type six secretion system

1 Chapter 1: Introduction

This study looks at the arginine specific aminopeptidase autotransporter protein of *Pseudomonas aeruginosa* (AaaA) in the context of cystic fibrosis (CF) lung infections. This chapter presents the following:

1.1 *Pseudomonas aeruginosa*
- i. General
- ii. Metabolism
- iii. Virulence
- iv. *P. aeruginosa* as biofilm forming bacterium
- v. Regulatory network

1.2 Cystic Fibrosis
- vi. Cause and pathogenesis of CF
- vii. Microbiome of the CF airway
- viii. *P. aeruginosa* as a CF pathogen

1.3 Autotransporters
- ix. The secretion systems in gram negative bacteria
- x. The type V secretion system
- xi. Mechanism of autotransporter secretion to cell exterior
- xii. Autotransporters in *P. aeruginosa*
- xiii. AaaA

1.1 Pseudomonas aeruginosa

Pseudomonas aeruginosa is a highly adaptive Gram-negative bacterial species, able to thrive in a diverse range of environments (Kung *et al* 2010). These include water, soil, plants and animals including humans (Rahme *et al* 1995). In humans it can cause serious urinary tract, burn wound, and respiratory infections; the latter including those found in lung cancer, chronic obstructive pulmonary disease (COPD), bronchiectasis and cystic fibrosis patients (Berghmans *et al* 2003; Papi *et al* 2006; Monsó *et al* 1995; Nicotra *et al* 1995; Oliver *et al* 2000; Smith *et al* 1996).

At *P. aeruginosa's* disposal is an extensive genome of 6.3 mega bases (Mb) comprised of 5,570 predicted open reading frames (ORFs). It shows a high degree of plasticity, facilitating the bacterium's high adaptability, with evidence showing a large amount of gene rearrangement and acquisition (Stover *et al* 2000).

The *Genera Pseudomonas* currently includes the largest number of strains in the Gram-negative division of bacteria. In 2014 there were 144 strains classified as

belonging to *Pseudomonas* and that number continues to grow (Gomila *et al* 2015). The species *P. aeruginosa* can be broadly divided into 3 groups as defined by the International *Pseudomonas aeruginosa* Consortium (Freschi *et al* 2015). Notably, group 1 includes the strain PAO1, group 2 includes PA14 and group 3 is dominated by PA7 (Figure 1.1.1). Further sequence comparison using core-genome analysis (Harvest), suggested that *P. aeruginosa* has on average a genetic core size 17.5% of the total genome.

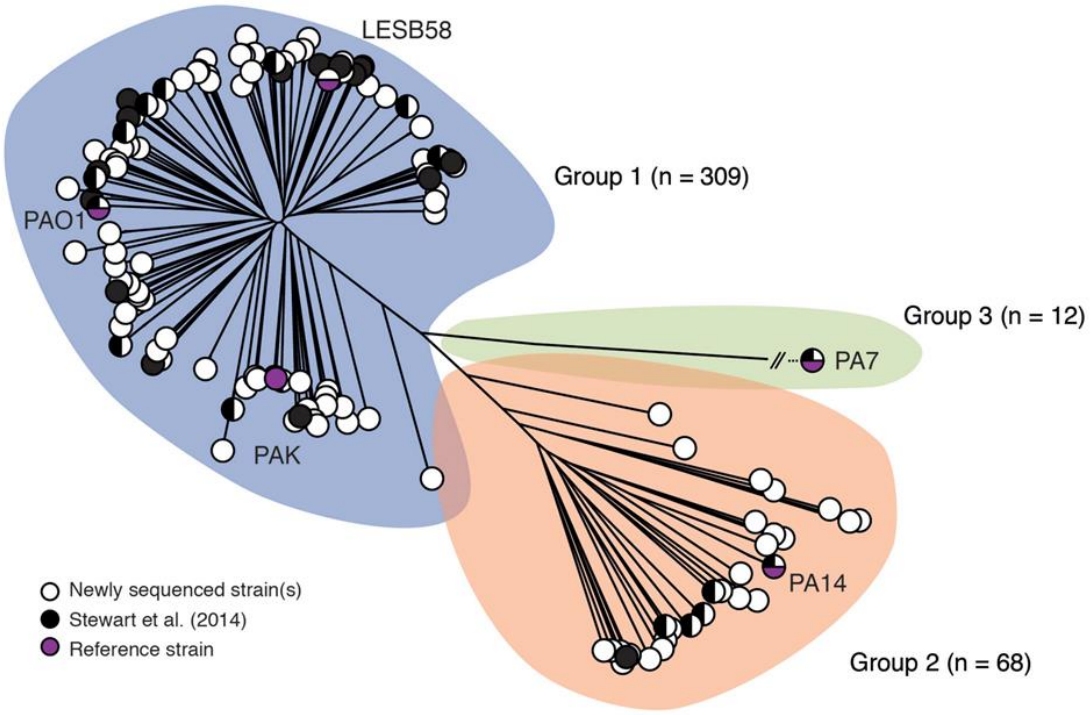


Figure 1.1.1: *P. aeruginosa* phylogenetic tree. The diagram shows the 3 major groups of 389 *P. aeruginosa* strains in an unrooted phylogenetic tree of maximum likelihood, created using core genome SNP comparison. White circles show the strains newly sequenced by Freschi *et al*, black circles show the strains previously analysed by Stewart *et al* 2014 and the purple circles highlight the strains used as a reference in the study. The number of strains assigned to each group is shown, group 1 containing the majority. Adapted from Freschi *et al* (2015).

1.1.1 Metabolism

Possession of a large genome has equipped *P. aeruginosa* with a versatile metabolism. Preferentially, the bacterium will aerobically generate energy. However, it is also able to successfully propagate in oxygen limited environments and is consequentially known as a facultative anaerobe (Arai 2011).

1.1.1.1 Aerobic respiration

Five terminal oxidases are known to be utilized by *P. aeruginosa*. Three of these are cytochrome c oxidases, the other 2 being quinol oxidases (Fujiwara *et al* 1992; Matsushita *et al* 1983, 1982; Preisig *et al* 1993; Comolli *et al* 2004). Table

1.1.1 outlines each oxidase. These vary in affinity to oxygen which is likely to increase the bacterium's environmental adaptability. Regulation of these is principally from the transcriptional regulator ANR, the two-component transcriptional regulator RoxSR (Arai 2011, 2014) and RpoS, the stationary phase sigma factor (Fujita *et al* 1994). ANR is an oxygen sensor and upregulates genes involved in anaerobic survival when oxygen concentration is low (Lazazzera *et al* 1996; Ye *et al* 1995). It has been found to activate the transcription of the Cbb_3-2 cytochrome c oxidase, needed under conditions of reduced oxygen concentration. RoxSR is thought to act in response to the redox status of the respiratory chain and upregulates both Cbb_3-1 and Cbb_3-2 as well as the quinol oxidases. It works in conjunction with RpoS to regulate levels of the low oxygen affinity aa_3 oxidase (Kawakami *et al* 2010).

Oxidase	Group	Regulation	Oxygen affinity	Role
Cbb_3-1	Cytochrome c oxidase	Upregulated by RoxSR	High	Dominant oxidase expressed
Cbb_3-2	Cytochrome c oxidase	Upregulated by ANR Upregulated by RoxSR	High	Upregulated in low oxygen or stationary phase conditions
aa_3	Cytochrome c oxidase	Downregulated by RoxSR Upregulated by RpoS	Low	Induced under carbon, nitrogen or iron starvation
Bo_3	Quinol oxidase	Upregulated by RoxSR	Low	Induced under iron starvation or presence of s-nitrosoglutathione (NO producer)
CIO	Quinol oxidase	Downregulated by ANR Upregulated by RoxSR Upregulated by RpoS	Low	Important low oxygen concentrations when cyanide concentrations inhibit haem-copper oxidases Expressed under conditions of copper starvation

Table 1.1.1: The aerobic oxidases possessed by *P. aeruginosa*. Based on Arai 2011 (Arai 2011, 2014; Kawakami *et al* 2010; Fujiwara *et al* 1992; Matsushita *et al* 1983, 1982; Preisig *et al* 1993; Comolli *et al* 2004; Fujita *et al* 1994; Lazazzera *et al* 1996; Ye *et al* 1995).

P. aeruginosa consumes available carbon sources in an ordered hierarchy according to its preferences (NG and Dawes 1967; Rojo 2010). When preferred compounds are present, assimilation of alternative sources of nutrition are repressed. This phenomenon is called carbon catabolite repression (CCR) (Rojo 2010) and allows metabolically versatile bacteria to optimise their resources in order to maximise growth. Expression of virulence factors are often linked to CCR, as many of them function in gaining access to novel carbon sources (Gorke and Stulke 2008). In contrast to *E. coli*, glucose does not appear to play a central metabolic role in *Pseudomonas* species, which generally prioritise the

consumption of amino acids and some organic acids. Supporting this, succinate and acetate presence represses gluconate, glycerol, fructose and mannitol assimilatory genes (Collier *et al* 1996). Last in the hierarchy are the hydrocarbons (Moreno *et al* 2010). There is even an ordering of utilization within the amino acids. In *Pseudomonas putida,* proline, alanine, glutamate, glutamine, histidine, arginine, lysine, asparagine and aspartate availability represses assimilation of valine, isoleucine, leucine, threonine, phenylalanine, tyrosine, glycine and serine (Rojo 2010). The complex and highly structured nutrient assimilatory mechanisms of *Pseudomonas* highlight this *Genus*' versatility and the importance in considering the wider metabolic consequences of tinkering with a specific part of its network.

1.1.1.1.1 Arginine metabolism in aerobic conditions: part 1, the catabolic pathways

P. aeruginosa possesses 4 arginine catabolic pathways. One of these, the arginine deiminase (ADI) pathway, is applicable in anaerobic conditions and will be discussed later. The aerobically operating pathways include the arginine succinyltransferase (AST) pathway, the arginine decarboxylase (ADC) pathway and the arginine dehydrogenase, or transaminase (ADH, or ATA) pathway. *P. aeruginosa* also employs a racemization route for the conversion of D-arginine to L-arginine. In aerobic conditions the AST pathway is preferred (Yang and Lu 2007; Li and Lu 2009; Itoh 1997; Vander Wauven *et al* 1984).

Figure 1.1.2 depicts the AST pathway. The *aruCFGDBE* operon encodes the enzymes required by this pathway until glutamate is produced. Following the production of glutamate, the *gdhB* gene facilitates conversion of glutamate into 2-ketoglutarate. Induction of *aruCFGDBE* and *gdhB* is by ArgR, responding to the presence of arginine (Lu *et al* 2004; Li and Lu 2009; Itoh 1997). When the AST pathway is disabled, the ADH (ATA) pathway is activated (Figure 1.1.3). Unlike the AST pathway, ArgR is not responsible for the induction. In fact, *argR* mutant strains show upregulation of this pathway, due to inactivation of the AST route. Instead, the *aruHI* operon is activated by the AruRS two-component system (TCS) which responds to arginine activation (Yang and Lu 2007; Lu *et al* 2004; Li and Lu 2009).

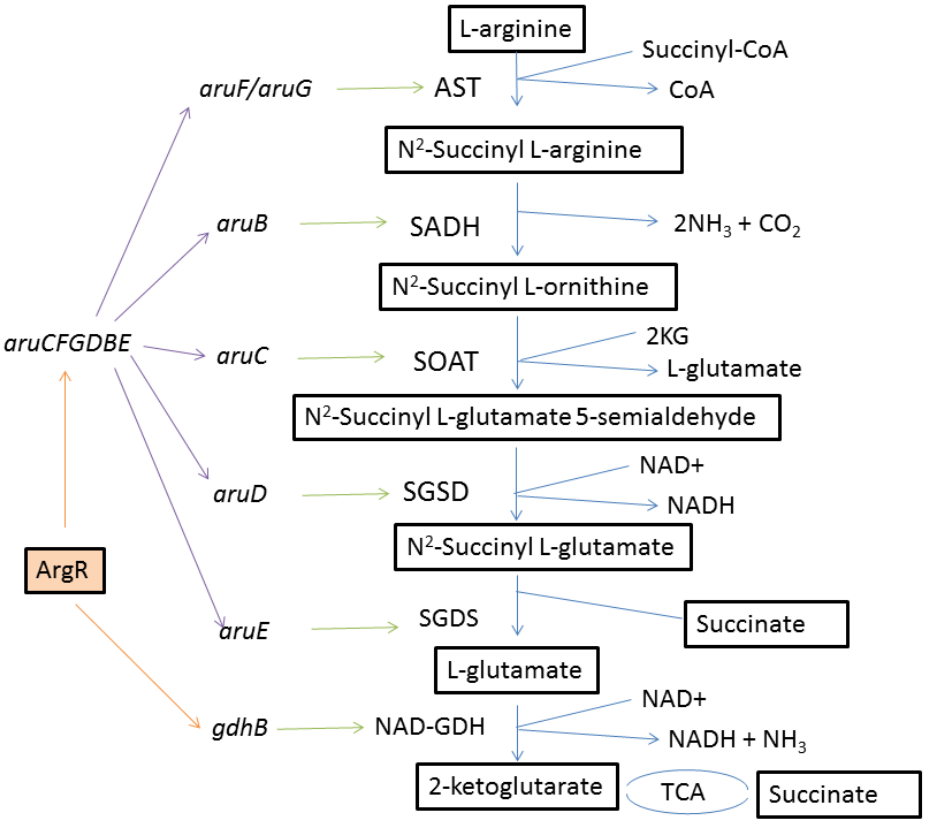


Figure 1.1.2: The arginine succinyltransferase (AST) pathway. L-arginine is converted by the arginine succinyltransferase (AST) enzyme to N2-Succinyl L-arginine releasing CoA. N2-Succinyl L-arginine is then converted to N2-Succinyl L-ornithine by N2-Succinylarginine dihydrolase (SADH), releasing ammonia and carbon dioxide. N2-Succinyl L-ornithine is converted to N2-Succinyl L-glutamate 5-semialdehyde by N2-Succinylornithine 5-aminotransferase (SOAT) with the release of L-glutamate. N2-Succinyl L-glutamate 5-semialdehyde is converted to N2-Succinyl L-glutamate by N-Succinylglutamate 5-semialdehyde dehydrogenase (SGSD) with the conversion of NAD+ to NADH. N2-Succinyl L-glutamate is converted to L-glutamate and succinate by N-Succinylglutamate desuccinylase (SGDS). Succinate enters the TCA cycle while L-glutamate is converted by the NAD+ dependent glutamate dehydrogenase (NAD-GDH) to 2-ketoglutarate with the conversion of NAD+ to NADH and release of ammonia. The 2-ketoglutarate enters the TCA cycle. The operon *aruCFGDBE* encodes AST, SADH, SOAT, SGSD and SGDS. The gene *gdhB* encodes NAD-GDH. Both *aruCFGDBE* and *gdhB* are upregulated by ArgR (Yang and Lu 2007; Li and Lu 2009; Itoh 1997; Lu and Abdelal 2001; Nakada and Itoh 2003).

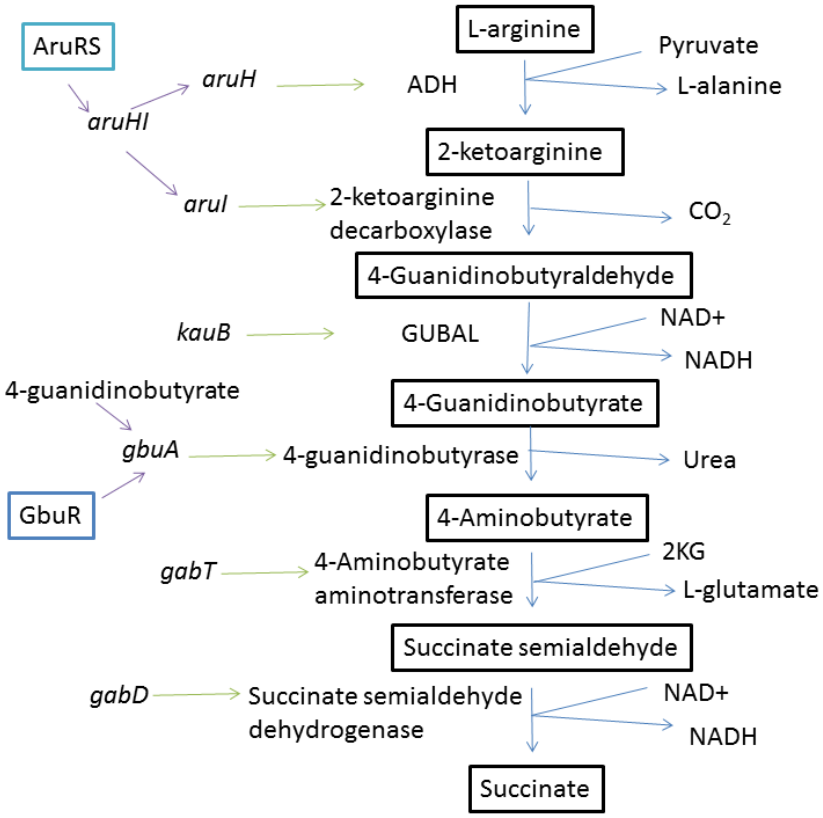


Figure 1.1.3: The arginine dehydrogenase (ADH, or ATA) pathway. L-arginine is converted to 2-ketoarginine with the L-arginine dehydrogenase (ADH) enzyme, with the addition of pyruvate and release of alanine. The 2-ketoarginine decarboxylase enzyme converts 2-ketoarginine to 4-guanidinobutyralehyde with the release of CO_2. The 4-guanidinobutyraldehyde dehydrogenase (GUBAL) enzyme converts 4-guanidinobutyralehyde to 4-guanidinobutyrate with the conversion of NAD+ to NADH. The 4-guanidinobutyrase enzyme converts 4-guanidinobutyrate to 4-aminobutyrate with the release of urea. The 4-aminobutyrate aminotransferase converts 4-aminobutyrate to succinate semialdehyde with the input of 2-ketoglutamate (2KG) and release of glutamate. Finally, succinate semialdehyde dehydrogenase converts succinate semialdehyde to succinate with the conversion of NAD+ to NADH. Succinate enters the TCA cycle (not shown). Regulation of the *aruHI* operon encoding ADH and 2-ketoarginine carboxylase is through AruRS which responds to arginine. The *gbu* gene, which encodes the 4-guanidinobutyrase enzyme, is regulated by Gbu and its substrate 4-guanidinobutyrate (Yang and Lu 2007; Li and Lu 2009; Itoh 1997).

In the ADC pathway, arginine is converted to agmatine and putrescine (Figure 1.1.4). The purpose of this pathway is hypothesised to be for putrescine provision which can be converted to spermidine (Nakada and Itoh 2003). In replacement of ArgR regulation, agmatine, N-carbamoylputrescine and arginine upregulate *aguBA* (agmatine deiminase operon) and N-carbamoylputrescine amidohydrolase, which convert agmatine to putrescine (Mercenier *et al* 1980). Addtionally, the ADC pathway appears to be under the control of CCR and nitrogen repression. Mercenier *et al* (1980) reported that succinate or citrate repressed this pathway in arginine or agmatine containing media; a combination of succinate and ammonia or glutamine repressed agmatine deiminase and N-carbamoylputrescine amidohydrolase.

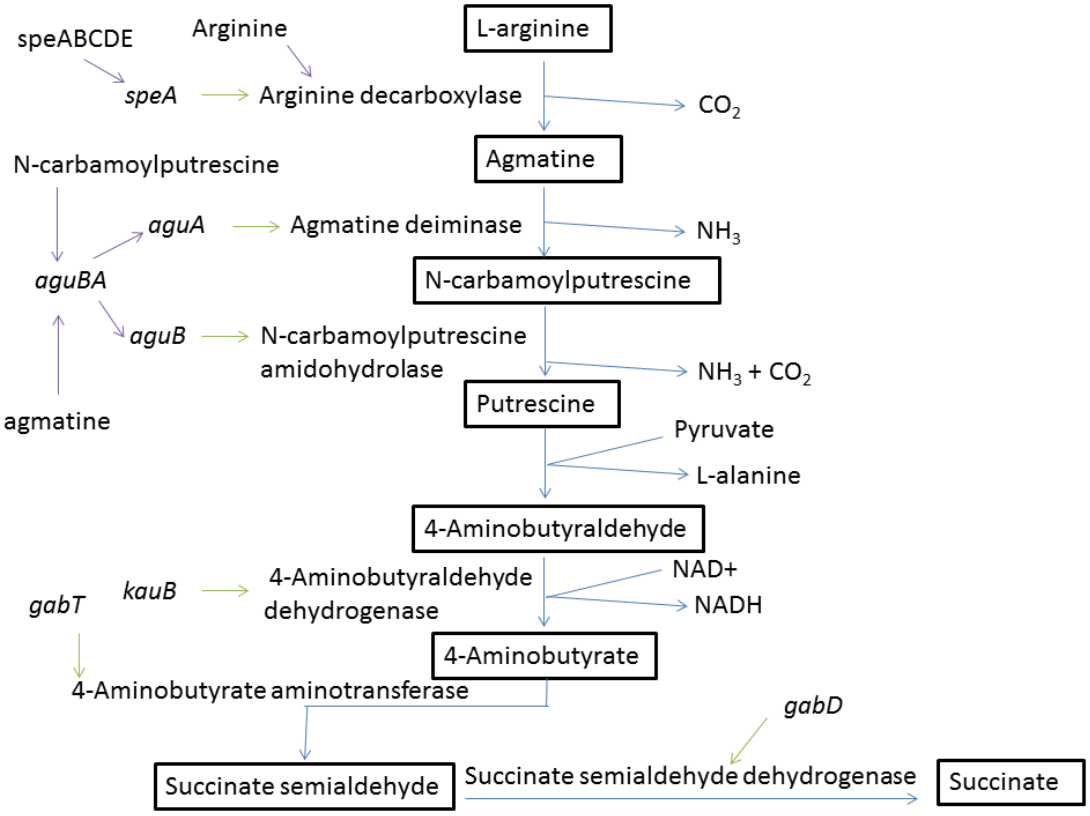


Figure 1.1.4: The ADC pathway. L-arginine is converted to agmatine by arginine decarboxylase (ADC) with the release of ammonia. Agmatine is converted to N-carbamoylputrescine by agmatine deiminase. N-carbamoylputrescine is converted to putrescine by N-carbamoylputrescine amidohydrolase with the release of ammonia and carbon dioxide. Putrescine can then be converted to 4-amminobutyraldehyde with the addition of pyruvate and release of alanine. The enzyme 4-aminobutyrate dehydrogenase then converts 4-amminobutyraldehyde to 4-aminobutyrate with the conversion of NAD+ to NADH. Penultimately, 4-aminobutyrate is converted to succinate semialdehyde with 4-aminobutyrate aminotransferase. Succinate semialdehyde is then converted to succinate by succinate semialdehyde dehydrogenase. When only arginine is available for growth, the arginine decarboxylase is activated. This enzyme is encoded on the operon *speABCDE*. Agmatine deiminase and N-carbamoylputrescine amidohydrolase are encoded on the *aguBA* operon. Both agmatine and N-carbamoylputrescine upregulate activity of these enzymes but not arginine (Mercenier *et al* 1980; Nakada and Itoh 2003).

Compared to the AST, ADH, ADC and ADI pathways which metabolise the L-form of arginine, the D-arginine dehydrogenase (DADH) pathway (Figure 1.1.5) can support *P. aeruginosa* growth when D-arginine is the sole source of carbon and nitrogen. This is achieved through a racemization process, a 2 step conversion of D-arginine to L-arginine by DADH and an anabolic L-arginine dehydrogenase encoded on the *dauBAR* operon. D-arginine upregulates *dauBAR* and 2-ketoarginine, the intermediate between L and D arginine forms, activates DADH. A principle purpose of this pathway is to provide L-arginine for the AST and ADH (ATA) pathways (Li and Lu 2009; Haas *et al* 1984; Jann *et al* 1988).

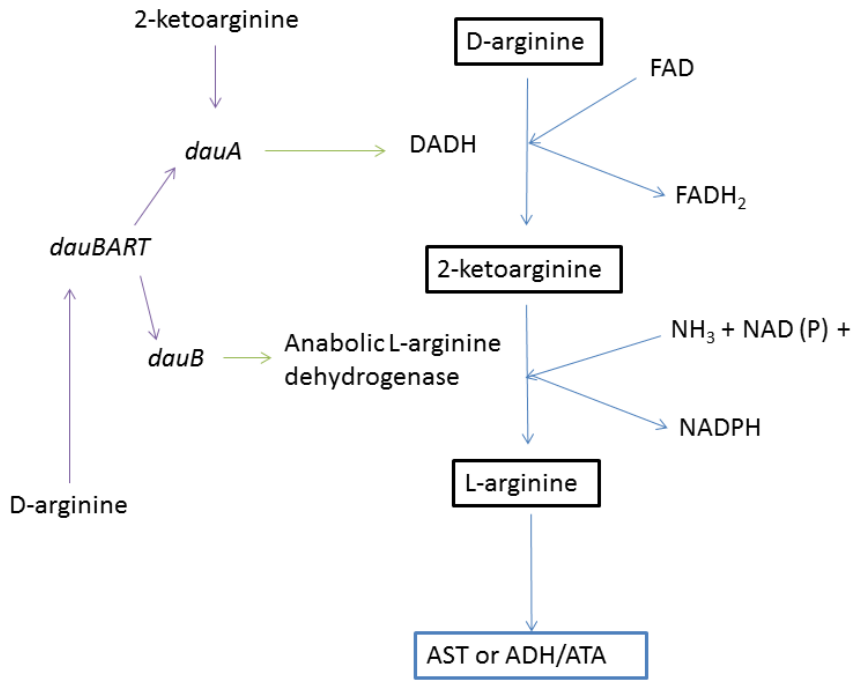


Figure 1.1.5: The D-arginine dehydrogenase pathway. D-arginine is converted to 2-ketoarginine by the D-arginine dehydrogenase (DADH) encoded by *dauA*. FAD is converted to $FADH_2$. Ammonia and 2-ketoarginine are converted to L-arginine by the anabolic L-arginine dehydrogenase encoded by *dauB*. NAD (P)+ is converted to NADH. L-arginine can then be fed into the AST or ADH/ATA pathway. The genes *dauA* and *dauB* are part of the *dauBART* operon which is upregulated by D-arginine. DADH (*dauA*) is upregulated by 2-ketoarginine in addition to D-arginine (Li and Lu 2009; Haas *et al* 1984; Jann *et al* 1988).

1.1.1.1.2 Arginine metabolism in aerobic conditions: part 2, the anabolic pathways

The arginine anabolic pathways in *P. aeruginosa* rely on the initial availability of L-glutamate and L-glutamine to generate carbamoyl phosphate and L-ornithine which are converted to citrulline, L-arginosuccinate and L-arginine. The presence of L arginine, L-ornithine, 2-aminobutanoate and zinc ions inhibits different parts of the process (Cunin *et al* 1986). Figure 1.1.6 outlines this pathway and the points at which inhibition can occur.

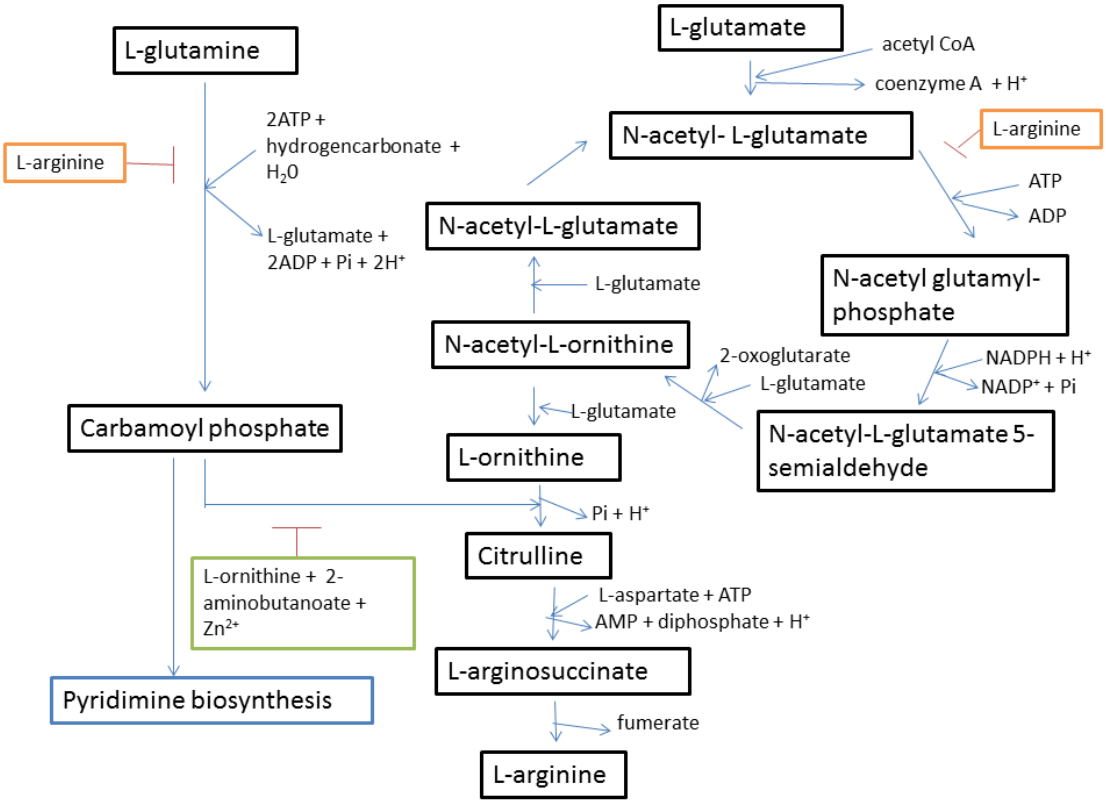


Figure 1.1.6: The arginine anabolic pathways. The starting amino acids glutamine and glutamate begin this pathway. L-glutamate procedes through a cycle to generate L-ornithine which is combined with carbamoyl phosphate (the product of L-glutamine) to form citrulline followed by L-arginosuccinate and finally L-arginine. The presence of L-arginine inhibits the conversion of L-glutamine to carbamoyl phosphate and the production of N-acetyl glutamyl-phosphate from N-acetyl-L-glutamate. The presence of ornithine, 2-aminobutanoate and zinc ions inhibits the production of citrulline from carbamoyl phosphate and ornithine (Cunin *et al* 1986). Figure based on the pathway presented in biocyc.

1.1.1.2 P. aeruginosa is adapted for microaerophilic conditions

Cbb_3-1 and Cbb_3-2 (Table 1.1.1) are highly expressed even in oxygen abundant conditions (Comolli *et al* 2004). The lower oxygen affinity enzymes are maintained at reduced concentrations in the absence of stress or starvation (Kawakami *et al* 2010) and appear to function primarily to support growth under these sub-optimal conditions. This is in contrast to other bacterial species (Mouncy *et al* 1998; Preisig *et al* 1996; Otten *et al* 2001) and suggests that *P. aeruginosa* is particularly well adapted to microaerobic environments. Many of the environments inhabited by *P. aeruginosa* are microaerobic or cause the bacteria to reduce the concentration of oxygen reaching its cells. For example, alginate is produced profusely in CF isolates and this has been found to slow the diffusion of oxygen (Linker and Jones 1996; Govan and Harris 1986; Davies *et al* 1993). The environment of the CF airway is microaerobic to anaerobic, a location where *P. aeruginosa* successfully persists (Worlitzsch *et al* 2002). Additionally, the

production of biosurfacants such as rhamnolipids reduces oxygen penetration into liquids, reducing the oxygen reaching the cells (Sabra *et al* 2002).

1.1.1.3 Anaerobic respiration

In the absence of oxygen, *P. aeruginosa* can use nitrate or nitrite as alternate electron acceptors through the denitrification pathway outlined in Figure 1.1.7. The genes involved in the denitrification process are activated when oxygen is limited, in combination with nitrate or nitrite availability (Palmer *et al* 2007).

Figure 1.1.7 outlines the denitrification pathway. Three nitrate reductases are known to be utilised by *P. aeruginosa*: Nar, Nap and Nas. Nap may also play a redox regulatory function (Gavira *et al* 2002; Flanagan *et al* 1999) and Nas a nitrate assimilatory function (Berks *et al* 1995).

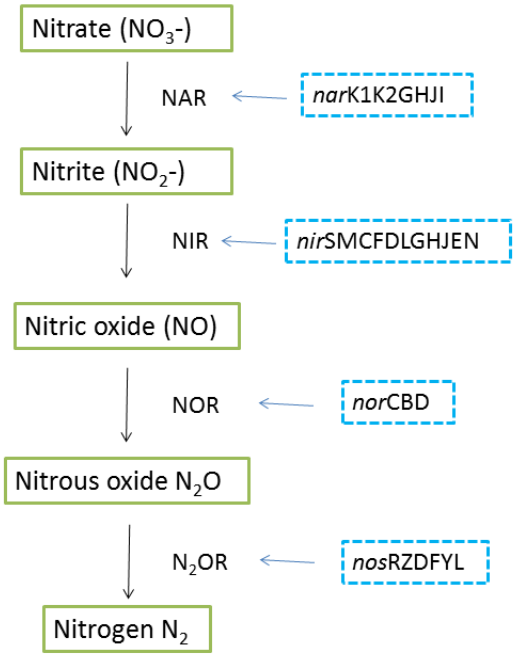


Figure 1.1.7: The denitrification pathway in *P. aeruginosa*. Nitrate (NO_3-) is reduced with the nitrate reductase Nar encoded by the *narK1K2GHJI* operon. Nitrite (NO_2-) is reduced with the nitrite reductase Nir encoded by the *nirSMCFDLGHJEN* operon. Nitric oxide (NO) is converted into nitrous oxide (N_2O) with Nor, a nitric reductase encoded by *norCBD,* and the nitrous reductase N_2OR (*nosRZDFYL* operon) completes the process through conversion of nitrous oxide into nitrogen. (Berks *et al* 1995; Arai 2011; Palmer *et al* 2007).

Regulation of the genes involved in the denitrification cascade (Figure 1.1.8) is largely by the *E. coli* FNR analogs, ANR and DNR (Hasegawa *et al* 1998), and the nitrate sensing TCS NarXL (Rabin *et al* 1993; Stewart *et al* 2003; Hartig *et al* 1999). Nar expression (*narK1K2GHJI*) responds to ANR, DNR and NarXL (Nadine *et al* 1999; Haas *et al* 1995; Arai *et al* 1991; 1994; 1995). As these regulators respond to limited oxygen and abundant nitrate, these conditions are central to

denitrification pathway activation. Nir (*nirSMCFDLGHJEN*) is regulated by NirQ (Silvestrini *et al* 1989; 1994). NirQ balances NO concentration which when high, is toxic to the cell (Arai *et al* 1998; Jungst and Zumft 1992). NirQ is regulated by DNR, which is controlled by ANR and NarXL. The *norCBD* (Nor) operon, is also under NirQ regulation (Schreiber *et al* 2007; Arai *et al* 2003).The last reductase in the cascade, N_2OR (*nosRZDFYL*) is under DNR regulation. NarXL and ANR both regulate expression from *dnr* (Arai *et al* 1997; Trunk *et al* 2010).

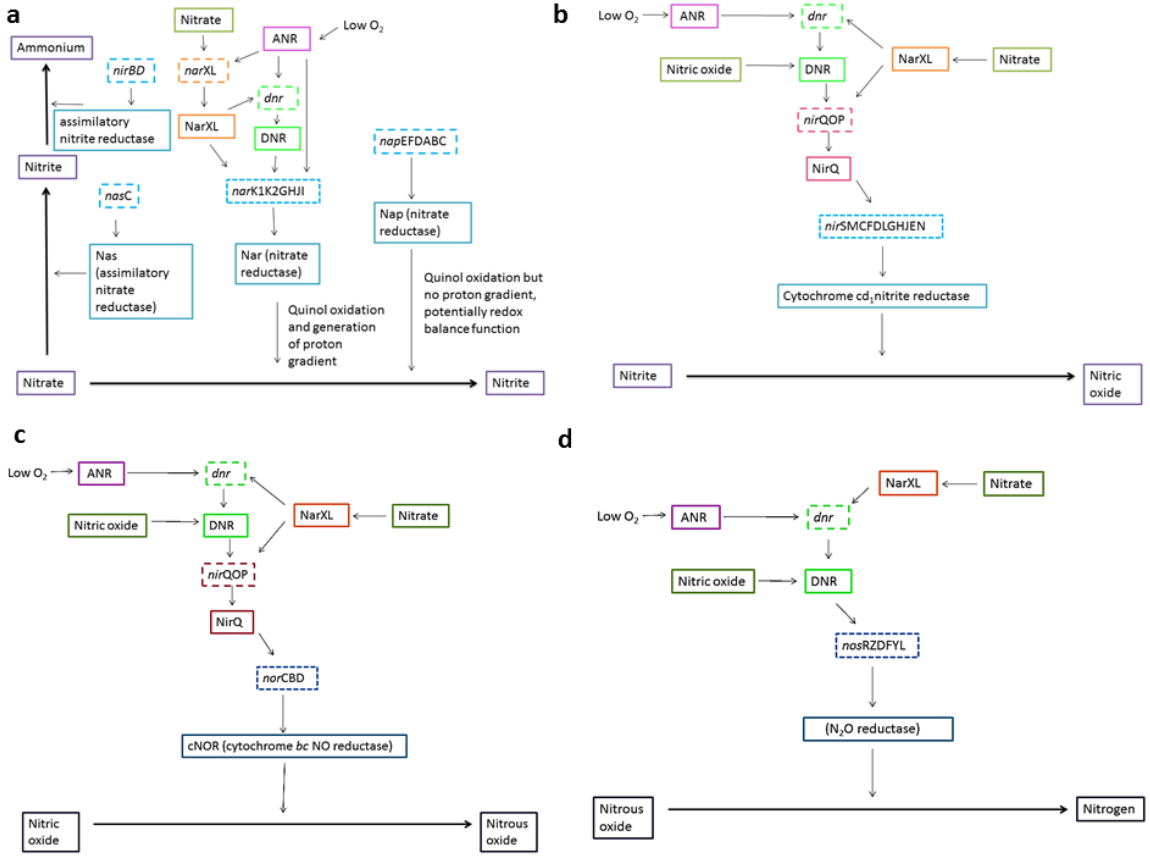


Figure 1.1.8: A detailed outline of each step in the *P. aeruginosa* denitrification pathway. Reductases are shown in blue outlined boxes, operons for the reductases shown in blue dashed outlined boxes. Regulator genes or operons are shown in dashed boxes and regulators in solid outline boxes. In Panel A, there are 3 reductases. While Nas and Nap perform nitrate assimilatory and probable redox balancing roles respectively, Nar reduces nitrate to nitrite by quinol oxidation which generates a proton gradient across the membrane. Nar is expressed from the *narK1K2GHJI* operon which responds to ANR, DNR and NarXL regulation (Nadine *et al* 1999; Haas *et al* 1995; Arai *et al* 1991; 1994; 1995). In Panel B nitrite is reduced to nitric oxide by the cytochrome cd1 nitrite reductase. This reductase is encoded by the *nirSMCFDLGHJEN* operon (Silvestrini *et al* 1989; 1994) which is regulated by NirQ. NirQ is under DNR and NarXL control (Arai *et al* 1998; Jungst and Zumft 1992). In Panel C, NOR reduces nitric oxide to nitrous oxide. NOR is regulated by NirQ (Schreiber *et al* 2007; Arai *et al* 2003). In Panel D, nitrous oxide is reduced to nitrogen by N_2O reductase which is regulated by DNR (Arai *et al* 1997; Trunk *et al* 2010).

In addition to anaerobic respiration using the denitrification cascade, *P. aeruginosa* can survive in anoxic conditions using the energy sources arginine and pyruvate. Pyruvate fermentation allows survival but not growth. In aerobic or anaerobic conditions where nitrate is available, pyruvate is metabolised to acetate which is utilized in the Krebs cycle. When conditions become anaerobic without available nitrate, pyruvate is converted into 3 products: lactate, acetate and succinate (Figure 1.1.9). This process occurs even in the presence in available arginine and the two processes are likely to complement each other due to the low pH generated from the acidic pyruvate fermentation products and the high pH resulting from ammonia release by arginine fermentation. The operon which encodes the phosphotransacetylase (PtA) and the acetate kinase (Ack), *ack-pta* is under ANR and integration host factor (IHF) regulation (Eschbach *et al* 2004).

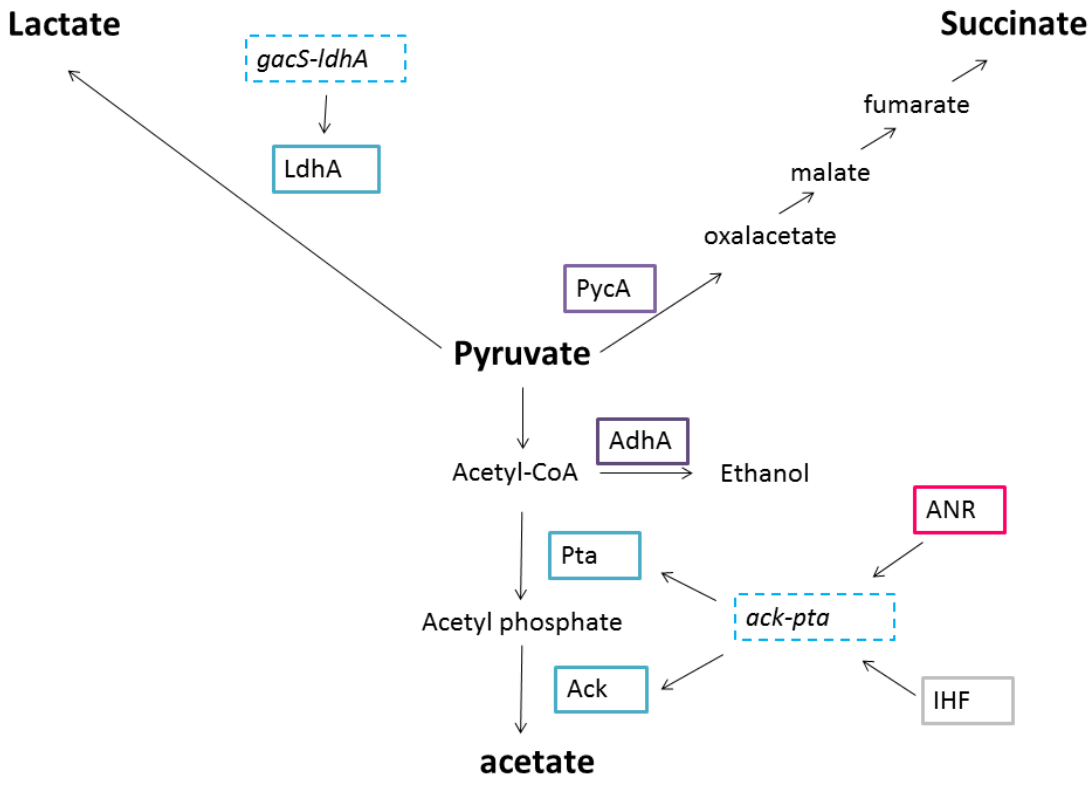


Figure 1.1.9: A simplified diagram of pyruvate fermentation in *P. aeruginosa*. Pyruvate is converted into acetate, lactase and succinate in an anaerobic environment devoid of nitrate. The *gacS-ldh* and *ack-pta* operon are essential to this pathway. The NADH-dependent lactate dehydrogenase LdhA is encoded by *gacS-ldh*. Encoded by *ack-pta* is the acetate kinase Ack and phosphotransacetylase Pta. AdhA is alcohol dehydrogenase and PycA is pyruvate carboxylase. The *ack-pta* operon is regulated by ANR and IHF. Based on Eschbach *et al* 2004.

When arginine is available, *P. aeruginosa* is able to grow slowly in anaerobic environments lacking a nitrate source using the arginine deiminase (ADI) pathway (Figure 1.1.10). At least 30-40 mM arginine is required to support growth in a complex medium such as yeast extract (Vander Wauven *et al* 1984).

Arginine enters the cell through the arginine/ornithine antiporter (Verhoogt *et al* 1992; Luthi *et al* 1990) and is converted to ornithine in a series of reactions catalysed by the enzymes arginine deiminase (ADI), catabolic ornithine carbamoyltransferase (cOTC) and carbamate kinase (CK) (Stalon *et al* 1967; Luthi *et al* 1990; 1986; Thauer *et al* 1997). The ADI pathway enzymes and ornithine/arginine antiporter are encoded on the *arcDABC* operon; *arcD* expressing the antiporter, *arcA* expressing ADI, *arcB* expressing cOTC and *arcC* expressing CK (Vander Wauven *et al* 1984; Rella *et al* 1985; Luthi *et al* 1986; Baur *et al* 1989). The *arcDABC* operon responds to low oxygen tensions through ANR activation, while the global arginine regulator, ArgR, also upregulates it. Nitrate availability represses this pathway through NarXL inhibition as the more efficient denitrification pathway is prioritised. Metabolites also influence the ADI pathway, with glucose, fumarate, citrate and pyruvate repressing it, while carbon, phosphate and energy shortage encourage its activation (Mercenier *et al* 1980).

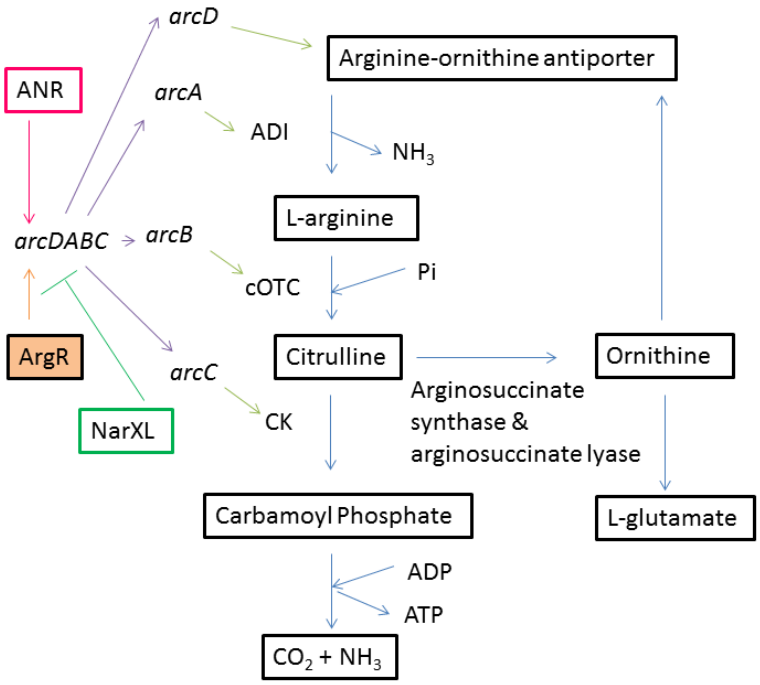


Figure 1.1.10: The arginine deiminase (ADI) pathway. Arginine enters the cell through the arginine-ornithine antiporter and is converted to citrulline by the arginine deiminase (ADI) enzyme. Citrulline is then converted to carbamoyl phosphate by the catabolic ornithine carbamoyltransferase (cOTC) with the addition of phosphate (Pi). Ornithine is released as a by-product and can either be transported outside of the cell through the arginine-ornithine antiporter or converted to L-glutamate by the *aruCFGDBE* operon. Each molecule of carbamoyl phosphate is used to generate 1 molecule of ATP with the assistance of the carbamate kinase enzyme (CK). Carbon dioxide and ammonia is released (Lu *et al* 2001; Maghnouj *et al* 1998).

1.1.2 Virulence

In addition to its metabolic versatility, *P. aeruginosa* is in possession of several virulence factors which facilitate host colonisation and damage. Table 1.1.2 outlines some of these virulence factors and their functions.

Virulence factor group	Virulence factor	Function and enhancement of pathogenesis	Genetics	Regulation	References
Proteases	**Protease IV**	A lysine specific serine endoprotease which degrades immunoglobulins, complement, fibrinogen and plasminogen. Involved in iron scavenging by degradation of lactoferrin and transferrin.	*piv*	LasR regulated	Engel *et al* 1998; Conibear *et al* 2012; Wilderman *et al* 2001
	Alkaline protease (AprA)	A metalloprotease which degrades the α_1-protease inhibitor, complement, laminin, matrix metalloproteinases, human γ interferon and tumour necrosis factor.	*aprA*	LasR and iron deficiency upregulates this enzyme (by PvdS)	Morihara *et al* 1979; Hong and Ghebrehiwet, 1992; Heck *et al* 1986; Twining *et al* 1993; Horvat and Parmely 1988; Laarman *et al* 2012; Shigematsu *et al* 2001; Gambello *et al* 1993
	Elastase: Elastase A (LasA) Elastase B (LasB)	Attacks intercellular tight junctions. LasB has been found to cause damage to host tissues, immunoglobulin, coagulator, complement, a-proteinase inhibitor, cytokines and chemokines and pulmonary surfactant. LasA has staphylolytic activity.	*lasB* gene *lasA* gene	LasR regulates *lasA* and *lasB*	Wretlind and Pavlovskis 1983; Kuang *et al* 2011; Kessler *et al* 1998; Van der plas *et al* 2016; Azghani 1996; Morihara 1964; Schultz and Miller 1974; Schmidtchen *et al* 2002
	***P. aeruginosa* small protease (PasP)**	Causes corneal damage and is able to degrade complement C3, fibrinogen and antimicrobial peptide LL-37.	*pasP*	Computational evidence from the Pseudomonas genome database places *pasP* in an operon with PA0422, a hypothetical protein, the association between these and	Marquart *et al* 2005; Tang *et al* 2013 Winsor *et al* 2016

				their regulation has not yet been proven experimentally.	
Phenazines	**Pyocyanin (PCN)**	A secondary metabolite which is a blue redox-active zwitterion. Causes cellular damage including to that of the respiratory tract, disrupts important enzyme (protease, catalase) and ion (calcium) balances and depletes cellular glutathione (GSH). PCN also disturbs vascular homeostasis and targets the immune response, specifically by attacking RANTES and IL-8 levels, in addition to inducing neutrophil apoptosis.	Two *phzABCDEFG* operons mediate PCN synthesis from chorismate with the contribution of the *phzH*, *phzM* and *phzS* genes.	The QS system including the *lasR-lasI, rhlR-rhlI* and *mvfR-haq* systems. The GacA-GacS and Vfr global regulatory systems have also been implicated in PCN regulation.	Lau *et al* 2004; Wilson *et al* 1988; Mavrodi *et al* 2001; Fuqua *et al* 2001; Gallagher *et al* 2002; Cao *et al* 2001; McKnight *et al* 2000; Diggle *et al* 2003; Kamath *et al* 1995; Denning *et al* 1998; Britigan *et al* 1999, 2003; O'Malley *et al* 2004
	Pyoverdin (Pvd)	The primary siderophore (iron scavenging and transport). Iron is an important cofactor for metabolic enzymes and consequentially both growth and biofilm development are affected when iron cannot be sequestered. There are 3 types of pyoverdin found in *P. aeruginosa* which each recognise a specific receptor. The molecule consists of a dihydroquinoline-type chromophore linked to a peptide.	The pyoverdine backbone is constructed using PvdL, PvdI, PvdJ and PvdD. PvdA, PvdF and PvdH are also needed in the synthesis process. PvdE, an ABC transporter, exports the precursor protein to the periplasm, where PvdQ further processes it. The chromophore is formed by Tyr and Dab with the probable help of PvdN, PvdO and PvdP. PvdRT-OpmQ, an efflux pump, transports pyoverdine across the outer membrane.	Fur and PvdS	Lamont *et al* 2009; Meyer *et al* 1996; Banin *et al* 2005; Patriquin *et al* 2008; Schalk and Guillon 2013
	Pyochelin (Pch)	Siderophore which is also found to chelate Zn (II), Cu(II), Co(II), Ni(II) and Mo (VI) and therefore may be involved in recovering these ions in addition to iron. Shows a lower affinity for iron than pyoverdine. When pyoverdine is absent, production of pyochelin increases, suggesting that it has more of a supportive role in iron acquisition. Supports biofilm development.	*pchDABC* operon	Fur and *pchR* (activatior of pyochelin biosynthesis)	Lamont *et al* 2009 Brandel *et al* 2012 Braud *et al* 2009 Serino *et al* 1997

Exoenzymes	**Exoenzyme S**	An extracellular ADP-ribosyltransferase which has been shown to affect host cytoskeletal structure, cell morphology and antiphagocytic activity as well as inhibit DNA synthesis, disrupt cell adhesions and promote microvillus effacement. Two forms of exoenzyme S exist which are immunologically related: exoenzyme S (49kDa) and exoenzyme T (53kDa). Secretion occurs through a type III secretion system.	*exoS* and *exoT*	Induction by ion chelator presence (e.g. EDTA), while repression occurs from the presence of zinc or calcium. The exoenzyme S regulon includes ExsC and ExsA proteins and exsB, a cis-acting RNA region.	Iglewski *et al* 1978; Yahr *et al* 1995; Frank 1997; Rocha *et al* 2003; Fraylick *et al* 2002 McGuffie *et al* 1998; Goehring *et al;* 1999 Frithz-Lindsten *et al* 1997.
	Exoenzyme U	Acute cytotoxin with phospholipase activity. Secreted by the type III secretion system.	*exoU*	*exoU* and *exoY* are part of the exoenzyme S regulon. Low ion concentration and a temperature of 37°C induce the exoenzyme S regulon. Human serum, eukaryotic cell contact and higher NaCl concentration also upregulate this regulon.	Sato *et al* 2003 Vance *et al* 2005
	Exoenzyme Y	Presence of ExoU is an indicator of lung injury, bacterial dissemination and sepsis. Adenylate cyclase which is secreted by the type III system.	*exoY*		Yahr *et al* 1998
Exotoxins	***Pseudomonas* Exotoxin A (PE)**	A member of the two-component AB toxin family where the enzyme (A) is coupled to a cell binding domain (B). It is secreted from the bacterium using Sec and type II secretion systems. Once it enters the host through CD91 receptor binding, protein synthesis is halted and apoptosis occurs.	*toxA* (exotoxin A precursor)	The regulation is complex having an association with iron uptake and bacterial glucose metabolism, presence of certain amino acids and growth temperature.	Michalska and Wolf 2015; Domenighini and Rappuoli, 1996; Swanson *et al* 1999
Rhamnolipids	**Rhamnolipids**	Primarily have a surfactant role through their glycosyl activity. Have been implicated in immune system modulation, antimicrobial activity, surface motility and biofilm development.	*rhlAB and rhlC*	*las* and *rhl* systems, particularly the *rhl* system	Pearson *et al* 1997; Abdel-Mawgoud *et al* 2010; Koch *et al* 1991; McClure *et al* 1992; Itoh *et al* 1971); Tremblay *et al* 2007

Phospholipase C (PLC)	**PlcN (non-haemolytic) , PlcB, and PlcH (Haemolytic)**	All forms of PLC cause hydrolysis of phosphatidylcholine and PlcH can also hydrolyse sphingomyelin. PlcH is involved in phosphate scavenging and provision of osmoprotectants, in addition to vascular permeability and organ damage. PlcH also suppresses the neutrophil respiratory burst and phospholipid chemotaxis. PlcB is important for chemotaxis by twitching towards phospholipids.	*plcHR, plcB,* and *plcN*	Inorganic phosphate, PhoB (PlcB, PlcHR, PlcN)	Meyers *et al* 1992; Terada *et al* 1999; Barker *et al* 2004; Shortridge *et al* 1992
Pili/fimbrae	**Type IV pili**	Allows twitching motility and has a role in biofilm structure. Type IV pili have also been found to regulate virulence factors.	More than 40 genes make up the structure and regulate the type 4 pilus structure. Amongst these are *pilA* which is the precursor and *pilD* which processes the *pilA* encoded precursor.	*pilA* expression relies on RpoN.	Costerton *et al* 1999; Persat *et al* 2015; Klausen *et al* 2003; Ishimoto and Lory 1989; Strom and Lory 1986; Leighton *et al* 2015
Flagella	**Flagellum**	Allows motility and chemotaxis toward preferred substances. Involved in biofilm formation and dispersal. It is immunogenic, promoting phagocytosis and mucin binding which can cause cells to be cleared quicker by the host than their flagellum lacking counterparts. CF isolates show selection for flagella lacking strains.	Three clusters of genes in non-contiguous regions.	RpoN, FleQ, FleR and FliA	Feldman *et al* 2017; O'Toole and Kolter 1998; Luzar *et al* 1985; Dasgupta *et al* 2003

Lipopolysaccharide (LPS)	**LPS**	The outer membrane permeability barrier, conferring resistance to phagocytosis and serum in Gram-negative bacteria. LPS consists of 3 parts: lipid A, rough core oligosaccharide and O-antigenic side chain (presence determines smooth colony phenotype). There appears to be a bias toward the absence of O-antigen (rough phenotype) as well as a specific type of lipid A in CF isolates. Healthy CFTR channel binding to *P. aeruginosa* LPS has been linked to pathogen clearance.	The genetics behind LPS are complex and here only summarised. The LPS core biosynthesis requires *galU* (UTP-glucose-1-phosphate uridylyltransferase) and *algC* (bifunctional phosphomannomutase/phosphoglucomutase). The core viability and drug resistance is supported by *wapP, wapQ, waaC and waaF*. The O-antigen biosynthetic locus contains 11 distinct biosynthetic loci all placed between the *nimP/ihfB* and *wbpM* genes.	The loss of the O-antigen in CF isolates has been linked with the *mucA* mutation found within many of these isolates.	Darveau and Hancock 1983; Tokuda 2009; Pier *et al* 1996, 1997, 2007; Ernst *et al* 1999; Hancock *et al* 1983; Raymond *et al* 2002; Sousa *et al* 2004
Exopolysaccharide	**Pel, Psl and alginate**	A major part of the biofilm extracellular matrix. Primary functions are adhesion and protection, including resistance to the immune system and antibiotic therapy. Overexpression of alginate is a phenotypic trait particular to the CF lung.	Biosynthesis and regulation of alginate genes map onto 5 loci in *P. aeruginosa*. They are organised into 3 clusters of genes: structural, regulatory and genetic switching. More is described in a later section.	The switch between a non-mucoid and mucoid phenotype is largely mediated by: *algT* (*algU*), *algN* (*mucA* and *mucB*), *algM* (*mucC*) and *algW/Y* (*mucD*).	May *et al* 1991 Muhammadi and Nuzhat Ahmed 2007

Table 1.1.2: Predominant virulence factors of *P. aeruginosa*.

1.1.3 *P. aeruginosa* as a biofilm forming bacterium

P. aeruginosa, along with a complex metabolic machinery and an extensive array of virulence weaponry, owes its success to the ability to form a biofilm (Kenna *et al* 2007). In contrast to planktonic growth, biofilms involve multiple cells existing in close proximity to each other, which can be single or multi-species (O'Toole *et al* 2000). Strictly speaking, bacterial communities are only classed as biofilms if the cells are sessile, embedded in a self-made extracellular matrix, have altered growth rates, show differences in gene transcription and are irreversibly attached to a surface or to each other (Donlan 2012). *P. aeruginosa* has been shown to form biofilms in the context of catheter infections (Khoury *et al* 1992), industrial settings (Costerton *et al* 1987), infected wounds (Watters *et al* 2013; Schaber *et al* 2007) and in the CF lung (Worlitzsch *et al* 2002).

The biofilm mode of growth is abundant in nature and confers protective benefits, allowing survival in hostile environments in addition to facilitating cell dispersal, permitting exploitation of new habitats (Luanne Hall-Stoodley *et al* 2004). Furthermore, mature biofilms have increased antimicrobial and phagocytic resistance, advantageous traits during host colonisation (Lewis 2001). In CF infections, biofilm formation has been linked to increased persistence of *P. aeruginosa* in the lung (Khoury *et al* 1992).

1.1.2.1 Extracellular matrix, alginate and the mucoid phenotype

The biofilm matrix consists of exopolysaccharides (Matsukawa and Greenberg 2004), DNA (Whitchurch *et al* 2002) and proteins (Costerton *et al* 1995). These facilitate cell adhesion and aggregation, additionally contributing to the cohesion, hydration and substance exchange of the biofilm (Flemming and Wingender 2010).

Exopolysaccharides help form a scaffold which facilitates biofilm stability. Three principle polysaccharides are produced by *P. aeruginosa*: alginate, Pel and Psl (Ryder *et al* 2007; Ghafoor *et al* 2011). Classification of a strain as mucoid depends on the relative amount of alginate in respect to Pel/Psl forming the extracellular matrix (ECM) (Ma *et al* 2009; Ma *et al* 2012; Mann and Wozniak 2012). In addition to the structural stability it provides, alginate helps retain water and nutrients. Alginate is a linear, unbranched polymer comprised of D-mannuronic acid and L-gluluronic acid (Ertesvag and Valla 1998) whereas Psl consists of D-mannose, L-rhamnose and D-glucose (Byrd *et al* 2009). Pel is a glucose-rich polysaccharide, but the structure has not yet been elucidated (Rasamiravaka *et al* 2015; Friedman and Kolter 2004; Franklin *et al* 2011).

DNA secreted (eDNA) by bacteria is an integral part of viable *P. aeruginosa* biofilms. DNaseI treated biofilms are easily dispersed by sodium dodecyl sulphate (SDS) (Whitchurch *et al* 2002). In addition to facilitating the cellular interconnection (Flemming and Wingender 2010; Whitchurch *et al* 2002; Allesen-Holm *et al* 2006), eDNA acts as a nutrient source in times of starvation (Finkel and Kolter 2013; Mulcahy *et al* 2010). Gloag *et al* (2013) found that eDNA can even facilitate twitching-mediated motility by maintaining cell alignments. In a pathogenic setting, DNA secreted by bacteria may excite the host inflammatory response (Lipford *et al* 1998) resulting in host-cell tissue damage.

1.1.2.2 Motility appendages: how movement impacts biofilm structure

Flagella, facilitating *P. aeruginosa* swarming and swimming motilities (Kohler *et al* 2000; Masduki *et al* 1995; Deziel *et al* 2001) have been implicated in biofilm formation (Costerton *et al* 1999; O'Toole *et al* 2000; Stoodley *et al* 2002). Although there are differences in opinion as to the exact role this appendage plays, which may be environmentally dependent (Klausen *et al* 2003; Shrout *et al* 2006), studies agree that it is important for cell dispersal (Costerton *et al* 1999; O'Toole *et al* 2000; Stoodley *et al* 2002; Klausen *et al* 2003), allowing colonisation of new niches. Type IV pili, involved in a surface-attached motility called twitching (Whitchurch *et al* 1991; Merz *et al* 2000), are associated with microcolony formation (Klausen *et al* 2003) and surface-dependent microcolony expansion (Costerton *et al* 1999; O'Toole *et al* 2000; Stoodley *et al* 2002).

1.1.2.3 Nutritional effect on biofilm phenotype

The type of carbon source in the environment of a developing biofilm can impact the type of architecture observed. Two broad types of biofilm structure are described *in vitro*. One which has a highly structured 'mushroom-like' phenotype, which is the result of growth on a glucose containing minimal medium and the other has a flat appearance, the phenotype resulting from growth using a citrate, succinate, or cas- amino acid containing minimal medium (Costerton *et al* 1999; O'Toole *et al* 2000; Stoodley *et al* 2002; Klausen *et al* 2003; Shrout *et al* 2006).

The mechanisms by which nutrition influences biofilm phenotype, appears to involve Crc, a global carbon metabolism regulator (O'Toole *et al* 2000). Shrout *et al* (2006) suggests that flagella-mediated motility along a biofilm surface is under Crc control which influences cellular dispersion. However, the relationship between nutrition and biofilm formation is largely unchartered territory.

Free-floating biofilms grown in artificial sputum media (ASM) (Davies *et al* 2017) did not appear to need Type IV pili. It is possible that the type of nutrient sources

available in ASM encourage a biofilm type unaided by Type IV pili. Alternatively, different attachment mechanisms may be required when the biofilms are not anchored to a surface. If biofilms in the CF lung mainly exhibit this free-floating phenotype, targeting Type IV pili may not be an appropriate strategy.

1.1.2.4 Formation of a P. aeruginosa biofilm

Biofilm formation requires a complex coordination of gene expression that may vary according to nutrition, location and the presence of other microbial life. Rather than a linear process, biofilm formation should be viewed as a cycle (Rasamiravaka *et al* 2015). Different forms can be obtained depending on the strain and nutrient availability (Shrout *et al* 2006). Notably, the literature is biased in favour of *in vitro* biofilms due to the difficulty of studying the *in vivo* counterparts. It has been recognised that differences between laboratory and naturally derived biofilms are likely to exist (Lebeaux *et al* 2013; Roberts *et al* 2015) and a direct comparison of the 2 systems is required to more fully understand this. These comparisons are largely in their infancy (Chua *et al* 2015; Dalton *et al* 2011; Li *et al* 2015) which necessitates that the following sections describe the *in vitro* biofilm. This type of biofilm is sensitive to the physical conditions imposed on it in the laboratory, including the growth medium, flow, humidity, mechanical manipulation and attaching surface.

The typical stages of *in vitro* biofilm formation are summarised in Figure 1.1.11. The early events consist of a reversible adhesion stage, followed by an irreversible attachment stage with microcolony formation. After this a more structured and 3 dimensional layout is achieved as the microcolonies expand and coverage is extended. Bacteria are then dispersed from this mature biofilm and new niches colonised (Rasamiravaka *et al* 2015; Costerton *et al* 1999; O'Toole *et al* 2000; Stoodley *et al* 2002; Klausen *et al* 2003).

1.1.2.4.1 Stages in development

1.1.2.4.1.1 Stage I (reversible attachment)

Planktonic cells encounter a surface and form an initial attachment. In the 'mushroom' biofilm type, flagella were found to mediate transport to the surface (Costerton *et al* 1999; O'Toole *et al* 2000; Stoodley *et al* 2002). In the 'flat' biofilm type, flagella and Type IV pili do not appear necessary for initial attachment (Klausen *et al* 2003). *In vivo,* eDNA can facilitate initial attachment by binding to expired neutrophil F-actin and forming bundles (Wei and Ma 2013; Parks *et al* 2009).

1.1.2.4.1.2 Stage 2 (irreversible attachment) and Stage 3 (beginning of structured biofilm)

Initial microcolonies form and the ECM begins to develop. The expression of *algC*, involved in alginate production, climbs at this stage (Davies and Geesey 1995). Crc is also important, most notably for supporting Type IV pili action (Whiteley *et al* 2001). In the 'mushroom' biofilm, Type IV pili mediate bacterial movement along the surface, allowing them to aggregate and form microcolonies (Costerton *et al* 1999; O'Toole *et al* 2000; Stoodley *et al* 2002). The alignment of adjacent cells is assisted by eDNA (Wei and Ma 2013; Gloag *et al* 2013) and transcription of *algC*, *algD*, and *algU* occurs (Davies and Geesey 1995). In 'flat' biofilms, microcolonies form without flagella or Type IV pili involvement. However when the microcolonies reach a certain size, Type IV pili appear important for bacterial expansion across microcolonies as *ΔpilA* mutant strains form increasingly large microcolonies by clonal growth (Klausen *et al* 2003).

1.1.2.4.1.3 Stage 4 (structured and heterogeneous) and stage 5 (dispersal)

Formation of a mature, structured and differentiated biofilm with an established ECM occurs at stage 4. The presence of eDNA can act as a nutrient source and defence against antibiotic attack (Wei and Ma 2013; Mulcahy *et al* 2008; Finkel and Kolter 2001). Some cells leave the biofilm and revert to a planktonic form for exploration of new destinations. A reduction of *algC* expression in areas of the biofilm intended for dispersal may prime these cells to leave the community (Davies and Geesey 1995). In the 'mushroom' biofilm, thick, biocide-resistant, biofilms form. Presence of eDNA in the mushroom stalks is (Wei and Ma 2013; Allesen-Holm *et al* 2006) hindered by mutation of *lasI*, resulting in a thin, easily dispersed biofilm phenotype (Davies *et al* 1998). 'Flat' style biofilms spread into a flat layer unless deficient in Type IV pili, which results in isolated, expanded microcolonies. Deletion of the flagella component *fliM,* produced 'hilly' biofilms of increased biomass, which is likely due to decreased dispersal. The flagella deficient strain has a competitive advantage in biofilms and a conversion to a non-motile phenotype could occur *in vivo* as a consequence of intra-biofilm selection (Klausen *et al* 2003). In support of this, a large proportion of *P. aeruginosa* CF isolates are non-flagellated (Luzar and Montie 1985; Mahenthiralingam *et al* 1994).

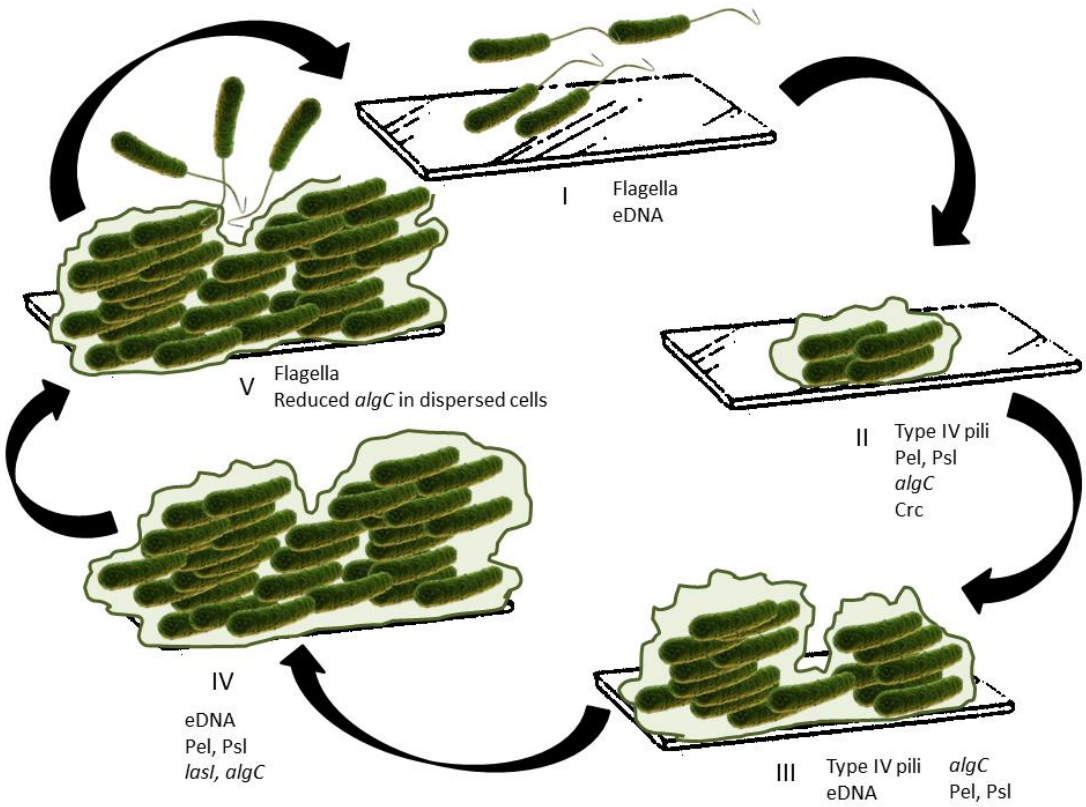


Figure 1.1.11: The stages of biofilm development. Stage I: initial attachment. Stage II: irreversible attachment (microcolony formation). Stage III: microcolony expansion and beginning of more structured settlement. Stage IV: increased coverage and maturation of biofilm. Stage V: dispersal. Not mentioned in this cartoon principally depicting an *in vitro* biofilm, are the raised expression of the phage genes of the bacteriophage *Pf1* which causes the formation of small colony variants (Jefferson 2004, Whiteley *et al* 2001; Webb *et al* 2004). Information: Rasamiravaka *et al* 2015; Costerton *et al* 1999; O'Toole *et al* 2000. Labels are from Yang *et al* 2011; Davies and Geesey 1995; Whiteley *et al* 2001; O'Toole *et al* 2000; Klausen *et al* 2003. Picture components are from the following websites. Slide: http://teachertech.rice.edu/Participants/louviere/vms/science/labequipment.html. *P. aeruginosa*: http://www.thesilveredge.com/pseudomonas.shtml#.WO39B_nF92E.

1.1.2.5 Global regulation systems involved in P. aeruginosa biofilms

In an *in vivo* context and particularly that of a pathogenic environment, *P. aeruginosa* must employ a mode of growth which maximises its success in a particular niche. Co-ordination of planktonic and biofilm lifestyles is mediated by global regulation systems. The global secondary messenger bis-(3'-5')-cyclic dimeric guanosine monophosphate (c-di-GMP), is one such regulator. The intracellular concentration of c-di-GMP determines a sessile or planktonic mode of growth, with high concentrations promoting biofilm formation by encouraging surface adhesion, cell aggregation and ECM production (Hengge 2009; Romling *et al* 2005). Maintenance of c-di-GMP is largely by diguanylate cyclase (DGC) and phosphodiesterase (PDE), which respond to environmental and intracellular inputs (Figure 1.1.12) (Hengge 2009). These include oxygen, light, starvation and extracellular substances such as antimicrobials (Jenal and Malone 2006; Ryan *et al* 2006). The c-di-GMP molecule binds to a diverse range of effectors including

the PilZ protein family, FleQ and PelD (Hickman and Harwood 2008; Lee *et al* 2007; Benach *et al* 2007).

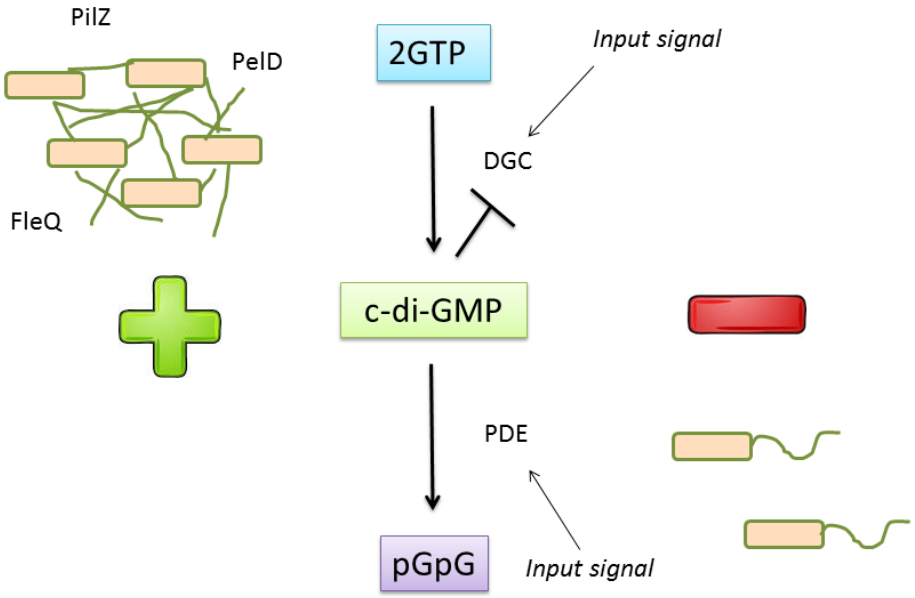


Figure 1.1.12: The balance of c-di-GMP promotes a biofilm or planktonic existence. The secondary messenger bis-(3′-5′)-cyclic dimeric guanosine monophosphate (c-di-GMP) is formed from 2 GTP molecules with the aid of diguanylate cyclase (DGC). A negative feedback loop maintains an upper limit c-di-GMP by inhibition of DGC. The level of c-di-GMP is reduced by phosphodiesterase (PDE), which catalyses the conversion of c-di-GMP to 5'-phosphoguanylyl-(3'-5')-guanosine (pGpG). A higher concentration of c-di-GMP promotes biofilm formation, while a lower concentration, a planktonic mode of growth. The activity of DGC versus PDE is controlled by a diverse variety of input factors. The effect of c-di-GMP is mediated through several targets which include the PilZ protein family, FleQ and PelD. Based on information provided by Hengge 2009; Romling *et al* 2005; Jenal and Malone 2006; Ryan *et al* 2006; Hickman and Harwood 2008; Lee *et al* 2007; Benach *et al* 2007.

In *P. aeruginosa*, TCS are central for coordinating bacterial adaptive responses to environmental conditions (Rodrigue *et al* 2000). The involvement of two TCSs, in association with the quorum sensing system, were found to regulate biofilm formation and facilitate successful host invasion. These are the GacS/GacA and the RetS/LadS systems (Rasamiravaka *et al* 2015). Together they form the basis of the acute/chronic switch (Mikkelsen *et al* 2011), which is further detailed in Figure 1.1.13.

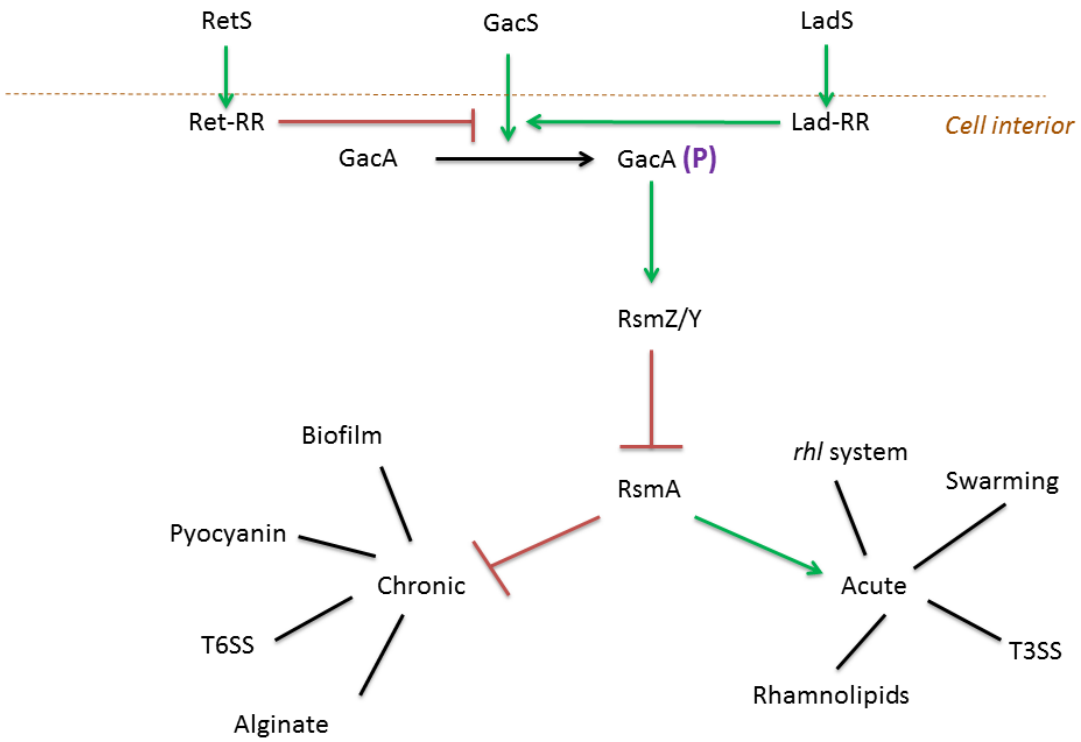


Figure 1.1.13: Biofilm regulation in *P. aeruginosa*. Green arrows indicate stimulation and red arrows inhibition. RR = response regulator. GacS is autophosphorylated in response to environmental signals. This phosphorylation status is then transferred to GacA, the response regulator. Phosphorylated GacA stimulates the production of RsmZ and RsmY, regulatory RNAs. These rRNAs bind to RsmA, a RNA binding protein, inhibiting it. RsmA inhibits traits associated with a more chronic cell state and upregulates traits which aid the bacterium in forming acute infection. RetS and LadS act on GacS in an antagonistic manner (Jimenez 2012; Goodman *et al* 2004; Ventre *et al* 2006; Mikkelsen *et al* 2011).

1.1.2.6 P. aeruginosa biofilms in the CF environment

In 1999, Costerton and colleagues linked poor treatment outcomes with biofilm formation in CF airway *P. aeruginosa* infections. A number of other studies have also indicated biofilm formation occurs in CF airway *P. aeruginosa* infections. However, the details of how *P. aeruginosa* biofilms are established in the respiratory tract of CF patients remain undefined (Moreau-Marquis *et al* 2009). For example, opposing data exists regarding the initial site of colonisation. Worlitzsch *et al* (2002) presented evidence to show *P. aeruginosa* forms clusters of cells within the mucus layer and is not in contact with the respiratory epithelial cells (also McDonnell *et al* 2015). Contesting this, other studies show that *P. aeruginosa* binds to epithelial cells, growing directly on or inside them (Haussler *et al* 2003; Chi *et al* 1991; Garcia-Medina *et al* 2005; Darling *et al* 2004; Lanotte *et al* 2004). If this is the case, *P. aeruginosa* biofilms found within the mucus layer could be a secondary niche exploited by the bacterium (Figure 1.1.14).

In vitro models have attempted to replicate particular conditions found with the CF airway environment (Davies *et al* 2017; Lebeaux *et al* 2013; Anderson *et al* 2008; Kirchner *et al* 2012; Sriramulu *et al* 2005), but complete recreation is difficult due to its complexity. The *P. aeruginosa* infected CF airway includes abnormal epithelial cells, oxygen deprived areas, and a thick mucus containing mucin proteins, actin and eDNA from neutrophil necrosis (Whitchurch *et al* 2000; Matsukawa and Greenberg 2004; Allesen-Holm *et al* 2006). Thicker mucus has been suggested to promote biofilm formation by impeding bacterial movement and assisting in the accumulation of QS molecules (Matsui *et al* 2006). However, the water content of CF mucus is under considerable debate, with a high variation between patients observed. Furthermore, the variation did not correlate with *P. aeruginosa* colonisation (Deneuville *et al* 1997). The mucin proteins themselves were shown to provide attachment sites for *P. aeruginosa* on a glass slide (Landry *et al* 2006), but the importance of mucin for *in vivo* biofilm establishment is yet to be definitively determined.

P. aeruginosa pulmonary isolates often exhibit particular phenotypes including mucoidy (Gacesa 1998), absence of flagella (Garrett *et al* 1999), absence of Type IV pili, auxotrophy, hypermutability, loss of known virulence factors, slower growth in rich media and resistance to antimicrobials (Mahenthiralingam *et al* 1994; Smith *et al* 2006; Ciofu *et al* 2010; Winstanley *et al* 2016). The loss of motility found in *P. aeruginosa* CF isolates would appear at odds with the evidence of biofilm formation in these strains. As observed in the case of *in vitro* biofilms, motility appendages seem more important in certain conditions and this may apply in the CF environment. A study examining *P. aeruginosa* clinical isolates observed no correlation between biofilm production and Type IV pili (Head and Yu 2004) suggesting that the presence of motility appendages are not essential for biofilm formation in the context of CF.

A high degree of diversity is often found in the isolates from CF patients (Winstanley *et al* 2016; Workentine *et al* 2013; Mowat *et al* 2011; Fothergill *et al* 2010; Ashish *et al* 2013; Darch *et al* 2014; Jorth *et al* 2015; Clark *et al* 2015) and this could be due to the variability in sources they can be acquired from. Different niches within the lung may promote different traits and antibiotics encourage diversification within a biofilm (Boles *et al* 2004). Evidence against pre-infection isolate diversity being the principle source of variability seen in CF isolates has been procured by Darch *et al* (2014) and additionally the highly represented Liverpool Epidemic Strain (LES), shows high variability between patients (Mowat *et al* 2011; Fothergill *et al* 2010; Williams *et al* 2016).

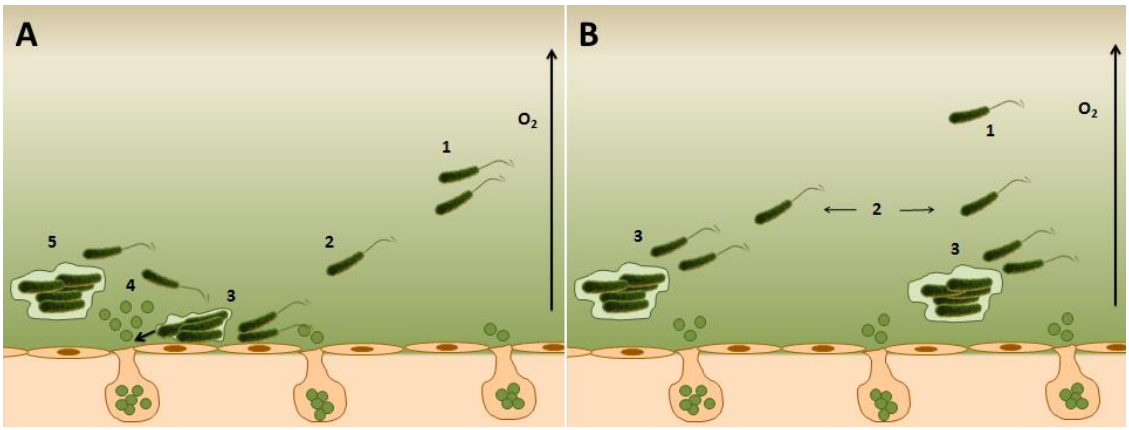


Figure 1.1.14: Two potential modes of initial colonisation of the CF airway by *P. aeruginosa*. Potential colonisation mode A: *P. aeruginosa* enters the respiratory tract (1) and travels through the layers of mucus (2) until reaching the epithelium (3). Here the *P. aeruginosa* attach to the epithelial surface and form a biofilm. The presence of this biofilm induces goblet cells to secrete more mucus (4) which allow dispersed bacterial cells from the previous biofilm community to colonise a new niche: the luminal space adjacent to the epithelium but not in contact with it (5). Potential colonisation mode B: *P. aeruginosa* enters the respiratory tract (1) and travel down to the deeper layers where the mucus is thicker, in part due to increased goblet cell secretions (2). The cells form biofilms in this environment, near to the epithelium but not attached (3). Based on the references: Worlitzsch *et al* (2002); McDonnell *et al* 2015; Haussler *et al* 2003; Chi *et al* 1991; Garcia-Medina *et al* 2005; Darling *et al* 2004; Lanotte *et al* 2004.

1.1.2.6.1 Mucoidy in CF isolated *P. aeruginosa*

Overproduction of alginate is characteristic of *P. aeruginosa* isolated from the CF airway (Pedersen *et al* 1990; Bragonzi *et al* 2005; Lam *et al* 1980). These isolates are termed mucoid and are typically difficult to clear (Boucher *et al* 1997). Specifically why mucoidy is advantageous to *P. aeruginosa* of the CF respiratory tract is not yet known, however it is probably linked with immune defence, dehydration, antibiotic usage, nutrient deprivation and oxygen limitation (Mathee *et al* 1999; Bayer *et al* 1990; Berry *et al* 1989; DeVault *et al* 1990; Speert *et al* 1990; Terry *et al* 1991; Bagge *et al* 2004).

Frequently, non-mucoid, environmental *P. aeruginosa* colonises the respiratory tract, where it then becomes mucoid. Following this, a reversion to non-mucoidy can occur (Ciofu *et al* 2008). Alginate production is under the control of the *algD* promoter, which is principally activated by the sigma factor AlgT (σ^{22}). In addition to direct activation, AlgT can also promote expression from *algD* through other regulatory proteins (Govan and Deretic 1996). AlgT belongs to an operon containing the genes *mucA, mucB, mucC* and *mucD* (Ciofu *et al* 2008). The conversion to mucoidy occurs by a mutation in *mucA,* resulting in the constitutive expression of alginate due to the abolishment of negative control over AlgT. The *mucB* and *mucD* genes also produce more alginate upon mutation, but have less of an effect than modification of *mucA* (Ciofu *et al* 2008). The inflation of AlgT

levels has other cellular effects besides that of alginate overproduction as it is usually involved in the regulation of heat shock, osmotic balance and protection against reactive oxygen species (Yu *et al* 1995; Martin *et al* 1994; Firoved *et al* 2002). Therefore, the mucoid phenotype is a relatively unstable one and consequently there is often a reversion back to normal alginate levels. The mechanism for this reversion is reported to occur most frequently through a second mutation in the *algT* gene (Devries and Ohman 1994). However, a study by Ciofu and colleagues (2008), found that this mechanism is underrepresented *in vivo*. Other pathways to reverse mucoidy can occur through restoration of MucA to wild-type functionality or by secondary site mutations in other alginate regulatory genes (Devries and Ohman 1994; Ciofu *et al* 2008; Schurr *et al* 1994).

1.1.2.7 Biofilm resistance to antimicrobials and the immune system

That biofilms are more resistant to attack from both immune and anti-microbial molecules is well documented (Brooun *et al* 2000; Nickel *et al* 1985; Mah *et al* 2003; Drenkard 2003; Stewart and Costerton 2001; Mah and O'Toole 2001). This does not appear to be due to individual cell resistance mechanisms, however (Costerton *et al* 1999; Sun *et al* 2013; Singh *et al* 2009), and is attributed to the biofilm community-style living as a whole (Spoering and Lewis 2001; Stewart and Costerton 2001). As a consequence of their inherent resistance, biofilms can act as reserves which replenish the bacterial population following a course of antibiotics (Marrie *et al* 1982). This is believed to occur in chronic *P. aeruginosa* infection of CF airways, where symptoms are reduced or eliminated by antimicrobial removal of planktonic cells, but which have little effect on biofilm eradication (de Beer *et al* 1994; Chen and Stewart 1996; Lu *et al* 1998; Burns *et al* 2001).

There are 3 mechanisms which are thought to contribute to biofilm-mediated antibiotic resistance. Firstly, the antimicrobials must penetrate the biofilm. Evidence suggests that antimicrobial progress through the outer layers is impeded and is deactivated prior to reaching the deeper areas (Cheema *et al* 1986; Stewart *et al* 1998). Secondly, antibiotics are more effective on rapidly dividing cells. Within a biofilm are nutritionally limited areas populated by slow-growing cells. This limits the effectiveness of the antimicrobial agent (Brown *et al* 1988). Thirdly, the heterogeneity of a biofilm means that there is a variation in cell phenotype. Some of these phenotypes are potentially resistant to particular antimicrobials (Costerton *et al* 1999). In all cases, a proportion of the biofilm would survive antibiotic attack.

1.1.3 Regulation

1.1.3.1 Sigma factors in P. aeruginosa

Sigma factors form part of the RNA polymerase complex when joined to the core polymerase enzyme, recognising specific promoters and thereby increasing transcriptional selectivity (Campbell *et al* 2002; Murakami *et al* 2002). Being a necessary component of the transcriptional machinery, (Burgess *et al* 1969) they play an important part in the regulatory network of bacteria. Usually, they recognise a particular nucleotide motif upstream of the gene to be transcribed, the classic example being the sigma 70 factors which recognise -35/-10 promoters (Potvin *et al* 2008; Gruber and Gross 2003). They can be divided by the types of promoters they target, for example the alternative sigma factors and the extra-cytoplasmic function sigma factors (ECF) which contribute to a bacterium's adaptability and virulence (Potvin *et al* 2008; Schulz *et al* 2015). In *P. aeruginosa*, there are at least 25 different sigma factors (Potvin *et al* 2008). These are summarised in Table 1.1.3.

Sigma factor group	Sigma factor	Description
σ70	RpoD σ70	Binds to a large number of housekeeping gene promoters. Stimulates promoters during exponential phase (Fujita *et al* 1994). Recognises **T**AtAA**T** at the -10 and **TTG**c**C**c at the -35 sites (Dominguez-Cuevas and Sylvia 2004.
σ32	RpoH σ32	Heat-shock induction response.
σE	AlgU σE	Transcription dependent on AlgU σE. Heat shock and mucoidy.
σ28	FilA (RpoF or σ28)	Flagellin biosynthesis.
σS	RpoS (σS or σ38)	Regulates QS (Whiteley *et al* 2000) Activates genes at the beginning of stationary phase (Latifi *et al* 1996).
σ54	RpoN (σ54 or σN or NtrA)	Nitrate assimilation, motility, pili formation and cell-cell communication (Ishimoto and Lory 1989; Totten *et al* 1990). Consensus binding motif of -12GC and -24GG. Transcriptional activator needed.
σECF	Various including PvdS	Regulate genes which provide bacteria with advantages in particular environments. Many linked to OM ferric-siderophore receptors.

Table 1.1.3: Sigma factors in *P. aeruginosa*. Based on the information provided by Potvin *et al* 2008.

1.1.3.1.1 RpoN (sigma54), the alternative sigma factor

RpoN, also named σ^{54} and NtrA, is an alternative sigma factor, unusual in the regard of requiring an obligatory cognate ATP-dependent transcriptional activator to allow the RNA polymerase (RNAP) holoenzyme to melt, and begin transcribing the DNA (Buck *et al* 2000). The activator usually binds upstream of the RpoN

binding site and often requires an integration host factor (IHF) binding site to bring it into contact with the rest of the holoenzyme (Bertoni *et al* 1998). In contrast to the majority of sigma factors, the binding motif for RpoN follows a -24/-12 format with a highly conserved binding motif of GG-10bp-GC (Merik 1993).

RpoN has been linked to gene repression by both direct and indirect mechanisms. It is thought to repress gene transcription directly by sigma factor competition. RpoN binding sites can overlap or interact with other sigma factor binding sites with a more typical -35/-10 arrangement (Schaerer *et al* 2015). Figure 1.1.15 by Schaefer *et al* (2015) illustrates how RpoN mediated sigma factor competition could occur when the respective binding sites are situated in different locations.

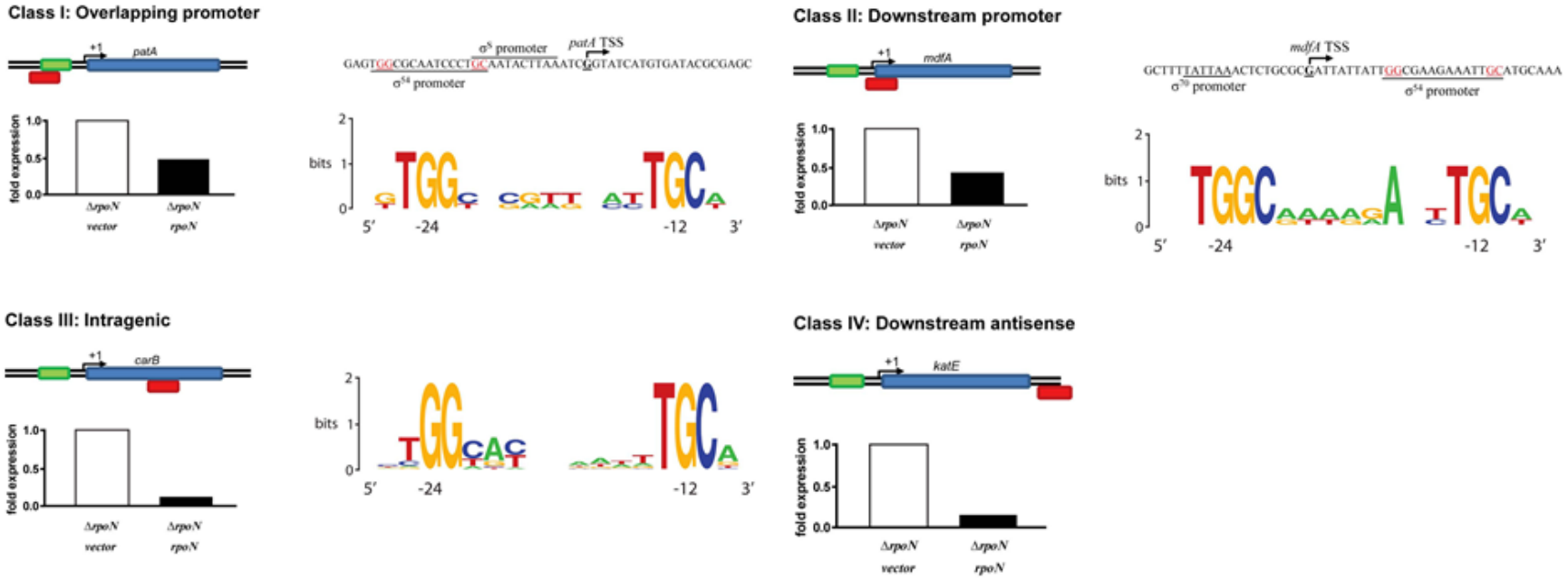


Figure 1.1.15: How RpoN can mediate gene repression (Figure adapted from Schaerer *et al* 2015). There are 4 classes of promoters which have found to be repressed by RpoN, grouped according to the location of the RpoN binding motif. Class I: competitive binding due to overlapping -35/-10 and -24/-12 promoters. Class II: a RpoN binding site downstream from the -35/-10 motif, blocks transcription. Class III: an intragenic RpoN binding motif blocks full transcription of the gene. Class IV: the RpoN motif is located downstream of the gene and on the anti-sense strand. The forth class has only one member and therefore does not currently have a consensus sequence (Schaerer *et al* 2015).

RpoN regulates nitrate assimilation and glutamine synthase genes (Hirschman *et al* 1985; Hunt and Magasanik 1985; Jones *et al* 1994; Totten *et al* 1990) and is implicated in the transcription of an assortment of other genes such as those involved in motility (Ishimoto and Lory 1989; Jones *et al* 1994). In *Bacillus subtilis* RpoN was found to regulate arginine and ornithine utilisation (Gardan *et al* 1997). Recognition of both arginine and nitrate promoters by RpoN could be an important component in the linkage between the two metabolic systems.

1.1.3.2 The Quorum Sensing system

Quorum sensing (QS) allows microbes to sense the bacterial density of their surroundings. It facilitates communication between neighbouring cells and upregulates genes appropriate for the numbers of individuals present (Miller and Bassler 2001). A typical QS system consists of a signalling molecule (autoinducer), and a receptor system which recognises the signal molecule. Upon attainment of a critical concentration of autoinducer (the quorum threshold), density dependent gene transcription is induced and a surge in signal molecule generation occurs (Waters and Bassler 2005; Hibbing *et al* 2010). QS systems in bacteria are frequently composed of more than one system (Schauder and Bassler 2001).

P. aeruginosa possesses 4 QS systems arranged into a hierarchy. The *lasIR* system sits at the 'top' of the hierarchy and when its autoinducer N-(3-oxododecanoyl) homoserine lactone (3-oxo-C12-HSL) (Papenfort and Bassler 2016; Wai-Leung and Bassler 2009) binds to its receptor *lasR*, the other systems are activated including the next in the hierarchy: the *rhlIR* system (Lee and Zhang 2015). The *rhl* autoinducer N-butyryl homoserine lactone (C4-HSL) (Papenfort and Bassler 2016; Wai-Leung and Bassler 2009) is recognised by RhlR and upregulates *rhlR* and *rhlI,* in addition to regulating transcription of the genes in its regulon (Lee and Zhang 2015). The third autoinducer is 2-heptyl-3-hydroxy-4-quinolone (PQS) (Pesci *et al* 1999; Gallagher *et al* 2002) which is recognised by PqsR (Gallagher *et al* 2002). It is activated by the *lasIR* system and repressed by *rhlIR* system while it activates the *rhlIR* system. The last system involves the 2-(2-hydroxyphenyl)-thiazole-4-carbaldehyde (IQS) autoinducer and activates itself in response to *lasR* activation (Lee *et al* 2013).

These intercellular communication systems are instrumental in regards to bacterial virulence and biofilm formation; *P. aeruginosa* QS mutants showing decreased virulence in mouse models (Rumbaugh *et al* 1999; Nealson and Hastings 1979; Pearson *et al* 2000; Davies *et al* 1998). The virulence genes

currently identified as being regulated by the *las* system are elastase, LasA protease, alkaline protease and exotoxin A (Whiteley *et al* 1999; Gambello *et al* 1993; Pearson *et al* 1997). The *rhl* system has been implicated in the regulation of cyanide, pyocyanin and lectin virulence factors (Brint and ohman 1995; Latifi *et al* 1996; Pearson *et al* 1995; Winson *et al* 1995). QS allows the cell to coordinate its expression profile with the environment (Wagner *et al* 2003): it is therefore highly instrumental in the adaptability of *P. aeruginosa*.

1.2 Cystic Fibrosis

1.1.4 Cause and Pathogenesis of Cystic Fibrosis

Cystic Fibrosis (CF) is a recessive monogenic disease, varying in prevalence across ethnic groups. In Europe, it is reported to occur once in every 2000-3000 births (WHO 2017). The symptoms, which manifest in diverse forms in multiple organs (Figure 1.2.1), stem from an imbalance of chloride ions across epithelial cell membranes (Welsh and Smith 1993; Boucher 2002). This is due to a loss of function mutation in the Cystic Fibrosis Transmembrane Conductance Regulator (CFTR) gene which codes for a chloride ion transportation channel (Riordan *et al* 1989; Welsh and Smith 1993; Cheng *et al* 1990; Gregory *et al* 1990; Anderson *et al* 1991). There are 6 classes of CFTR mutation which are summarised in Figure 1.2.2 below. The channel is situated on the apical membrane of epithelial cells (Denning *et al* 1992) lining the airways and digestive system. This results in a deficit in chloride ions in the fluid lining the epithelial wall of these passage ways. Sodium ions respond to the reduction in negative charge created by the absence of chloride ions, reducing the concentration of sodium in the lumen. In consequence to the change in electrochemical gradient, the osmotic potential of the luminal fluid is lowered and it becomes increasingly dehydrated (Matsui *et al* 1998; Elborn and Vallieres 2014). The hyperviscous surface fluid obstructs the digestive and airway passages contributing to persistent coughing, malnutrition and a high incidence of lung infections (Matsui *et al* 1998; Boucher 2004).

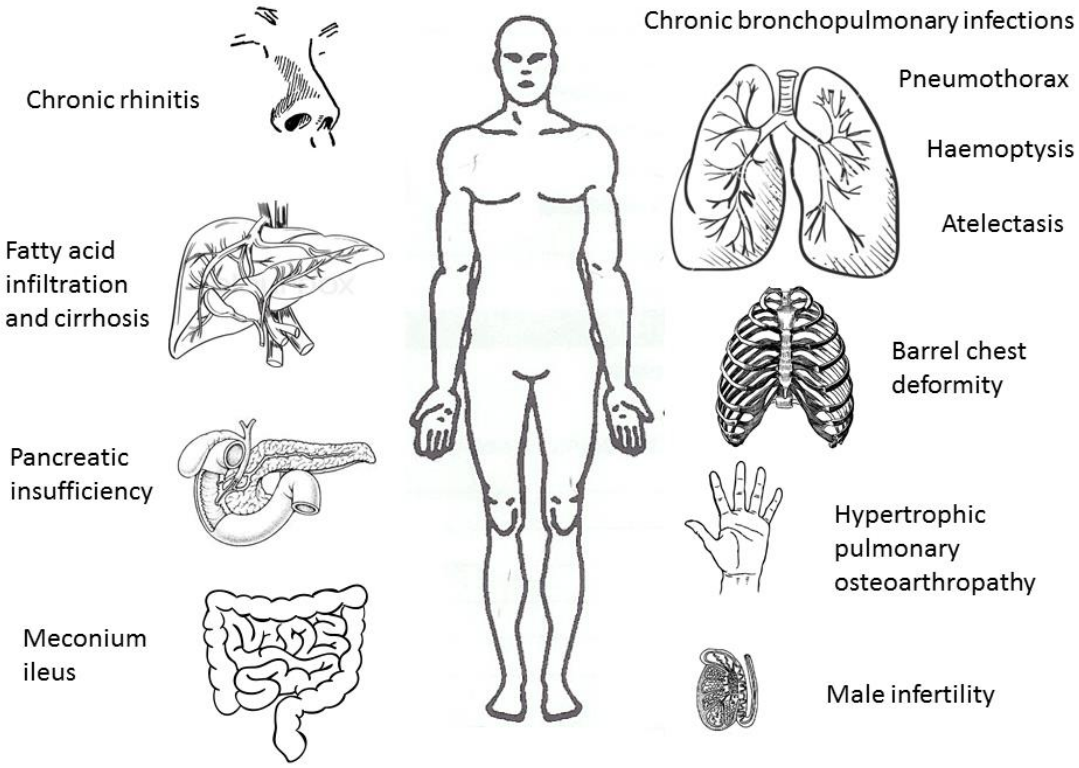


Figure 1.2.1: An overview of the symptoms experienced by Cystic Fibrosis patients. The more typical effects seen with CF are chronic rhinitis, chronic bronchopulmonary infections, male infertility and meconium ileus. The more severe manifestations are fatty acid infiltration and cirrhosis, haemoptysis, pneumothorax, atelectasis, barrel chest deformity and hypertrophic pulmonary osteoarthropathy. Information based on: Kerem *et al* 2005; Smyth *et al* 2014; Zielenski 2000; Knowles and Drumm 2012; Sinaasappel *et al* (2002); Smyth *et al* 2005; Kaplan *et al* (1968); Koch *et al* (2008); Nash *et al* (2008). Pictures are from various sources: Body=Medical Image Annotations.Com (2008); Lung= Vector Shock; Liver= ColourBox (2014); Pancreas= kamontgomery-Communication Networks; Intestine=ClipArt; Ribcage=ClipArt (ETC); Hand= ClipArt; Testes=WikiEducator; Nose=ClipArt.

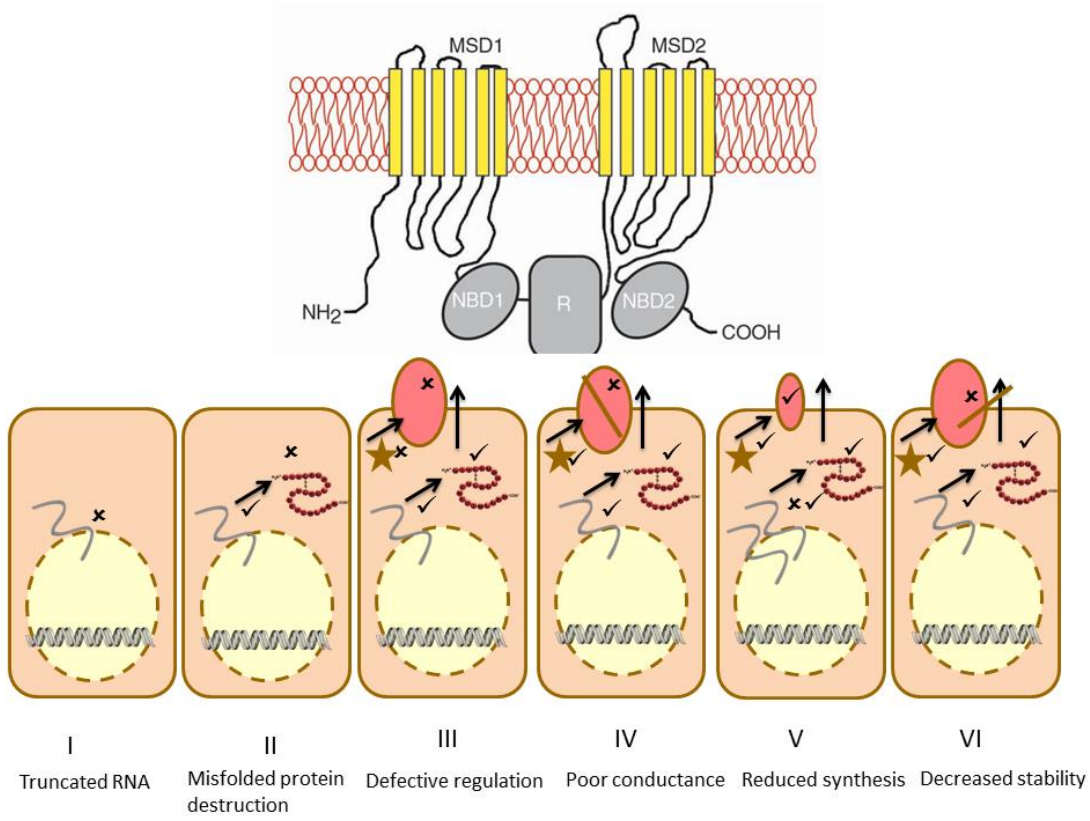


Figure 1.2.2: The structure of the CFTR receptor and the 6 classes of mutations. Top: the CFTR channel structure (picture taken from the Cystic Fibrosis Genetic Analysis Consortium). From left to right: the N-terminus is followed by the first membrane spanning domain (MSD1) consisting of 6 alpha helices. This is connected with the first nuclear binding domain (NBD1), linked with the R domain. The R domain is also linked with the second membrane spanning domain (MSD2), also 6 alpha helices, which is followed by the second nuclear binding domain (NBD2) and subsequently, the C-terminus (Fuller *et al* 1992; Mornon 2009; Cant *et al* 2014; Gadsby *et al* 2006). A central pore (Linsdell 2006) selectively facilitates the transport of anions including chloride, gluconate and bicarbonate (Anderson *et al* 1991; Hug *et al* 2003; Briel *et al* 1998). The CFTR is regulated by adenosine 3',5'-cyclic monophosphate (cAMP) (Gadsby *et al* 2006; Sheppard and Welsh 1999). **Bottom:** the 6 classes of CFTR mutations. Class 1: CFTR synthesis does not occur due to stop codons or splicing defects. Class 2: synthesis of CFTR occurs, however it takes an immature form (i.e. only partially glycosylated) and is misfolded, triggering degradation by the ubiquitin-proteosomal pathway. It is not released from the endoplasmic reticulum (ER). Class 3: synthesis and transportation of the CFTR protein to the plasma membrane occurs but CFTR fails to become normally activated and regulated by cAMP or ATP. Class 4: synthesis and expression of CFTR occurs but there is a reduction in the effectiveness of chloride conductance. Class 5: There is a partial defect in the processing or synthesis of CFTR. Class 6-CFTR is synthesised and transported to the plasma membrane but the effectiveness of ion conductance other than chloride is reduced (Riordan *et al* 1989; Kerem *et al* 1990; Kerem *et al* 1989; Welsh and Smith 1993; Zielenski 2000).

1.1.5 Altered microbiota of the CF respiratory system and how this is linked to the susceptibility of these patients for contracting lung infection

The CF airway plays host to a complex polymicrobial community (Filkins and Tool 2015; Van der Gast *et al* 2010), the composition of which is unique to each individual patient (de Dios Caballero). This has been demonstrated by culture based assays (Govan and Nelson 1992) and more recently by culture-independent techniques such as 16S gene sequencing (de Dios Caballero; Rogers *et al* 2004; O'Toole 2018). As more data is gathered, a picture of a much wider

and more complex community of microbial life is emerging. This has highlighted the importance of considering the whole microbiome, in combination with the traditional approach of reducing the numbers of key pathogens such as *P. aeruginosa* (Smith *et al* 2014; O' Toole 2018).

Microbes which have been identified in CF patient airways include *Pseudomonas aeruginosa, Staphylococcus aureus, Haemophilus influenza, Burkholderia cepacia, Mycobacterium abscessus, Steptococcus sp., Prevotella sp., Veillonella sp., Neisseria sp., Porphorymonas sp.,* and *Catonella sp.* (Filkins and Tool 2015; Van der Gast *et al* 2010; de Dios Caballero). The presence of anaerobes including *Stenotrophomonas maltophilia, Achromobacter sp., Ralstonia, Pandoraea, Prevotella, Veillonella, Propionibacterium, Actinomyces* and *Acinetobacter*, has also been acknowledged by molecular methods and Bronchoalveolar lavage (BAL) (Rogers et al 2004; Tunney et al 2008). In addition to bacterial species, fungi and viruses have been identified in the CF airway. These include *Candida, Malassezia, Aspergillus*, as well as influenza and respiratory syncytial virus (Etherington et al 2014; Willger et al 2014; Gilligan 2014). Table 1.2.1 outlines each of the microbes above.

The identified microbes can be divided depending on their prevalence in CF patient airways. The term 'satellite taxa' was used by Van der Gast *et al* (2010) to refer to bacteria which show a high variability in presence between patients. The unique combination of microbial species forms a bacterial footprint which is specific to the individual and in some cases can influence clinical outcomes (Acosta *et al* 2018). Although a fairly new area of study, investigations of the interactions between these resident microbes have shown the existence of cooperative and competitive relationships. For example, Nair *et al* (2014) noticed that *Staphylococcus aureus* cooperates with *C. albicans, H. influenzae*, and influenza virus, while competing with *P. aeruginosa* and *Streptococcus pneumoniae*. The completion of more studies of this nature will be useful for furthering our understanding of the link between the presence of certain microbial combinations and lung function. It also has the potential to lead to a more personalised antibiotic treatment regimen.

Some similarities have been observed in the timeline of CF respiratory disease progression. Generally, children and young adults show a more wide ranging microbiota than older patients where a decline in microbial diversity is observed (LiPuma 2014; Brown *et al* 2014; Rogers *et al* 2004) *S. aureus* and *H. influenza* are typically observed first in young patients, followed by *B. cepacia* and *P.*

aeruginosa (Filkins and Tool 2015). The shift in pathogen type as the patient ages has been attributed to pathogen adaption, competitive interactions between microbes, and antibiotic usage (O'Toole *et al* 2018; Acosta *et al* 2018; Smith *et al* 2014; Winstanley *et al* 2016).

Microbe	**Description**	**High or low prevalence in the CF community**	**Reference (s)**
Staphylococcus aureus	Gram-positive cocci, opportunistic.	Highly variable depending on patient location and age, typically declining with patient age.	Prevalence: Hurley 2018 Description: Boucher and Corey 2008
Haemophilus influenza	Gram-negative coccobacillus, with or without a capsule. Can grow aerobically and anaerobically. Either capsulated or non-capsulated. Non-capsulated forms more commonly found in CF airways.	Prevalent in early years.	Description: King 2012 Prevalence: Armstrong *et al* 1996
Burkholderia	Aerobic Gram-negative bacillus which prefers aquatic environments. Some species can cause severe lung function decline in CF patients.	*B. multivorans* appears to be the most prevalent currently, replacing *B. cenocepacia*.	Description: Coenye *et al* 2001 Prevalence: Zlosnik *et al* 2015
Steptococcus sp.	Gram-positive cocci. Two groups (A and B) can both cause pathogenic disease in humans.	High prevalence.	Description: Parks *et al* 2015 Prevalence: Acosta *et al* 2018
Stenotrophomonas maltophilia	Opportunistic, aerobic, Gram-negative rod.	Fairly prevalent, isolated from about 30% of patients. Denoted a 'satalite' family of the CF airway by van der Gast *et al* (2011).	Description: Brooke *et al* 2012 Prevalence: Waters *et al* 2011; van der Gast *et al* (2011)

Microbe	Description	High or low prevalence in the CF community	Reference (s)
Achromobacter xylosoxidans	Opportunistic, Gram-negative bacilli. Generally aerobic but can grow anaerobically.	Fairly prevalent, mainly in older patients, found to be 17.9% in a study by Baets *et al* (2007) but the prevalence varies greatly between studies from 2-30% (LiPuma *et al* 2010).	Description: Swenson and Sadikot 2014 Prevalence: Baets *et al* (2007); LiPuma *et al* 2010
Mycobacterium abscessus	Aerobic, Gram-positive bacillus. Found in soil and water, can cause non tuberculous lung disease and soft tissue infections.	Found in about 10% of CF patients.	Description: Hypolite et al 2015; Lee *et al* 2015 Prevalence: Skolnik *et al* 2016
Prevotella sp.	Anaerobic, Gram-negative bacilli.	Fairly prevalent	Description: Gilpin *et al* 2017 Prevalence: Acosta *et al* 2018; Gilpin *et al* 2017; Tunney *et al* 2008
Veillonella sp.	Gram-negative, anaerobic cocci, associated with oral biofilms.	Low prevalence but denoted a core family in van der Gast *et al* (2011).	Description: Rovery *et al* 2005 Prevalence: Acosta *et al* 2018 Interactions: Mashima and Nakazawa 2015
Neisseria sp.	Gram-negative diplococci	Fairly prevalent, but this prevalence decreases in patients with moderate or severe lung disease.	Description: Liu *et al* 2015 Prevalence: Acosta *et al* 2018
Porphorymonas sp.	Gram-negative anaerobic bacilli	Low prevalence (Acosta et al 2018), but denoted a core family in van der Gast *et al* (2011).	Description: Falagas and Siakavellas 1999 Prevalence: Acosta *et al* 2018

Microbe	Description	High or low prevalence in the CF community	Reference (s)
Catonella sp.	Gram-negative anaerobe	Fairly prevalent, denoted a 'core' taxa of the CF airway by van der Gast *et al* (2011).	Description: Moore and Moore 1994 Prevalence: van der Gast et al 2011
Ralstonia	Gram-negative non-fermenters	Quite low prevalence, but rising. Found to be 2.1% in 2014-2016 (Green *et al* 2016).	Description: Green *et al* 2016 Prevalence: Green *et al* 2016
Pandoraea	Aerobic, Gram-negative bacilli. Found in soil, water, food and human respiratory tracts.	Considered an emerging infection, numbers may be underestimated due to misidentification as other bacteria such as *Ralstonia.*	Description: Costello *et al* 2011 Prevalence: Atkinson *et al* 2006
Propionibacterium	Gram-positive, anaerobic bacilli, a commensal of human skin and most well-known for associations with acne.	Where anaerobic bacteria were detected, *Propionibacterium* was recovered frequently.	Description: Achermann *et al* 2014 Prevalence: Tunney *et al* 2008
Acinetobacter	Aerobic, Gram-negative coccobacilli. Found in soil, water, food and mucosal membranes of humans and animals.	Several species types identified, the general prevalence in CF airways is not yet well-known.	Description: Wong *et al* 2017 Prevalence: LiPuma 2010
Actinomyces	Gram-positive bacilli, facultative anaerobes.	Low prevalence. Denoted a 'satalite' class of the CF airway by van der Gast *et al* (2011).	Description: Kononen and Wade 2015 Prevalence: Acosta *et al* 2018; van der Gast *et al* 2011

Microbe	Description	High or low prevalence in the CF community	Reference (s)
Candida	Opportunistic fungal (yeast) member of the human gut flora	Frequently isolated, *C. albicans* found in about 3 quarters of CF patients (75-78%) in by 2 studies quoted in LiPuma 2010.	Description: Nobile and Johnson 2015 Prevalence: LiPuma 2010
Malassezia	Yeast-like fungi. Commensals which can cause chronic disease in the predisposed.	Frequency may be underreported due to poor detection by culture based methods. Nagano *et al* 2010 found 2.6% of patient sputum samples contained *Malassezia.*	Description: Thayikkannu *et al* 2015 Prevalence: Nagano *et al* 2010
Aspergillus	Airborne saprophytic fungi, which can cause disease in immunocompromised patients.	*A. fumigatus* is the most prevalent filamentous fungus isolated from CF airways. A wide range of prevalence rates reported 6-60%. Found more often in older patients.	Description: Latge 1999 Prevalence: LiPuma 2010
Influenza (both A and B) viruses	From the family *Orthomyxoviridae,* influenza viruses show high genetic variation. Their genome is composed of negative-sense, single-stranded, segmented RNA.	Fairly low prevalence. Closely follows respiratory syncytial virus in prevalence. Its presence is dependent on the season, methodology and patient age.	Description: Taubenberger and Morens 2008 Prevalence: LiPuma 2010
Respiratory syncytial virus (RSV)	From the genus *Orthopneumovirus,* RSV is enveloped and spherical, with a non-segmented, negative RNA genome. A problem for those with vulnerable immune systems including young children and the elderly.	Fairly low prevalence. RSV is typically the most frequently detected virus in the CF airway. Its presence is dependent on the season, methodology and patient age.	Description: Griffiths *et al* 2017 Prevalence: LiPuma 2010

Microbe	Description	High or low prevalence in the CF community	Reference (s)
Parainfluenza virus and adenovirus	Parainfluenza viruses are medium sized and enveloped, with a negative-sense RNA genome. They are of the *Paramyxoviridae* family. Adenoviruses belong to the *Mastadenovirus* genus. They are non-enveloped, with a double-stranded DNA genome.	Low frequency	Description: Henrickson 2003; Ghebremedhin 2014 Prevalence: LiPuma 2010

Table 1.2.1: Microbial life discovered in the CF respiratory tract. Note that this is not an exhaustive list and prevalence values may vary depending on the study.

Of all the pathogens found to colonise the CF airway, chronic *P. aeruginosa* infection appears to be of the greatest clinical significance. This is due to its persistence despite extensive antibiotic treatment (Bryan *et al* 1972; Kobayashi *et al* 1972; Lyczak *et al* 2002), stimulating an inflammatory response which leads to tissue damage and loss of lung function (Konstan *et al* 1995). Whether inflammation occurs prior to, or following bacterial infection has not been definitively proven, with studies showing evidence of elevated levels of neutrophil elastase in the lungs of patients with no culturable bacteria detected (Birrer *et al* 1994; Konstan *et al* 1994; Khan *et al* 1995). Whether or not the immune system is already primed when *P. aeruginosa* invades, its presence correlates with an increase in IL-8 (DiMango *et al* 1995), increased activated complement (C3a) (Schoitz *et al* 1979) and a high amount of neutralising antibodies against several cellular components (Doring and Hoiby 1983; Jensen *et al* 2010). These result in neutrophil recruitment and accumulation, causing an abnormal depletion of oxygen due to the generation of superoxide, a product of the respiratory burst. Rather than clearing the biofilm communities of *P. aeruginosa*, the surrounding host tissues sustain considerable damage (Jensen *et al* 2010).

1.1.6 *P. aeruginosa* as a CF pathogen

The high incidence of *P. aeruginosa* infection in CF patient airways (Cystic Fibrosis Patient Registry 2015) indicates the suitability of this environment for the bacterium. A large majority of *P. aeruginosa* strains found in CF patients appear to be environmental (Gibson *et al* 2003), indicating that the bacterium is adapting to the CF airway environment upon colonisation. There are several reported theories of why *P. aeruginosa* is particularly adept at establishing infection in CF patients (Worlitzsch *et al* 2002; Anderson *et al* 2008; Matsui *et al* 1998; Goldman

et al 1997; Pier *et al* 1996; 1997; de Bentzmann *et al* 1996; Pezzulo *et al* 2012). Although their individual impact on successful colonisation is still unclear, it is likely that they work in concert to outcompete host immune and clearance defences.

The physiological environment of the CF airway differs from that of the normal respiratory tract. Dehydrated and hyperviscous mucous and airway surface liquid layers result in poor mucociliary clearance and mucous layer thickening. In certain areas this thickening can obstruct the airway, forming a mucous plug (Boucher 2004). Within the thickened mucous and especially inside the plugs, a steep oxygen gradient forms which *P. aeruginosa* colonise. The bacteria contribute to the depletion of oxygen and the environment becomes increasingly hypoxic (Worlitzsch *et al* 2002). Undoubtedly, the high degree of metabolic flexibility *P. aeruginosa* possesses confers a distinct survival advantage in this environment and observations that its operating machinery is adjusted along a continuing gradient of oxygen availability has been observed by Alvarez-Ortega and Harwood (2007). Not only does the thickened mucous allow growth of *P. aeruginosa*, the oxygen deprived conditions have been linked to the generation of a mucoid phenotype which overproduces alginate (May *et al* 1991; Cunin *et al* 1986; Anderson *et al* 2008; Doring *et al* 2000). This colony morphology has been linked with increased persistence, tissue damaging inflammation and resistance to antibiotic treatment (Kenna *et al* 2007).

Two opposing models have been proposed to explain the effect of altered ion concentrations on the clearance of *P. aeruginosa* from the lung (Lyczack *et al* 2002; Boucher 2002). The first has been referred to above and is currently the more accepted theory. It is known as the 'mechanical clearance' hypothesis, proposing that a sufficient sodium chloride concentration of around 150 mM should be maintained to ensure that the layer of fluid situated between the epithelium and the thicker particle trapping mucous, be sufficiently hydrated for efficient removal by cilia beating. Dehydration of this layer in CF would result in poor clearance, allowing microbial establishment (Matsui *et al* 1998; Tarran *et al* 2001). Abnormal chloride secretions could also disturb the normal functioning of the cilia (Wills *et al* 1997). The alternative theory focuses instead on the properties of the airway surface liquid which promote antimicrobial action by the innate immune system. It has been named the 'chemical shield' hypothesis and reasons that a low NaCl concentration (<50 mM) allows normal neutrophil functioning and effectiveness of some groups of antimicrobial peptides. The researchers propose that the NaCl concentration is higher in CF and this impairs

removal of pathogens from the airway surface liquid (Goldman *et al* 1997; Smith *et al* 1996; Zabner *et al* 1998). Although the authors present intriguing evidence to support this second hypothesis, it is difficult to prove (Lyczak *et al* 2002) due to the complexity of antimicrobial molecules in CF airway surface liquid, (Travis *et al* 2001), and evidence suggesting salt concentration is the same as in normal lungs (Travis *et al* 1999).

Alongside the ion concentration theories, there are also studies which focus on bacterial-host cell binding. Pier *et al* (1996; 1997) found that *P. aeruginosa* recognise healthy CFTR as a receptor and the binding of the bacterium to this channel induces epithelial cell internalisation. Epithelial cells containing multiple bacterial cells can then be cleared from the immune system (Albert *et al* 1998). Conversely, increased binding between glycolipid asialo-ganglioside M1 (aGM1) receptors and *P. aeruginosa* has been associated with reduced clearance. The number of aGM1 receptors escalates with tissue damage, when cell repair is occurring. Inflammation of the airways, either prior to or from previous exposure of *P. aeruginosa* could increase the success of subsequent invasions (de Bentzmann *et al* 1996; Feldman *et al* 1998).

The pH of the CF airway was found to be lower than normal due to another function of healthy CFTR channels: bicarbonate (HCO_3) ion transport. The lack of HCO_3 ions reaching the airway surface causes a decrease in pH (Ballard *et al* 1999; Poulsen *et al* 1994; Poulsen and Machen 1996). Pezzulo *et al* (2012) found that pH correlated with airway bactericidal efficacy, with CF pig airway surface liquid (ASL) presenting a lower pH and impaired killing ability than healthy counterparts. Increasing and decreasing the pH of the fluid, raised and lowered the bactericidal effectiveness, respectively. Tate *et al* (2002) measured the pH of exhaled air from healthy controls, stable CF and exacerbating CF patients. Both CF groups had more acidic exhalations than the healthy controls and interestingly the exhalations from the exacerbating group were more acidic than the stable ones correlating with a higher state of inflammation.

A summary of the theories discussed above is presented in Figure 1.2.3.

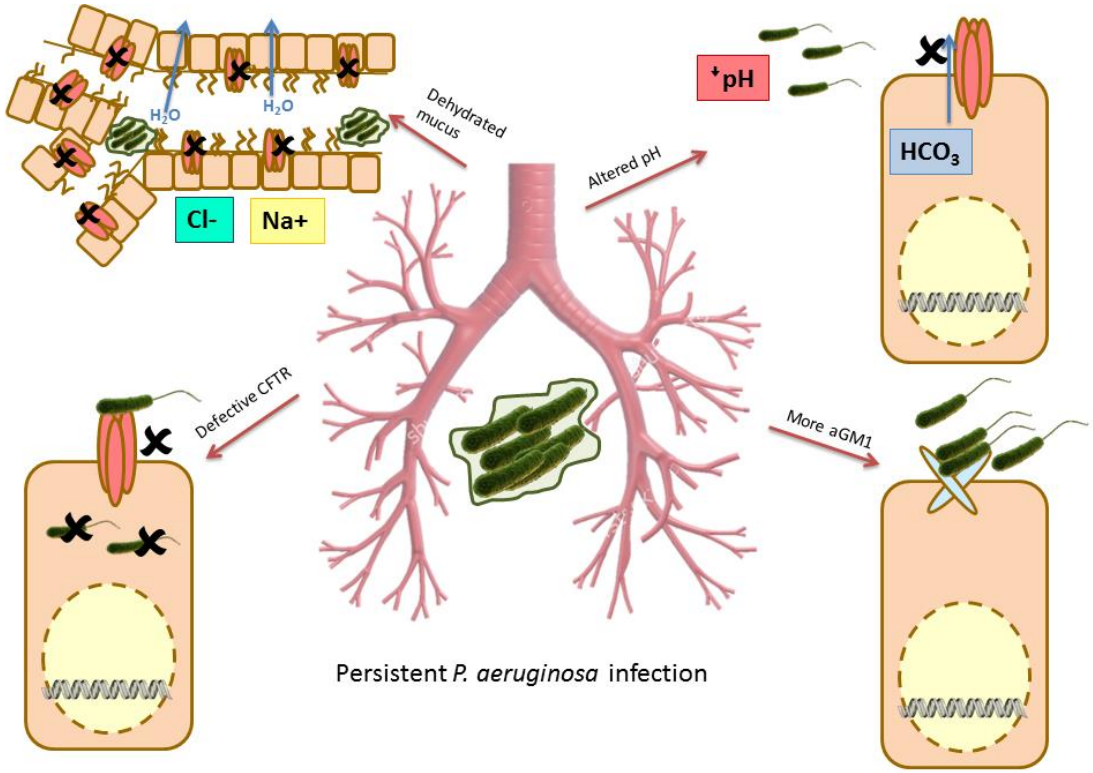


Figure 1.2.3: *P. aeruginosa* as a successful CF airway pathogen: a summary diagram. Dehydrated mucus in the lumen, caused by defective transport of chloride ions (Cl-) and following lack of sodium ions (Na+), impairs clearance of P. aeruginosa. An altered pH of the airway surface fluid occurs due to defective bicarbonate (HCO3) transport by the cystic fibrosis transmembrane conductance regulator (CFTR). Increased glycolipid asialo-ganglioside M1 (aGM1) receptors in damaged tissue encourage increased binding of P. aeruginosa. Defective CFTR is unable to bind and internalise P. aeruginosa which would normally reduce bacterial numbers in the lumen. References: Matsui *et al* 1998; Tarran *et al* 2001; Wills *et al* 1997; Worlitzsch *et al* 2002; Pier *et al* (1996; 1997); de Bentzmann *et al* 1996; Feldman *et al* 1998; Pezzulo *et al* (2012). Picture references: airway central diagram by Shuttershock, *P. aeruginosa* http://www.thesilveredge.com/pseudomonas.shtml#.WO39B_nF92E.

1.1.7 *P. aeruginosa* as a clinically important pathogen outside of the CF airway

In addition to its prowess as a CF respiratory pathogen, *P. aeruginosa* colonisation has been assoiated with other patient groups, in a number of different sites of the body (Berghmans *et al* 2003; Papi *et al* 2006; Monsó *et al* 1995; Nicotra *et al* 1995; Oliver *et al* 2000; Smith *et al* 1996). Generally speaking, *P. aeruginosa* is mainly a problem for people with disadvantaged immune systems and therefore is more often observed in hospitalised patients (Goldberg 2010). The exploited disadvantage in immune defence can be a breach of the body's natural barriers or defects in other areas of the immune response such as the recruitment of neutrophils (Goldberg 2010).

One type of high risk category for *P. aeruginosa* infections are indivduals with a foreign body present, such as a ventilator tube or catheter. Like with CF airway

infections, resistance of *P. aeruginosa* to antibiotics in ventilator assocated pneumonia (VAP) and catheter-assocatied urinary tract infections (CAUTI) are at least in part attributed to biofilm growth (Ramirez-Estrada *et al* 2016). Additionally, evidence suggests that some of the same global regulators as in CF are involved, for example c-di-GMP is instrumental in successful colonisation of the kidenys in CAUTI (Cole and Lee 2016). However, *P. aeruginosa* VAP infection is more aggressive, rapidly spreading from the ventilation tube to the lower respiratory tract. The immune response to VAP is therefore more tailored to an acute infection with acute leucocytosis and fever (Fricks-Lima *et al* 2012).

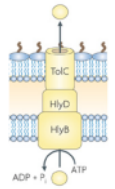
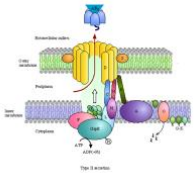
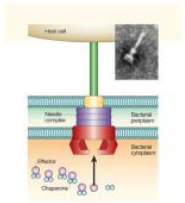
As well as foreign body associated infections, *P. aeruginosa* is also a cause of soft tissue infections which can be divided into acute and chronic types. An example of acute soft tissue *P. aeruginosa* infections, are burn wounds. These typically spread swiftly thoughout the body and can result in death in a matter of days. For a wound to be classified as chronic there needs to be an absence of movement through the process of healing in a timely manner (Turner *et al* 2014). A large category of chronic wounds infected by *P. aeruginosa* are those of diabetic ulcers, where a break in the skin and poor circulation leave patients vulnerable to colonisation by opportunistic pathogens. Observation of *P. aeruginosa* infected chronic wounds showed that a biofilm mode of growth was favoured (Kirketerp-Møller *et al* 2011; James *et al* 2008). In contrast with *S. aureus*, which is frequently isolated alongside *P. aeruginosa* in chronic wounds, *P. aeruginosa* was normally located deep within the tissue away from the surface (Kirketerp-Møller *et al* 2011). The relative fitness of *P. aeruginosa* in this environment was found to correlate with differential expression in metabolic genes, highlighting the important role of metabolic flexibility in chronic infection (Turner *et al* 2014).

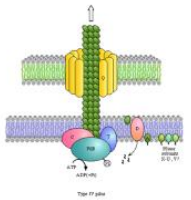
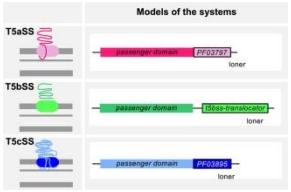
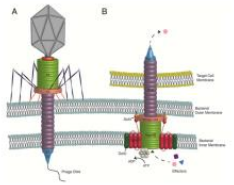
Looking at this information together, an interesting extension of the work presented in this thesis would be to compare the relevance of arginine metabolism, and by extension the arginine specific aminopeptidase autotransporter, in different infection models. The hypothesis here is that the arginine specific aminopeptidase autotransporter would have a greater role in less aggressive, more chronic infections.

1.3 Autotransporter Proteins

1.1.8 Secretion systems in *P. aeruginosa*

Table 1.3.1 summarises the secretion systems of bacteria. The symbol (*) indicates that this system has been found in *P. aeruginosa.*

Secretion System	Structure	Mechanism of secretion	Function (general) and effector proteins	Picture	Reference(s)
T1SS (*)	Also called ATP-binding cassette (ABC) transporters, this class consists of 3 components: an ABC, an outer membrane channel (OMF) and a membrane fusion protein (MFP).	One step system.	Secrete a variety of proteins from the cytoplasm to the extracellular space. Example effector: alkaline protease, AprA	 Picture from Fronzes *et al* 2009	Costa *et al* 2015; Filloux 2011;
T2SS (*)	Consists of 12 to 15 components called Xcp in *Pseudomonas.* Four parts including an OM complex, pseudopilus, an IM platform and a cytoplasmic ATPase make up this system.	Two step system involving *Tat* and *Sec* pathways to facilitate transport across the inner membrane. The folded protein is then passed through the periplasm and outer membrane.	Secretes various enzymes that facilitate growth and survival in the host or certain environmental niches. Example effector: LapA (low molecular weight alkaline protease)	 Picture from Kegg pathways (http://hultgren.wustl.edu/UTI89/map-nolabel/map03090.html)	Parizad *et al* 2016; Costa *et al* 2015; Filloux 2011;
T3SS (*)	A needle-like complex which crosses both the inner and outer membrane. There are about 25 proteins of which it is composed. Some of these form a base of stacked rings spanning both membranes and the others form a needle which extends from the OM into the extracellular space.	One step system. Facilitated by chaperones and translocator proteins which form pores in the host membrane and are secreted though the 'needle', a helical tube. Along with the translocator proteins, effector proteins pass through the needle and into the host cell.	Transports bacterial effectors to the cytoplasm or plasma membrane of eukaryotic cells. These can then initiate or disrupt intracellar processes, facilitating bacterial colonisation. T3SSs are upregulated in acute virulence and downregulated during biofilm growth. Example effector: ExoS,T,U,Y	 Picture from Stebbins and Galan 2003	Costa *et al* 2015 ; Filloux 2011; Goodman *et al* 2004

T4SS	Typically consist of 12 proteins (in *E. coli*). These are arranged into scaffold, translocation apparatus and pilus components.	One step system. The pilus of the T4SS is a tube-like structure which connects 2 cells, allowing the passage of DNA or proteins to pass from the donor cell to the receiving one.	These are able to transport DNA (important for conjugation) as well as proteins into other bacteria or eukaryotic cells. Example effector: not present in *P. aeruginosa*	 Picture from Kegg pathways (http://hultgren.wustl.edu/UTI89/map-nolabel/map03090.html)	Costa *et al* 2015
T5SS (*)	The substrate itself contains the machinery necessary for its own secretion. This includes a signal peptide N-terminal sequence which directs the protein towards the Sec machinery in the IM and a beta-barrel domain which facilitates transport across the OM. There are 5 subgroups (Va to Ve). *P. aeruginosa* has been found to possess proteins in group Va, Vb and Vd.	Two step system involving the Sec apparatus. The peptide is directed to the IM, Sec complex and passes through the periplasm where the beta-barrel then mediates transport through the OM in concert with the Bam complex.	Mainly virulence factor secretion as well as cell to cell adhesion and proteins involved in biofilm formation. Example effector: EstA, AaaA	 Picture from Abby *et al* 2016	Costa *et al* 2015; Wilhelm *et al* 1999; Kida *et al* 2008; da Mata Madeira *et al* 2016
T6SS (*)	Composed of 13 core components and an assortment of accessory modules. The structure has 2 main parts: a membrane cluster which contains IM proteins homologous to the ones employed by the T4SS, and a tail which is related to the contractile tails possessed by bacteriophages.	One step system. Thought to be similar to the mechanism employed by bacteriophage. The tail contracts following an extracellular cue which causes an inner tube within the tail to be pushed out of the bacterial membrane and across a target cell envelope.	Toxic effectors are transported into both bacterial and eukaryotic cells by this system. Contributes to bacterial pathogenicity and competitive advantages. In fact, *P. aeruginosa* has 2 groups of T6SS. The first (T6SS-1) specialises in bacterial-bacterial interactions and the second (T6SS-2) in bacterial-host relations. Example effector: Tse1,2,3 (bacterial toxin)	 Picture from Records *et al* 2011	Costa *et al* 2015; Filloux 2011

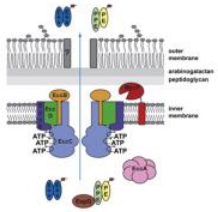
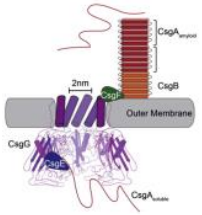
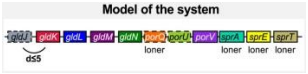
T7SS or chaperone -usher secretion pathway	Contains an ATPase and a putative membrane channel through which folded protein substrates are transported.	This could be a one or a two-step process depending on whether certain components are found to be inserted into the OM or not. Currently only insertion into the IM has been suggested. Specific secretion chaperone-like proteins could be involved in a similar way to that of the T3SS. An AAA+ ATPase is also involved. Substrates are targeted to the inner membrane and then are translocated across both membranes to the cell exterior. It is thought that some components form a pore large enough through which the folded substrates are transported.	Employed by mycobacteria, both essential for virulence and viability. The substrate to be transported takes the form of a heterodimer with 4 helices arranged in a bundle. Example effector: not present in *P. aeruginosa*	 Picture from Houben *et al* 2014	Houben *et al* 2014
T8SS	Also called nucleation–precipitation secretion. The periplasmic component, CsgE is directed towards the OM pore forming protein CsgG. CsgF connects with CsgG on the surface of the cell.	Secretion of the curli subunits CsgA and CsgB is achieved while they are in an unstructured, insoluble form. CsgE is a periplasmic component which directs the proteins to the OM component, CsgG which forms a pore in the outer membrane. CsgF then helps the proteins assemble on the surface of the cell.	Secretion of the protein components for the construction of extracellular amyloid fibers (Curli). Curli contribute to structural and adhesive qualities useful for biofilm formation. Example effector: not present in *P. aeruginosa*	 Picture from Evans *et al* 2014	Evans *et al* 2014
T9SS	Five proteins are spread between the IM and the OM. These proteins are from *Porphyromonas.* PorL and PorM reside in the inner membrane, PorN in the periplasm and PorK and PorP in the OM. The Sec pathway has also shown to be involved in the initial transportation step across the IM.	This is thought to be a two-step process involving Sec machinery. The inner components PorL and PorM have been suggested to act as an energy transferring complex. PorK and PorP potentially form a ring structure in the outer membrane allowing passage to the outside of the cell. These proteins are from *Porphyromonas* and this system has not yet been found in *Pseudomonas*.	Secretion of toxins, adhesins, chitinases or S-layer proteases. Example effector: not present in *P. aeruginosa*	 Picture from Abby *et al* 2016	Vincent *et al* 2017

Table 1.3.1: Secretion systems in Gram-negative bacteria.

1.1.9 The Type V Secretion System

Autotransporters (ATs) are polypeptide molecules transported across the bacterial membrane by the type V secretion system (T5SS). They have a specific, multi-component structure which facilitates their journey from cell interior to outer membrane (OM). The process is believed to be energy independent and does not involve the use of ATP or a proton gradient across the OM (Thanassi *et al* 2005). In comparison to the other secretion systems available in the arsenal of *P. aeruginosa*, the T5SS is simplistic (Cascales and Christie 2003; Henderson *et al* 2000) (Table 1.3.1). All ATs are composed of 3 main domains. These are summarised in Figure 1.3.1. The first domain following the N-terminus is the signal peptide (SP) which allows efficient localisation to the Sec complex and subsequent passage through the inner membrane (IM). This region is typically 20-30 amino acids in length and shows a fairly high amount of diversity in sequence (Dautin and Bernstein 2007). Following the SP is the passenger domain. These are generally quite variable in size ranging from less than 20 kDa to more than 400 kDa. Although differing greatly in sequence, the general structure of passenger domains are highly conserved (Dautin and Bernstein 2007). At the C-terminus, resides the beta(β)-barrel domain. This is normally about 30 kDa, varying less in size than the passenger domain. They possess a large level of sequence diversity, lacking universal sequence motifs, although the architectural structure appears to be conserved (Dautin and Bernstein 2007).

Autotransporter proteins have been divided into 5 subgroups from Va to Ve (Leo *et al* 2012). The first class, of which the prototype IgA protease is a member, are also called the classical ATs and are expressed as a single polypeptide (Leo *et al* 2012). The β-barrels of this type of AT are typically composed of 12 strands. The arginine specific aminopeptidase autotransporter of *P. aeruginosa* (AaaA) appears to be part of this group (Luckett *et al* 2012). The second group is also named the two-partner secretion (TPS) system (Henderson *et al* 2004; Jacob- Dubuisson *et al* 2004; Benz and Schmidt 2011) where the passenger and β-barrel translocation domains are expressed as 2 separate peptides. The β-barrel containing peptide also contains a polypeptide transport associated (POTRA) domain which helps the passenger peptide connect with the β-pore (Leo *et al* 2012; Fan *et al* 2016). The mechanism of transport appears to be the same as the Va group of ATs, but the β-barrels are typically 16-stranded instead of 12 (Leo *et al* 2012). Vc, or trimeric ATs, usually have passenger functions as adhesins. The structure of the peptide is the same as Va peptides, however 3 of these peptides are transported separately

through Sec, their β-barrel domains (which contain 4 strands of the channel) combining into a 12 stranded pore at the OM (Szczesny and Lupas 2008; Linke *et al* 2006). A class D (Vd) seems to be a combination of Va and Vb in that it is expressed as one peptide, but the β-barrel and the passenger are separated by a POTRA domain (Salacha *et al* 2010). The Ve group is also called the inverted AT group and are represented by intimin and invasin proteins. These have the same structure as the Va group but in reverse (Tsai *et al* 2010; Oberhettingher *et al* 2014).



Figure 1.3.1: The structure of a typical autotransporter protein. From left to right: Signal peptide (IM transportation), passenger (functional) domain, β-barrel (OM transportation) (Dautin and Bernstein 2007). Many autotransporter peptides contain a linker region between passenger and β-barrel which aids in hairpin formation and translocation across the OM (Leo *et al* 2012).

The autotransporter family is broad and includes a large number of polypeptides with a variety of functions, typically as adhesins, cytotoxins, degradative enzymes and other virulence proteins (Dautin and Bernstein 2007). The most famous autotransporters are the secreted serine protease autotransporters of *Enterobacteriaceae* (SPATES) (Ulsen *et al* 2014; Celik *et al* 2012; Bodelon *et al* 2009). These possess passenger domains with a trypsin-like serine protease at the N-terminus (Henderson and Nataro 2001; Dutta *et al* 2002). Some also have a long SP sequence, the function of which has not yet been agreed upon. Earlier studies focusing on the EspP and Hbp proteins suggest that the extension helps with the cotranslational targeting of proteins via the signal recognition particle (SRP) pathway (Peterson *et al* 2003; Sijbrandi *et al* 2003), while subsequent investigations hypothesise that the function of this longer signal peptide mediates post-translational translocation across the IM (Desvaux *et al* 2007; Chevalier *et al* 2004; Henderson *et al* 2004). A study by Szabady *et al* (2005) suggests that a longer SP helps reduce misfolding in the periplasm, in contrast to the findings of Leyton *et al* (2010) which discount all of these possibilities. The SPATES can also have an asparagine-asparagine motif dividing passenger and beta-barrel domains (Ulsen *et al* 2014; Dautin 2010; Ruiz-Perez and Nataro 2014).

1.1.9.1 Mechanism

The mechanism employed by ATs to travel through the bacterial membrane was first investigated in the immunoglobulin A (IgA1) protease (Klauser *et al* 1992). There are 3 main stages in the AT's journey to the extracellular space: crossing

the IM, the periplasm and the OM. This is outlined in Figure 1.3.2 and later figures will expand on this in more detail. The mechanism of passenger domain transversal of the OM is still debated and the conflicting theories are here summarised in Figure 1.3.3.

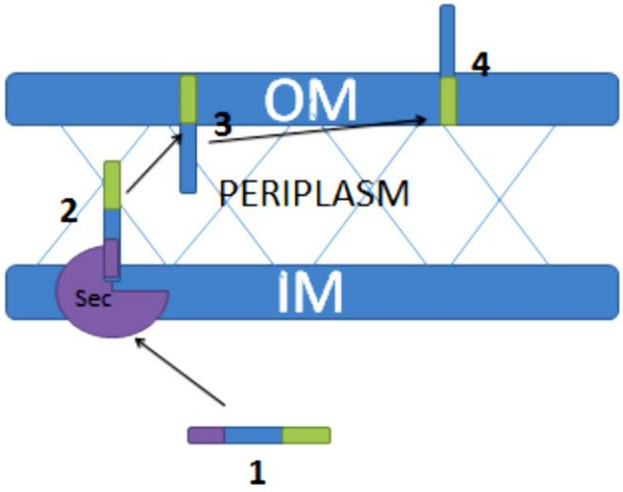


Figure 1.3.2: Overview of the autotransporter mechanism of secretion. The signal peptide directs the autotransporter to the Sec complex and is then subsequently cleaved from the molecule. The nature of Sec pathway means that the autotransporter must enter the periplasm in a linear, unfolded conformation (Brandon *et al* 2003, Sijbrandi *et al* 2003; Peterson *et al* 2006). Once in the periplasm, the signal peptide remains attached to the Sec complex and is slowly cleaved from the other autotransporter domains (Szabady *et al* 2005), which continue to be transported through the OM. The mechanism whereby this is done is still only partially understood and is discussed in Figure 1.3.3. Once though the OM, the passenger can remain associated with the membrane or be released into the extracellular milieu by subsequent cleavage (Benstein 2015).

It was first thought that the β-barrel alone was sufficient to allow the passenger domain to pass from periplasm to cell exterior (Pohlner *et al* 1987). β-barrel insertion into the OM, and formation of a cylindrical channel, was confirmed by X-ray crystallography (Oomen *et al* 2004; Barnard *et al* 2007) and mutational studies (Pavlova *et al* 2013; Leyton *et al* 2014). The hair-pin model was then proposed to explain how the passenger could cross the OM, by the threading of the passenger through the β-pore (Figure 1.3.3; Leva and Bernstein 2009; Junker *et al* 2009). The problem with this model was that the channel does not appear big enough for this to occur. The pore size was found to be ~17-20 A in diameter, which would allow either 1 alpha (α)-helix or 2 linearized peptide strands through at a time (Sauri *et al* 2012; Oomen *et al* 2004; Barnard *et al* 2007; van den Berg, 2010; Tajima *et al* 2010; Zhai *et al* 2011). Evidence by a number of studies however, indicates that passenger domains with tertiary structure pass though the β-barrel (Veiga *et al* 2004; Skillman *et al* 2005; Kang'ethe and Bernstein 2013) and the linker region, thought to be the static side of the hairpin inside the

channel, takes the form of an α-helix (Leva *et al* 2008; Peterson *et al* 2010). Along with findings showing the channel should not be able to expand when formed (Khalid and Sansom 2006; Tian and Bernstein 2010) the hairpin model was thrown into dispute. If the channel alone is not sufficient for passenger secretion, it would indicate that other OM proteins could be aiding the process. Indeed, studies have shown that when translocation is halted, passenger domains reside in the vicinity of an Omp85 family protein, BamA (Leva and Bernstein 2009). BamA appears to assist the β-barrel throughout translocation, potentially by facilitating a conformational change in the β-barrel channel to allow the passenger to pass through (Leva *et al* 2011; Sauri *et al* 2009). This has led to a second model being proposed which involves the β-barrel folding in the periplasm with the 'hairpin' incorporated inside with the help of molecular chaperones. The β-barrel is then inserted into the OM with the help of the Bam complex. It then has been speculated that BamA and the β-barrel could form a hybrid channel, increasing the pore size and allowing the passenger through in a harpin-motion manner (Bernstein 2015).

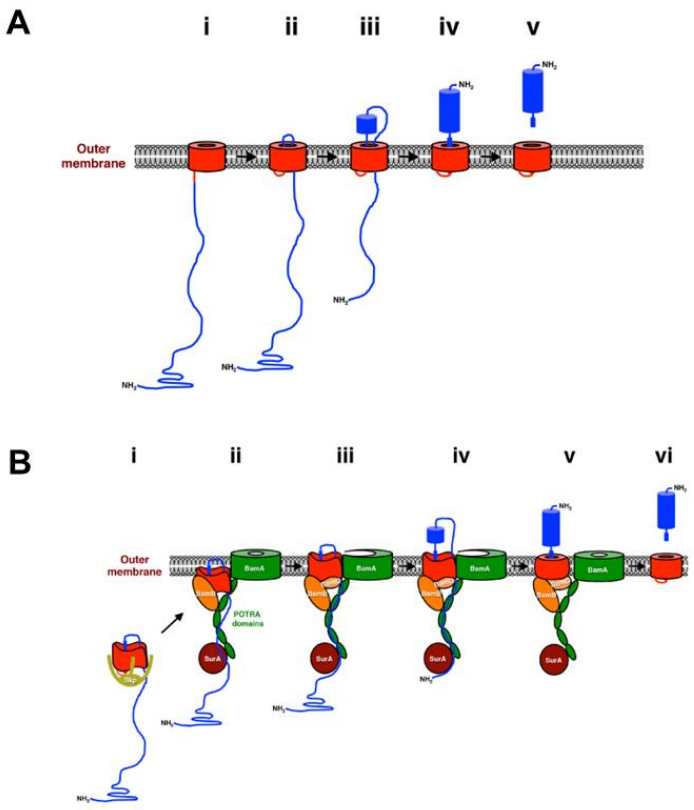


Figure 1.3.3: Models for how autotransporter proteins cross the outer membrane. Part A: hairpin model involving only the β-barrel. Once the β-barrel incorporates into the OM, the C-terminus of the passenger is inserted into the channel in a 'hairpin' conformation and gradually threaded through with the N-terminus reaching the extracellular space last (Pohlner et al 1987; Henderson 2004). Part B: BamA and chaperone assisted model with hairpin movement of the passenger through the OM. The β-barrel is inserted into the OM with the help of the Bam complex and then the β-barrel channel is held in an extended open conformation by BamA. The passenger travels through in the hair-pin manner described in part A (Leva *et al* 2011; Sauri *et al* 2009; Bernstein 2015). Figure adapted from Bernstein (2015).

1.3.3 Type V secretion systems in *P. aeruginosa*

In *P. aeruginosa*, 3 classical autotransporter proteins (Va) were identified from the PAO1 genome (Stover *et al* 2000) as having sequences resembling those of ATs and were subsequently investigated. These have now been named EstA (Wilhelm *et al* 1999), EprS (Kida *et al* 2013) and AaaA (Luckett *et al* 2012). Proteins belonging to the TPS system (Vb) (Kida *et al* 2008) and the type 5 d (Vd) (da Mata Madeira *et al* 2016) secretion system have also been found.

EstA is an autotransporter esterase (Wilhelm *et al* 1999), instrumental for *P. aeruginosa* virulence and biofilm formation in chronic respiratory infection (Potvin *et al* 2003; Wilhelm *et al* 2007). The role EstA plays in virulence and biofilm formation has been attributed to rhamnolipid production (Wilhelm *et al* 2007), which have been linked to adverse effects on cilia in the trachea (Read *et al* 1992), impairment of the macrophage phagocytic response (McClure and Schiller

1996), action as hemolysins (Abdel-Mawgoud *et al* 2010) and cell detachment from biofilms (Boles *et al* 2005). Interestingly, the passenger domain of EstA remains firmly attached to the OM by covalent interaction (Wilhelm *et al* 1999). This is unusual for the passenger domains of ATs, which more commonly maintain attachment by non-covelent interactions if they are not released from the OM (Dautin and Bernstein 2007).

EprS is a serine protease with exo and endo peptidase action, preferentially hydrolysing peptides terminating with arginine or lysine (Kida *et al* 2013). The serine protease autotransporters of *Enterobacteriacease* (SPATES) are characterised to be highly expressed and important for virulence in *Enterobacteriacease*. Belonging to this category, the Proteus toxic agglutinin (Pta) shares the closest sequence identity (56% similarity) with EprS and high conservation of the catalytic domains between these two proteases have been observed. EprS is released from the bacterial surface following the transport of the passenger domain across the OM. How this is achieved has not yet been determined (Kida *et al* 2013).

There are at least 5 TPS system proteins present in the genome of *P. aeruginosa*: PA2462–PA2463; Tps2: PA0040–PA0041; Tps3: PA4624–PA4625; Tps4: PA4540–PA4541 and Tps5: PA0690–PA0692 but not all of these have been tested experimentally (Filloux 2011). Of interest, the Tps3 mentioned above encodes the CdrA/CdrB proteins which have been shown to encourage biofilm formation and bacterial auto-aggregation (Borlee *et al* 2010). Another TPS system (Tps4) encodes a protein pair with trypsin-like serine protease motif called LepA/LepB (Kida *et al* 2008).

PlpD is an active lipase recognising phosphatidylinositols, a component of eukaryotic cell membranes. It consists of 788 residues, including an N-terminal SP, catalytic domain and C-terminal β-barrel. The β-barrel and catalytic domain are joined by a POTRA domain, placing this protein in the Vd subcategory. Its catalytic domain is similar to that of patatin (da Mata Madeira *et al* 2016; Salacha *et al* 2010).

1.3.4 The arginine specific aminopeptidase autotransporter of *P. aeruginosa* (AaaA)

AaaA is an AT shown to be specific for the cleavage of arginine from the N-terminus of peptide molecules (Luckett *et al* 2012). It is a member of the T5SS, type Va group and part of the M28.005 family of proteins. The M28 family includes amino and carboxy peptidases, including the aminopeptidase A of

Streptomyces griseus (SGAP) and the leucine-specific aminopeptidase of *Vibrio proteolyticus* (VpAP) (Chevrierl *et al* 1994; Gilboa *et al* 2001; Ben-Meir *et al* 1993; Stamper *et al* 2004; Gilboa *et al* 2000; Bzymek *et al* 2005; Greenblatt *et al* 1997; Luckett *et al* 2012). Mapping the sequence of AaaA against other members of the group revealed that active site residues in the catalytic pocket of the passenger domain were 100% conserved (Figure 1.3.4). Furthermore, mutation of 7 residues within the predicted active site attenuated activity. The current model for the active site conformation is that a glutamic acid and either a tyrosine or histidine, work in concert with 2 interacting zinc ligands (Fundoiano-Hershcovitz *et al* 2004; Hershcovitz *et al* 2007; Luckett *et al* 2012). Whether AaaA has a catalytic mechanism similar to that of SGAP has not yet been confirmed, as not all of the central catalytic residues for SGAP were mutated in AaaA. Rather than being released into the extracellular space, AaaA remains tethered to the OM, where it is vulnerable to trypsin degradation (Luckett *et al* 2012). This indicates that the product produced by AaaA is useful for the cell to have close at hand.

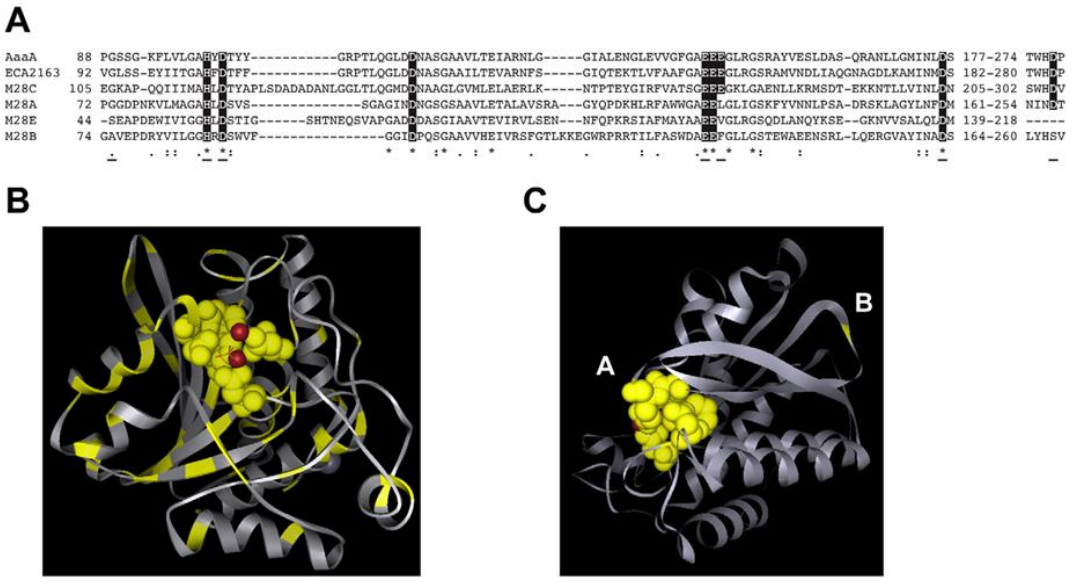


Figure 1.3.4: Predicted catalytic residues and active site pocket of AaaA, from Luckett *et al* 2012 (showing parts A-C). Part A shows a ClustalW2 multiple sequence alignment of the predicted active site regions in enzymes representing the 4 M28 subfamilies in addition to an M28C autotransporter from Pectobacterium caratovora ECA2163 and AaaA. Asterisks indicate identical residues and cols/full stops, similar ones. Residues highlighted by black boxes have been shown to be functional. The underlined regions are those chosen for site-directed mutagenesis. The UniProt database software (http://www.uniprot.org/) was used in the study to acquire the sequences shown. **Part B**: showing the crystal structure of the M28.003 founding aminopeptidase (SGAP). Residues conserved between this protein and AaaA are highlighted in yellow. **Part C**: predicted structure of AaaA based on an alignment with the crystal structure of SGAP as the guide. The yellow coloured residues were mutated, all within the active site region (Ca) apart from a control residue (Cb).

Employment of an enzyme activity assay which measures the rate at which an amino acid coupled to the chromophore P-nitroanilide is cleaved, revealed that

AaaA is able to specifically release arginine. Indeed, when AaaA was removed from the genome this cleavage of arginine from P-nitroanilide reduces to a background level. Additionally, the removal of viable AaaA by mutation abolished the ability of *P. aeruginosa* to grow in conditions where the only nutrient source were peptides containing an N terminal arginine (Luckett *et al* 2012; Lu *et al* 1999; Leisinger *et al* 1972). Only when the terminal arginine was adjacent to a lysine or another arginine, was AaaA unable to release the terminal arginine from peptide chains and growth was consequentially unsupported. The adjacent amino acid to the N terminal arginine seems to improve or reduce the efficiency of arginine release by AaaA and the best arginine utilised growth was seen with an isoleucine or valine residue bonded with the terminal arginine. This evidence indicated that AaaA has a principle role in providing the bacterium with a source of unbound L-arginine, likely to be most important upon a lack of the free amino acid in the environment (Luckett *et al* 2012).

The influence AaaA has on *P. aeruginosa* fitness *in vivo* was tested by infecting a mouse wound model with PAO1 wild-type and PAO1 *ΔaaaA* strains. Both strains were equally pathogenic in an acute situation, but in chronic conditions the Δ*aaaA* mutant showed attenuated virulence (Rumbaugh *et al* 2009; Luckett *et al* 2012). The absence of AaaA also caused changes in the host immune response including lower levels of tumour necrosis factor alpha (TNFα) and interleukin 1 alpha (IL-1α) that are associated with *P. aeruginosa* infection (Yanagihara *et al* 2000; Horino *et al* 2009). Murine chemokines (KC) and cyclooxygenase-2 (COX-2), usually elevated in response to *P. aeruginosa* (Cole *et al* 2000; Sadikot *et al* 2007; Luckett *et al* 2012), were also found at lower levels in hosts infected with PAO1 *ΔaaaA*. The difference in these immune factor levels between WT and Δ*aaaA* mutant *P. aeruginosa* infections is likely due to the number of bacteria present in the tissue. One of the reasons for the Δ*aaaA* mutant strain's attenuated virulence could be due to a growth disadvantage *in vivo*. A combination of hypoxic areas with a lack of nitrate and arginine sources could place PAO1 Δ*aaaA* at a disadvantage. Additionally, in chronic infections, *P. aeruginosa* is likely to grow as a biofilm (Hoiby *et al* 2010; Bjarnsholt *et al* 2010; Costerton *et al* 1981; Yoon *et al* 2002; Moreau-Marquis 2008), exacerbating conditions of oxygen deprivation and nutrient starvation. Supporting this Luckett *et al* (2012), found clusters of cells in the skin secretions of mice infected with the PAO1 WT and these were notably absent in the *ΔaaaA* mutant.

Increased arginine concentrations could also have an immunomodulatory effect. To investigate if arginine released by AaaA had such an effect on the host

immune system, host factors known to respond to arginine availability, nitric oxide synthase (iNOS) and arginase (Arg1 and Arg2), (Frank *et al* 2002) were measured and found to be lower in the wound colonised by PAO1 *ΔaaaA* with iNOS levels elevating after 8 days of infection. During an injury iNOS and arginase levels compete for a limited pool of available arginine (Frank *et al* 2002; Luckett *et al* 2012). It is possible that arginine release from peptides by *P. aeruginosa* disrupts the balance, disrupting this part of the immune response (Luckett *et al* 2012). The arginases catalyse arginine to ornithine and urea which leads to the TH2 alternative response in macrophages (Ishino *et al* 1987; Luckett *et al* 2012) whereas iNOS combines arginine with oxygen to form NO, inhibiting bacterial growth as part of the TH1 classical pathway. In the WT, the generation of arginine by AaaA could increase the supply of arginine available for arginase and iNOS. This would tip the balance in favour of arginase activity, reducing the arginine available for the iNOS response. Whether or not this is the case is still unproven but it is an interesting theory to be explored in the future. Additional influences of AaaA on bacterial virulence *in vivo* remain undiscovered; AaaA could activate another bacterial protein on its surface or deactivate a host protein with an antimicrobial function (Luckett *et al* 2012). Although the work in this thesis aims to shed light on the contribution AaaA could play in *P. aeruginosa* CF infections, the immune component is not investigated and this would be an exciting avenue to pursue in the future.

1.4 Conclusion

The literature suggests that AaaA could contribute to the success of *P. aeruginosa* as a CF pathogen in a number of ways. These include supporting growth in oxygen and nutrient limited conditions, maintenance of a favourable pH and manipulation of the host's immune response. This thesis focuses primarily on the former of these, also with the goal of furthering understanding of the protein structure, leading to drug design and better treatment outcomes.

1.5 Aims

The following areas of interest are pursued in this work:

- **Chapter 3:** Control of AaaA by cellular regulators and development of a qRT-PCR assay as an investigative tool
- **Chapter 4:** AaaA importance in *P. aeruginosa* CF isolates and CF relevant conditions
- **Chapter 5:** Development of a recombinant version of AaaA protein suitable for crystallisation and cell-free inhibitor assays

- **Chapter 6:** The correspondence between AaaA and biofilm formation by *P. aeruginosa* in a range of environmental conditions and strain backgrounds

2 Chapter 2: Materials and Methods

2.1 General Chemicals

Unless stated, Sigma Aldrich was the source of the chemicals used in this work.

2.2 Bacterial Strain Storage and Growth Conditions

All bacterial strains were grown and cultured in accordance with Luckett *et al* (2012) unless otherwise stated. Strains were stored at -80°C in screw top Eppendorf tubes. A final glycerol concentration of 25% was used for all of the bacterial stocks. Before conducting an experiment using *Pseudomonas aeruginosa*, the frozen strain was plated and the following day an overnight culture was made from an isolated colony. The media used for culturing was Lysogeny Broth (LB) unless stated differently and a volume of 5 ml for liquid cultures was used unless indicated. The overnight cultures were grown in 50 ml falcon tubes (Fischer Scientific). Unless otherwise stated, freshly plated *P. aeruginosa* strains were always used to avoid differences in strain behaviour due to mutation. Antibiotic concentrations for *Pseudomonas* strains were 125-150 µg/ml Tetracycline and 20-30 µg/ml Gentamycin. For *E. coli* strains 100 µg/ml Ampicillin and 10 µg/ml Tetracycline were added to cultures. Strains included in this thesis are summarised in Table 2.12.1.

2.2.1 Microaerobic growth

Growth of bacteria in microaerobic conditions was conducted in a microaerobic cabinet unless otherwise stated. The media was allowed to adjust to the oxygen tension of the cabinet for an hour before the bacteria was added. Shaking was conducted at 200 rpm to ensure an even distribution of cells throughout the broth. Samples were taken inside the cabinet and subsequently processed on the bench.

2.3 Optical density ($OD_{600\ nm}$)

The same spectrometer (Thermo Scientific) was used in all experiments to measure cell density prior to normalisation. A volume of 1 ml was placed into a cuvette (Fischer Scientific) and the readings compared to a blank medium sample. Readings greater than 1.0 $OD_{600\ nm}$ were diluted to fall within the range of accuracy of the spectrometer. The values measured by this spectrometer differ from the $OD_{600\ nm}$ value measured by the Tecan Infinate 200 and are therefore not directly comparable.

It should be noted that a relative growth curve to determine absolute cell number was only conducted for specific experiments and is indicated where this is the case.

2.4 Transfer of genetic material into bacteria

The vectors and plasmids used in this study were either conjugated or transformed into *P. aeruginosa* as is described in Sambrook *et al* (1989).

2.4.1 Conjugation

The *E. coli* strain S17-1 *λpir* was used in conjugation reactions (Table 2.12.1) as the donor strain. Conjugations were performed based on Westfall *et al* (2004).

Single colonies of *E. coli* S17-1 *λpir* and the recipient *P. aeruginosa* strain were grown overnight in 10 ml of LB at 200 rpm. *E. coli* S17-1 *λpir* was grown at 37°C while *P. aeruginosa* was grown at 42 ^{o}C to reduce the effect of the restriction/modification system. One millilitre from each of the overnight cultures was transferred into Eppendorf tubes and subsequently washed twice with LB using a microfuge to centrifuge the cells (Biofuge Pico Heraeus) for 5 min at 2571 X g. The pellet was then resuspended in 50 µl of LB. The donor and recipient strains were combined at a ratio of 1:1 unless otherwise stated and 40 µl taken for plating. The cells were plated onto well dried LB agar plates and incubated for 6 hours at 30 ^{o}C. Following this, the cells were scraped off using a sterile loop and placed into an Eppendorf tube containing 1 ml of LB. One hundred millilitres of this suspension was plated onto *Pseudomonas* isolation agar (PIA) plates containing the appropriate antibiotic for selection.

2.4.2 Transformation

The *E. coli* strains DH5 alpha and BL21 (DE3) were used in transformation reactions (Table 2.12.1). *P. aeruginosa* strains (Table 2.12.1) were also transformed using the method below with the exception that a 42 ^{o}C overnight growth temperature was used. Usually electroporation was the transformation method of choice (Farinha & Kropinski 1990), but in some cases cells were made chemically competent and transformed by heat shock.

2.4.2.1 Electroporation

Strains were grown overnight in 10 ml LB at 37 ^{o}C, 200 rpm. The resulting cultures were centrifuged at 2571 X g at 4 ^{o}C for 5 min (Sigma 3K36) and resuspended in 20 ml pre-chilled 10% glycerol. The resuspended cultures were again centrifuged at the same speed, time and temperature and resuspended in 1

ml of pre-chilled 10% glycerol. At this point the cell suspension was transferred to a microcentrifuge tube and centrifuged as the previous in the Sigma 3K36. The supernatant and any dead cells were removed and 100 µl of pre-chilled 10% glycerol added. To 50 µl of this 400 ng of DNA was added and combined using gentle pipetting. Following 10-30 minutes incubation on ice, the cell and DNA mixture was transferred to an electroporation cuvette and the Biorad micropulser used to transfer the DNA inside the cell by an electric pulse. The efficiency of the electroporation was checked using the Time/ms setting. A value of greater than 4 was assumed to be promising. Directly following electroporation, 950 µl of SOC medium was added to the cuvette and this was then placed in the 37 ^{o}C incubator for 1 hour. The cells were then transferred to a microcentrifuge tube and centrifuged at 2571 X g for 5 minutes at room temperature. The supernatant was removed and the cells resuspended in 100 µl of LB. Ten microliters was taken and plated onto one LB plate containing the appropriate antibiotic for selection and the remainder of the 100 µl was deposited onto another plate. Following spreading and drying, the plates were placed in the 37 ^{o}C incubator for 24 hrs.

2.4.2.2 Screening of colonies following transfer of DNA

In the case of the miniCTX-*lux* vector, post-conjugation and post-transformation plates were viewed under the light camera (Hamamatsus, Wasabi software) and colonies selected which produced light.

Where light or fluorescent colony selection was not possible, colonies were screened by a combination of colony PCR (see PCR section) and restriction digest.

Some of the post-conjugation plates were covered in a lawn which did not allow selection of single colonies. In these incidences, a small loop was taken from the plate and restreaked onto another plate to allow better separation of colonies. Colonies were then picked from this plate.

Following selection, clones were sequenced using the service provided by Source Bioscience.

2.5 DNA manipulation

Plasmid DNA was purified using a plasmid purification kit (Sigma Aldrich) according to the manufacturer's instructions. Chromosomal DNA was extracted by the use of a genomic DNA kit (Promega wizard) according to the manufacturer's instructions. Purification of DNA was achieved by using the DNA clean up kit (Qiagen). Various gel extraction kits were trialled during the course of this project which includes Qiagen, Bioline and Monarch NEB suppliers.

2.5.1 PCR

For the identification of *aaaA* by PCR the following conditions were used: an initial denaturation of 95 ^{o}C for 4 mins followed by 30 cycles of denaturation (95°C) 30s, annealing (62°C) 30s and extension (72°C) 2 min. A 10 min final extension of 72°C followed cycle number 30. In the case of colony PCRs a colony from an agar plate was taken with a sterile loop and placed into 50 µl of sterile distilled water; 3 µl of this was added to the PCR reaction. In PCR reactions where chromosomally extracted DNA was used as template, 2 µl (~1 µg DNA) was added per 25 µl reaction. PAO1 Nottingham chromosomal extract was used a positive control and a no template control (NTC) was also included. Gotaq hot-start green master mix (Promega) was used, unless for PCRs where the object was to sequence the product and in that case Q5 (NEB) replaced the Gotaq master mix. The oligonucleotide primers used in this assay are shown in Table 2.5.2. These were synthesised by Sigma-Aldrich. PCR products were visualised on 0.7% agarose gels unless stated otherwise. Agarose gel electrophoresis in 16 TAE buffer (80 mM Tris-acetate pH 7.8, 19 mM EDTA) was performed using the standard methods quoted in Sambrook *et al* (1989).

For the amplification of the *aaaA* promoter region, LESB65 upstream and downstream regions and the truncated *aaaA* gene version 2 & 3 (*aaaAt2 & aaaAt3*), the following conditions were used with reaction specific annealing temperatures and extension times. An initial denaturation of 95°C for 4 mins followed by 30 cycles of denaturation (95°C) 30s, annealing (Table 2.5.1) 30s and extension (72°C), Table 2.5.1. A 10 min final extension of 72°C followed cycle number 30. The controls and amount of reagents remained the same as for the identification of the *aaaA* OFR with the exception that the genomic control was extracted from LESB65 when amplifying from this strain.

2.5.2 Cloning

The cloning in this thesis and associated work included the construction of an inducible PAO1 *ΔaaaA* strain (PAO1 *ΔaaaA* miniCTX::*araC::aaaA*), the creation of two recombinant versions of AaaA protein (*aaaAt2* and *aaaAt3*), and in collaboration with the university of Liverpool, a LESB65 *ΔaaaA* strain. Table 2.5.2 below shows the primers used for each project and the associated annealing temperature. Where restriction enzymes were used, these were from Promega and the manufacturer's instructions were followed. There was an exception in the case of NdeI used in the cloning of *aaaAt2* and *aaaAt3.* A fast digest NdeI by Thermo scientific was allowed to cut for 2 hours before the addition of the

corresponding Thermo Scientific EcoRI and another 1 µl of NdeI for a further digestion of 1.5 hours. Band recovery and DNA extraction was achieved by use of a gel extraction kit (Qiagen). The DNA was quantified by Nanodrop Spectrometry and then was then ligated using T4 ligase and buffer (Promega) overnight at 16 ^{o}C followed by 1 hr room temperature incubation. The equation shown in Figure 2.5.1 was used to calculate the relative quantities of vector and insert. The ligated product was transformed into electrically competent *E. coli* DH5 alpha cells or *E. coli* S17-λpir by electroporation. Colonies were selected on plates containing the appropriate antibiotic.

$$\text{mass insert ng} = \frac{(\text{mass vector 50ng}) \text{ X } (\text{size of insert kb})}{(\text{size of vector kb})} \text{ X (insert:vector)}$$

Figure 2.5.1: Ligation equation used in cloning work. Provided in the manufacturer's instructions (Promega).

The software packages DNAstar (Lazergene) software and Snapgene viewer assisted with the *in silico* design of cloning strategies, primer design and other sequence analysis. Template sequences were taken from the PAO1 reference strain on the *Pseudomonas* genome database. The Sigma Aldrich website (http://www.sigmaaldrich.com/technical-documents/articles/biology/probe-design-services.html) was utilized for the checking of secondary structures.

2.5.3 Tables relevant to nucleic acid manipulation

PCR reaction	Primer pair	Annealing temperature °C	Extension time
Amplifying passenger domain *aaaA*	E1-F E1-R	62	2 min
Amplifying upstream region *aaaA*	PromF PromR	68	45 sec
Amplifying upstream region *aaaA* (LES-like)	UF_aaaA_LES PromR	68	45 sec
Amplifying *aaaA* downstream	DF_aaaA DR_aaaA	68	45 sec
Amplifying *aaaAt2*	aaaAt2_F aaaAt2_R	59.8	1.2 min
Amplifying *aaaAt3*	aaaASV_F aaaAt2_R	60	1.2 min
qRT-PCR *aaaA*, *PA0329* and *16S*	aaaA_7 PA0329_1 16S-PD	60	1 min

Table 2.5.1: Amplification conditions used in this work.

Primer target	Sequence	Short-hand name	Source
aaaA ORF	5'CAGGATTC**ATG**TTCAAACCATTAGCTGTCGCTG3'	E1-F	Paredes 2014
	5'GCTATCGATTTAGTGATGGTGATGGTGATGGAACTGC CAGTTCACCC**TGA**G3'	E1-R	
aaaA Promoter	5'- TATCTCGAGAGCTGAGGCCTGGCGGC -3'	PromF	Paredes 2014
	5'- TATGAATTCGAACACGGCACTTTCCTCTG -3'	PromR	
aaaA Promoter when deletion region was present and for *aaaA* ORF deletion LESB65	5' TATACTAGTCTTCGGATTGGCGGTGAAG 3'	UF_*aaaA*_LES	This study
aaaAt2 cloning	5' ATACAT**ATG**TATCAATACGGGGAATACGCC 3'	aaaAt2_F	This study
	5' TATGAATTC**TTA**ATGGTGGTGGTGATGATG GTCGTGCAGGCGGGTCAGT 3'	aaaAt2_R	
aaaA ORF start for truncation without signal peptide	5'- TATCAT**ATG**TTCAAACCATTAGCTGTCGCTG -3'	aaaASV_F	Paredes 2014
	5' TATGAATTC**TTA**ATGGTGGTGGTGATGATG GTCGTGCAGGCGGGTCAGT 3'	aaaAt2_R	This study
Sequencing T7	Source Bioscience inclusive		Source Bioscience
Sequencing M13	Source Bioscience inclusive		Source Bioscience
SDM RpoN	5'CGTGCTCCAGAGACATGAAAC**ta**TCCGCATCCT**aa**TTT CCGCG3'	RpoN_SDM_F	This study
	5'CGCGGAAA**tt**AGGATGCGGA**ta**GTTTCATGTCTCTGGA GCACG3'	RpoN_SDM_R	
	5'CGTGCTCCAGAGACATGAAACGGTCCGCATCCTGCTT TCCGCG3'	RpoN_unmutated_F	
qRT-PCR *aaaA* set 5	5'TCCCGGTGTTGTTCCTCGAC3'	aaaA5_F	This study
	5'ACTTCCTTGTTGTCCTCGGC3'	aaaA5_R	

qRT-PCR *aaaA* set 7	5'GTCACCGGCGACAAGATGTA3'	aaaA7_F	This study
	5'CAGGATCTGTTCGCGGTAGG3'	aaaA7_R	
qRT-PCR *PA0329* set 1	5'TGAAGAAAGCGAAAGACGGC3'	PA03291_F	This study
	5'TGGCCTTGTACAGTTCGCTG3'	PA03291_R	
qRT-PCR *aaaA* set 4	5'TCATTCTCACCAGCGAACTGT3'	PA03294_F	This study
	5'GTGGCCTTGAGCACGAAGTG3'	PA03294_R	

Table 2.5.2: Table of Primers. Bold uppercase indicates start and stop codons, bold lowercase indicates bases which differ from the template for site-directed mutagenesis, underlined bases indicate introduced restriction sites.

2.6 RNA

2.6.1 RNA extraction

Overnights of each strain (3 separate colonies per strain) were grown in the appropriate condition for 18 hours. These were then normalised and added to fresh media to a final OD_{600} of 0.01. Samples were collected every 2 hours by the transferral of 600 µl to a clean tube containing 1, 200 µl of RNA protect. This was in accordance with the manufacturer's recommendations of a 2 part: 1 part RNA Protect (Qiagen) to bacterial culture respectively. The mixture was incubated at room temperature for 5 min and subsequently vortexed for 5 sec. The tubes were then centrifuged at 2571 xg (Sigma 3K36), the supernatant removed and the pellet frozen at – 80°C for no longer than 1 month. Following this, RNA was extracted using the Qiagen RNeasy minikit. Protocol number 4 for chemical lysis of cells was followed and subsequently Protocol number 7 for RNA extraction was followed. The RNA was eluted into 30 µl of nuclease free water and further concentrated by passing through the column a second time. The concentration of nucleic acid was assessed using the nanodrop spectrometer. Samples showing substantial reagent or protein contamination were discarded at this stage. A PCR using *aaaA* ORF primers (E1-F and E1-R Table 2.5.2) was performed which confirmed the presence of DNA. DNAse (ambion) was then added according to manufacturer's instructions and the sample incubated at 37°C for 30 mins. The DNAse inhibitor was then added, incubated with the sample and subsequently removed by centrifugation as according to the manufacturer's instructions. To determine whether the digestion of DNA had been completely successful, a PCR using the *aaaA* ORF primers was performed and compared to the samples from the 'before digestion' PCR. The RNA was then reassessed in the nanodrop for

quantity and contamination. When found to be of sufficient concentration and purity, further analysis for integrity was performed in the Bioanalzer (Aligent).

2.6.2 RNA conversion to cDNA

The GoScript™ Reverse Transcription System (Promega) was used for the generation of cDNA. The RNA concentration was normalised to 0.2 µg/ml. Random primers 0.5 µg were combined with the RNA and nuclease free dH_20 in a total volume of 5 µl according to the manufacturer's instructions. These were incubated at 70°C for 5 minutes. The mixture was then chilled on ice for 5 minutes and then pulse spun in a myfuge (benchmark) for 10 sec. The tube was then stored on ice while the reverse transcription mix was prepared. The components for this mix can be found in the manufacturer's protocol. The reverse transcription mix and the primers plus RNA mix were combined and then incubated at 25°C to anneal, followed by an hour at 42°C to extend. The temperature variations required were executed by the T3000 thermocycler (Biometra, Thistle Scientific). The Nanodrop Spectrometer was used to measure the concentration and the cDNA stored at -20 ^{o}C. Before qRT-PCR the cDNA concentration was adjusted to 1 µg and the reverse transcriptase inactivated by incubating in a heat block for 15 mins at 70°C.

2.6.3 RT-qPCR endogenous reference screening

A panel of 6 housekeeping genes: *RpoD, 16S, ProC, OprM, GyrB, Adk,* were tested using the GeNorm kit (PrimerDesign). The protocol provided by PrimerDesign was followed and all reagents were sourced from that company.

Each well of an optical clear 96 well clear plate (Applied Biosystems, Part No. 4306737) was filled with the appropriate master mix and subsequently the cDNA was added. Biological triplicates and technical duplicates were included.

The reaction was run in the 7500 real time PCR system (Applied Biosystems) for the durations specified by the manufacturer. All qPCR work was conducted in a designated area with a UV lamp served cabinet.

Analysis was achieved by using the online tool RefFinder (Xie *et al* 2012).

2.6.4 Primer efficiency testing

The primer pair efficiencies were tested using a standard curve. The DNA standards ranged from 500 ng to 0.005 ng in a 1:9 dilution series. The concentrations of these were assessed using the Nanodrop Spectrometer. Each primer pair (1 µl of each 10 µM F and 10 µM R) and 10 µl master mix of assorted

type (e.g. Luna qPCR mix NEB) were combined with 2 µl nuclease free H_20, vortexed for 2 sec and pulse spun (myfuge benchmark). To each well of a 95 well white plate (Primerdesign), 15 µl of this master mix was added. Subsequently, 5 µl of a DNA mixture was added: 4 µl nuclease free water and 1 µl of DNA standard. Each DNA standard was added in triplicate with the inclusion of a water only NTC. The plate was sealed (Thermo Fischer) and centrifuged for 2 mins at 1,788 xg in centrifuge 5430 (Eppendorf). Once the plate had been placed in the ABI 7500 qPCR machine, the run was started and the cycles followed the sequence quoted in Table 2.6.1. The ABI software was used post amplification to produce a melt curve.

	Step	**Time**	**Temperature °C**
	Enzyme activation	2 min	95
40 x Cycles	Denaturation	15 sec	95
	Annealing and Extension	1 min	60
	Melt curve analysis		

Table 2.6.1: Temperature cycling used in qRT-PCR assays.

2.6.5 qRT-PCR for gene expression in different growth conditions

The standardised cDNA (1 µg/µl) was mixed 1:4 in nuclease free water in autoclaved and irradiated PCR tubes. Master mix (FastStart Universal SYBR Green Master (Rox) by Roche under Sigma Aldrich) was combined with either 16S primer, aaaA7 primer or PA0329-1 primer pairs in the manner described in the previous section. Five 96 well plates containing master mix with one of the 3 primer sets were set up. To one of these, cDNA was added and placed in the thermocycler. Four of these were stored at 4°C and cDNA added directly prior to running the reaction. All 5 plates were run during the same day.

2.7 P-nitroanilide degradation assay

To measure AaaA activity, a colourimetric assay using the molecule L-arginine-P-nitroanilide was utilised. When P-nitroanilide was released from L-arginine, a yellow colour was observed and the concentration of this quantified using an automated plate reader (Anthos LUCY).

Strains were assayed in minimal media P (MMP) prepared according to Haas, D *et al* (1997) containing Na_2HPO_4 10.4 mM, KH_2PO_4 4.8 mM, $MgSO_4$ 1.7 mM, $FeSO_4$ 6.6 µM (Sigma). L-arginine- P-nitroanilide was added at a final concentration of 0.5 mM.

Overnight cultures were added to fresh media at a 1:10 dilution and grown until a mid to late exponential growth phase was reached (0.5-0.8 $OD_{600\ nm}$ unit). The variability of CF isolate growth rate resulted in large differences in OD and therefore cultures were allowed to grow until the point where the slowest growing isolate reached an OD of at least 0.5. This occurred after 3-3.5 hrs of growth. The cells were then washed 2 times in MMP with centrifugation at 3707 Xg for 10 minutes (CF strains) or 5 minutes (PA01-N) to separate the pellet from supernatant. Following the final centrifugation, the supernatant was discarded and the pellet resuspended in 5 ml of MMP. The suspension was then adjusted by dilution in MMP to an optical density of 0.5. For each bacterial strain, 3 wells in a sterile clear bottomed 96 well plate (greiger bio1 F bottom) were prepared with 150 µl of the 1 mM working solution of arginine-p-nitroanilide and 150 µl of the $OD_{600\ nm}$ 0.5 bacterial suspensions. The degradation of arginine-p-nitroanilide was determined by 1h measurements of $OD_{405\ nm}$ for 24 h at 37°C in an automated plate reader (Anthos Lucy 1).

For assays involving the *E. coli* BL21 (DE3) pET21a overexpressing strains, the final resuspension of bacteria was adjusted to 0.25 $OD_{600\ nm}$ due to the high concentration of AaaA protein present in the cells.

Note that in assays where the growth differed substantially between strains (for example between CF isolates), once a strain reached exponential phase they were suspended in MMP and kept on the bench (room temperature). This proceeded until all strains reached exponential and the assay could be continued.

2.7.1 Inhibitor Assays

In the cell-free, protein L-arginine-P-nitroanilide assays, 150 µl of dialysed AaaAt was added to 150 µl 1 mM L-arginine-P-nitroanilide. Phenanthroline and EDTA were added at concentrations of 0.1 mM to 1 mM. This was achieved by preparing a 100 mM stock solution of inhibitor and adding 1 µl to 10 µl respectively to the normalised cultures.

In the whole cell assays, the inhibitor was added as in the cell-free assays described above.

2.7.2 Specialised conditions

Please see the Tecan section below for details of media adjustment. Both the growth media and MMP was adjusted unless otherwise stated.

2.8 Tecan assay to measure gene expression using the miniCTX-*lux* transcriptional reporter

Overnight cultures were washed 2 times in fresh media and resuspended in a volume equal to that of the original culture (10 ml unless stated otherwise). The cultures were normalised to an $OD_{600\ nm}$ of 0.1. A volume of 200 µl was added in triplicate to Greiner 96 well flat black microtitre plates. To prevent evaporation wells surrounding the samples were always inoculated with media. Cell density ($OD_{600\ nm}$) and bioluminescence were measured in an Infinite 200 (Tecan). Readings were taken every 30 minutes, during the course of the run a temperature of 37 ^{o}C was maintained and no shaking was included.

2.8.1 Specialised Media

When a change in media was used in order to observe the expression of *aaaA* in different conditions, 5 ml cultures were grown overnight in the media of choice, washed in the media of choice and resuspended in this media. Cultures were then normalised to $OD_{600\ nm}$ 0.1 as previously described.

2.8.1.1 Artificial sputum media (Palmer et al 2007)

The artificial sputum media used in this work follows the guidelines of Palmer and colleagues (2007). Here it is abbreviated ASM rather than SCFM. Components were sterilised by filtration and batches were kept no longer than 1 month at 4°C. Table 2.8.1 shows the composition of this media.

Order	Chemical	Amount	Of 100x stock
1	NaCl dH2O	3.03 g 640 ml	
2	NaH2PO4	10 ml	0.13 M
	NH4CI	10 ml	0.228 M
	KNO3	10 ml	0.0348 M
	K2SO4	10 ml	0.0271 M
	MOPS	10 ml	1 M
3	Amino acids	190 ml total	
	Aspartame		82.7 M
	Threonine		107.2 M
	Serine		144.6 M
	Glutamic Acid		154.9 M
	Proline		166 M
	Glycine		120.3 M
	Alanine		178 M
	Cysteine		16 M
	Valine		111.7 M
	Methionine		63.3 M
	Isoleucine		112.1 M
	Leucine		160.9 M
	Tyrosine		80.2 M
	Phenylalanine		53 M
	Ornithine-HCI		67.6 M
	Lysine		212.8 M
	Histidine		51.9 M
	Tryptophan		1.3 M
	Arginine		30.6 M
	Tryptophan		1.3 M
4	HCl	To pH 6.8	1 M
5	dH2O	To 950 ml	
6	CaCl2	10 ml	0.175 M
	MgCl2	10 ml	0.0606 M
	Glucose	10 ml	0.3 M
7	L-Lactic acid	10 ml	0.93 M
	Fe(111)504.7H20	10 ml	0.00036 M

Table 2.8.1: Composition of ASM used in this thesis based on the protocol by Palmer *et al* (2007).

2.8.1.2 Minimal media cocktail composition

The minimal media cocktail solution was based contains 8.33 mM of each amino acid noted in Table 2.8.2 in a total volume of 1 L. This resulted in a total amino acid content of 99.96 mM. For a 9.99 mM final concentration of amino acids this could be reduced to 0.833 mM. To facilitate longer storage (up to 3 months) of individual components, 7 separate solutions were made and sterilised by filtration. These were combined when required. The final solution was adjusted to

pH 7 and filter sterilised. Storage of the combined solution did not exceed 1 week at room temperature.

Solution	Component	Amount (g)	Volume made up to
I	Phenylalanine	1.38 g	100 ml dH_2O
II	Valine	0.98 g	100 ml dH_2O
	Alanine	0.74 g	
III	Threonine	0.99 g	100 ml dH_2O
	Serine	0.88 g	
IV	Aspartate	1.11 g	9.1 ml of 36%** HCl added to 80 ml dH_2O
V	Glutamic acid	1.26 g	Amino acids and NaOH
	Tyrosine	1.51 g	were dissolved in 80 ml of
	NaOH pellets	4 g	dH_2O, and the solution made up to 100 ml dH_2O.
VI	Isoleucine	1.09 g	100 ml dH_2O
	Leucine	1.09 g	
VII	Na_2HPO_4	1.47 g	400 ml dH_2O
	KH_2PO_4	0.65 g	
	$MgSO_4$	0.20 g	
	$C4H_4Na2O_4 \cdot 6H2O$	2.70 g	
	Cysteine	1.01 g	
	Methionine	1.24 g	
	$FeSO_4.7H_20$	0.0001 g	

Table 2.8.2: Minimal media cocktail composition.

2.8.2 Changes to assay to investigate CF specific conditions

2.8.2.1 Microaerobic conditions

Overnight cultures were grown in a microaerobic cabinet. They were then washed and normalised as usual with media acclimatised to the oxygen tension of the cabinet. The 96 well plate was set up inside the cabinet and sealed with a clear film (Thermo Fischer) which did not permit gas exchange. The experiment then proceeded as usual.

2.8.2.2 Nitrate comparison

To compare the expression and activity of AaaA when more nitrate was present, 10 mM (0.62 g/L KNO_3, 0.53 g/L NH_4Cl) and 100 mM (6.20 g/L KNO_3, 5.35 g/L NH_4Cl) of either KNO_3 or NH_4Cl was added to LB media. The two nitrate sources had a similar percentage of nitrogen per molecule (22.59% in KNO_3 and 26.19% NH_4Cl).

MMP was not adjusted in this experiment due to the potential influence of NH_4Cl on the pH which could have affected the protein activity.

2.8.2.3 NaCl comparison

Three representative NaCl conditions were chosen based on a study by Havasi *et al* (2008). The study compared growth of PAO1 in 0.9%, 2% and 7% NaCl

concentrations. Growth was impaired in the 7% condition but not the 2% or 0.9% categories where only the motility differed. To avoid adverse effects on growth but still identify any effects of NaCl on AaaA, the total concentration of NaCl was kept below 2%. Table 2.8.3 below shows the composition of each NaCl adjusted media solution.

LB	**Tryptone Yeast extract (g/L)**	**Added NaCl (g/L)**	**Final concentration of NaCl (g/L)**	**Final concentration of NaCl (mM)**
Low NaCl	10 5	0	0.055	0.9
Medium NaCl	10 5	10	10.055	172
High NaCl	10 5	17	17.055	291
MMP	**Na_2HPO_4 KH_2PO_4 $MgSO_4$ $FeSO_4$ (g/L)**	**Added NaCl (g/L)**	**Final concentration of NaCl (g/ L)**	**Final concentration of NaCl (mM)**
Low NaCl	1.47 0.648 0.2 0.001	0.055	0.055	0.9
Medium NaCl	1.47 0.648 0.2 0.001	10	10.055	172
High NaCl	1.47 0.648 0.2 0.001	17	17.055	291

Table 2.8.3: NaCl concentrations used in the NaCl comparison experiment.

2.8.2.4 pH comparison

The media was buffered with sodium phosphate to represent pH 5.8, pH 6.2, pH 6.8 and pH 7.2. Different ratios of NaH_2PO_4 and Na_2HPO_4 were combined to a final concentration of 0.1 M and autoclaved. These are shown in Table 2.8.4. From this, 100 ml was combined with 900 ml of media for a final buffer concentration of 0.01M.

For the activity assay, both the growth medium and MMP were adjusted for pH. As MMP is already buffered by Na_2HPO_4 and KH_2PO_4, these were replaced with the NaH_2PO_4:Na_2HPO_4 solution as is detailed above.

x ml 0.2 M Na_2HPO_4	x ml 0.2 M NaH_2PO_4	pH 25 °C
4.0	46.0	5.8
9.25	40.75	6.2
24.5	25.5	6.8
36.0	14.0	7.2

Table 2.8.4: Ratio of Na_2HPO_4 and NaH_2PO_4 for a 0.1 M 100 ml stock solution at different pHs.

2.9 Phenotypic Assays

2.9.1 Motility

Please see Table 2.9.1 for media composition of plates. Plates were prepared by adding 10 ml of a filtered D-glucose 20% w/v stock solution to 400 ml media following autoclaving (final concentration 0.5%). The media was then poured into plates (25 ml per plate) and dried for 30 mins to set. Following this, the plates were dried in a ventilated cabinet for 45 mins.

Immediately following completion of plate drying, 3 µl of overnight culture (18 hours) was either dropped onto the surface of the plate (swarming) or inoculated at a depth half-way between the surface and bottom of the plate (swimming) in the centre of each plate. In the case of twitching, a sterile tooth pick was used to pick a colony off a plate and then stabbed to the bottom of the plate 10 times. Each sample was done in triplicate.

The plates were incubated at 37 ^{o}C for 16 hours in the case of swimming and swarming and 22 hours for twitching. Racks were used to avoid the plates touching each other. For twitching assays, the plates were placed in a humidified chamber consisting of a base of damp paper towel, separated from the sample plates by a barrier of empty plates and with a surrounding plastic bag, sealed with tape. The plates were photographed immediately after this incubation period with the exception of the twitching plates which were dried first at 50°C. The agar from the twitching plates was removed and the base of the plate stained with 1% crystal violet to facilitate visualisation of the halo.

	Media for motility composition			
	Agar type	*Grams per litre*	*Media type*	*Grams per litre*
Swimming	Bacto Agar	5	Nutrient Broth No.2	8
Swarming	Agar Technical	3	Nutrient Broth No.2	25
			Yeast extract	5
Twitching	Agar Technical	10	Yeast Extract	5
			Tryptone	10
			NaCl	10

Table 2.9.1: Media for motility assays.

2.9.2 Pyocyanin

The method used was based on that described by Essar *et al* (1990). Overnight cultures were normalised to an $OD_{600\ nm}$ of 1.0. This was then added to LB broth at a 1:100 concentration so that the total volume was 20 ml. To allow sufficient aeration, 200 ml flasks were used. These were incubated at 37 ^{o}C with shaking at 200 rpm, for 18 hours. Following this, 4.5 ml of chloroform was added to each 7.5 ml of filter sterilized culture. The samples were vortexed for 10 seconds and then centrifuged for 10 mins at 9.390 xg (Sigma 3K36) 4°C. The bottom, blue, chloroform layer was transferred to another tube and mixed with 1.5 ml of 0.2 M HCl. This solution was vortexed for 10 seconds and then centrifuged for 2 mins at 9.390 xg (Sigma 3K36) 4°C. The resulting HCl containing, pink top layer was drawn off by pipette and the absorbance measured at a wavelength of 520 nm in a spectrometer (Thermo scientific). Samples were done in triplicate.

To calculate the pyocyanin concentration (µg/ml), the absorbance value was multiplied by 17.072 and then further multiplied by 1.5 to account for loss of volume.

2.9.3 Elastase

A method similar to the one described by Naughton and Sanger (1961) was used to determine elastase activity. Overnight cultures were grown in LB media at 37°C 200 rpm for 18 hours. The cultures were normalised OD_{600} 1.0 and 0.1 ml combined with 10 ml of fresh LB in 100 ml conical flasks. A media only control

was included. The cultures were grown for a further 16 hours using the same conditions previously described. Following this the cultures were spun at 9.390 xg (Sigma 3K36) and the supernatants filtered with a 0.22 µM filter. Five hundred microliters of supernatant was combined with 500 µl 20 mg/ ml elastin-Congo red (ECR) solution (Table 2.9.2) in Eppendorf tubes. Regular vortexing of the Congo-red ECR solution was required to discourage sedimentation of the elastin-Congo red. The tubes were incubated for 4 hours at 37°C, 200 rpm. They were then centrifuged at 16060 xg (Biofuge Pico Heraeus) for 3 min. From each tube 800 µl of supernatant was transferred to a cuvette and absorbance read at 495 nm using the spectrometer (Thermo Scientific) which was normalised by the media only control as a blank.

Elastin-Congo red (ECR) solution		
Component	*Amount*	*Final pH*
Tris	2.42 g	7.5
$CaCl_2$	38.94 mg	
dH_2O	Up to 200 ml	

Table 2.9.2: Elastin-Congo red solution preparation.

2.10 Biofilm

2.10.1 Microscopy

Strains were transformed with *pBK-MiniTn7(Gm)-GFP* and helper plasmid *pUX-BF13(Amp)* plasmids (kindly donated by Dr Diana Palenzuela) to allow them to be visualised under the microscope. The plasmid DNA was extracted and transformed as has been previously described. Where tagged strains were not used, Syto9 (Thermo Fischer) was added to a final concentration of 1 µg/ml and Propidium iodide (PI) at a final concentration of 4 µg/ml.

A Ziess LSM 700 Zen microscope (Carl Zeiss, Ltd, Welwyn, UK) was used for all confocal analysis. The gain was adjusted between experiments to allow for inter-experiment fluorescence variation and use of different dyes or tags, but the same gain maintained within the same imaging session. A typical gain ranged from 400-700. The pinhole was set at 1.0 AU and laser intensity was 15 %. An averaging of 4 was selected. The required wavelength was selected using the drop down list provided by the software. The selections were eGFP for GFP tagged cells, PI for PI stained samples and Syto11 for Syto9 stained samples. Objectives 5-40x were used and quoted where used.

2.10.2 8-well chamber slide assay (microchambers)

Overnight cultures were washed twice in fresh media and normalised to an $OD_{600\ nm}$ of 0.05. Of this normalised culture 500 µl was added to an 8 well chamber slide (Lab-Tek^{R}II chamber slide^{TM}). The slide was incubated at 37 ^{o}C statically. Unless otherwise indicated, the slides were incubated for 48 hours. Following incubation, the supernatant was drawn off with a pipette and the biofilms were viewed using the confocal microscope (Zeiss) at 5x or 10x magnification. Where washing was used, 200 µl of media was added to the wells and placed on a rotary shaker for 5 minutes at room temperature and then removed.

2.10.3 Bioflux

Overnight cultures were washed twice and resuspended in ASM (or alternative media where specified) and normalised to an OD_{600} of 0.05. Where appropriate this ASM contained one or more dyes at the concentrations mentioned previously. To a 48 well Bioflux plate covered by the clear film supplied by the manufacturer, a section of the film was removed to allow entry to the wells to be used in the particular experiment. To the inlet well 100 µl of media was added taking care not to introduce air bubbles to the system. The plate lid (sterilised by swabbing with ethanol) was then screwed on using the provided screwdriver. The plate was attached to the Bioflux pump system by the capillaries for priming. The software Fluxion was used to program the Bioflux and the shear was set to 5 dyn for 5 minutes or until the inner circle in the outlet was filled with media. The associated temperature control platform was set at 37°C and remained at this temperature for the duration of the experiment. The plate was then disconnected from the capillaries, the lid removed and 70 µl of normalised culture added to the outlet well. Media was added to a total of 1200 µl to the inlet well and the resterilised plate lid replaced. The plate was connected to the Bioflux system and the following sequence followed: 2 seconds at a shear of 2 dyn, 30 minutes no flow, 14 hours at a shear of 0.5 dyn and 1 hour at a shear of 0. 25 dyn. Following the completion of the Bioflux run, the plate was disconnected, the lid removed and imaging proceed with using the confocal microscope (Zeiss).

2.10.4 Congo red colony biofilm assay

The method used was based on the described protocol in Dietrich *et al* (2013). The plates were made by dissolving 1% agar and 1% tryptone in dH_20 and autoclaving. The media was cooled to 55°C before the addition of 20 µg/ml Coomassie brilliant blue and 40 µg/ml Congo red. The plates were poured by

adding 60 ml of media to each 10 cm square petri dish. These were allowed to dry at room temperature for 24 hours with closed lids.

A single colony for each strain and replicate was taken from an LB plate and grown in LB media for 12 hours (aerobic) or 36 hours (microaerobic) at 37°C 200 rpm. If microaerobic, these were placed in a sealed jar with a microaerobic sachet (CampyGen, Thermo Scientific). Ten microliters of these cultures was spotted onto the dried Congo red plates. The plates were then incubated at room temperature (23-25°C) for the desired number of days. Photographs were taken with a digital camera (Nikon).

2.10.5 Floating biofilm assay in ASM

Falcon tubes containing 5 ml of ASM (Palmer *et al* 2007) were inoculated with a colony picked from an LB agar plate or a 1 µl loop of frozen glycerol stock where specified. The tubes were incubated for 18 hours at 37°C with shaking at 200 rpm. Photographs were taken with a digital camera (Nikon).

2.10.6 *ex vivo* pig lung model

Harrison and Diggle (2016) describe the protocol used here for bacterial growth on *ex vivo* pig lung (EVPL) bronchiole tissue sections. A local butcher (JT Beedham & Sons) supplied lungs from a specific pig herd. These were collected on the day of delivery from the abattoir, kept cool during transportation and directly dissected upon arrival to the laboratory. The laboratory used for dissection purposes was not used for microbial work and a sterile technique was followed to minimise introduction of environmental bacteria to the tissue. The desired sections of lung were seared with a hot, ethanol sterilised pallet knife to sterilise the surface and a razor blade used to carefully expose the bronchioles. Sections of 1-5 cm were gently liberated from the surrounding tissue using a razor blade and forceps and placed into a petri dish. A 1:1 solution of RPMI and Dulbecco's modified Eagle medium (DMEM) supplemented with 50 µg/ ml ampicillin was used to wash the bronchioles. During this process remaining alveolar tissue was removed using a razor blade, scissors and forceps. Sections of bronchiole were then cut across the lumen into 0.5 cm pieces using scissors and forceps. The diameter of bronchiole used here was between 0.5 cm and 1 cm if the entire circumference of the bronchiole was used (preferred). Bronchioles which exceeded this diameter (1.5-5 cm) were cut across the diameter to equal a size similar to the 0.5-1 cm sections. A further wash with the RPMI-DMEM media was followed by a wash with ASM media (Palmer *et al* 2007) made as previously described with the exclusion of glucose and addition of 50 µg/ ml ampicillin.

The sections of bronchiole were placed in the wells of a 24 well plate filled with a 400 µl 0.8% w/v agarose-ASM (no glucose, 50 µg /ml ampicillin) gel and transported to the microbiology laboratory. Five hundred microliters of the ASM was added to each well. A 30G hypodermic needle was used to pierce the tissue with a colony (or without a colony in the mock infected control). The plates were placed into a humidified 37°C incubator and left for either 24 hours (CFU count) or 24-72 hours (histology analysis) with a rotation of 60 rpm.

To perform the CFU count the bronchioles were washed in PBS and then added to a tube of 500 µl PBS with 18 2.38 mm metal beads (Mo Bio) which were sterilised by autoclaving. A Precellys 24 homogenizer was used to bead-beat the tissue sections. The bronchioles did not completely disintegrate but the disruption dislodged the bacteria into the surrounding liquid. A serial dilution was performed and 10 µl aliquots (dropping method) were plated on LB agar in triplicate to obtain single colonies. To generate the histology images, the bronchioles were washed in PBS and placed in formalin before transportation to the histology department in the QMC for sectioning and staining with Gram or haematoxylin and eosin (H&E) stain. The sections were imaged using the Nikon Eclipse 50i Microscope.

2.10.7 Murine *P. aeruginosa* respiratory infection model (Liverpool University)

For the murine respiratory infection model, a method developed in Liverpool using a natural respiratory inhalation route of infection was followed. This method involved infecting the murine host (Balb/c) intranasally with a dose of *P. aeruginosa* grown to mid-log phase and suspended in 50 µl PBS. Intranasal infection has been shown to be an effective strategy for increased time periods of lung colonisation (Fothergill *et al* 2014; Waters *et al* 2017).

Optimisation of bacterial growth, number of doses, starting quantity of bacteria per dose, and mouse strain type, was conducted with PAO1 and PAO1 *ΔaaaA*. From this, the efficiency of colonisation and accuracy of CFU count was observed to be best when the inoculum was prepared directly from an agar plate.

Using a dose of 8x10^{6}, Balb/c mice were infected with the PAO1 WT and *ΔaaaA* mutant. Colony forming units (CFUs) were recovered from the homogenised lungs and nasopharynx following infection with PAO1 WT or PAO1 *ΔaaaA* over 5 days. Ten mice were used per time point (5 mice for time zero) to ensure statistically significant differences could be detected.

2.11 Statistical analysis

Statistical analyses were performed using the GraphPad Prism 6 Software. At least 3 independent biological replicates were included for each experiment (unless indicated) and the standard deviation from the mean calculated. The standard deviation has been presented graphically as error bars. To assess the significance of differences between samples or experimental conditions, the data was loaded into GraphPad and a test selected according to the number of categories and normality of the data. In the majority of cases a Students t-test or analysis of variance (ANOVA) was performed, while their non-parametric alternatives Mann-Whitney U and Kruskal-Wallis were selected when the program detected that the data was not normally distributed. A non-significant result is indicated by 'ns', a P value of <0.05 by 1 asterisk, <0.01 by 2 asterisks, <0.001 by 3 asterisks and <0.0001 by 4 asterisks.

2.12 Strain and Plasmid Tables

Strain name	**Strain description**	**Antibiotic resistance**	**Source**
Section 1: PAO1 and derivatives			
Wild-type PAO1 Nottingham		None	ATCC15692
PAO1 Nottingham *ΔaaaA*	Deletion mutant of *aaaA*	None	Luckett *et al* 2012
PAO1 T7:gfp	PAO1 tagged with a chromosomally integrated green fluorescent protein	Gentamycin	This study
PAO1 *ΔaaaA* T7:gfp	PAO1 *ΔaaaA* tagged with a chromosomally integrated green fluorescent protein	Gentamycin	This study
PAO1 *ΔaaaA pME6032:aaaA*	*pME6032* with full length aaaA ORF under Ptac control	Tetracycline	Luckett *et al* 2012
PAO1 *ΔaaaA pME6032*	*pME6032* with no insert	Tetracycline	Luckett *et al* 2012
PAO1 *ΔaaaA* miniCTX*::aaaA*	miniCTX with full length *aaaA* insert (promoter and ORF)	Tetracycline	Paredes 2014
PAO1 *ΔaaaA* miniCTX*::aaaA T7:gfp*	PAO1 *ΔaaaA* miniCTX*::aaaA* tagged with a chromosomally integrated green fluorescent protein	Gentamycin	This study
PAO1 *ΔaaaA* miniCTX	miniCTX with no insert	Tetracycline	Paredes 2014
PAO1 miniCTX*::araC::aaaA*	miniCTX with full length *aaaA* ORF under *araBAD* control	Tetracycline	This study
PAO1 *ΔaaaA* miniCTX*::araC::aaaA*	miniCTX with full length *aaaA* ORF under *araBAD* control		
PAO1-N pMini-CTX-*lux*:P*aaaA*	PA01 Nottingham with miniCTX-*lux aaaA* promoter fusion	Tetracycline	Paredes 2014

PAO1-N *ΔaaaA* MiniCTX-*lux*:P*aaaA*	PA01 Nottingham Δ*aaaA* with miniCTX-*lux aaaA* promoter fusion	Tetracycline	Paredes 2014
PAO1			Bleves from: Heurlier *et al* (2003)
PAO1 *ΔrpoN* (PA06358)	Deletion mutant of *rpoN*		Bleves from: Heurlier *et al* (2003)
PAO1 *ΔrpoN att Tn7:rpoN*$^{+}$	Complemented *ΔrpoN*	Gentamycin	Bleves from: Heurlier *et al* (2003)
PAO1 miniCTX-*lux*::P*aaaA*	PAO1 with miniCTX-*lux aaaA* promoter fusion	Tetracycline	This study
PAO1 *ΔrpoN* miniCTX-*lux*::P*aaaA*	PAO1 *ΔrpoN* with miniCTX-*lux aaaA* promoter fusion	Tetracycline	This study
PAO1 *ΔrpoN att Tn7:rpoN*$^{+}$miniCTX-*lux*::P*aaaA*	Complemented *ΔrpoN* with miniCTX-*lux aaaA* promoter fusion	Tetracycline, Gentamycin	This study
PAO1 miniCTX-*lux*::P*kan*	PAO1 with miniCTX-*lux kan* promoter fusion	Tetracycline	This study
PAO1 *ΔrpoN* miniCTX-*lux*::P*kan*	PAO1 *ΔrpoN* with miniCTX-*lux kan* promoter fusion	Tetracycline	This study
PAO1 ΔrpoN *ΔrpoN att Tn7:rpoN*$^{+}$ miniCTX-*lux*::P*kan*	Complemented *ΔrpoN* with miniCTX-*lux kan* promoter fusion	Tetracycline, Gentamycin	This study
	PA14 and derivatives		
PA14		None	Dietrich *et al* (2013)
PA14 *ΔaaaA*	Deletion mutant of *aaaA*	None	Dietrich *et al* (2013)
PA14 *Δphz*	Deletion mutant of *phz*	None	Dietrich *et al* (2013)
PA14 *Δphz ΔaaaA*	Deletion mutant of *phz* and *aaaA*	None	Dietrich *et al* (2013)
	LES and derivatives		
LESB65	Liverpool epidemic strain subtype 65		Waters (unpublished)
LESB65 *ΔaaaA*	Deletion mutant of *aaaA* in LESB65		Waters (unpublished)
	E. coli strains		
E. coli DH5α	Cloning strain		Darch 2013
E. coli BL21 (DE3) *pET21a (+)*	*pET21a* with no insert	Ampicillin	Paredes 2014
E. coli BL21 (DE3) *pET21a:aaaAt*	*pET21a* with truncated *aaaA* insert	Ampicillin	Paredes 2014
E. coli BL21 (DE3) *pET21:aaaA*	*pET21a* with full length *aaaA* insert	Ampicillin	Paredes 2014
E. coli BL21 (DE3) pET21a:aaaAt2	*pET21a* with truncated *aaaA* insert	Ampicillin	This study
E. coli BL21 (DE3) *pET21a:aaaAt3*	*pET21a* with truncated *aaaA* insert	Ampicillin	This study

E. coli S17-1 λpir	*E. coli* strain capable of conjugation *into P. aeruginosa*	None	Paredes 2014
E. coli S17-1 λpir miniCTX-*lux*:*PaaaA*	*S17* with miniCTX-*lux* plus *aaaA* promoter. Used for conjugation purposes.	Tetracycline	Paredes 2014
E. coli S17-1 λpir miniCTX-*lux*:*Pkan*	*S17-1 λpir* with miniCTX-*lux* plus a kanamycin promoter. Used for conjugation purposes.	Tetracycline	Paredes 2014
	Cystic Fibrosis clinical isolates		
13w406983	CF clinical isolate	Untested	Holden, Microbiology
13w409030	CF clinical isolate	Untested	Holden, Microbiology
13w402129	CF clinical isolate	Untested	Holden, Microbiology
13w408484	CF clinical isolate	Untested	Holden, Microbiology
13w405098	CF clinical isolate	Untested	Holden, Microbiology
13w413326	CF clinical isolate	Untested	Holden, Microbiology
13w412971	CF clinical isolate	Untested	Holden, Microbiology
13w409892	CF clinical isolate	Untested	Holden, Microbiology
13w607570	CF clinical isolate	Untested	Holden, Microbiology
13w402393	CF clinical isolate	Untested	Holden, Microbiology
SED 1	CF clinical isolate from single patient	Untested	Darch *et al* 2014
SED 2	CF clinical isolate from single patient	Untested	Darch *et al* 2014
SED 3	CF clinical isolate from single patient	Untested	Darch *et al* 2014
SED 4	CF clinical isolate from single patient	Untested	Darch *et al* 2014
SED 5	CF clinical isolate from single patient	Untested	Darch *et al* 2014
SED 6	CF clinical isolate from single patient	Untested	Darch *et al* 2014
SED 7	CF clinical isolate from single patient	Untested	Darch *et al* 2014
SED 8	CF clinical isolate from single patient	Untested	Darch *et al* 2014
13w607570 miniCTX-*lux*:: P*aaaA*	CF570 conjugated with miniCTX-l*ux*:: P*aaaA*	Tetracycline	This project

13w409030 miniCTX-*lux*:: P*aaaA*	CF030 conjugated with miniCTX-*lux*:: P*aaaA*	Tetracycline	This project
13w402129 miniCTX-*lux*:: P*aaaA*	CF129 conjugated with miniCTX-*lux*:: P*aaaA*	Tetracycline	This project
13w408484 miniCTX-*lux*:: P*aaaA*	CF484 conjugated with miniCTX-*lux*:: P*aaaA*	Tetracycline	This project
13w405098 miniCTX-*lux*:: P*aaaA*	CF098 conjugated with miniCTX-*lux*:: P*aaaA*	Tetracycline	This project
13w413326 miniCTX-*lux*:: P*aaaA*	CF326 conjugated with miniCTX-*lux*:: P*aaaA*	Tetracycline	This project
13w412971 miniCTX-*lux*:: P*aaaA*	CF971 conjugated with miniCTX-*lux*:: P*aaaA*	Tetracycline	This project
13w409892 miniCTX-*lux*:: P*aaaA*	CF892 conjugated with miniCTX-*lux*:: P*aaaA*	Tetracycline	This project
13w406983 miniCTX-*lux*:: P*aaaA*	CF983 conjugated with miniCTX-*lux*:: P*aaaA*	Tetracycline	This project
13w402393 miniCTX-*lux*:: P*aaaA*	CF393 conjugated with miniCTX-*lux*:: P*aaaA*	Tetracycline	This project
13w408484 miniCTX-*lux*:: P*kan*	CF484 conjugated with miniCTX-*lux*:: P*kan*	Tetracycline	This project
13w409892 miniCTX-*lux*:: P*kan*	CF892 conjugated with miniCTX-*lux*:: P*kan*	Tetracycline	This project
13w607570 miniCTX-*lux*:: P*kan*	CF570 conjugated with miniCTX-l*ux*:: P*kan*	Tetracycline	This project
13w402393 miniCTX-*lux*:: P*kan*	CF393 conjugated with miniCTX-*lux*:: P*kan*	Tetracycline	This project

Table 2.12.1: Bacterial strains used in this study.

Plasmid backbone	Plasmid name	Description	Antibiotic R'	Reference
pME6032	*pME6032:aaaA*	Shuttle vector with an IPTG inducible Ptac promoter. Fused with the *aaaA* ORF	Tetracycline	Luckett *et al* 2012.
miniCTX-1	miniCTX::*aaaA*	Integrating vector which recombines at the attB site in the *P. aeruginosa* chromosome. Containing the *aaaA* ORF under control of its own promoter.	Tetracycline	Luckett *et al* 2012.
	miniCTX::araC::*aaaA*	miniCTX containing an arabinose inducible promoter system and *aaaA* ORF.	Tetracycline	This study
miniCTX-*lux*	miniCTX-*lux*::*PaaaA*	miniCTX with *luxCDABE* genes creating luminescence when promoter is activated. With *aaaA* promoter fusion.	Tetracycline	Paredes (thesis, 2014)
	miniCTX-*lux*::*Pkan*	As previous but with *kan* promoter fusion.	Tetracycline	Paredes (thesis, 2014)
pET21a (+)	*pET21a::aaaAFL*	Protein expression vector with a T7 promoter (IPTG inducible). Containing full length *aaaA* ORF.	Ampicillin	
	pET21a::aaaAt1	First truncated version of *aaaA* lacking a beta-barrel. Previously called *pET21a::aaaA-SV* but is renamed here for clarity.	Ampicillin	Paredes (thesis, 2014)
	pET21a::aaaAt2	Second truncated version of *aaaA* lacking a beta-barrel but slight extension of c-terminus and no signal peptide.	Ampicillin	This study
	pET21a::aaaAt3	Third truncated version of *aaaA* lacking a beta-barrel but slight extension of c-terminus.	Ampicillin	This study
pGemT-easy		T-tailed vector for subcloning purposes	Ampicillin	Promega
pbluescriptKS		Suicide vector for subcloning purposes.	Ampicillin	Palenzuela (thesis, 2016)
pla33	*pla33::araC::aaaA*	Plasmid used to image *aaaA* in *E. coli* cells. Used here to transfer *araC::aaaA* to miniCTX-1.	Chloramphenicol	Ashawesh(thesis 2016).

Table 2.12.2 plasmids used in this study.

3 Chapter 3: Regulation of AaaA and development of a qRT-PCR assay for the improved investigation of gene expression in response to internal regulators and extracellular factors

3.1 Introduction

To fully understand the relationship between AaaA and the environment surrounding *P. aeruginosa*, the regulatory network surrounding AaaA must be considered. Extensive investigation of this network was initiated by Dr Esteban Paredes Osses. This chapter aims to move further with the investigation, evaluate which forces are likely to have the largest impact on AaaA by forming new models, and develop a tool which will facilitate future work in this area.

3.1.1 Background

3.1.1.1 Overview of key regulatory elements in P. aeruginosa

A model of the *P. aeruginosa* regulatory network was developed by Galán-Vásquez and colleagues (2011) using pooled RT-PCR, gel-shift assays, and DNA-foot printing data from the literature. To give an indication of the size of this network, there were 1020 interactions from 690 genes (only 12% of the total *Pseudomonas* genome). This 12% of genes included 54% of the currently identified sigma factors and 16% of the known transcription factors (TFs). The analysis placed the regulatory network of *P. aeruginosa* as the third most complex system to be reported in bacteria.

From the vast web of regulatory elements, a few systems are predicted to interact with *aaaA*. The global regulatory systems of c-di-GMP (biofilm co-ordination) Ret/Gac/Rsm (acute/chronic switch) and QS (cell density) could regulate *aaaA* indirectly through their relationship with biofilm and virulence, and are considered in this chapter (Hengge 2009; Romling *et al* 2005; Jimenez 2012; Rasamiravaka *et al* 2015; Nealson and Hastings 1979; Pearson *et al* 2000; Davies *et al* 1998). Additionally, regulators of metabolic pathways associated with AaaA were found to affect *aaaA* promoter (*PaaaA*) activation in a study by Dr Esteban Paredes Osses (thesis, 2014) using a miniCTX-*lux* based transcriptional reporter.

How *aaaA* could fit within these regulatory systems is discussed in more detail in the following sections.

3.1.1.2 How the metabolic requirements of P. aeruginosa influence aaaA expression

There are 4 L-arginine catalytic pathways, 3 of these operating in oxygenated conditions. The arginine succinyltransferase (AST) pathway, the arginine dehydrogenase pathway/ arginine transaminase ADH (or ATA) pathway and arginine carboxylase (ADC) pathway function in aerobic conditions. When oxygen is no longer abundant, the arginine deiminase (ADI) pathway can be used to produce ATP though the catalysis of arginine. (Yang and Lu 2007; Li and Lu 2009; Itoh 1997; Vander Wauven *et al* 1984). Figure 3.1.1 shows these pathways.

The main route of activation for these pathways is through the arginine availability. In aerobic conditions, the arginine sensing regulator ArgR, encoded on the *aotJQMOP-argR* operon, responds to the presence of arginine by binding to recognised motifs, controlling gene expression in a negative or positive manner (Nishijyo *et al* 1998; Lu *et al* 2004; Park *et al* 1997). ArgR stimulates expression of the AST pathway genes encoded on the *aruCFGDBE* operon, which simultaneously inhibits the ADH pathway (Lu *et al* 2004; Li and Lu 2009; Itoh 1997). While the ADH pathway is not activated by ArgR, it responds to the presence of arginine through the two-component system (TCS), AruRS, which upregulates *aruH* (Lu *et al* 2004; Li and Lu 2009; Itoh 1997). The ADC pathway is not responsive to ArgR, but is stimulated by arginine, agmatine and N-carbamoylputrescine. When oxygen is no longer abundant, ArgR upregulates the ADI pathway operon, *arcDABC* (Maghnouj *et al* 1998) and arginine-ornithine transportation operon, *aotJQMOP-argR,* which also transcribes more ArgR (Nishijyo *et al* 1998; Lu *et al* 2004).

In addition to arginine obtainability, *P. aeruginosa* selects which metabolic pathways are required by the availability of oxygen. The oxygen sensor ANR activates *arcDABC* (ADI pathway) when oxygen is limited (Maghnouj *et al* 1998). This occurs in the absence of a nitrate source; the TCS NarXL has been found to repress *arcDABC* when a source of nitrate or nitrite is available (Hasegawa *et al* 1998; Eschbach *et al* 2004; Mercenier *et al* 1980).

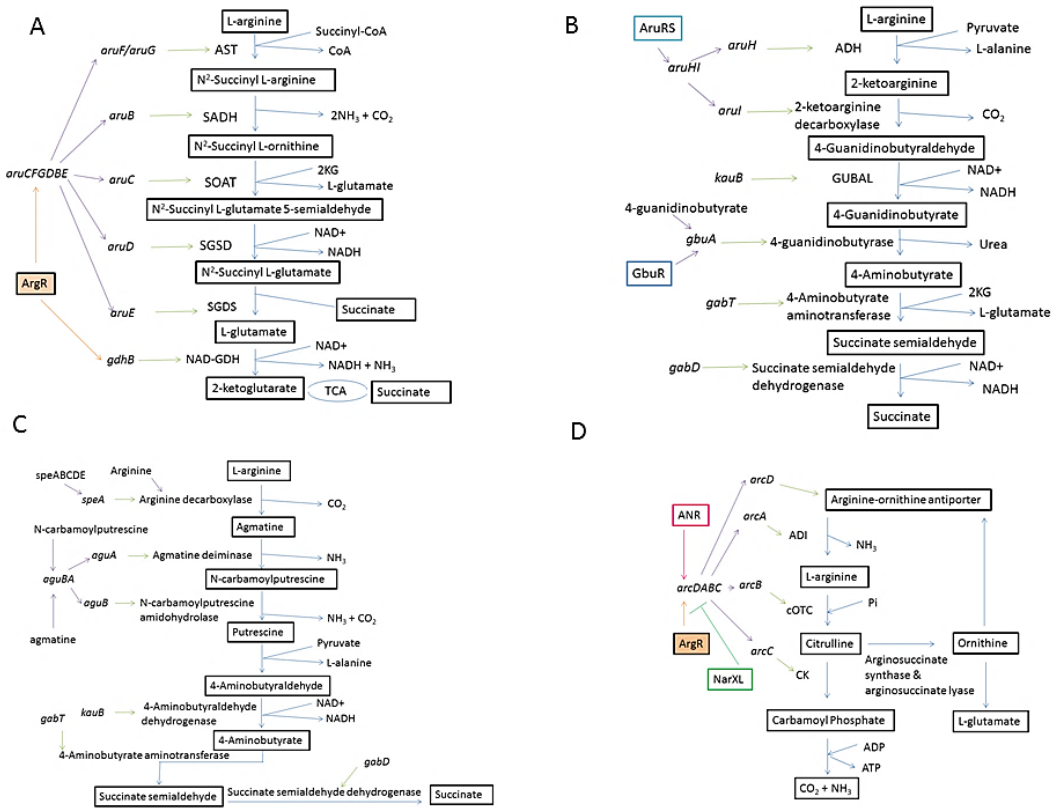


Figure 3.1.1: Summary of the 4 L-arginine catabolic pathways in *P. aeruginosa* and their regulatory influences. A) = arginine succinyltransferase pathway (AST), B) the arginine dehydrogenase pathway/ arginine transaminase pathway ADH (or ATA), C) the arginine carboxylase pathway (ADC), and D) arginine deiminase pathway (ADI). ArgR =arginine sensing regulator which upregulates AST and ADI pathway genes. AruRS =arginine sensing two-component system which upregulates the ADH pathway genes. ANR = anaerobic sensor which upregulates the ADI pathway genes. NarXL= two component sensing regulator which inhibits the ADI pathway genes when nitrate is available. GbuR = upregulates the enzyme 4-guanidinobutyrase of the ADH pathway. For a more detailed view and individual references please see the original figures in the main introduction.

Investigations by Paredes (thesis, 2014), Luckett *et al* (2012), and Lu *et al* (2004), linked AaaA with regulators of the catabolic arginine pathways mentioned above. As an arginine-releasing enzyme, it would be intuitive for AaaA to be required by *P. aeruginosa* when there was a deficit of arginine. It was thought that ArgR would repress *aaaA* expression in a similar way to the repression of the arginine synthesis pathways (Park *et al* 1997). However, the data from Paredes (thesis, 2014), and Lu *et al* (2004), show that ArgR activation stimulates *aaaA* expression (Paredes Osses 2014, Lu *et al* 2004). Results show that *aaaA* expression does not respond to an arginine deficit *per se* and rather is repressed when arginine is processed through the pathways operational in aerobic conditions (Paredes Osses thesis 2014). This is depicted in Figure 3.1.2. This could insure that the action of AaaA is limited through negative feedback in aerobic conditions, while presence of arginine in anaerobic conditions would affect AaaA differently. Through what mechanism this could occur is still unknown.

In support of the model in Figure 3.1.2, Paredes (2014) showed that components of the ADI pathway activated *PaaaA*. Additionally, ANR was found to have a positive regulatory effect on *aaaA* expression (Paredes 2014). This upregulation could be occurring indirectly through the ADI pathway, through direct binding to P*aaaA,* or through an unknown mechanism. This is investigated later in the chapter.

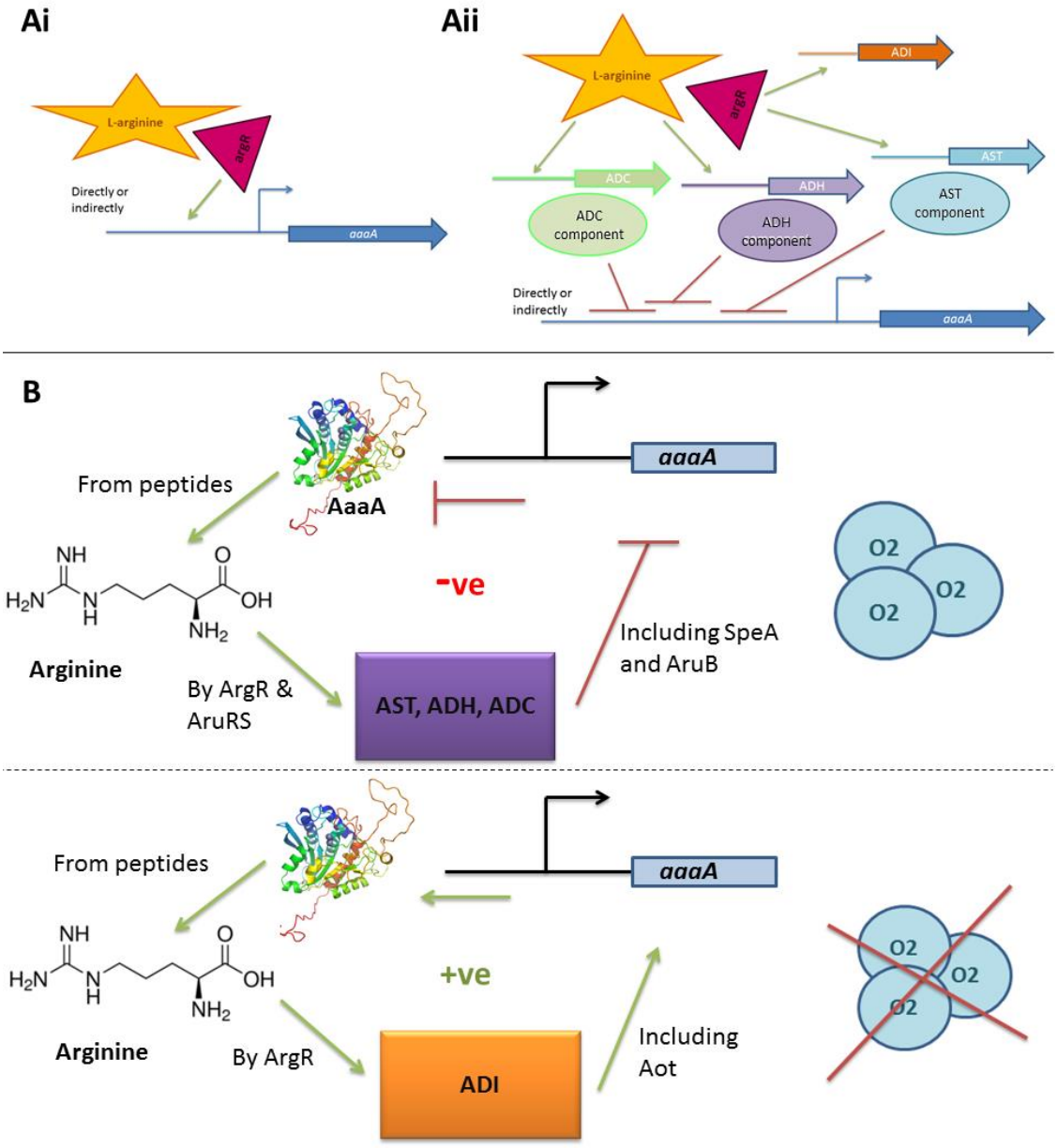


Figure 3.1.2: Model of relationship between arginine, arginine catabolic pathways, and AaaA. Panel A: How AaaA could respond to arginine through the global arginine sensor ArgR. Ai) although counter-intuitive, argR stimulates rather than inhibits *aaaA* expression. Aii) Arginine stimulates operation of the arginine catalytic pathways in either an argR dependent (ADI, AST) or independent manner (ADH, ADC). Components of the AST, ADH and ADC pathway inhibit *aaaA* expression. Green arrows represent a positive influence on expression and red arrows an inhibitory effect. ADI=arginine deiminase pathway, ADC=arginine decarboxylase pathway, ADH (ATA))=arginine dehydrogenase/transaminase pathway, AST=arginine succinyltransferase pathway. Based on data by: Paredes Osses (2014) and Lu *et al* (2004). Panel B: Hypothesis of how the metabolic feedback loops differ in different oxygen tensions. Data from Paredes Osses (2014) suggests that *aaaA* expression is under a negative feedback loop in aerobic conditions and under a positive feedback loop in anaerobic conditions. ADI=arginine deiminase pathway, ADC=arginine decarboxylase pathway, ADH (ATA))=arginine dehydrogenase/transaminase pathway, AST=arginine succinyltransferase pathway.

In addition to the ADI pathway, the activation of ANR stimulates the expression of denitrification pathway enzymes encoded on *narK1K2GHJI* and *nirSMCFDLGHJEN* operons. Together with ANR, NarXL activates the denitrification pathway in

response to exogenous nitrate (Nadine *et al* 1999; Haas *et al* 1995; Arai *et al* 1991; 1994; 1995; 1998; Jungst and Zumft 1992). The response regulator, NarL, simultaneously represses *arcDABC* (Mercenier *et al* 1980). This ensures that when nitrate is available in oxygen limited conditions, the preferred pathway for energy generation is denitrification. Thus, when nitrate is available, *aaaA* transcription would not be stimulated by the ADI pathway. Nitrate may also inhibit the *aaaA* promoter directly which will be explored in this chapter. Figure 3.1.3 illustrates this.

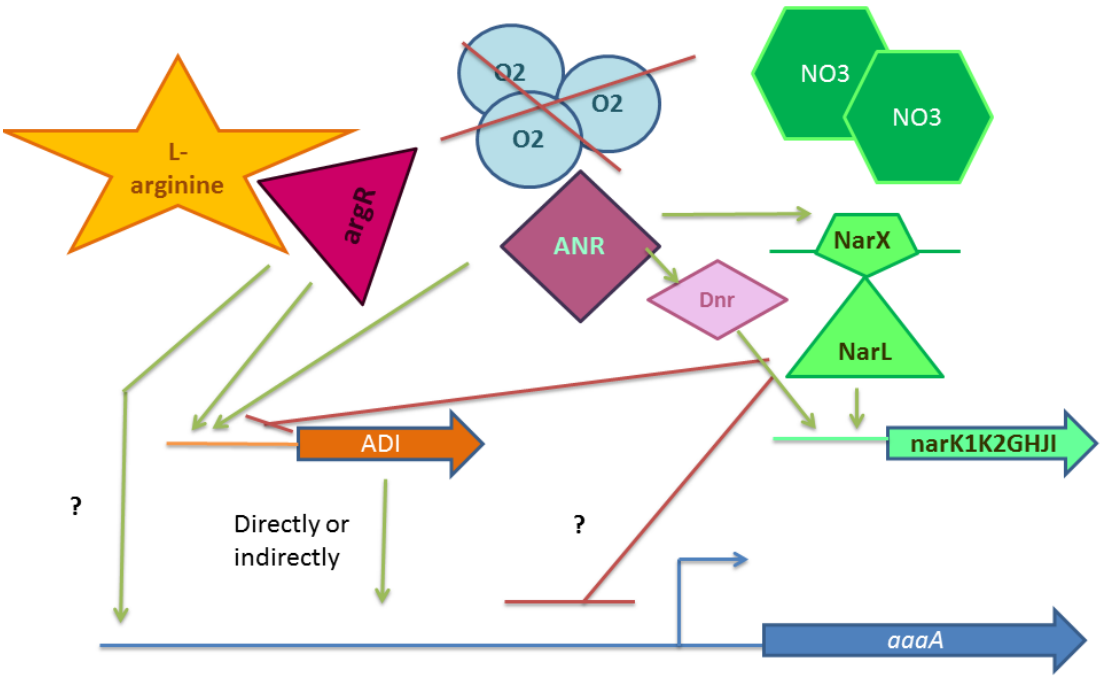


Figure 3.1.3: How oxygen and nitrogen availability could influence *aaaA* expression through the regulators ANR, NarXL and ArgR. ArgR and ANR act positively on the ADI pathway enzyme transcription, while ANR and NarL act positively on the denitrification enzyme transcription. NarL inhibits the ADI pathway enzyme transcription. NarL and ArgR could act directly on *aaaA* expression. Green arrows represent a positive influence on expression and red arrows an inhibitory effect. ADI=arginine deiminase pathway, ADC=arginine decarboxylase pathway, ADH (ATA))=arginine dehydrogenase/transaminase pathway, AST=arginine succinyltransferase pathway. Based on data by: Paredes (2014); Nadine *et al* (1999); Haas *et al* (1995); Arai *et al* (1991; 1994; 1995; 1998); Jungst and Zumft (1992); Mercenier *et al* (1980).

Further to the arginine catabolic pathways, Paredes (2014) found that elements of the arginine biosynthetic pathway (*argF, argG* and *argJ)* were able to activate *PaaaA.* When arginine is available, these genes are repressed by ArgR (Lu *et al* 2004). As both the arginine biosynthetic genes and ArgR activate *aaaA* expression it is reasonable to conjecture that arginine is only a small piece of the complex regulation network of *aaaA*. The hypothesis presented here is that the principle function of *aaaA* is to support energy generation in oxygen limited conditions and is not a general method of arginine acquisition.

3.1.1.3 AaaA may respond to microbial density through the QS molecule RhlR

As mentioned in the main introduction, RhlR is the response regulator of the RhlIR QS system which is regulated by the LasIR system (Lee and Zhang 2015). These systems respond to cell density, influencing virulence factors such as cyanide, pyocyanin, and motility (Brint and ohman 1995; Latifi *et al* 1996; Pearson *et al* 1995; Winson *et al* 1995). The coordination of bacterial individuals is necessary for the appropriate strategy to be employed effectively: acute and virulent or chronic and persisting (Balasubramanian *et al* 2015).

RhlR was found to have a negative effect on *aaaA* transcription (Paredes 2014). Control by RhlR could help tailor arginine release for different cell densities and this could be important for biofilm maintenance. In fact, in Paredes (2014) and subsequent experiments in this thesis using the miniCTX-*lux* reporter show a peak of P*aaaA* expression at ~4 hours, corresponding with the earlier part of exponential phase. This could be partially coordinated by RhlR. Whether the repressive effect of RhlR is direct or indirect is explored in this chapter.

3.1.1.4 The interaction of aaaA with RNA polymerase: sigma factor RpoN, its associated regulators, and DNA bending proteins

The sigma factors of *P. aeruginosa* were discussed in the main introduction. They are classed according to the type of promoter they target (Campbell *et al* 2002; Murakami *et al* 2002). Of interest to this work is the alternative sigma factor group which target genes contributing to bacterial adaptability or virulence (Potvin *et al* 2008; Schulz *et al* 2015). The alternative sigma factor RpoN (σ^{54} and NtrA) facilitates uptake of nitrate and production of glutamine (Totten *et al* 1990) and was found to repress *aaaA* expression (Paredes 2014). RpoN may therefore be a dominant player in the nitrate-mediated repression of *aaaA*; however this is not the only system RpoN controls. RpoN was found to activate *rhlR* (Thompson *et al* 2003) which also represses *aaaA* expression (Paredes 2014). Thus RpoN could exert its repressive effects through this route. Whether RpoN also interacts with *PaaaA* to repress it directly is explored in this chapter (Figure 3.1.4 A & B).

The mechanism of RpoN mediated repression-activation is particular (Schaerer *et al* 2015) and worth outlining briefly. When RpoN binds to its target promoter it initially forms a closed confirmation. Depending on the binding site location, this can repress gene expression by steric interference. To transition to an open confirmation, RpoN requires the binding of an ATP-hydrolysing transcriptional activator. This usually interacts with the DNA upstream of the RpoN binding site

and connects to the polymerase-RpoN complex with the aid of DNA bending integration host factor protein (IHF) (Bertoni *et al* 1998). The gene can then be transcribed. The ATP-hydrolysing transcriptional activators of RpoN are also called enhancer binding proteins (EBPs) (Bush and Dixon 2012; Rappas *et al* 2007) and their association with *PaaaA* is explored in this chapter. To date, Paredes (2014) showed that 2 EBPs, Sfa2 and Sfa3, contributed to *aaaA* upregulation. Sfa2 and Sfa3 are encoded at the T6SS genetic locus and associate with RpoN to control expression of one of the encoded genes, H2-T6SS (Sana *et al* 2013). Whether these EBPs activate *PaaaA* directly or indirectly is investigated in this chapter (Figure 3.1.4 C & D).

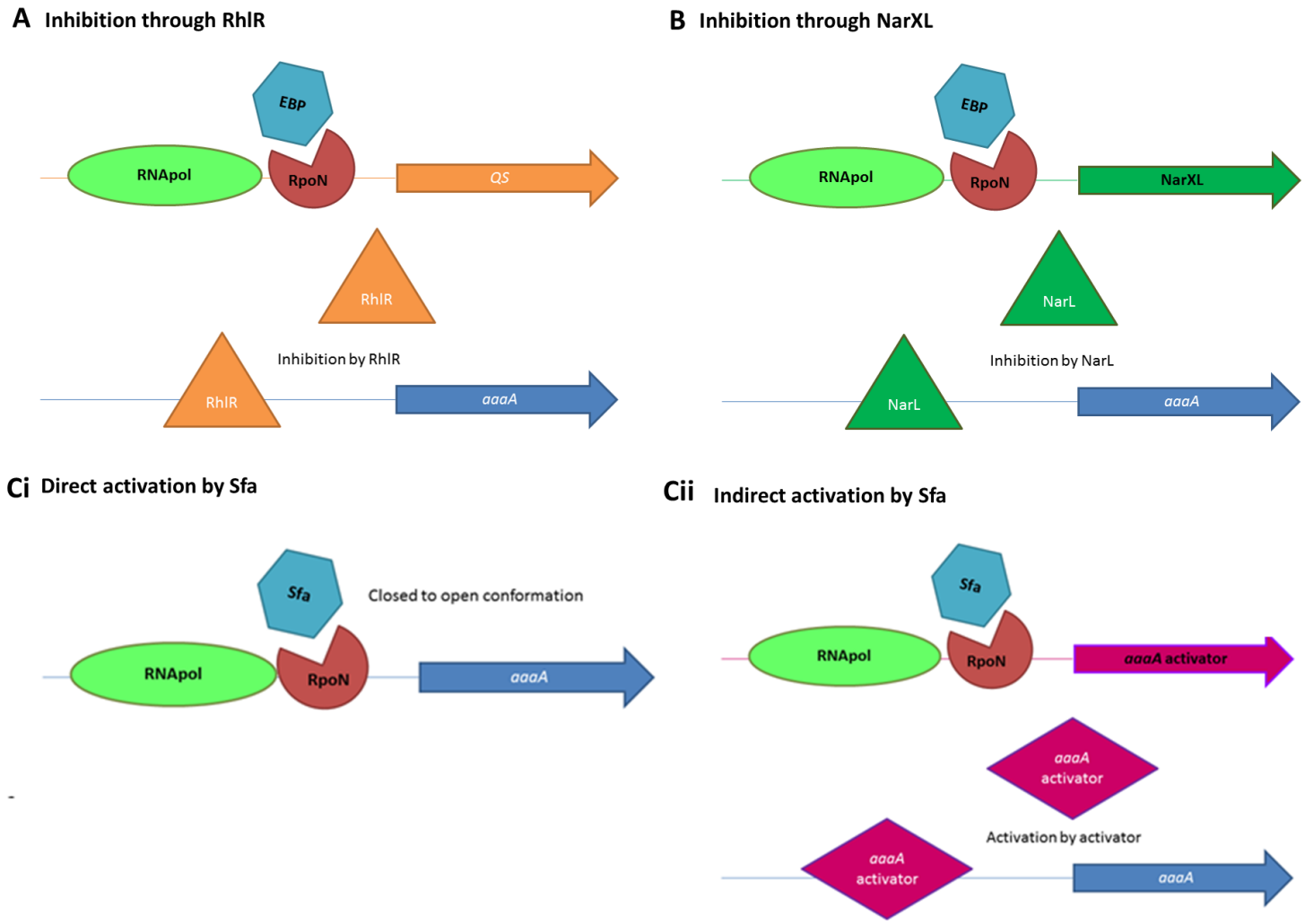


Figure 3.1.4: RpoN could inhibit *aaaA* directly or indirectly. Panel A: RhlR was found to negatively control *aaaA* expression (Paredes Osses 2014). RpoN could activate the QS genes which would repress *aaaA* directly or indirectly. Panel B: RpoN upregulates the genes involved in the denitrification cascade and the nitrate sensing two-component system NarXL (Totten *et al* 1990). NarXL could repress *PaaaA* either directly or through repression of the ADI pathway genes. Panel C: the EBP Sfa could facilitate transcription of *aaaA* by either opening the RpoN complex at *PaaaA* (i) or by opening the RpoN complex at another gene locus which coded for an activator of *PaaaA* (ii). Information from Sana *et al* (2013), Schaerer *et al* (2015) Bertoni *et al* (1998).

Also known to affect the RNA polymerase's ability to transcribe a gene, are the histone-like nucleoid-structuring proteins (H-NS) of *E. coli*. Two of these identified in *P. aeruginosa* are MvaT and MvaU. Unlike RpoN and the sigma factors, their action is not confined by the recognition of specific motifs and they bind instead to curved sections of DNA with a high AT content (Winardhi *et al* 2014; Castang *et al* 2008; Worrell thesis, 2005; Falconi *et al* 1993). Interestingly MvaT and MvaU have been found to repress the *aotJQMOP-argR* operon directly (Li *et al* 2009). They were also found to repress *aaaA* expression (Paredes 2014) possibly due to the reduced production of ArgR and AotJ, or through direct repression of *PaaaA*. This is investigated here. A double MvaT/MvaU deletion mutant eliminated pyocyanin production (Li *et al* 2009). It is possible that MvaT and MvaU could be influential on the anaerobic metabolic pathways through arginine influx and pyocyanin production and their effect on *aaaA* could be an extension of this.

3.1.1.5 Autoregulation of AaaA

An autoregulation loop exists where production of AaaA inhibits further expression of itself. When the *aaaA* open reading frame (ORF) was deleted, expression from the *aaaA* promoter was increased (Darch 2013, Paredes 2014 and this chapter). This negative feedback does not appear to be mediated by arginine; addition of exogenous arginine did not inhibit further *aaaA* expression (Paredes 2014). This correlates with the hypothesis that a deficit of arginine is not the greatest predictor of *aaaA* upregulation. Therefore there must be another mechanism, or more likely multiple mechanisms, at work. This could occur through an RNA silencing mechanism, the binding of the enzyme to its own promoter, through a regulator which is upregulated upon translation of AaaA, or through a regulator responding to a metabolite produced from AaaA activity. Figure 3.1.5 illustrates these possible mechanisms. This chapter considers the RNA silencing mechanism and the metabolite-regulator route is investigated in Chapters 4 & 6.

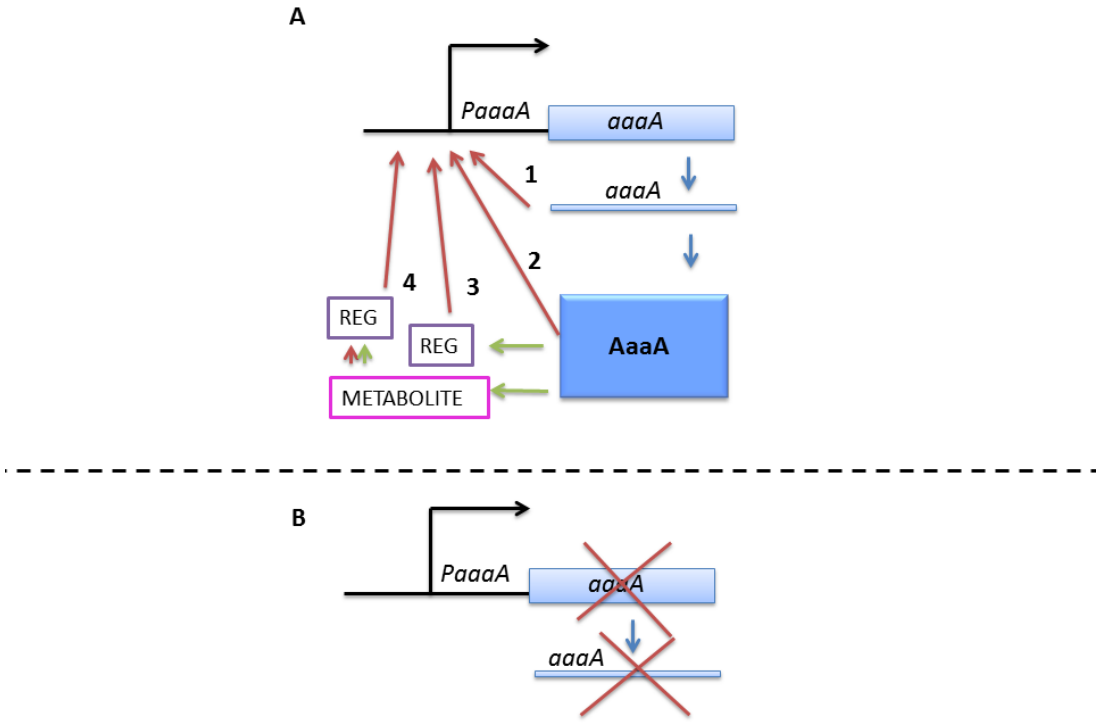


Figure 3.1.5: Autoregulation of *aaaA* could be mediated at different stages. Panel A: when a functional copy of *aaaA* is present negative regulation could occur by: (1) The RNA transcript, (2) directly from AaaA protein-DNA interaction, (3) regulator responding to the AaaA protein, or (4) regulator responding to a downstream metabolite produced by the activity of AaaA. Panel B: when *aaaA* is deleted negative feedback does not occur. Regulator is abbreviated to REG.

3.1.1.6 Other factors which may affect aaaA expression

Additional advantages can be gained from the release of arginine from exogenous peptides. For example, the basic properties of arginine could balance the acidic pH which has been linked to the infected CF airway environment (Ballard *et al* 1999; Poulsen *et al* 1994; Poulsen and Machen 1996). Additionally, Luckett *et al* (2012) suggested *aaaA* might have an immunomodulatory role. The authors noted that nitric oxide synthase (iNOS) and arginase activity, which share arginine as a substrate, differed in WT and *ΔaaaA P. aeruginosa* strains infecting a murine burn wound. AaaA could potentially throw the host response out of balance by increasing the availability of arginine. This would reduce iNOS activity in favour of arginase activity, lessening NO production and bacterial killing. Although outside the scope of this work, it should be recognised that *aaaA* transcription may also respond to factors associated with the host immune system. A final possibility is that peptidases can be involved in the modification of other *P. aeruginosa* peptidases or host proteins to facilitate, modify or disrupt functionality (Luckett *et al* 2012). The relationship of AaaA with other peptidases is explored in section 3.2.2.

3.1.2 Chapter aims

The following aims are addressed in this chapter:

- Investigation of regulators which could directly interact with *PaaaA* and their significance for the *in vivo* environment
- Identification of protein networks associated with *aaaA*
- Development of an *aaaA* tailored qRT-PCR assay to facilitate further investigation of its regulation

3.2 Results

3.2.1 Promoter analysis of *aaaA* suggests the existence of a complex regulatory network

Scrutiny of the upstream region of a gene can reveal potential regulators by the identification of stretches of sequence associated with TF or sigma factor binding (Hernandez-Garcia and Finer 2013). Using the data from Paredes (2014) to guide the search, the upstream region of *aaaA* was analysed by manual mining of the literature and use of the tool Prodoric Virtual Footprint (Munch *et al* 2005), to identify conserved regulator binding motifs.

Table 3.2.1 shows the possible sigma factor binding sites and Table 3.2.2 shows the possible TF binding sites in the *aaaA* sequence found by Virtual Footprint.

3.2.1.1 A note on the orientation of transcription factor binding motifs

The *aaaA* gene is encoded on the negative strand. Non palindromic TF binding motifs where the reported consensus reads in the same direction as *aaaA* are marked as such in the TF table. The alternatively reading (reverse complement of the reported consensus) TF binding sites have also been included in the table because evidence suggests that the orientation of the motif is not always influential on gene expression. A study by Lis and Walther (2016) found that the orientation of TF binding motifs did not affect gene expression, while Ishihama (2010) and Lobell & Schleif (1991) describe TFs to be effective (in general) when binding in either orientation to the RNA polymerase and this can be mediated through DNA bending proteins such as IHF and H-NS. Figure 3.2.1 illustrates this point.

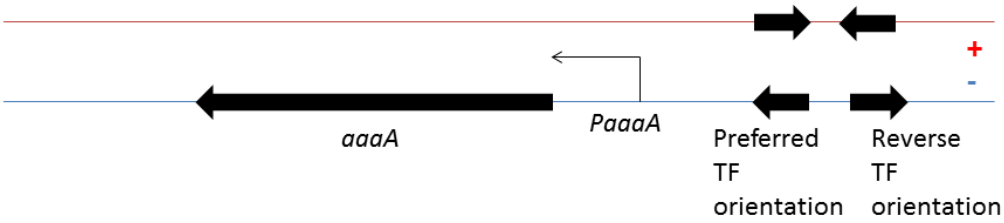


Figure 3.2.1: The *aaaA* gene is encoded on the negative strand and transcription factors which also read in this direction will be indicated. Transcription factor is abbreviated to TF.

Sigma factor	Motif found	Reading same direction as *aaaA*?	From	To	In expected location?	Discount?	Additional comments
AlgU -10	GGTCTCAG	yes	-320	-312	not -10	yes	No -10
AlgU -35	TGGAACTTGC	no	-442	-443	not -35	yes	
Sig70	TACGAT	no	-25	-20	around -16GTG or +5ATG	yes	Other strand and no -35
Sig70	TACGTT	no	-127	-122	not -10	yes	Other strand and no -10
Sig70	TTTCAT	no	-77	-72	not -10	yes	Other strand and no -10
SigB (-10)	GACGGGAAGTAA	no	-235	-224	not -10	yes	Other strand and no -10
SigB (-10)	GAAGGGAATGCA	no	-252	-241	not -10	yes	Other strand and no -10
SigB (-10)	CAGAGGAAAGTG	yes	-13	-2	minus 10 GTG	yes	no corresponding -35
SigB (-35)	ACCGTTTCATGT	no	-79	-68	minus 35 ATG	yes	Other strand and no corresponding -10
SigE (-35)	TTTCATGTCTC	no	-82	-72	minus 40 ATG	yes	Other strand and no corresponding -10
SigE (-35)	TGGCATAGAGC	no	-387	-377	not -35	yes	Other stand and no -35
SigE (-35)	AGTGTTACTTG	no	-187	-177	not -35	yes	Other strand and no -35
SigH (-10)	ATCGAATGAT	no	-40	-31	around -8 ATG	yes	on other strand and no -35
SigH (-10)	AGGGAATGCA	no	-252	-243	not -10	yes	Other strand and no -10
SigH (-10)	CACGAATTGA	no	-97	-88	not -35	yes	Other strand and no -35
SigH (-35)	CCAGGAGTTGAA	yes	-223	-212	not -35	yes	No -35
SigH (-35)	GAAGGGAATGCA	no	-252	-241	not -35	yes	Other strand and no -35

Table 3.2.1: Identified Sigma Factors using the tool Virtual Footprint (Prodoric). All were discounted from further investigation for the location, reading direction and missing half of the binding sites. RpoN was included as a searched sigma factor but not identified. Sensitivity was set at 0.8, core sensitivity/size was 0.9/. The start of the *aaaA* ORF was counted from the GTG start predicted by the *Pseudomonas* genome database.

Sigma factor	Consensus	Motif found	Reading same direction as *aaaA*?	From	To	Discount?	Additional comments
ArgR	TGTCGCNNNNNNGNAANNNNN	TGTCGCTACGTTGTAA	-	-131	-116	No	Lu *et al* (2004)
IHF	A/T-ATCAA-NNNN-TT-A/G	CTGCATTCCCTTCCGC	+	-253	-238	No	
IHF	A/T-ATCAA-NNNN-TT-A/G	TGGCAGCGGCTTGGAC	-	-148	-133	No	
NarL	TACC/TNA/CT	TAACACT	+	-183	-177	no	after Rhlr PBS and just before another NarL PBS
NarL	TACC/TNA/CT	TACCGAC	+	-21	-15	yes	after putative transcription start and only half motif
NarL	TACC/TNA/CT	TACTTCC	+	-234	-228	no, but unlikely	close to Rhlr PBS
NarL	TACC/TNA/CT	TGTCTCT	-	-83	-77	no	after IHF PBS, close to RpoN PBS, half motif, (NT also found)
NarL	TACC/TNA/CT	TGCCTCT	+	-167	-161	No	first half (NT also found)
NarL	TACC/TNA/CT	TCTCTCT	+	-163	-157	No	second half (NT also found)
RhlR	(N)2CTNCCAG(N)2TTNGNAGN	CTTCACCGACTGCACG	-	-354	-339	yes	far upstream and other orientation
RhlR	(N)2CTNCCAG(N)2TTNGNAGN	+CTTCCCGTCCCAGGAG -CTCCTGGGACGGGAAG	+/-	-232	-217	no	
Fur (8mer)	GATAATGATAATCATTATC	TGAAAATG	-	-201	-194	yes	only one part of hexamer repeat
Fur (8mer)	GATAATGATAATCATTATC	TTGTAACT	-	-133	-126	yes	only one part of hexamer repeat
Fur (8mer)	GATAATGATAATCATTATC	AGGAAAGT	+	-10	-3	yes	only one part of hexamer repeat
ArcA	GTTAACTAAATGTTA	TGTTACTTGC	-	-188	-179	no	
FleQ	Box1:CGCCTAAAAATTGACAGTT Box2:CATTAGATTGACGTTAATC	TGTCGCTACGT	-	-126	-116	no	identified also by Nick Tucker
FleQ	Box1:CGCCTAAAAATTGACAGTT Box2:CATTAGATTGACGTTAATC	TGTCGGTACGA	-	-24	-14	no	after putative start of transcription, typical binding site more than 100 bp upstream
FleQ	Box1:CGCCTAAAAATTGACAGTT Box2:CATTAGATTGACGTTAATC	CGTCGCTGAGA	-	-318	-308	no	far upstream

GlnG (NtrC)	TGCACCATAATGGTGC A	TGGTGC	-	-30	-25	yes	far upstream and opposite orientation
GlnG (NtrC)	TGCACCATAATGGTGC A	TGGTGG	-	-418	-413	yes	far upstream and opposite orientation
GlnG (NtrC)	TGCACCATAATGGTGC A	TGCTCC	+	-89	-84	no	

Table 3.2.2: Identified Transcription Factors using the tool Virtual Footprint (Prodoric). Whether they were accepted or discounted from further investigation was decided by the location, reading direction and completeness of the binding sites. Sensitivity was set at 0.8, core sensitivity/size was 0.9/. The start of the *aaaA* ORF was counted from the GTG start predicted by the *Pseudomonas* genome database. PBS=putative binding site; NT = Dr Nick Tucker. The consensus sequences were taken from: Lavrrar and McIntosh (2003); Lu *et al* (2004); Tyson *et al* 1993; Craig and Nash (1984); Hervas *et al* (2008); Baraquet *et al* (2012); Schuster *et al* (2004).

3.2.1.2 A RpoN binding site and transcriptional start site location were identified in the aaaA upstream region

In the beginning of the *aaaA* gene investigation, Dr Owen Darch (2013) attempted to find the promoter. This was more difficult than expected and even the use of several *in silico* based tools did not identify any promoter predictions in 1000 bp of upstream (UPS) sequence. The predicted location of the transcriptional start site was also unclear as there were two possibilities: that of the GTG predicted by the *Pseudomonas* genome database and an ATG start 78 bp upstream from this. The use of SignalP software (Petersen *et al* 2011) showed that the GTG start was more likely to allow signal peptide cleavage to occur. Dr Esteban Paredes Osses (2014) moved further with this by construction of the miniCTX-*lux* fusion with P*aaaA*, but extensive promoter interrogation was not pursued. To further understand how *aaaA* is transcribed, the *aaaA* sequence was here analysed for sigma factor binding sites using Virtual Footprint. Table 3.2.1 shows the multiple sigma factor sites identified by the program and why they were discounted.

A different approach was then taken. Manual combing of the UPS for an RpoN binding site, which experimental data most closely linked with *aaaA*, was facilitated by the consensus sequence reported by Barrios *et al* (1999) (Figure 3.2.2). With the kind help of Dr Nick Tucker, a putative RpoN binding site was identified and along with this the putative transcription start site (Figure 3.2.2).

Following this, the location of a Shine-Dalgarno (SD) or ribosome binding site (RBS) sequence was looked for. The *Pseudomonas* Database had not found one automatically and the likelihood of the translation start site being a GTG codon decreases the probability of finding one. However, a manual search found a possible site where 4 out of the 6 conserved bases (5'-AGGAGG-3) resided 9 bp before the GTG codon and would therefore be within the desired proximity range (Ma *et al* 2002; Omotajo *et al* 2015) (Figure 3.2.2).

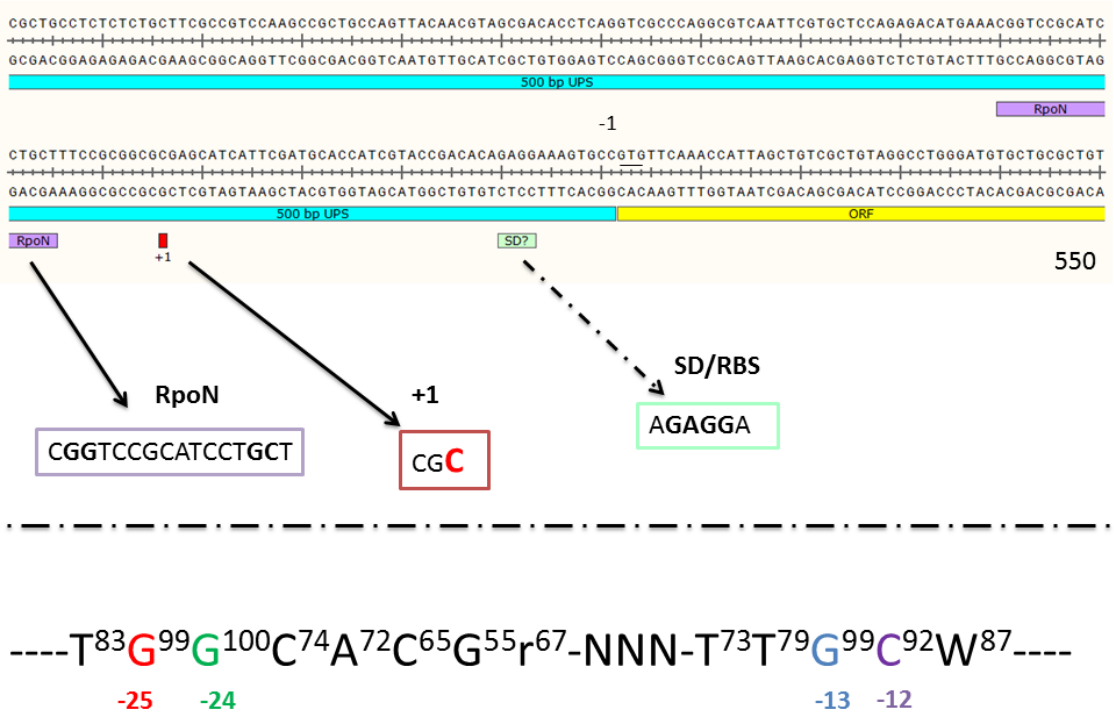


Figure 3.2.2: A putative binding site for RpoN was found in the *aaaA* 500 bp UPS region. Top section: the RpoN binding site has the conserved -25/-24 GG and -13/-12 GC bases with the conserved 10 base pairs dividing these two locations. This is shown in purple. If the site is valid and is indeed in the correct location, the start of transcription should be the nucleotide marked in red. The Shine-dalgarno (or ribosome binding site) is possibly at the location shown in mint-green. Bottom section: the consensus RpoN sequence with the probability of base conservation. This work was achieved with the help of Dr Nick Tucker and the information provided in Barrios *et al* (1999); Ma *et al* (2002); Omotajo *et al* (2015).

3.2.1.3 Regulator binding sites associated with metabolism were identified in the aaaA upstream region

3.2.1.3.1 A putative ArgR binding motif was identified in the *aaaA* UPS

ArgR was found to positively affect *aaaA* expression (Paredes 2014). To investigate whether ArgR was binding directly to the *aaaA* UPS, manual literature searching and Virtual Footprint software was utilised. A putative ArgR binding motif was revealed in the *aaaA* UPS region (Figure 3.2.3). The location of the ArgR binding motif was further confirmed by a study of the ArgR regulon by Lu *et al* (2004), which identified AaaA as one of the target genes. The presence of an ArgR site suggests that it interacts with *PaaaA* directly.

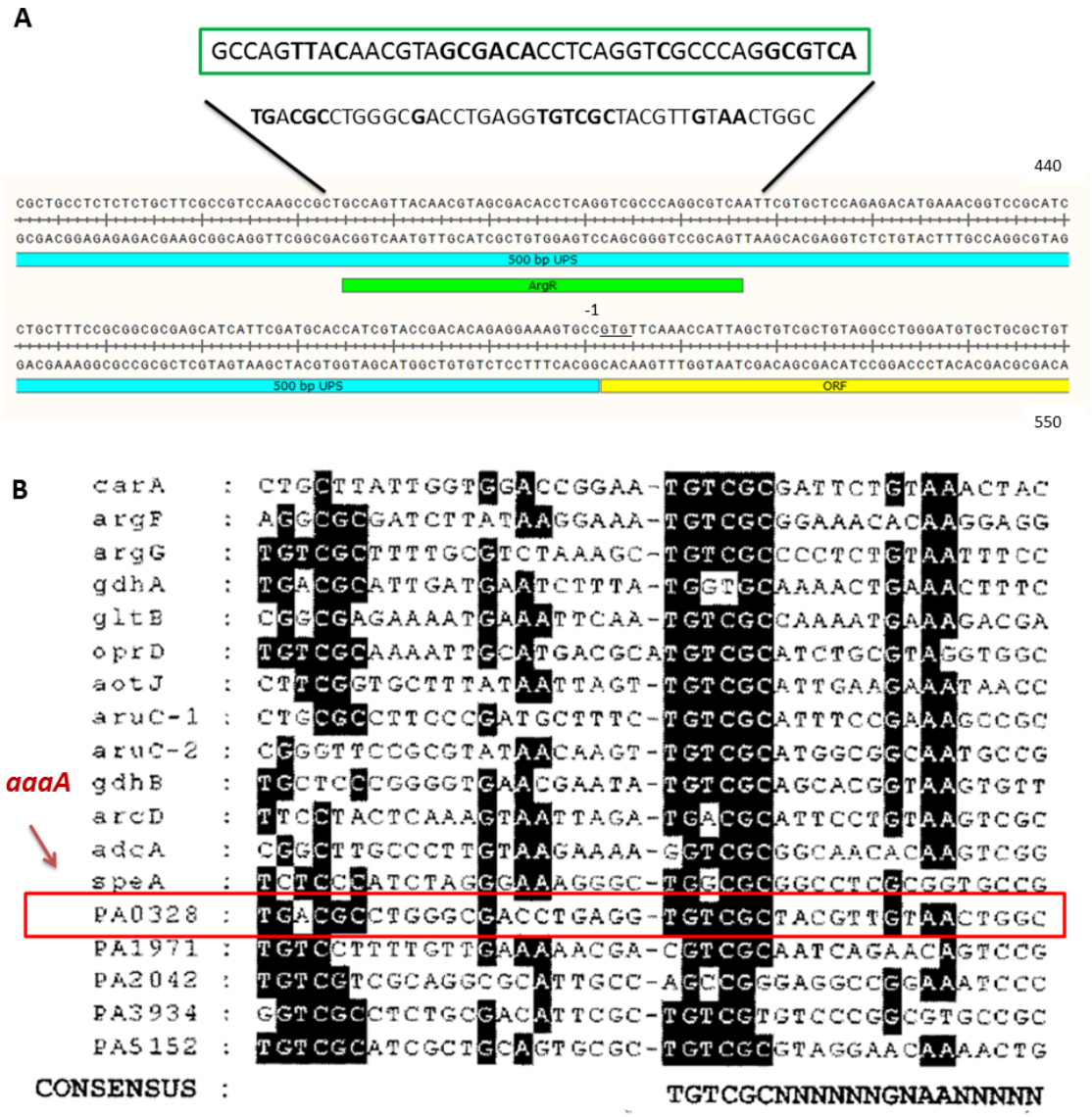


Figure 3.2.3: A putative ArgR binding site was identified in the 500 bp UPS *aaaA* upstream region. Panel A: ArgR putative binding site in the *aaaA* UPS. The lime green box shows the ArgR binding sequence as it appears in the direction of the *aaaA* gene. The sequence below the lime green box shows the ArgR binding sequence as it is presented by Lu *et al* (2004). Conserved residues are shown in bold. Panel B: ArgR site found by Lu *et al* (2004). *PA0328* = *aaaA* and is highlighted by a red box.

3.2.1.3.2 A series of NarXL binding motifs were identified in the *aaaA* UPS

While arginine upregulates P*aaaA* through ArgR (Paredes 2014), it was hypothesised that exogenous nitrate should inhibit *PaaaA.* The nitrate sensing TCS NarXL was found to repress the *arcDABC* operon (ADI pathway) by steric interference of an ArgR binding site, when nitrate was present (Benkert *et al* 2008). Inhibition of *aaaA* expression could either occur indirectly through reduced activation from ADI pathway components or by direct binding of NarL to *PaaaA.* To investigate whether NarL could bind directly to *PaaaA*, Virtual Footprint was used to search for putative binding motifs.

Several putative NarL binding sites were identified by the software which have been included in Table 3.2.2. One was discounted due to its location after the transcription start. The 2 putative NarL binding sites which are most likely to be genuine are located either side of the putative ArgR binding site with one of these directly upstream of RpoN. These were also found by Dr Nick Tucker during his assistance with locating RpoN. Figure 3.2.4 shows the location of the putative NarL binding sites.

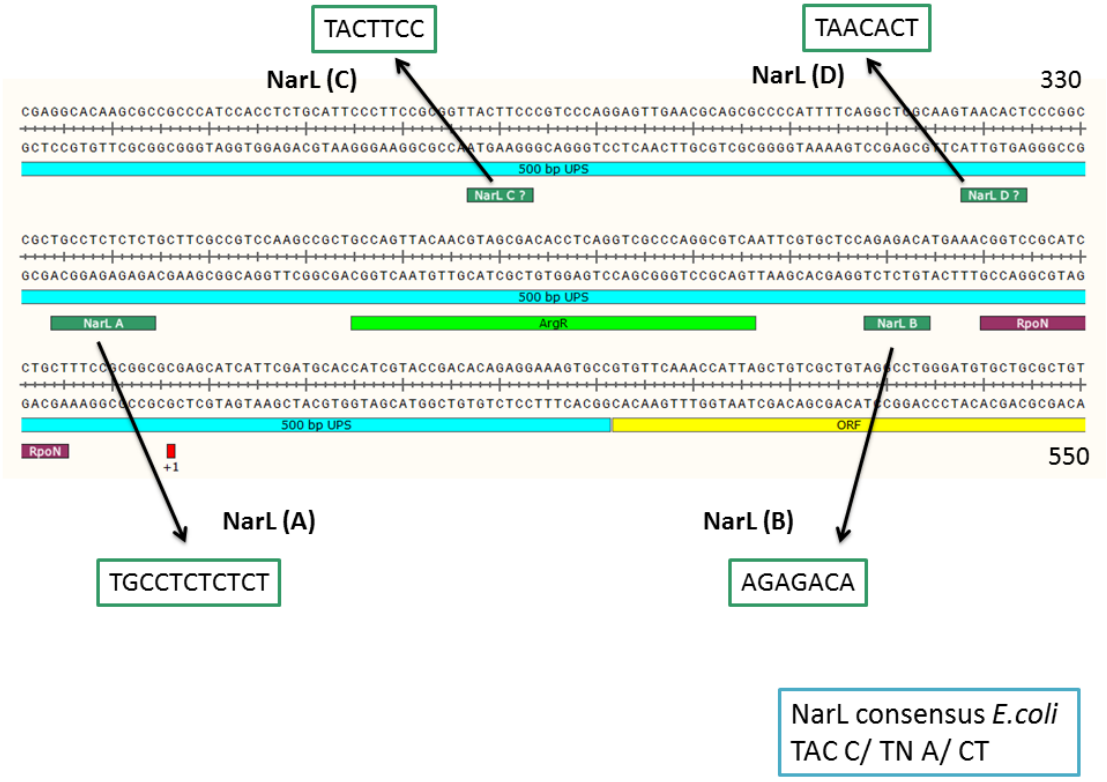


Figure 3.2.4: Putative NarL binding sites were identified in the *aaaA* 500 bp UPS region. The sites were identified by the Virtual Footprint software and with the kind assistance of Dr Nick Tucker. Green boxes show the putative NarL binding sites. The consensus sequence identified by Tyson *et al* 1993 is shown at the bottom of the figure for comparison. The lime green box is the putative ArgR transcription site and the mauve box is the putative RpoN binding site. The red box is the putative start of transcription.

3.2.1.3.3 Two IHF binding motifs were identified in the aaaA UPS

IHF is thought to facilitate activation of RpoN by bringing it into contact with EBPs through DNA bending (Friedman *et al* 1988; Freundlich *et al* 1992). It recognises an asymmetrical motif identified by Craig and Nash (1984) shown in Figure 3.2.5. To determine if IHF could bind to the *aaaA* UPS region, manual sequence analysis and use of Virtual Footprint were employed. Two IHF motifs were identified (Figure 3.2.5).The most interesting site is relatively close to RpoN, overlapping the first part of the putative ArgR binding site. This strengthens the probability of the RpoN site being genuine.

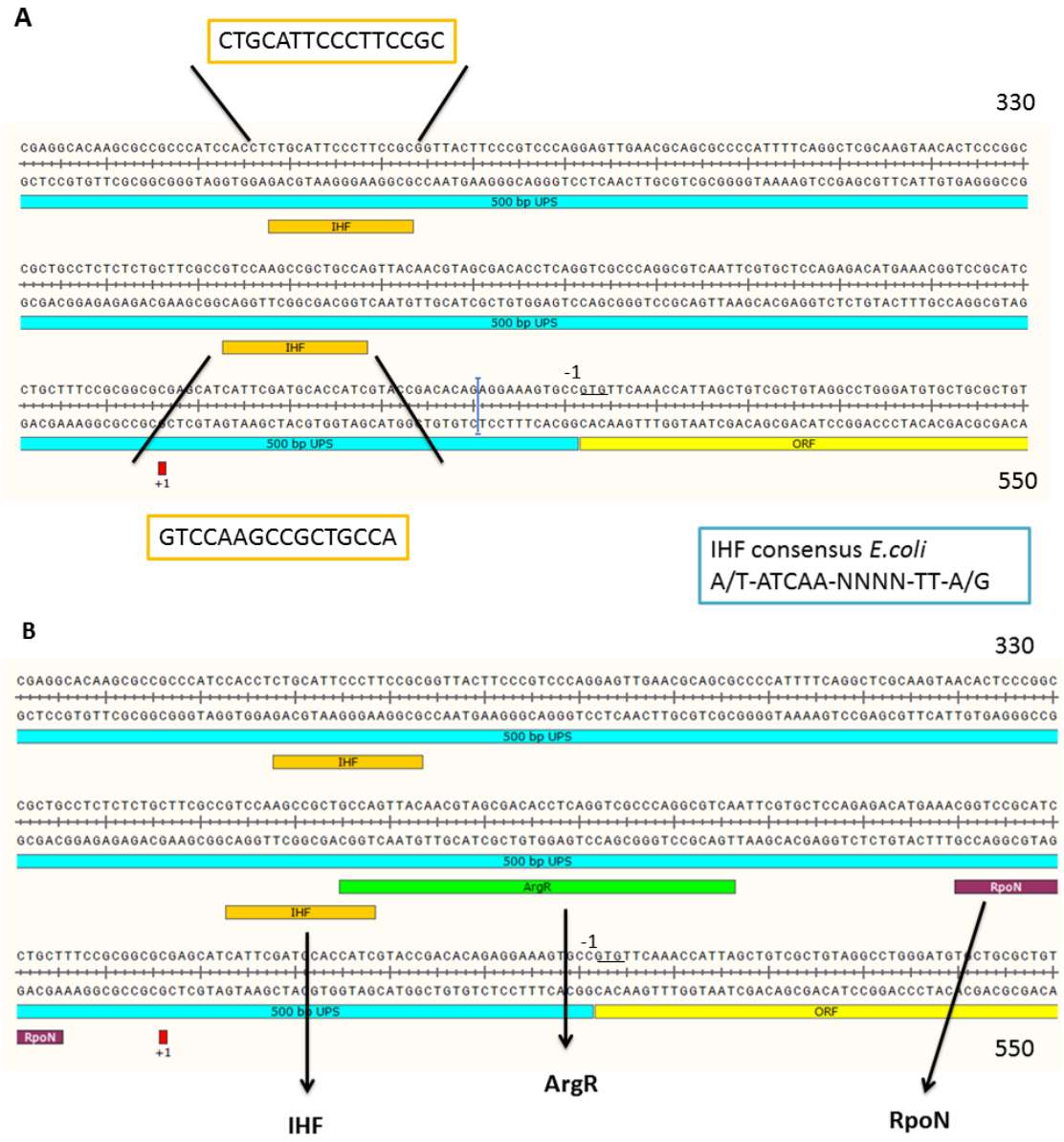


Figure 3.2.5: Two putative IHF binding sites were identified in the 500 bp *aaaA* upstream region. Panel A: IHF putative binding site in the *aaaA* UPS. The sites were identified by Virtual Footprint and manual identification using the consensus by Craig and Nash (1984) which is shown at the bottom of the figure for comparison. Orange boxes show the IHF sites. The red box is the putative start of transcription. Panel B: location of IHF putative binding sites in relation to other putative binding sites. One putative IHF site overlaps a putative ArgR binding site and is in a good location to bring the RpoN binding site into contact with other transcription regulator sites. Orange boxes show IHF, the green box shows ArgR and the mauve box shows RpoN putative binding sites. The red box shows the putative start of transcription.

3.2.1.3.4 A NtrC (GlnG) binding motif was identified in the *aaaA* UPS

The *glnALG* operon in *E. coli* consists of GlnA, a glutamate synthase which converts ammonia and glutamate to glutamine when nitrate is limited, and two response regulators GlnL (NR II) and GlnG (NR I) which upregulate GlnA (Sheng-Ping Shiau *et al* 1993; Backman *et al* 1981). The analogous system in *P. aeruginosa* consists of GlnA and a TCS regulator NtrB/NtrC (*Pseudomonas* genome database). NtrB is the sensor and NtrC is the response regulator which

activates pathways that can provide alternative sources of nitrogen in nitrogen limited conditions (Janssen *et al* 1982). Furthermore, NtrC contains an ATP binding domain for the opening of RpoN-RNA polymerase complexes (UniProtKB - P0AFB8 (NTRC_ECOLI); *Pseudomonas* genome database).

To investigate whether NtrC could be interacting with the *aaaA* UPS, the Virtual Footprint software was used to search for the conserved binding motif. A putative binding site a little upstream from RpoN was found. Using the consensus sequence reported by Hervas *et al* (2008), this was extended to highlight the full site. Figure 3.2.6 shows the location of the identified binding site.

The NtrC binding motif found in the *aaaA* promoter overlaps the NarL (B) putative binding site. It is likely that only one of the sites is genuine or there is steric competition between the regulators which represses RpoN activation in nitrate rich conditions and activates RpoN in nitrate limited environments.

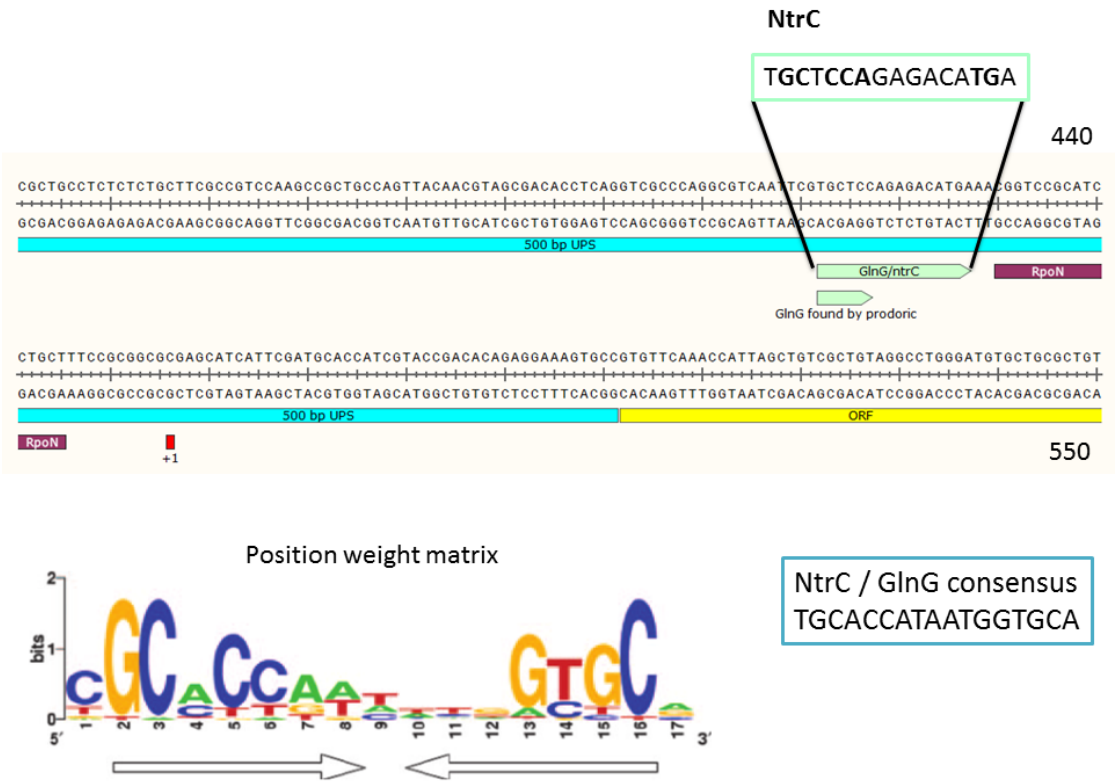


Figure 3.2.6: A putative NtrC binding site was identified in the 500 bp *aaaA* UPS region. The sites were identified by Virtual Footprint and manual identification using the consensus by Hervas *et al* (2008). The position weight matrix and consensus sequence identified by Hervas *et al* (2008), is shown at the bottom of the figure for comparison. The mint green box shows the NtrC putative binding site. The red box is the putative start of transcription. The mauve box shows the putative RpoN site.

3.2.1.3.5 An ArcA binding motif was identified in the aaaA UPS

Paredes (2014) observed that ArcD from the ADI pathway upregulated *aaaA*. From the *arcDABC* operon, ArcA and ArcB form a TCS where ArcA is the response regulator. When phosphorylated, ArcA is able to bind directly to DNA and forms part of a nucleoprotein complex (Jeon *et al* 2001; Luchi and Lin 1992; Sawers and Suppmann 1992). Metabolic pathways operating in aerobic conditions are repressed by ArcA (Gunsalus and Park 1994), whereas ArcA activates the fermentative pathways (Brondsted and Atlung 1994). The regulons of the anaerobic sensor FNR and ArcA considerably overlap; with FNR responsible for genetic control in anaerobic conditions and ArcA having a greater role in microaerobic conditions (Salmon *et al* 2005; Perrenoud and Sauer 2005; Alexeeva *et al* 2003; Levanon *et al* 2004).

ArcA can also interfere with other regulator binding sites and it has been known to antagonise H- NS action (Govantes *et al* 2000 and Park *et al* 2003).

To investigate if *aaaA* transcription could respond positively to the ADI pathway by direct binding of ArcA, Virtual Footprint was used to search for binding motifs. A putative ArcA binding site was found in the *aaaA* upstream region. The binding consensus for ArcA is reported in Favorov *et al* (2005) and is shown in Figure 3.2.7.

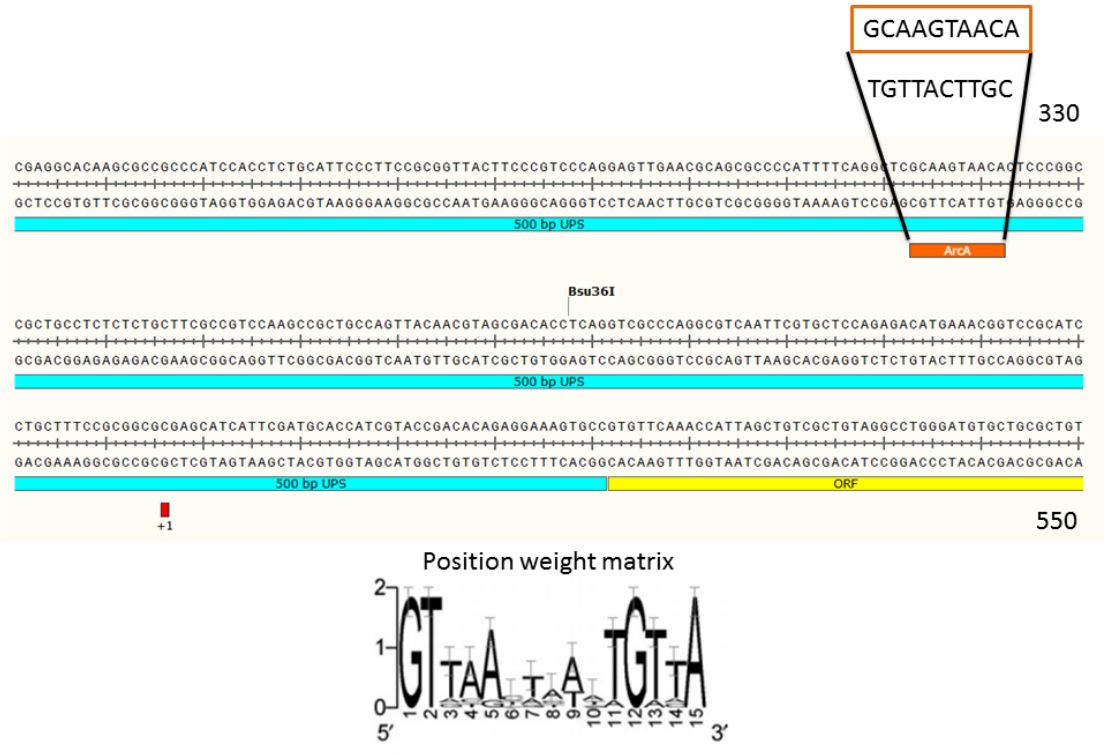


Figure 3.2.7: A putative ArcA binding site was identified in the 500 bp *aaaA* UPS region. The sites were identified by Virtual Footprint. The position weight matrix consensus sequence identified by Favorov *et al* (2005) is shown at the bottom of the figure for comparison. The orange box shows the location of the ArcA putative binding site. The red box is the putative start of transcription.

3.2.1.4 RhlR could bind to the aaaA promoter

RhlR was previously found to have a repressive effect on *PaaaA* (Paredes 2014). Both LasR and RhlR have been found to bind to conserved palindromic sequences upstream of the coding region. These sections of sequence have been termed *las-rhl* boxes (Pessi and Haas 2000; Anderson *et al* 1999; Whiteley and Greenberg 2001; Rust *et al* 1996). Schuster *et al* (2004) investigated the *las-rhl* boxes further to divide them into LasR co-operative, LasR non-cooperative and RhlR-only. These are shown in (Figure 3.2.8).

To investigate whether RhlR could interact directly with the *aaaA* UPS, Virtual Footprint was used to find 3 possible RlhR binding sites (Table 3.2.2). These were further investigated by manual analysis and 1 binding location accepted as a putative binding site. The sequence found in the *aaaA* sequence (Figure 3.2.8)

shows similarity with the RhlR specific binding motif. Along with the experimental data, it looks likely that *aaaA* is under RhlR control and this can be tested further by site-directed mutagenesis.

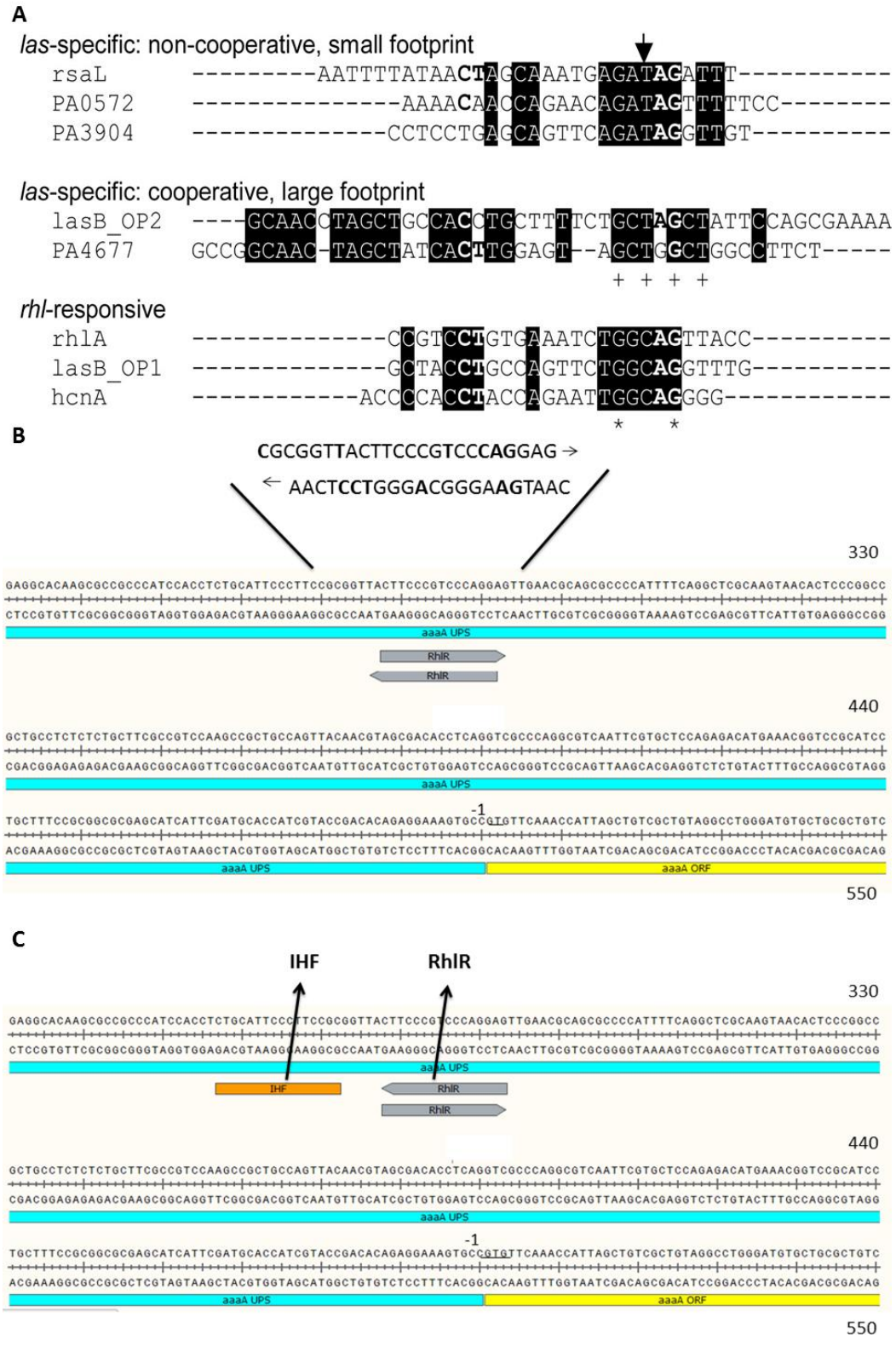


Figure 3.2.8: A putative RhlR binding site was identified in the 500 bp *aaaA* UPS region. Panel A: RhlR binding sequence investigated by Schuster *et al* (2004). Figure adapted from Schuster *et al* (2004). Arrow indicates the important difference in bases between the Las and RhlR specific binding motifs. Asterisk and plus signs indicate complete conservation of bases across 8 sequences. Panel B: RhlR putative binding site in the *aaaA* UPS. The sites were identified by Virtual Footprint. The location of the putative RhlR binding site is shown in grey. Residues in bold match the consensus sequence identified by Schuster *et al* 2004. Panel C: proximity of the putative RhlR binding motifs to an IHF binding motif.

3.2.1.5 The enhancer binding protein FleQ potentially binds to the aaaA promoter

FleQ is an enhancer binding protein (EBP) of RpoN. It is associated with the control of biofilm related genes through interaction with c-di-GMP and flagellin genes through a mechanism which is not yet fully understood. FleQ can both activate and repress its target genes and typically interacts with RpoN by binding >100 bp upstream from the transcription start site. The connection with RpoN is facilitated through a DNA bending mechanism (Baraquet *et al* 2012). An alternative regulatory mechanism can also be mediated by FleQ which does not necessitate RpoN. Baraquet *et al* (2012) showed this to be the case at the *pelA* promoter. Two FleQ sites flank the transcription start site and they interact with each other though FleN to distort the DNA and presumably block DNA polymerase binding. Activation of gene transcription occurs when c-di-GMP associates with the complex and presumably adjusts the DNA configuration.

To investigate whether any FleQ binding sites were present in the *aaaA* UPS, Virtual Footprint was used to identify 3 potential FleQ binding sites. One was far upstream and seemed unlikely to be genuine. The other two are located either side of the putative transcription start site. The first overlaps with the putative ArgR binding site (Figure 3.2.9). Investigation of these sites will be two-fold: first to determine if they are genuine and second to elucidate whether the first site acts in conjunction with RpoN or if the two sites work together in a mechanism similar to the one described by Baraquet *et al* (2012).

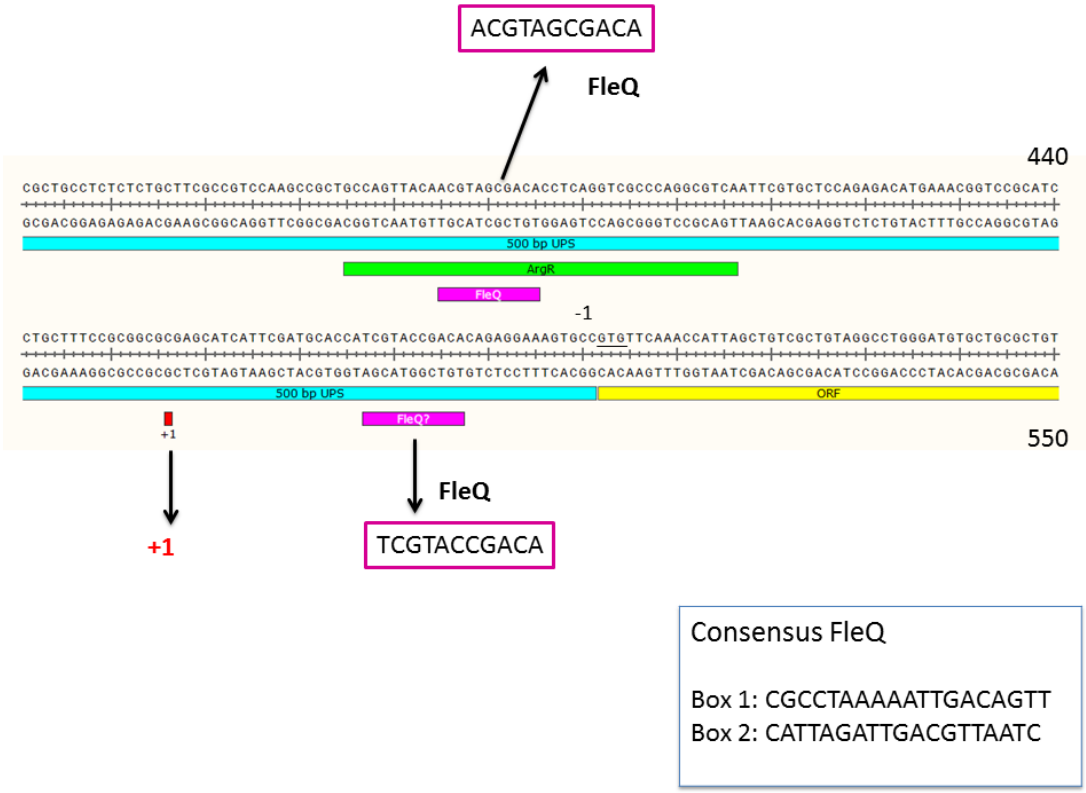


Figure 3.2.9: Putative FleQ binding sites were identified in the 500 bp *aaaA* UPS region. The sites were identified by Virtual Footprint. The location of the putative FleQ binding sites are shown in pink. The consensus sequence for FleQ (Baraquet *et al* 2012) is shown at the bottom of the figure.

3.2.2 STRING database analysis places aaaA between diverse gene networks

The STRING database predicts associations between genes. It was based on the principle that protein interactions should not be confined to direct physical binding. It makes use of complete sequenced genomes to determine co-occurrence, genetic location proximity, co-expression, gene fusions and experimental associations between genes (Christian von Mering *et al* 2003). The STRING database was used here to identify new potential parts of the AaaA regulatory network that had not yet been considered. It was hoped that this might provide some of the missing links, leading to better elucidation of the mechanisms controlling AaaA expression. The results are presented in Figure 3.2.10 and Figure 3.2.11. The information provided for each connected gene was taken from the *Pseudomonas* genome database unless a specific reference is given.

AaaA, also called PA0328, is represented by the red central node. It is surrounded by 10 nodes. The majority of these are either co-occurrence links which means that the genes are found together across genomes or text mining which derives connectivity from literature references.

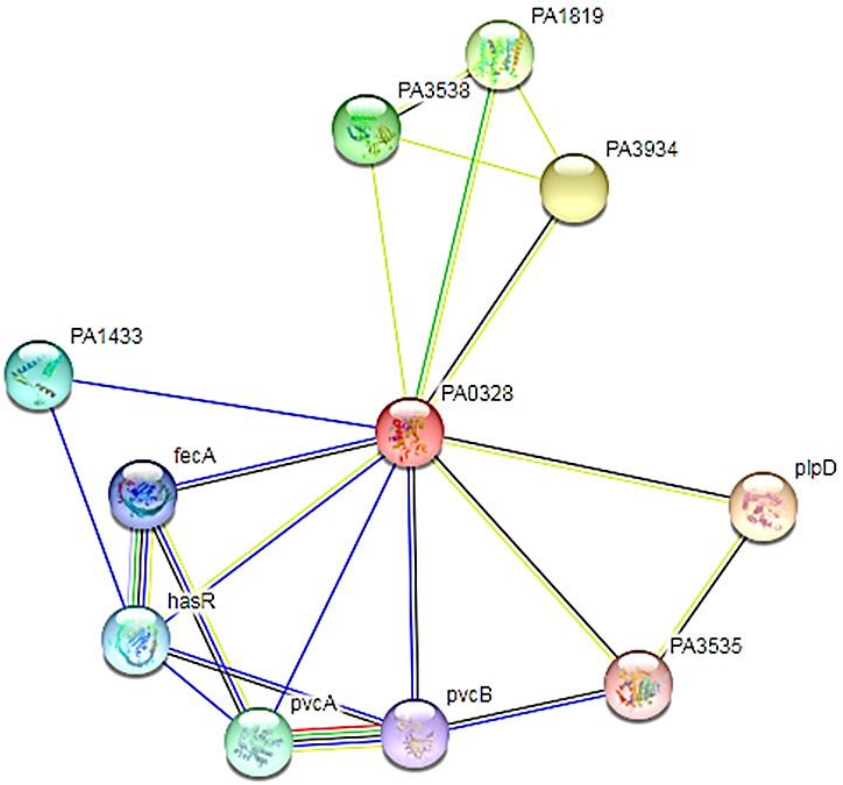


Figure 3.2.10: Output from the STRING database on 21-05-2018 shows the connections known about *aaaA* (here *PA0328*). Also called *PA0328*, *aaaA* is represented by the red central node. A blue connection line represents a predicted interaction due to gene co-occurrence. A black connection line represents co-expression, a green line is a predicted interaction due to gene neighbourhood. A red line represents a predicted interaction due to gene fusions. A yellow line represents a connection generated by text mining.

3.2.2.1 The ArgR regulon connects AaaA with hypothetical proteins

PA3538, PA1819, and *PA3934* are inter-connected with each other and *aaaA* by text mining. In addition, *aaaA* is connected to *PA1819* by genetic location and to *PA3934* by co-expression. The common link between all of these genes is that they are preceded by an ArgR binding motif. *PA3538* is also directly preceded by *argF* and the 2 genes could share the same promoter. *PA3538* is predicted to function as an ATP binding component of an ABC transporter which locates to the inner membrane (IM). *PA1819* is a probable amino acid permease located to the IM and is directly downstream of *cadA* (lysine decarboxylase). They likely share the same the promoter under the control of ArgR. *PA3934* is a conserved hypothetical oligopeptide transporter located to the IM and its upstream region contains putative ArgR and AmzR binding sites. Promoter activation by AmrZ was demonstrated by Xu *et al* (2016) in the transcription of *algD* which has links with mucoidy. AmrZ also has been associated with control of Pel and Psl production, twitching and flagella-mediated motility, and metabolism of c-di-GMP. These are necessary for biofilm development (Xu *et al* 2016; Baynham *et al* 2006; Jones *et al* 2013; Jones *et al* 2014; Martínez-Granero *et al* 2004; Tart *et al* 2006).

Whether the expression of *PA3538, PA1819*, and *PA3934* influence *aaaA* transcription or *vice versa*, cannot be construed from this data but it appears that they all belong to the ArgR network.

3.2.2.2 AaaA is connected to other Type V secretion system proteins

The *plpD* and *PA3535* genes are also connected to *aaaA* by text mining and co-expression. Interestingly, these appear to be Type V secretion system proteins. The gene *plpD*, also called patatin-like protein, is localised to the outer membrane (OM) and is classified as a Type Vd autotransporter. It is believed to have lipase activity. No binding motifs have yet been found in the upstream region. *PA3535* is a probable serine protease with a predicted β-barrel domain and expected proteolysis activity from a serine-type endopeptidase. It is predicted to be regulated by *lasR* and is directly upstream of the *argF* and *PA3538* genes. The autotransporter status and OM enzyme activity function connects these genes with *aaaA*.

3.2.2.3 AaaA has links with iron sequestering machinery

The genes *pvcA* and *pvcB* are implicated in pyoverdine synthesis, paerucumarin biosynthesis and isonitrile biosynthesis pathways. The *pvcA* and *pvcA* genes produce the paerucumarin biosynthesis cytoplasmic proteins PvcA and PvcB. They are both connected to *aaaA* through co-occurrence and *pvcA* is co-expressed. The gene *fecA* produces the Fe (III) dicitrate transport protein FecA. It is an OM protein that is predicted to transport ferric iron and siderophores. Its mutant phenotype suggests that it also transports citrate. It is co-expressed with *aaaA* and is highly connected with *hasR* which is also connected to *aaaA* through co-occurrence. The gene *hasR* produces the heme uptake outer membrane receptor HasR precursor which is an OM protein involved in heme transport. *PA1433* is a conserved hypothetical protein, predicted to be involved in signal transduction, forming an integral part of the membrane. It is connected to *aaaA* and *hasR* through gene co-occurrence. To conclude, this group has iron uptake and OM locations in common. Similar putative regulator binding sites to *aaaA* have not yet been found.

3.2.2.4 Directly upstream of aaaA is PA0329

PA0329 is a conserved hypothetical protein which is relatively small (110 bp, predicted 11.8kDa), with an unknown function. It is situated directly upstream of *aaaA*. It appears to be well conserved between *P. aeruginosa* genomes which will be presented in the following chapter. The absence of this gene from the STRING network of *aaaA* prompted an investigation of the *PA0329* network. It was found

to be co-expressed, linked by experimental data (microarray), and sharing the same genetic neighbourhood with *aaaA* (Figure 3.2.11). This places the connection with *aaaA* as the strongest in the *PA0329* network. It was decided to investigate this connection later in this chapter using qRT-PCR.

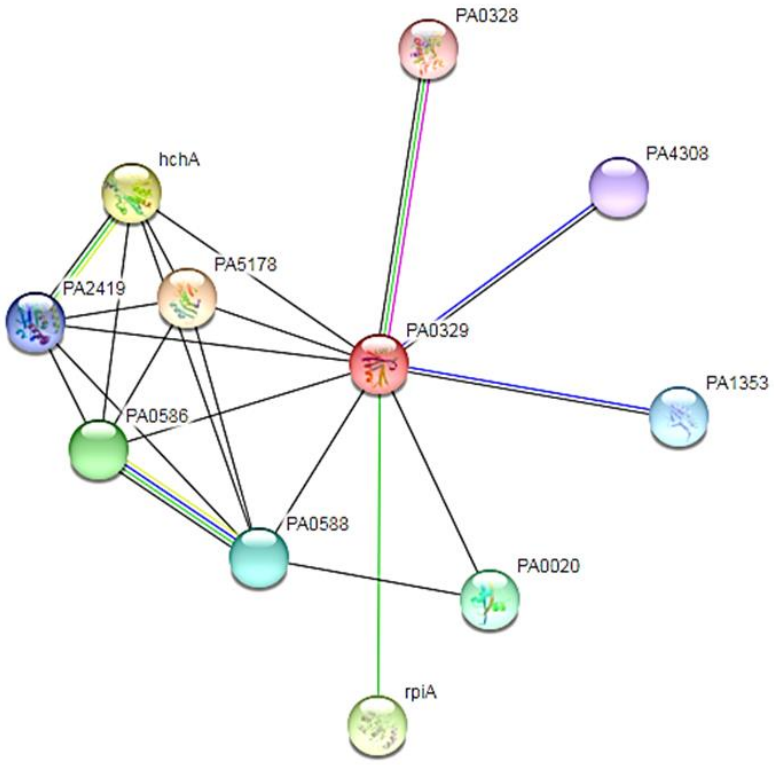


Figure 3.2.11: Output from the STRING database on 21-05-2018 shows the connections known about *PA0329*. PA0329 is represented by the red central node. *PA0328 (aaaA)* is represented by the pink node that is connected only to *PA0329* and no other nodes. A blue connection line represents a predicted interaction due to gene co-occurrence. A black connection line represents co-expression, a green line is a predicted interaction due to gene neighbourhood. A pink line represents experimentally determined connections.

3.2.2.5 PA0329 has an AmzR putative binding site in its upstream region.

A neighbouring gene *rpiA*, is a ribose 5-phosphate isomerase and is the first of the 3 adjacent genes ending with *aaaA*. Although there is no evidence yet that it is co-expressed in *PA0329*, there is a putative binding site for the global TF, AmrZ within the *rpiA* ORF which overlaps with the 500 bp UPS region of *PA0329*. A previously mentioned, AmrZ regulates genes involved in biofilm formation (Xu *et al* 2016; Baynham *et al* 2006; Jones *et al* 2013; Jones *et al* 2014; Martínez-Granero *et al* 2004; Tart *et al* 2006) and it is possible that *rpiA* and *PA0329* are recruited during this process.

3.2.2.6 The other genes in the PA0329 network are mostly predicted proteins with enzymatic function

There is a dense network of hypothetical proteins including *PA5178*, *PA0021*, *PA0588*, *PA0586*, *PA2419* and *hchA* associated with PA0329. These are a mixture of putative metabolic enzymes and supporting proteins. No regulatory connections have been found but they have not yet been extensively investigated.

Also hypothetical proteins, *PA4308* (putative ATPase and helicase) and *PA1353* (putative glyoxalase/bleomycin resistance) genes are co-expressed and co-occur with *PA0329*. No identified regulator motif of interest has yet been found.

3.2.3 DNA curvature analysis of the promoter for MvaT/MvaU binding reveals region overlapping the putative RpoN site

A previously mentioned, MvaT and MvaU were found to repress *aaaA* expression (Paredes 2014). They are homologous to the H-NS proteins in *E. coli*, affecting gene transcription by targeting areas of DNA sequence showing high curvature and AT content (Winardhi *et al* 2014; Castang *et al* 2008). These regions are typically found in the promoter regions of genes (Wang and Rodwell 1991; Rosenthal and Rodwell 1998).

The program BEND-IT (Vlahovicek *et al* 2003) predicts DNA curvature using statistically derived dinucleotide geometries (roll, tilt and twist angles) based on 3D structures or other measurements such as electrophoretic mobility shift analysis, nucleosome binding or DNaseI digestion assays (Goodsell and Dickerson, 1994). Experimentally tested curved motifs produce curvature values of 5-25°/helical turn whereas straight motifs produce values of less than 5°/helical turn (Vlahovicek *et al* 2003).

To investigate whether potential MvaT or MvaU binding sites exist in *PaaaA*, the 500 bp UPS region of *aaaA* was analysed using BEND-IT. Figure 3.2.12 shows the output from this analysis. Seven peaks of curvature were identified at -450 bp, -410 bp, -360 bp, -310 bp, -200 bp, -80 bp and -50 bp. Three curvature peaks corresponded with high AT content: the -450 bp, -200 bp and -80 bp peaks. The -200 bp and -80 bp peaks curvature versus AT content are the most defined and in an interesting location. Table 3.2.3 shows the peak location in comparison to sigma and transcription factor putative binding sites. Of particular interest is RpoN, which is -71 to -54 bp. This corresponds to the -80 peak of high curvature and low GC content. The length of the RpoN binding motif correlates well with the size of the peak.

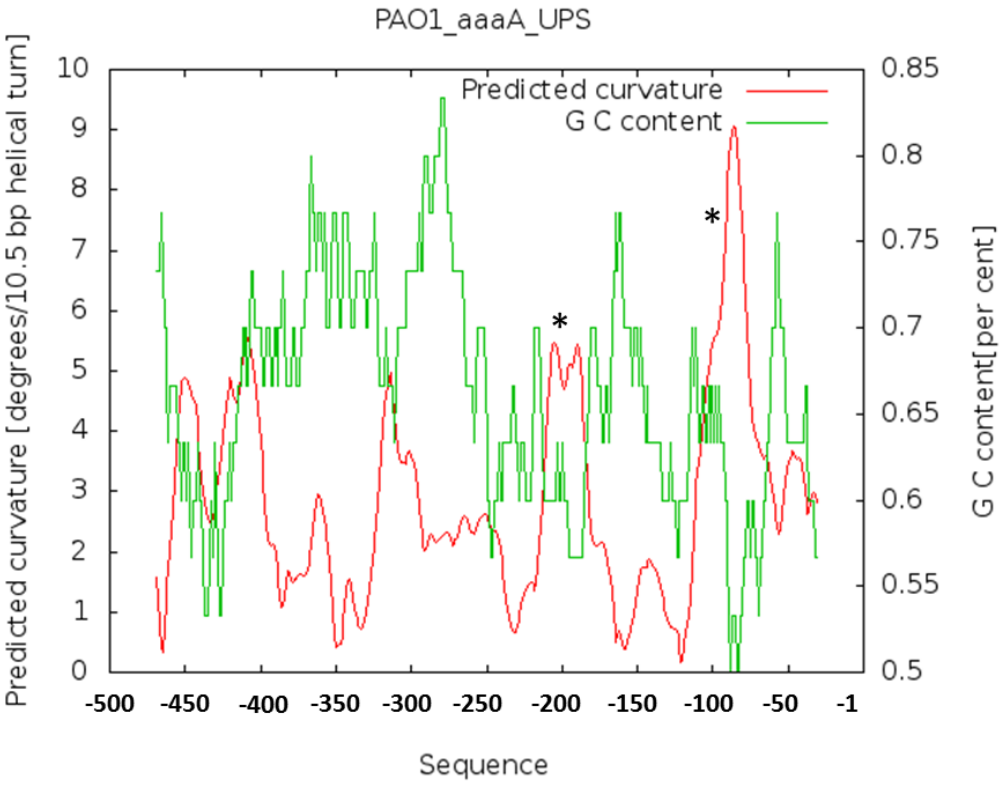


Figure 3.2.12: Curvature prediction and GC content of the *aaaA* 500 bp upstream region shows at least 7 peaks of curvature. To generate the curvature and AT content graph, the *aaaA* UPS was input into the BEND-IT software (Vlahovicek *et al* 2003). Motifs above 5°/helical turn are considered to be curved. The red line represents curvature and the green line represents the AT content. There at least 7 peaks of curvature: 1 at -450 bp, 2 at -410 bp, 3 at -360, 4 at -310 bp, 5 at -200 bp, 6 at -80 bp and 7 at -50 bp. The first peak (-450 bp), fifth peak (-200 bp) and sixth peak (-80 bp) correspond to high AT content, whereas the others do not. Asterisks indicate the most likely binding locations of MvaT and/or MvaU.

Base pair number of high curvature peak	High AT?	Putative site of interest	Base pair number range of putative site of interest
-450	Yes	None identified	
-410	No	None identified	
-360	No	None identified	
-310	No	None identified	
-200	Yes	Fur	-200 to -193
		ArcA	-187 to -178
		NarL	-182 to -176
-80	Yes	RpoN	-71 to -54
		NtrC	-88 to -73
		NarL	-82 to -76
-50	No	Putative start of transcription	-44

Table 3.2.3: Curvature peak location in the *aaaA* UPS in relation to putative sites of transcription or sigma factors.

3.2.4 The negative regulation problem and significance of oxygen

Past data by Paredes (2014), showed that bioluminescence driven from the *aaaA* promoter in the PAO1 *ΔaaaA* strain exceeded that of the PAO1 WT strain. To further confirm this effect and illustrate the scale of the *PaaaA* activation, PAO1 and PAO1 *ΔaaaA P. aeruginosa* strains containing an integrated miniCTX-*lux* reporter fused with either the *PaaaA* or constitutive *Pkan* control, were grown overnight in aerated LB at 37°C 200 rpm. The cultures were washed in fresh media and standardised to OD $_{600}$ 0.1 before addition to a 96 well plate. This was incubated in a tecan plate reader for 24 hours at 37°C.The bioluminescence emitted from the cultures is measured in relative lux units (RLU) and is normalised by cell density (OD $_{600}$). The RLU/ OD $_{600}$ is proportional to the activation of the fused promoter and in the following chapter the system will be discussed in greater detail.

Figure 3.2.13 shows the difference in bioluminescence corresponding to *aaaA* promoter activation is much higher in the PAO1 *ΔaaaA* strain ($P<0.0001$).

Although there is a difference in bioluminescence from *Pkan* activation between WT and mutant strains, this difference is small with less confidence of significance ($P<0.05$).

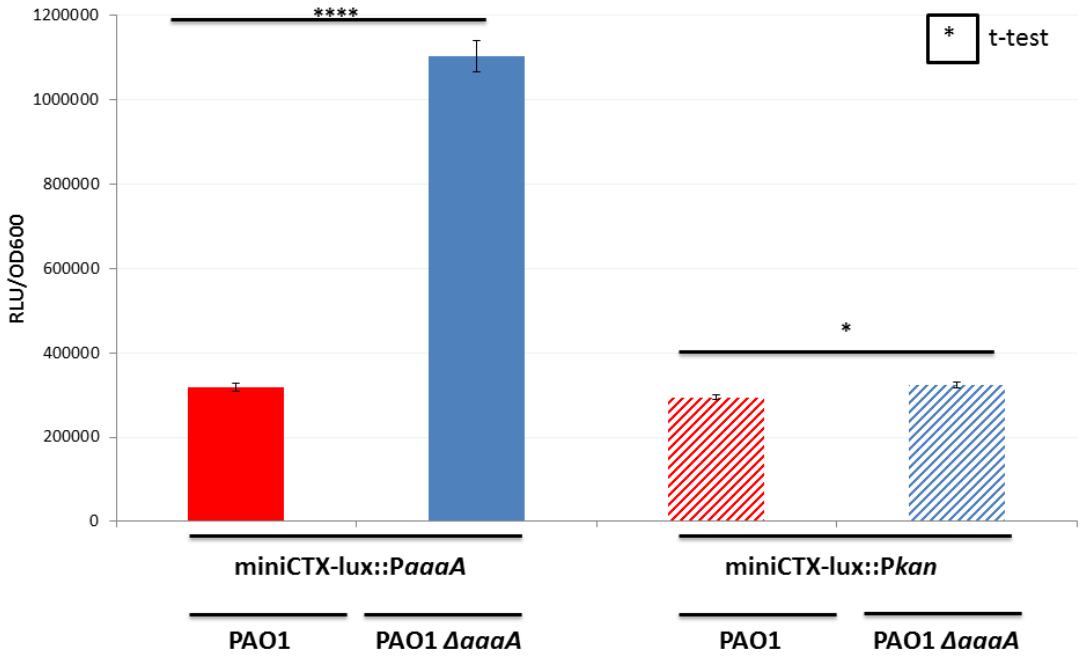


Figure 3.2.13: Activation of the *aaaA* promoter is higher in the PAO1 *ΔaaaA* strain than the WT. PAO1 and PAO1 *ΔaaaA* with miniCTX-*lux*::*PaaaA* or miniCTX-*lux*::*Pkan* were grown overnight in LB media, washed 3x and standardised to OD_{600} 0.1. They were then added to a 96 well plate, allowing the growth (OD_{600}) and luminescence (RLU) to be measured over 24 hours at 37°C by a tecan plate reader. The luminescence corresponds to activation of *PaaaA* or *Pkan* and is presented as the AUC of the RLU/OD_{600}. Three biological replicates (x9 technical) over 3 separate experiments were used and each bar represents the average of these. The error bars show the standard deviation from the mean. A t-test was performed between PAO1 and PAO1 *ΔaaaA*. The level of significance is shown by ns (non-significant), * ($P<0.05$) and **** ($P<0.0001$).

3.2.5 RpoN may not repress *aaaA* expression consistently

How *aaaA* is transcribed is still unknown. Paredes (2014) found that *PaaaA* showed more activation in a PA14 *ΔrpoN* mutant than in the PA14 WT. This indicated that RpoN is able to repress *PaaaA*. Correlating with this data, microarray gene expression data included on the *Pseudomonas* genome database, shows a data set where *aaaA* expression is compared in PAO1 *kinB* mutant strains and PAO1 *kinB rpoN* double mutant strains. The data set shows a consistent increase in *aaaA* expression in the PAO1 *kinB rpoN* double mutant strains compared to the *kinB* only mutant strains (Figure 3.2.14).

To further validate the data in Paredes (2014) using the PAO1 strain background and including a complemented control, PAO1, PAO1 *ΔrpoN*, and PAO1 *ΔrpoN att* T7::*rpoN*$^{+}$ strains (kindly donated by Dr Sophie Bleves) were conjugated with miniCTX-*lux*::P*aaaA* and miniCTX-*lux*::P*kan* reporters. These strains were then grown overnight in aerated LB containing 0.4% glutamine (*ΔrpoN* strains are

auxotrophic for glutamine) at 37°C 200 rpm. The cultures were washed in fresh media and standardised to OD $_{600}$ 0.1 before addition to a 96 well plate. The bioluminescence (RLU) emitted from the cultures was measured by a tecan plate reader over 24 hours and normalised by cell density (OD $_{600}$).

Intriguingly, there was no difference in *PaaaA* activation between PAO1 and PAO1 *ΔrpoN* (Figure 3.2.15). The PAO1 *ΔrpoN att* T7::*rpoN*$^{+}$ strain showed greater *PaaaA* activation which is the reverse of expectations. The PAO1 *ΔrpoN att* T7::*rpoN*$^{+}$ strain also showed greater *Pkan* activation and therefore the complementation may be affecting the miniCTX-*lux* reporter in a non-specific manner. Addition of 0.4% glutamine did not significantly affect the activation of *PaaaA*.

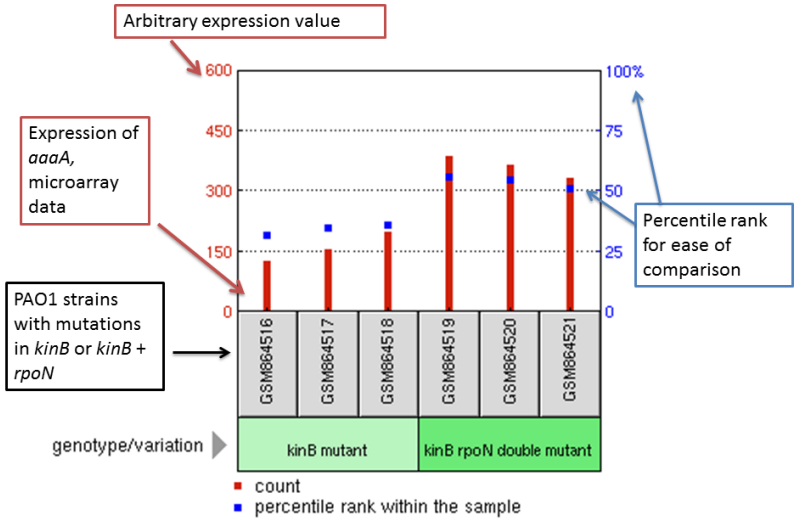


Figure 3.2.14: GEO expression data presented on the *Pseudomonas* genome database shows that *aaaA* expression increases in the *rpoN* mutant strains of PAO1. This correlates with Paredes (2014). The experimental conditions were not detailed on the site.

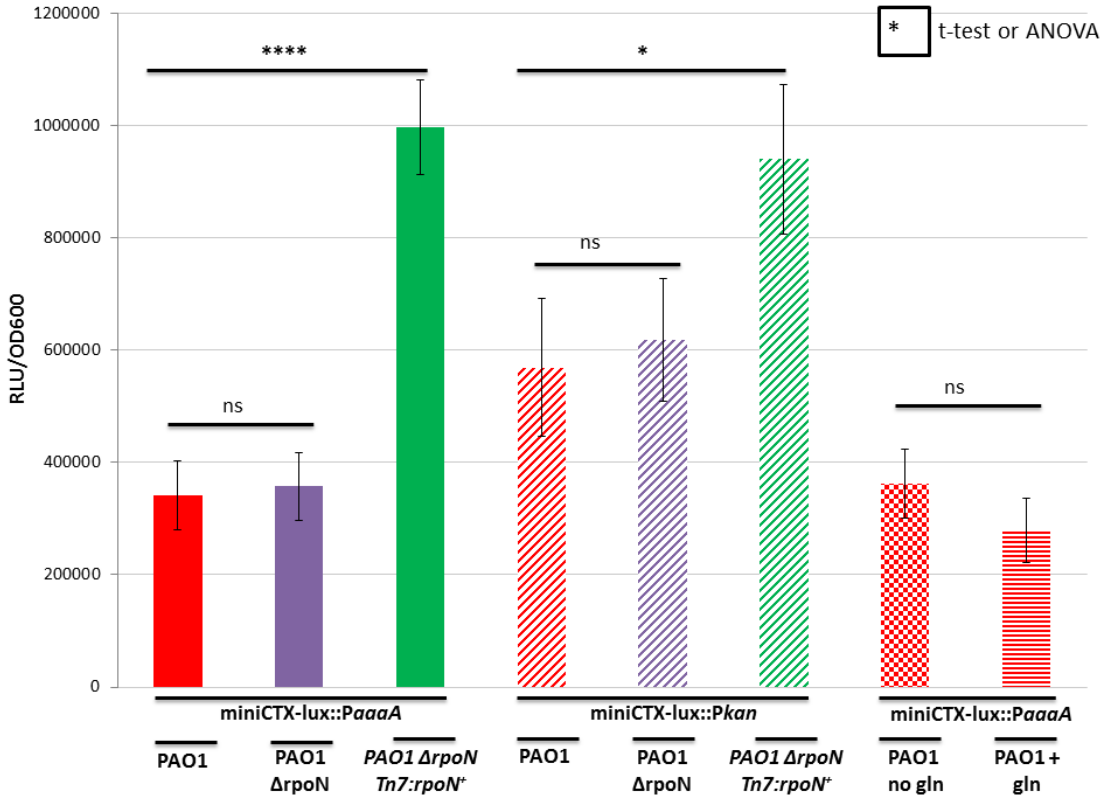


Figure 3.2.15: RpoN does not reduce P*aaaA* activation, opposing expectation, while the complemented strain shows increased promoter activation in *PaaaA* and *Pkan*. PAO1, PAO1 *ΔrpoN*, and PAO1 *ΔrpoN att T7::rpoN* with miniCTX-*lux*::*PaaaA* or miniCTX-*lux*::*Pkan* were grown overnight in LB media containing 0.4 % glutamine, washed 3x and standardised to OD_{600} 0.1. They were then added to a 96 well plate, allowing the growth (OD_{600}) and luminescence (RLU) to be measured over 24 hours at 37°C by a tecan plate reader. The luminescence corresponds to activation of *PaaaA* or *Pkan* and is presented as the AUC of the RLU/OD_{600}. Three biological replicates (x9 technical) over 3 separate experiments were used and each bar represents the average of these. The error bars show the standard deviation from the mean. A t-test was conducted between PAO1 and PAO1 *ΔrpoN* strains and PAO1 with and without glutamine controls (gln, no gln). An ANOVA was performed between PAO1, PAO1 *ΔrpoN*, and PAO1 *ΔrpoN att T7::rpoN* strains. The level of significance is shown by ns (non-significant), * (P<0.05) and **** (P<0.0001).

3.2.6 Development of a qRT-PCR assay to complement miniCTX-*lux* data

The experiments using miniCTX-*lux* have 2 principle caveats: firstly they do not distinguish between direct and indirect regulatory effects, and secondly they do not control for specific conditions which could affect how regulators such as RpoN interact with *aaaA*. The first requirement can be addressed by site-directed mutagenesis and the second by qRT-PCR. With this aim a qRT-PCR assay was developed. To pilot-test the assay *aaaA* expression was compared in 4 conditions: aerobic LB; aerobic artificial sputum media (ASM, Palmer *et al* 2007 version); microaerobic LB; and microaerobic ASM.

An advantage of qRT-PCR is that the expression of more than one gene can be measured from one sample. In addition to *aaaA* expression, *PA0329* expression was tested for a dual purpose: (1) to investigate if expression of *PA0329* and *aaaA* are connected and responding to similar environmental differences as suggested by STRING, and (2) to function as an internal control (different from the endogenous reference gene) for assay performance. Expression of *aaaA* was predicted to be complex, responding to numerous conditions and regulators. Thus, it was foreseen that the expression pattern of *aaaA* may be difficult to interpret.

The relative, comparative C_T method of qRT-PCR was used here (Figure 3.2.16). This compares the expression of a target gene in a particular sample with the expression of that gene in other samples. To measure DNA amplification, the fluorescent Sybr Green dye method was used. Sybr Green binds to amplified double stranded DNA PCR product and the fluorescent signal is detected. The alternative approach using target specific probes (e.g. TaqMan) is expensive and probes have to be designed specifically for each target. The disadvantage of Sybr Green is the ubiquity of its binding: non-specific products or DNA contamination will also be detected (Morrison *et al* 1998). Post reaction melt-curve analysis (sequential temperature increase) is used to ensure other products are not being amplified by comparing product specific melting temperatures. This is detected by a drop in Sybr Green fluorescence from the dissociation of the two DNA strands (Ririe *et al* 1997). This data will be included in the optimisation section.

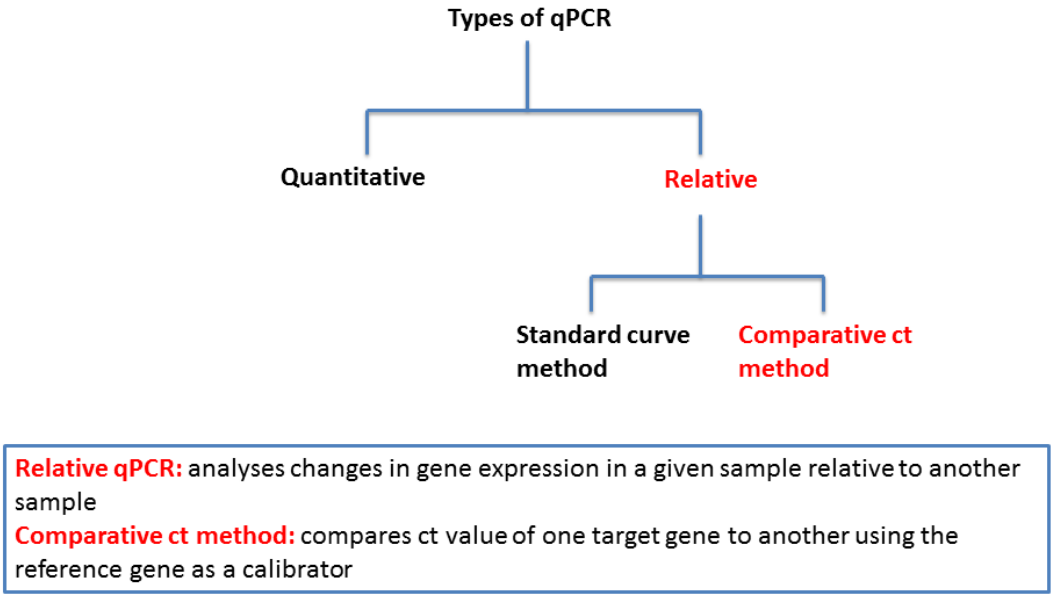


Figure 3.2.16: From the different categories of qRT-PCR, the relative, comparative C_T method is used here. This method relies on a endogenous reference gene to calibrate target gene expression. Text highlighted in red shows the methods which were chosen and black text shows alternative options.

3.2.6.1 Stage 1: extraction conditions

To identify the best time point during *P. aeruginosa* growth in which to compare *aaaA* expression, a representative sample for lag, exponential and stationary phase was collected. In aerobic cultures this was at 2, 4 and 8 hours and in microaerobic cultures at 2, 24, and 36 hours (Figure 3.2.17). RNA protect was immediately added to the samples upon isolation: 600 µl culture for 1.2 ml of RNA protect. This ensured the RNA was stabilised before pelleting and freezing of the cells at -80 ^{o}C. For each strain (PAO1 and PAO1 *ΔaaaA*) and condition 3 biological replicates were obtained.

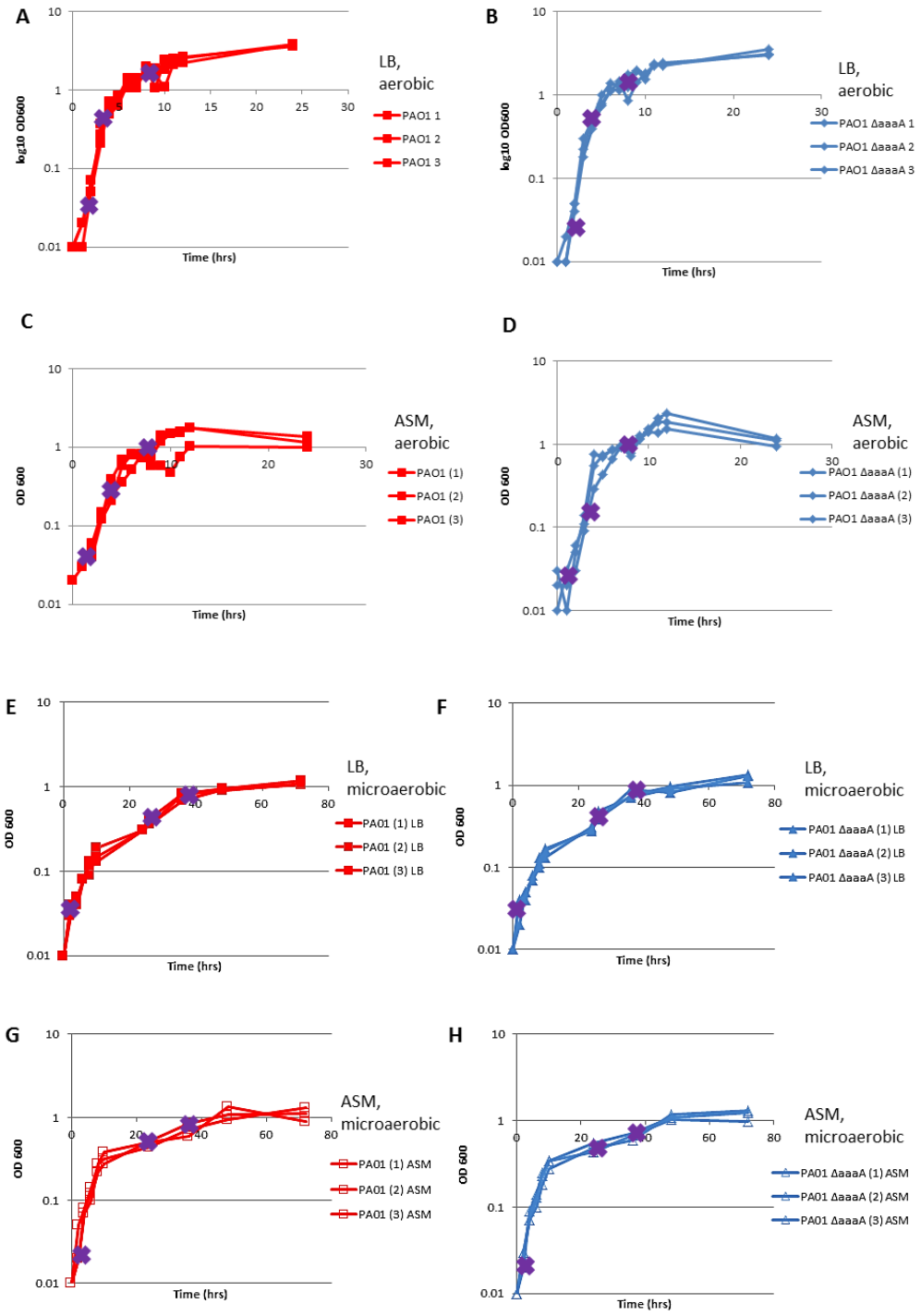


Figure 3.2.17: Sampling points representative of lag, exponential, and early stationary phase were selected along growth curves of PAO1 and PAO1 *ΔaaaA* strains in aerobic LB, aerobic ASM, microaerobic LB and microaerobic ASM. Three separate colonies for each growth condition were picked, overnights grown for 18 hours in the appropriate condition (microaerobic in a microaerobic cabinet) and standardised to OD_{600} 0.01. Sampling points included at 2, 4 and 8 hours for the aerobic conditions and 2, 24 and 36 hours for the microaerobic curves. Graphs A to D show PAO1 and PAO1 *ΔaaaA* grown in aerobic LB or ASM. Graphs E to H show PAO1 and PAO1 *ΔaaaA* grown in microaerobic LB or ASM. The purple crosses indicate where the time points intersected the growth curves.

3.2.6.2 Stage 2: RNA extraction optimisation and conversion to cDNA

To extract the total RNA from the cell samples the Qiagen RNeasy kit was used. A lysozyme buffer (materials and methods) in combination with the kit lysis buffer

was used for cell lysis of the frozen-thawed sample pellet. The manufacturer's instructions were then followed to extract the RNA. The Extracted RNA was incubated with TURBO DNAse (ambion) and tested by PCR, using *aaaA* specific primers (E1F and E1R: 5'-CAGGATTCATGTTCAAACCATTAGCTGTCGCTG and 5'-GCTATCGATTTAGTGATGGTGATGGTGATGGAACTGCCAGTTCACCCTGAG by Paredes 2014), to ensure any residual DNA was eliminated (Figure 3.2.18). The final concentrations were tested by the Nanodrop spectrometer. Table 3.2.4 shows the final concentrations. Where yields were lower than expected, future experiments could improve this by increasing the sample volume and concentrating it before processing. Low yield or quality samples were avoided: an asterisk next to the replicate number in Table 3.2.4 indicates that a sample was discarded. The Bioanalyzer (Aligent) was used to test the RNA sample purity and the RIN is quoted where identified by the bioanalyzer. A score of 10 is high quality and a score of 1 is low quality. A representative gel picture was also shown by the bioanalyzer and the quality of this was given an arbitrary score (good, medium or poor) in addition to the RIN. Due to the low yield and quality of the 2 hr time point samples (lag phase), these were omitted from the qRT-PCR analysis.

The RNA samples were standardised to 200 ng/ µl and then converted to cDNA using the Promega GoTaq 2-Step RT-qPCR System kit. This yielded cDNA of 1000 ng / µl with slight variation between batches. For consistency, the samples were standardised to 1000 ng/ µl and 1 µl from this was added to each qPCR reaction.

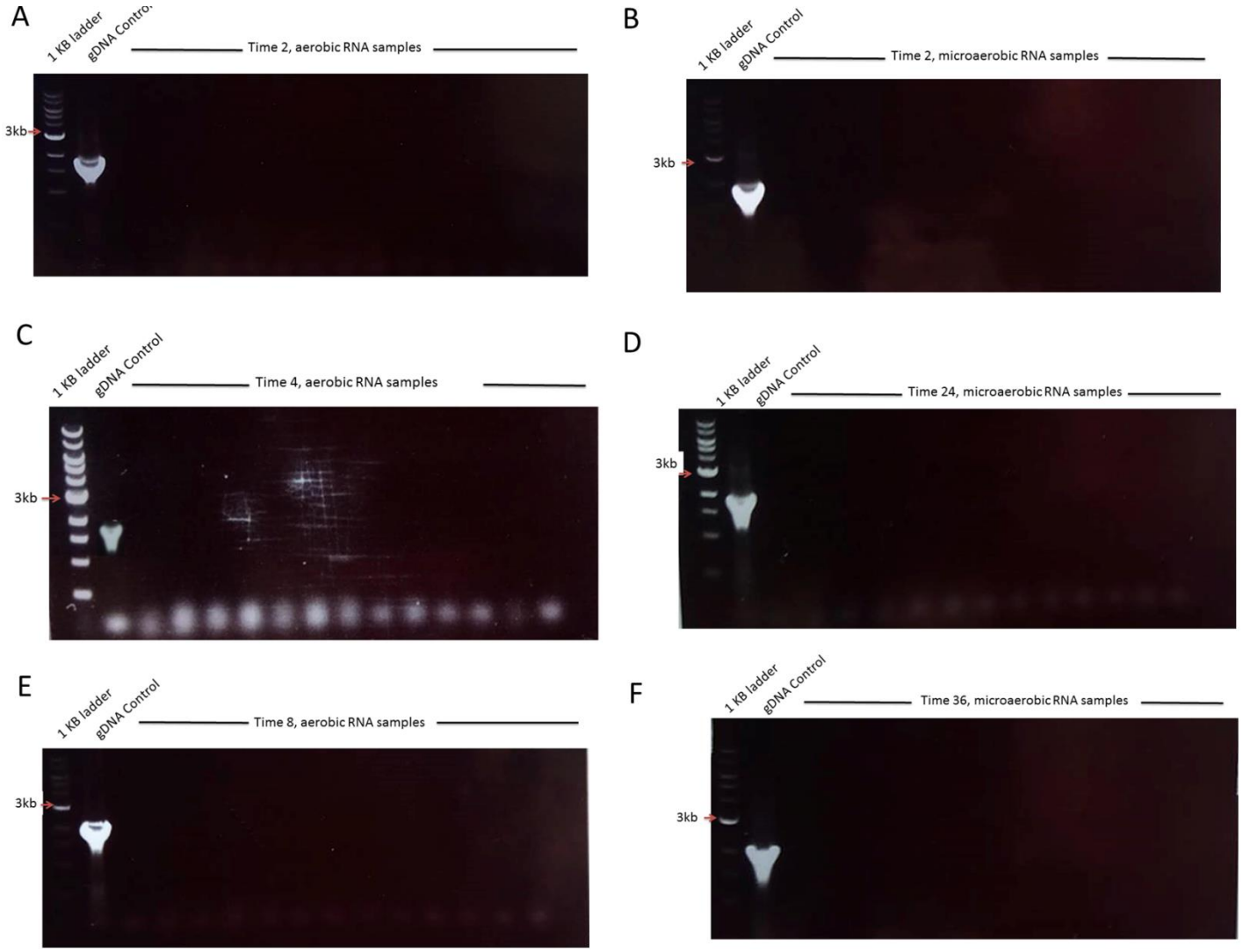


Figure 3.2.18: DNA was digested successfully in all RNA samples using TURBO DNase (Ambion). A-F shows each batch of RNA samples tested for DNA. The PCR reaction was conducted as detailed in the materials and methods with *aaaA* Fwd and Rev, E1F and E1R: 5'-CAGGATTCATGTTCAAACCATTAGCTGTCGCTG and 5'-GCTATCGATTTAGTGATGGTGATGGTGATGGAACTGCCAGTTCACCCTGAG primers by Paredes 2014). The genomic control was gDNA from PAO1.

Replicate number	Time	Condition	Strain	Concentration ng/µl	Quality (RIN)
1	T2	LB, aerobic	PAO1	33.32	10
2	T2	LB, aerobic	PAO1	21.40	8.4
3	T2	LB, aerobic	PAO1	24.49	2.6
1	T2	LB, aerobic	PAO1 Δ*aaaA*	14.24	2.6
2	T2	LB, aerobic	PAO1 Δ*aaaA*	17.01	2.6
3	T2	LB, aerobic	PAO1 Δ*aaaA*	27.16	
1	T2	ASM, aerobic	PAO1	22.5	
2	T2	ASM, aerobic	PAO1	4.5	
3	T2	ASM, aerobic	PAO1	-16.9	
1	T2	ASM, aerobic	PAO1 Δ*aaaA*	-17.1	
2	T2	ASM, aerobic	PAO1 Δ*aaaA*	-12.5	
3	T2	ASM, aerobic	PAO1 Δ*aaaA*	-8.6	
1	T4	LB, aerobic	PAO1	78.01	10
2	T4	LB, aerobic	PAO1	219.64	10
3	T4	LB, aerobic	PAO1	287.12	10
1	T4	LB, aerobic	PAO1 Δ*aaaA*	274.86	
2	T4	LB, aerobic	PAO1 Δ*aaaA*	149.15	
3	T4	LB, aerobic	PAO1 Δ*aaaA*	352.64	
1	T4	ASM, aerobic	PAO1	150	8.7
2*	T4	ASM, aerobic	PAO1	6.7	2.7
3	T4	ASM, aerobic	PAO1	63.6	
1*	T4	ASM, aerobic	PAO1 Δ*aaaA*	3.6	
2*	T4	ASM, aerobic	PAO1 Δ*aaaA*	35.2	
3	T4	ASM, aerobic	PAO1 Δ*aaaA*	38.2	10
1	T8	LB, aerobic	PAO1	185.75	9.5
2	T8	LB, aerobic	PAO1	147.43	10
3*	T8	LB, aerobic	PAO1	1.84	
1	T8	LB, aerobic	PAO1 Δ*aaaA*	252.77	10
2	T8	LB, aerobic	PAO1 Δ*aaaA*	235.49	10
3	T8	LB, aerobic	PAO1 Δ*aaaA*	250.66	10
1	T8	ASM, aerobic	PAO1	441.11	9.9
2	T8	ASM, aerobic	PAO1	224.13	
3	T8	ASM, aerobic	PAO1	47.34	
1	T8	ASM, aerobic	PAO1 Δ*aaaA*	33.12	
2*	T8	ASM, aerobic	PAO1 Δ*aaaA*	4.40	
3	T8	ASM, aerobic	PAO1 Δ*aaaA*	177.88	10
1	T2	LB, microaerobic	PAO1	?	
2	T2	LB, microaerobic	PAO1	?	
3	T2	LB, microaerobic	PAO1	?	
1	T2	LB, microaerobic	PAO1 Δ*aaaA*	?	
2	T2	LB, microaerobic	PAO1 Δ*aaaA*	?	
3	T2	LB, microaerobic	PAO1 Δ*aaaA*	?	
1	T2	ASM, microaerobic	PAO1	?	
2	T2	ASM, microaerobic	PAO1	?	
3	T2	ASM, microaerobic	PAO1	?	
1	T2	ASM, microaerobic	PAO1 Δ*aaaA*	?	
2	T2	ASM, microaerobic	PAO1 Δ*aaaA*	?	
3	T2	ASM, microaerobic	PAO1 Δ*aaaA*	?	
1*	T24	LB, microaerobic	PAO1	2.10	
2	T24	LB, microaerobic	PAO1	102.86	
3	T24	LB, microaerobic	PAO1	106.51	
1	T24	LB, microaerobic	PAO1 Δ*aaaA*	121.53	5.6
2	T24	LB, microaerobic	PAO1 Δ*aaaA*	117.82	
3*	T24	LB, microaerobic	PAO1 Δ*aaaA*	8.52	
1*	T24	ASM, microaerobic	PAO1	65.27	2.7

2	T24	ASM, microaerobic	PAO1	85.39	
3	T24	ASM, microaerobic	PAO1	79.77	
1	T24	ASM, microaerobic	PAO1 Δ*aaaA*	2.11	9.5
2*	T24	ASM, microaerobic	PAO1 Δ*aaaA*	75.52	
3	T24	ASM, microaerobic	PAO1 Δ*aaaA*	69.30	
1	T36	LB, microaerobic	PAO1	100.09	9.6
2	T36	LB, microaerobic	PAO1	45.00	
3	T36	LB, microaerobic	PAO1	165.90	
1	T36	LB, microaerobic	PAO1 Δ*aaaA*	118.70	
2	T36	LB, microaerobic	PAO1 Δ*aaaA*	29.12	
3	T36	LB, microaerobic	PAO1 Δ*aaaA*	87.55	
1	T36	ASM, microaerobic	PAO1	66.67	
2*	T36	ASM, microaerobic	PAO1	7.00	
3	T36	ASM, microaerobic	PAO1	45.03	9.9
1	T36	ASM, microaerobic	PAO1 Δ*aaaA*	47.90	
2	T36	ASM, microaerobic	PAO1 Δ*aaaA*	23.24	
3	T36	ASM, microaerobic	PAO1 Δ*aaaA*	27.36	

Table 3.2.4: RNA yield and quality from extraction process after DNA digestion. Green shading represents a good RNA sample as judged by the bioanalyzer gel picture, blue shows slight deterioration and orange show a very degraded sample. An asterisk indicates samples which were omitted from the qRT-PCR because of poor yield or quality. The lag phase (T2) samples were also not taken forward because of generally low yields.

3.2.6.3 Stage 3: reference gene selection, primer validation and assay optimisation

3.2.6.3.1 Endogenous reference gene selection

A reference gene (s) is included to ensure the comparison between samples is standardised (Pfaffl 2004).

To ensure that the endogenous reference gene used in these assays was consistently expressed in all the conditions tested, a set of 6 potentially suitable genes were tested across the spectrum of samples to be investigated using the geNorm kit by Primerdesign. These were *16S*, *gyrB*, *rpoD*, *proC*, *oprM* and *adk*. A working concentration of 300 nM of primer (including Fwd and Rev) was added per 20 µl reaction and the manufacturer's instructions followed. To analyse the data the online tool RefFinder was used (Xie *et al* 2012) which compares the different methods of assessing reference gene stability and presents the consensus of these in the form of the geometric mean (Figure 3.2.19). The *16S* gene was the most stable across the samples, followed by *gyrB*. Due to cost and time constraints only one reference gene was used: 16S. However, in future experiments the *gyrB* reference gene could also be included for greater confidence.

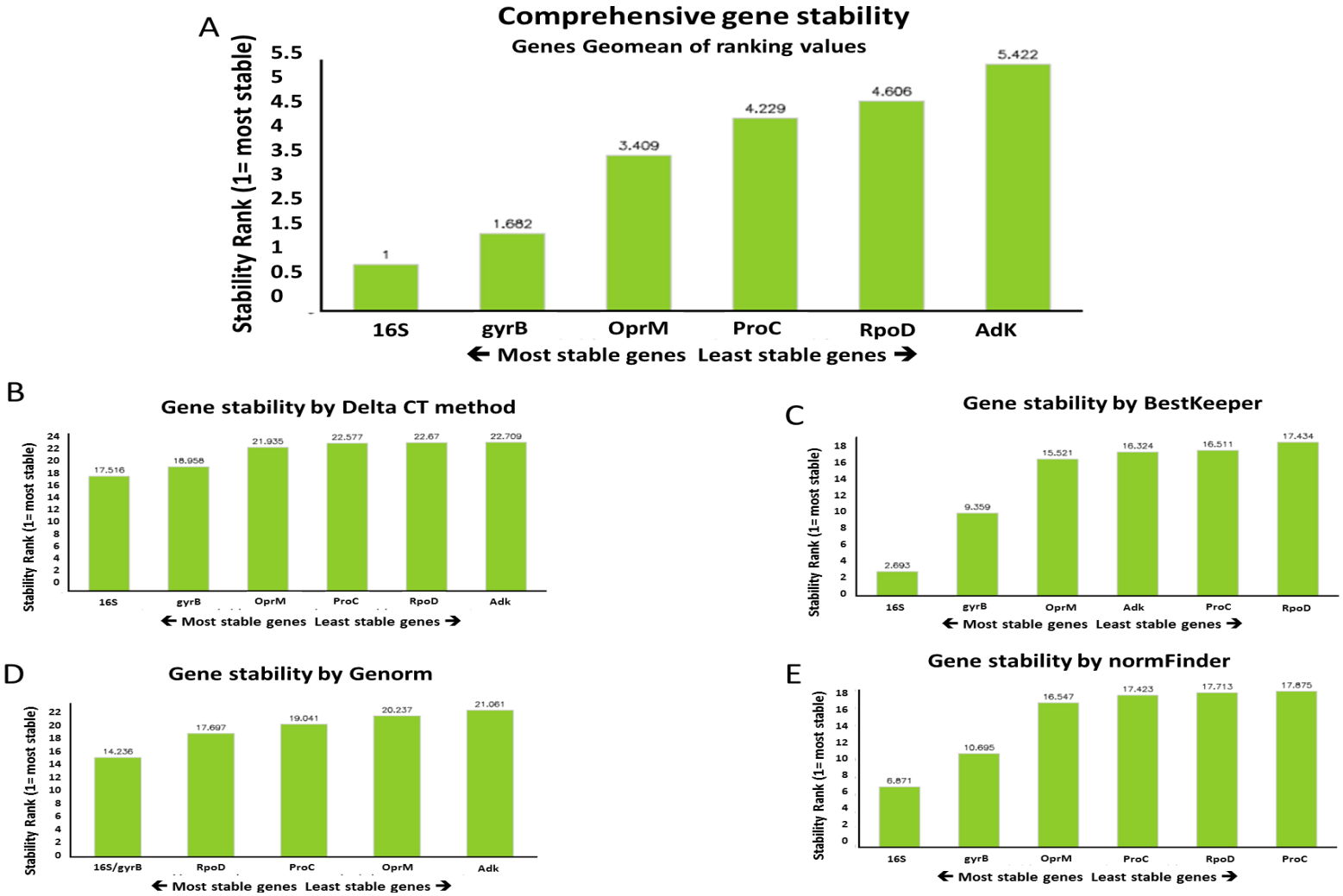
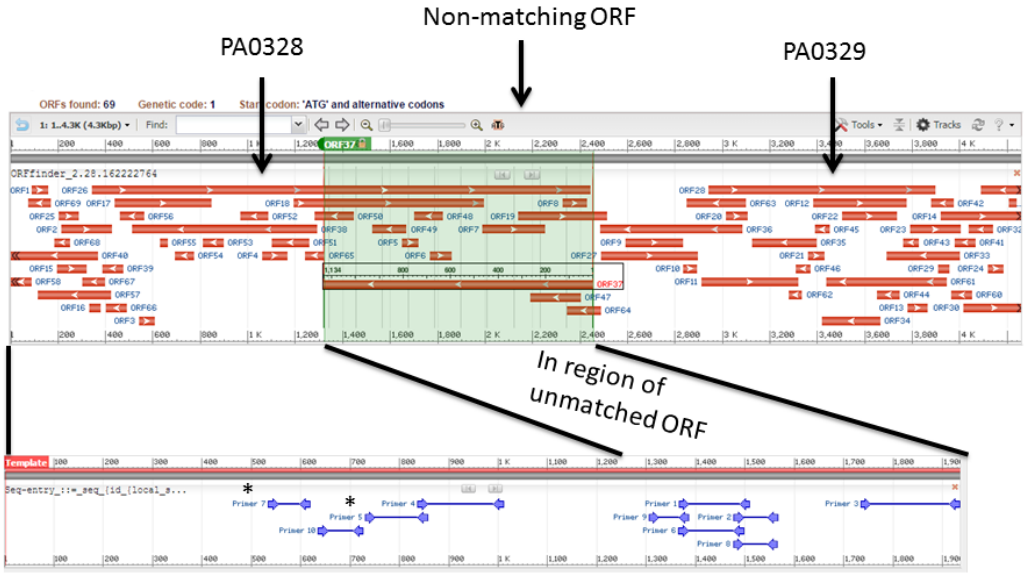


Figure 3.2.19: Reference gene selection using the online tool RefFinder shows *16S* to be the most stable in the conditions tested. A panel of endogenous reference gene candidates (*16S*, *gyrB*, *rpoD*, *proC*, *oprM* and *adk)* were tested for stability of expression in each sample to be investigated using the geNorm kit by PrimerDesign. A working concentration of 300 nM of primer (including Fwd and Rev) was added per 20 µl reaction and the manufacturer's instructions followed. All methods of analysis showed 16S to be the most stably expressed across all the samples with *gyrB* being the second most stable. Reference = Xie *et al* (2012).

3.2.6.3.2 Design of *aaaA* and *PA0329* primers and testing of their efficiency

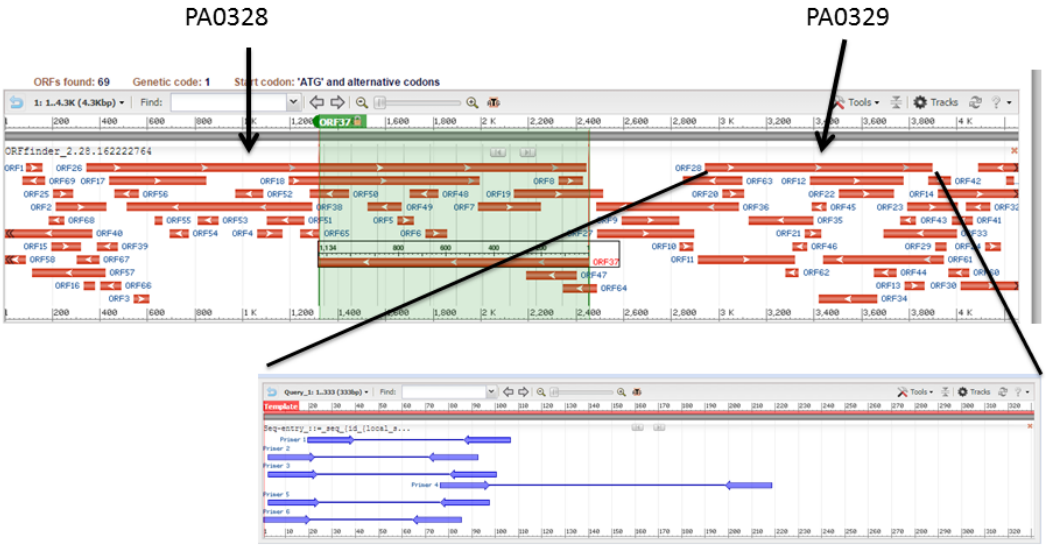
Using the NCBI primer design and BLAST tool, a number of potential primer pairs were identified and 2 pairs selected for trial based on length, specificity, and secondary structure (Figure 3.2.20). Because *aaaA* regulation is complex and not fully understood, the ORF sequence was analysed by the NCBI ORF finder to check for alternative ORFs within or overlapping with *aaaA* which could reduce assay specificity. A number of potential alternative ORFs were revealed which will be further analysed in Chapter 6. Although the primer hybridisation site could not be located in a region of *aaaA* with no overlapping alternative ORFs, the majority of the putative ORFs had no associated promoters and are unlikely to be genuine (Chapter 6). The ORF which could be transcribed from a predicted promoter (ORF 52 in this figure) does not overlap with the primer hybridisation sites. The region of ORF 37 (ORF 11 in Chapter 6) was also avoided because of its size and start site location.



Primer pair *aaaA*	Fwd 5'-3'	Rev 5'-3'	Product length bp	Binding location
5	TCCCGGTGTTGTTCCTCGAC	ACTTCCTTGTTGTCCTCGGC	127	Fwd 731-750 Rev 857-838
7	GTCACCGGCGACAAGATGTA	CAGGATCTGTTCGCGGTAGG	84	Fwd 535-554 Rev 618-599

Figure 3.2.20: Design and choosing of qRT-PCR primers for *aaaA* amplification by the NCBI BLAST Primer design tool. Chosen primers are shown with asterisks and included in the table at the bottom of the figure. The use of the NCBI ORF finder was also employed so that any potential reverse coding or internal ORFs in the *aaaA* ORF sequence would be identified and avoided if possible. More information on this is discussed in Chapter 6. Note that the direction of coding for *aaaA* and *PA0329* is from right to left (negative strand).

In addition to designing primers for *aaaA*, primers were also identified and chosen for *PA0329* using the NCBI BLAST Primer design tool. A number of potential primer pairs were identified and 2 pairs selected for trial based on length, specificity, and secondary structure (Figure 3.2.21).



Primer pair PA0329	Fwd 5'-3'	Rev 5'-3'	Product length bp	Binding location
1	TGAAGAAAGCGAAAGACGGC	TGGCCTTGTACAGTTCGCTG	87	Fwd 20-39 Rev 106-87
4	TCATTCTCACCAGCGAACTGT	GTGGCCTTGAGCACGAAGTG	142	Fwd 77-97 Rev 218-199

Figure 3.2.21: Design and selection of qRT-PCR primers for *PA0329* amplification by the NCBI BLAST Primer design tool. Chosen primers are included in the table at the bottom of the figure. The use of the NCBI ORF finder was also employed so that any potential reverse coding or internal ORFs in the *PA0329* ORF sequence would be identified and avoided if possible. Note that the direction of coding for *aaaA* and *PA0329* is from right to left (negative strand).

To achieve primer efficiencies in the range of 90-110% as stipulated by the MIQE guidelines, the two sets of *aaaA* and *PA0329* primers were tested in different master mixes, at different concentrations, different annealing temperatures and different gDNA concentrations. A standard curve was produced for each gene using 5 DNA standards in duplicate and a representative repeat is shown in Figure 3.2.22. The final conditions used are presented in Table 3.2.5.

These were accepted as the primer specific conditions to use in this assay. Although the efficiencies of one or the other primer sets might have been better with a different master mix or different annealing temp (62°C was slightly better for *aaaA*), these conditions represented the best compromise for use of the same assay conditions for both targets. The more generic qRT-PCR methods and conditions are presented in Chapter 2.

Primer pair	Accepted concentration mM	Accepted master mix	Annealing temperature	DNA concentration range (ng)	Final efficiency
aaaA_5	Not accepted	n/a	n/a	n/a	n/a
aaaA_7	0.25	AB Power Sybergreen	60	1000 -0.1	87.62%
PA0329_1	0.25	AB Power Sybergreen	60	1000 -0.1	98.61%
PA0329_4	Not accepted	n/a	n/a	n/a	n/a

Table 3.2.5: Optimised qRT-PCR conditions for the detection of *aaaA* and *PA0329* transcripts. The primer pairs *aaaA_7* and *PA0329_1* were more efficient for amplification of their respective genes.

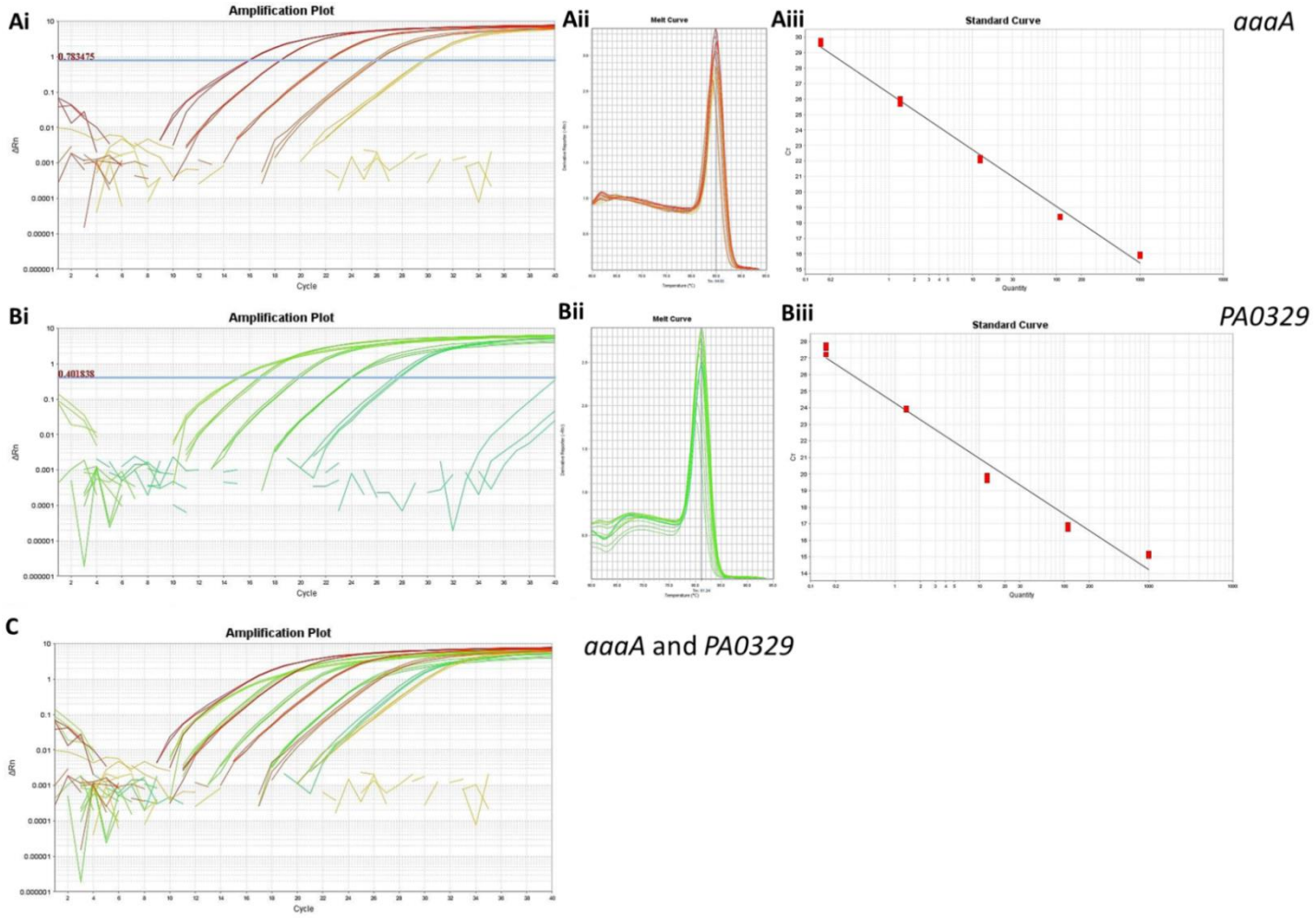


Figure 3.2.22: Optimised primer efficiencies for primer pairs aaaA_7 and PA0329_1 show efficiencies close to 90% for aaaA_7 and close to 100% for PA0329_1. Panel A=*aaaA*. Panel B=*PA0329*. Panel C=*aaaA* and *PA0329*. (i) Amplification plot. (ii) melt curve analysis. (iii) Standard curve. The AB Power Sybrgreen mastermix was combined with 0.25 mM primer. To each well of a 96 well plate, 15 µl was added. Five microliters of 1000-0.1 ng gDNA (PAO1) was added to the appropriate wells and the sealed plate centrifuged. It was then placed in a thermocycler with the annealing and extension at 60 °C. A subsequent melt-curve analysis was conducted to check for non-specific amplification. The primer efficiency was calculated from the standard curve where 100% corresponds to 3.3 cycles between each DNA standard.

3.2.6.4 Stage 4: Results from the assay

Using the conditions and primers previously described, *aaaA* and *PA0329* expression were tested. Each primer set was added to separate wells, i.e. they were not multiplexed. With further optimisation, this could be achieved in the future. The master mix was combined and added to all plates on the same day and the plates kept at 4°C while the run proceeded for previous plates. Three experimental repeats were included for each sample and where possible 3 biological replicates of each condition were included. RNA samples of poor quality were excluded (Table 3.2.4). This data should be viewed as a preliminary sample of *aaaA* expression using a new method and is intended to provide a tool for future investigation of *aaaA* expression. To help with the data interpretation, Table 3.2.6 shows a glossary of terms used in this analysis.

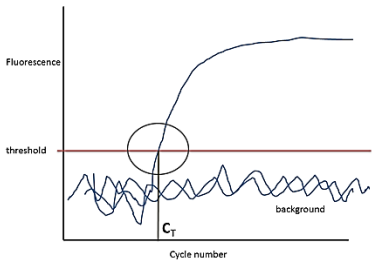
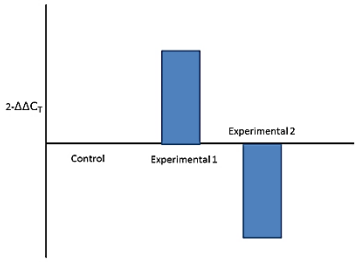
qRT-PCR glossary of terms			
Term	*Full name*	*What it means*	*Explanatory figure*
C_T	C_T value	The cycle number where the quantity of PCR product crosses the detection threshold. The lower the CT, the higher the starting amount of RNA transcript (relatively)	
Δ C_T	Delta C_T	To standardise target gene C_T values, the reference gene (16S) is subtracted from the target gene	C_T (target) – C_T (ref)=ΔC_T
ΔΔ C_T	Delta, delta C_T	Target gene expression in an experimental condition is compared to a control condition (LB, aerobic)	ΔC_T (exp) – ΔC_T (ctrl)=ΔΔC_T
2 - ΔΔ C_T	Fold change	How much the target gene expression changes in the experimental conditions versus the control condition	
ΔC_T SD	Standard deviation of delta C_T	This is calculated by the square root of the sum of squared target and reference gene standard deviations across biological replicates	S=√(SDtarget^2 + SDreference^2)
2 - ΔΔ C_T upper range	Lower range of fold change	The standard deviation of delta C_T is added to the delta delta C_T and then this is subtracted from 2 to get the lower fold change limit	2 - (ΔC_T – ΔC_T SD)
2 - ΔΔ C_T lower range	Upper range of fold change	The standard deviation of delta C_T is subtracted from the delta delta C_T and then this is subtracted from 2 to get the upper fold change limit	2 - (ΔC_T – ΔC_T SD)

Table 3.2.6: qRT-PCR terms used in the following section. Information was obtained from the Applied Biosystems qPCR manual.

3.2.6.4.1 At both exponential and early stationary phase, *aaaA* expression is low, making it difficult to make significant conclusions

Figure 3.2.23 (A) shows the fold change in *aaaA* expression in comparison to the aerobic, LB condition at exponential phase: time point 4 (aerobic) or 24 (microaerobic). In general, the ΔC_T values were high (expression of *aaaA* was low), making it difficult to distinguish between negative and positive samples.

Consequently statistical analysis could not distinguish between the different conditions and no significant differences were found. The primer efficiency was in the accepted efficiency range, so the high ΔC_T values were likely because *aaaA* expression was low, even in microaerobic conditions. To resolve this, future experiments should increase the cell density or amount of cDNA added to each reaction.

Figure 3.2.23 (B) shows the fold change in *aaaA* expression in comparison to the aerobic, LB condition at the early stationary phase: time point 8 (aerobic) or time point 36 (microaerobic). Similar to the exponential time point, the ΔC_T values were high (low *aaaA* expression). Again, the statistical analysis found no significant difference between the conditions.

3.2.6.4.2 There was much better detection of *PA0329* and this gene is potentially upregulated in microaerobic conditions during exponential phase

Figure 3.2.23 (C) shows the fold change in *PA0329* expression in comparison to the aerobic, LB condition at the exponential phase: time point 4 (aerobic) or 24 (microaerobic). This gene was detected at much earlier cycles (higher expression). Interestingly, in microaerobic conditions *PA0329* expression appears higher and this difference is significant in the PAO1 *ΔaaaA* strain background. Because the differences are small, repetition of this test with a higher sample number could be a helpful next step.

Figure 3.2.23 (D) shows the fold change in *PA0329* expression in comparison to the aerobic, LB condition at the early stationary phase: time point 8 (aerobic) or 36 (microaerobic). At this time point there were no significant differences from the control condition (LB, aerobic) except in the microaerobic LB condition (PAO1 WT background). Although not significant, there appears to be a general trend of higher expression in aerobic conditions at this time point.

3.2.6.4.3 A slight trend for higher *aaaA* expression in exponential phase is not significant

Figure 3.2.24 (A) shows the comparison of *aaaA* expression in the exponential phase and early stationary phase samples. Although it looks like there is a slight trend for the exponential phase samples to have lower ΔC_T values (higher *aaaA* expression) than the early stationary phase samples in aerobic conditions, these were not found to be significant. This could be due to the generally high ΔC_T values. The difficulty of detecting *aaaA* transcripts in microaerobic conditions in this experiment does not allow comparisons to be made.

3.2.6.4.4 A trend of higher *PA0329* expression in early stationary phase for aerobic conditions is not consistently significant

Figure 3.2.24 (B) shows the comparison of *PA0329* expression in the exponential phase and early stationary phase samples. The ΔC_T values were lower (higher *PA0329* expression) in the early stationary phase than the exponential phase in the aerobic samples. However, the only significant difference found between time points in *PA0329* expression was in the PAO1 *ΔaaaA* strain background in aerobic, LB conditions. In the microaerobic samples this difference decreases so that expression at both time points is similar.

3.2.6.4.5 Expression of *aaaA* and *PA0329* are not significantly different in 3 of 4 aerobic conditions tested but *PA0329* expression appears generally higher

Figure 3.2.25 compares *aaaA* and *PA0329* expression in each condition, at both time points. The ΔC_T values (expression) of the two genes are not significantly different in aerobic LB (exponential only) and aerobic ASM (exponential and early stationary). Qualitatively *PA0329* expression is higher than *aaaA* however. Because of the poor detection of *aaaA* in the microaerobic samples, these have been omitted from the comparison.

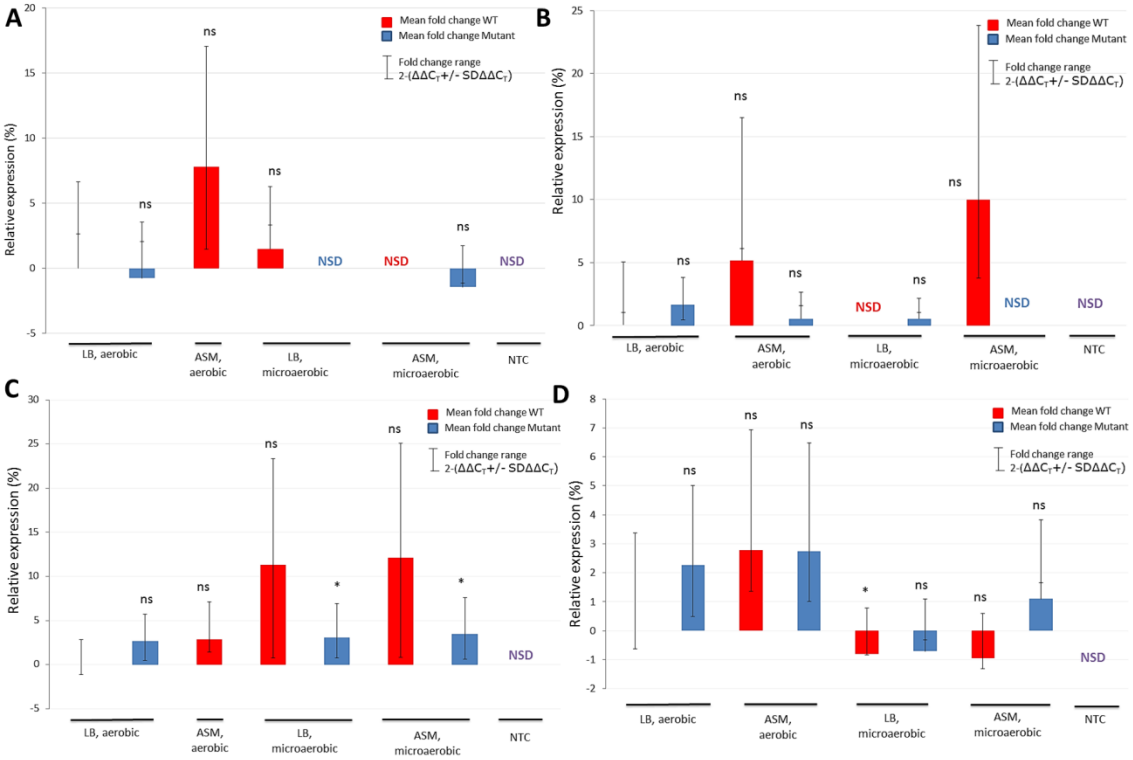


Figure 3.2.23: Relative expression of *aaaA* and *PA0329* expression in different conditions at exponential and early stationary phase, show no significant differences in *aaaA* expression and a significant increase in *PA0329* expression in the PAO1 *ΔaaaA* microaerobic samples . A= *aaaA* expression at exponential phase; B = *aaaA* expression at early stationary phase; C= *PA0329* expression at exponential phase; D= *PA0329* expression at early stationary phase. PAO1 and PAO1 *ΔaaaA* were grown in 4 different conditions: aerobic LB, aerobic ASM, microaerobic LB or microaerobic ASM. When exponential (4 hrs aerobic, 24 hrs microaerobic) or early stationary (8 hrs aerobic, 36 hrs microaerobic) phase was reached, the samples were mixed with RNA protect, lysed, and the RNA extracted. Following DNA removal and conversion to cDNA, 1 µg of cDNA was added per qRT-PCR reaction and gene specific primers used to amplify *aaaA* or *PA0329*. Each bar shows the mean fold-change in expression compared to PAO1 grown in LB, aerobic conditions. Red bars=PAO1, blue bars=PAO1 *ΔaaaA*. The error bars shows the fold change range calculated by including the standard deviation of the $\Delta C_T/\Delta\Delta C_T$ in the fold change calculations. The Livak method was used to calculate the ΔC_T and $\Delta\Delta C_T$ values with the reference gene being 16S and the control condition being WT, LB, aerobic. Three biological replicates were included where possible for each strain in each condition (at least 2 were included). The significant differences were calculated using the ΔCT and ΔCT SD values with a one-way ANOVA comparing deviation from the control sample (aerobic, LB). The RNA for the ASM aerobic mutant strain was not of sufficient quality to be included and is therefore absent from the graph. NSD = no signal detected up to 40 cycles. The detected signals after 35 cycles are included in this analysis which is why some mutant strains and NTC replicates show a value. NTC = no template control.

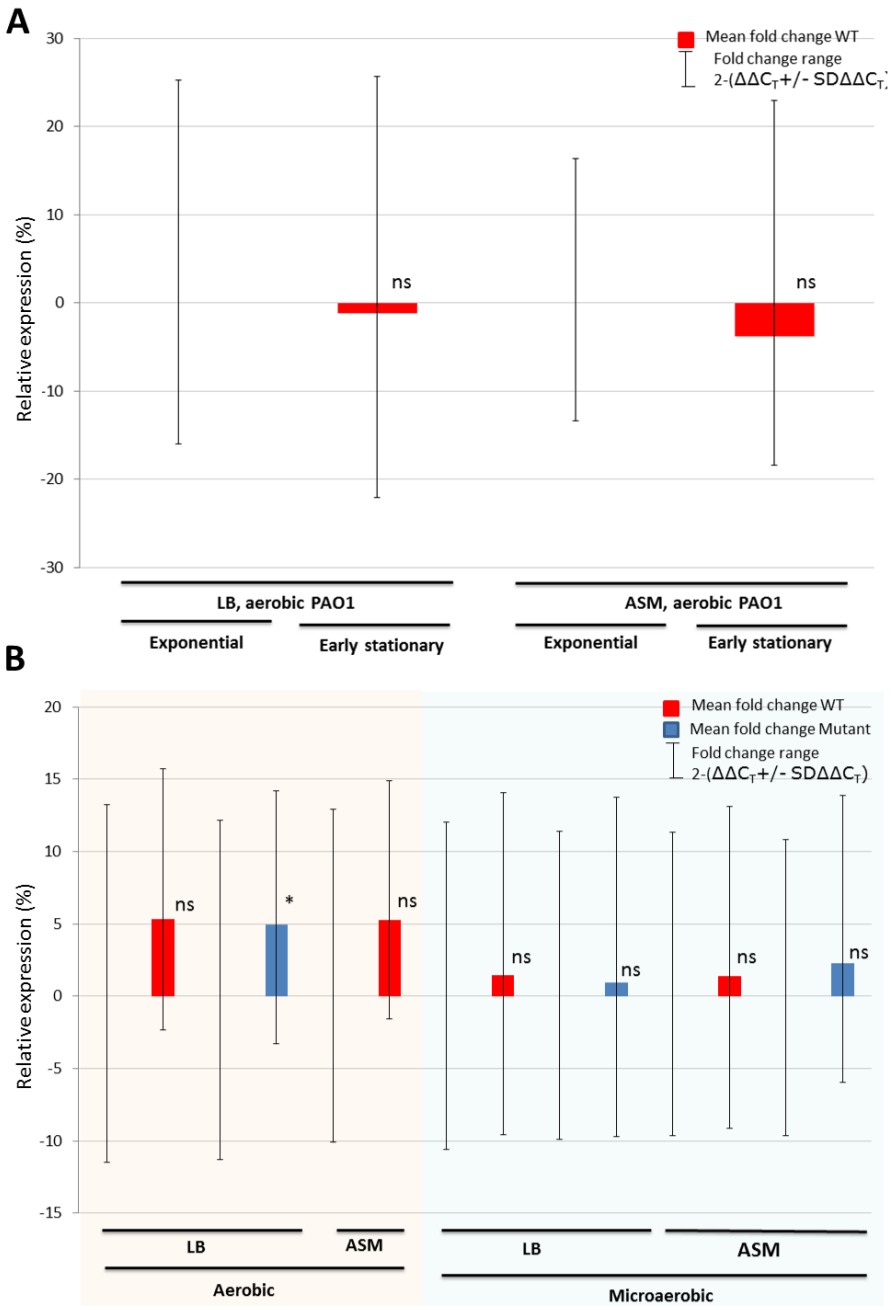


Figure 3.2.24: Differences in gene expression between growth phases in PAO1 and PAO1 *ΔaaaA* backgrounds are mostly insignificant. Panel A: relative expression in *aaaA* expression. Panel B: relative expression in *PA0329* expression. PAO1 and PAO1 *ΔaaaA* were grown in 4 different conditions: aerobic LB, aerobic ASM, microaerobic LB or microaerobic ASM. When exponential (4 hrs aerobic, 24 hrs microaerobic) or early stationary (8 hrs aerobic, 36 hrs microaerobic) phase was reached, the samples were mixed with RNA protect, lysed, and the RNA extracted. Following DNA removal and conversion to cDNA, 1 µg of cDNA was added per qRT-PCR reaction and gene specific primers used to amplify *aaaA* or *PA0329*. Each bar shows the mean fold-change in gene expression in early stationary compared to exponential. Red bars=PAO1, blue bars=PAO1 *ΔaaaA*. A signal was not detected for *aaaA* in microaerobic LB early stationary and in microaerobic ASM exponential and so microaerobic samples are omitted from graph A. The non-detected, no-template controls were also not included in the graph to facilitate ease of interpretation. The error bars show the fold change range calculated by including the standard deviation of the $\Delta C_T/\Delta\Delta C_T$ in the fold change calculations. The Livak method was used to calculate the ΔC_T and $\Delta\Delta C_T$ values with the reference gene being 16S and the control condition being exponential phase. Three biological replicates were included where possible for each strain in each condition. The significant differences were calculated using the ΔCT and ΔCT SD values with repeated non-paired t-tests performed on the 2 time points grown in equivalent conditions (e.g. aerobic LB 4 hours and 8 hours). NS = non-significant; * = P<0.05; **=P<0.01.

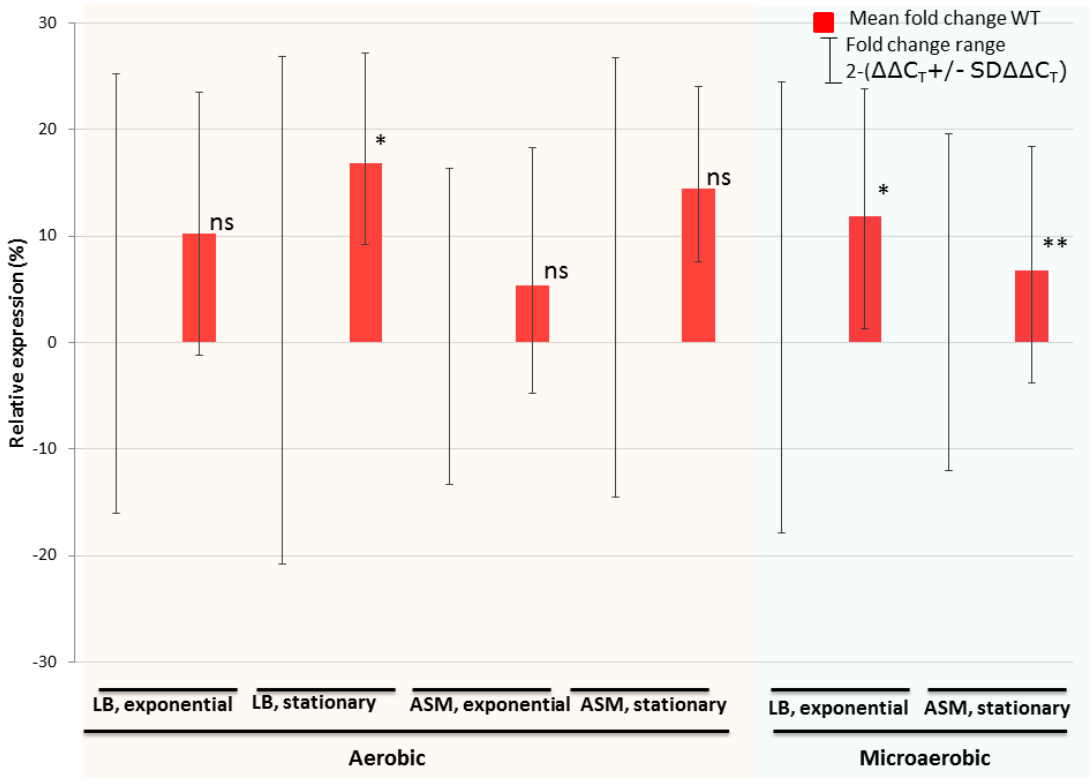


Figure 3.2.25: Relative expression of *PA0329* expression from *aaaA* expression in exponential and early stationary phase samples in the PAO1 strain show generally higher expression in *PA0329* but this is only significant in microaerobic and aerobic LB stationary phase samples. PAO1 was grown in 4 different conditions: aerobic LB, aerobic ASM, microaerobic LB or microaerobic ASM. When exponential (4 hrs aerobic, 24 hrs microaerobic) or early stationary (8 hours aerobic, 36 hours microaerobic) phase was reached, the samples were mixed with RNA protect, lysed, and the RNA extracted. Following DNA removal and conversion to cDNA, 1 µg of cDNA was added per qRT-PCR reaction and gene specific primers used to amplify *aaaA* or *PA0329*. Each red bar shows the mean fold-change in *PA0329* expression compared *aaaA*. A signal was not detected for *aaaA* in microaerobic LB early stationary and in microaerobic ASM exponential and have been omitted from the graph. The non-detected, no-template controls were also not included in the graph. The error bars show the fold change range calculated by including the standard deviation of the $\Delta C_T/\Delta\Delta C_T$ in the fold change calculations. The Livak method was used to calculate the ΔC_T and $\Delta\Delta C_T$ values with the reference gene being 16S and the control condition being *aaaA*. Three biological replicates were included where possible for each strain in each condition. The significant differences were calculated using the ΔCT and ΔCT SD values with repeated non-paired t-tests performed on the 2 genes grown in equivalent conditions (e.g. *aaaA* aerobic LB 4 hours and *PA0329* aerobic LB 4 hours). NS = non-significant; * = P<0.05; **=P<0.01.

3.3 Discussion

To better understand the advantage that AaaA could give *P. aeruginosa* in causing persistent lung infections in CF patients, it is important to identify the factors involved in its regulation. The regulation of *aaaA* appears to be multifaceted and complex, suggesting that this gene is required under precise conditions. The current chapter aimed to lay the foundations for further discovery by outlining some possible sources of regulation, attempting to map these into a plausible model and developing a tool to test this model: qRT-PCR.

3.3.1 Promoter analysis

Dr Esteban Paredes Osses (2014) identified a number of potential regulators of *aaaA* by using a miniCTX-*lux* based reporter system to measure the expression of *aaaA* in different transposon mutants. To complement this, the promoter of *aaaA* was analysed here *in silico.* Several putative regulator binding sites were found and, if genuine, these could interact with each other to modulate *aaaA* expression in different conditions. Figure 3.3.2 below presents a model to show how this interaction could occur.

3.3.1.1 RpoN and the mystery of aaaA transcription

The *aaaA* transcription start site has been difficult to place. Dr Owen Darch (2013) was not able to find the signature -10 and -35 sigma factor binding sites in the UPS. The hypothesis that transcription could be mediated by the alternative sigma factor RpoN, was generated by Paredes' (2014) demonstration of increased *PaaaA* activation in a PA14 *ΔrpoN* mutant. A putative RpoN site was identified here, suggesting RpoN may interact directly with *PaaaA*. This can now be confirmed by site-directed mutagenesis. Verification of the RpoN putative binding site is only the beginning in understanding how it controls *aaaA* expression. One hypothesis which assumes RpoN is the only sigma factor to interact directly with *PaaaA* involves the EBP, NtrC, interacting with a closed RpoN complex in nitrate-limited conditions to permit transcription. FleQ could also interact with RpoN in this way in the presence of c-di-GMP (Baraquet *et al* 2012) when biofilm formation is required.

An alternative hypothesis of RpoN mediated transcription is that it could compete with another sigma factor such as RpoS, the binding of one sigma factor sterically blocking the other. A variation of this could also occur where the binding of RpoN could sterically block the passage of the RNA polymerase activated by the other sigma factor (Schaefer *et al* 2015). However, an RpoS putative binding site in a location for these hypotheses to be correct was not found. Nevertheless, this

could be investigated further by comparing P*aaaA* activation in *Δrpos*, *ΔrpoN*, and *ΔrpoSΔrpoN* mutants using the miniCTX-*lux* reporter.

RpoN could also work with another sigma factor in the manner described in an interesting study by Zafar *et al* (2014), which demonstrates a two transcript feedback mechanism (Figure 3.3.1). An RpoS promoter overlaps a downstream RpoN promoter. When the RpoS site is activated a longer transcript is copied which includes a non-translated region containing an RBS (SD) site. This is translated into protein. When the RpoN site is activated however, a shorter transcript is copied which has less of an untranslated region lacking the RBS. The transcript is not translated and instead inhibits translation of the longer transcript. This permits negative feedback at the RNA level. As *aaaA* shows 2 potential start codons, control through this mechanism is a possibility. The levels of *aaaA* transcript produced in *ΔrpoN* and *ΔrpoS* mutant strains could be compared using qRT-PCR to test this hypothesis.

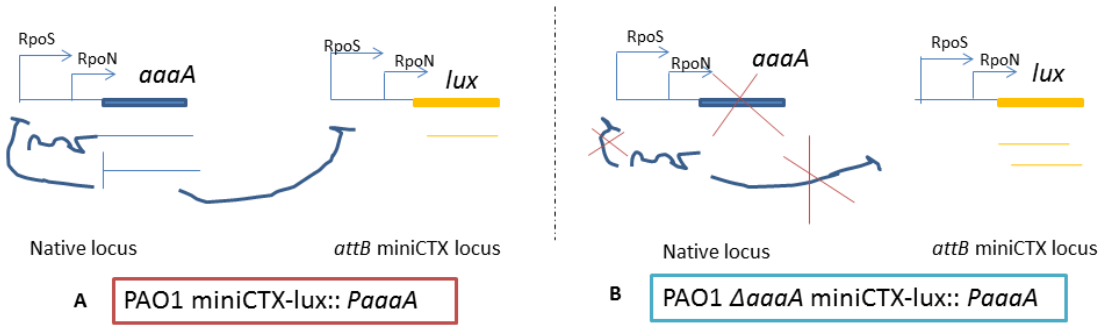


Figure 3.3.1: Potential mechanism of RpoN mediated control of *PaaaA* activation. Based on Zafar *et al* (2013), 2 transcripts are copied from 2 overlapping promoters. The more upstream RpoS promoter permits a longer transcript which allows translation. The more downstream RpoN promoter copies a shorter transcript which is untranslated and inhibits further promoter activation. Panel A and B show how this could affect the results generated by the miniCTX-*lux* reporter. Perpendicular arrows indicate inhibition.

3.3.1.2 Activators of aaaA are likely to be arginine, limited-oxygen and limited-nitrate

Three putative binding sites for regulatory proteins were found in the *aaaA* UPS region which should stimulate its expression. These were NtrC, ArgR and ArcA. NtrC has already been discussed and would activate *PaaaA* in nitrate-limited conditions. ArgR responds arginine presence by activating pathways associated with arginine catalysis. Paredes (2014) found that *aaaA* expression decreased in a *ΔargR* mutant and the addition of exogenous arginine to LB increases *aaaA* expression. This supports the model proposed in the introduction where P*aaaA* is activated in the presence of arginine and inhibited when that arginine is processed though the aerobic catalytic pathways. It also presents a positive

feedback mechanism where the product of *aaaA* activity (arginine) encourages the production of more protein. The presence of a putative ArcA site is particularly interesting because if genuine it explains how the ADI pathway is able to stimulate *aaaA* expression. This supports the hypothesis that P*aaaA* activation is increased in conditions of low oxygen where arginine is available and nitrate is limited. Site directed mutagenesis and use of qRT-PCR to measure *aaaA* expression in an *ΔarcA* mutant could be used to further confirm this.

3.3.1.3 Inhibitors of aaaA respond to nitrate abundance and cell density

The response regulator of the nitrate-sensing TCS, NarXL, represses expression from the *arcDABC* promoter (ADI pathway) by steric interference of ArgR binding (Benkert *et al* 2008). Although the putative NarL binding sites identified in the *aaaA* UPS do not overlap the putative ArgR binding site, 2 of the sites are close in location and could interfere with ArgR binding. NarL could also prevent ArcA activation through its inhibition of the *arcDABC* operon. From either mechanism, presence of nitrate would override activation of the *aaaA* promoter. The abundance of a nitrate source in the media used for to test *PaaaA* activation makes it likely that such inhibition was occurring in the experiments to date. However, growing *Pseudomonas aeruginosa* in microaerobic conditions without a nitrogen source is not easy. To circumvent this in future experiments a *narL/aaaA* double knock out mutant could be made to use as a control.

RhlR was found to have an inhibitory effect on *aaaA* in Paredes (2014). An RhlR putative binding site was found in the *aaaA* UPS suggesting direct interaction. RhlR is under the control of RpoN (Thompson *et al* 2003). It is possible that part of the RpoN repressive effect is mediated through RhlR binding. To test this, a double *ΔrhlR ΔrpoN* mutant could be compared with *ΔrhlR* and *ΔrpoN* single mutants to observe any differences in inhibitory effect.

3.3.1.4 MvaU/MvaT could act antagonistically with ArcA or FleQ

A region of DNA corresponding with the putative RpoN binding site shows the curvature and AT content typical of an MvaU/MvaT binding site. If this binding site is genuine, *aaaA* could be under a state of repression unless certain transcriptional activators are present. This could contribute to the low expression of *aaaA* observed by qRT-PCR. ArcA has been implicated in antagonising the action of MvaT/MvaU and this relationship could occur at *PaaaA* (Govantes *et al* 2000; Park *et al* 2003; Paredes 2014).

FleQ could also work together with MvaT/MvaU DNA bending to control *aaaA* expression in response to c-di-GMP during biofilm development. In an RpoN

independent manner, FleQ can bind to itself either side of the promoter and interact with FleN and c-di-GMP to distort the DNA structure. This could prevent the binding of repressors (Baraquet *et al* 2012).

3.3.1.5 For the future

Regulation at the *aaaA* promoter appears to include fine-tuned interactions of multiple systems. Investigating which of these are operating could be achieved by a combination of site-directed mutagenesis and qRT-PCR. Promoter pull down is also an option. Revealing the direct regulation networks governing expression of *aaaA* would aid in elucidating its function *in vivo*, thereby revealing how it supports *P. aeruginosa* in a host environment.

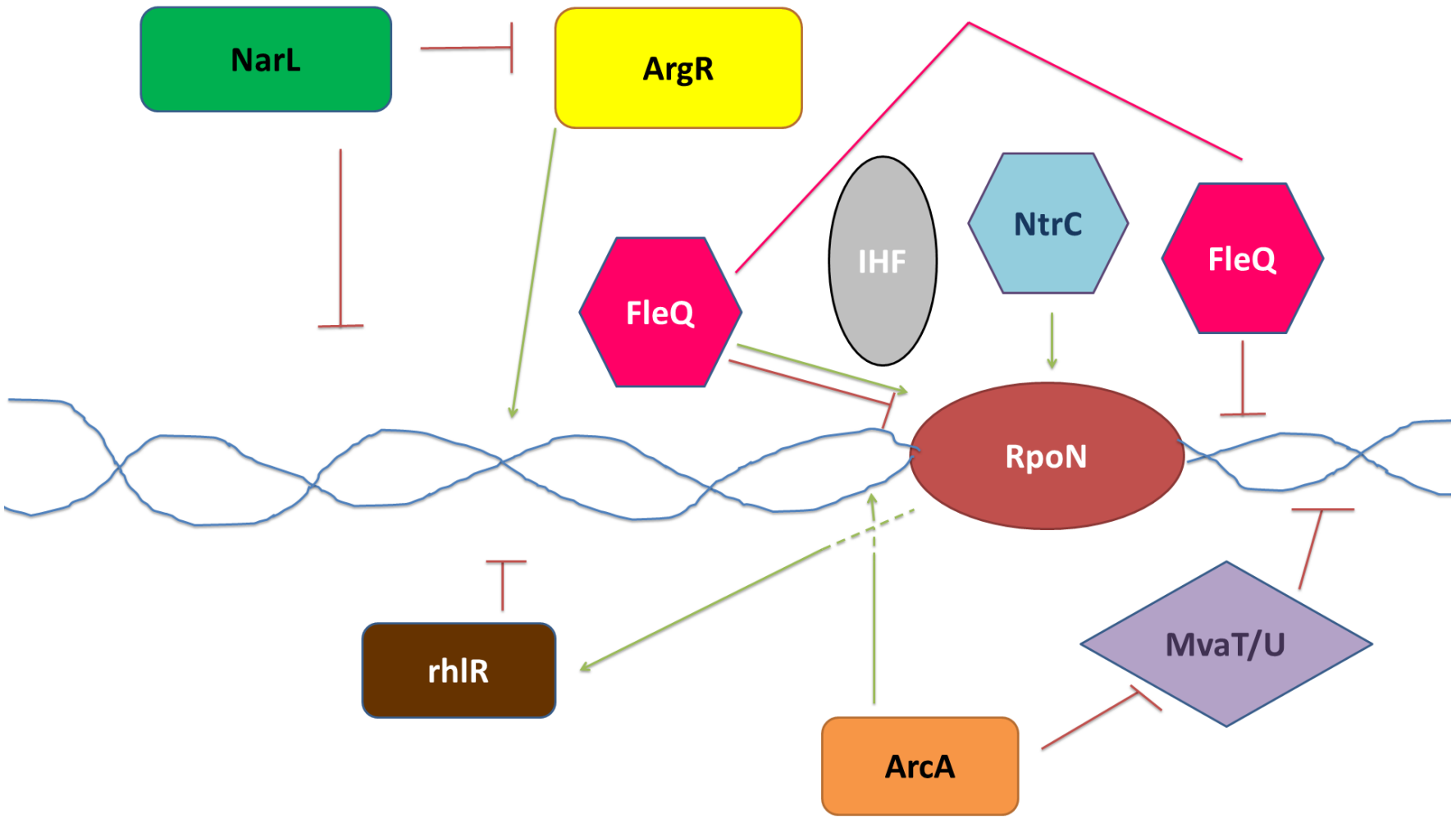


Figure 3.3.2: How the putative *PaaaA*-binding regulators of *aaaA* expression could interact with each other. Red arrows represent inhibitory interactions and green arrows activating interactions. Interactions could be through steric competition, DNA bending, or protein-protein interactions. References: Baraquet *et al* 2012; Thompson *et al* 2003; Benkert *et al* 2008; Govantes *et al* 2000 and Park *et al* 2003).

3.3.2 The association of *aaaA* with other genes: STRING database findings

In addition to the *in silico* promoter analysis, possible connections *aaaA* could have to proteins in *P. aeruginosa* was investigated using the STRING database. One group of putatively connected genes shared upstream putative ArgR binding motifs. Although the functions of these genes have not yet been determined, the presence of ArgR binding sites could link them to arginine metabolism. Further investigation of these genes may fill in a missing piece of the puzzle of *aaaA* regulation.

The second group of putatively connected genes belong to the Type V secretion group of proteins and are OM enzymes (lipase and endopeptidase). This suggests a similar function, location and secretion mechanism. It would be interesting to see whether they have any regulators manging their expression in common. Primers could be designed for qRT-PCR to compare differences in expression of these genes in different regulator mutant backgrounds with differences in *aaaA* expression.

Iron acquisition and *aaaA* seem to be related according to the STRING results. It is possible that when *P. aeruginosa* resides in certain *in vivo* settings it is experiencing low oxygen and low iron conditions simultaneously. Mashburn *et al* (2005) noted that 5% of the *P. aeruginosa* genome is expressed differently *in vivo* and that this 5% includes iron acquisition and genes involved in low oxygen growth. This would suggest that co-expression of *aaaA* and iron acquisition genes could occur when *P. aeruginosa* grows in such environments. Iron acquisition gene expression could also be affected by oxidative stress instigated by the host immune system. Hi Dao *et al* (1999) found that presence of reactive oxygen species decreased pyoverdine production, which the authors hypothesised was a mechanism of decreasing the damage from oxidising agents. This would link to *aaaA's* potential role in modulating the host immune defence system by disrupting the balance of NO production (Luckett *et al* 2012).

3.3.3 In line with previous data, *PaaaA* activation is reduced in the PAO1 WT, but this cannot be explained by RpoN mediated repression

Comparison of PAO1 miniCTX-*lux*::P*aaaA* and PAO1 *ΔaaaA* miniCTX-*lux*::P*aaaA* strains demonstrated that *PaaaA* in the PAO1 *ΔaaaA* mutant is activated more than in the PAO1 WT. This supports the negative regulation loop hypothesis. In Figure 3.1.5 (introduction) some mechanisms are proposed. (1) Repression occurs at the RNA level: this could occur by the dual transcript mechanism

described above and can be tested by qRT-PCR. (2) Repression is mediated by a direct AaaA enzyme-DNA interaction: this is unlikely as AaaA does not have a DNA binding domain and is OM localised (Luckett *et al* 2012). (3) A regulator responds to AaaA localisation to the OM: this has not been investigated here. (4) A downstream metabolite from AaaA activity stimulates TF inhibition of AaaA. This could be through MvaT/MvaU and RpoN or another factor.

Paredes (2014) found RpoN reduced *PaaaA* activation in a PA14 background. Repetition of the experiment in a PAO1 background with a complemented control did not find a difference. The problem is, we do not know how RpoN is interacting with *aaaA*. To understand this discrepancy, and determine if *aaaA* autoregulation and RpoN are related, a combination of site-directed mutagenesis and qRT-PCR analysis can be utlilised.

3.3.4 qRT-PCR development

The miniCTX-*lux* reporter system has limitations. Valid conclusions rely on the luminescence output being influenced solely by the fused promoter, and this is not always the case (Paredes, 2014). The integration site was shown to be neutral (Hoang *et al* 2000), but if there were regulatory elements of *aaaA* encoded in the ORF which have not yet been identified, these would be missing from the fusion. Due to the *aaaA* regulatory network complexity, use of another investigatory tool to complement the miniCTX-*lux* reporter data would be helpful in unravelling the unknowns. For this purpose an *aaaA* specific qRT-PCR assay was developed. This technique also has the advantage of comparing expression of multiple genes in multiple conditions. Four conditions were chosen to pilot- test this assay: aerobic LB; aerobic artificial sputum media (ASM, Palmer *et al* 2007 version); microaerobic LB; and microaerobic ASM. Differences in *aaaA* expression between these conditions could help link the environment with the previously discussed *aaaA* regulatory network.

3.3.4.1 Some technical considerations for further use

To provide suitable representation of *aaaA* expression across the growth stages, samples were taken at lag, exponential, and early stationary phase. A volume of 600 µl was mixed 1:2 with RNA protect. This proved to be too dilute for significant conclusions to be drawn and in future it would be recommended to take 2-5 ml and concentrate the cells by centrifugation before adding the RNA protect.

The Qiagen RNeasy method of extraction did not cope with the small amount of total RNA available in the lag phase samples but was otherwise a suitable method

of extraction. The removal DNA by TURBO DNase (ambion) effectively removed DNA contamination and would be recommended for future use. The cDNA conversion by the Promega GoTaq 2-Step RT-qPCR System was also efficient and produced a high and consistent yield from a relatively low starting concentration of RNA.

To choose an endogenous reference gene which would be consistently expressed in all experimental conditions the geNorm kit by PrimerDesign was a convenient and consistent option. Six genes were included in the kit of which *16S* was found to be the most stable and *gyrb* the second most stable (Bustin *et al* 2009). These reference genes could be used in future experiments using the conditions tested here. In new strain backgrounds or environmental conditions another reference gene screen would need to be conducted with the same panel of genes (MIQE guidelines; Bustin *et al* 2009).

To be able to use the Livak method of comparative expression analysis, the primer efficiencies should be close to 100% (Bustin *et al* 2009), preferably between 90% and 110%. The primer pairs for *aaaA* and *PA0329* were designed using the NCBI tool and tested for efficiency using the standard curve method. The pairs showing the best efficiencies were chosen and can be used in future assays. The Roche Sybergreen master mix was found to be the best compromise between *aaaA* and *PA0329* efficiencies.

3.3.4.2 Expression of aaaA is very low and the assay requires adjustment to compensate

3.3.4.2.1 The expression of *aaaA* is low in all conditions tested compared to *PA0329*

The expression of *aaaA* and *PA0329* across the 4 different conditions was investigated. At both time points the expression of *aaaA* in these samples appeared to be generally low which made the significant difference between the positive and negative samples smaller. It also resulted in an undetectable signal in some sample groups. Wild-type *aaaA* is unable to be detected by immunoblot (Paredes 2014), suggesting that the expression is low rather than the assay particularly insensitive. Now this has been determined, future assays should increase the cell sample concentration. It may also be helpful to increase the concentration of cDNA added to each reaction, for example to 2 or 3 µg rather than 1 µg.

From past miniCTX-*lux* reporter data (Paredes 2014) and from the *in silico* promoter analysis, *aaaA* expression was predicted to increase in low oxygen concentrations. In this test, a significant difference between media type or oxygen tension was not found. Future experiments will need to confirm this because the generally low expression (high C_T values) makes the data difficult to interpret.

The expression of *PA0329* was much higher, leading to earlier detection of the PCR product. Interestingly the expression of this gene appeared to increase in microaerobic conditions (at exponential phase), although this was only significant in the PAO1 *ΔaaaA* background. The function of *PA0329* is unknown. If this gene is upregulated in microaerobic conditions specifically at exponential phase, this suggests that it contributes to *P. aeruginosa* survival in low oxygen environments.

3.3.4.2.2 Gene expression of *aaaA* and *PA0329* in exponential and early stationary phase does not significantly differ in the majority of conditions tested

Comparison of *aaaA* expression at the exponential and early stationary phase for selection of the most appropriate sampling point for future assays did not show a significant difference. This could be because of the generally low expression and further confirmation with a higher RNA concentration is required. It is predicted that if a difference between growth phases in *aaaA* expression exists, this will be at exponential. If differences in expression are revealed in future experiments, the time point with the highest *aaaA* expression can be chosen.

PA0329 expression was not significantly different between time points in the microaerobic conditions. There was also no significant difference in the aerobic conditions except in the PAO1 *ΔaaaA* LB samples where *PA0329* expression was higher in stationary phase. This suggests that the exponential phase time point would be suitable for further investigations of *PA0329* expression.

3.3.4.2.3 There could be an association between *aaaA* and *PA0329*

The STRING database output suggested a connection between the expression of *aaaA* and *PA0329*. The preliminary results shown here suggest that they could be co-expressed. There are significant differences in expression between the 2 genes in microaerobic conditions, but this could be because it was more difficult to get detectable signal for *aaaA* in these conditions. A repeat experiment with a higher cell concentration would be useful to determine if this difference was an experimental artefact or if the two genes are expressed differently under low oxygen conditions. As *PA0329* expression increased in microaerobic conditions at

exponential phase, the two genes could be associated by upregulation in low oxygenated environments which may or may not be dependent on cell density.

3.3.4.2.4 The two transcript autoregulation hypothesis could be tested using this assay with a small amendment

One hypothesis for *aaaA* autoregulation was by the production of 2 transcripts from 2 sigma factor binding sites, where one shorter transcript would inhibit production of a second longer translatable transcript. The primers designed in this chapter hybridise within the *aaaA* ORF and thus to either length transcript. To test this hypothesis, the primers designed here could be compared to a primer set which would hybridise just prior to the putative RpoN promoter dependent start of transcription.

3.3.4.2.5 Future priorities

This assay could be improved by a higher concentration of cells and inclusion of a second endogenous reference gene. Once these issues have been addressed, this assay can be used to test a number of hypotheses including *aaaA* expression in the background of various regulator mutants in microaerobic conditions.

3.3.5 Final conclusions

The *aaaA* gene appears to be under the regulation of multiple systems ensuring that AaaA can rescue the cell in nitrate and oxygen limited conditions. There is a possible link with biofilm formation through FleQ and c-di-GMP and Chapter 6 investigates this link further. To study these overlapping systems, different environmental conditions and regulator knockouts will have to be examined. Future investigation using qRT-PCR and site-directed mutagenesis can now be pursued to validate the putative regulator binding sites and place *aaaA* more firmly within its regulation network. The next chapter investigates AaaA in the context of environmental conditions and strain backgrounds relevant to the CF airway.

4 Chapter 4: The Relationship of AaaA with Cystic Fibrosis

Utilisation of a panel of cystic fibrosis isolates to investigate the relationship between the arginine specific aminopeptidase autotransporter of *P. aeruginosa* and the Cystic Fibrosis airway.

4.1 Introduction

In this chapter the role of the arginine specific amino peptidase (AaaA) in the context of the cystic fibrosis (CF) lung is investigated. The central questions here are:

- Is AaaA needed in the CF airway for *P. aeruginosa* persistence?
- When does the action of AaaA give *P. aeruginosa* an advantage in the CF airway?
- What is the role of AaaA in the CF airway?

To investigate these in a non-invasive manner, expression and activity of AaaA was tested in a panel of *P. aeruginosa* CF isolates. To see whether AaaA correlated with any particular traits, a range of phenotypic tests were performed to build a profile for each strain.

Figure 4.1.1 and Figure 4.1.2 below show the isolates that were studied.

Strain ID	Shorthand reference	Derived from
13W409030	CF 030	Unknown epidemic strain
13W405098	CF 098	Liverpool epidemic strain
13W402129	CF 129	Liverpool epidemic strain
13W413326	CF 326	Liverpool epidemic strain
13W402393	CF 393	Unknown epidemic strain
13W408484	CF 484	Unknown epidemic strain
13W407570	CF 570	Liverpool epidemic strain
13W409892	CF 892	Unknown epidemic strain
13W412971	CF 971	Unknown epidemic strain
13W406983	CF 983	Liverpool epidemic strain

Figure 4.1.1: *P. aeruginosa* clinical isolates from Cystic Fibrosis patient sputum. Kindly donated by Dr Matthew Hurley and his team in the QMC Microbiology department.

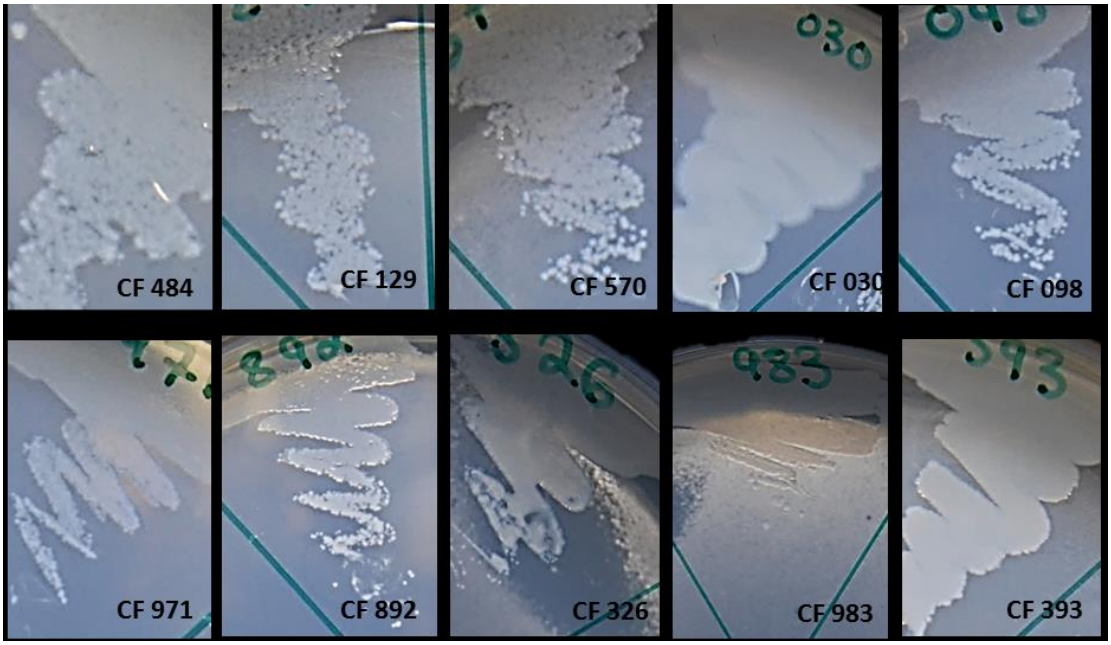


Figure 4.1.2: Three CF isolates exhibited mucoid phenotypes or failed to generate defined colonies: CF 326, CF 393 and CF 030. The indicated strains were grown overnight on LB agar plates at 37°C.

4.1.1 Background

P. aeruginosa seems to be a particularly tenacious member of the CF airway microbiota and in some cases is so successful that it defies both immune (Jensen *et al* 2010), and antibiotic attack (Bryan *et al* 1972; Kobayashi *et al* 1972; Lyczak *et al* 2002) in addition to the challenges arising from an environment low in

oxygen (Worlitzsch *et al* 2002; Hassett *et al* 2009; Rogers *et al* 2004). The adaption of *P. aeruginosa* to the specific environment of the CF airway has likely been heavily aided by its metabolic flexibility (Palmer *et al* 2005; Arai 2011). As was discussed in Chapter 1*, P. aeruginosa* contains mechanisms to generate ATP in conditions where oxygen is not available. This includes using nitrate as an alternative electron acceptor through the denitrification pathway (Berks *et al* 1995; Arai 2011; Palmer *et al* 2007), the fermentation of pyruvate (Eschbach *et al* 2004) and the fermentation of arginine using the arginine deiminase (ADI) pathway (Maghnouj *et al* 1998).

The availability of oxygen in the CF airway has been found to be in short supply (Worlitzsch *et al* 2002; Hassett *et al* 2009; Rogers *et al* 2004; Worlitzsch *et al* 2009; Tunney *et al* 2008). Worlitzsch *et al* (2002) demonstrated that the high number of bacteria and related neutrophil attack resulted in an oxygen deficit within CF mucus which increased with depth from the surface. Additionally, isolation of a high quantity of anaerobic bacteria from the CF airway indicates that environments favourable to these bacteria exist (Jones 2011; Rogers *et al* 2004; Worlitzsch *et al* 2009; Tunney *et al* 2008). Although the exact location of *P. aeruginosa's* residence in the CF airway has been contested by different studies (Hassett *et al* 2009; Worlitzsch *et al* 2002), the researchers agree that the bacteria migrate to and from communities close (or directly adjacent) to the epithelial layer in the deeper layers of mucus, and are consequently exposed to hypoxic conditions.

In response to oxygen paucity, *P. aeruginosa* utilizes nitrogen as an electron acceptor. In an extensive study by Quinn and colleagues (2014), the transcription of different metabolic pathways was compared between CF sputum and healthy control saliva samples. It was found that nitrate reductases were over-represented in CF sputum. Furthermore, Kolpen *et al* (2014) found a continual generation of N_2O and depletion of NO_3 in CF mucus. Interestingly, although plenty of denitrification pathway genes were expressed, there was a lack of genes encoding the other half of the nitrate cycle, the oxidative reactions. This correlates with an accumulation of ammonia found in the surrounding environment, which is a product of an incomplete nitrogen cycle. Together, this suggests *P. aeruginosa* exists in a state of reduction with an imbalance of NAD+/NADH, making the action of electron shutting molecules such as redox active phenazines, vitally important (Quinn *et al* 2014). A reliance on nitrogen in hypoxic conditions makes acquisition of nitrate sources imperative. The amount of nitrate in CF sputum (approximately 400 μM with a maximum of 1 mM) is

sufficient for bacterial growth by denitrification (Line *et al* 2014; Grasemann *et al* 1998; Palmer *et al* 2007; Kolpen *et al* 2014) and is composed of ammonium, nitrate and nitrogen containing amino acids (Gaston *et al* 2002; Barth and Pitt 1996; Thomas *et al* 2000).

Nitrogen ions originate from multiple sources. One route is through host ingestion of food containing nitrate and nitrite. This passes through the digestive tract and is either excreted through the kidneys or absorbed into the bloodstream, where it reaches the tissues (Lundberg, Weitzberg and Gladwin 2008). Another source of nitrogen could be generated by inducible nitric oxide synthase (iNOS) activity, an immune system component which converts L-arginine into the reactive oxygen species nitric oxide (NO). Elevated levels of exhaled NO can indicate upper respiratory inflammation and theoretically should predict airway inflammation occurring in CF patients (Robbins and Grisham 1997). This is not the case however, and could be due to iNOS inhibition or the trapping of NO in the abnormally thick mucus layer where it is oxidised to nitrate (Figure 4.1.3). Sputum sample evaluation showed increased NO_3 and NO_2 concentrations in exacerbating CF patients; (Jones *et al* 2000 and Linnane *et al* 1998) demonstrating that host generation of NO could be exploited by *P. aeruginosa* to support growth. Evidence also suggests that iNOS is outcompeted for its substrate L-arginine. Grasemann *et al* (2006) found reduced L-arginine concentrations in the plasma of CF patients undergoing pulmonary exacerbations (71% of the control L-arginine concentration) which increased after antibiotic treatment. Depletion by *P. aeruginosa* arginine fermentation or increased consumption of arginine by host immune system mechanisms could be responsible. Grasemann *et al* (2005) showed that the enzyme arginase, which shares L-arginine as a substrate, exhibited increased activity in CF sputum. It is also possible that other mechanisms contribute to NO consumption, including its conversion into inactive nitrosylated NO, which is mediated by pyocyanin (Linnane *et al* 1998).

When sources of nitrate and oxygen are depleted, *P. aeruginosa* can generate ATP from arginine using the ADI pathway (Verhoogt *et al* 1992; Stalon *et al* 1967; Luthi *et al* 1990; 1986). A reduced amount of bioavailable arginine was measured in CF patient airways in comparison to the healthy controls, particularly during times of exacerbation. Plasma concentrations of arginine were reported as 48 (+/- 20) during an exacerbation, whereas control levels were 68 (+/- 19) (Grasemann *et al* 2006). This indicates that in CF, arginine could be a limited

resource. The release of arginine from peptides could therefore support *P. aeruginosa* growth in areas of low oxygen concentration.

Pyruvate can be fermented to support *P. aeruginosa* survival. The products can be acetate, lactate or succinate. The anaerobic regulator ANR promotes the pyruvate to acetate pathway (Eschbach *et al* 2004) which is aided by phenazine redox cycling (Glasser 2014). The advantage of producing acetate is that it can be coupled with ATP synthesis using acetate kinase (Glasser 2014). Quinn *et al* (2014) identified pyruvate metabolism as the switch between fermentation and oxidative phosphorylation, supporting Glasser's (2014) theory that pyruvate can maintain survival of *P. aeruginosa* through this phenazine-acetate-ATP link.

A reduced pH has been observed in CF airways (Ballard *et al* 1999; Poulsen *et al* 1994; Poulsen and Machen 1996). This has been linked to reduced efficacy in bacterial killing mechanisms (Pezzulo *et al* 2012). The reduction in host defence strategies likely plays another part in aiding *P. aeruginosa's* continued residence. However, a lower pH would be less favourable for bacterial growth (Tsuji *et al* 1981) and therefore it would make sense for the bacterium to contain a coping mechanism for this. Conversely, the end product of denitrification and an incomplete nitrogen cycle is basic (ammonia) (Gaston *et al* 2002; Barth and Pitt 1996; Thomas *et al* 2000) which may help balance the pH in *P. aeruginosa's* immediate environment. Arginine itself contains a basic side chain and has been proposed as a way of increasing the pH of biofilms, facilitating their destruction by antibiotic action (Boriello *et al* 2006; Lebeaux *et al* 2014). Increased supplies of arginine may help to regulate pH in a primarily acidic environment. AaaA could also be useful in fulfilling this purpose.

A fine-tuned metabolic balancing system appears to be occurring to maintain a favourable growth environment for *P. aeruginosa* in the CF airway. AaaA may contribute to this balance by modulating the levels of free arginine available in its vicinity. Another layer to the environmental complexity is the biofilm mode of growth *P. aeruginosa* typically chooses in the CF lung (Worlitzsch *et al* 2002). Upon entering the CF lung, *P. aeruginosa* migrates deep into the mucus layer and switches from a planktonic to a sessile mode of growth in close proximity or in conjunction with the airway epithelial cells (Haussler *et al* 2003; Chi *et al* 1991; Garcia-Medina *et al* 2005; Darling *et al* 2004; Lanotte *et al* 2004; Worlitzsch *et al* 2002). The environment becomes increasingly anaerobic, is viscous with ample neutrophil derived eDNA and mucin proteins in addition to its own secreted ECM. Over time, the favouring of certain mutations, such as in *lasR, rpoN* and *mucA,*

has been observed (Yang *et al* 2011; Smith *et al* 2006; Boucher *et al* 1997). The acute/chronic switch, comprised of the GacS/GacA/RetS/LadS systems, (Goodman *et al* 2004, 2009; Ventre *et al* 2006; Mikkelsen *et al* 2011) is also seen to swing towards the chronic setting (Jimenez *et al* 2012). This would stimulate the expression of biofilm related genes such as *pel* and the Type VI secretion system, while decreasing the expression of acute virulence (excluding pyocyanin) and motility genes (Goodman *et al* 2004; Jimenez *et al* 2012). The majority of isolates investigated here are epidemic CF strains and are therefore likely to contain at least one of these mutations and be in a chronic mode of survival. In contrast, the PAO1 and PAO1 *ΔaaaA* strains (Nottingham subtype) are laboratory adapted and consequently not in a chronic state. This could influence how AaaA is utilized by *P. aeruginosa* as it was hypothesised that AaaA is required more in a chronic background. This hypothesis is supported by a burn wound PAO1 infection model (Luckett *et al* 2012) where the mutation of *aaaA* had no effect in the acute condition. The surrounding environment is also likely to influence the *aaaA* upregulation. To allow for this, some of the conditions typical of the CF lung were investigated, including a range of NaCl, nitrate, pH and oxygen concentrations, to examine whether any of these has a particular effect upon AaaA.

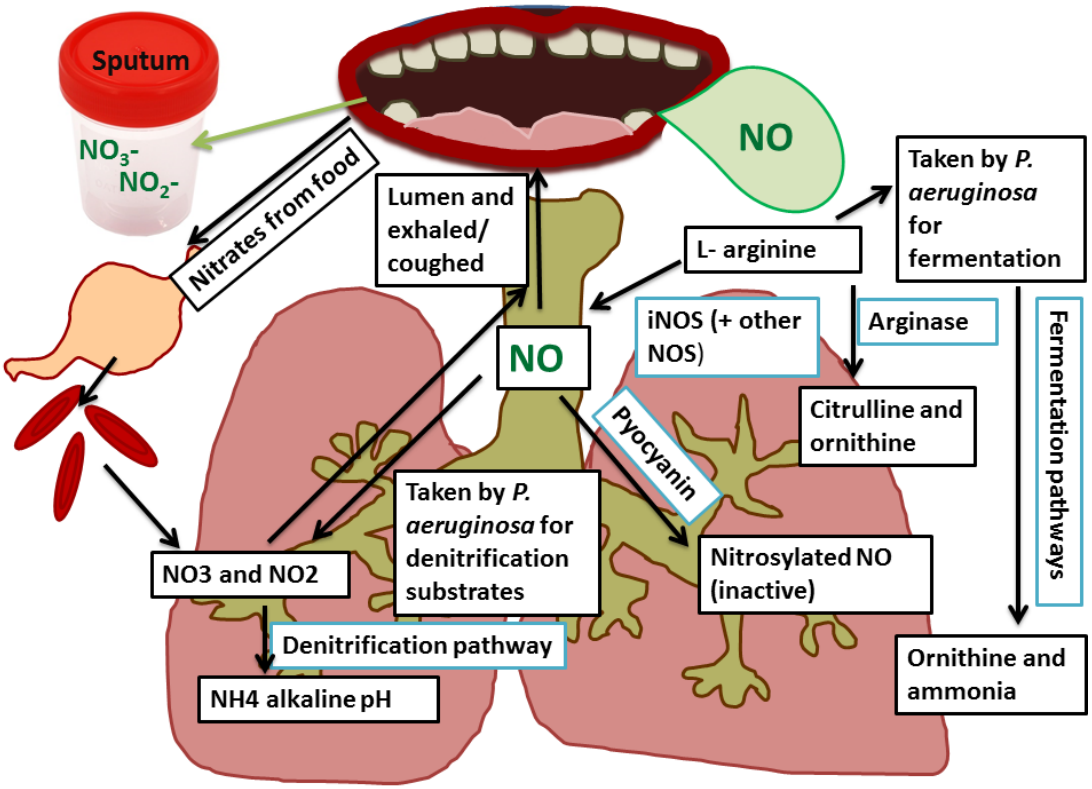


Figure 4.1.3: Where does the nitric oxide (NO) go? Levels of exhaled NO are lower than expected in CF. A combination of mechanical obstruction (thick mucus), bacterial influence though denitrification, pyocyanin mediated inactivation and arginine depletion, and increased arginase activity could be responsible. A side effect of denitrification and arginine fermentation could be a localised increase in pH. Based on the research by Quinn *et al* (2014); Kolpen *et al* (2014) ; Lundberg, Weitzberg and Gladwin (2008); Robbins and Grisham (1997) Jones *et al* (2000); Linnane *et al* 1998; Grasemann *et al* 2005, 2006, Gaston *et al* (2002); Barth and Pitt (1996); Thomas *et al* (2000). Sputum pot cartoon was taken from AliExpress.

To determine the importance of AaaA to *P. aeruginosa* CF isolates in the CF airway and how environmental factors influence the requirement for this enzyme, the *aaaA* sequences were analysed, the relative expression tested and the activity measured in different conditions. To see if AaaA correlated with particular phenotypes or virulence factors, a representative battery of phenotypic tests were employed on the CF isolates and patterns searched for.

4.1.2 A note on media choice and naming

More biologically relevant than LB, artificial sputum media (here termed ASM) was used in some experiments. Bacteria grown in this media have previously shown a pattern of gene expression closer to that seen *in vivo*. There is some variation in the type of ASM recipes available. The ASM composition used follows the method described in Palmer *et al* (2007). There it is called synthetic CF sputum media (SCFM) and does not contain mucin or eDNA. The more defined SCFM was chosen due to the interest in metabolic interactions in this study. It is also permissive of use in different phenotypic tests.

4.2 Results

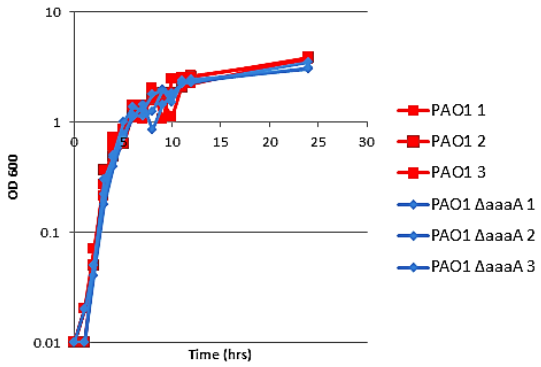
4.2.1 Characterisation of Cystic Fibrosis isolates

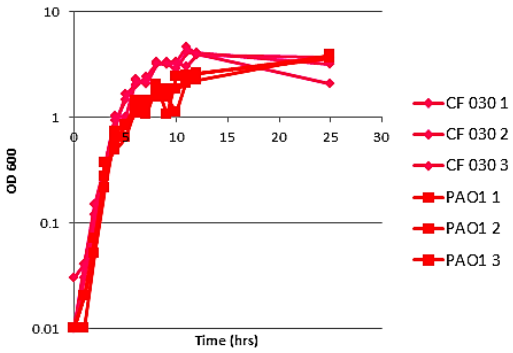
To investigate the role(s) AaaA could play in the context of the cystic fibrosis airway, the CF isolates were tested for phenotypic traits including growth, elastase production, motility, pyocyanin and biofilm production. This aimed to provide a better understanding of the general characteristics of the CF isolates and reveal if any traits correspond with a greater requirement for AaaA.

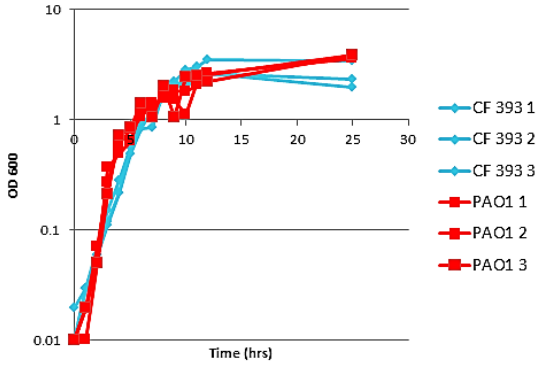
4.2.1.1 Cystic Fibrosis strains differ in growth rate

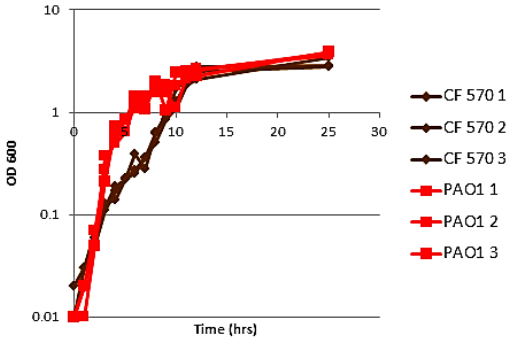
To observe differences in growth rate between the CF isolates, the 10 strains were grown in 4 conditions: (1) aerobic, LB (2) aerobic ASM (3) microaerobic, LB (4) and microaerobic ASM. The aerobic conditions were created using a 50 ml starting volume standardised to an OD_{600} of 0.01 in 500 ml flasks. Vigorous shaking at 200 rpm was maintained throughout to ensure good oxygenation of the culture. The OD_{600} was taken every hour for 12 hours and then after 24 hours. To establish microaerobic conditions, overnight cultures were grown in a microaerobic cabinet and standardised to OD_{600} 0.1. A volume of 200 µl was loaded onto a 96 well plate and the plate sealed with a clear film to prevent gas exchange inside the microaerobic cabinet. The plate was then incubated in a tecan plate reader which was largely static and the OD_{600} taken every 30 minutes.

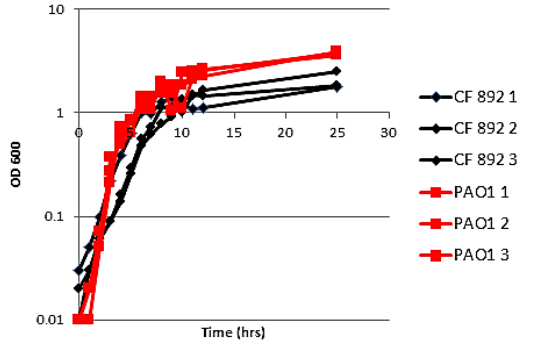
Figure 4.2.1 shows the growth of the CF isolates in well oxygenated, LB media. It can be seen that CF 030 was the only isolate to exceed the growth of PAO1. Strains with a slower exponential than PAO1 include CF 570, CF 983, CF 098, CF 129, CF 971 and CF 326. CF 892 had a slightly lower OD_{600} upon reaching stationary phase. The similarity between replicate growth curves for each strain is apparent by the closely matching plots for each strain, with no substantial differences.

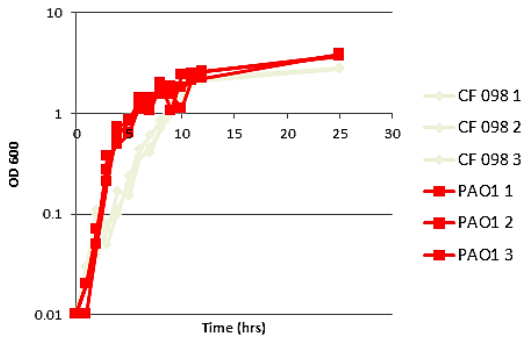

OD 600
Time (hrs)
PAO1 1
PAO1 2
PAO1 3
PAO1 ΔaaaA 1
PAO1 ΔaaaA 2
PAO1 ΔaaaA 3

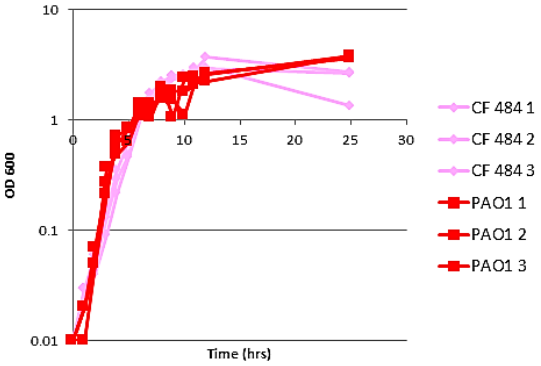

OD 600
Time (hrs)
CF 030 1
CF 030 2
CF 030 3
PAO1 1
PAO1 2
PAO1 3

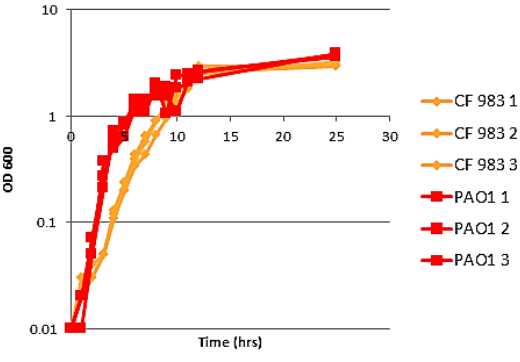

OD 600
Time (hrs)
CF 393 1
CF 393 2
CF 393 3
PAO1 1
PAO1 2
PAO1 3


OD 600
Time (hrs)
CF 570 1
CF 570 2
CF 570 3
PAO1 1
PAO1 2
PAO1 3


OD 600
Time (hrs)
CF 892 1
CF 892 2
CF 892 3
PAO1 1
PAO1 2
PAO1 3


OD 600
Time (hrs)
CF 098 1
CF 098 2
CF 098 3
PAO1 1
PAO1 2
PAO1 3


OD 600
Time (hrs)
CF 484 1
CF 484 2
CF 484 3
PAO1 1
PAO1 2
PAO1 3


OD 600
Time (hrs)
CF 983 1
CF 983 2
CF 983 3
PAO1 1
PAO1 2
PAO1 3

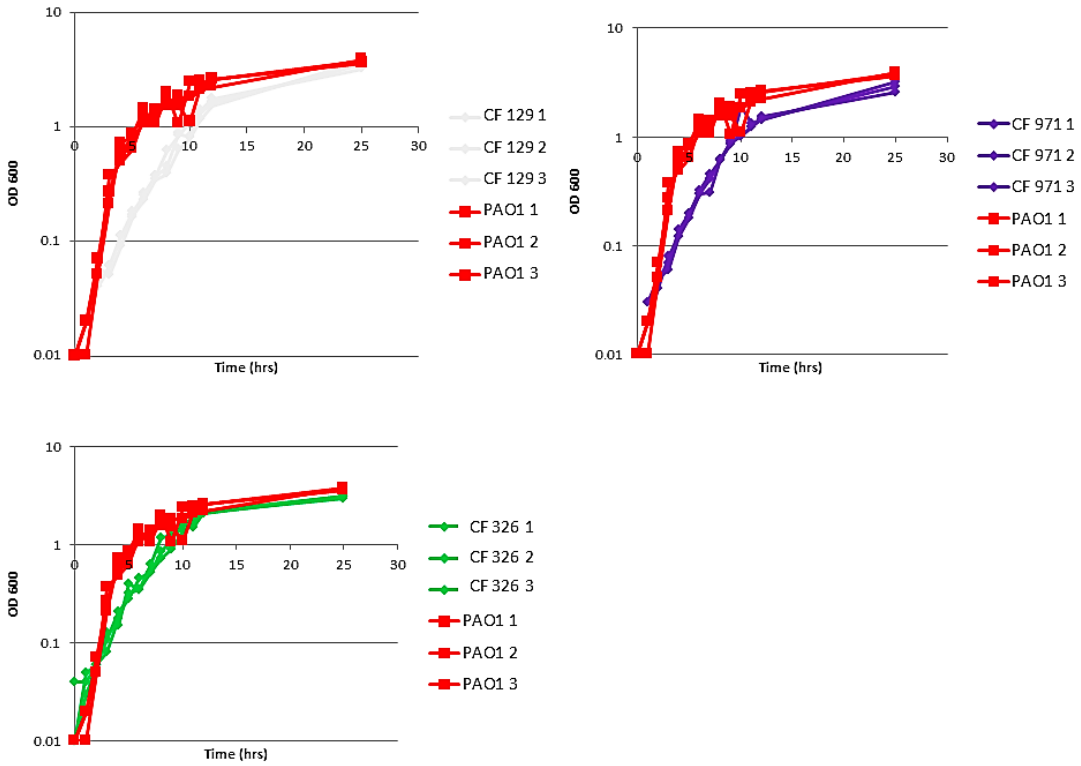
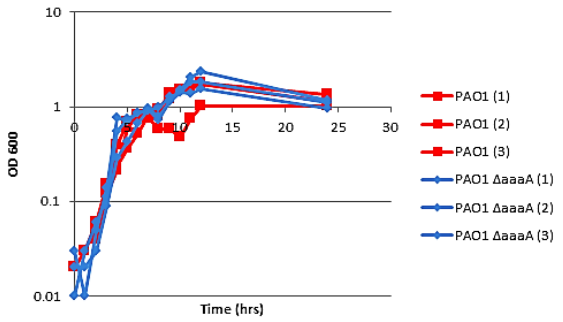
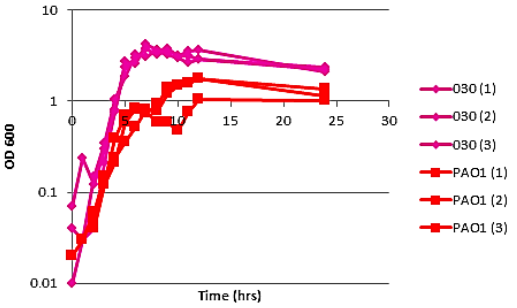
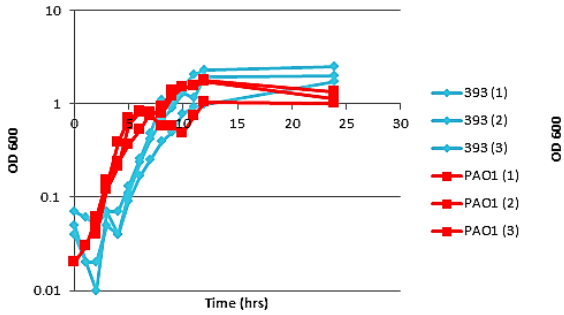


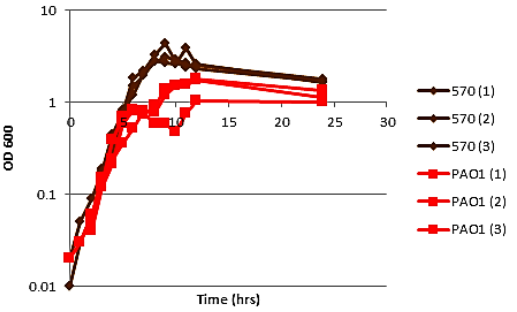
Figure 4.2.1: All CF isolates differed to PAO1 at some point during the growth curve in aerated, LB media. All CF isolates plus PA01 (red squares) and the *ΔaaaA* mutant were grown in LB aerobically over 24 hours. The OD_{600} values taken at the indicated time points are shown plotted against time on a logarithmic scale. Each CF isolate or the *ΔaaaA* mutant is indicated by the diamonds in assorted colours. Each line corresponds to one biological replicate of the triplicate growth curves.

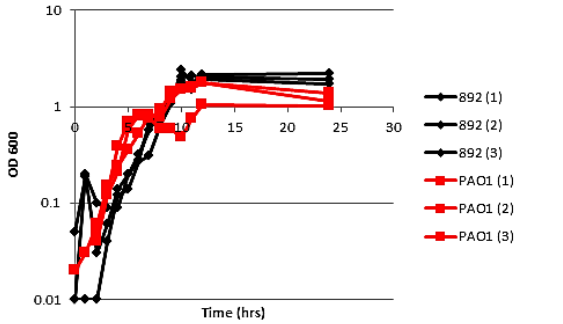
Figure 4.2.2 shows the growth of the CF isolates in well oxygenated ASM. In this media, more isolates exhibited growth profiles that mirrored PAO1. Exceeding the growth of PAO1 was CF 030 and CF 326. Equal to or slightly exceeding the growth of PAO1 were the isolates CF 570, CF 098 and CF 484. Lagging behind PAO1 were CF 393, CF 892 and CF 983. CF 129 lagged behind PAO1 initially but slightly exceeded it at the beginning of stationary phase. CF 971 did not grow at all in ASM.

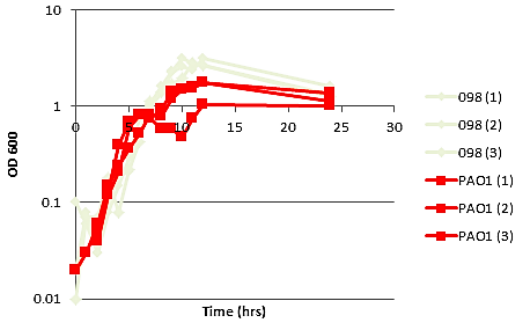

OD 600
Time (hrs)
PAO1 (1)
PAO1 (2)
PAO1 (3)
PAO1 ΔaaaA (1)
PAO1 ΔaaaA (2)
PAO1 ΔaaaA (3)

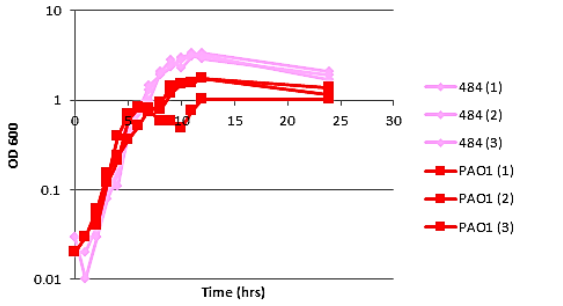

OD 600
Time (hrs)
030 (1)
030 (2)
030 (3)
PAO1 (1)
PAO1 (2)
PAO1 (3)

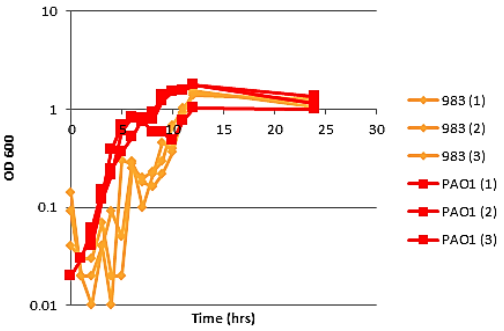

OD 600
Time (hrs)
393 (1)
393 (2)
393 (3)
PAO1 (1)
PAO1 (2)
PAO1 (3)


OD 600
Time (hrs)
570 (1)
570 (2)
570 (3)
PAO1 (1)
PAO1 (2)
PAO1 (3)


OD 600
Time (hrs)
892 (1)
892 (2)
892 (3)
PAO1 (1)
PAO1 (2)
PAO1 (3)


OD 600
Time (hrs)
098 (1)
098 (2)
098 (3)
PAO1 (1)
PAO1 (2)
PAO1 (3)


OD 600
Time (hrs)
484 (1)
484 (2)
484 (3)
PAO1 (1)
PAO1 (2)
PAO1 (3)


OD 600
Time (hrs)
983 (1)
983 (2)
983 (3)
PAO1 (1)
PAO1 (2)
PAO1 (3)

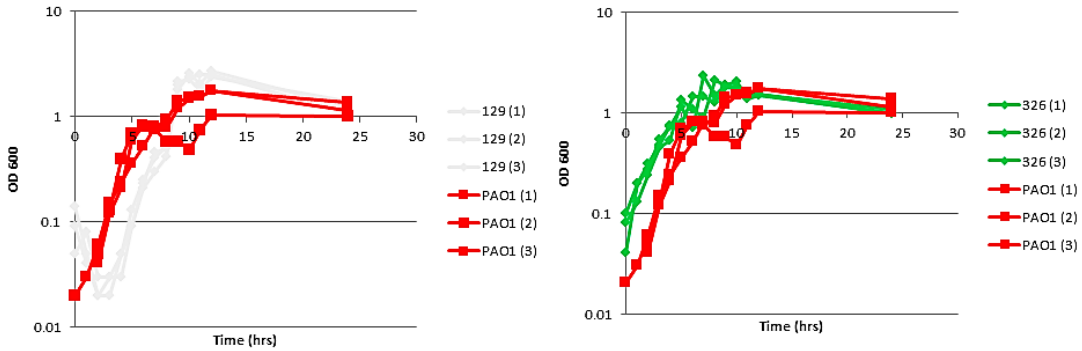
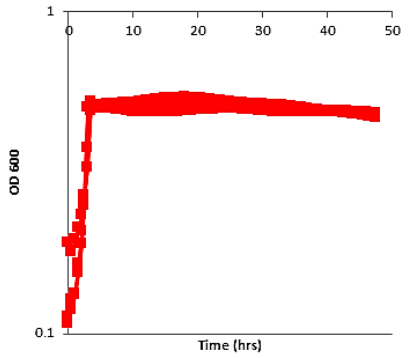
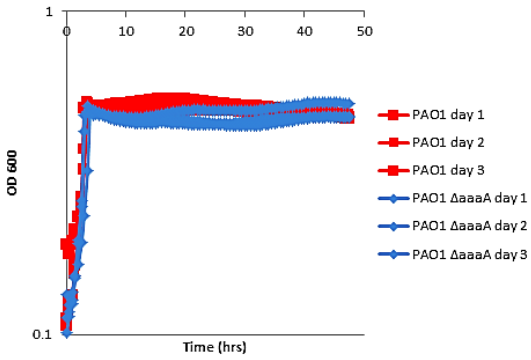
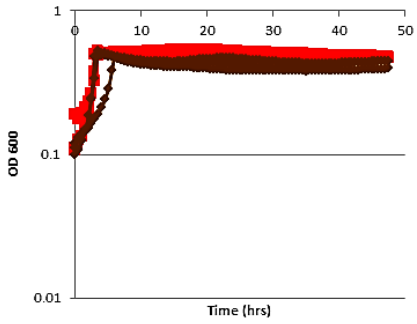


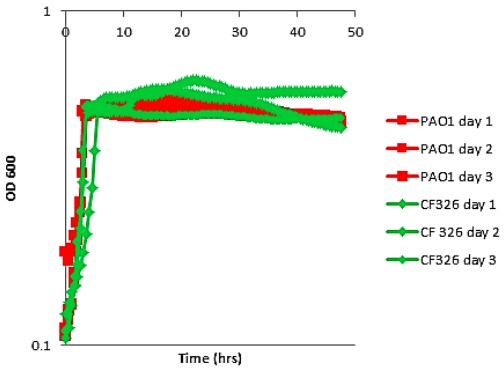
Figure 4.2.2: All CF isolates differed to PAO1 at some point during the growth curve in aerated, artificial sputum media. All CF isolates plus PA01 (red squares) and the *ΔaaaA* mutant were grown in ASM aerobically over 24 hours. The OD_{600} values taken at the indicated time points are shown plotted against time on a logarithmic scale. Each CF isolate or the *ΔaaaA* mutant is indicated by the diamonds in assorted colours. Each line corresponds to one biological replicate of the triplicate growth curves. CF971 did not grow in this media and the overnight culture of CF 484 needed 2 days to grow to be sufficient for standardisation. Variation between the biological replicates in some of the isolates was a consequence of a clumping phenotype observed. Notably this included CF393, CF983 and to a lesser extent PAO1.

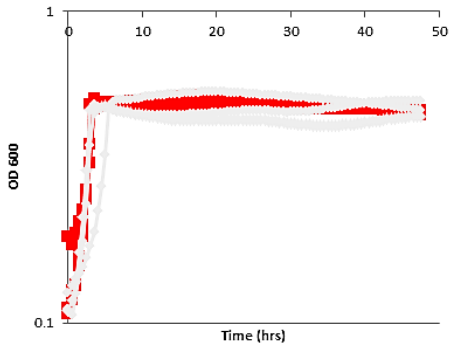
Figure 4.2.3 shows the microaerobic growth of the CF isolates in LB media. All of the strains show a very short lag and exponential phase. The experiment was continued for 48 hours rather than 24 due to the slow growth observed in the PAO1 and PAO1 *ΔaaaA* strains during a manual microaerobic growth curve (results shown in microaerobic activity section). The smaller volumes and static conditions used in the tecan appear to have rendered this extension unnecessary however. Very little difference in growth between the isolates and the PAO1 control was observed in these conditions. CF 983, CF 484 and CF 971 slightly lag behind. CF 393 also seems to lag slightly but there is greater variation in the biological replicates of this strain than the others. The clumping phenotype associated with CF 393 is likely the cause of this variation.

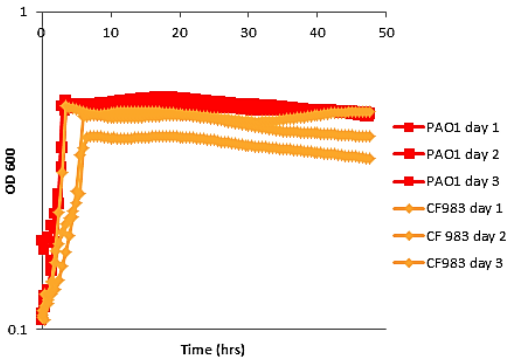

1
0
10
20
30
40
50
OD 600
0.1
Time (hrs)
PAO1 day 1
PAO1 day 2
PAO1 day 3

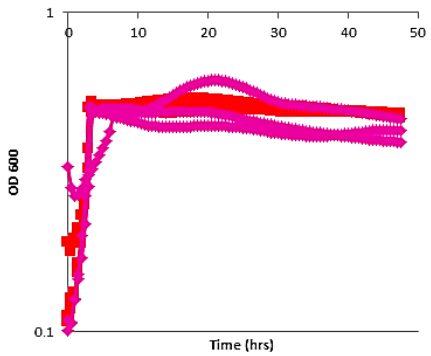

1
0
10
20
30
40
50
OD 600
0.1
Time (hrs)
PAO1 day 1
PAO1 day 2
PAO1 day 3
PAO1 ΔaaaA day 1
PAO1 ΔaaaA day 2
PAO1 ΔaaaA day 3

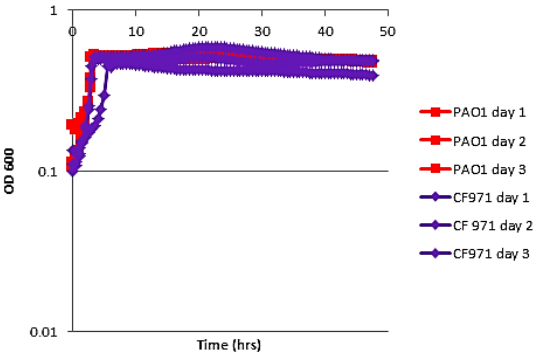

1
0
10
20
30
40
50
OD 600
0.1
0.01
Time (hrs)
PAO1 day 1
PAO1 day 2
PAO1 day 3
CF570 day 1
CF 570 day 2
CF570 day 3


1
0
10
20
30
40
50
OD 600
0.1
Time (hrs)
PAO1 day 1
PAO1 day 2
PAO1 day 3
CF326 day 1
CF 326 day 2
CF326 day 3


1
0
10
20
30
40
50
OD 600
0.1
Time (hrs)
PAO1 day 1
PAO1 day 2
PAO1 day 3
CF129 day 1
CF 129 day 2
CF129 day 3


1
0
10
20
30
40
50
OD 600
0.1
Time (hrs)
PAO1 day 1
PAO1 day 2
PAO1 day 3
CF983 day 1
CF 983 day 2
CF983 day 3


1
0
10
20
30
40
50
OD 600
0.1
Time (hrs)
PAO1 day 1
PAO1 day 2
PAO1 day 3
CF030 day 1
CF 030 day 2
CF030 day 3


1
0
10
20
30
40
50
OD 600
0.1
0.01
Time (hrs)
PAO1 day 1
PAO1 day 2
PAO1 day 3
CF971 day 1
CF 971 day 2
CF971 day 3

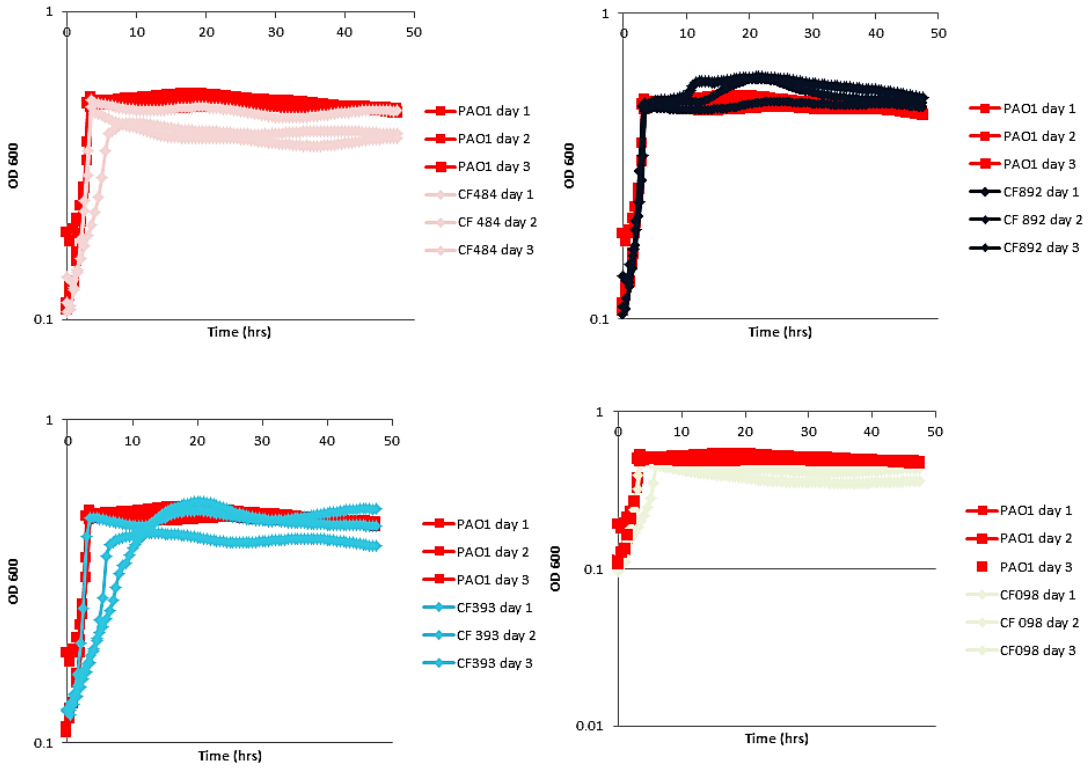
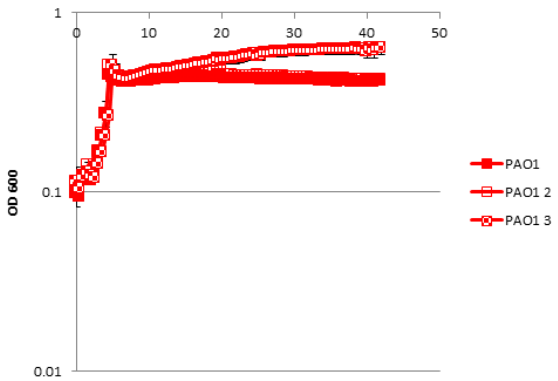
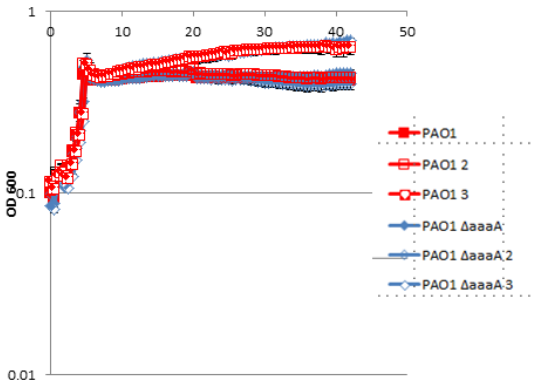
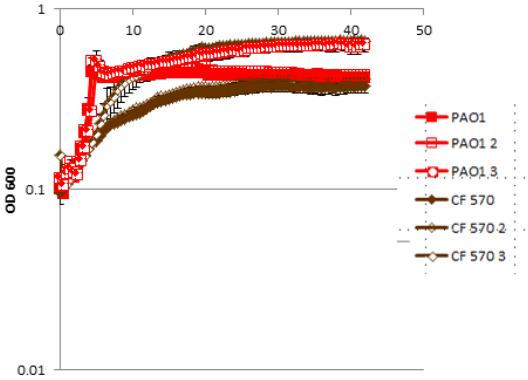


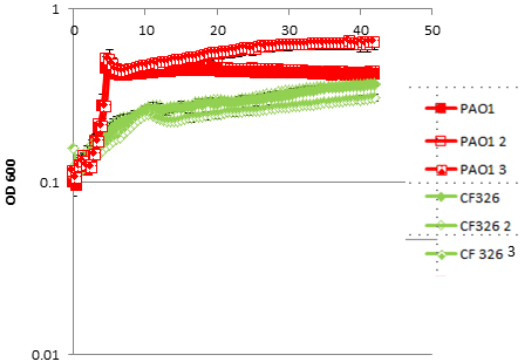
Figure 4.2.3: All CF isolates differed to PAO1 at some point during the growth curve in microaerobic, LB media. All CF isolates plus PA01 (red squares) and the *ΔaaaA* mutant were grown in LB microaerobically over 24 hours in a sealed 96 well plate using a tecan plate reader. The OD_{600} values taken at the indicated time points are shown plotted against time on a logarithmic scale. Each CF isolate or the *ΔaaaA* mutant is indicated by the diamonds in assorted colours. Each line corresponds to one biological replicate of the triplicate growth curves.

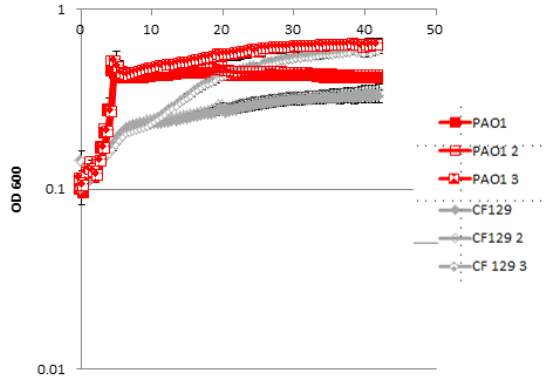
Figure 4.2.4 shows the microaerobic growth of the CF isolates in ASM. The short lag phase exhibited was also observed during growth in LB. The PAO1 control grew similarly in the ASM and LB. In contrast, in this low oxygen condition, the exchange of LB for ASM had more of an impact on the CF isolates, with only CF 030 growing as quickly as PAO1. CF 326, CF 129, CF 983 and CF 393 show greatly increased lag and exponential phase times.

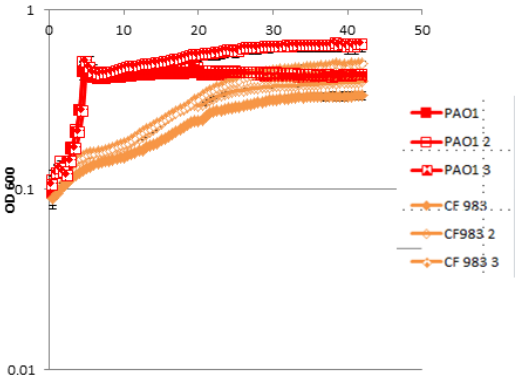

OD 600
1
0.1
0.01
0
10
20
30
40
50
PAO1
PAO1 2
PAO1 3

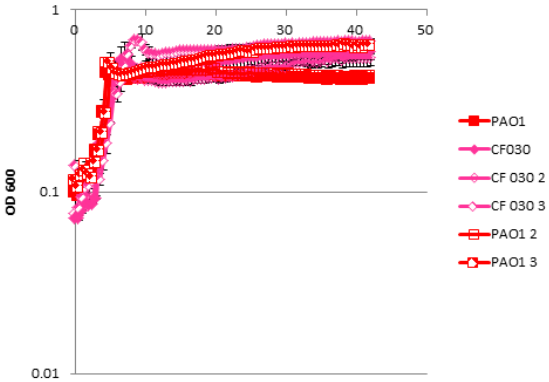

OD 600
1
0.1
0.01
0
10
20
30
40
50
PAO1
PAO1 2
PAO1 3
PAO1 ΔaaaA
PAO1 ΔaaaA 2
PAO1 ΔaaaA 3

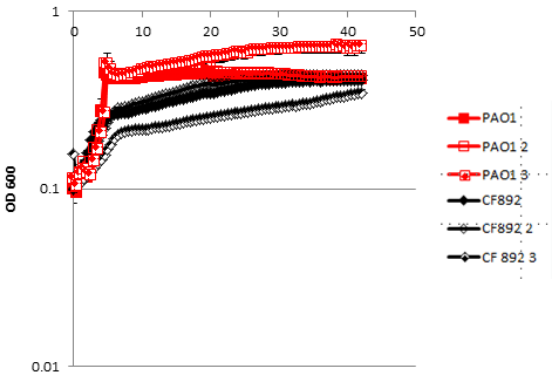

OD 600
1
0.1
0.01
0
10
20
30
40
50
PAO1
PAO1 2
PAO1 3
CF 570
CF 570 2
CF 570 3


OD 600
1
0.1
0.01
0
10
20
30
40
50
PAO1
PAO1 2
PAO1 3
CF326
CF326 2
CF 326 3


OD 600
1
0.1
0.01
0
10
20
30
40
50
PAO1
PAO1 2
PAO1 3
CF129
CF129 2
CF 129 3


OD 600
1
0.1
0.01
0
10
20
30
40
50
PAO1
PAO1 2
PAO1 3
CF 983
CF983 2
CF 983 3


OD 600
1
0.1
0.01
0
10
20
30
40
50
PAO1
CF030
CF 030 2
CF 030 3
PAO1 2
PAO1 3


OD 600
1
0.1
0.01
0
10
20
30
40
50
PAO1
PAO1 2
PAO1 3
CF892
CF892 2
CF 892 3

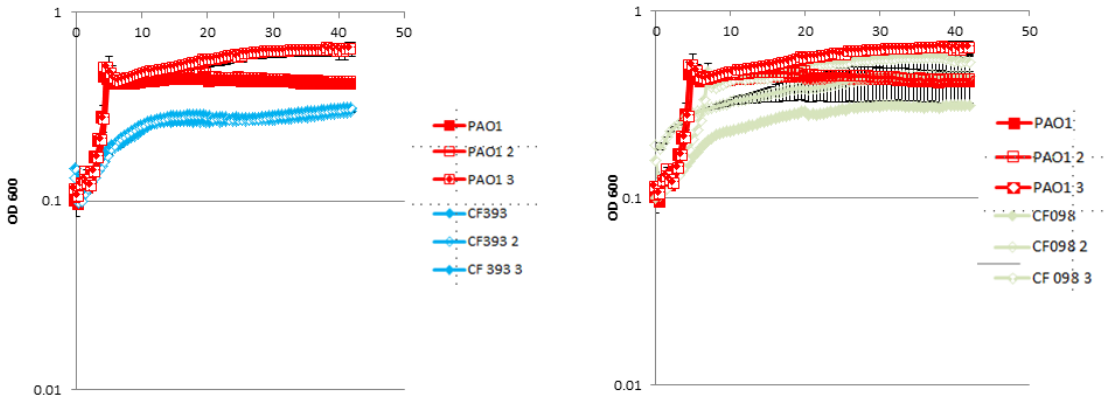


Figure 4.2.4: All CF isolates differed to PAO1 at some point during the growth curve in microaerobic, ASM media. All CF isolates plus PA01 (red squares) and the *ΔaaaA* mutant were grown in ASM microaerobically over 24 hours in a sealed 96 well plate using a tecan plate reader. The OD_{600} values taken at the indicated time points are shown plotted against time on a logarithmic scale. Each CF isolate or the *ΔaaaA* mutant is indicated by the diamonds in assorted colours. Each line corresponds to one biological replicate of the triplicate growth curves. CF 971 is not included as this isolate does not grow in the ASM used here; CF 484 is not included due to difficulties in getting this isolate to grow in ASM, requiring 2 days of overnight growth rather than one.

4.2.1.2 Isolates show a general lack of motility

Motility is an important attribute for *P. aeruginosa* virulence. It is mediated by flagella (swimming) and Type IV pili (twitching) and can occur with directional coordination (swarming) (Kohler *et al* 2000). The following experiments tested which CF isolates exhibited these motility behaviours.

To observe if the CF isolates were able to swarm, a plate-based swarming assay was performed. Kohler *et al* (2000) found that the onset of swarming is induced by the presence of particular carbon and nitrogen sources in addition to a suitable agar concentration (0.5-0.7%). Glutamate and aspartate were found to be the best nitrogen providers to induce swarming. The best carbon source to stimulate swarming was glucose, while succinate was completely ineffective. The media used here included glucose and peptone (in nutrient broth no.2 Sigma) as carbon and nitrate sources respectively. The plates were incubated for 18 hours at 37°C.

A general lack of swarming ability was observed (Figure 4.2.5). Only one isolate, CF 030, appeared to move across the plate in the 18 hours incubation time. The phenotype differs considerably from that of the PAO1 strains, both of which swarm equally regardless of the mutation in *aaaA*. One isolate, CF 098, shows a mushrooming effect which is likely due to individual cells mutating to a more motile phenotype.

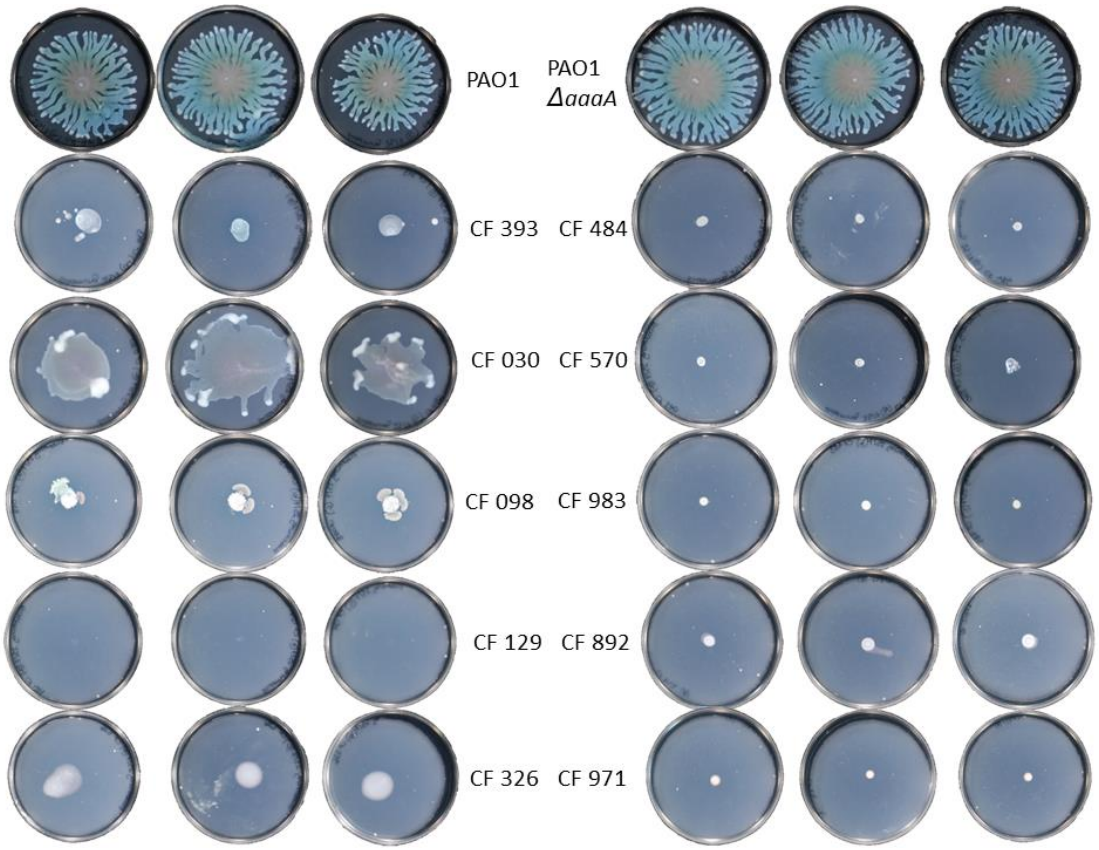


Figure 4.2.5: CF isolates differ from PAO1 in their capacity to swarm. A drop of normalised culture was spotted onto the surface of swarming agar plates and these were allowed to incubate for 18 hours at 37°C. Each plate represents a biological replicate. Only the PAO1 derived strains show the typical swarming phenotype, although CF 030 has been able to move across the plate a similar distance.

Following this, a plate-based swimming assay was performed to test the ability of the isolates to move using flagella. Swimming occurs in low density liquids of less than 0.4 % agar (Kohler *et al* 2000). The bacteria move through the body of the medium rather than across the surface and it does not require the QS system or rhamnolipids as with swarming (Dae-Gon Ha *et al* 2014). In this case (Figure 4.2.6) only isolate CF 030 shows the capacity to swim. CF 030 swims almost as well as PAO1; there is no apparent difference in the PAO1 Δ*aaaA* mutant. One of the CF 892 replicates exhibited asymmetrical movement, but has been discounted here as a mutation occurring during the experiment on the basis of its asymmetry and the other two replicates' immobility.

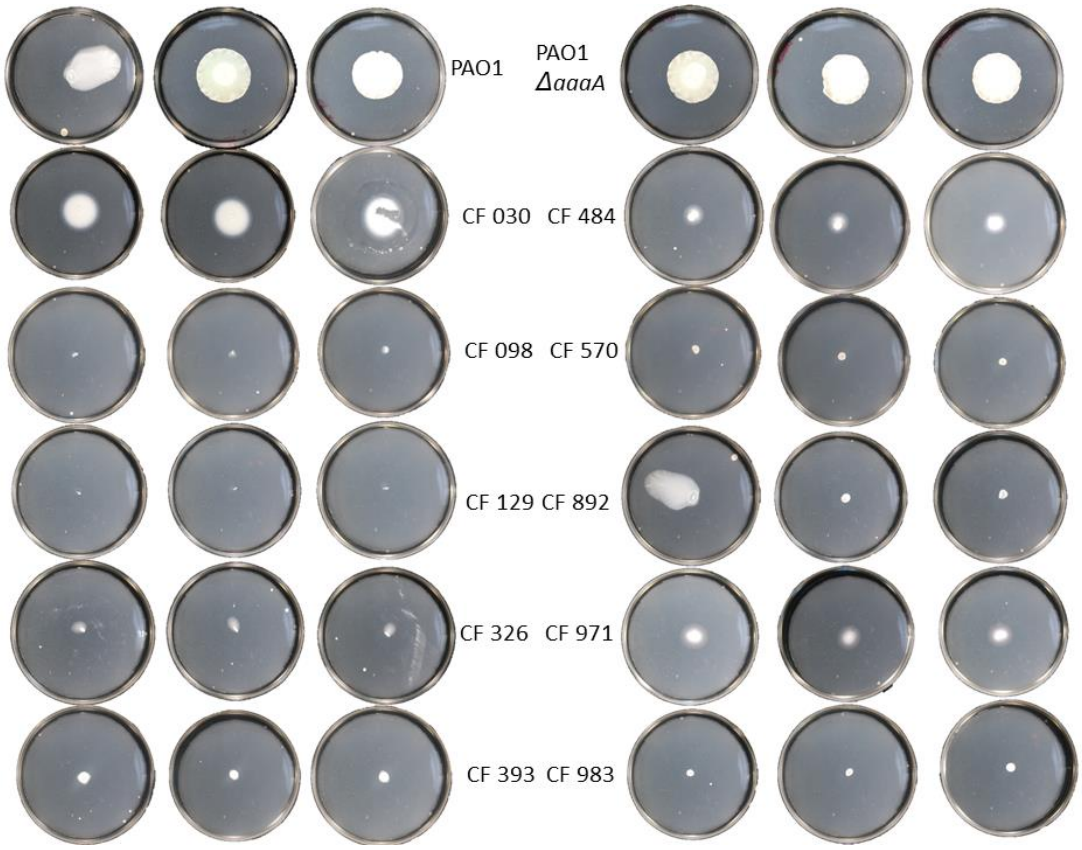


Figure 4.2.6 CF isolates differ from PAO1 in their capacity to swim. A drop of normalised culture was inserted at a depth roughly equidistant from the surface and bottom of the plate and these were allowed to incubate for 18 hours at 37oC. Each plate represents a biological replicate. The CF isolate 030, swims almost as well as the PAO1 derived strains. CF971 and CF484 appear to have moved slightly, however there is a large difference in the motility shown by these and PAO1. The remainder of the CF isolates seem to have not moved, or moved very little.

Swarming and swimming motility assays test movement associated with the flagellum. To examine the mobility of the CF isolates specifically using Type-IV pili, a twitching assay was performed. This movement occurs along a surface (either biological or abiotic), the cells inching along using the contraction and relaxation of the pili (O'Toole and Kolter 1998; Kohler *et al* 2000). Because of this, there is a higher agar percentage in twitching media than the other motility assays and a thinner layer is spread on the plates. A colony was taken for each strain with a sterile tooth pick and stabbed 10 times to the centre-bottom of the petri dish. Following incubation (22 hours), a halo could be observed on the bottom of the plate. The media was then removed and the halos stained with 10% crystal violet for better visualisation. In this assay (Figure 4.2.7) there again does not appear to be much movement occurring in the isolates. The CF isolates 892 and 098 show a slight twitching phenotype when compared to the other strains which do not appear to be twitching. The PAO1 strains show the twitching motility and there is no apparent difference in the PAO1 *ΔaaaA* mutant.

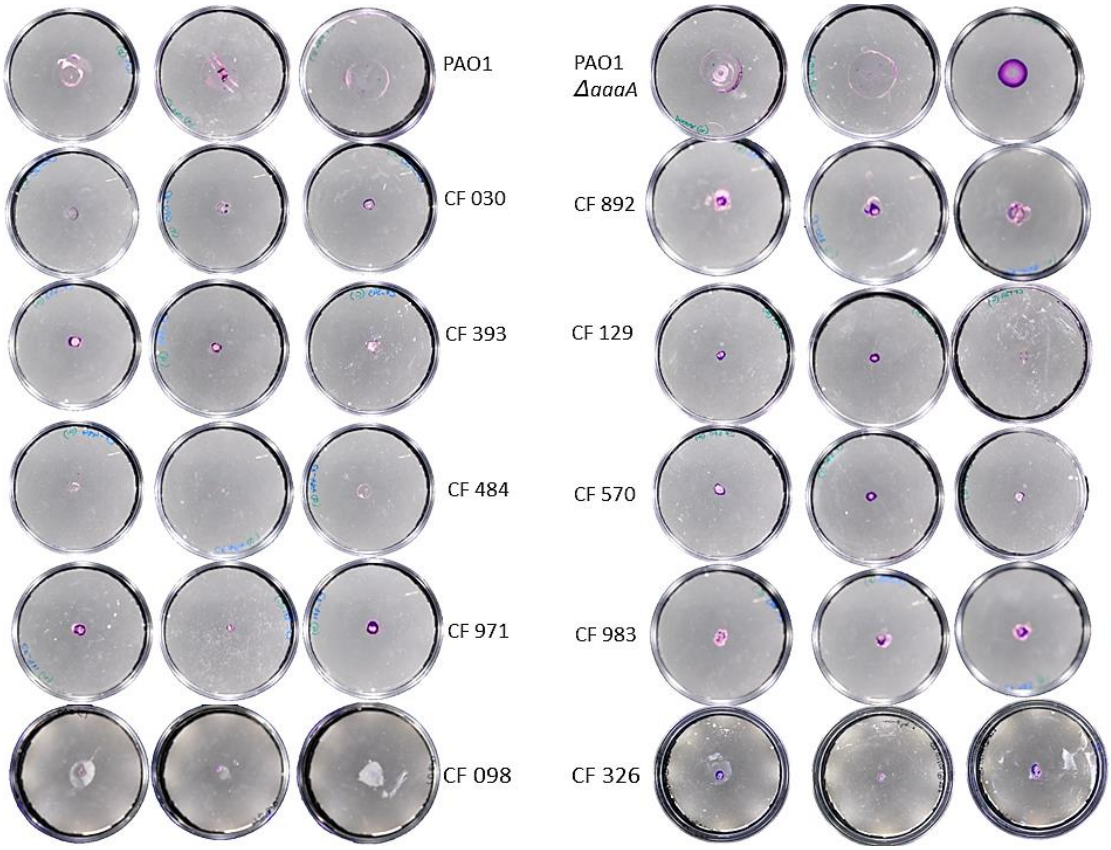


Figure 4.2.7 CF isolates differ from PAO1 in their capacity to twitch. A colony was inserted with a cocktail stick at bottom of the plate, between the plastic and the agar, and these were allowed to incubate for 22 hours at 37°C. Each plate represents a biological replicate. The CF isolates 892 and 098 seem to show some twitching motility but not as noticeable as PA01. The remainder of the CF isolates seem to have not moved, or moved very little.

4.2.1.3 CF isolates produce negligible elastase

Elastase is produced by *P. aeruginosa* to attack the junctions between cells and consequently facilitates greater invasion of host tissue (Wretlind and Pavlovskis 1983). A high production of this enzyme can therefore indicate a strain is expressing virulence factors suitable for an acute stage of infection. The elastase assay used here involves measuring the extent of Congo red release from an elastin-Congo red complex. The more bonds cleaved between elastin and Congo red, the greater the absorbance at OD_{495} (Naughton and Sanger 1961). The bacteria were grown in aerobic, LB media and the experiment performed 3 times with 3 technical replicates included for each strain.

None of the CF isolates showed elastase activity equalling the PAO1 strains (Figure 4.2.8). One of the isolates, CF 326 showed a level of Congo red-elastase dissociation similar to that of the *ΔlasB* mutant strain. In addition to a lack of LasB, other enzymes with redundant activity may also be diminished in the other CF isolates as elastolytic activities measured in these strains were lower than the *ΔlasB* mutant.

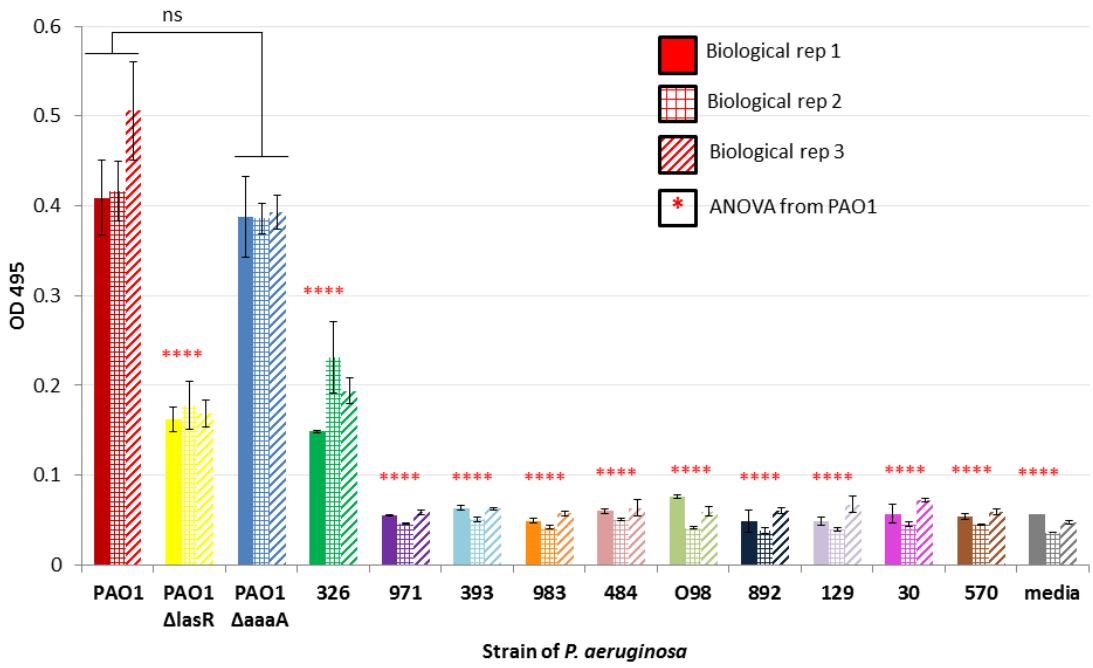


Figure 4.2.8: Elastase activity is low in the CF isolates in comparison to PAO1. Bacteria were grown overnight aerobically in LB and standardised to OD 600 1.0. The cultures were then diluted 1:100 in fresh LB and allowed to grow for 16 hours. Following filter sterilisation, the supernatants were mixed with the elastin-Congo red solution (1:1) and incubated for 4 hours at 37°C 200 rpm. The remaining insoluble particles were sedimented by centrifugation, the supernatant removed and the OD_{495} read from these which corresponds to the cleavage of elastin from Congo red. ECR buffer was used as a blank. Each colour represents a different strain while each pattern represents a different biological replicate. Error bars represent the standard deviation across 3 technical replicates. A t-test was performed between PAO1 and PAO1 *ΔaaaA* and found to be non-significant (ns). An ANOVA using PAO1 as the comparison reference was performed and significant results indicated by red asterisk. Four asterisks = P<0.0001.

4.2.1.4 In LB media, pyocyanin production by the CF isolates is low

Pyocyanin has been assigned virulence factor status, and its production within a host can cause disruption to the immune system. These include damage to the cilia lining the respiratory tract (Wilson *et al* 1987), interference with vascular homeostasis mechanisms, for example that of prostaglandin I_2 and nitic oxide (Kamath *et al* 1995), and causing an increase in IL-8 production (Denning *et al* 1998) while simultaneously inducing neutrophil destruction (Usher *et al* 2002). As well as its role in virulence, pyocyanin is an electron acceptor and helps balance the oxidative state of the cell (Price-Whelan *et al* 2007). As oxygen availability has been hypothesised to be a principle trigger in *P. aeruginosa's* requirement of AaaA, it was thought that it would be interesting to see if differences in pyocyanin production could be correlated with AaaA activity. To reveal any differences in pyocyanin production existing between the CF isolates, a pyocyanin assay was performed in LB medium. The 25 ml cultures were grown in 200 ml flasks in a 200 rpm shaking 37°C incubator for 18 hours. A chloroform-HCL extraction was proceeded with and the absorbance value at 520 nm taken in a spectrometer.

Only CF 892 produced a quantifiable amount of pyocyanin which was greater than the amount produced by PAO1 and PAO1 (Figure 4.2.9) Δ*aaaA*. More isolates produced pyocyanin in ASM (CF 098 and CF 393), but this has not yet been quantified.

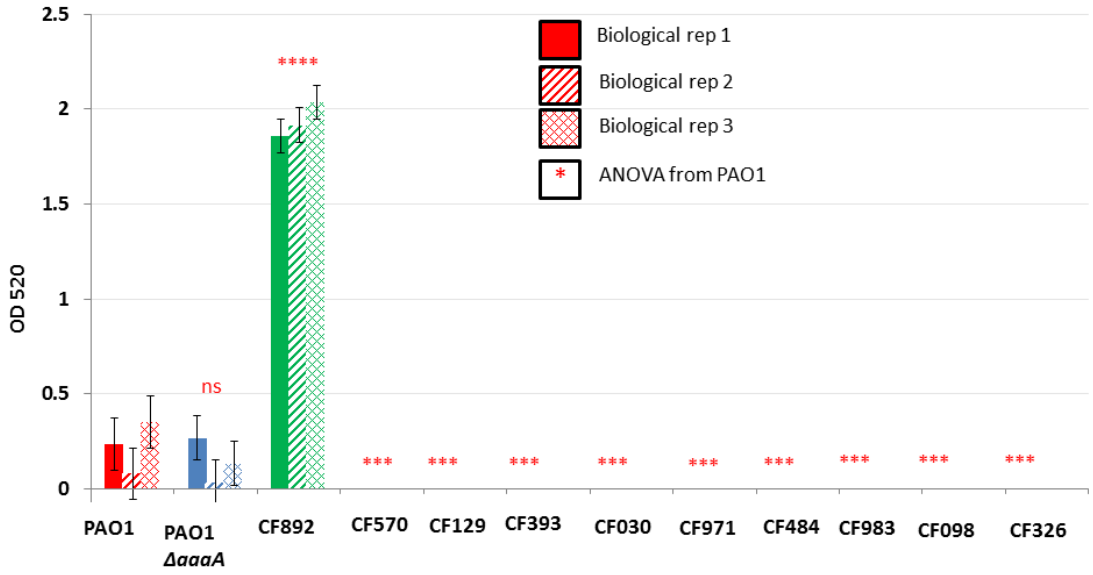


Figure 4.2.9: The majority of CF isolates do not produce detectable pyocyanin when grown in LB, aerobically. Bacteria were grown overnight aerobically in LB for 18 hours at 37°C 200 rpm. The supernatants were then filter sterilised and chloroform-HCL extraction process used to isolate the pyocyanin. The amount of pyocyanin produced by each strain was quantified by taking the absorbance reading at the OD_{520}. Each colour represents a different isolate; each pattern represents a separate biological repeat performed on a different day. Error bars represent variation between the 3 technical isolates. An ANOVA using PAO1 as the comparison reference was performed: significant results are indicated by red asterisk and non-significant are indicated by ns. Three asterisks = P<0.001; four asterisks = P<0.0001.

4.2.1.5 Biofilm production varies among CF isolates and these differ structurally from PAO1

4.2.1.5.1 Colony biofilms show phenotypic variations across isolates: CF 326, CF 892 and CF 030 produce less EPS, and while some CF isolates appear more rugose than PAO1, deep wrinkles corresponding to poor inner colony survival are absent

Freeman *et al* (1989) described a plate assay to view microcolony biofilms. A modified form of this test was employed to reveal the presence of interesting phenotypes which could be observed between the CF isolates. Plates are made with Congo red and Coomassie brilliant blue and late exponential/ early stationary phase culture spotted onto them. Originally, the Congo red plate assay was used to detect the presence of 'slime' or extracellular matrix production in the Gram-positive *Staphylococci* (Freeman *et al* 1989). Black colonies were noted to produce EPS and red ones were not. However, this colour difference was found by Rajkumar *et al* (2016) not to apply in the same way to non-fermenting Gram

negative bacteria such as *Pseudomonas*. Friedman and Kolter (2003) observed that PA14 with mutated *pel,* important for the composition of the extracellular matrix, loses the dark red colour seen in the wild-type. Further to this, Solano *et al* (2003) showed that the red colour of the colonies is due to Congo red adsorption. Thus, it will be considered here that white or pale colonies may be deficient in extracellular matrix components. A particularly interesting phenotype for *Pseudomonas* species is a wrinkly or rugose appearance. A study by Ray *et al* (2012) on the organism *Vibrio fischeri*, reports that this phenotype can be used as an indicator of the biofilm formation and can be semi quantitative if desired. However, this is contradicted somewhat by studies conducted by Dietrich *et al* (2013, 2008) which link the appearance of wrinkles with a lack of phenazine molecule production. The wrinkles are the biofilm's way of rebalancing the state of redox by increasing surface area. There is a similar contradiction with regard to colony biofilm size, Ray *et al* (2012) note that a greater diameter is indicative of a higher biofilm producing strain whereas Dietrich *et al* (2013) attribute the increase in size to a greater requirement for oxygen. Although diameter was not measured, a rough comparison was made by eye.

For this assay, colony biofilms were incubated for 6 days, and on day one (Figure 4.2.10) differences were already seen between the strains. Both CF 892 and CF 393 show a marbled appearance suggesting the formation of wrinkles. Others show differences in texture and colour but are less obvious. PAO1 and PAO1 Δ*aaaA* strains are opaque, smooth and red with a defined border. Some isolates are more transparent than others, particularly CF 971, CF 484, CF 983 and CF 129. Some isolates have more of a border with CF 098, CF 971 and CF 484 having the most noticeable thin margins, while CF 030 has a thick white edge and central region. A central darker spot is shared by CF 098, CF 030, CF 484 and possibly CF 129 and CF 971 although there is some difference in replicates in these. A darker central region may be the start of internal wrinkling as observed by Ray *et al* (2012). Most colonies are circular but CF 983 and CF 129 appear to have some unidirectional spreading. All are a pink colour.

On day 2, PAO1 and PAO1 Δ*aaaA* strains show a bulls eye appearance. CF 098, CF 971 and CF 484 do this to a lesser extent. CF 892 starts to emit a substance or group of cells from the central circular colony which is unidirectional. CF 570, CF 030, CF 129 and CF 971, CF 098, CF 484, and CF 393 to a lesser extent, developed a white border. The majority of the strains excluding CF 892, CF 030, CF 326, CF 983 and CF 393 developed a deeper pigmentation. CF 030 and CF 393 show the start of wrinkle development. Day 3 is very similar to day 2.

Changes that occur on day 4 include the replacement of the bulls eye appearance of PAO1, PAO1 Δ*aaaA*, CF 098 and most of CF 971 with a more uniform red colour. CF 484 darkened in colour but still shows a bulls eye pattern. CF 892 shows further thickening and spreading of the outer layer and CF 393 developed a thick white border. The outer layer of CF 030 increased in thickness relative to the inner circle and developed more obvious crenulations.

On days 5 and 6 (Figure 4.2.11) there is a greater divergence of phenotype between isolates. PAO1 and PAO1 Δ*aaaA* strains show concentric rings around a lighter centre and have a white band which could be a halo surrounding the colony. CF 098 is a darker shade of red than PAO1 and has an internal border but less of a white ring. CF 892 is surrounded by a large area of substance which could be cells growing in a different pattern or a secreted product. It is very different from that of PAO1. CF 570 is more similar to PAO1 but with a lighter middle section and with a pink outer ring inside the white layer. CF 030 appears wrinkly and like CF 892 appears to have 2 parts: an internal ring and a thick outer band. A translucent layer coats the outside and one of the biological isolates seems to have another colony budding off which is interesting because the only the translucent layers touch. CF 971 shares the dark red shade of CF 098 and looks very similar in terms of size and texture. CF 484 is similar to PAO1 but with less of a white outer ring and more of a graduation from the inside (light) to the outside (dark) colour. CF 983 is a paler colour, smoother and less circular than the majority of the other strains. CF 129 shares the asymmetry with CF 983 but has a more defined border. CF 030 is the whitest of the colonies (light pink), has a white outer layer and internal border. CF 393 looks similar to a wax seal with an outer layer oozing out from the central circular colony. There is a double ring border.

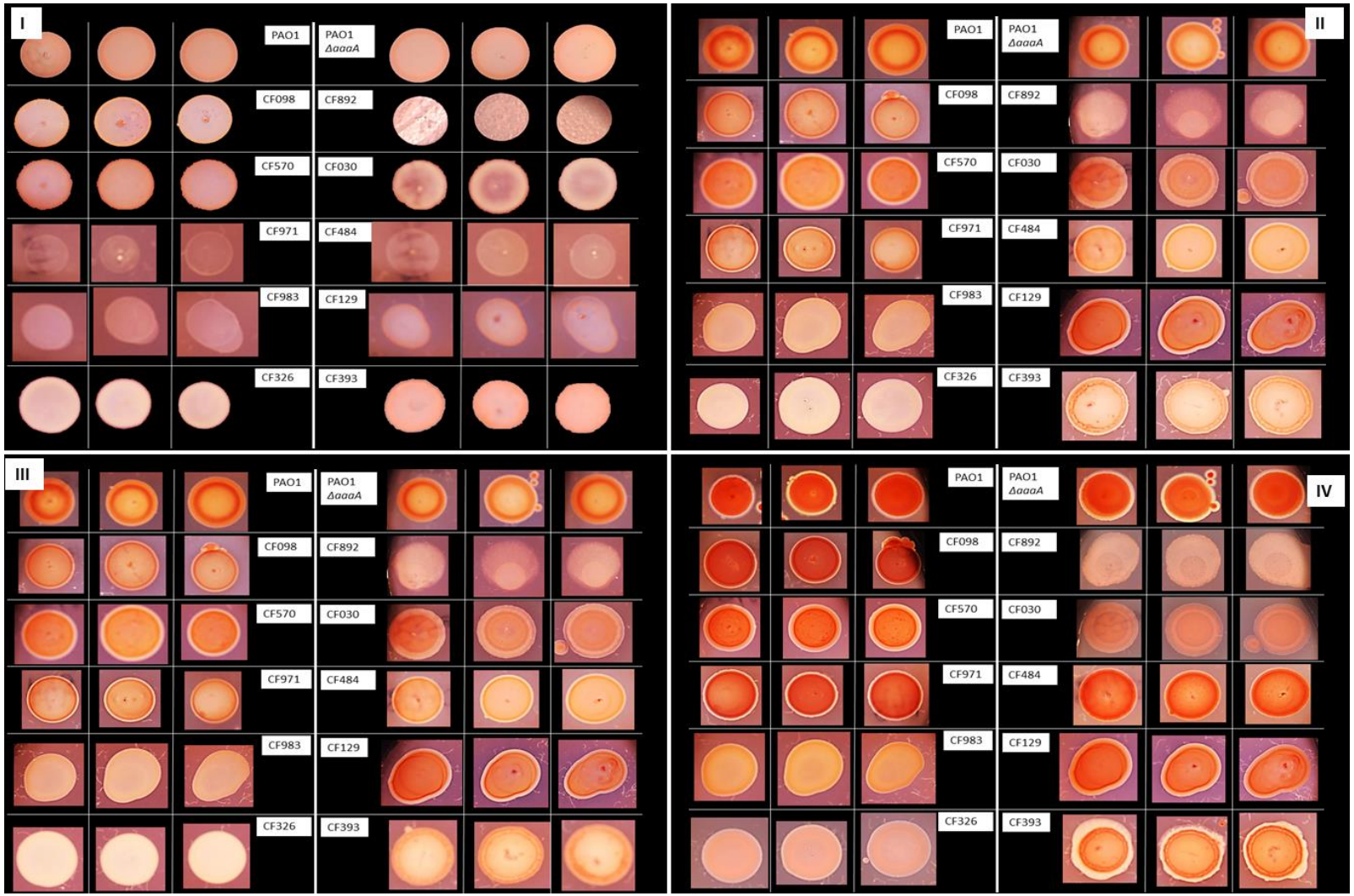


Figure 4.2.10: Congo red colony biofilms produced by CF isolates on days 1-4 show variation in colour, shape, size and rugosity. Overnight cultures were grown in LB, aerobically. Following standardisation, a drop of culture was pipetted onto Congo red, Coomassie plates and incubated at room temperature. Three biological replicates were included for each strain. I day 1; II day 2, III day 3, IV day 4. Note that the background was removed from some colonies when the contrast from the background was low.

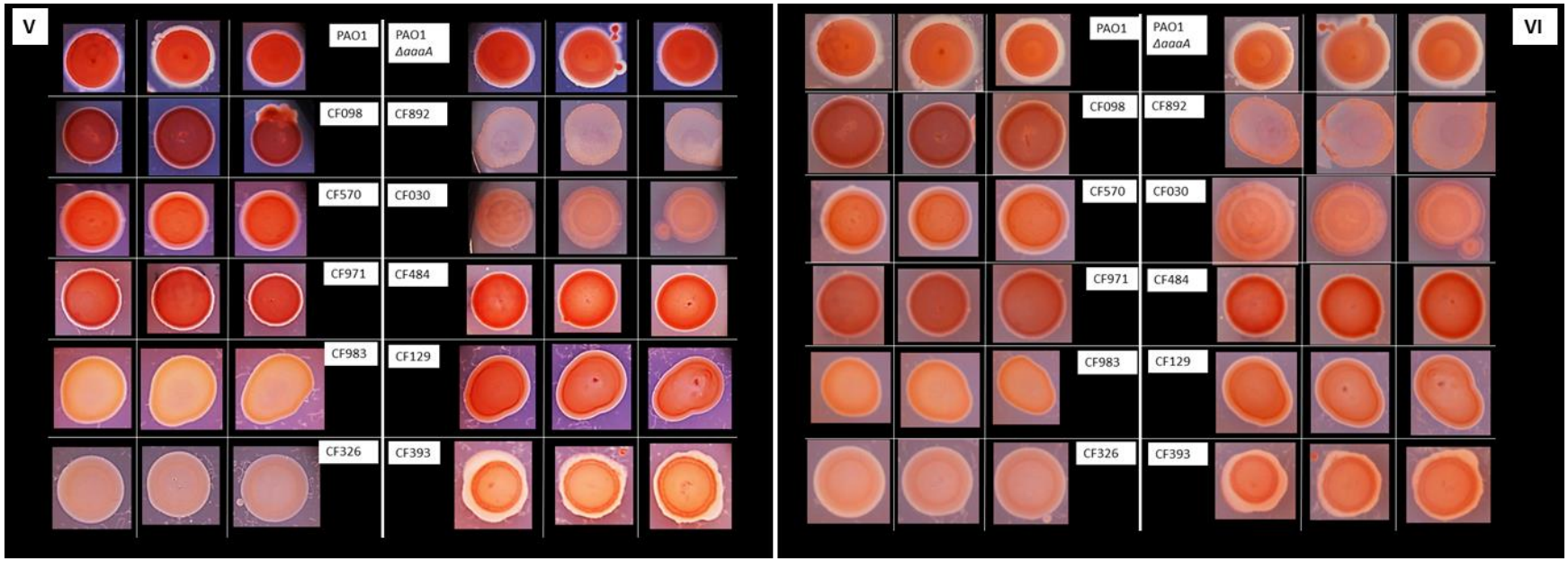


Figure 4.2.11 Congo red colony biofilms produced by CF isolates on days 5-6 show variation in colour, shape, size and rugosity. Overnight cultures were grown in LB, aerobically. Following standardisation, a drop of culture was pipetted onto Congo red, Coomassie plates and incubated at room temperature. Three biological replicates were included for each strain. V day 5 and VI day 6.

4.2.1.5.2 Floating biofilms

Floating biofilm cultures have been obtained by Wright *et al* (2013) where a small quantity of overnight culture is added to a tube of ASM (Kirchner *et al* 2012 and Sriramulu *et al* 2005) and shaken at 37°C, 200 rpm for varying amounts of time. When a clump of cells is observed floating in the media, this can be indicative of biofilm growth. It is perhaps more relevant than growth on a glass or plastic surface to a CF airway environment where biofilms have been observed to be mainly 5-17 μm away from airway epithelial cells (Worlitzsch *et al* 2002). To see whether the CF isolates would form this floating biofilm phenotype, ASM (Palmer *et al* 2007) was added to 50 ml falcons and each falcon inoculated with a colony from an LB agar plate. The cultures were grown overnight for 18 hours and photographed the next day. The experiment was conducted 3 times to provide biological triplicates.

Only one of the CF isolates formed a noticeable clump in the media (Figure 4.2.12). This was CF 393. This isolate was chosen as one of three to be imaged in detail using the Bioflux and confocal microscope. Although the remainder did not clump, further biofilm tests indicated that this was not an indicator of biofilm forming capability but rather that they were unable to form biofilms in the particular conditions created by this assay. The PAO1 controls are shown below in Figure 4.2.13 and are further discussed in Chapter 6.

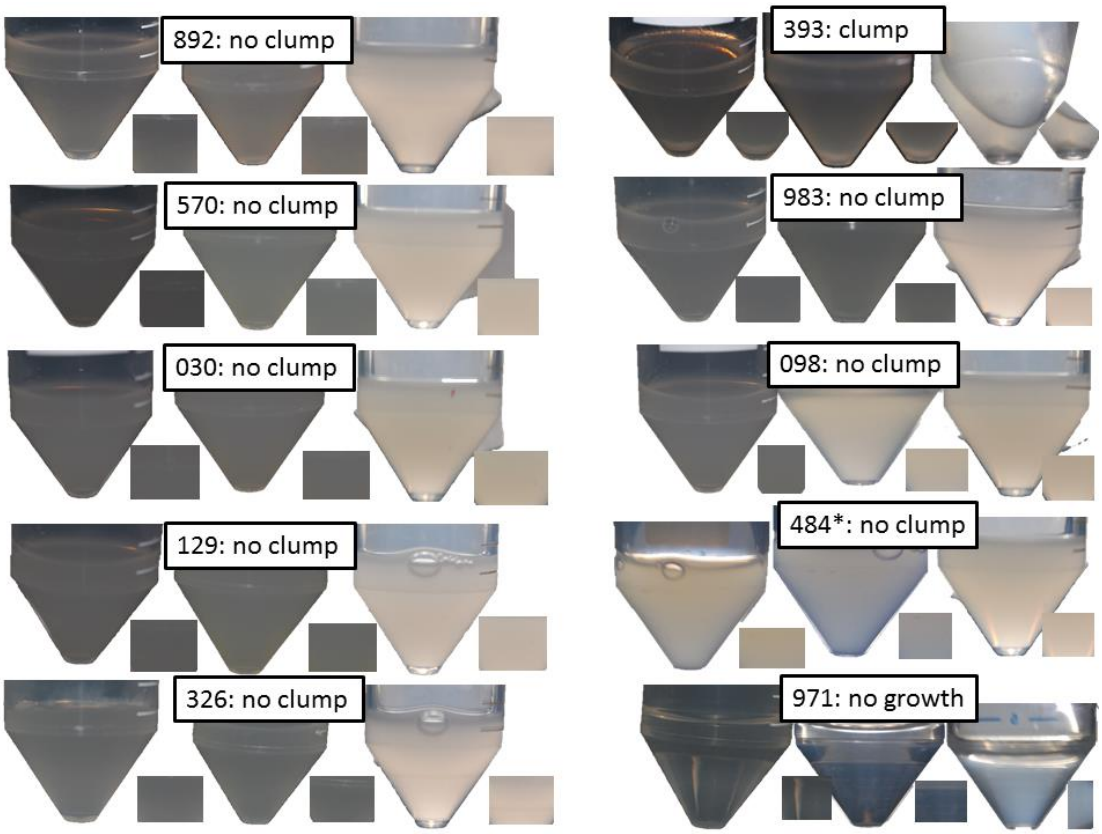


Figure 4.2.12: Only CF 393 showed a clumping phenotype in the floating biofilm assay. Five millilitres of ASM was inoculated with a single colony of a CF isolate and incubated at 37°C 200rpm for 18hrs. Photographs were taken with a digital camera (Nikon). CF 971 was not able to grow at all in this medium. The experiment was performed 3 times with a different biological replicate of each isolate.

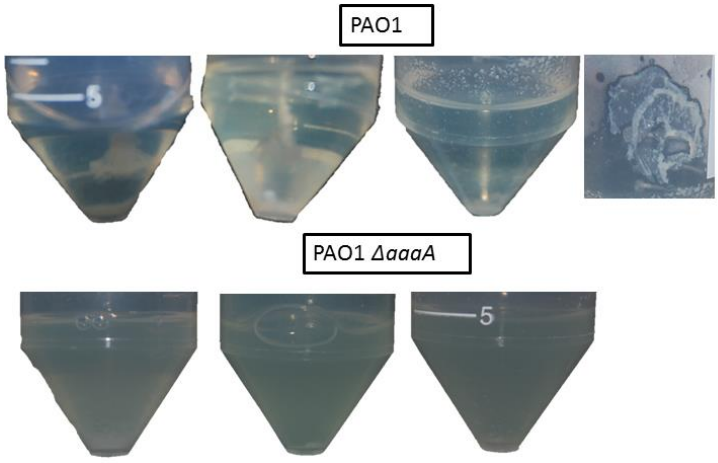


Figure 4.2.13: The PAO1 WT shows a clumping phenotype in the floating biofilm assay. Five millilitres of ASM was inoculated with a single colony of a CF isolate and incubated at 37°C 200rpm for 18hrs. Photographs were taken with a digital camera (Nikon). The experiment was performed 3 times with a different biological replicate of each isolate.

4.2.1.5.3 Three selected CF isolates form different biofilms when grown in a flow channel (Bioflux)

Although the above methods of *in vitro* biofilm growth provide a general picture at the biofilm capabilities and phenotypes of the *P. aeruginosa* isolates and have the advantage of being able to screen large numbers of samples in parallel, imaging by confocal microscopy allows a more detailed picture of the biofilm structure produced. Three isolates were selected on the basis of their differing expression of *aaaA* (section 4.2.4), varying phenotypes with the previous biofilm assays and differences in the promoter regions of *aaaA* (see promoter comparison section of this chapter where this is presented). The biofilms were grown using a Bioflux system where the bacteria are seeded into a microfluidic channel connecting 2 wells: the inlet and the outlet. Media is pumped from the inlet to the outlet at a chosen flow (shear) rate (dyne/cm^2). One dyne/cm^2 is equivalent to 0.1 Pascals. In this case a shear of 0.5 dyne/cm^2 was used. Using this method, the developing biofilm receives a continuous fresh source of nutrients. The Bioflux system available was not able to be adapted to microaerobic or anaerobic conditions so the biofilms seen here may differ from those produced under oxygen deprivation.

ASM (Palmer *et al* 2007) without eDNA or mucin was chosen as the growth media. The use of ASM produces biofilms which are more self-clustering and less adherent to abiotic surfaces in the case of PAO1 (Kirchner *et al* 2012, Davies *et al* 2017). The PAO1 control produced a self-clustering phenotype, leading to the conclusion that neither mucin nor eDNA are essential to the clumping and did not need to be present in our experiments for this reason (Figure 4.2.14). The biofilms were allowed to develop for 15 hours which was the amount of time that it took the majority of the inlet media to be passed to the outlet. Incubation was maintained at 37°C using a hot plate. To image the cells, Syto9/Propidium iodide (PI) (live/dead) stain was added to the inlet media (ASM) at concentrations of 1 µM/4 µM per µl of media.

The clustering phenotype of PAO1 (Figure 4.2.14) increased from the left to the right of the channel. There was some adhesion to the sides of the channel, but additionally there were large microcolonies suspended in the middle. The low level of PI staining (red patches) indicated that the majority of the cells within the biofilm were alive. CF 326 (Figure 4.2.15) showed a thicker and flatter growth with a general absence of the large microcolonies produced by PAO1. Most of the cells appear green ('alive') as PI ('dead') staining was at a low level. CF 983 (Figure 4.2.16) shows a more clustering phenotype than CF 326. These clusters

were more interconnected than the separate spheres produced by PAO1, and there was a relatively high quantity of red ('dead') cells. CF 393 (Figure 4.2.17) exhibited more clustering than the other two CF isolates, with the biofilm structure being intermediate between CF 983 and PAO1. More spherical microcolonies formed but there were also interconnected flatter sections of biofilm. There were very few red ('dead') cells.

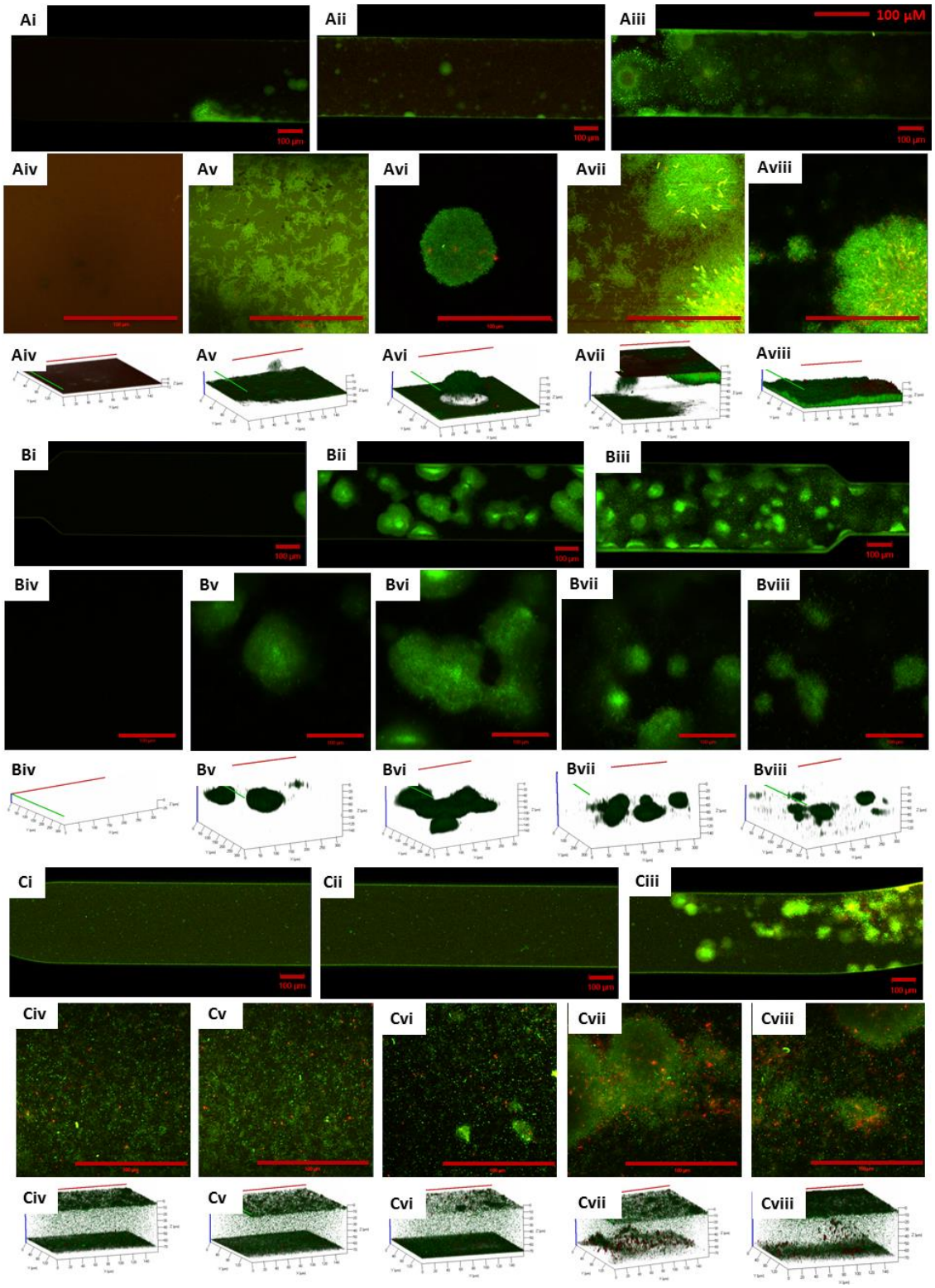


Figure 4.2.14: PAO1 grown in a Bioflux system in ASM media produces a biofilm which is highly clustered. Biofilms were grown for 15 hours in ASM at 37°C**.** Syto9 and PI were added to the inlet media at a ratio of 1:4. Images were taken across the channel using confocal microscopy (Zeiss) with the left hand pictures corresponding to the left (inlet) side of the channel and each picture moving along the channel to the right hand (outlet) side. Three biological replicates are shown and indicated by A, B, C. Two magnifications are shown: 5x and 20x/40x. Numbers i, ii and iii represent the 5x images and numbers from iv represent the 20x/40x images from z stacks.

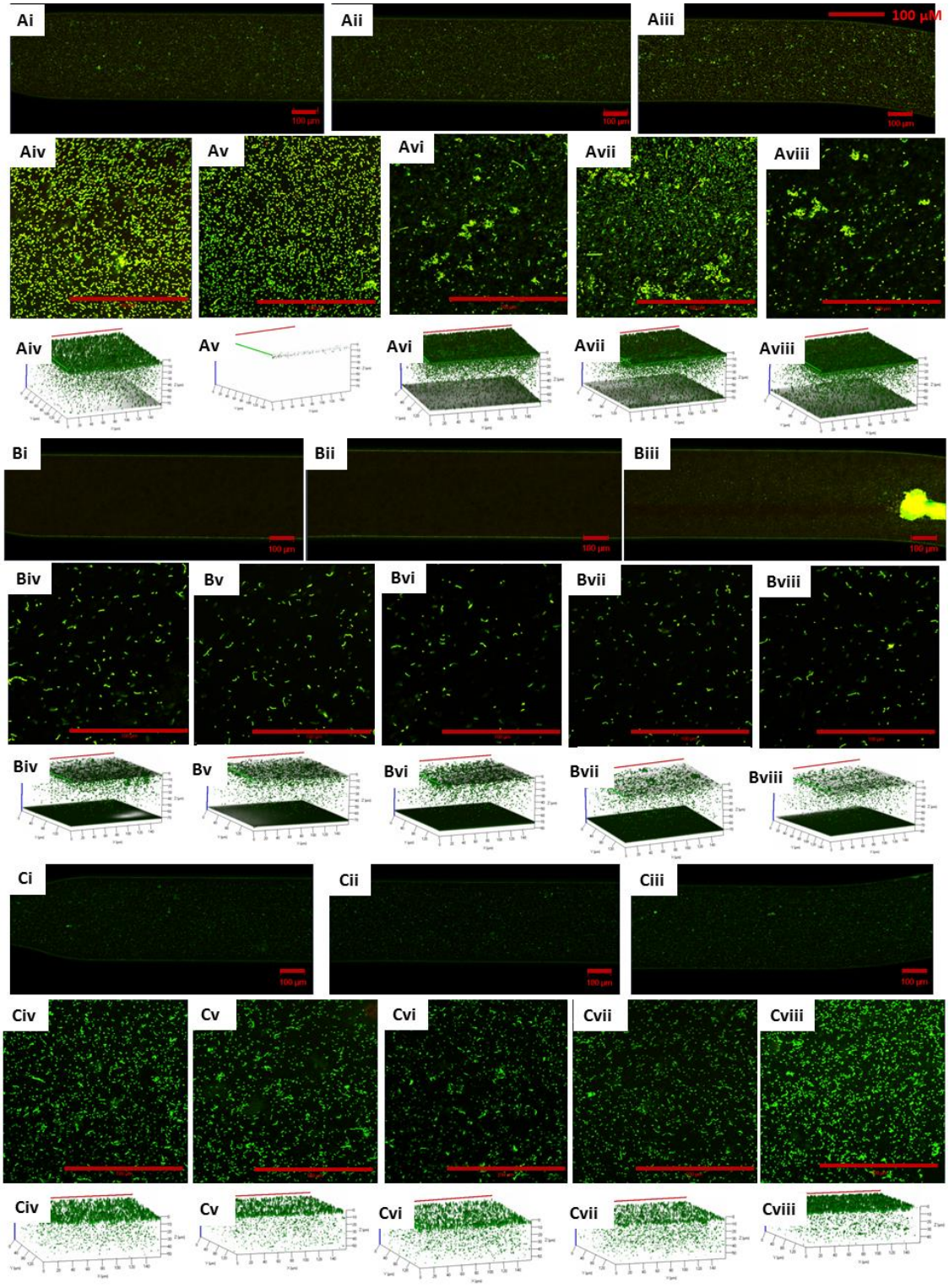


Figure 4.2.15: CF 326 grown in a Bioflux system in ASM media produces a biofilm which has more evenly spaced, smaller microcolonies than PAO1. Biofilms were grown for 15 hours in ASM at 37oC. Syto9 and PI were added to the inlet media at a ratio of 1:4. Images were taken across the channel using confocal microscopy (Zeiss) with the left hand pictures corresponding to the left (inlet) side of the channel and each picture moving along the channel to the right hand (outlet) side. Three biological replicates are shown and indicated by A, B, C. Two magnifications are shown: 5x and 40x. Numbers i, ii and iii represent the 5x images and numbers from iv represent the 40x images from z stacks.

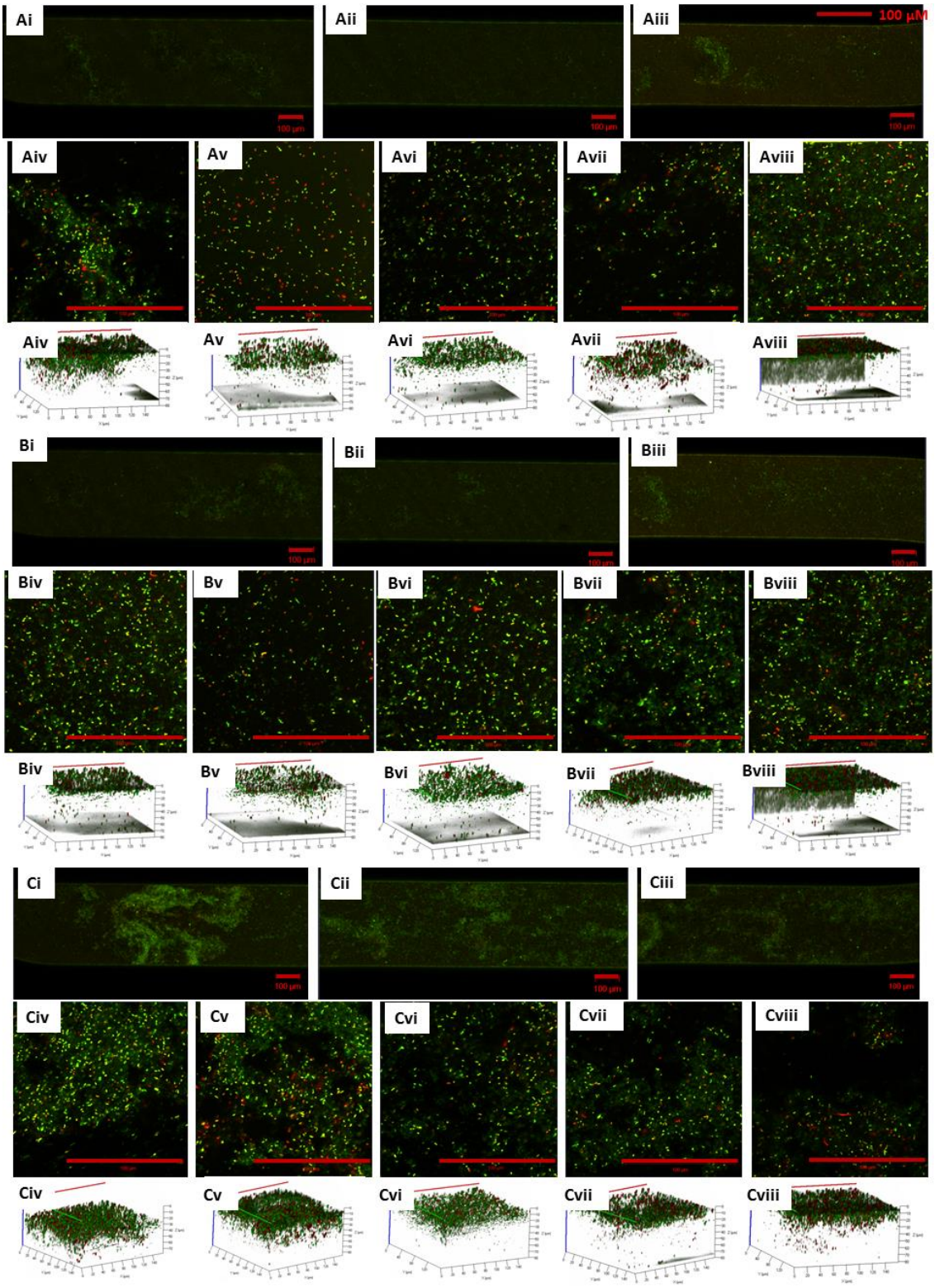


Figure 4.2.16: CF 983 grown in a Bioflux system in ASM media produces a biofilm which has more evenly spaced, smaller microcolonies and more red (dead) areas than PAO1. Biofilms were grown for 15 hours in ASM at 37°C. Syto9 and PI were added to the inlet media at a ratio of 1:4. Images were taken across the channel using confocal microscopy (Zeiss) with the left hand pictures corresponding to the left (inlet) side of the channel and each picture moving along the channel to the right hand (outlet) side. Three biological replicates are shown and indicated by A, B, C. Two magnifications are shown: 5x and 40x. Numbers i, ii and iii represent the 5x images and numbers from iv represent the 40x images from z stacks.

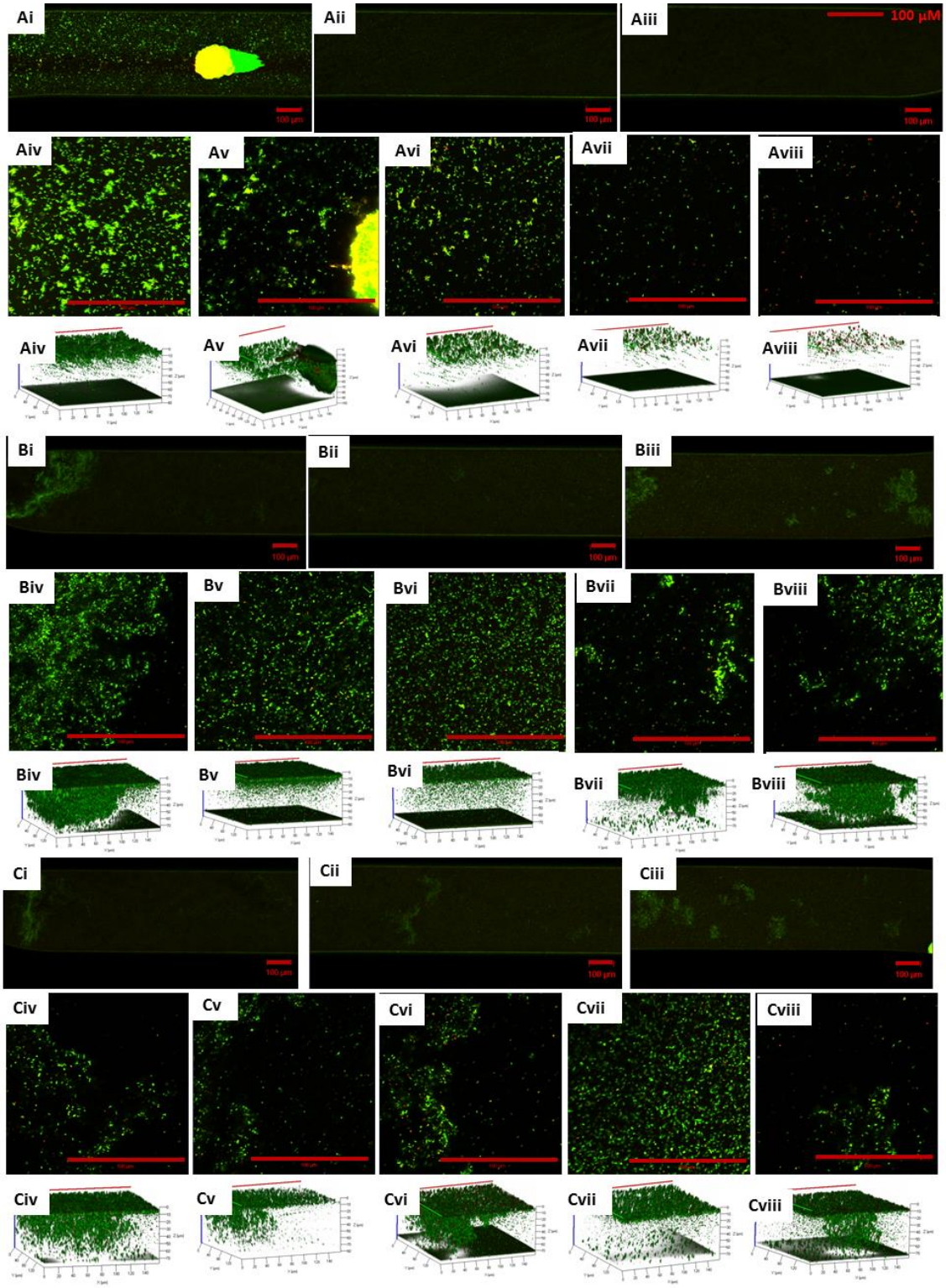


Figure 4.2.17: CF 393 grown in a Bioflux system in ASM media produces a biofilm which shows the beginning of large microcolonies forming similar to PAO1. Biofilms were grown for 15 hours in ASM at 37°C. Syto9 and PI were added to the inlet media at a ratio of 1:4. Images were taken across the channel using confocal microscopy (Zeiss) with the left hand pictures corresponding to the left (inlet) side of the channel and each picture moving along the channel to the right hand (outlet) side. Three biological replicates are shown and indicated by A, B, C. Two magnifications are shown: 5x and 40x. Numbers i, ii and iii represent the 5x images and numbers from iv represent the 40x images from z stacks.

4.2.2 The role of AaaA in cystic fibrosis isolates

4.2.2.1 The aaaA gene is conserved across cystic fibrosis isolates

To determine whether AaaA was required by *P. aeruginosa* within the environment of the CF lung, 2 panels of isolates were screened by colony PCR for the presence of the *aaaA* gene (Figure 4.2.18 and Figure 4.2.19). One panel (Figure 4.2.18) was comprised of *P. aeruginosa* isolated from different patients. The second panel (Figure 4.2.19) consisted of multiple isolates taken from the same patient. In all the bacteria tested, *aaaA* was present. The differences in the PCR product band intensity are likely due to the differences in initial DNA template concentration present, which could not be quantified since colony PCR was employed for this initial screen.

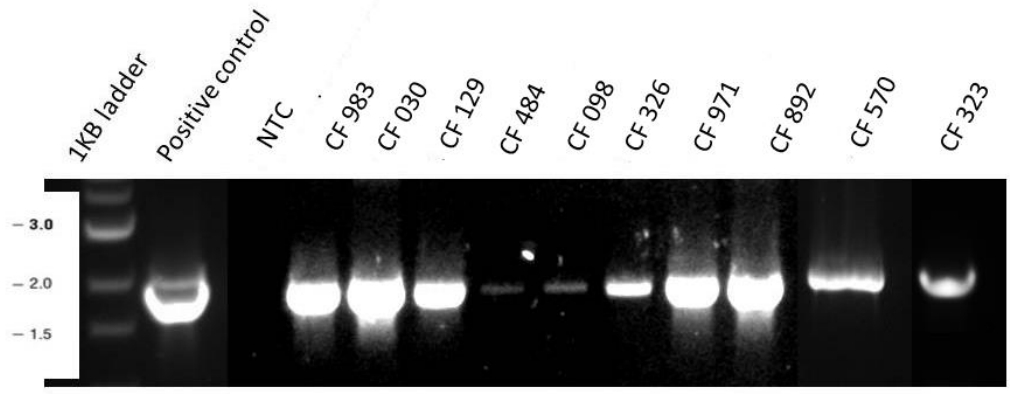


Figure 4.2.18: The *aaaA* gene is present in *P. aeruginosa* isolated from a range of CF patients. The results were obtained by colony PCR using PAO1 as the positive control and a no template control (NTC) as a negative. The primer pair used was aaaA ORF (E1F and E1R) 5'-CAGGATTCATGTTCAAACCATTAGCTGTCGCTG and 5'-GCTATCGATTTAGTGATGGTGATGGTGATGGAACTGCCAGTTCACCCTGAG (originally designed by Dr Esteban Paredes 2014). The expected product of 1944 bp is shown.

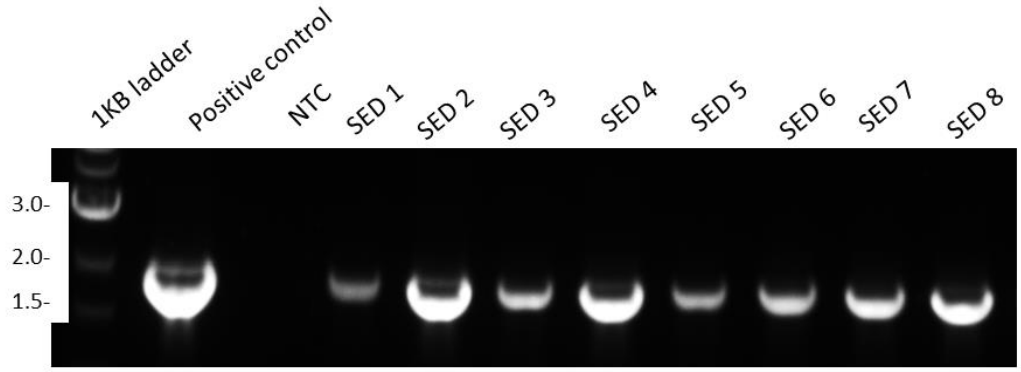


Figure 4.2.19: The *aaaA* gene is present in multiple *P. aeruginosa* strains isolated from a single CF patient (from Darch *et al* 2015). The results were obtained by colony PCR using PAO1 as the positive control and a no template control (NTC) as a negative. The primer pair used was aaaA ORF (E1F and E1R) 5'-CAGGATTCATGTTCAAACCATTAGCTGTCGCTG and 5'-GCTATCGATTTAGTGATGGTGATGGTGATGGAACTGCCAGTTCACCCTGAG (originally designed by Dr Esteban Paredes 2014). The expected product of 1944 bp is shown.

.

4.2.2.2 The open reading frame of aaaA shows high sequence conservation

Having ascertained that all isolates tested contained a copy of *aaaA*, potential differences between the sequences were investigated. The alignment is shown below (Figure 4.2.20). The residues predicted to be responsible for protein activity were conserved, suggesting that the original arrangement is important for the maintenance of enzyme activity. There were, however, some SNPs found in the CF isolate AaaA passenger domains, mainly occurring towards the C terminus of the protein.

Common to all the CF isolates apart from CF 393 is a change in the lysine found at position 55 to glutamate. It is found in the middle of an alpha helix which is on the outside of the protein structure. Glutamate, as well as lysine, is an amino acid that works well in such a structure and it may be that there is little effect on the functioning of the protein. However, the side chain of lysine is sometimes involved in supporting the protein structure by generation of a salt bridge. Glutamate is negatively charged whilst lysine has a positive charge.

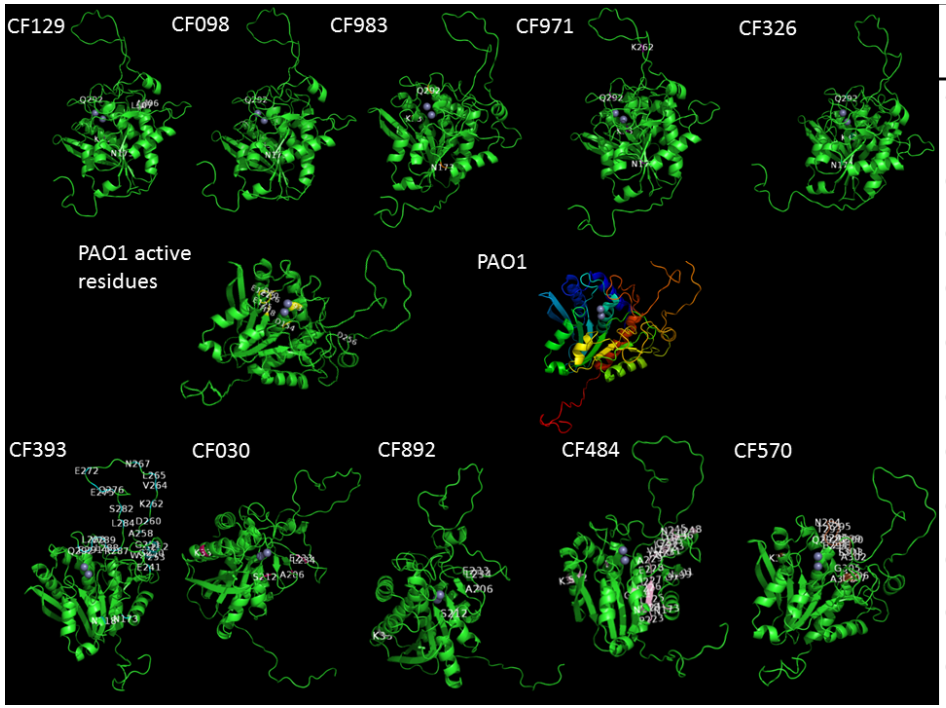
A group of CF isolates showing a similar mutation pattern includes CF 129, CF 098, CF 983, CF 971 and CF 326 (Figure 4.2.21). They share the previously mentioned lysine to glutamate exchange (position 55), a change from asparagine to serine (position 195) and the replacement of glutamine with leucine (position 314). CF 570 also appears similar to this group but does not contain the asparagine to serine mutation and has some extra changes nearer the C-terminus (Figure 4.2.24:). Position 195 is just before the start of an alpha helix, the change to serine may help stabilise this part of the structure as it can act in a similar way to proline by facilitating a tight turn. The substitution of leucine for glutamine at position 314 changes the residue from a polar to a hydrophobic one. The position is in the centre of an alpha loop, facing towards the active site of the protein but has not been identified as one of the active residues.

CF 030 and CF 892 appear to show a different pattern of mutations to the previous group and closely resemble each other in terms of the residue changes showing a change from A to T (position 228) and EL to GT (position 255-256) (Figure 4.2.22). Position 228 is on a loop following a beta sheet, bordering the active site pocket but at a fair distance away. Alanine is a small amino acid which is non polar but not particularly hydrophobic. Its side chain is non-reactive but can play a role in substrate recognition. Threonine is polar, but not a strongly hydrophilic, amino acid. It more often has a role in the active site. Perhaps this substitution for a more reactive amino acid increases the catalytic function of AaaA, or its increased polarity helps stabilise the structure. Positions 255 and 256 are on a loop in close proximity to the A-T (position 228) substitution. Glycine, with only hydrogen in its side chain has high conformational flexibility, more than glutamate which is bigger and is a polar amino acid. The adjacent leucine is substituted for threonine. Both threonine and leucine contain C-beta branches and so are more bulky and less flexible than other amino acids. The combination with glycine probably helps create the tight angle needed for the loop. Threonine is more polar than leucine which is hydrophobic and so may alter the structure

through its interaction with the outside of the protein. Threonine also has a more reactive side chain than leucine.

CF 393 and CF 484 were found to contain a much greater number of changes in the AaaA ORF than the other CF isolates (Figure 4.2.23). They show more similarity to each other than the other strains but have several individual mutations distinct from the other (Figure 4.2.24:). The similar mutations are at position 270 (isoleucine to valine) and position 240 (asparagine to isoleucine). Isoleucine to valine is a substitution which should not cause too much difference; they are both hydrophobic, C-beta branched amino acids. The position at the end of the alpha-helix is unlikely to be involved in catalytic functions. Asparagine's substitution with isoleucine also occurs at the end of an alpha-helix. The polar amino acid is changed to a bulkier hydrophobic one and may support a tighter angle of the helix end toward the centre of the protein.

The substitutions unique to CF 393 happen further towards the C terminus than the substitutions in CF 484. There is very little overlap apart from the above mentioned (Figure 4.2.24:). They occupy a large block rather than single changes. In CF 393 the changes can be seen to occur principally on the large loop and adjoining alpha helix. In CF 484 the changes occur on a loop closer to the centre of the protein and on a fairly central beta sheet.



	55K	100H; 102D	115	147-149EEE	176D	195N	270I	228A	240N	255-256EL	277D	314Q
Active		H ; D	D	EEE	D						D	
CF 129	K→E					N→S						Q→L
CF 098	K→E					N→S						Q→L
CF 983	K→E					N→S						Q→L
CF 971	K→E					N→S						Q→L
CF 326	K→E					N→S						Q→L
CF 393						N→S	I→V		N→I			
CF 030	K→E							A→T		EL→GT		
CF 892	K→E							A→T		EL→GT		
CF 484	K→E					N→C	I→V		N→I			
CF 570	K→E											Q→L

Figure 4.2.20: AaaA passenger domain mutations in CF isolates do not overlap with active site residues indicating that this is conserved. Figure left: each structure shown is the AaaA passenger domain starting at position 22 and ending at position 370. The SNPs found to occur in each CF isolate are marked. At the centre left of the figure is the AaaA passenger domain with the active site residues indicated. These active residues come from an alignment with SGAP and were validated by Luckett *et al* (2012). Table right: common changes occurring in the CF AaaA sequences. These Include lysine (K) to glutamate (E) at position 55, asparagine (N) to serine (S) at position 195 and glutamine (Q) to leucine (L) at position 314. CF isolates 393 and 484 show the greatest amount of change and isolates CF 129, 098, 983, 971 and 326 show a similar pattern of mutations. Sequencing was outsourced to Source Bioscience, the NCBI protein alignment tool was used to compare sequences and the Pymol software used to create the image.

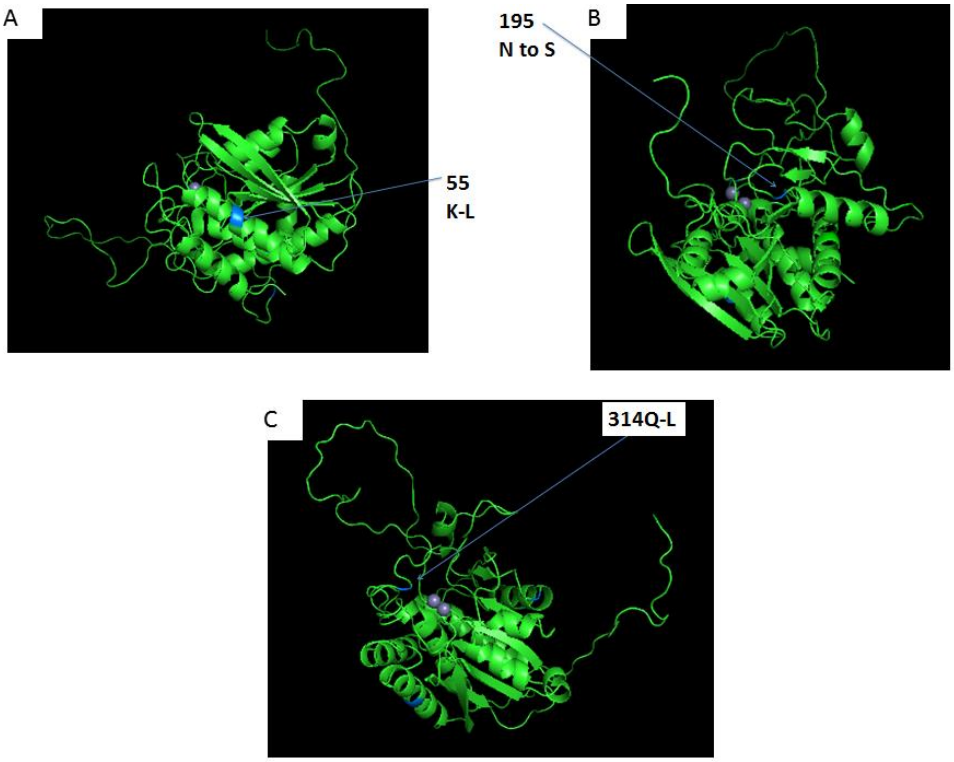


Figure 4.2.21: Common mutation pattern 1. A: position 55 lysine (K) to glutamate (E). B: position 195 asparagine (N) to serine (S). C: position 314 glutamine (Q) to leucine (L). Images created using Pymol.

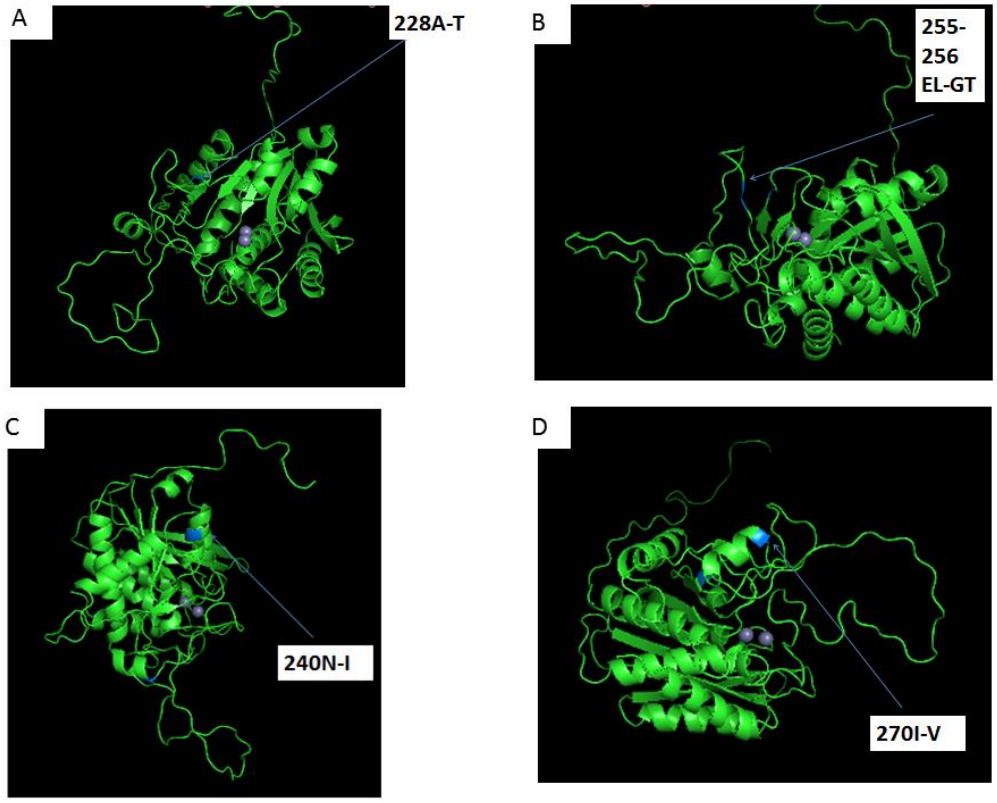


Figure 4.2.22: Common mutation pattern 2 (A and B) and 3 (C and D). A: position 228 alanine (A) to threonine (T). B: position 255 and 256 glutamate (E) and leucine (L) to glycine (G) and threonine (T). C: position 240 asparagine (N) to isoleucine (I). D: position 270 isoleucine (I) to valine (V). Images created using Pymol.

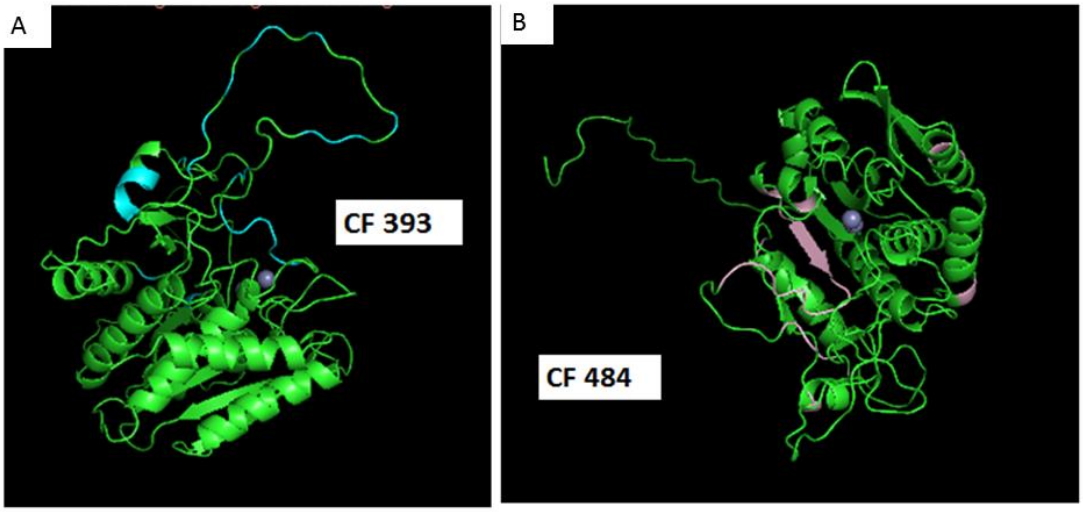


Figure 4.2.23: Mutation patterns in CF 393 (A) and CF 484 (B). CF 393 showing more external changes and CF 484 more internal changes. Images created using Pymol.

	CF 570	CF 971	CF 484	CF 393	CF 129
27E			E-Q		
54S			S-C		
221G			G-R		
223N			N-D		
236G			G-C		
246-252VLFIEAT			VLFIEAT-GVVHRGD		
256L			L-W		
258D			D-T		
260			Insertion S		
263E			E-P	E-K	
264O			O-T		
266-267DN			DN-RF		
271I			I-V		
272-277 PGGSTW-				PGGSTW—RRLNLA(R)	
280A				A-G	
282D				D-G	
284K		K-Q		K-Q	
285K				K-G	
287-289VLN				VLN-TDH	
292				Insertion R	
296E				E-H	
298IEQR				IEQR- HXVTH	
306S				S-P	
308L				L-A	
308-312RLVLE				RLVLE-PGAGS	

312-324 EQTNADLLA	EQTNADLLASTAS- D*PTPTCWP
327-330 GALA	GALA- APWP
328-329AL	AL-RP
335D	D-N

Figure 4.2.24: Mutations unique to individual isolates in the AaaA passenger domain. Asterisks indicate a deletion.

4.2.2.3 In comparison to PAO1, the majority of CF isolate aaaA promoters contain an 169 bp deletion region which is shared by LES

To ascertain whether AaaA could be differentially regulated in the CF isolates, it was necessary to determine any changes to the sequence upstream of the AaaA ORF. To do this, the promoters were amplified by PCR for the purpose of sequence analysis. The primers used were PromF (5'-TATCTCGAGAGCTGAGGCCTGGCGGC) and PromR (5'-TATGAATTCGAACACGGCACTTTCCTCTG) originally designed and used by Paredes (2014). Interestingly, many of the isolates contained *aaaA* promoters which could not be amplified even though the PAO1 control was positive. To investigate whether the promoters could be so different that one or both of the primers were not able to hybridise, an alignment of several published *aaaA* promoter sequences (inclusive of 500 bp upstream of the ORF) belonging to a range of different *P. aeruginosa* strains was performed by an MSc student, Mr Monir Mohammad (Masters dissertation 2015) using the NCBI BLAST tool. It was found that several strains including the Liverpool epidemic strains (LES) contained a 169 bp–deletion region which spanned across the hybridisation site of the forward primer. Following this interesting finding by Monir, the 500 bp section of sequence was expanded to include the first 133 bp of *PA0329*. The details of the query sequence used as the BLAST template are noted in Figure 4.2.25 and the results from the search are detailed in Table 4.2.2. This investigation was expanded with the help of Dr Diana Palenzuela Bretones to include several wound *P. aeruginosa* isolates. These are marked by a blue font colour. The deletion region is seen in strains isolated from diverse environments and not exclusively found in clinically isolated *P. aeruginosa*.

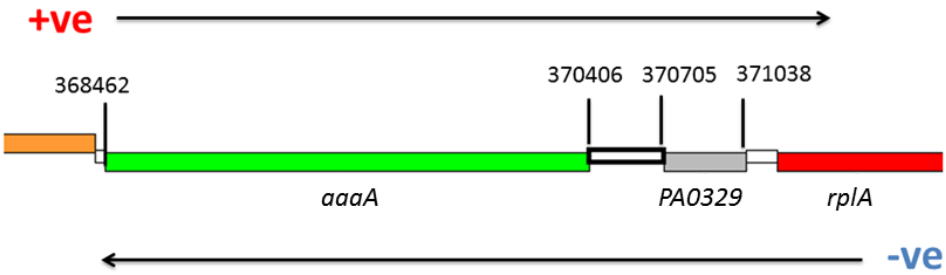
The results from the BLAST alignment showed that there were 2 different sequence types: one containing a deletion from the 333bp query (PAO1) to 502 bp of the PA01 promoter (first 169 bases of the intergenic region between

PA0329 and *aaaA*). A schematic of the 2 types of upstream region region is shown in Figure 4.2.25. Group 1 is similar to the PAO1 reference, and group 2 contains the deletion region in respect of PAO1. Many of the CF isolates in this work were derived from LESB and therefore there was a high likelihood that these would contain the deletion region. The original forward primer used for amplifying the promoter region is homologous to a stretch of sequence within the deletion region. A new forward promoter primer was designed (UF_aaaA_LES, 5' tatactagtCTTCGGATTGGCGGTGAAG 3') using the LESB65 sequence as a guide and the PCR repeated. This was largely successful except for CF 030 and CF 393, which was not altogether surprising as these isolates were not derived from LESB (Figure 4.1.1). However, it was difficult to get sufficient amplification with either the original or new forward primer, suggesting that in both regions there were substantial changes to the sequence. A sequence for CF 393 was generated with the original primer, but not for CF 030. The alignment is shown in Figure 4.2.26 and a phylogenetic tree illustrates the proximity of the isolates to the PAO1 or LESB65 lineage. The mismatches of the CF isolate sequences with the PAO1 reference are also included in Figure 4.2.26. Apart from CF 393, the mutations imitate that of LESB65. The conserved nature of these changes indicates that they may be selected for in the CF lung.

Mapping the changes seen between the CF isolate sequences and the PAO1 reference shows that some of these overlap with putative regulator binding sites (Figure 4.2.27). The identified regulator binding sites containing SNPs are ArgR and NarL (1 of 4 sites found). Interestingly, at least 6 of the changed bases in the regulator binding sites can be seen in several other *P. aeruginosa* strains including, PA7, DK2, PA1R, M18 and the LES groups. None of the SNPs appeared in the RpoN site and so could indicate a need for conservation. The deletion region began just after the hybridisation site of the LESB65 primer and contained 3 NarL, both IHF, ArcA and RhlR putative binding sites (not shown in figure).

A

Strain in Pseudomonas genome database	Ref seq	Locus tags	Genomic location	Ortholog group (Pseudomonas)
PAO1 reference sequence	NP_249019.1	PA0329	370706 - 371038 (- strand)	POG000321 (391 members)
	NP_249020.1 (*aaaA* ORF)	Intergenic region between PA0329 and PA0328 (*aaaA*)	370406-370705(- strand) Finishing at start of *aaaA* ORF)	POG000320 (344 members, starting *aaaA* ORF)



B

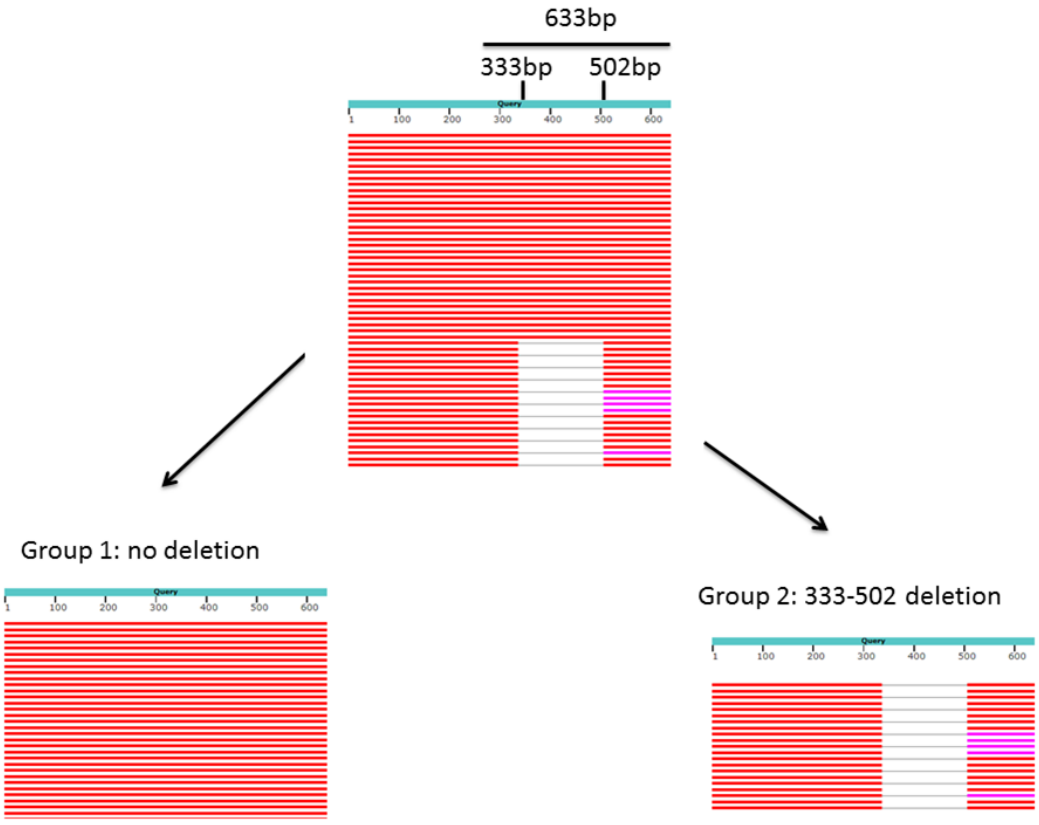


Figure 4.2.25: Some strains of *P. aeruginosa* have a deletion of 169bp at the beginning of the intergenic region between *PA0329* and *aaaA*. Part A: 633 bp of the PAO1 reference sequence (*Pseudomonas* Genome Database) ending at the *aaaA* start codon and beginning at the PA0329 start codon, was entered into an NCBI BLASTN search. The genomic coordinates are shown on the cartoon. Part B: two types of alignment were identified, sequences which contained a 169 bp deletion between base 333 and base 502 (first part of the intergenic following the *PAO329* ORF) and sequences which did not contain this deletion. The sequences not containing the deletion have been assigned to group 1 and the deletion containing sequences assigned to group 2. The figures were taken and adapted from the NCBI results window.

Group 1 (no deletion)		**Group 2 (deletion)**	
Strain	**Total mismatches in aligned**	**Strain**	**Total mismatches in aligned**
Pseudomonas aeruginosa strain ATCC 15692, complete genome	0	*Pseudomonas aeruginosa* strain PA_D21, complete genome	5
Pseudomonas aeruginosa genome assembly PAO1OR, chromosome	0	*Pseudomonas aeruginosa* strain PA_D5, complete genome	5
Pseudomonas aeruginosa PAO1-VE13 genome	0	*Pseudomonas aeruginosa* strain PA_D25, complete genome	5
Pseudomonas aeruginosa PAO1-VE2 genome	0	*Pseudomonas aeruginosa* strain PA_D22, complete genome	5
Pseudomonas aeruginosa PAO581 genome	0	*Pseudomonas aeruginosa* strain PA_D16, complete genome	5
Pseudomonas aeruginosa PAO1, complete genome	0	*Pseudomonas aeruginosa* strain PA_D9, complete genome	5
Pseudomonas aeruginosa strain 12-4-4(59), complete genome	1	*Pseudomonas aeruginosa* strain PA_D2, complete genome	5
Pseudomonas aeruginosa strain L10, complete genome	2	*Pseudomonas aeruginosa* strain PA_D1, complete genome	5
Pseudomonas aeruginosa strain M1608, complete genome	2	*Pseudomonas aeruginosa* strain N17-1, complete genome	11
Pseudomonas aeruginosa isolate PA14Or_reads genome assembly, chromosome: PA14OR	2	*Pseudomonas aeruginosa* strain N15-01092, complete sequence	10
Pseudomonas aeruginosa strain BAMCPA07-48, complete genome	2	*Pseudomonas aeruginosa* DSM 50071, complete genome	10
Pseudomonas aeruginosa strain M37351, complete genome	2	*Pseudomonas aeruginosa* genome assembly NCTC10332, chromosome : 1	10
Pseudomonas aeruginosa UCBPP-PA14, complete genome	2	*Pseudomonas aeruginosa* strain AR_0353 chromosome, complete	6

Pseudomonas aeruginosa MTB-1, complete genome 3

Pseudomonas aeruginosa strain Cu1510, complete genome 4

Pseudomonas aeruginosa DNA, complete genome, strain: IOMTU 133 4

Pseudomonas aeruginosa strain PB353 chromosome, complete genome 5

Pseudomonas aeruginosa strain PB354 chromosome, complete genome 5

Pseudomonas aeruginosa DHS01, complete genome 6

Pseudomonas aeruginosa strain USDA-ARS-USMARC-41639, complete genome 6

Pseudomonas aeruginosa strain T63266, complete genome 6

Pseudomonas sp. AK6U chromosome, complete genome 7

Pseudomonas aeruginosa strain Pa1242, complete genome 8

Pseudomonas aeruginosa strain CCBH4851 genome 8

Pseudomonas aeruginosa strain W45909, complete genome 8

Pseudomonas aeruginosa strain W16407, complete genome 8

genome

Pseudomonas aeruginosa strain PB368 chromosome, complete genome 6

Pseudomonas aeruginosa strain PB369 chromosome, complete genome 6

Pseudomonas aeruginosa strain 12939 chromosome, complete genome 6

Pseudomonas aeruginosa strain Ocean-1155, complete genome 6

Pseudomonas aeruginosa strain Ocean-1175, complete genome 6

Pseudomonas aeruginosa C-NN2 isolate early isolate NN2 (clone C) genome assembly, chromosome: I 12

Pseudomonas aeruginosa strain Pa58, complete genome 6

Pseudomonas aeruginosa strain M8A4 genome 6

Pseudomonas aeruginosa strain PASGNDM699, complete genome 6

Pseudomonas aeruginosa strain PASGNDM345, complete genome 6

Pseudomonas aeruginosa strain W36662, complete genome 12

Pseudomonas aeruginosa strain PA_154197, complete genome 6

Pseudomonas aeruginosa isolate B10W, complete genome 6

Pseudomonas aeruginosa strain PA7790, complete genome	8
Pseudomonas aeruginosa strain PA11803, complete genome	8
Pseudomonas aeruginosa strain PA8281, complete genome	8
Pseudomonas aeruginosa strain PA1088, complete genome	8
Pseudomonas aeruginosa strain FA-HZ1, complete genome	8
Pseudomonas aeruginosa strain H47921, complete genome	8
Pseudomonas aeruginosa strain PSE305, genome	8
Pseudomonas aeruginosa c7447m genome	10
PA-W25|scaffold_1	19
PA-W48|scaffold_2	19
PA-W18|scaffold_6	25
PA-W42|scaffold_6	25
Pseudomonas aeruginosa strain DN1, complete genome	6
Pseudomonas aeruginosa DNA, complete genome, strain: NCGM257	8
Pseudomonas aeruginosa VRFPA04, complete genome	6
Pseudomonas aeruginosa B136-33, complete genome	6
Pseudomonas aeruginosa strain AR_0095 chromosome, complete genome	12
Pseudomonas aeruginosa strain AR_0357 chromosome, complete genome	7
Pseudomonas aeruginosa strain AR_0230 chromosome, complete genome	12
Pseudomonas aeruginosa strain AR_0354 chromosome, complete genome	7
Pseudomonas aeruginosa strain F5677 chromosome, complete genome	12
Pseudomonas aeruginosa isolate RW109 genome assembly, chromosome: Main chromosome	12
Pseudomonas aeruginosa strain PB350 chromosome, complete genome	7
Pseudomonas aeruginosa strain PB367 chromosome, complete genome	7

PA-W15|scaffold_5	21	*Pseudomonas aeruginosa* strain Pb18 genome	12
PA-W14|scaffold_3	24	*Pseudomonas aeruginosa* strain M28A1 genome	12
PA-W28|scaffold_5	19	*Pseudomonas aeruginosa* strain M8A1 genome	13
PA-W38|scaffold_7	19	*Pseudomonas aeruginosa* strain F63912, complete genome	12
PA-W3|scaffold_1	25	*Pseudomonas aeruginosa* PAK chromosome, complete genome	12
PA-W5|scaffold_6	25	*Pseudomonas aeruginosa* strain X78812, complete genome	13
PA-W31|scaffold_6	25	*Pseudomonas aeruginosa* strain T38079, complete genome	12
PA-W39|scaffold_6	25	*Pseudomonas aeruginosa* strain S86968, complete genome	12
PA-W35|scaffold_3	21	*Pseudomonas aeruginosa* strain W60856, complete genome	12
PA-W45|scaffold_6	19	*Pseudomonas aeruginosa* strain H27930, complete genome	12
PA-W41|scaffold_1	19	*Pseudomonas aeruginosa* strain H5708, complete genome	12
PA-W23|scaffold_6	25	*Pseudomonas aeruginosa* strain F23197, complete genome	13
PA-W10|scaffold_3	41	*Pseudomonas aeruginosa* strain E6130952, complete genome	7
PA-W7|scaffold_3	40	*Pseudomonas aeruginosa* strain RIVM-EMC2982, complete genome	12
PA-W44|scaffold_5	18	*Pseudomonas aeruginosa* strain F9670, complete genome	12
PA-W12|scaffold_3	40	*Pseudomonas aeruginosa* strain T52373, complete genome	12
PA-W33|scaffold_1	23	*Pseudomonas aeruginosa* strain F30658, complete genome	12
PA-W46|scaffold_5	41	*Pseudomonas aeruginosa* LESlike4 sequence	12

Pseudomonas aeruginosa LESlike1 sequence	12
Pseudomonas aeruginosa LESB65 sequence	12
Pseudomonas aeruginosa LES400 sequence	12
Pseudomonas aeruginosa LESlike7 sequence	12
Pseudomonas aeruginosa LESlike5 sequence	12
Pseudomonas aeruginosa YL84, complete genome	12
Pseudomonas aeruginosa PA38182, complete genome	12
Pseudomonas aeruginosa SCV20265, complete genome	12
Pseudomonas aeruginosa LES431, complete genome	12
Pseudomonas aeruginosa PA1R, complete genome	12
PA-W27|scaffold_6	20
PA-W21|scaffold_0	37
PA-W22|scaffold_8	6
PA-W16|scaffold_7	6
PA-W17|scaffold_5	37

PA-W2|scaffold_4	4
PA-W29|scaffold_4	6
PA-W47|scaffold_3	37
PA-W49|scaffold_12	33
PA-W13|scaffold_1	21
PA-W40|scaffold_2	23
PA-W32|scaffold_2	37
PA-W20|scaffold_0	37
PA-W26|scaffold_0	6
PA-W43|scaffold_4	26
PA-W8|scaffold_5	23
PA-W30|scaffold_1	7
PA-W19|scaffold_6	7
PA-W24|scaffold_6	37
PA-W6|scaffold_4	21

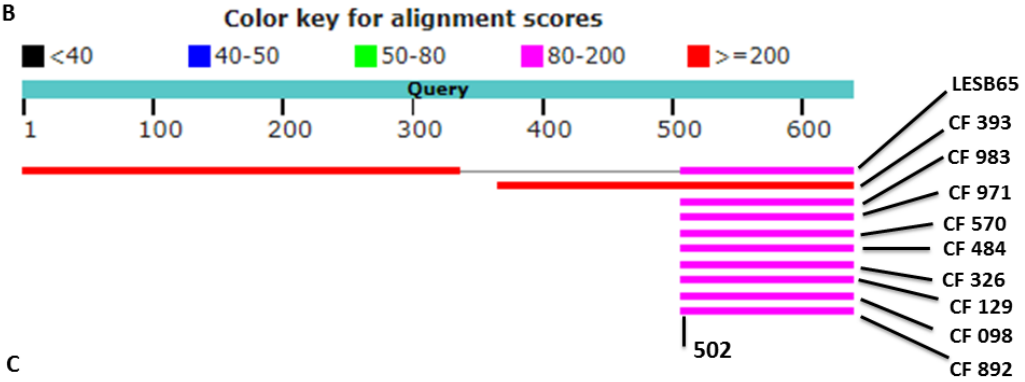
PA-W36|scaffold_3	34
PA-W37|scaffold_4	30
PA-W9|scaffold_2	37
PA-W34|scaffold_6	37
PA-W1|scaffold_6	80
PA-W11|scaffold_1	34
PA-W4|scaffold_3	37

Table 4.2.1: Identities of the sequences belonging to group 1 or group 2. Note that LESB65 and the LES-like sequences are in group 2 in addition to the PAK strain. Neither group contains exclusively clinical strains. The number of mismatches for each sequence is also included to demonstrate the relatively low amount of change aside from the deletion. The alignment was performed using the NCBI BLASTN tool.

A



B



C

	185A	207G	301A	369C	507A	509G	511A	520T	528C	539A	547-548C	550A	552A
CF393				C→DEL									
LESB65	A→G	G→A	A→G			G→C	A→G	T→G	C→A	A→C	TC→CA	A→C	A→G
CF983						G→C	A→G	T→G	C→A	A→C	TC→CA	A→C	A→G
CF971						G→C	A→G	T→G	C→A	A→C	TC→CA	A→C	A→G
CF570						G→C	A→G	T→G	C→A	A→C	TC→CA	A→C	A→G
CF484						G→C	A→G	T→G	C→A	A→C	TC→CA	A→C	A→G
CF326						G→C	A→G	T→G	C→A	A→C	TC→CA	A→C	A→G
CF129						G→C	A→G	T→G	C→A	A→C	TC→CA	A→C	A→G
CF098						G→C	A→G	T→G	C→A	A→C	TC→CA	A→C	A→G
CF182					A→G	G→C	A→G	T→G	C→A	A→C	TC→CA	A→C	A→G

D

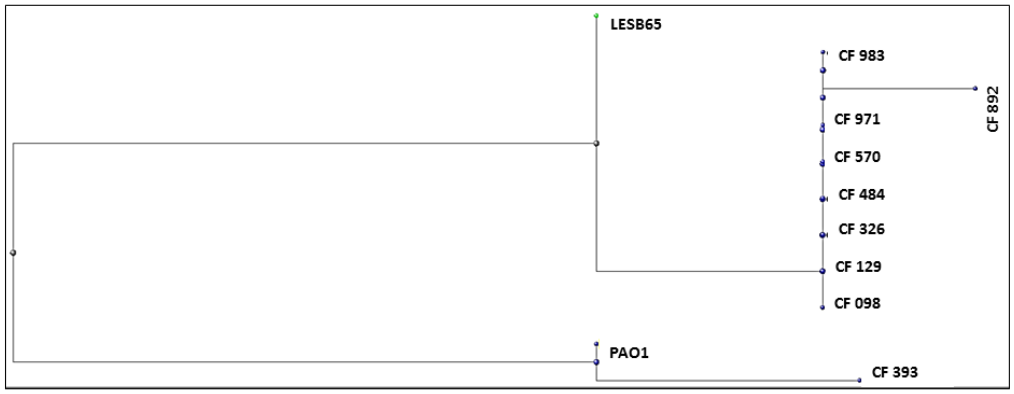


Figure 4.2.26: Most of the CF isolates have the deletion identified in Fig 3.31, and a sequence with good homology to LESB65. Panel A: PCR products produced using the original promoter primer and the new promoter primer to amplify the genomic DNA were applied to an agarose gel prior to sequencing. In red are the strains which did not amplify well using the new promoter primer. Panel B: phylogenetic tree constructed using NCBI, default settings. The pattern of mutations seen in 8 of the isolates is identical to LESB65 (indicated by pink lines) apart from 1 extra SNP in CF892. CF 393 shows a different profile, not having the deletion, and showing a high level of similarity to the PAO1 reference (represented by the red line). The first 360 bases of PAO1 are absent in the CF isolate sequences as the forward primer hybridizes after this. Panel C: table of mutations from the PAO1 reference sequence. Panel D: phylogenetic tree constructed using NCBI default settings.

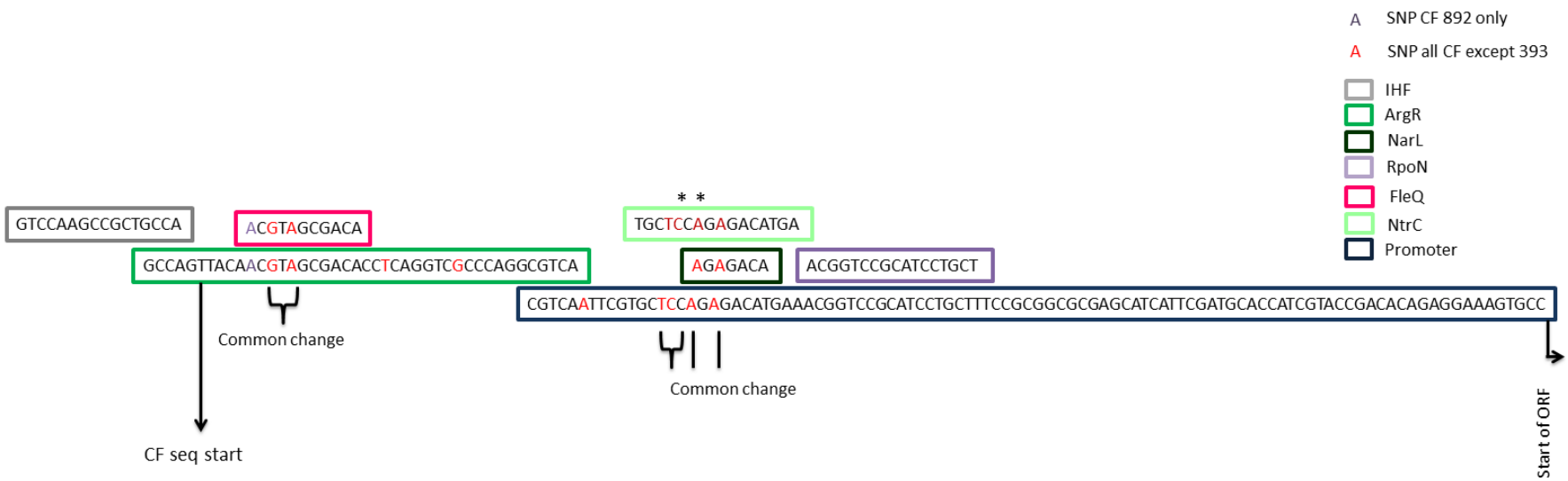


Figure 4.2.27: Single nucleotide changes to the upstream region of *aaaA* shared by the CF isolates intersect with some identified putative regulatory sites. Putative regulator binding sites were found using a combination of manual publication searching, PRODORIC and assistance by Prof. Nick Tucker (RpoN) (chapter 3) which are represented by coloured boxes. The promoter was identified by Dr Owen Darch (2013) which is represented by a dark blue box. Grey=IHF, green=ArgR, pink= FleQ, mint green= NtrC, dark green =one of the NarL sites, purple=RpoN. Changes between the PAO1 reference and the CF isolates/ LESB65 (excluding CF 393), are marked by a change in font colour to red. One change specific to CF 892 is marked on in purple font. Changes that are seen to occur across several strain groups in the BLAST analysis are marked with black indications and 'common change'. The asterisks show a coincidence of a SNP with a conserved base in a putative binding motif. The last base on the right is the base prior to the start of the *aaaA* ORF.

4.2.3 Investigation of conditions relevant to the Cystic Fibrosis airway: PAO1 and PAO1 *ΔaaaA* strains

In this section the expression and activity of AaaA was tested in the conditions outlined below:

- Expression
    1. Addition of nitrate
    2. Different NaCl concentrations
    3. pH range
- Activity
    1. ASM and LB in aerobic and microaerobic conditions
    2. Addition of nitrate
    3. Different NaCl concentrations
    4. pH range

4.2.3.1 The activation of the aaaA promoter can be measured using a lux-based reporter system

To observe differences in the expression of *aaaA*, a mini-CTX vector containing a fusion between the *aaaA* promoter and *luxCDABE* genes (designed and constructed by Paredes 2014) was introduced into PAO1, PAO1 *ΔaaaA* and the CF isolates by conjugation or transformation. The mini-CTX system, developed by Hoang *et al* (2000), is able to insert into a neutral site in the *P. aeruginosa* chromosome (*attB*) by integrase mediated recombination. The resistance cassette (tetracycline) and integrase sequences can be subsequently removed *in vivo* using the flanking *flp* recombinase target (FRT) sites. The resistance cassette however was not removed in this study to facilitate selective growth (Figure 4.2.28).

A kanamycin promoter was fused with the *luxCDABE* genes (Paredes 2014) to provide a control exhibiting constitutive gene expression.

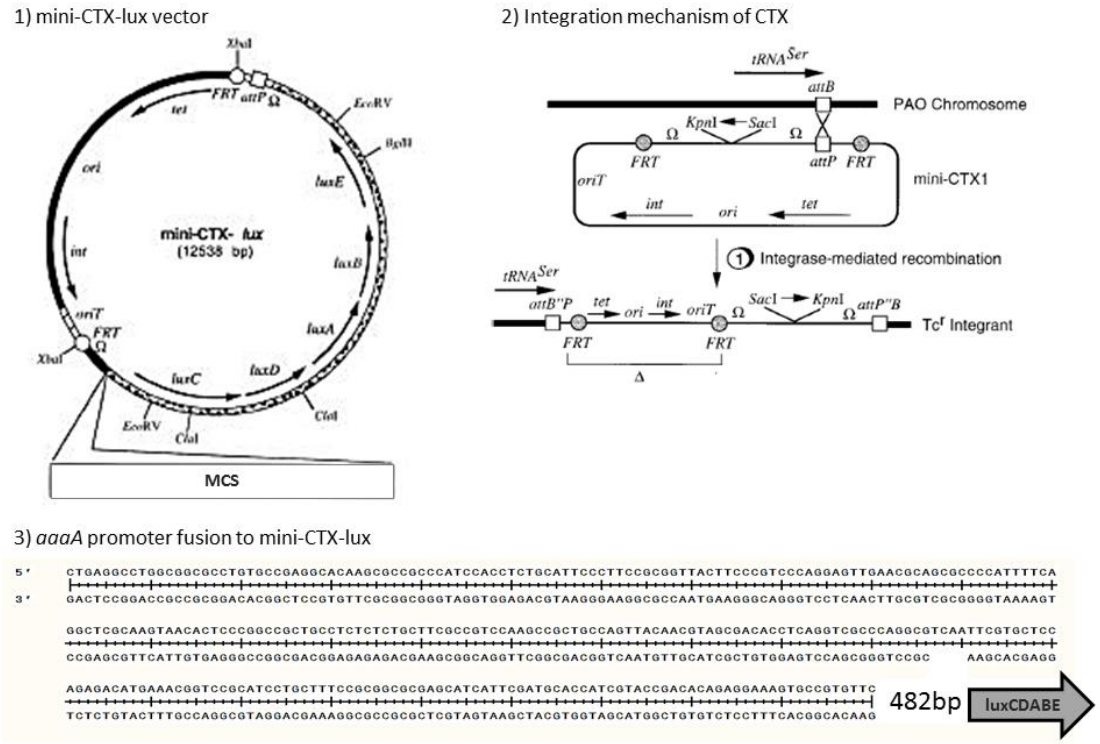


Figure 4.2.28: Construction of strains to measure *aaaA* expression using the miniCTX-*lux* reporter. (Panel 1) Diagram taken from Becher and Schweizer (2000) showing the miniCTX-*lux* vector. (Panel 2) Explanatory figure taken from Hoang *et al* (2000) showing the method mini-CTX uses for insertion into the *P. aeruginosa* chromosome. The *attP* site on mini-CTX recognises the *attB* site on the *P. aeruginosa* chromosome and the encoded integrase facilitates recombination at these sites. (Panel 3) The *aaaA* promoter sequence inserted into the MCS of miniCTX-*lux*, upstream of the *luxCDABE* genes. This was achieved by Paredes (2014) prior to this work.

4.2.3.2 Addition of exogenous nitrate to LB media does not affect aaaA expression

P. aeruginosa utilises nitrate as an alternative electron acceptor (Berks *et al* 1995; Arai 2011; Palmer *et al* 2007), which is detected by NarX/NarL (Nadine *et al* 1999; Haas *et al* 1995; Arai *et al* 1991; 1994; 1995). Putative NarL binding sites were found in the *aaaA* upstream region (Chapter 3) and could have an inhibitory role. Schobert and Jahn (2010) described a hierarchy of substrate preference for *P. aeruginosa* when oxygen is unavailable (depicted in Figure 4.2.29). It is likely that *aaaA* expression is dependent upon the nitrate availability.

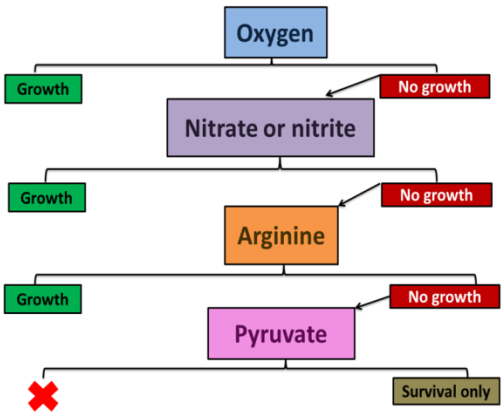


Figure 4.2.29: Metabolic hierarchy of *P. aeruginosa.* Based on the information from Schobert and Jahn (2010). Oxygen is the preferred electron acceptor. When this is not available nitrate or nitrite can be used instead as alternative electron acceptors. When nitrate is unavailable, arginine can sustain growth through the deiminase pathway and pyruvate can allow survival.

To investigate the effect of exogenous nitrate on *aaaA* expression, overnight cultures of PAO1 and PAO1 *ΔaaaA*, containing either the miniCTX-*lux*::*PaaaA* or miniCTX-*lux*::*Pkan* fusions, were grown in either LB, LB with the addition of a 10 mM nitrate source or 100 mM nitrate source. These cultures were washed and standardised in the appropriate media. The luminescence emitted from the activated *PaaaA* and *Pkan* promoters was measured in a tecan plate reader over the course of 24 hours.

Contrary to expectations, there is no reduction in *aaaA* promoter activation when KNO_3 (Figure 4.2.30) or NH_4Cl (Figure 4.2.31) is added to LB media. Furthermore, there appears to be more activation of the *aaaA* promoter expression in the higher concentrations of both KNO_3 and NH_3Cl indicating that higher concentrations of a nitrate source increase P*aaaA* activation in aerobic conditions. However as this effect is shared in the kanamycin promoter control counterparts, nitrate may also be affecting transcription of *lux* genes non-specifically, masking the *aaaA* specific results.

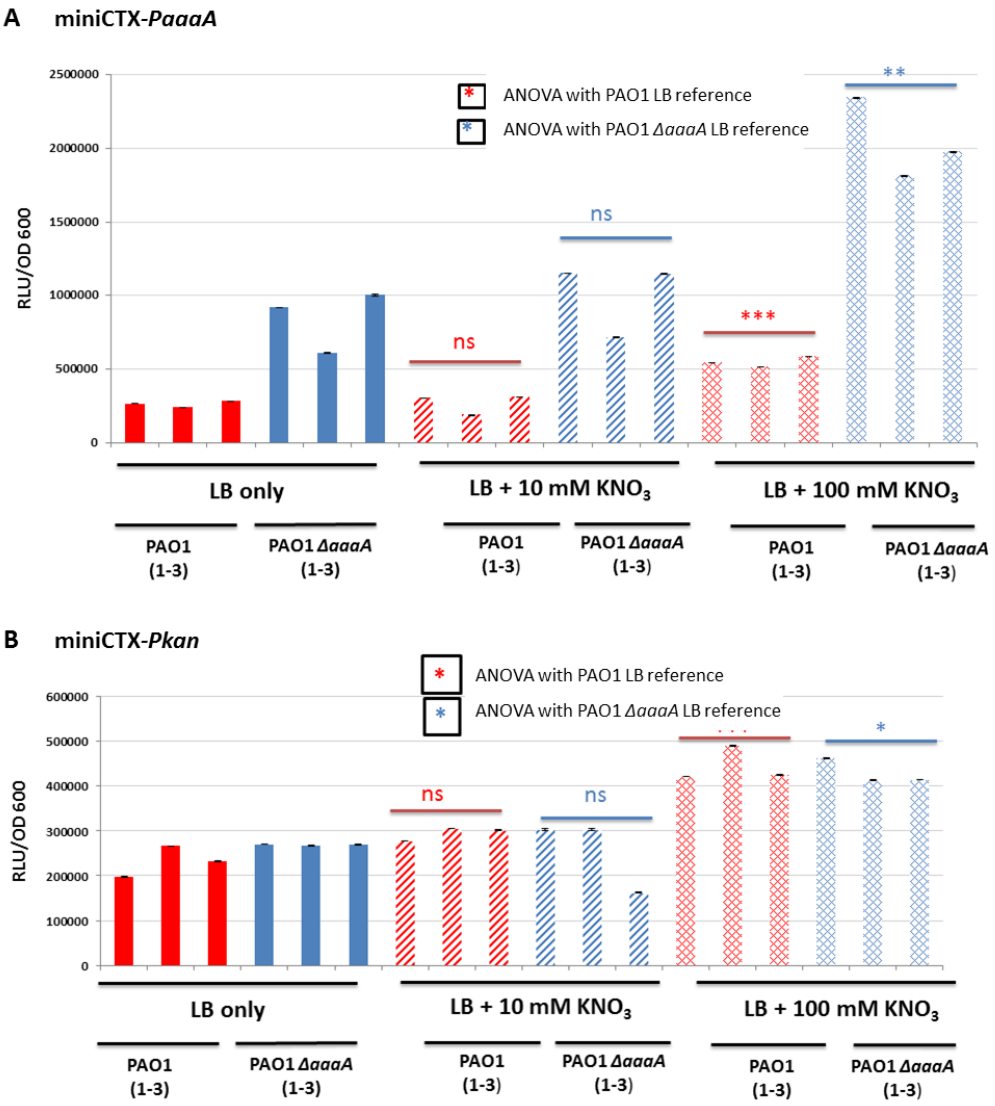


Figure 4.2.30: In LB media, activation of the *aaaA* promoter is not reduced by addition of KNO_3. PAO1 miniCTX-*lux*::P*aaaA*, PAO1 *ΔaaaA* miniCTX-*lux*::P*aaaA,* PAO1 miniCTX-*lux*::P*kan,* and PAO1 *ΔaaaA* miniCTX-*lux*::P*kan* were grown overnight in LB media or KNO_3 enriched LB media , washed 3x and standardised to OD_{600} 0.1. They were then added to a 96 well plate, allowing the growth (OD_{600}) and luminescence (RLU) to be measured over 24 hours by a tecan plate reader. The luminescence corresponds to activation of *PaaaA* or *Pkan* and is presented as the AUC of the RLU/OD_{600}. Panel A: P*aaaA*. Panel B: P*kan* constitutive control. Three biological replicates of each strain in each condition are shown as separate bars, the standard deviation between the 3 technical replicates of these are shown by the error bars. An ANOVA was performed with the LB control condition as the reference and the level of significance represent by 1 or more * or ns.

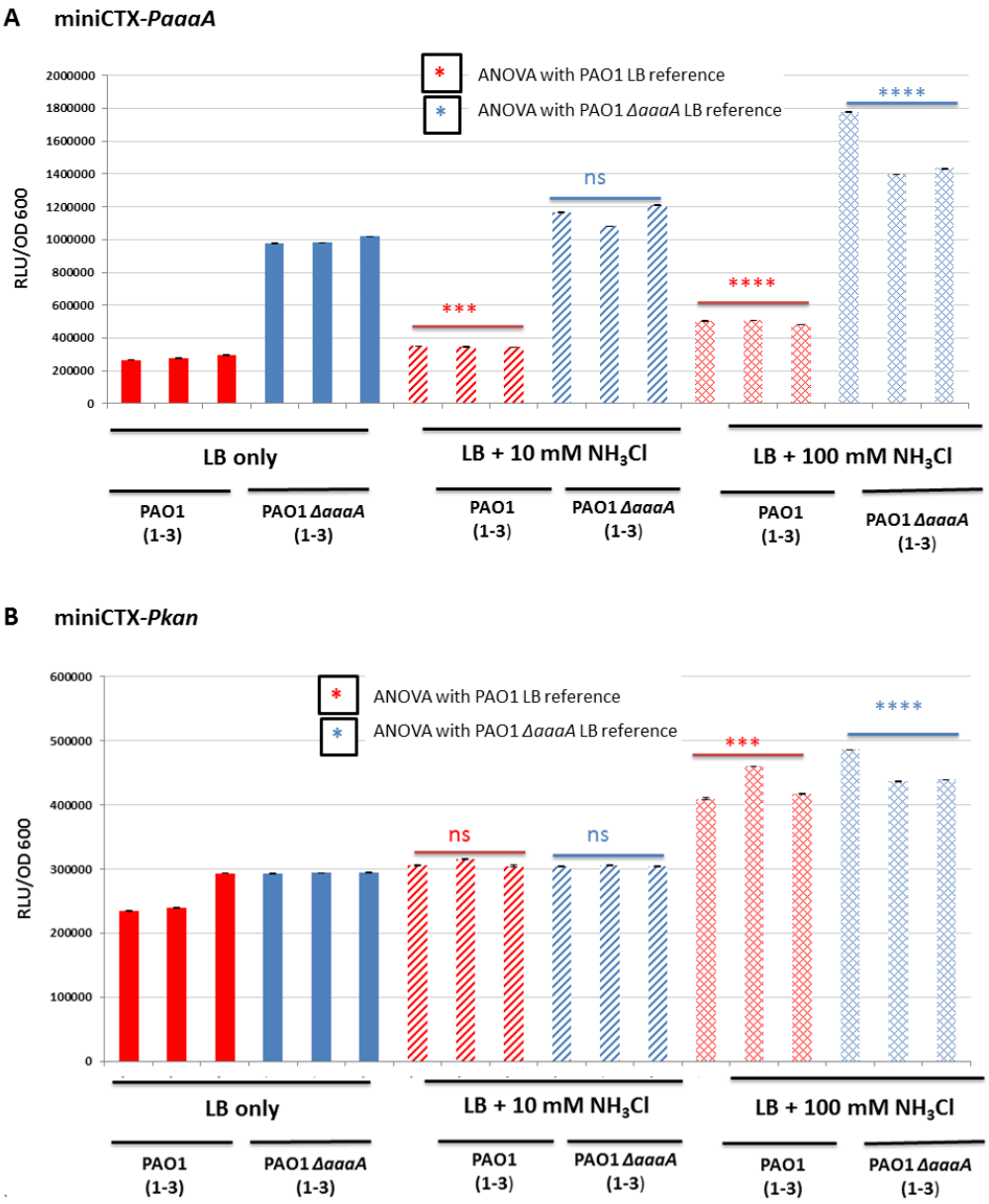


Figure 4.2.31: In LB media, activation of the *aaaA* promoter is not reduced by addition of NH_4Cl. PAO1 miniCTX-*lux*::P*aaaA*, PAO1 *ΔaaaA* miniCTX-*lux*::P*aaaA,* PAO1 miniCTX-*lux*::P*kan,* and PAO1 *ΔaaaA* miniCTX-*lux*::P*kan* were grown overnight in LB media or NH_4Cl enriched LB media , washed 3x and standardised to OD_{600} 0.1. They were then added to a 96 well plate, allowing the growth (OD_{600}) and luminescence (RLU) to be measured over 24 hours by a tecan plate reader. The luminescence corresponds to activation of *PaaaA* or *Pkan* and is presented as the AUC of the RLU/OD_{600}. Panel A: P*aaaA*. Panel B: P*kan* constitutive control. Three biological replicates of each strain in each condition are shown as separate bars, the standard deviation between the 3 technical replicates of these are shown by the error bars. An ANOVA was performed with the LB control condition as the reference and the level of significance represent by 1 or more * or ns.

4.2.3.3 Activation of PaaaA is unaffected by NaCl concentration in the PAO1 WT, while PaaaA activation is increased in PAO1 ΔaaaA grown in higher NaCl concentrations

In CF patients the abnormal secretion of chloride ions into the airway lumen has been theorised to result in dehydrated mucus impairing ciliary beating and clearance of microbial invaders. Although the level of fluid is disrupted due to this osmotic imbalance, the overall concentration of NaCl is not thought to be significantly higher (Matsui *et al* 1998; Tarran *et al* 2001; Wills *et al* 1997). Some studies suggest however, that the NaCl concentration in the airway lumen is higher than normal and this results in diminished efficacy of host defence mechanisms (Goldman *et al* 1997; Smith *et al* 1996; Zabner *et al* 1998). Although this second hypothesis may not be correct, it was thought that an investigation into how AaaA might be affected in different salt concentrations would be interesting.

To observe any differences in the expression of *aaaA* when varying NaCl concentrations are present in the environment, PAO1 and PAO1 Δ*aaaA,* containing either the miniCTX-*lux*::*PaaaA* or miniCTX-*lux*::*Pkan* fusions, were grown overnight in 3 different LB broth solutions containing either 0.055 g/L (0.9 mM), 10.055 g/L (172.1 mM) or 17.055 g/L (291.8 mM) concentrations of NaCl. Following the washing and standardisation of the cultures in the appropriate media, the activation (emitted luminescence) of the *PaaaA* and *Pkan* promoters was measured in a tecan plate reader over the course of 24 hours.

At higher concentrations of NaCl, more activation of the *aaaA* promoter can be seen to occur in the PAO1 Δ*aaaA* mutant strain but not the PAO1 WT (Figure 4.2.32). There is a possibility that this is due to the generally higher activation of *PaaaA* in the PAO1 *ΔaaaA* strain (Chapter 3). The activation of *Pkan* is not significantly different in any of the NaCl concentrations. The greatest reproducibility for both *Pkan* and *PaaaA* activation data is observed in the mid NaCl concentration (typical of standard LB broth).

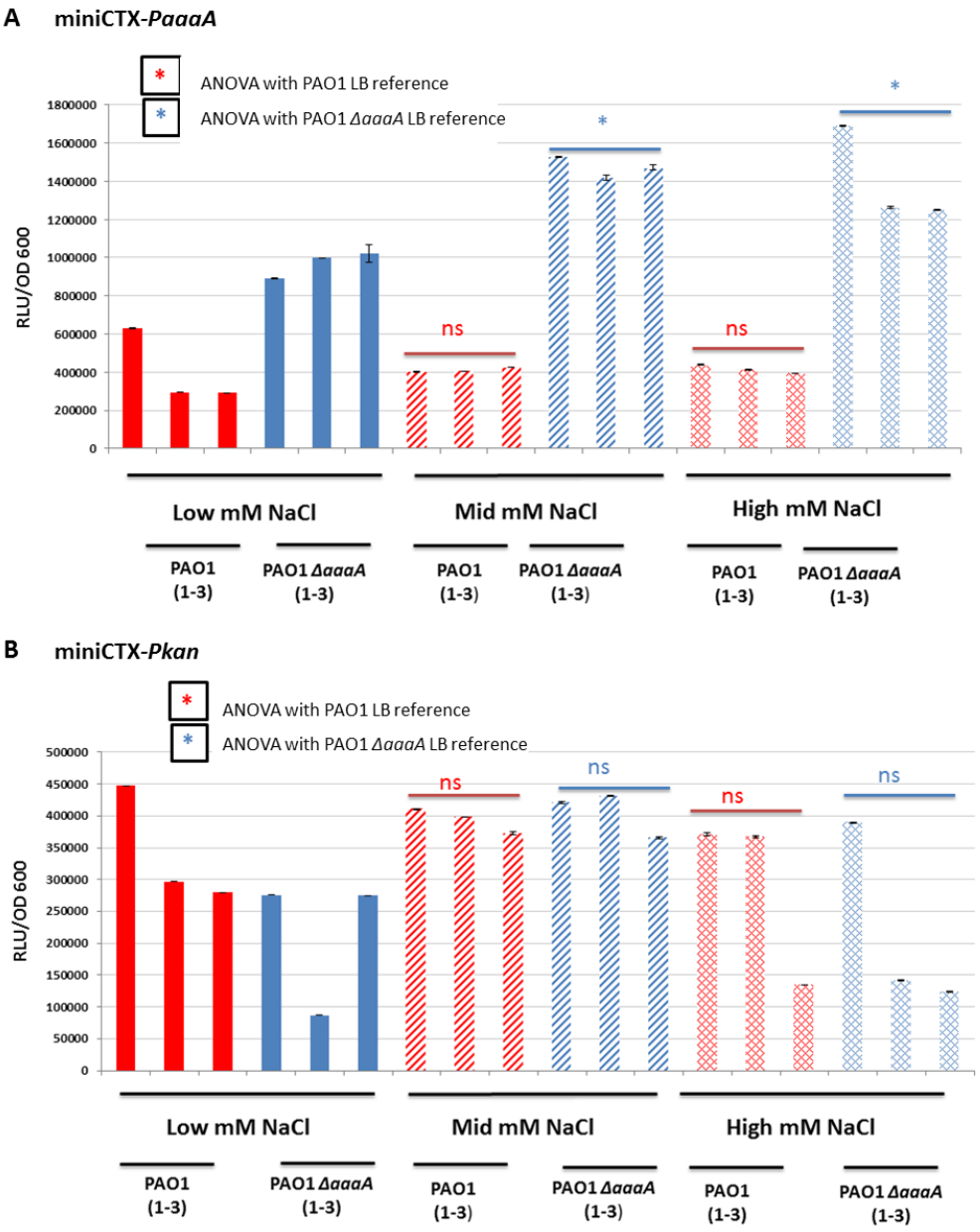


Figure 4.2.32: In LB media, activation of the *aaaA* promoter is increased in higher NaCl concentrations in the PAO1 *ΔaaaA* mutant but not the PAO1 WT strain. PAO1 miniCTX-*lux*::P*aaaA*, PAO1 *ΔaaaA* miniCTX-*lux*::P*aaaA,* PAO1 miniCTX-*lux*::P*kan,* and PAO1 *ΔaaaA* miniCTX-*lux*::P*kan* were grown overnight in LB media of 3 different NaCl concntrations (0.9 mM, 172.1 mM or 291.8 mM) , washed 3x and standardised to OD_{600} 0.1. They were then added to a 96 well plate, allowing the growth (OD_{600}) and luminescence (RLU) to be measured over 24 hours by a tecan plate reader. The luminescence corresponds to activation of *PaaaA* or *Pkan* and is presented as the AUC of the RLU/OD_{600}. Panel A: P*aaaA*. Panel B: P*kan* constitutive control. Three biological replicates of each strain in each condition are shown as separate bars, the standard deviation between the 3 technical replicates of these are shown by the error bars. An ANOVA was performed with the LB control condition as the reference and the level of significance represent by 1 or more * or ns.

4.2.3.4 The activation of the aaaA promoter is the same when grown in LB buffered to 5.8, 6.2 or 6.8.

In CF patients, differences in the pH of respiratory fluids have been linked with poorer outcomes in pathogen clearance (Pezzulo *et al* 2012). To observe how *aaaA* expression differed when *P. aeruginosa* was grown in media buffered to different pH values the following procedure was undertaken.

Overnight cultures of PAO1 and PAO1 *ΔaaaA*, containing either the miniCTX-*lux*::*PaaaA* or miniCTX-*lux*::*Pkan* fusions, were grown in LB with the addition of one of four different phosphate buffers corresponding to either pH 5.8, pH 6.2, pH 6.8 or pH 7.2. These cultures were washed and standardised in the appropriate media. The luminescence emitted from the activated *PaaaA* and *Pkan* promoters was measured in a tecan plate reader over the course of 24 hours.

There was no significant difference in the activation of *PaaaA* or *Pkan* in LB buffered to 5.8, 6.2 or 6.8 (Figure 4.2.33). Note that there is one less biological repeat in the *Pkan* control experiment due to time restraints but this is unlikely to have had influenced the experimental outcome.

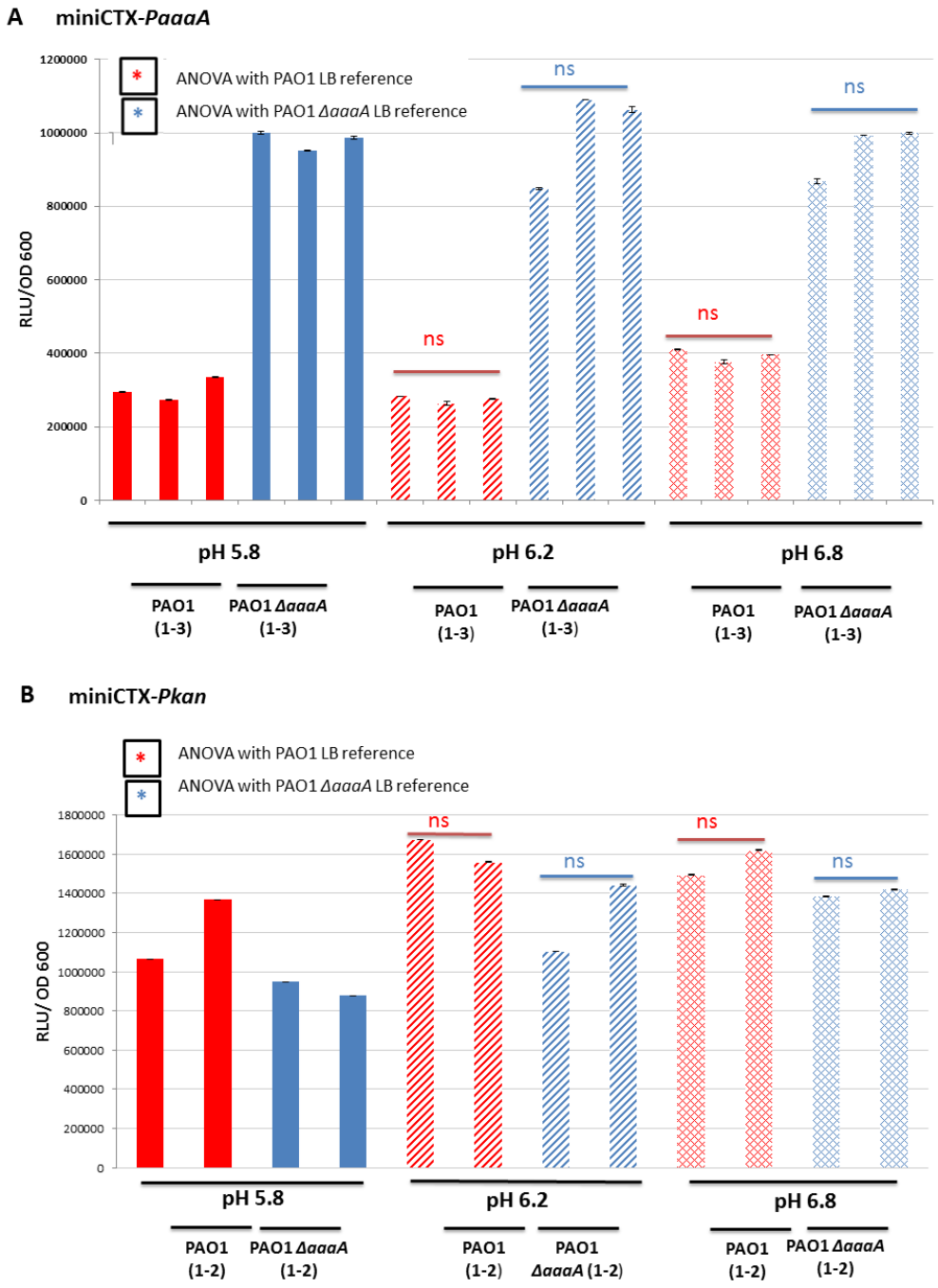


Figure 4.2.33: In LB media, pH values between 5.8 and 6.8 do not affect the activation of *PaaaA*. PAO1 miniCTX-*lux*::P*aaaA*, PAO1 *ΔaaaA* miniCTX-*lux*::P*aaaA,* PAO1 miniCTX-*lux*::P*kan,* and PAO1 *ΔaaaA* miniCTX-*lux*::P*kan* were grown overnight in LB media buffered to 3 different pHs (5.8, 6.2 and 6.8), washed 3x and standardised to OD_{600} 0.1. They were then added to a 96 well plate, allowing the growth (OD_{600}) and luminescence (RLU) to be measured over 24 hours by a tecan plate reader. The luminescence corresponds to activation of *PaaaA* or *Pkan* and is presented as the AUC of the RLU/OD_{600}. Panel A: P*aaaA*. Panel B: P*kan* constitutive control. Three biological replicates of each strain in each condition are shown as separate bars, the standard deviation between the 3 technical replicates of these are shown by the error bars. An ANOVA was performed with the LB control condition as the reference and the level of significance represent by 1 or more * or ns.

4.2.3.5 Oxygen concentration affects the miniCTX-lux reporter

As previously mentioned, oxygen concentration was hypothesised to affect *aaaA* expression. To test whether the miniCTX-*lux* reporter could be used to test this, a preliminary comparison was conducted with aerobic and microaerobic growth conditions.

Overnight cultures of PAO1 and PAO1 *ΔaaaA*, containing the miniCTX-*lux*::*Pkan* fusion, were grown in LB in aerated or microaerobic conditions (cabinet). The aerobic cultures were washed and standardised as normal and added to one side of a 96 well plate. The microaerobic cultures were washed, standardised and added to the other side of the 96 well plate in the microaerobic cabinet. The side of the plate containing the microaerobic culture was sealed with a clear film which did not permit gas exchange. The luminescence emitted from the activated *Pkan* promoter was measured in a tecan plate reader over the course of 24 hours.

The activation of *Pkan* was affected by a reduction in oxygen concentration (Figure 4.2.34). This type of experiment is therefore not suitable for testing the effect of oxygen concentration on *aaaA* expression.

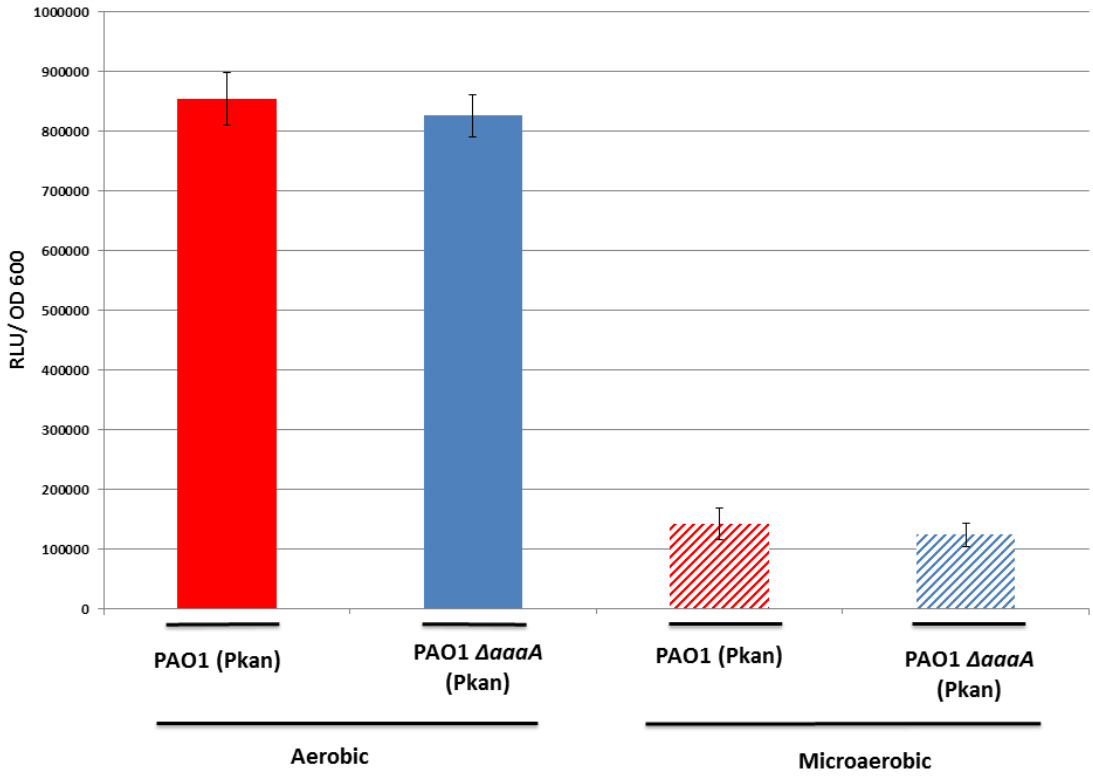


Figure 4.2.34: The miniCTX-*lux* reporter driven by a constitutive promoter (*Pkan*) produces less bioluminescence when oxygen is limited. PA01 and the *ΔaaaA* mutant containing the constitutively expressing miniCTX-*lux*::*Pkan* were grown in aerobic and microaerobic conditions in LB. Microaerobic and aerobic experiments were performed together on the same plate with a gas impermeable film covering the part of the plate dedicated to the microaerobic conditions. The bioluminescence divided by OD_{600} is plotted as the AUC. The error bars represent the standard deviation between 3 technical replicates.

4.2.3.6 The activity of AaaA can be determined by the cleavage of L-arginine-p-nitroanilide

Dr Owen Darch (2013) demonstrated the activity of AaaA can be measured in a medium which keeps cells in a state of suspended growth. This medium is minimal media P (MMP) and was developed by Lesinger *et al* (1972). MMP consists of salts and iron buffered to a pH of 7. *P. aeruginosa* did not grow in MMP, thus the amount of AaaA should be approximately equal at the start and end of the assay. The level of background was low and accounted for by the inclusion of an AaaA negative control. The substrate L-arginine P-nitroanilide is mixed with the bacterially attached AaaA and the enzyme cleaves this to yield L-arginine and P-nitroaniline, a yellow dye which is detected at an optical density of 405 nm. The concentration of the dye is proportional to the activity of the enzyme (Figure 4.2.35).

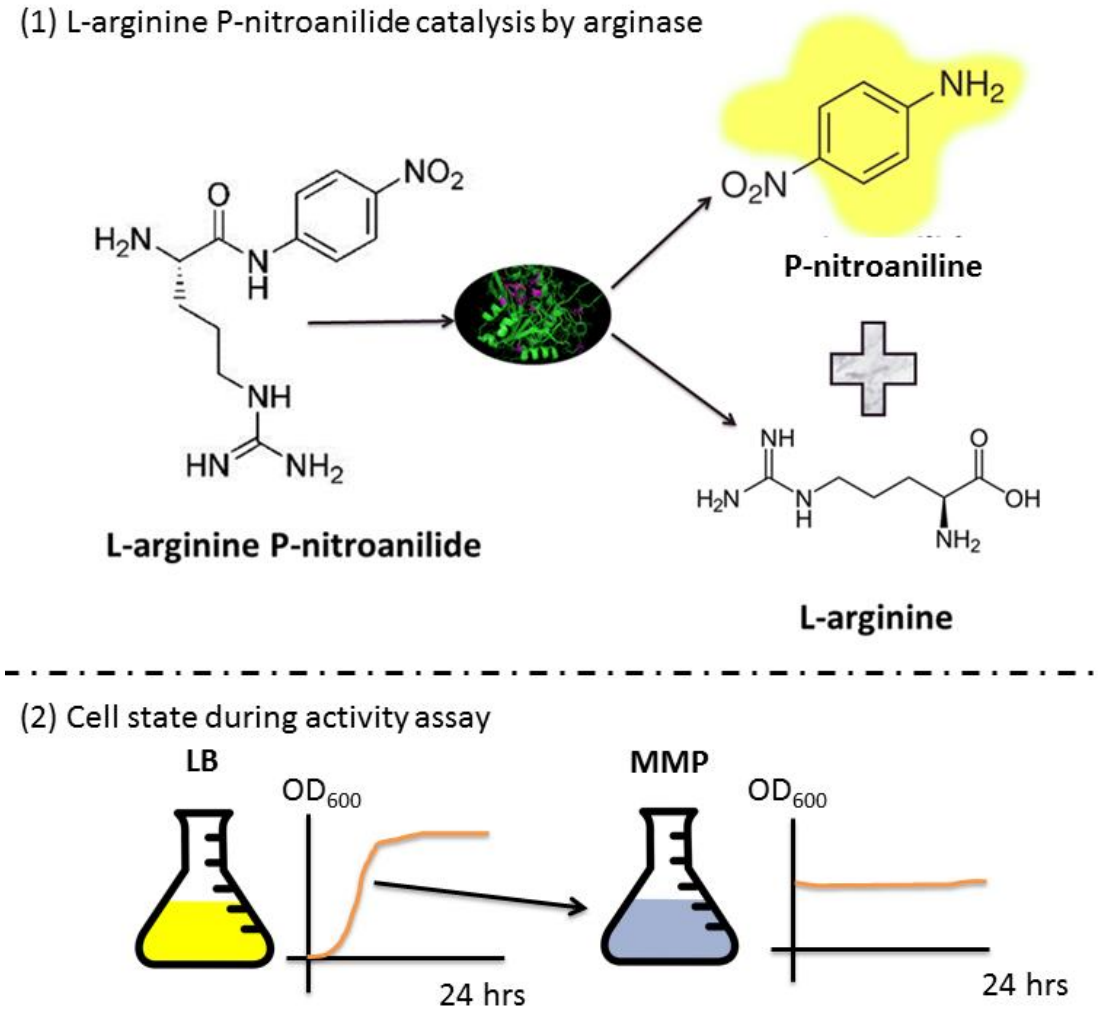


Figure 4.2.35 The AaaA activity assay measures hydrolysis of L-arginine coupled to the dye P-nitroanilide and can be used to test activity of cell-associated enzyme as the bacteria are not growing and the background non-specific activity is low. (Panel 1) L-arginine P-nitroanilide is catalysed by AaaA to yield separate molecules of arginine and P-nitroaniline. The liberated P-nitroaniline is detected at $OD_{405\ nm}$. (Panel 1) Bacterial cultures are grown to exponential phase and suspended in minimal media P (MMP) which keeps the cells in a suspended state of growth. This should keep the number of AaaA molecules the same throughout the course of the assay. Arginine molecule taken from Nanne (2015). Arginine P-nitroanilide dihydrochloride molecule taken from Sigma Aldrich product page CAS Number 40127-11-5. P-nitroaniline molecule taken from Sigma Aldrich page CAS Number 100-01-6.

4.2.3.7 Activity of AaaA differs in response to the media type and oxygen availability

A comparison of AaaA activity in 2 different media and oxygen availabilities was conducted to investigate whether AaaA was responsive to either CF relevant condition.

To see whether the activity of AaaA differed when *P. aeruginosa* was grown in ASM rather than that of LB, the experiment was adjusted by growing the overnight cultures in ASM, diluting them 1:10 in fresh ASM, continuing to grow until exponential phase (0.4-0.6 OD_{600}) and proceeding with the experiment as

normal: washing them in MMP before normalisation and incubating with the substrate L-arginine P nitroanilide.

In ASM media the activity of PAO1 appears to be less than in LB media (Figure 4.2.36). This is particularly useful to consider when comparing biofilms grown in different media.

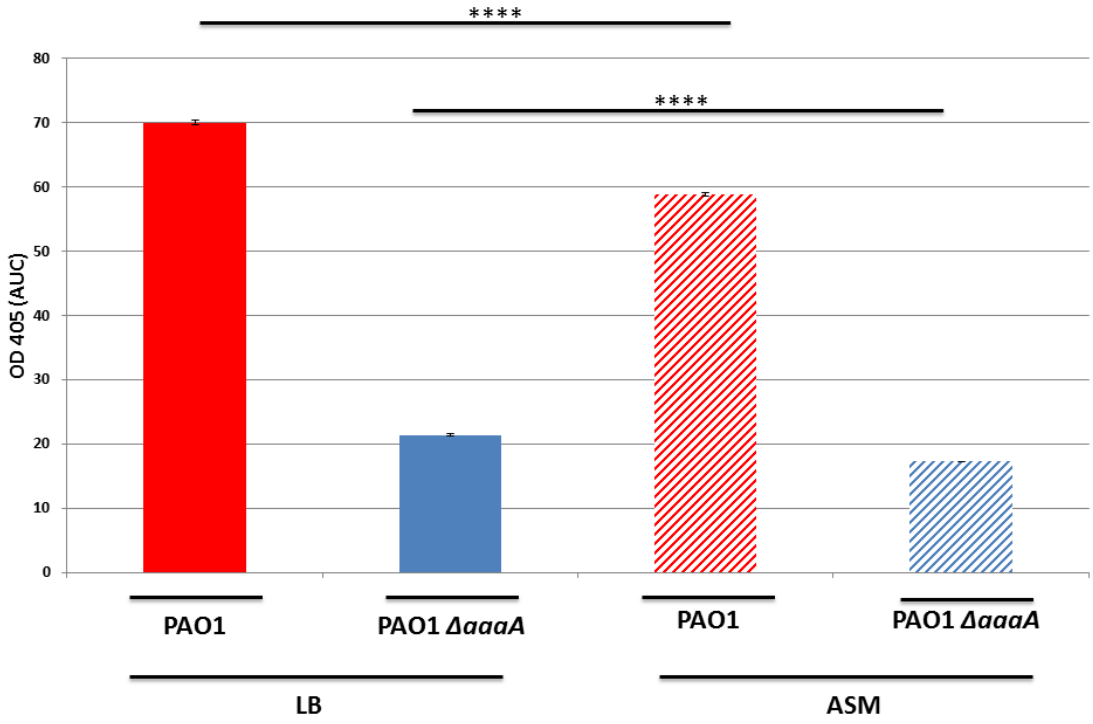


Figure 4.2.36: PAO1 and the PAO1 *ΔaaaA* mutant have lower AaaA activities in ASM compared to in LB media when cells are grown aerobically. PAO1 = red and the PAO1 *ΔaaaA* = blue. PAO1 and PAO1 *ΔaaaA* were grown in aerobic LB or ASM media until exponential phase. The cultures were washed 3x in MMP and standardised to OD_{600} 1.0. The cells were then incubated with the AaaA substrate L-arginine-p-nitroanilide for 24 hours at 37°C. The OD_{405} is representative of the p-nitroaniline dye cleavage from original molecule. Each bar shows the AUC of the OD_{405}. Three biological replicates (x 9 technical) are represented by error bars showing the standard deviation between the repeats. A t test was performed between the media and **** represents a P value of <0.0001.

To investigate the activity shown by the AaaA enzyme in microaerobic cultures, PAO1 and PAO1 *ΔaaaA* were grown in microaerobic LB and ASM media and samples manually collected during the course of growth (Figure 4.2.37 A). The microaerobic cultures reached exponential phase at 24 hours (Time point 24). The sampled cells were washed in MMP and mixed with L-arginine p-nitroanilide as is detailed in Chapter 2. Once the culture was mixed with the substrate, the assay proceeded for 24 hours. Over this time, the L-arginine p-nitroanilide substrate was degraded at a speed dependent on the amount of active L-arginine specific aminopeptidase enzyme present. The time point in which the activity reached the plateau phase of the assay was taken as the 'end point' and these plotted on the graph. This measurement is used instead of the AUC because apart

from the 24 hour growth point sample, fewer measurements were taken than normal during the 24 hours of L-arginine-p-nitroanilide incubation due to the number of samples.

Figure 4.2.37 (B) shows the level of L-arginine p-nitroanilide substrate degradation (proportional to AaaA activity) for each time point in a microaerobic growth curve. The substrate degradation (AaaA activity) appears to be relatively constant in PAO1 cells grown in LB. The slight raise in peptide bond cleavage (activity) when exponential phase is reached may be nonspecific as it was also discernible in the negative control, PAO1 *ΔaaaA*. L-arginine p-nitroanilide degration (AaaA activity) in PAO1 grown in ASM is similar to that of the LB grown culture but the raise in activity at 4 hours is more pronounced. Interestingly more degradation (activity) is seen in the PAO1 *ΔaaaA* control grown in LB than was seen in the ASM media. This suggests another method of arginine cleavage from peptide termini in *P. aeruginosa* may exist and be upregulated in a richer/more complex medium.

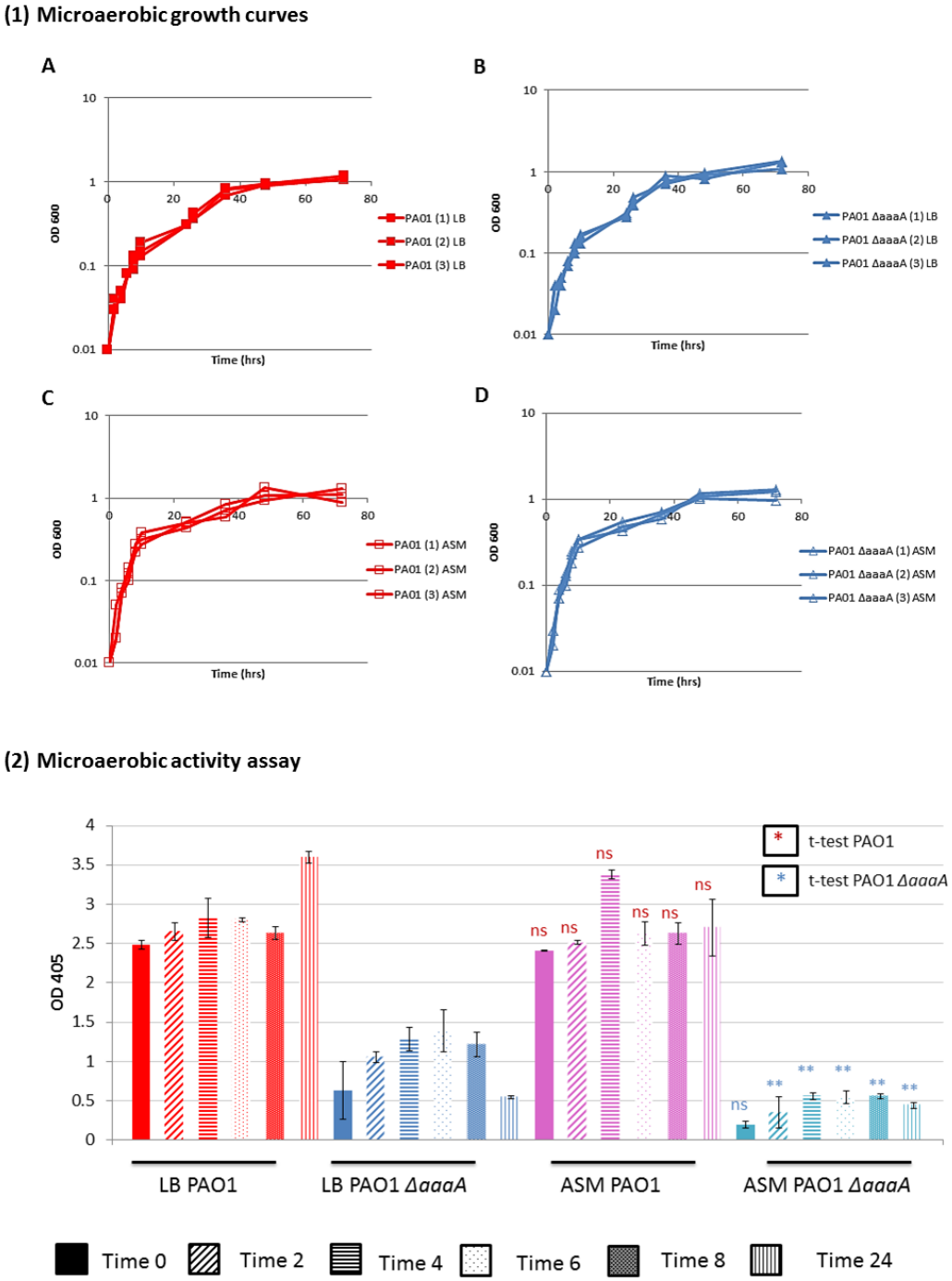


Figure 4.2.37: In microaerobic conditions, the level of L-arginine p-nitroanilide degradation (representing AaaA activity) differs between LB and ASM at all time points above 0 in PAO1 *ΔaaaA* but not PAO1. Panel 1: Microaerobic growth of PAO1 and PAO1 *ΔaaaA* in LB and ASM using manual sampling. A: PAO1 growth in LB. B: PAO1 *ΔaaaA* growth in LB. C: PAO1 growth in ASM. D: PAO1 *ΔaaaA* growth in ASM. Microaerobic conditions were maintained using a microaerobic cabinet. Values indicate the OD_{600} taken at each time point (every hour for 12 hours and then once every 24 hours). Each line corresponds to one biological replicate. Panel 2: PAO1 and PAO1 *ΔaaaA* were grown in microaerobic LB and ASM media and samples manually collected during the course of growth. The sampled cells were washed in MMP and incubated with L-arginine p-nitroanilide for 24 hours at 37°C. The OD_{405} is representative of the p-nitroaniline dye cleavage from original molecule. Each bar represents a sample taken along the growth curve and the OD_{405nm} value shown is the end point value of the assay (the 24 hour reading of the activity curve). The standard deviation between 3 biological replicates are represented by each error bar. A series of t-tests were performed between LB and ASM samples. The symbol ** indicates a P value <0.01, ns = non-significant.

To compare the activity of AaaA in this experiment to the AaaA activity in aerobic conditions, the exponential phase microaerobic sample (time point 24) was incubated with the L-arginine-p-nitroanilide substrate for 24 hours and measurements taken as usual throughout the experiment. The amount of substrate degradation (OD_{405}) observed for each time point was divided by the starting concentration of cells (OD_{600} of the 24 hour growth time point) and multiplied by 1.0 (the OD_{600} used in the other, aerobic activity assay). The AUC was calculated from these normalised activity values. The formula below shows the calculation used for clarity.

$$Normalised\ activity\ value = 1.0\left(\frac{OD405}{OD600}\right)$$

Consistent with the expectation that greater AaaA activity would be observed in oxygen restricted environments, more than double the L-arginine p-nitroanilide degradation (activity) was measured from PAO1 grown microaerobically in LB (Figure 4.2.38).

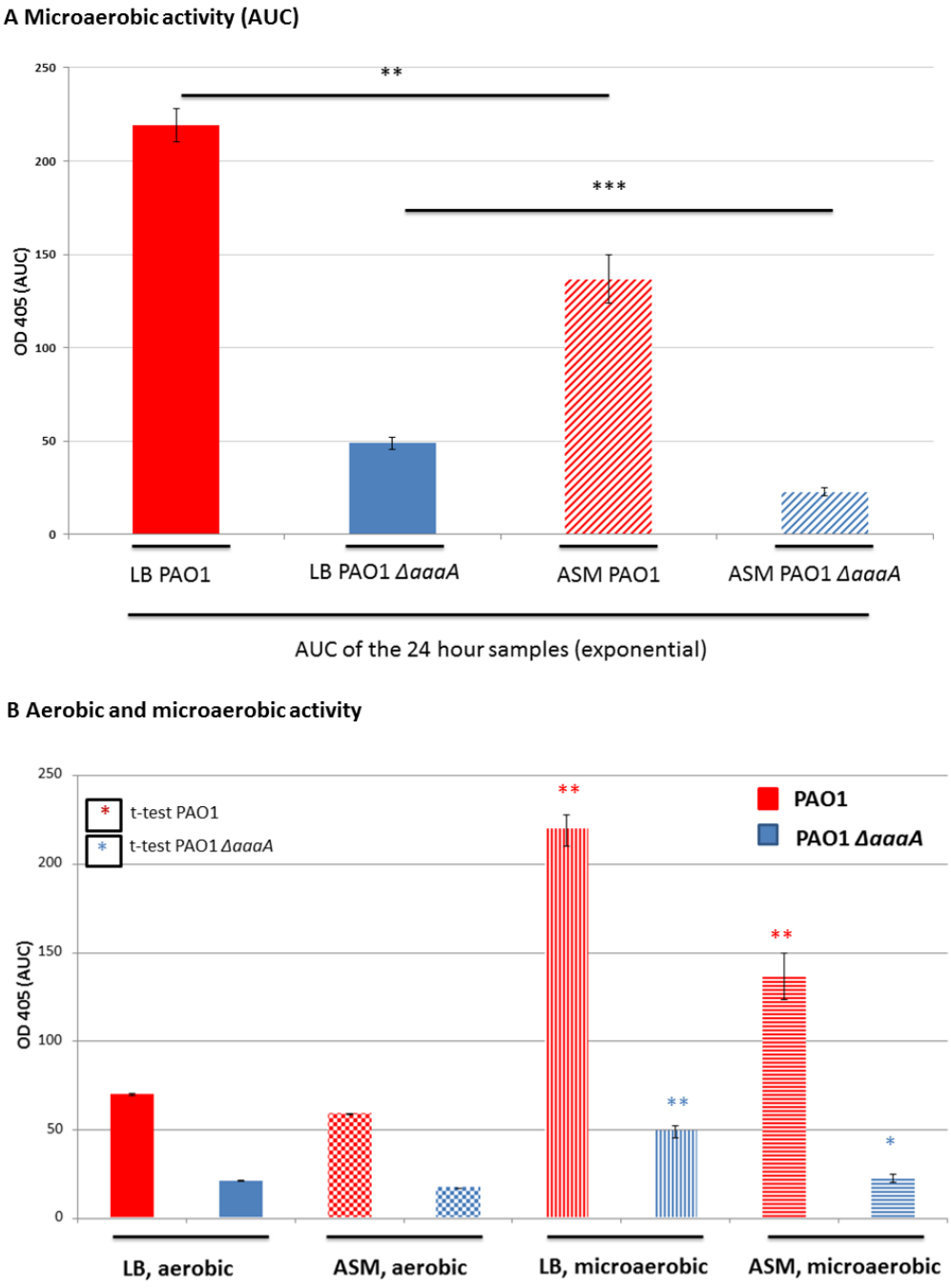


Figure 4.2.38: The amount of L-arginine p-nitroanilide degration (AaaA activity) is different in ASM and substantially increases when the oxygen concentration is lower in PAO1 and PAO1 *ΔaaaA* strains. Panel A: PAO1 and PAO1 *ΔaaaA* were grown in LB and ASM under microaerobic conditions and cells collected at the 24 hour (exponential) growth point. The sampled cells were washed in MMP and incubated with L-arginine p-nitroanilide for 24 hours at 37°C. The OD_{405} is representative of the p-nitroaniline dye cleavage from original molecule. The OD_{405} values were normalised by dividing by the OD_{600} of the samples and multiplying by 1.0. Panel B: PAO1 and PAO1 *ΔaaaA* grown and treated in the manner described in Panel A, were compared with PAO1 and PAO1 *ΔaaaA* grown in LB and ASM under aerobic conditions. These cells were harvested at exponential phase, washed in MMP and standardised to OD_{600} 1.0. Incubation with L-arginine p-nitroanilide proceeded for 24 hours at 37°C. Error bars show the standard deviation between 3 biological replicates (X 9 technical). Red bars correspond to AaaA activity in PAO1 and blue bars correspond to AaaA activity in PAO1 *ΔaaaA*. A t-test was performed and the level of significance represent by 1 or more * or ns.

4.2.3.8 Exogenous nitrate had no effect on AaaA activity in PAO1

To investigate the effect of exogenous nitrate on AaaA activity, overnight cultures of PAO1 and PAO1 *ΔaaaA* were grown in either LB or LB with the addition of a 10 mM or 100 mM nitrate source (KNO_3 or NH_4Cl). The overnights were diluted 1:10 in the appropriate media and grown until exponential phase was reached (0.4-0.6 OD_{600}). The cells were then washed in MMP, standardised, and incubated with L-arginine-p-nitroanilide for 24 hours at 37°C as is detailed in Chapter 2.

No significant difference was seen in L-arginine p-nitroanilide degration (AaaA activity) between the nitrate concentrations when either source of nitrate was added (Figure 4.2.39).

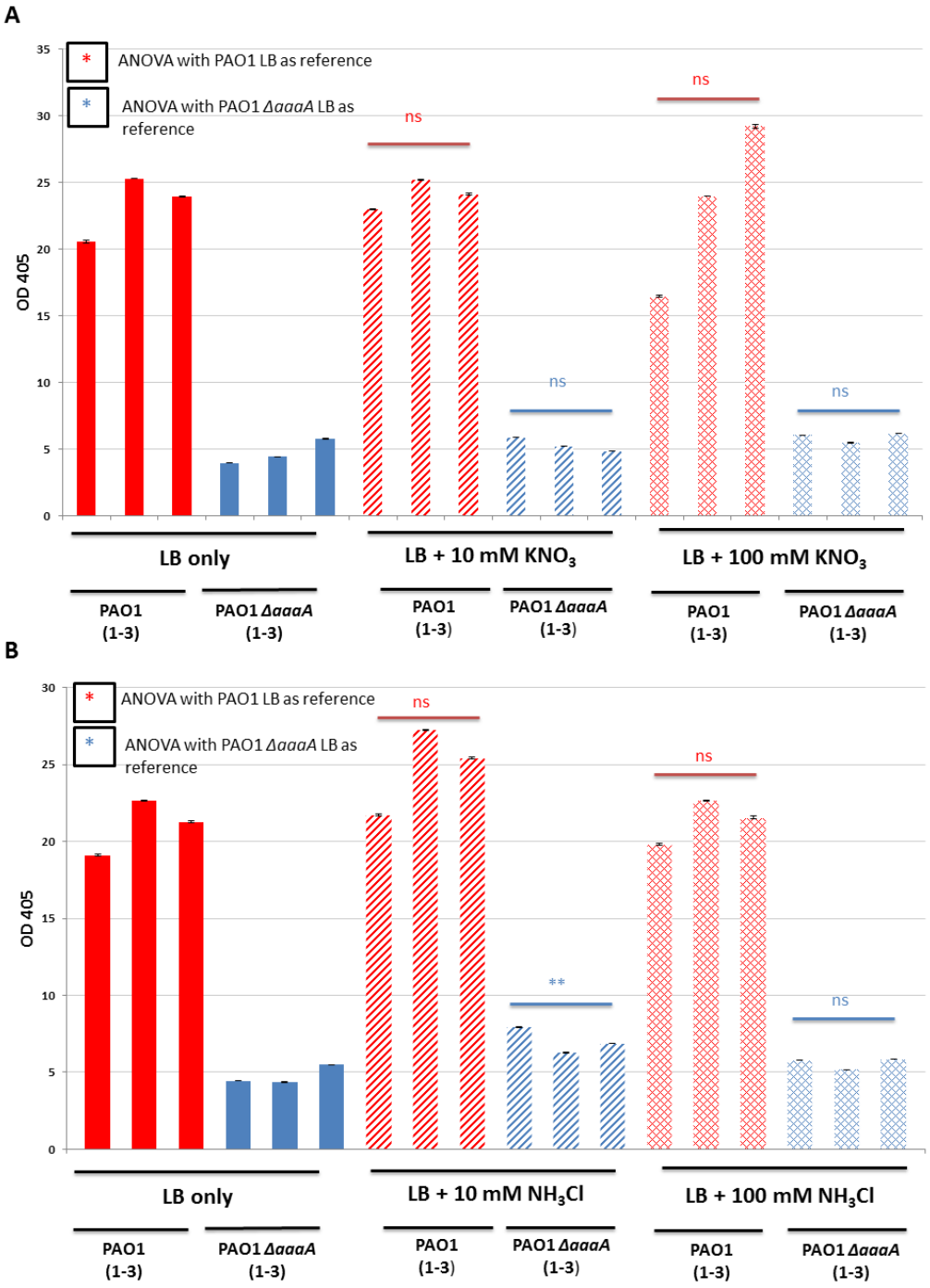


Figure 4.2.39 Addition of exogenous KNO_3 and NH_3Cl does not affect the amount of L-arginine p-nitroanilide degration (AaaA activity) in LB media. PAO1 and PAO1 *ΔaaaA* were grown in LB, or LB enriched with a 10 mM or 100 mM nitrate source, until exponential phase. The cultures were washed 3x in MMP and standardised to OD_{600} 0.5. The cells were then incubated with the AaaA substrate L-arginine-p-nitroanilide for 24 hours at 37°C. The OD_{405} is representative of the p-nitroaniline dye cleavage from original molecule. Each bar shows the AUC of the OD_{405}. PAO1 = red and the PAO1 *ΔaaaA* = blue. Three biological replicates (x 9 technical) are represented by error bars showing the standard deviation between the repeats. An ANOVA was performed between the media with PAO1 or PAO1 *ΔaaaA* grown in LB only as the reference and the level of significance is represented by 1 or more * or by ns. Panel A: KNO_3. Panel B: NH_4Cl.

3.2.3.6 In LB medium, NaCl concentration does not affect AaaA activity within the range tested

To investigate whether NaCl concentration affected AaaA activity, PAO1 and PAO1 Δ*aaaA* strains were grown overnight in 3 different LB broth solutions containing either a 0.055g/L (0.9 mM), 10.055g/L (172.1 mM) or 17.055g/L (291.8 mM) concentration of NaCl. The overnights were diluted 1:10 in the appropriate media and grown until exponential phase was reached (0.4-0.6 OD_{600}). The cells were then washed in MMP which was adjusted to the appropriate NaCl concentration, standardised, and incubated with L-arginine-p-nitroanilide for 24 hours at 37°C as is detailed in Chapter 2.

No significant difference was seen in L-arginine p-nitroanilide degradation (AaaA activity) between the NaCl concentrations in PAO1 (Figure 4.2.40). The background (OD 405 observed in PAO1 *ΔaaaA* control) was slightly lower in the medium concentration of NaCl.

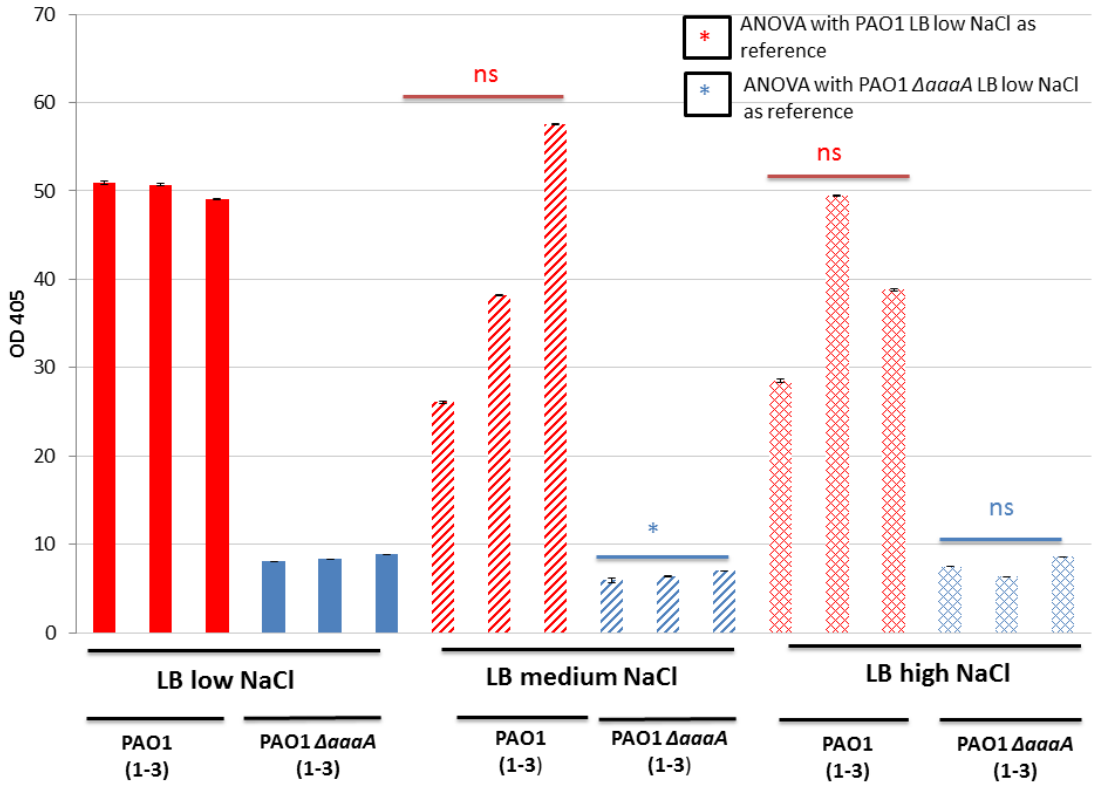


Figure 4.2.40: NaCl concentration does not affect the amount of L-arginine p-nitroanilide degradation (AaaA activity) in LB media in the range tested. PAO1 and PAO1 *ΔaaaA* were grown in LB, containing either a 0.9 mM, 172.1 mM or 291.8 mM concentration of NaCl , until exponential phase. The cultures were washed 3x in MMP adjusted to the appropriated NaCl concentration and standardised to OD $_{600}$ 0.5. The cells were then incubated with the AaaA substrate L-arginine-p-nitroanilide for 24 hours at 37°C. The OD $_{405}$ is representative of the p-nitroaniline dye cleavage from original molecule. Each bar shows the AUC of the OD $_{405}$. PAO1 = red and the PAO1 *ΔaaaA* = blue. Three biological replicates (x 9 technical) are represented by error bars showing the standard deviation between the repeats. An ANOVA was performed between the media with PAO1 or PAO1 *ΔaaaA* as the reference and the level of significance is represented by 1 or more * or by ns.

3.2.3.7 In LB medium, AaaA activity is increased at a higher pH

To see whether AaaA activity differed when cells were grown at different pH values, PAO1 and PAO1 Δ*aaaA* were grown overnight in LB with the addition of one of four different phosphate buffers corresponding to either pH 5.8, pH 6.2, pH 6.8 or pH 7.2. The overnights were diluted 1:10 in the appropriate media and grown until exponential phase was reached (0.4-0.6 OD $_{600}$). The cells were then washed in MMP which was adjusted to the appropriate pH concentration by excluding the KH_2PO_4 and Na_2HPO_4 component and replacing with a 1:10 addition of the phosphate buffer (see materials and methods). The cells were standardised and incubated with L-arginine-p-nitroanilide for 24 hours at 37°C as is detailed in Chapter 2.

Contrary to expectations, L-arginine p-nitroanilide degradation (AaaA activity) was found to be increased in the higher pH adjusted media. AaaA activity was lower in pH 5.8 and pH 6.2 and higher in pH 6.8 and pH 7.2 (Figure 4.2.41).

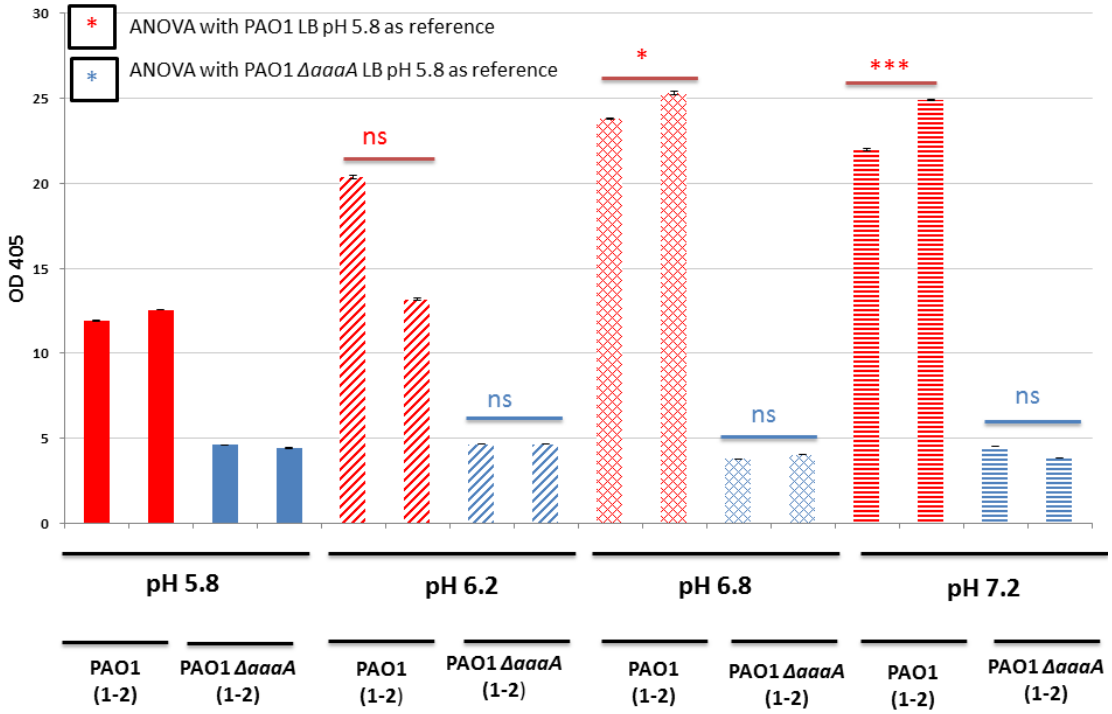


Figure 4.2.41: The amount of L-arginine p-nitroanilide degradation (AaaA activity) is higher at pH 6.8 and pH 7.2 than pH 5.8 and pH 6.2. PAO1 and PAO1 *ΔaaaA* were grown in LB buffered to a pH of 5.8, 6.2, 6.8 or 7.2, until exponential phase. The cultures were washed 3x in MMP adjusted to the appropriate pH and standardised to OD_{600} 0.5. The cells were then incubated with the AaaA substrate L-arginine-p-nitroanilide for 24 hours at 37°C. The OD_{405} is representative of the p-nitroaniline dye cleavage from original molecule. Each bar shows the AUC of the OD_{405}. PAO1 = red and the PAO1 *ΔaaaA* = blue. Two biological replicates (x 6 technical) are represented by error bars showing the standard deviation between the repeats. An ANOVA was performed between the media with PAO1 or PAO1 *ΔaaaA* as the reference and the level of significance is represented by 1 or more * or by ns.

4.2.4 Investigation of conditions relevant to the Cystic Fibrosis airway in the CF isolates

In this section, the following conditions are investigated in the CF isolates:

1. The expression and activity of AaaA in LB
2. The expression and activity of AaaA in ASM
3. The expression and activity of AaaA in different nitrate concentrations
4. The expression and activity of AaaA in different NaCl concentrations

4.2.4.1 A note on the miniCTX-lux reporter integration in the CF isolates

Some of the CF isolates were incalcitrant to integration of the reporter and were thus omitted from this analysis. For the CF isolates that did initially receive the reporter, subsequent growth deficiencies and cell lysis hampered maintenance of the reporter and thus it was only possible to conduct 2 biological repeats (performed in 2 separate experiments) for each CF isolate in some investigations. It will be indicated where this applies. Even storage at -80°C could not overcome this genetic instability, and not even the constitutive Kanomycin reporter could be

maintained in some of the CF isolates. Although retransformation was an option, an alternative approach was optimized to investigate *aaaA* expression, qRT-PCR (Chapter 3) as it offers greater flexibility in that it can be utilized in low oxygen environments and could serve to validate the data shown here for the transcriptional reporter. The reduction of bioluminescence produced by the constitutive *Pkan* reporter has been presented in Figure 4.2.34.

4.2.4.2 PaaaA activation in CF isolates grown in LB is generally low but this does not correlate with AaaA activity

To establish variation between the CF isolates and PAO1 strains in *PaaaA* activation and AaaA activity, the bacteria were tested using the miniCTX-*lux* reporter assay and the AaaA activity assay in the manner which has been previously described.

In LB medium, the CF isolates showed a generally low activation of the *PaaaA* promoter which was significantly different from both PAO1 and PAO1 *ΔaaaA* strains (Figure 4.2.42). The typical peak seen at around 4 hours in the PAO1 strain was also absent in these isolates, suggesting a difference in regulation (data not shown). Isolate CF 484 exhibited the highest *PaaaA* activation, exceeding that of the PAO1 *ΔaaaA* mutant. The relatively high P*aaaA* activation levels of CF 570 were lower than those measured in PAO1 *ΔaaaA* mutant. CF 393 and CF 129 showed an *PaaaA* activation at levels similar to PAO1 WT level but still significantly different. CF 983 and CF 971 show the lowest activation of *PaaaA*. The kanamycin controls differ between the PAO1 strains and the CF isolates, suggesting that the strain background is affecting the reporter bioluminescence in an *aaaA* independent manner. Most notably CF 892 produced very low levels of luminescence driven by the kanamycin promoter. This makes interpreting these expression results difficult, particularly because the kanamycin data is unavailable for several of the isolates.

The CF isolates show varying amounts of activity (Figure 4.2.43), which is above baseline levels but lower than PAO1. CF 326 and CF 030 show higher activity and CF 570, CF 892 and CF 098 show lower activity. For comparison, the within patient CF isolates (Darch *et al* 2015), SED 1-8 were tested. All isolates showed an activity higher than baseline but lower than PAO1. SED 4 showed the highest activity, while SED 5 and SED 6 were close behind this. SED 7 and SED 3 showed an activity which was lower than the other isolates.

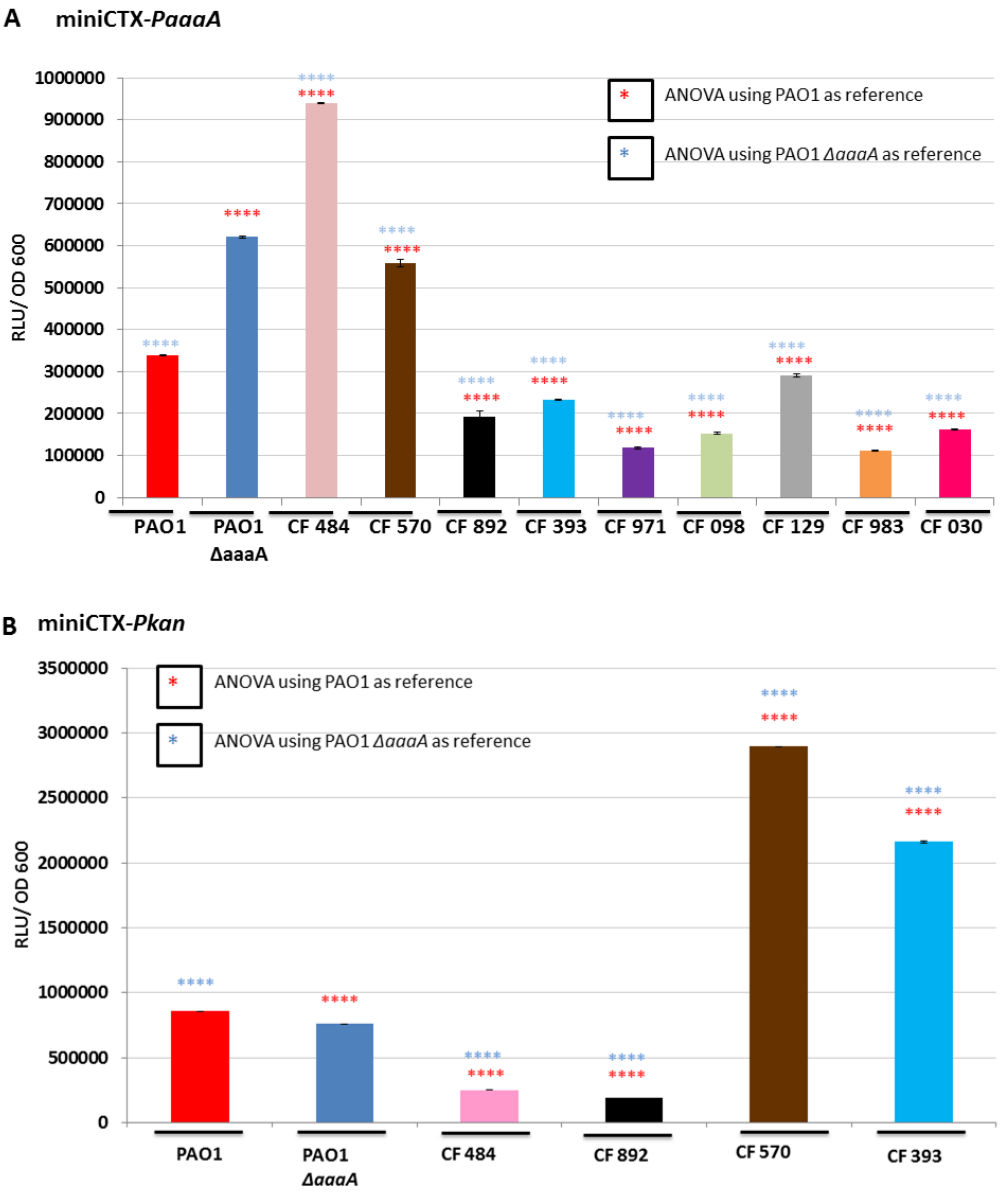


Figure 4.2.42: In aerobic LB media, CF isolates exhibit variation in *PaaaA* activation, while the *Pkan* promoter does not consistently drive luminescence. PAO1, PAO1 *ΔaaaA* and CF isolates with integrated miniCTX-*lux*::P*aaaA*, or miniCTX-*lux*::P*kan,* were grown overnight in LB media, washed 3x and standardised to OD_{600} 0.1. They were then added to a 96 well plate, allowing the growth (OD_{600}) and luminescence (RLU) to be measured over 24 hours by a tecan plate reader. The luminescence corresponds to activation of *PaaaA* or *Pkan* and is presented as the AUC of the RLU/OD_{600}. Each bar represents the average of 3 biological (9 technical) repeats for PAO1 and PAO1 *ΔaaaA* and for the CF isolates with miniCTX-*lux*::P*kan;* only 2 biological repeats (x6 technical) are included for some of the CF isolates with miniCTX-*lux*::P*aaaA*. Error bars show the standard deviation between the repeats. An ANOVA was performed with PAO1 or PAO1 *ΔaaaA* as the reference and the level of significance represented by 1 or more * or ns.

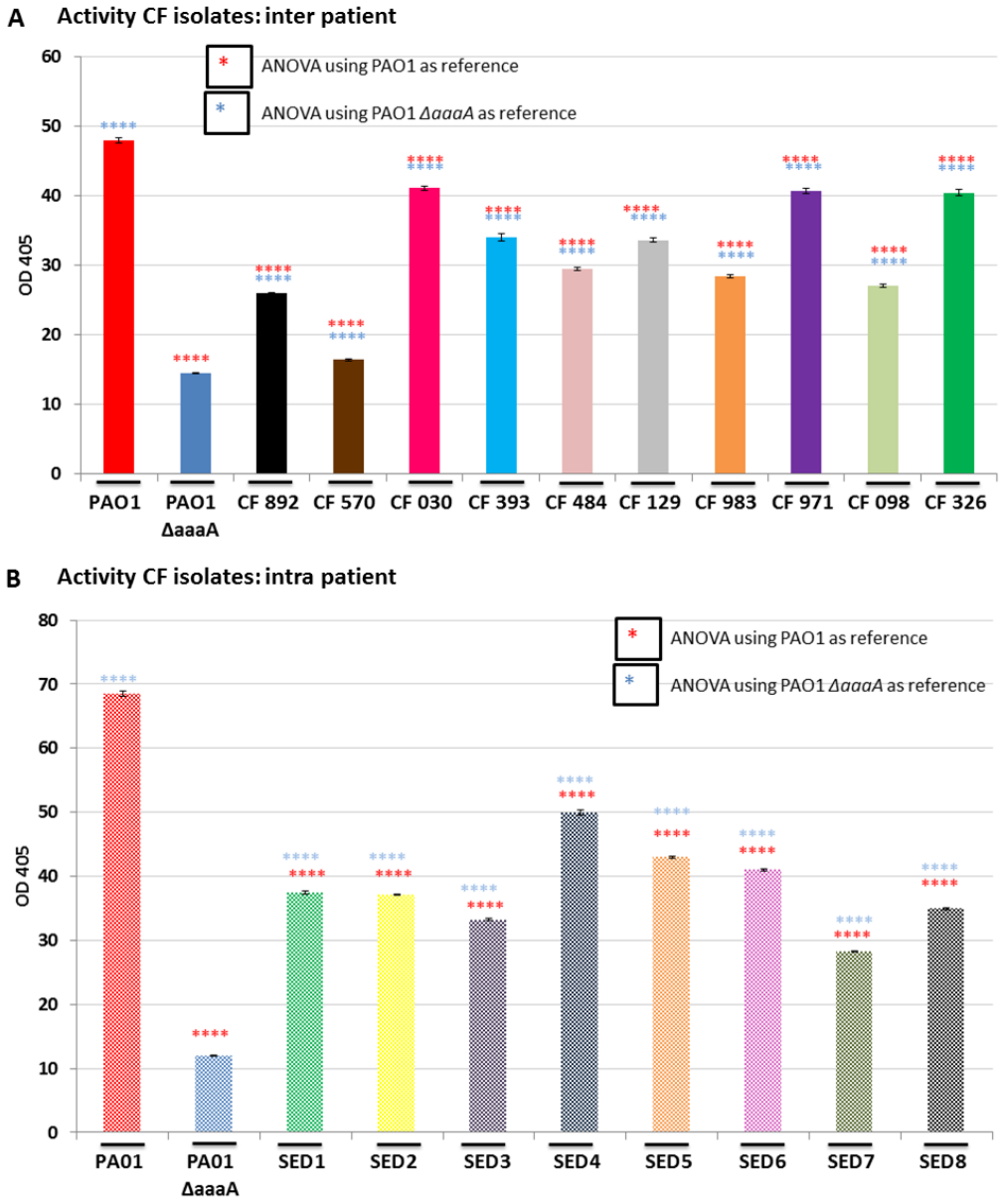


Figure 4.2.43: All CF isolates exhibit more than the baseline AaaA activity when grown aerobically in LB. PAO1, PAO1 *ΔaaaA* and the CF isolates were grown in LB until exponential phase. The cultures were washed 3x in MMP and standardised to OD_{600} 0.5. The cells were then incubated with the AaaA substrate L-arginine-p-nitroanilide for 24 hours at 37°C. The OD_{405} is representative of the p-nitroaniline dye cleavage from original molecule. Each bar shows the AUC of the OD_{405}. The 3 biological replicates (x 9 technical replicates) are represented by the error bars showing the standard deviation between these repeats. An ANOVA was performed with PAO1 or PAO1 *ΔaaaA* as the reference and the level of significance represented by 1 or more * or ns.

4.2.4.3 PaaaA activation in CF isolates grown in ASM is different to that of LB and AaaA activity is generally higher in ASM

ASM is used elsewhere in this thesis to more closely mimic the CF airway environment. *P. aeruginosa* gene expression was closer to *in vivo* conditions in ASM than LB (Palmer *et al* 2007). AaaA activity was found to be less in ASM than LB in the PAO1 WT. To see if a similar effect existed in the CF isolates, the activation of the *aaaA* promoter and the activity of the AaaA enzyme were tested in ASM and LB in the CF isolates. The miniCTX-*lux* reporter assay and the AaaA activity assay were performed in the manner which has previously been described.

There was a difference in *PaaaA* activation in ASM compared to LB (Figure 4.2.44 Ai). This was consistent across the CF isolates. However, whether the *PaaaA* promoter increased or decreased in ASM differed between the *P. aeruginosa* strains. The PAO1 and PAO1 *ΔaaaA* strains both showed reduced luminescence in ASM from both the *PaaaA* and *Pkan* promoters. CF 892 also showed reduced *PaaaA* activation in ASM. CF 484, CF 570, and CF 393 showed an increase in *PaaaA* activation when grown in ASM.

Moreover, the lack of a consistent control for bioluminescence levels (*Pkan* activation, Figure 4.2.44) made it apparent that either an alternative control or approach was necessary to monitor the expression of *aaaA* in different environmental conditions with the CF isolates.

Aside from CF isolate CF 098, the activity of AaaA was increased in the CF isolates grown in ASM compared to LB (Figure 4.2.44 B). This was also the case for the PAO1 control which differs from Figure 4.2.36, and may be a consequence of the modified experimental set up to accommodate the slow growth of the CF isolates (materials and methods).

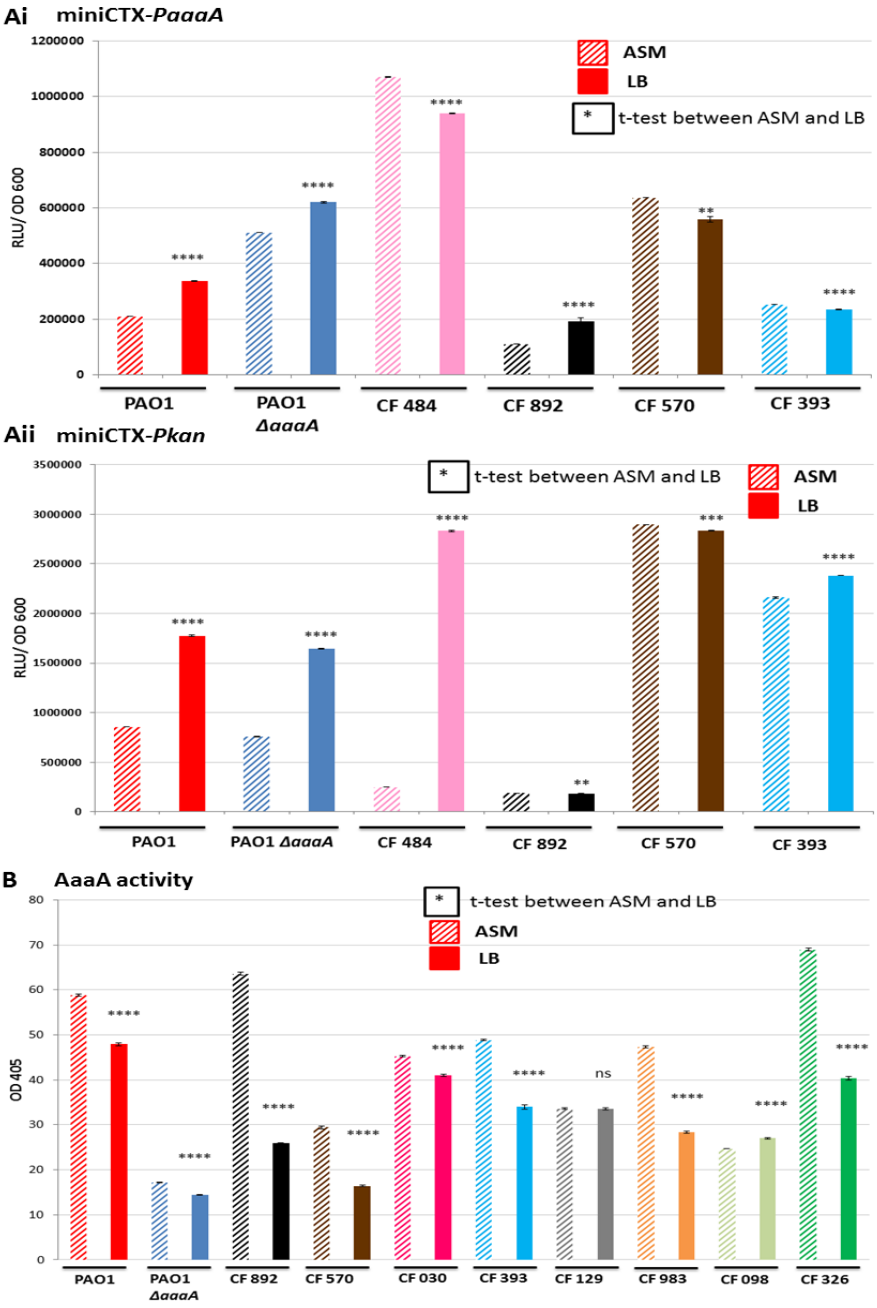


Figure 4.2.44: The activation of *PaaaA* is different in CF isolates grown in ASM compared to LB, however the kanamycin promoter did not drive comparable levels of bioluminescence in ASM and LB when integrated into CF isolates grown in aerobically. AaaA activity in CF isolates increases in ASM. Panel A: Bioluminescence produced from *PaaaA* (i) and *Pkan*. PAO1, PAO1 *ΔaaaA* and CF isolates with integrated miniCTX-*lux*::P*aaaA*, or miniCTX-*lux*::P*kan,* were grown overnight in LB media or ASM, washed 3x and standardised to OD_{600} 0.1. They were then added to a 96 well plate, allowing the growth (OD_{600}) and luminescence (RLU) to be measured over 24 hours by a tecan plate reader. The luminescence corresponds to activation of *PaaaA* or *Pkan* and is presented as the AUC of the RLU/OD_{600}. Each bar represents the average of 3 biological (9 technical) repeats for PAO1 and PAO1 *ΔaaaA* and for the CF isolates with miniCTX-*lux*::P*kan;* only 2 biological repeats (x6 technical) are included for some of the CF isolates with miniCTX-*lux*::P*aaaA*. Error bars show the standard deviation between the repeats. Panel B: AaaA activity. PAO1, PAO1 *ΔaaaA* and the CF isolates were grown in LB or ASM until exponential phase. The cultures were washed 3x in MMP and standardised to OD_{600} 0.5. The cells were then incubated with the AaaA substrate L-arginine-p-nitroanilide for 24 hours at 37°C. The OD_{405} is representative of the p-nitroaniline dye cleavage from original molecule. Each bar shows the AUC of the OD_{405}. The 3 biological replicates (x 9 technical replicates) are represented by the error bars showing the standard deviation between these repeats. A t-test was performed for each strain between LB and ASM media and the level of significance represented by 1 or more * or ns.

4.2.4.4 KNO_3 addition to LB media potentially increases PaaaA activation in CF isolates and does not decrease AaaA activity in all isolates

To investigate the effect of exogenous nitrate on *PaaaA* activation and AaaA activity in the CF isolates, PAO1, PAO1 *ΔaaaA* and the CF isolates were tested in LB and 10 mM KNO_3 in the manner which has previously been described for the miniCTX-*lux* reporter assay and the AaaA activity assay.

The CF isolates grown in nitrate enriched LB generally showed a slight decrease in *aaaA* expression (Figure 4.2.45 A). This difference was more noticeable in CF 892 and CF 484. Notably, this was also seen in PAO1 for this set of experiments and may be due to the reason outlined in 4.3.3.2.2. Unfortunately there were growth issues with the CF isolates containing the miniCTX-*lux::Pkan* construct which were not resolved in time for inclusion in this thesis. These results should therefore be considered a preliminary test, prior to future qRT-PCR data.

In the CF isolates, AaaA activity differed between LB and LB with 10 mM KNO_3 added. However, whether this increased or decreased depended on the isolate (Figure 4.2.45 B).

AaaA activity increased in PAO1 *ΔaaaA* (background), CF 030, CF 892, CF 983, and CF 098, in response to additional nitrate. AaaA activity decreased in strains CF 971, CF 129, CF 326 and CF 393 in nitrate enriched media. AaaA activity was not significantly different in PAO1 and CF 484 in either condition.

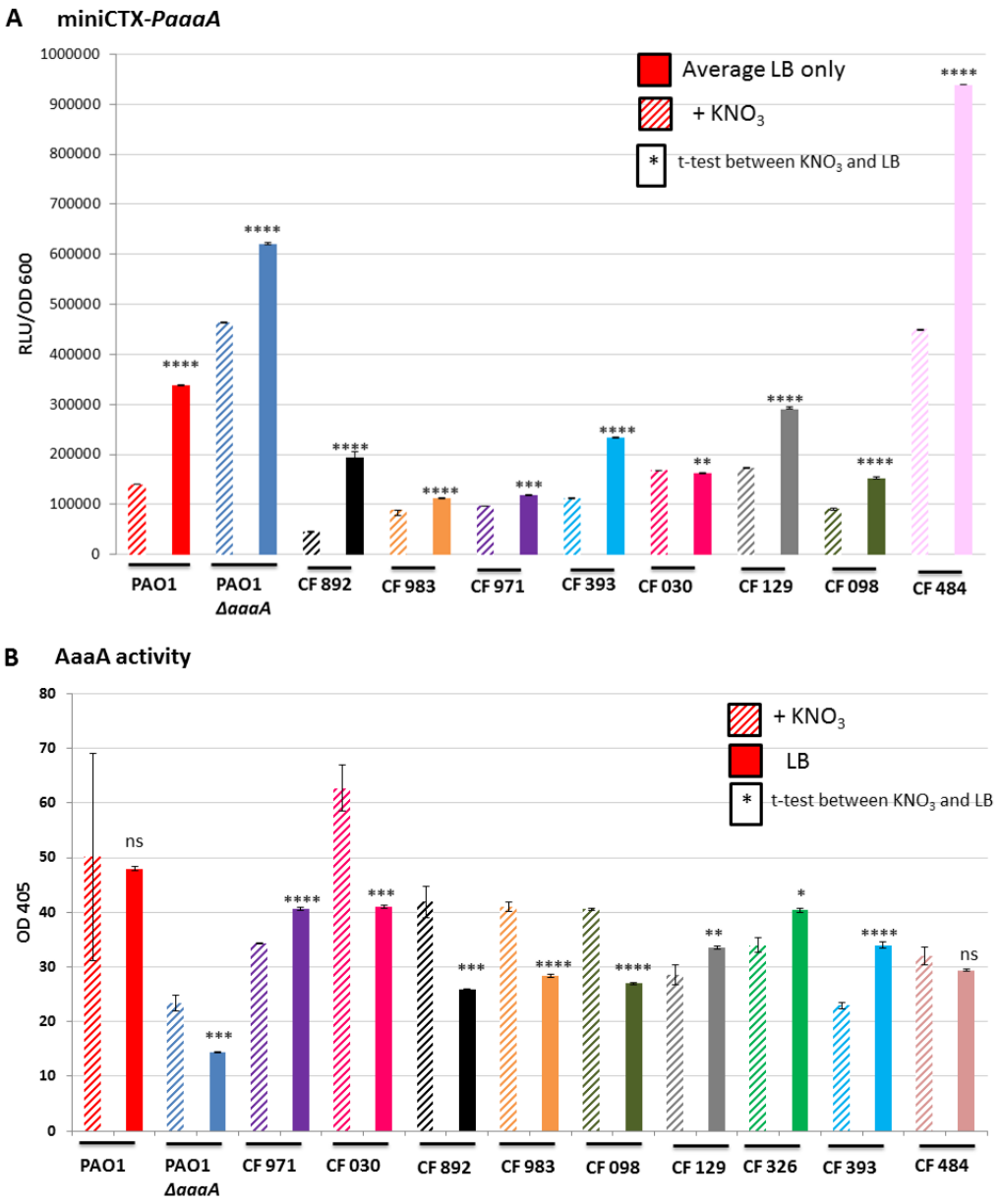


Figure 4.2.45 : CF isolates show a general increase in *PaaaA* activation in KNO_3 enriched media, while AaaA activity is affected differently depending on the CF isolate. Panel A: *PaaaA* activation in CF isolates in LB and LB media enriched with 10 mM KNO_3. PAO1, PAO1 *ΔaaaA* and CF isolates with integrated miniCTX-*lux*::*PaaaA*, were grown overnight in LB media or LB + 10 mM KNO_3, washed 3x and standardised to OD_{600} 0.1. They were then added to a 96 well plate, allowing the growth (OD_{600}) and luminescence (RLU) to be measured over 24 hours by a tecan plate reader. The luminescence corresponds to activation of *PaaaA* and is presented as the AUC of the RLU/OD_{600}. Each bar represents the average of 2 biological (6 technical) repeats. Error bars show the standard deviation between the repeats. Panel B: AaaA activity in CF isolates in LB and 10 mM KNO_3 enriched LB. PAO1, PAO1 *ΔaaaA* and the CF isolates were grown in LB or LB + KNO_3 until exponential phase. The cultures were washed 3x in MMP and standardised to OD_{600} 0.5. The cells were then incubated with the AaaA substrate L-arginine-p-nitroanilide for 24 hours at 37°C. The OD_{405} is representative of the p-nitroaniline dye cleavage from original molecule. Each bar shows the AUC of the OD_{405}. Error bars the standard deviation from 3 biological (x 9 technical) replicates for the LB condition and 2 biological replicates (x6 technical) for the additional nitrate condition. A t-test was performed for each strain between LB and LB + KNO3 conditions and the level of significance represented by 1 or more * or ns.

4.2.4.5 Higher NaCl concentrations in LB potentially cause a decrease in PaaaA activation in most CF isolates and lower NaCl concentrations result in less AaaA activity

To investigate the effect of NaCl concentration on *PaaaA* activation and AaaA activity in the CF isolates, PAO1, PAO1 *ΔaaaA* and the CF isolates were tested in LB with either 0.055 g/L (0.9 mM), 10.055 g/L (172.1 mM) or 17.055 g/L (291.8 mM) NaCl added. The miniCTX-*lux* reporter assay and the AaaA activity assay were proceeded with in the manner which has previously been described with the exception that no NaCl was added to the MMP.

In the CF isolates the most common pattern seen is less P*aaaA* activation in high NaCl containing LB (Figure 4.2.46 A). This occurs in PAO1, PAO1 Δ*aaaA,* CF 892, CF 983, CF 971, CF 393, CF 098 and CF 484. CF 129 and CF 030 show lower *PaaaA* activation in the middle concentration of NaCl with the second lowest activation occurring in the low NaCl condition. Unfortunately there were growth issues with the CF isolates containing the miniCTX-*lux*::*Pkan* construct which were not resolved in time for inclusion in this thesis. These results should therefore be considered a preliminary test, prior to future qRT-PCR data.

In contrast to the effect on *PaaaA* promoter activation, the activity of AaaA was lower in all the CF isolates and the PAO1 strains in the low NaCl condition (Figure 4.2.46). This excludes CF 326, CF 484 and CF 570 where the data is not available for this condition. In PAO1, CF 030, CF 971, CF 393, CF 326 and CF 484, AaaA activity was highest in the middle NaCl concentration. PAO1 Δ*aaaA,* CF 098, CF 983, CF 129 and CF 892, showed the highest AaaA activity in the high NaCl condition.

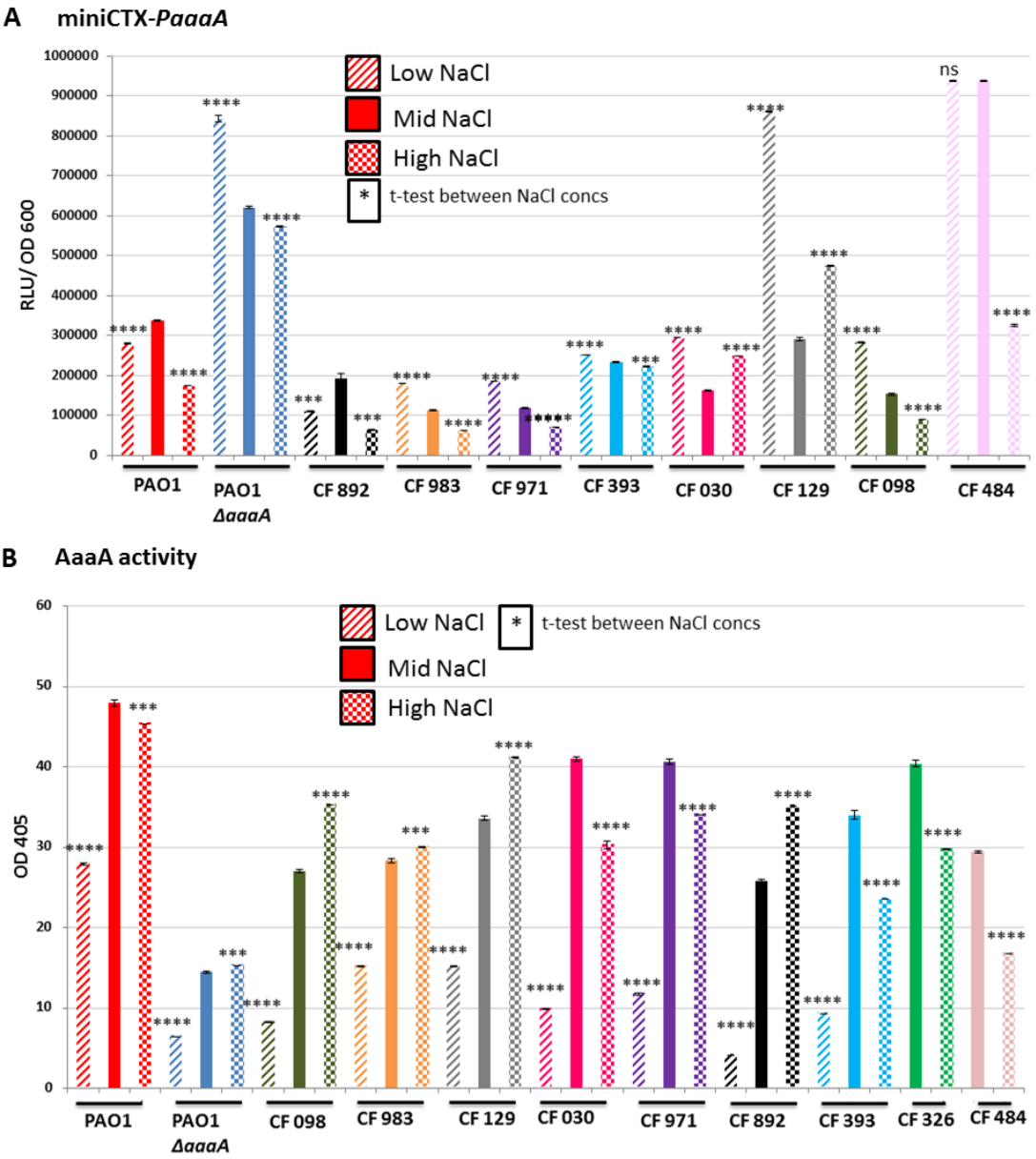


Figure 4.2.46: In most CF isolates less *PaaaA* activation is observed in high NaCl LB, while a lower AaaA activity correlates with a low concentration of NaCl. Panel A: *PaaaA* activation in CF isolates in LB with either 0.9 mM, 172.1 mM or 291.8 mM NaCl. PAO1, PAO1 *ΔaaaA* and CF isolates with integrated miniCTX-*lux*::*PaaaA*, were grown overnight in LB media of the appropriate NaCl concentration, washed 3x and standardised to OD_{600} 0.1. They were then added to a 96 well plate, allowing the growth (OD_{600}) and luminescence (RLU) to be measured over 24 hours by a tecan plate reader. The luminescence corresponds to activation of *PaaaA* and is presented as the AUC of the RLU/OD_{600}. Each bar represents the average of 2 biological (6 technical) repeats. Error bars show the standard deviation between the repeats. Panel B: AaaA activity in CF isolates in LB with either 0.9 mM, 172.1 mM or 291.8 mM NaCl. PAO1, PAO1 *ΔaaaA* and the CF isolates were grown in LB of appropriate NaCl concentration until exponential phase. The cultures were washed 3x in MMP and standardised to OD_{600} 0.5. The cells were then incubated with the AaaA substrate L-arginine-p-nitroanilide for 24 hours at 37°C. The OD_{405} is representative of the p-nitroaniline dye cleavage from original molecule. Each bar shows the AUC of the OD_{405}. Error bars the standard deviation from 3 biological (x 9 technical) replicates for the LB condition and 2 biological replicates (x6 technical) for the additional nitrate condition. A t-test was performed for each strain between LB middle NaCl and either low NaCl or high NaCl conditions and the level of significance represented by 1 or more * or ns.

4.2.5 CF isolate trait comparison and relationship to AaaA

Table 4.2.2 summarises the results in this chapter in order to identify any correlating traits.

P. aeruginosa strain	**Trait**								
	Growth A) aerobic, LB B) aerobic, ASM C) microaerobic, LB D) microaerobic, ASM	**Motility** A)Swarming B)Swimming C) Twitching	**Elastase production**	**Pyocyanin production**	**Biofilm** A) Tube B) Congo red C) Bioflux	**AaaA** A) Presence B ORF mutations C) Prom deletions	**AaaA** A)expression in LB B) Activity in LB	**Media and oxygenation effects on AaaA** A) expression B) activity	**CF specific conditions effect of AaaA** A) NaCl B) Nitrate C) pH
PAO1		A) Motile B) Motile C) Motile	Positive	Positive	B) Red, circular, thin edge, not wrinkly C)Large circular clumps, little dead cells	A) Yes B) n/a C) n/a	A)middle-low B)high	A) Higher in LB B)Higher in LB, higher in microaerobic	A) no difference in expression, no difference in activity B)no difference in expression, no difference in activity C) no difference in expression, activity highest at 6.8 and 7.2.
PAO1 *ΔaaaA*	A) same as PAO1 B) same as PAO1 C) same as PAO1 D) same as PAO1	A) Motile B) Motile C) Motile	Positive	Positive	B) As PAO1	A) no B) n/a C) n/a	A) high B)low	A) Higher in LB B)Higher in LB, higher in microaerobic	A) more expression middle NaCl, lower activity in middle NaCl B) no difference in expression, no difference in activity C) no difference in expression, activity consistent in all pHs.

CF 326	A) slightly slower than PAO1 B) faster than PAO1 C) Similar to PAO1 D) slower than PAO1	A) none/little B) none/little C) none/little	Slightly more than *ΔlasB* but less than the PAO1 strains	none	A) no clump B) white, an edge, not wrinkly. C) fairly homogenous,few dead cells and not clumpy.	A) Yes B) Group 1 (inc CF 129) C) Yes, LES-like	A) Unavailable B) high	A) data unavailable B) Higher in ASM	A)expression data unavailable, activity highest mid NaCl B)expression slightly decreased in nitrate media, activity decreased in nitrate media
CF 393	A) Similar to PAO1 B) similar to PAO1 C) Slightly slower to PAO1 D) slower than PAO1	A) none/little B) none/little C) none/little	none	none	A) Clumps B) orange, a particular edge C) Sparsely spaced big clusters surrounded by flatter regions. Less dead cells than CF 983 and most similar to PAO1.	A) Yes B)Group 3 (CF 393 and CF 484) C) No, PAO1-like	A) middle B) middle-high	A) Higher in ASM B) Higher in ASM	A)expression high in low NaCl media, activity highest mid NaCl B)expression slightly decreased in nitrate media, activity decreased in nitrate media
CF 892	A) Slightly slower than PAO1 B) Similar to PAO1 C) Similar to PAO1 D) slightly slower than PAO1	A) none/little B) none/little C) little	none	More than PAO1	A) no clump B) white, a particular edge, wrinkly C) not tested	A) Yes B)Group 2 (CF 030 and CF 892) C) Yes, LES-like	A) middle B) low	A) Higher in LB B) Higher in ASM	A)expression high in middle NaCl media, activity highest in high NaCl B)expression slightly decreased in nitrate media, activity increased in nitrate media
CF 484	A) Similar to PAO1 B) Similar to PAO1 C) Slightly slower than PAO1 D) slightly slower than PAO1	A) none/little B) none/little C) none/little	none	none	A) no clump B) red, an edge, not wrinkly C) not tested	A) Yes B) Group 3 (CF 393 and CF 484) C) Yes, LES-like	A) high B) average	A) Higher in ASM B) Higher in ASM	A) expression high in low and middle NaCl media, activity highest mid NaCl B)expression slightly decreased in nitrate media, activity increased in nitrate media
CF 971	A) Slightly slower than PAO1 B) No growth	A) none/little B) none/little	none	none	A) no clump B) red, an edge, not wrinkly C) not tested	A) Yes B)Group 1 (inc 129) C) Yes,	A) low B) high	A) data unavailable B) Higher in ASM	A)expression high in low NaCl media, activity highest mid NaCl

	C) Similar to PAO1 D) no growth	C) none/little				LES-like			B)expression slightly decreased in nitrate media, activity decreased in nitrate media
CF 030	A) Faster than PAO1 B) faster than PAO1 C) Similar to PAO1 D) Similar to PAO1	A) some B) some C) none/little	none	none	A) no clump B) beige, a particular edge, wrinkly C) not tested	A) Yes B) Group 2 (CF 030 and CF 892) C) Yes, LES-like	A) unavailable B) high	A) data unavailable B) Same in ASM	A)expression high in low NaCl media, activity highest mid NaCl B)expression slightly decreased in nitrate media, activity increased in nitrate media
CF 098	A)Slightly slower than PAO1 B) Similar to PAO1 C) Similar to PAO1 D) Slightly slower than PAO1	A) none/little B) none/little C) little	none	none	A) no clump B) red, an edge, not wrinkly C) not tested	A) Yes B) Group 1 (inc 129) C) Yes, LES-like	A) low-middle B) low-middle	A) data unavailable B) Higher in LB	A)expression high in low NaCl media, activity highest in high NaCl B)expression slightly decreased in nitrate media, activity increased in nitrate media
CF 983	A)Slightly slower than PAO1 B) Slower than PAO1 C) Slightly slower than PAO1 D) Slower than PAO1	A) none/little B) none/little C) none/little	none	none	A) no clump B) yellow, an edge, not wrinkly C) More dead cells than the others, big interconnected clumps, not circular.	A) Yes B)Group 1 (inc 129) C) Yes, LES-like	A) low B) middle	A) data unavailable B) Higher in ASM	A)expression high in low NaCl media, activity highest in high NaCl B)expression slightly decreased in nitrate media, activity increased in nitrate media
CF 570	A)Slightly slower than PAO1 B) Similar to PAO1 C) Similar to PAO1 D) Slightly slower than PAO1	A) none/little B) none/little C) none/little	none	none	A) no clump B) orange, an edge, possibly wrinkly C) not tested	A) Yes B) Group 1 (inc 129) C) Yes, LES-like	A) high B) low	A) Higher in ASM B) Higher in ASM	A) Expression data unavailable, not available B)expression slightly decreased in nitrate media, activity increased in nitrate media

CF 129	A)Slightly slower than PAO1 B) Similar to PAO1 C) Similar to PAO1 D) Slower than PAO1	A) none/little B) none/little C) none/little	none	none	A) no clump B) red, an edge, not wrinkly C) not tested	A) Yes B) Group 1 (inc 129) C) Yes, LES-like	A) middle-high B)middle	A) data unavailable B) Same in both	A)expression high in low NaCl media, activity highest in high NaCl B)expression slightly decreased in nitrate media, activity decreased in nitrate media

Table 4.2.2: Summary of results. Shading indicates similar phenotype groups within each category.

4.3 Discussion

In this chapter a panel of CF isolates were characterised, the presence and behaviour of *aaaA* analysed, and the effect of different CF specific conditions on the expression and activity of AaaA investigated. The goal of this has been to move further towards answering the central questions outlined in the introduction:

- Is AaaA needed in the CF airway for *P. aeruginosa* persistence?
- When does AaaA activity give *P. aeruginosa* an advantage in the CF airway?
- What is the role of AaaA in the CF airway?

The results indicate that AaaA is advantageous for *P. aeruginosa* infecting the CF airway; however the specific advantage that this enzyme gives the bacteria in such an environment is still not completely clear. It is likely that AaaA interacts in concert with other metabolic systems operating in oxygen deficient conditions to allow growth and survival in the depths of airway mucus. The following sections discuss this further.

4.3.1 Phenotypic characteristics of CF isolates

To place AaaA in the context of CF, a selection of phenotypic characteristics were analysed in a panel of *P. aeruginosa* strains isolated from different CF patients. The aims were (i) to identify any particular trait which could correlate with an increase or decrease in the strain's reliance on AaaA, and (ii) to see if a particular combination of traits encouraged or discouraged AaaA from being utilized.

4.3.1.1.1 Growth in different media and oxygen concentrations

Growth curves in aerobic and microaerobic LB and ASM were performed for PAO1, PAO1 *ΔaaaA*, and the CF isolates to identify differences between strains and media types. There was no difference between PAO1 and PAO1 *ΔaaaA* strains, even in the microaerobic conditions, which could be because of the high availability of carbon and nitrate sources in the media. It is hypothesised that AaaA principally supports the ADI pathway which is dependent on nitrate availability and oxygen tension (Mercenier *et al* 1980). Comparing biofilms instead of planktonic cultures, while using a nitrate-restricted media is perhaps more enlightening and is explored in Chapter 6.

CF isolate growth in aerobic LB was generally slower than PAO1 with the exception of CF 393 and CF 484 which grew at a similar speed, and CF 030 exceeding PAO1 growth. Exchange of LB with ASM resulted in more CF isolates outgrowing the PAO1 strains (CF 030, CF 484, CF 570 and CF 326) suggesting that they are perhaps more adapted to ASM than LB or that they were more flexible in their media choice than PAO1. In ASM, the pre-experiment overnight culture of CF 484 required 36 rather than 18 hours of growth to reach a cell density suitable for standardisation and so it should be noted that this isolate had a very long lag phase in ASM that is not represented in the graph. CF 393 and CF 983 showed the slowest growth, with CF 971 not growing at all (likely auxotrophic). As CF 393 grew relatively quickly in LB this was intriguing and is hypothesised to be due to a strong clumping phenotype in ASM.

In microaerobic LB cultures, none of the CF isolates exceeded PAO1 in growth rate, CF 983, CF 971, CF 484 and CF 393 growing slower. The slower growth was more pronounced in ASM, all of the isolates growing slower than PAO1 apart from CF 030. It was thought that the CF isolates may have the advantage in growth under microaerobic conditions as the CF airway would be low in oxygen (Worlitzsch *et al* 2002). However, the growth of *P. aeruginosa* in this environment is likely to be as part of a biofilm community (Worlitzsch *et al* 2002), and is not directly comparable to planktonic behaviour (Yang *et al* 2008; Sonderholm *et al* 2017; Singh *et al* 2017).

The generally slower growth in ASM than LB in microaerobic conditions may be a consequence of the increased nitrogen availability in LB (~1.83 g/L as quoted by the manufacturer from complex peptides), than ASM, (0.31 g/L from 2.61 g amino acids, KNO_3 and NH_3Cl, Figure 4.3.1) important in oxygen deficient conditions. The amount of arginine is also likely to be less in ASM but it is difficult to determine the total amount in LB. Although the complex peptides available in LB could mean AaaA-mediated arginine release was contributing to growth in the microaerobic cultures, the lack of difference between the WT and *ΔaaaA* mutant strains suggests that this is not a major factor in this experiment. Also to be considered is the automatic mode of growth used for (tecan plate reader) the microaerobic growth curves. The volume was much lower and for a better comparison these should be done manually. The oxygenation of the microaerobic cultures probably reduced from the initial cabinet controlled concentration during the experiment due to the impermeability of the plate seals.

$$\%N\ in\ molecule = \frac{MW\ N}{MW\ N\ containg\ molecule}$$

$$gN = \%N * \frac{total\ g\ of\ molecule}{100}$$

Figure 4.3.1: Formulae used in nitrogen percentage calculations. Where N = nitrogen, MW = molecular weight and g = grams.

4.3.1.1.2 Motility ability

The CF isolates showed very little motility indicating a lack of functional flagella and Type IV pili appendages, suggestive of a loss of such apparatus or associated support systems during a sustained period of sessile growth. Lowered motility of CF isolates has also been found by Cullen *et al* (2015), and is suggested to be downregulated by the GacS/GacA/RetS/LadS acute/chronic switch and related RhlIR QS system (Jimenez *et al* 2012) as motility (plus rhamnolipids required for swarming) and biofilm formation are alternative options chosen by Gac/ Ret/Lad (Kohler *et al*, 2000; Jimenez *et al* 2012). Although there is an association between motility and biofilm development, the sustainment of mature biofilms is less dependent on motility appendages (Costerton *et al* 1999; O'Toole *et al* 2000; Klausen *et al* 2003). Additionally, reliance of flagella and Type IV pili is likely to differ *in vivo* where nutritional and attachment sources diverge from the laboratory (Davies *et al* 2017; Worlitzsch *et al* 2002).

CF 030 showed movement across swarming and swimming plates, although the swarming looked different from the classical tentacle-like appearance seen in the PAO1 and PAO1 *ΔaaaA* strains. It is interesting that CF 030 also shows the fastest growth in planktonic cultures and appears to be less adapted to oxygen limited environments (colony biofilm section). Perhaps this strain has not accumulated as many genetic changes as the other isolates or it could have evolved from a biofilm community of cells to bud off and explore new niches.

4.3.1.1.3 Elastase production

Elastase production by *P. aeruginosa* forms part of its invasion artillery (Wretlind and Pavlovskis 1983). It is encoded by *lasB* which is regulated by the *las*, and to a lesser extent the *rhl* system (Pessi *et al* 2001; Pearson *et al* 1997). It is an acute virulence factor, causing tissue damage and attacking the host immune system (Cathcart *et al* 2011; Kon *et al* 1999), but it also plays a role in the initiation of biofilm development and alginate synthesis (Kamath *et al* 1998; Cathcart *et al* 2011). A high proportion of *P. aeruginosa* isolated from CF patients have been found to contain a mutation in *lasR* which correlates with a reduction

in oxygen mediated metabolism and an increase in nitrogen consumption (Hoffman *et al* 2010). It may be that the CF isolates have such a mutation. This could be further investigated by PCR and sequence analysis. Although not a direct indicator of acute virulence due to its secondary role in biofilm formation, the lack of elastase production could indicate that these *P. aeruginosa* strains were isolated from a mature biofilm and thereby, with the motility data, suggests that this group of isolates are in a chronic state. It was hypothesised that AaaA would be more important for sustaining growth in chronic situations where the dominant strategy was to persist rather than to invade. It would be interesting to compare the AaaA profiles of these isolates to *P. aeruginosa* in a more acute, virulent, mode of living.

4.3.1.1.4 Pyocyanin production

Pyocyanin is a potent virulence factor which attacks the host immune system (Wilson *et al* 1987; Kamath *et al* 1995; Usher *et al* 2002) Only CF 892 produced a measurable quantity of pyocyanin, and this was several times higher than PA01-N. A study by Carlsson *et al* (2011) found that strains of *P. aeruginosa* which were pyocyanin negative correlated with patients showing elevated levels of BPI-ANCA. BPI-ANCA are anti-neutrophil cytoplasmic antibodies specific to the granula bactericidal increasing protein. These were found to correlate with *P. aeruginosa* infection and a decline in patient health. The lower immune response induced by pyocyanin negative strains may facilitate increases in bacterial number and associated decline in airway tissue health. A study by Caldwell *et al* (2009) however claimed that the presence of pyocyanin caused more airway damage because it caused a switching of the immune response to a T helper type 2 response which encouraged goblet cell hyperplasia and metaplasia. Although pyocyanin has been found to be useful to CF isolates (Ran *et al* 2003; Sarkisova *et al* 2005) and has been associated with biofilm formation, switching off pyocyanin production could facilitate immune system evasion.

This immune evasion strategy has to be balanced with survival in hypoxic conditions; pyocyanin (encoded by *phz*) is an electron acceptor and helps to maintain an oxidative balance (Price-Whelan *et al* 2007). It is this role in cellular redox that is particularly interesting from the point of view of AaaA. Price-Whelan *et al* (2007) found that pyruvate production in stationary phase cultures was markedly reduced in the PA14 *Δphz* mutant and pyocyanin was able to complement this, indicating that pyruvate fermentation relies on the aid of phenazines to some extent. Glasser *et al* (2014) further elucidated the mechanism of phenazine redox cycling, showing that in anaerobic conditions it

enabled glucose and pyruvate oxidation to acetate and generation of ATP. Importantly however, they found that the redox state of the cell, represented by the ratio of NADH/NAD+, did not affect ATP generation from the ADI pathway. This generation of ATP in spite of an unfavourable redox ratio means that the ADI pathway could work as an alternative or 'back up' survival strategy for cells existing in an anaerobic environment (Figure 4.3.2). Knocking out *aaaA* does not appear to have caused an increase of pyocyanin, but perhaps more pyocyanin will be produced under low oxygen, arginine deficient conditions in the PAO1 *ΔaaaA* strain. This could be further investigated by the extraction of pyocyanin from biofilm cultures.

Further investigation is needed to determine whether the pyocyanin production of the CF isolates increases in different conditions. Observation during growth in ASM suggested that the pyocyanin production in some CF isolates (CF 098, CF 393) may be enhanced. This would be interesting to explore, in addition to investigating the effect of nitrate, arginine and oxygen concentrations.

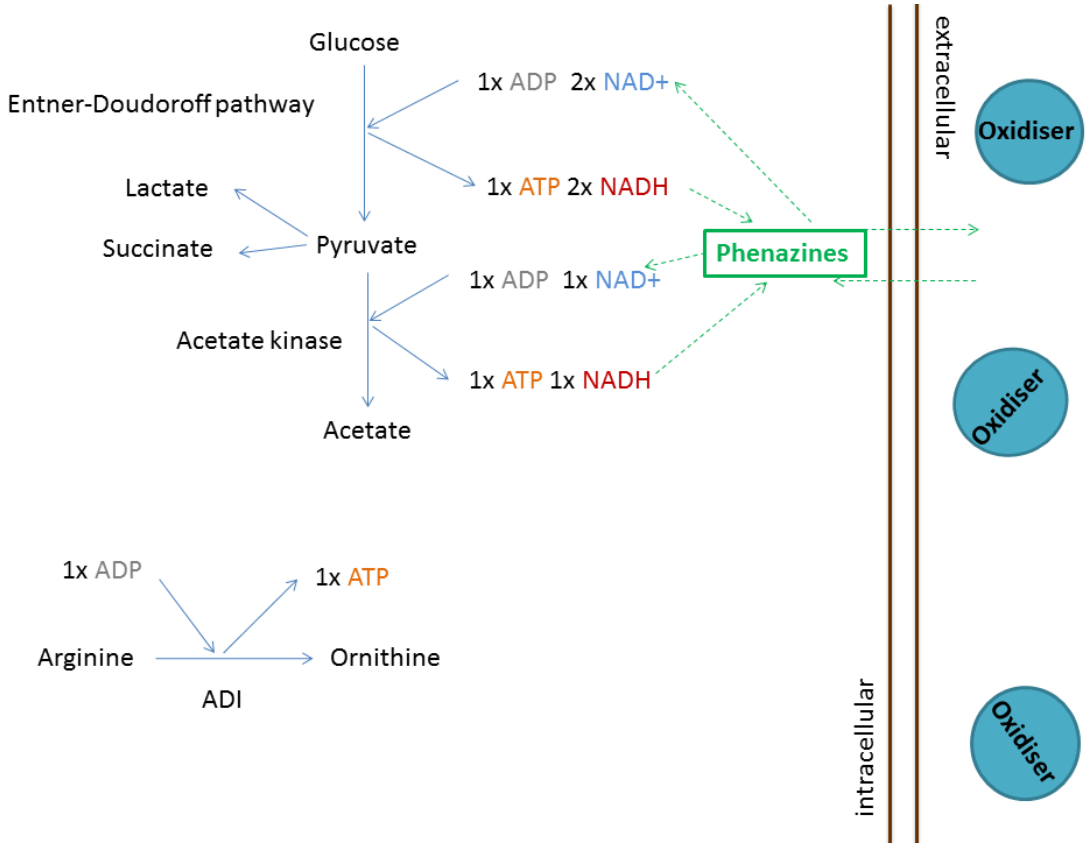


Figure 4.3.2: The redox cycling capabilities of phenazines allow ATP generation from glucose and pyruvate in anaerobic conditions but this is not required for functioning of the ADI pathway. The generation of ATP is coupled to the reduction of NAD+. Phenazines help to rebalance the NAD+/ NADH ratio by crossing the cell membrane and transporting electrons to extracellular oxidants. The generation of ATP by the arginine deiminase (ADI) pathway is not reliant on the cell being suitably oxidised (balanced NAD+/NADH ratio) and thus is independent of phenazine action. Based on the information from Glasser *et al* 2014 and Dietrich *et al* 2013.

4.3.1.1.5 Biofilm assays

Biofilms are complex structures which contain areas low in oxygen and nutrients (Stewart and Franklin 2008). Biofilms are a successful mode of growth in the CF airway, which are particularly difficult to eradicate, either by the host immune system or through antibiotic intervention (Mulcahy *et al* 2015). It was hypothesised that AaaA could support growth in the oxygen limited areas of a biofilm. From the growth, motility, elastase production and pyocyanin profiles, it appears likely that the CF isolates existed in a biofilm before extraction. To investigate the differences in biofilm formation existing between the isolates 3 different assays were chosen: a floating biofilm assay, a colony biofilm assay and a Bioflux system.

The floating biofilm assay was inspired by Wright *et al* (2013) and is thought to be a closer representation of *P. aeruginosa* biofilm formation in the CF airway, excluding possible epithelial cell attachment. Rather than growing the cells on a surface, a colony was simply added to a tube of ASM and grown for 18 hours to

see if they started to form 'clumps'. These suspended clumps or clusters of cells, indicate biofilm formation. Only CF 393 noticeably clumped. It was unexpected that so few of the isolates clumped; an extended time period seemed not to make any difference (data not shown). Potentially, the clumping phenotype could be increased with some adjustments. These cultures were grown aerobically with an ASM missing mucin proteins and eDNA, that if added would increase viscosity. Additionally, mucin may encourage the formation of larger cell clusters (Landry *et al* 2005) and mucin isolated from CF patients were covered with a glycoprotein (sialyl-Lewis) that *P. aeruginosa* readily binds to through the flagella (Jeffries *et al* 2016). Extracellular DNA is a biofilm matrix component and important in the initial stages of biofilm formation (Whitchurch *et al* 2002). Although *P. aeruginosa* can produce its own, the excess provided in the CF airway from damaged host cells (Dwyer *et al* 2014) could enhance biofilm formation. Adding these components to ASM could identify whether the lack of clumping was due to their absence.

Colony or microcolony biofilms were first used by Freeman *et al* (1989) to identify ECM production in gram-positive strains by spotting the colonies on Congo red plates and observing whether they turned black or red. The assay has been adapted for gram-negative strains, and used to observe the biofilm forming capacity of *P. aeruginosa* (Friedman and Kolter 2003; Dietrich *et al* 2013, 2008). Three phenotypes of particular interest were colour, wrinkling and size. A red colour has been understood here to mean an uptake of Congo red and production of some EPS components, for example Pel (Solano *et al* 2003). The colonies that remained pale after 6 days were CF 892, CF 030, CF 983, CF 326 and the edge of CF 393. CF 326 has a mucoid appearance when spread on plates and as a result may produce less Pel (Ghafoor *et al* 2011). CF 030 and CF 393 could also be mucoid but this is less obvious than CF 326. High alginate production does not seem to be a trait of CF 892 and CF 983.

Wrinkles have been hypothesised to be a strategy to increase surface area, indicating that colonies which wrinkle have a higher requirement for oxygen. For example, Dietrich *et al* (2013) found that *P. aeruginosa* unable to produce redox active phenazines formed wrinkly colonies. An earlier wrinkling starting time was thought to correlate with a higher inefficiency of survival at low oxygen densities (Dietrich *et al* 2013) and so the colonies were photographed daily. Although the wrinkles were not as obvious as in Dietrich *et al* (2013) a general roughness in colony appearance was apparent in some colonies and not others. The strain which showed this roughness the earliest in the experiment was CF 892, on day

1. On day 2 CF 030, the edges of CF 393 and also possibly CF 129 and CF 098 began to wrinkle. CF 570 showed slight wrinkling from day 4, and PAO1 and PAO1 Δ*aaaA* from day 5 with no difference between mutant Δ*aaaA* and WT phenotypes. It is possible that CF 030 is less adapted to a chronic lifestyle than some of the other isolates (faster growth and motile) and this is reflected in a lower aptitude for biofilm growth. This could indicate that it is more flexible than the other strains or earlier in the process of colonisation. CF 129, CF 098, CF 393 and CF 892 however, appear generally non-motile, slow growing and low virulence factor producing (elastase). CF 892 produced above average pyocyanin which is at odds with a high wrinkle phenotype (Dietrich *et al* 2013).

Colony size is another way that the cells can increase surface area and is also thought to correlate to a higher reliance for oxygen for growth (Dietrich *et al* 2013). The qualitatively bigger colonies were CF 892, CF 030, and CF 129, correlating with the wrinkling phenotype. Interestingly, CF 892 and CF 030 share a similar pattern of *aaaA* ORF changes. The fact that they are both more wrinkly and larger than the other strains and have this ORF similarity could mean that their AaaA proteins are less efficient than the other isolates, even though there is no change to the active residues. CF 030 does not have a particularly low activity assay profile however so further investigation is needed to uncover the mechanisms involved in producing these phenotypes.

To compare structural differences between CF isolate produced biofilms, a Bioflux system with confocal microscopy imaging was utilised. All isolates tested were able to form biofilms; however the structure of each was different. CF 326 is an isolate which exhibited relatively high AaaA activity, is high alginate producing, non-wrinkling, possesses a LES-typical *aaaA* promoter and showed the most common ORF change pattern. It produced the least clumpy looking biofilm which was surprising as it is the most obviously mucoid, in a tube of ASM forming a dense, thick slime. There was an absence of red fluorescence indicating a lack of dead cells. CF 393 showed middling AaaA activity, is the clumpiest of the isolates in ASM, has a PAO1-like *aaaA* promoter and an AaaA ORF with multiple changes to non-active residues. Of the isolates, CF 393 showed a biofilm structure the most similar to PAO1 forming large separate clusters, which were nonetheless bigger and more asymmetrical than the PAO1 phenotype. The similarity to PAO1 could stem from the possession of a similar *aaaA* promoter region. To investigate further, more isolates showing this promoter type could be tested using the Bioflux system. CF 393 also showed little evidence of dead cells. CF 983 has an AaaA activity which is a bit lower, a LES-like *aaaA* promoter and shows the most

common ORF change profile of the isolates. There were a higher amount of dead cells in the biofilms of CF 983 which could indicate this isolate was less adapt at growing in this environment. It could also be a consequence of the larger interconnected biofilms produced by this strain. The colony biofilm test suggested that it produces less EPS and may not be as good at growing at deeper, oxygen limited areas of a biofilm as some strains. This could be due to a lower AaaA activity, perhaps in conjunction with poor pyocyanin production. Further investigation is required to validate this hypothesis however.

An obvious correlation between an isolate's AaaA activity and biofilm structure is not apparent and it is likely many other factors are involved in addition to the ones investigated here. Additionally, AaaA activity measured in an activity assay does not account for the differences in regulation occurring in a biofilm from that of a planktonic culture. CF 983, which had lower AaaA activity than the other strains, showed more dead cells than the other biofilms and it would be interesting to investigate whether this could be due to this reduced activity.

4.3.2 AaaA in CF isolates

In this section the CF isolates were tested to see if they had retained the *aaaA* gene, a functional protein was expressed, and how this protein was utilised by the CF isolates: what is the cell responding to when it upregulates AaaA?

A PCR assay using primers designed by Paredes (2014) to amplify the ORF of AaaA showed that *aaaA* was present in all the CF isolates provided by the QMC Microbiology department (S.Holden). Further to this, 8 clones of *P. aeruginosa* isolated from a single CF patient (Darch *et al*, 2015) were tested to see whether the gene might have disappeared from some descendants of the original ancestor. Darch *et al* (2015) demonstrated that within the CF lung there are multiple related variants that could potentially inhabit specific niches. Phenotypic 'trade-offs' were found between traits such as growth rate and virulence factor (LasA and LasB) production for example. Perhaps in a mixed biofilm community only some cells need to specialize in cleaving arginine from the end of peptide chains using AaaA, and others can scavenge for the released arginine. Nonetheless the *aaaA* gene was present in all of these isolates, suggesting conservation of this gene in CF isolated *P. aeruginosa*. To determine if the gene continued to code for functional protein, the passenger (functional) domains of the AaaA ORF were sequenced and compared with the PAO1 reference sequence. Although the isolates differed in the amount and location of the protein residue changes they experienced, there were several in common. The most commonly

seen amino acid change was the replacement of lysine with glutamate at position 55. All of the isolates excepting CF 393 showed this change. The location of the change is in an external location, away from the active site. The change may affect the stability of the protein structure; it is unlikely to influence the active site. Comparing the activity measured in the P-nitroanilide assay of CF 393 with the other isolates does not indicate that this isolate has a particularly high or low AaaA activity. This is of course a crude comparison, not accounting for differences in regulation or other cellular processes.

The second highest frequency change seen (isolates CF 129, CF 098, CF 983, CF 971, CF 326, and CF 570) is at position 314, leucine to glutamine. This substitution of a polar amino acid with a hydrophobic one occurs close to the active site. Although not one of the identified active residues (Luckett *et al* 2012) which are H100, D102, D115, E147, E148, E149 and D176, this change could affect the shape of the active site and the spatial interaction between the substrate and active residues. It is hard to say whether this would increase or decrease the efficiency of catalysis without further experimentation using site-directed mutagenesis. The activity profiles vary between these isolates so there does not appear to have been a striking effect. The next frequently seen residue change is shared by CF 129, CF 098, CF 983, CF 971 and CF 326. This is the substitution of asparagine with serine at position 195. The change is likely to affect the stability of the protein structure, helping position the respecting alpha helix at tighter angle. It is unlikely to affect the functioning of the active site due to its location.

Another pattern of amino acid changes is shared by CF 030 and CF 892. One of these is the replacement of alanine with threonine at position 228, and the other a 2-base change from glutamate-leucine to glycine-threonine at position 255-256. These changes are close to each other structurally, fairly near the active site. The change from alanine to threonine results in an increase in polarity which could affect the positioning of the loop it is on. The side chain of alanine has been previously implicated in substrate recognition, but is otherwise non-reactive. Threonine in contrast more often has a role in the active site. The substitution of glutamate and leucine to glycine and threonine may alter the structure by creating a tighter loop. It is unlikely the structure of the active site would be substantially affected but without further investigation, this remains a slight possibility. The second pair of CF isolates with common mutations are 393 and 484, sharing the substitutions at position 270 (isoleucine to valine) and position 240 (asparagine to isoleucine). The former is unlikely to change either the

structure of the protein or the catalytic function of the active site as isoleucine and valine have similar properties. The second change may alter the structure slightly as the change from a polar to hydrophobic residue at the end of an alpha helix may result in tightening the configuration. Both CF 393 and CF 484 show large regions of change to the protein: in CF 393 these occur on a large loop and adjoining alpha helix, while in CF 484 the changes are more central and closer to the active site (although the active site itself is unchanged). The activity of AaaA in CF 484 is on the higher end of the scale so potentially these changes could have a positive effect on AaaA activity but this would need to be confirmed with further tests. CF 393 shows more clumping than the other strains and forms large clumps when grown as a biofilm in ASM, with few dead cells. The activity of its AaaA in LB is about average of the isolates. These features suggest that the changes in the AaaA protein of CF 393 are not having a substantial effect but like CF 484, this cannot be confirmed without further experimentation.

The differences in the AaaA ORF observed do not affect the active residues and only a few changes occur close to the active site. A correlation between particular groups of mutation pattern and differences in AaaA activity is not apparent. It may be that several of the residue changes affect neither the functioning, nor stability of AaaA. As mentioned by Luckett and colleagues (2012), AaaA has a low function density meaning that a very small part of the protein is responsible for activity (1%). However, the prevalence of specific patterns of amino acid change could indicate that they are advantageous in some manner; perhaps these mutations help stabilise the protein conformation. To evaluate significance of the residue changes in isolation from promoter diversity, the isolate ORF sequences could be fused with an artificial promoter (examples in Chapter 5). The activity could be assessed in an *E. coli* host or the proteins purified and tested in cell-free activity assays. To assess the effect of each individual residue change, site-directed mutagenesis could be employed.

Upon finding that AaaA should be functional in the CF isolates, the next question was whether CF isolates would regulate *aaaA* expression in response to different triggers to that of PAO1. A preliminary BLAST search of the *aaaA* upstream region revealed a 169 bp deletion region, in the first part of the intergenic region between *PA0329* and *aaaA*, was present in several *P. aeruginosa* strains. A clear divide between deletion-containing and PAO1-like sequences in phylogeny or environmental location was not observed. To see if the CF isolates had upstream regions showing similar deletion regions, they were sequenced and aligned with the PAO1 reference strain (no deletion) and LESB65 (deletion). All but CF 393

contained the deletion region and furthermore showed a series of SNPs which were identical to the LESB65 strain. Some of the isolates were LES derived and so this pattern could be inherited from a common ancestor. CF isolates 484, 892, 971 however also contained these SNPs and are not LESB65 derived. To see whether the deletion zone or SNPs could affect *aaaA* transcription, the changes were cross compared with putative regulation sites.

The deletion region contains 3 NarL, 2 IHF, an RhlR, and an ArcA putative binding site(s). NarL is part of a TCS system (NarX/NarL) which responds to available nitrate and inhibits the *arcDABC* operon, encoding the ADI enzyme (Mercenier *et al* 1980). The absence of a NarL binding site could prevent nitrate-mediated inhibition of *aaaA* upregulation. AaaA activity in response to nitrate was compared in the CF isolates but in aerobic LB and therefore an extension of this investigation should be to use a more defined media in oxygen limited conditions. RhlR was also predicted to have an inhibitory effect on aaaA (Paredes, 2014). ArcA on the other hand should have positive influence on transcription (Paredes, 2014). IHF is a DNA bending protein and can facilitate transcription factor binding (Moitoso *et al* 1989; Khrapunov *et al* 2006). Abolishment of this DNA bending site could reduce contact of EBPs or inhibitory transcription factors with RpoN, affecting the expression of *aaaA*. RpoN was found to have a negative effect on the expression of *aaaA* (Paredes 2014), in the right circumstances (Chapter 3). Due to the overwhelming deletion of putative repressor binding sites it was therefore expected that more *aaaA* expression should occur in the CF isolates than PAO1, which was not the case. To further investigate, site-directed mutagenesis on the RpoN binding site could be used to compare strains with and without the promoter deletion to see if a greater change in *aaaA* expression occurs in the IHF containing strains.

Some of the SNPs occurred in the ArgR motif. The ArgR motif in AaaA is 5'-**TG**A**CGC**CTGGG**C**<u></u>**G**ACCTG<u>A</u>GG-**TGTCGC**<u>T</u>A<u>C</u>G<u>T</u>T**G**T**AA**CTGGC-3' (Lu *et al* 2004) with the conserved bases in bold font and the SNPs underlined. As *aaaA* is on the negative strand, this reads 3- GCCAG**TT**A**C**AA<u>C</u>G<u>T</u>A**GCGACA**-CC<u>T</u>CAGGT**C**<u>G</u>CCCAG**GCG**T**CA**-5 in the sequence in Figure 4.2.27. None of the conserved bases have been affected and therefore the binding of ArgR is likely to be unimpeded. Other changes occurred in a second NarL site. The NarL binding sequence exists as a heptamer TACYYMT where Y= C or T and M =A or C. This heptamer is repeated after 2 nucleotides (Darwin *et al* 1997; Stewart and Bledsoe 2005). The second putative NarL binding sequence in *aaaA* is 3'-TCGTGC<u>T</u>*<u>CC</u>*<u>A</u>G<u>A</u>GACA-5' with the middle 2 nucleotides in italics and the changed

amino acids underlined. Here the final T of the first heptamer has been changed to a C which could reduce binding fidelity. The change of the middle C should not affect the binding as these nucleotides are not conserved. The start of the second heptamer AGA does not fit the conserved TMY format. The changes do not improve the likeness of the sequence to the conserved format and so it seems would have little effect. Overall, the changes in the second NarL binding site do not seem to have a large impact on binding. However this could be tested further by site-directed mutagenesis or promoter pull-down analysis. The NtrC putative binding site could have been affected by SNPs to 2 conserved bases. In THE sequence, TGCT**C**C**A**GAGACATGA, the bold font represents conserved bases and the underlined bases were affected by the SNPs. Although there was not time to investigate this further, it would be an interesting avenue to pursue using site-directed mutagenesis. The RpoN site was untouched by SNPs and thus may only be affected by the removal of the IHF site.

From these results it appears that the deletion, rather than the SNPs would have the greatest impact on regulator binding. Further work using site-directed mutagenesis, comparison in conditions stimulating and inhibiting regulator activation and promoter pull-down analysis would help move this analysis forward.

4.3.3 CF lung conditions effect on AaaA

To investigate whether AaaA could enhance the success of *P. aeruginosa* in relevant environments, the transcription and activity of this aminopeptidase were measured in conditions relevant to the CF airway. Increases in activity or upregulation could indicate a requirement for AaaA in these situations and help to elucidate its role.

4.3.3.1 Expression and activity of AaaA response in PAO1 and PAO1 ΔaaaA

4.3.3.1.1 Media type and oxygenation impact on AaaA

There was greater activity observed in PAO1 grown in LB as opposed to ASM in aerobic conditions, although this was quite small. This could be due to the greater availability of complex peptides available in LB than ASM which AaaA could excise L-arginine from (Palmer *et al* 2007). The presence of L-arginine initiates a positive feedback loop through ArgR (Lu *et al* 1999), which could continue to drive expression and subsequent activity of AaaA. There is also likely to be more free L-arginine in LB than ASM which could contribute to this feedback loop. Regulatory mechanisms are discussed in Chapter 6.

A larger difference in AaaA activity in the different media was seen in microaerobic conditions but only when the activity (OD_{405}) was normalised by cell number and the AUCs compared rather than the end points of the assay. Interestingly, there was a difference in the timing of peak AaaA activity in the microaerobic LB and ASM grown cells. In LB this peak was at the onset of exponential phase, whereas in ASM a peak was observed earlier in lag phase. However, as the activity was not measured in the late exponential and stationary phases of the growth curve it is not known whether there would be further peaks in these later phases. A peak of *aaaA* expression in aerobic LB conditions occurs at 4 hours which corresponds to early exponential phase. The expression of *aaaA* could be upregulated in this stage of growth (Chapter 6). This could be coordinated by the QS system through RhlR as previous data (Paredes 2014) and putative regulatory binding sites in the *aaaA* promoter (Chapter 3) support this. This could result in greater AaaA activity at exponential phase in comparison to earlier time points on the growth curve. Interestingly there was also a difference between the OD_{405} values in LB and ASM media in the PAO1 *ΔaaaA* control. This suggests that the background rate of L-arginine release in microaerobic conditions may be influenced by another aminopeptidase which is more stimulated by growth in LB than ASM.

There was a marked difference in AaaA activity between microaerobic and aerobic conditions in both media. Previous work by Paredes (2014), showed that components of the ADI pathway (AotJ and ArcD) and anaerobic sensor ANR had a stimulatory effect upon *aaaA* expression. This is corroborated by the similarity of regulator binding sites in the ADI encoding *arcDABC* operon with the putative binding sites in the *aaaA* upstream region. These include NarL (inhibitory), ArgR (stimulatory) and ArcA (stimulatory) binding sites (Mercenier *et al* 1980; Chapter 3). Furthermore, the greater importance of AaaA to *P. aeruginosa* in environments low in oxygen, agrees with the increased requirement for arginine in such conditions (Everett *et al* 2017; Vander Wauven *et al* 1984; Eschbach *et al* 2004). In contrast to the pathways operating in low oxygen conditions, an inhibitory effect upon *aaaA* expression was found to be the case (Paredes 2014) in the aerobically operating arginine catalytic pathways (AruB and SpeA). Together this data supports the hypothesis that AaaA aids the functioning of the ADI pathway and growth in hypoxic conditions (Figure 4.3.3).

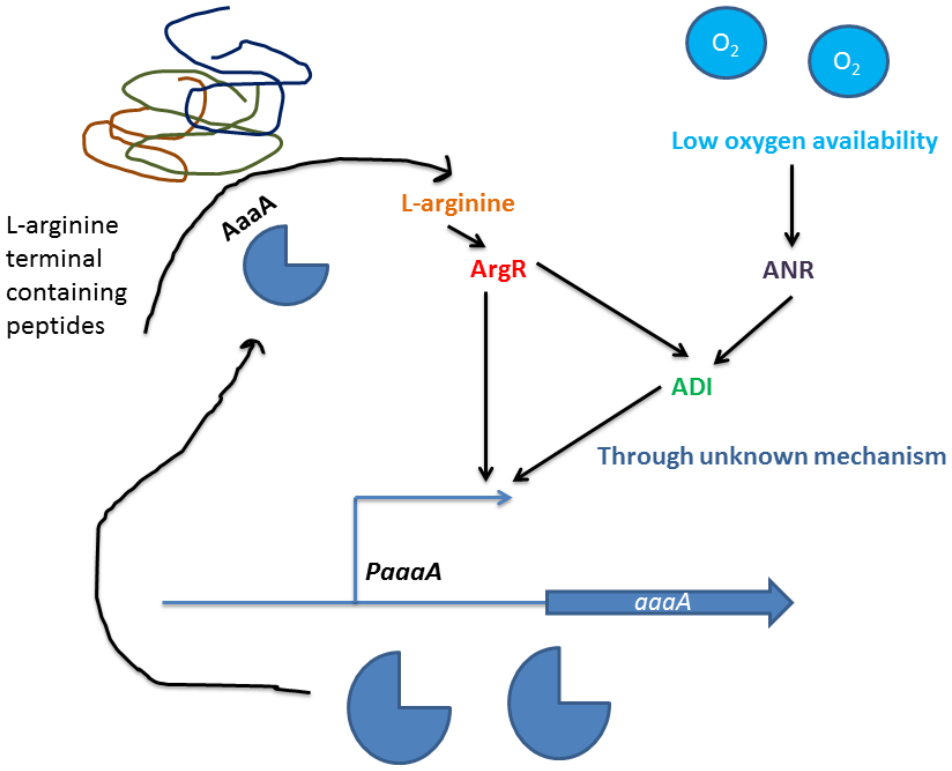


Figure 4.3.3: Microaerobic conditions stimulate AaaA activity when its substrate is present.

4.3.3.1.2 The relationship between nitrate availability and AaaA

When oxygen is unavailable as an electron acceptor, nitrate is able to fulfil that role through the denitrification pathway (Palmer *et al* 2007) which is upregulated by NarXL (Rabin *et al* 1993; Stewart *et al* 2003; Hartig *et al* 1999) through stimulation of *narK1K2GHJI* (Nadine *et al* 1999; Haas *et al* 1995; Arai *et al* 1991; 1994; 1995) and *dnr* (Hasegawa *et al* 1998). Simultaneously, NarL inhibits the *arcDABC* operon (Mercenier *et al* 1980). As discussed earlier, the ADI pathway and AaaA are connected with each other and it would be logical to assume that NarL would also inhibit *aaaA* transcription. Supporting this was the finding of putative NarL binding sites in the *aaaA* upstream region. Because of this, the effect of adding exogenous nitrate to the growth media of *P. aeruginosa* on *aaaA* expression and activity was investigated. This was hoped to support or discourage the hypothesis that NarXL inhibits *aaaA* transcription (Figure 4.3.4).

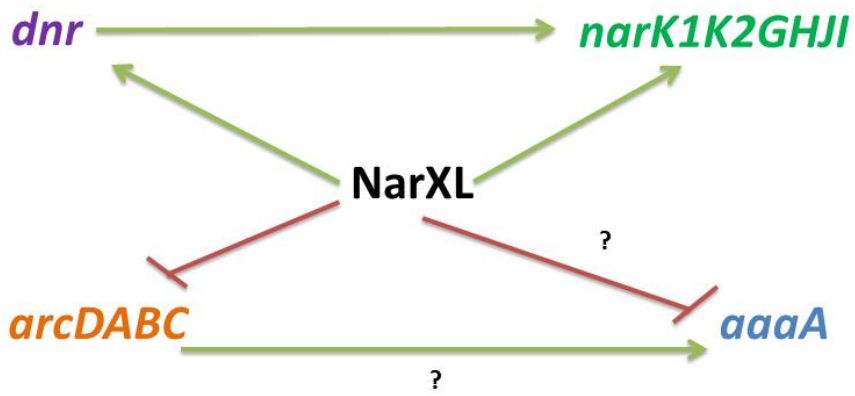


Figure 4.3.4: Hypothesis of the effect NarXL has on *aaaA* transcription.

Contrary to expectations, *aaaA* expression was higher in LB with an additional nitrogen source. This was consistent regardless the nitrogen containing molecule (KNO_3 or NH_4Cl). However, this effect was also seen for the kanamycin promoter and it may be that non *aaaA* specific mechanisms masking the effect on *aaaA*. These findings correlate with AaaA activity which was not affected by the addition of KNO_3 or NH_4Cl in LB. A substantial caveat of this experiment is that it used LB, a complex undefined media, which could vary in nitrate and nutrient content between batches and making the quantification of nitrogen molecules difficult. Furthermore the experiment was executed in aerobic conditions which are hypothesised to be less applicable for AaaA. This experiment should be repeated in oxygen limited conditions in a more defined media (Chapter 6).

4.3.3.1.3 How NaCl affects AaaA

How the concentration of NaCl varies from the norm in CF airways is a contended topic. Some studies suggest that higher amounts of NaCl are present in the airway lumen which contributes to the poor clearance of microbes from the airways by the host immune system (Goldman et al 1997; Smith et al 1996; Zabner et al 1998). Other studies dispute this and attribute the poor clearance of microbes to dehydrated mucus due to the osmotic imbalance caused by defective NaCl transport (Matsui et al 1998; Tarran et al 2001; Wills et al 1997). More NaCl in media has been linked to more surface adhesion (Cowell et al 1997) and less motility, particularly to flagella mediated motility (Soutourina et al 2001) and as AaaA was hypothesised to support biofilm development (Chapter 6), an association between NaCl and AaaA was considered. To investigate if NaCl concentration influenced *aaaA* expression and activity the *P. aeruginosa* strains were grown in 3 different LB broth solutions containing either an 0.9 mM, 172.1 mM or 291.8 mM concentration of NaCl.

Activation of the *PaaaA* promoter was not significantly affected in the PAO1 WT by NaCl concentration. However, *PaaaA* activation was stronger in the PAO1 *ΔaaaA* mutant grown in higher NaCl concentrations. This effect was not shared by the *Pkan* promoter. It is uncertain why NaCl should influence the *aaaA* promoter in the mutant but not the WT. There is a possibility that higher concentrations would have an effect on both strains and that the concentrations used in this experiment were too low to perceive a difference in the WT where promoter activation is lower (Chapter 3). There was no significant difference in AaaA activity between NaCl concentrations and it can be concluded that AaaA is not influenced by NaCl in the range tested.

4.3.3.1.4 How AaaA responds to pH variation

The pH of CF airways is reported to be lower than normal (Ballard et al 1999; Poulsen et al 1994; Poulsen and Machen 1996). A lower pH has been linked to bacterial growth impairments (Tsuji et al 1981). Arginine is a basic amino acid (Boriello et al 2006; Lebeaux et al 2014) and could help balance an acidic pH. If this were the case, AaaA would be instrumental in providing more free arginine. Perhaps more influential is the by-product of the ADI pathway, ammonia, which could also substantially balance an acidic pH (Lindgren *et al* 2014; Xiong *et al* 2014). It would follow that more transcription of *aaaA* should occur in lower pHs for this reason. However, this is not what was found here.

The *PaaaA* promoter was not differently activated in any of the pHs tested. AaaA activity was however higher in the higher pHs: 6.8 and 7.2. There is a possibility that a reduction in activity would be seen in higher pHs than 7.2. The pH of ASM is pH 6.8 and is thought to be the pH of the CF airway (Palmer et al 2007). That AaaA is highest at this pH is perhaps not surprising and a further experiment to test whether AaaA activity further increases with pH or declines after pH 7.2 would be useful to validate this correlation.

4.3.3.2 AaaA activity and expression in CF isolates

4.3.3.2.1 Influencing factors on AaaA activity in aerobic LB

The CF isolates showed levels of *PaaaA* activation and AaaA activity which were above baseline but lower than PAO1 in LB. There was a fair amount of variation between isolates in both *PaaaA* activation and AaaA activity. AaaA activity does not seem to correlate with promoter type (i.e. either showing the pattern of SNPs and 169 bp deletion similar to LES or a more PAO1 similar promoter), level of *PaaaA* activation or changes to ORF residues resulting in the cause of this variation to remain unknown (Figure 4.3.5). Because no obvious correlations

have been found from the findings presented here, the need to focus in more depth on a particular aspect of AaaA has become more apparent. Greater clarity could be achieved by examining each potential contributor (Figure 4.3.5) individually through site-directed mutagenesis and qRT-PCR.

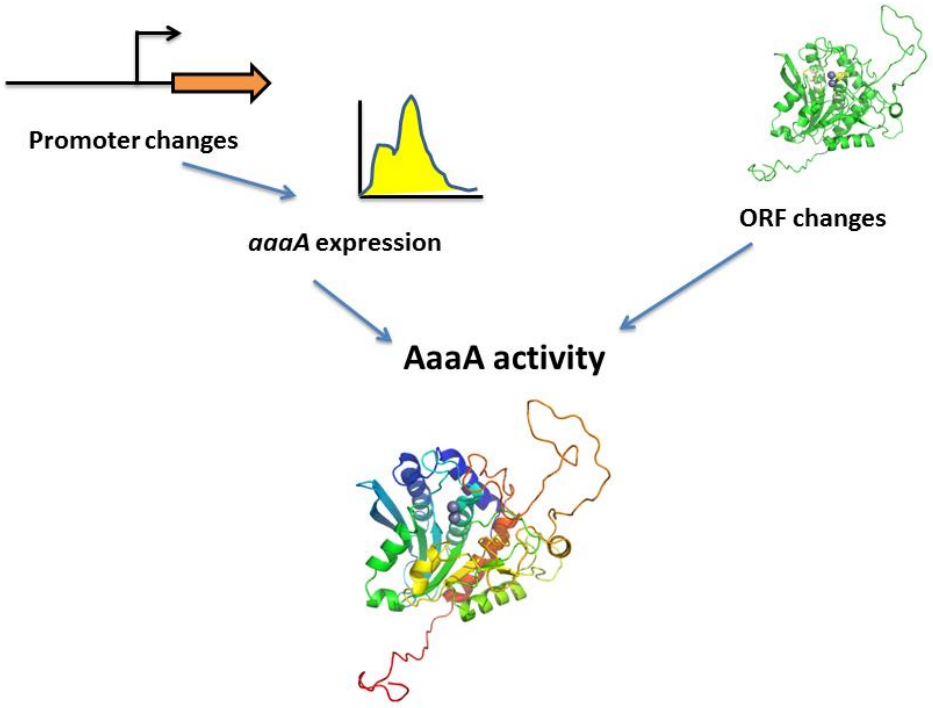


Figure 4.3.5: AaaA activity could be influenced by the relative expression and changes to the open reading frame (ORF).

In LB, aerobic conditions, P*aaaA* activation in CF 484 seems particularly high. The activity does not equate with this however, as it is around the average seen in the isolates. This could imply that factors other than the relative expression are at play, such as ORF differences. CF 484 has several changes to protein residues in the central region of the protein. They do not directly affect the active site but the interaction with the substrate could possibly be affected. Also showing a disparity between expression and activity, CF 570 shows a relatively high *PaaaA* activation and relatively low AaaA activity. There are a few more residue changes in the CF 570 ORF than the average here, but none affecting the active residues directly. CF 983 and CF 971 show the lowest activation of *PaaaA* of the CF isolates tested, but neither of these isolates showed particularly low AaaA activity. The isolates both share similar ORF changes (the common pattern) but the AaaA activity measured was different. CF 892 *PaaaA* activation was roughly in the middle of the CF isolates but the AaaA activity was one of the lowest. The residue changes in

the ORF are unlikely to be the cause in the lower activity as CF 030, which shows a similar pattern, has a much higher activity.

CF 030 and CF 393 *PaaaA* activation is similar and falls around the middle of the CF isolates. The AaaA activity of CF 030 is high in comparison to the majority of the other isolates and CF 393 AaaA activity is above the average. Unlike the other CF isolates, CF 393 possesses an *aaaA* upstream region more similar to PAO1 than LES. Unfortunately CF 030 was unable to be amplified so it is still unknown whether it is more similar to the LES or PAO1 type, but the fact that use of the LES specific forward primer would not allow amplification suggests that it does not have a LES-like promoter. CF 030 also exhibited the fastest growth of the isolates in aerobic conditions and showed swarming capabilities. CF 393 showed a biofilm structure and clumping behaviour more similar to PAO1 than to LES. CF 393 and CF 030 have different ORF residue change patterns. CF 030 has relatively few changes, while CF 393 has several changes to residues which are not shared by the other CF isolates. None of these are to active site residues however.

To compare the variation in AaaA activity in *P. aeruginosa* isolated from multiple patients to *P. aeruginosa* isolated from the same patient, the SED strains were also tested. These CF isolates also showed variation between themselves and PAO1 but this variation was smaller and the AaaA activity generally higher (mostly above OD_{405} 30). This may be because they come from the same ancestor in the same patient (Darch *et al* 2015). Further analysis of the *aaaA* ORF sequences and upstream regions would reveal how similar these are and whether they correlate with any of the other CF isolates.

Experimental limitations could also be making an association between *PaaaA* activation and AaaA activity difficult. The use of the miniCTX-*lux* reporter system in the CF isolates was problematic. The reporter was not accepted by many isolates and showed a lack of stability in those isolates where it was successfully integrated. The kanamycin constitutive control used was not reliable in the CF isolates either. This could indicate that there were differences in how the isolates were responding to their environment generally, potentially through global regulation differences, or the *lux*-reporter was instable in these conditions.

4.3.3.2.2 *PaaaA* activation and AaaA activity in ASM media compared to LB

In the CF isolates tested, *PaaaA* promoter activation varied in whether it was greater in LB or ASM depending on the isolate. The activity results were more consistent: aside from CF isolate CF 098, the activity of AaaA was increased in

the CF isolates grown in ASM compared to LB. This is the opposite than was observed with the PAO1 and PAO1 *ΔaaaA* comparison in LB and ASM. Why this is, is still not known. It could be correlated with the growth differences in LB and ASM. While PAO1 and PAO1 *ΔaaaA* showed enhanced growth in LB, this was not the case for several of the CF isolates.

4.3.3.2.3 Addition of KNO_3 to the growth media of CF isolates

Interestingly, in the 10 mM KNO_3 media, the CF strains showed a slight decrease in *aaaA* expression, in particular CF 892 and CF 484. This again defies expectations as the majority of the isolates have *aaaA* upstream regions containing the putative NarL and IHF spanning deletion region and theoretically should be less receptive of nitrate and NarL regulation. There is a second putative NarL binding site which retains its conserved nucleotides and is situated outside of the deleted region. This could be compensating for the loss of the other 'deleted' site, the 'deleted' site could not be a true site, or none of the NarL binding sites could be true as they are only putative and unconfirmed by experimentation. Site directed mutagenesis of the putative regulatory motifs would be helpful in answering this question. The kanamycin data is not available for this experiment, and rather than pursue this avenue, it is probably a better use of time to perform qRT-PCR analysis, facilitating the replication of the experiment under low oxygen concentrations.

AaaA activity differed in LB with 10 mM KNO_3 added compared to LB. However, whether this increased or decreased depended on the isolate and did correlate with promoter type. Both isolates possessing a LES-like promoter and CF 030 showed an increase in AaaA activity with KNO_3 addition. Similarly, both isolates containing a LES-like promoter and CF 393 showed a decrease in AaaA activity with KNO_3 addition. The testing in a more defined growth media and in microaerobic conditions would be a useful extension of this investigation.

4.3.3.2.4 NaCl effect on *PaaaA* activation and AaaA activity in CF isolates

The activation of P*aaaA* in the CF isolates varied. The most common pattern, shared by PAO1, PAO1 *ΔaaaA*, CF 892, CF 983, CF 971, CF 393, CF 098 and CF 484 was less P*aaaA* activation in high NaCl containing LB. CF 129 and CF 030 show lower *PaaaA* activation in the middle concentration of NaCl with the second lowest activation occurring in the low NaCl condition. Similarly to the KNO3 addtion experiment, the grouping of the isolates does not correlate with a promoter type .In addition the absence of *Pkan* activation data means that these

preliminary results would require further validation with another test such as qRT-PCR.

In contrast to the effect on *PaaaA* promoter activation, there was less AaaA activity in the lower NaCl concentration in all the CF isolates tested. This is different from the PAO1 and PAO1 *ΔaaaA* comparison. Because there is a link between a high NaCl concentration with reduced motility and increased attachment (Cowell *et al* 1998), NaCl could be affecting global regulation mechanisms such as the GacS/LadS acute/chronic switch system and the CF isolates could respond to smaller changes in NaCl than PAO1. Further testing with a wider range of NaCl concentrations could be conducted to explore this hypothesis. The difference in AaaA activity shown by the PAO1 control strains in the CF isolate experiment compared to the direct PAO1 and PAO1 *ΔaaaA* experiment, was unexpected and could be a consequence of being kept on the bench for 1-2 hours (materials and methods) when waiting for the slower growing CF isolates to reach exponential phase. Testing the activity along the growth curves could determine if this could be the case.

4.3.3.2.5 *PaaaA* activation and AaaA activity in the CF isolates

There was not sufficient time to investigate how the CF isolates respond to different pHs. It would be reasonable to assume that they would be better adapted to the pH of the CF airway and therefore it is likely we should see a similar pattern to PAO1 for AaaA activity and *PaaaA* activation.

4.3.4 Correlation of traits and final conclusions

That AaaA is being utilised by *P. aeruginosa* isolated from the CF lung has been confirmed in this Chapter. There is little change to the amino acid residues in the passenger (functional) domain in the majority of the isolates and no changes to the catalytic site amino acids. This indicates that there is a need for AaaA to remain functional. Additionally, the CF airway environment has not pushed the evolution of dramatic changes to the structure to increase the function. There is more of a divide between CF isolated *P. aeruginosa* and lab acclimatised PAO1 in the upstream-promoter region, indicating that any selection pressures on AaaA are acting on the regulation rather than on the protein itself. Interestingly, most of the isolates show an upstream profile almost identical to LESB65, even the isolates which are not LES derived. This suggests that this arrangement is advantageous for chronic infection of the CF airways and may also apply to other environments, as several other strains of *P. aeruginosa* were found to show this change in the BLAST analysis.

Characterisation of the CF isolates showed them to be as a whole non-motile, elastase negative, non-pyocyanin producing and fairly slow growing. CF 892 produced the most pyocyanin, CF 030 was the fastest grower and most motile isolate, and CF 326 produced the most elastase. None of these traits correlated with AaaA particularly. CF 393 produced the clumpiest biofilm and this had an AaaA profile most similar to PAO1 of the isolates. AaaA activity or expression is not unanimously higher or lower in the CF isolates (and by association chronic state *P. aeruginosa*), than the PAO1 strain. This makes it difficult to answer the central question of what role AaaA is playing to give *P. aeruginosa* an advantage. Additionally there was no difference between the PAO1 WT and PAO1 *ΔaaaA* strains in terms of growth (in either media or oxygen availability), motility, elastase production, pyocyanin production or Congo red biofilm production. Further investigation of the biofilm production capabilities of the two strains is explored in Chapter 6.

So what is AaaA needed for in the CF airway environment? The most striking finding here was the effect of oxygen availability on the activity of AaaA. This supports the hypothesis that AaaA is needed in oxygen deprived conditions specifically. The nutritional composition of its environment is also likely to play a role, but to a lesser extent. Disappointingly, the exogenous nitrate addition experiments yielded very little insight into the relationship between nitrate availability and arginine requirement. However, the huge caveat with this experiment is the availability of oxygen. Repeating these experiments in microaerobic or anaerobic conditions is an essential next step in pursuing this relationship. Additionally, looking at *aaaA* expression and activity in the background of a NarXL knockout (in oxygen limited conditions) would complement the exogenous nitrate experiment.

A moderate increase in NaCl concentration did not appear to have a substantial impact on AaaA. That a lower NaCl resulted in less AaaA activity in the CF isolates could be investigated further in a more extensive range of NaCl concentrations and cell-free protein activity assays. A pH of 6.8 is typical of CF according to Palmer *et al* (2007). This is the pH AaaA activity is highest at. Interestingly there is not more P*aaaA* activation or AaaA activity at lower pHs in which the release of arginine could help increase the pH to a more neutral value. This would seem to count against the hypothesis that AaaA could be employed in pH balancing. It is worth remembering that ample nitrate was present and a by-product of denitrification is ammonia (Gaston *et al* 2002; Barth and Pitt 1996; Thomas *et al* 2000). If nitrate was unavailable, *aaaA* expression might change in response to

lower pHs and this could investigated in the future. Nevertheless, from this and past data, it seems that the primary role of AaaA is supporting growth in oxygen limited conditions and work investigating this should take precedence.

Clearly, there is ample scope for further investigation, which should take place in oxygen limited conditions where nitrate availability is controlled for and phenazine/pyruvate availability is kept in mind. The next chapter looks at the production of recombinant AaaA for the purpose of structural analysis and inhibitor screening.

5 Chapter 5: Purification and Characterisation of AaaA

5.1 Introduction

AaaA is a promising therapeutic target for a number of reasons: it is exposed on the outside of the cell, is well conserved in clinical isolates, it contributes to chronic infections, and contains a highly conserved active site. As yet the structure of AaaA has only been predicted, based on its membership to the M28 family of proteins and using the crystal structure of peptidase A from *Streptomyces griseus* (SGAP) as a template. This chapter presents the progress made towards producing recombinant AaaA for the purpose of structural characterisation and inhibitor screening.

5.1.1 Background

Being an autotransporter (AT), AaaA has two translocation targeting domains (Ma *et al* 2003, Figure 5.1.1, Pohlner *et al* 1987). A signal peptide sequence at the N terminus guides AaaA from the ribosome to the IM and Sec apparatus, and is cleaved off during translocation to the periplasm (Dautin and Bernstein 2007). A beta-barrel (β-barrel) encoding sequence at the C-terminus facilitates transport through the OM (Pohlner *et al* 1987), but remains attached to tether AaaA to the bacterial surface. Only the central passenger domain bearing the functional protease is required for structural analysis in order to reveal potential targets of active site inhibition and to screen for effective inhibitors (Wilhelm *et al* 2011). The boundary of the amino-terminal signal peptide to the passenger domain can be predicted confidently using tools like SignalP, and there is an argument to leave it intact in order for AaaA to be translocated to the periplasm where folding would be assisted by chaperones. An intact signal peptide also provides the option of purifying AaaA from the periplasm, which would remove cytoplasmic contaminants.

A suitable C-terminal site to choose for severing the passenger domain from the β-barrel is harder to predict. This is because there is some evidence to suggest that the sequence between passenger and β-barrel may play a structurally important role. Celik *et al* (2017) found that a conserved alpha helix linker region (α-helix linker) located immediately upstream of the β-barrel sequence, is present in several ATs. In crystallised ATs this was structurally located inside the β-barrel

or just outside of it in the periplasm. This region was thought to be required for assembly of the β-barrel complex and subsequent cleavage of the passenger domain. Additionally, the presence of a linker in autotransporters which do not show passenger domain cleavage, led the authors to hypothesise that the linker could have another function, potentially aiding the early translocation of the passenger domain across the OM. A study by Rojas Lopez *et al* (2018) also suggests that the α-linker could facilitate protein folding in a subgroup of ATs. A conserved domain in the location of the α-linker called the autochaperone domain (AC) was found by structural analysis to be present in ATs with β-helical shaped passengers but not in α-helical globular shaped passengers. The majority of AT proteins have been found to include a passenger domain shaped into elongated β-helix surrounding a small typically globular catalytic segment (Yuan 2018). The autotransporter EstA of *P. aeruginosa* however, is one AT to have a smaller, more globular style passenger domain (van den Berg 2010). This appears to be more similar to the predicted structure of AaaA. It was therefore hypothesised that the protein folding of AaaA would not be affected by the cut site along the α-linker *per se*.

The decision to remove the β-barrel at all was also carefully considered. A number of protein structures of the AT family have been solved by purification strategies which include or exclude the β-barrel (Kahn *et al* 2012; Johnson *et al* 2012; Meng *et al* 2011; Otto *et al* 2005; van den Berg 2010). Some ATs which have been crystallised without their β-barrels are: EspP (Kahn *et al* 2012), Hap (Meng *et al* 2011) and Hbp (Otto *et al* 2005). Others which have been structurally solved with the full-length protein include: IgA1 protease (Johnson *et al* 2012) and EstA (van den Berg 2010). There is some evidence to suggest that the β-barrel could assist the passenger domain in more ways than translocation through the OM. Parts of the β-barrel have been implicated in supporting correct folding of passenger domains in the serine protease autotransporters of *Enterobacteriaceae* (SPATES) (Yuan 2018) of which group AaaA is closely associated. In particular, the mutation of one of the extracellular loops which the authors named L5, resulted in improper folding and protein degradation. However, the eventual goal of high throughput production clashes with the full-length protein purification approach. The production efficiency of membrane bound proteins in *E. coli* is low (Schlegel *et al* 2014) and therefore it was reasoned that a higher yield of protein could be reaped with a truncated version. In light of potential misfolding, the protein activity was tested as early as possible as a rough measure of correct folding before further steps were taken.

The previously predicted structure of the AaaA passenger domain (Luckett *et al* 2012) revealed a compact conformation with an identifiable active site that was confirmed by site directed mutagenesis of residues hypothesized to be key to the proteolytic activity from homology alignments (Figure 5.1.1). The substrates of AaaA have also been experimentally defined as peptides containing an N-terminal arginine (Luckett *et al* 2012). Not all peptides with this feature were equally well hydrolysed. The amino acid adjacent to the terminal arginine affects the efficiency of AaaA cleavage to some degree. The best efficiency was found to be when isoleucine or valine was the arginine's neighbour, while an adjacent lysine or arginine prevented cleavage (Luckett *et al* 2012). The active site is typical of a peptidase belonging to the M28 (M28.005 subgroup) family of proteins (Luckett *et* al 2012; Rawlings *et al* 2008). Within this group, AaaA shares the most similarity (64% ClustalW) to ECA2163 from *Pectobacterium carotovorum* (Darch 2013). Two zinc ligands are predicted to be tetrahedrally coordinated by histidine, aspartic acid and glutamic acid residues, forming a catalytic pocket (Luckett *et al* 2012, Fundoiano-Hershcovitz *et al* 2004; Chevrier *et al* 1996; Gilboa *et al* 2001). Several of the predicted catalytic residues in AaaA (Figure 5.1.1) contributed towards the activity of AaaA experimentally (Luckett *et al* 2012). Additionally, there was 100% conservation of the predicted catalytic residues when the protein sequence of AaaA was compared with other members of the M28 family (Luckett *et al* 2012). This high conservation is promising from the point of view of inhibitor design and development.

There is not a great deal of published work on the design and testing of inhibitors for AT proteins. An example of such a study can be found on the phospholipase autotransporter of *Fusobacterium nucleatum* (FlpA) however. Inhibitors for FlpA were identified in a study by Casasanta *et al* (2017) using activity assays and competition of the inhibitor with an active-site specific fluorescent probe (ActivX TAMRA-FP). In this chapter an AaaA specific activity assay is used to test inhibition by ion chelation which would need minimal adjustment to allow the testing of more specific inhibitors.

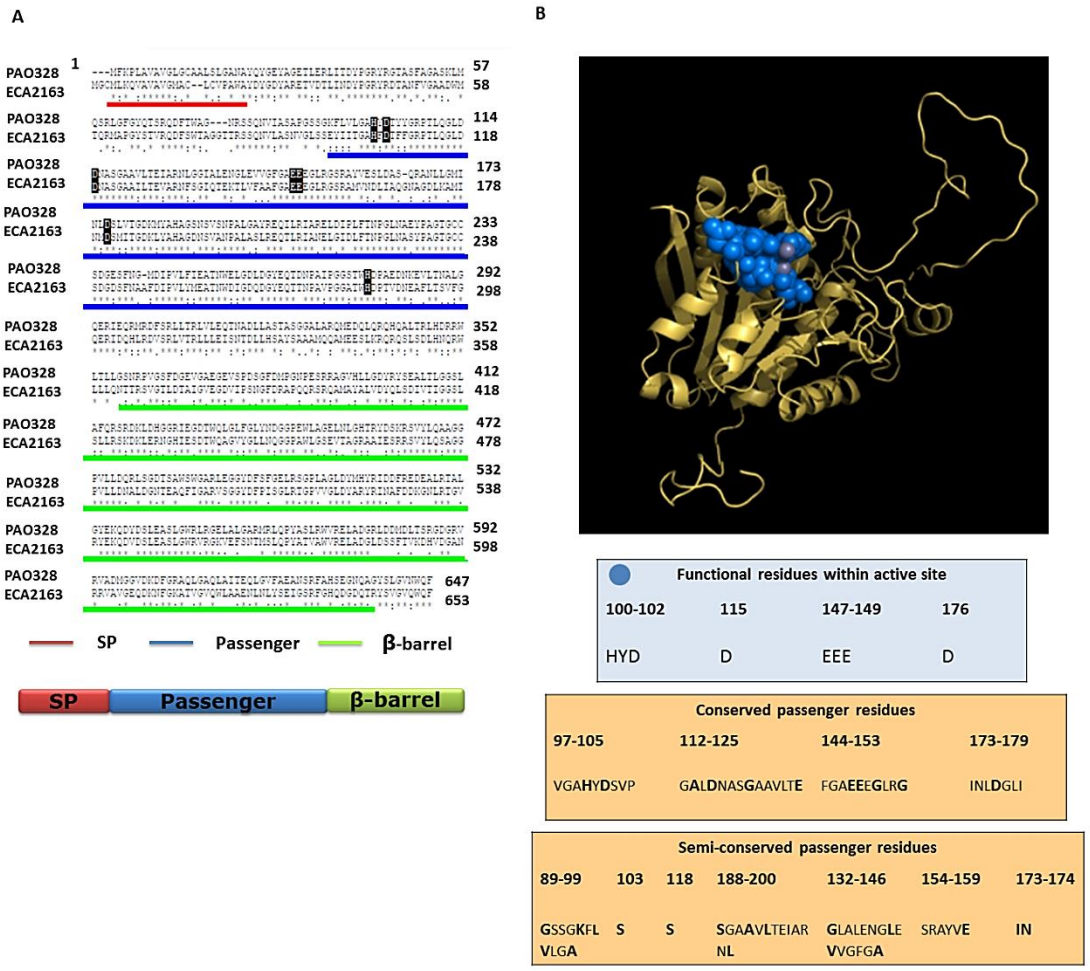


Figure 5.1.1: Structure of AaaA based on protein sequence comparison with SGAP highlighting active site residues. Panel A: sequence taken from Darch (2013) showing the full ORF of AaaA aligned with its closest member of the M28.005 subgroup, ECA2163 of Pectobacterium carotovorum with the domains indicated by coloured lines. Panel B: using the software Pymol, the predicted structure of AaaA (using SGAP as a scaffold) is shown with the conserved residues found to contribute to enzyme function (Luckett et al 2012) highlighted as blue spheres. The boxes below list the residues highlighted in blue with the orange panels listing additional conserved and semi-conserved residues for comparison.

5.2 Results

To study the activity of AaaA at a molecular and biochemical level and screen potential inhibitors, high levels of soluble, pure AaaA are required. As this protein naturally includes a membrane integrated component that will limit production levels and make purification more challenging, a series of truncations were engineered to remove the membrane-tethering β-barrel domain from the active aminopeptidase passenger domain. Table 5.2.1 outlines some basic properties of AaaA for use a reference when navigating the truncation processes. To maximise the yield of AaaA, the T7 promoter containing plasmid *pET21a (+)* was utilized as the expression vehicle, and this was hosted in *E. coli* BL21 (DE3).

	Information about the AaaA protein						
	Nucleotides (bp)	**Residues**	**Predicted size (kDa)**	**Size by blotting (kDa)**	**Predicted charge pH7**	**Kyte-Doolittle hydrophobicity value**	**Isoelectric point (pI) predicted**
Signal peptide	1-66 (66)	1-22 (22)	2.07		0.9		8.22
Between SP and Passenger	66-275 (209)	23-92 (69)	7.64		1.9		9.25
Passenger	276-875 (599)	93-292 (199)	21.25 (93-292) region) 28.88 (22-292)		-18.4 (93-292) -16.4 (22-292)	(93-292) -0.229 (GRAVY score) min (-2.711) and max (1.800) (22-292) -0.348 (GRAVY score) min (-2.711) and max (1.800)	4.35 (93-292) 4.57 (22-292)
α-helix Linker	875-1070 (195)	293-357 (64)	7.56		2.4		11.03
β-barrel	1070-1943 (870)	357-647 (290)	31.92		-12.8		5.00
Total protein	1-1943 (1943)	1-647 (647)	70.4	85	-25.65	-0.412 (GRAVY score) min(-2.767), max (2.367)	4.59

Table 5.2.1: Basic properties of the AaaA protein. Information from (Luckett *et al* 2012; *Pseudomonas* genome database). ProteinCalculator (http://protcalc.sourceforge.net) was used to predict size, charge and isoelectric point). Min and max hydrophobicity Kyte-Doolittle values were predicted using the ExPEASy online tool (https://web.expasy.org/cgi-bin/protscale/protscale.pl?1)window set at 9. The GRAVY value is calculated by adding the hydropathy value for each residue and dividing by the length of the sequence (Kyte and Doolittle 1982).

5.2.1 Truncating AaaA for purification, structural analysis and inhibitor screening: version 1

5.2.1.1 Production of truncated AaaA

The design and construction for the first truncated AaaA (AaaAt1) was generated by Dr Esteban Paredes Osses (thesis, 2014). The section of *aaaA* selected to be placed in *pET21a (+)* began at the start of the ORF and ended at nucleotide 1011 (codon TTG), residue 337 (leucine). As such, the signal peptide remained intact, allowing passage through the IM by interaction with the Sec complex and the β-barrel was removed with the additional removal of part of an α-linker at the C-terminus of the passenger domain. Figure 5.2.1 shows in detail the cloning process and how the truncation affected the protein structure.

The enzymes NdeI and EcoRI were included in the primers SV-fwd and SV-rev respectively. These are shown in Figure 5.2.1. NdeI was chosen as a restriction enzyme due to the inclusion of the start codon ATG in its sequence. The GTG start of *aaaA* was replaced by this to keep the protein sequence in frame with the *pET21a (+)* promoter and ribosomal binding site (RBS). A stop codon TGA was

added to the reverse primer before the EcoR1 cutting site to prevent unwanted read through. A full length version of *aaaA* was also cloned (Darch 2013) with the same restriction sites to be used as a control alongside empty *pET21a (+).* The plasmids were transformed into *E. coli* BL21 (DE3) cells for protein production.

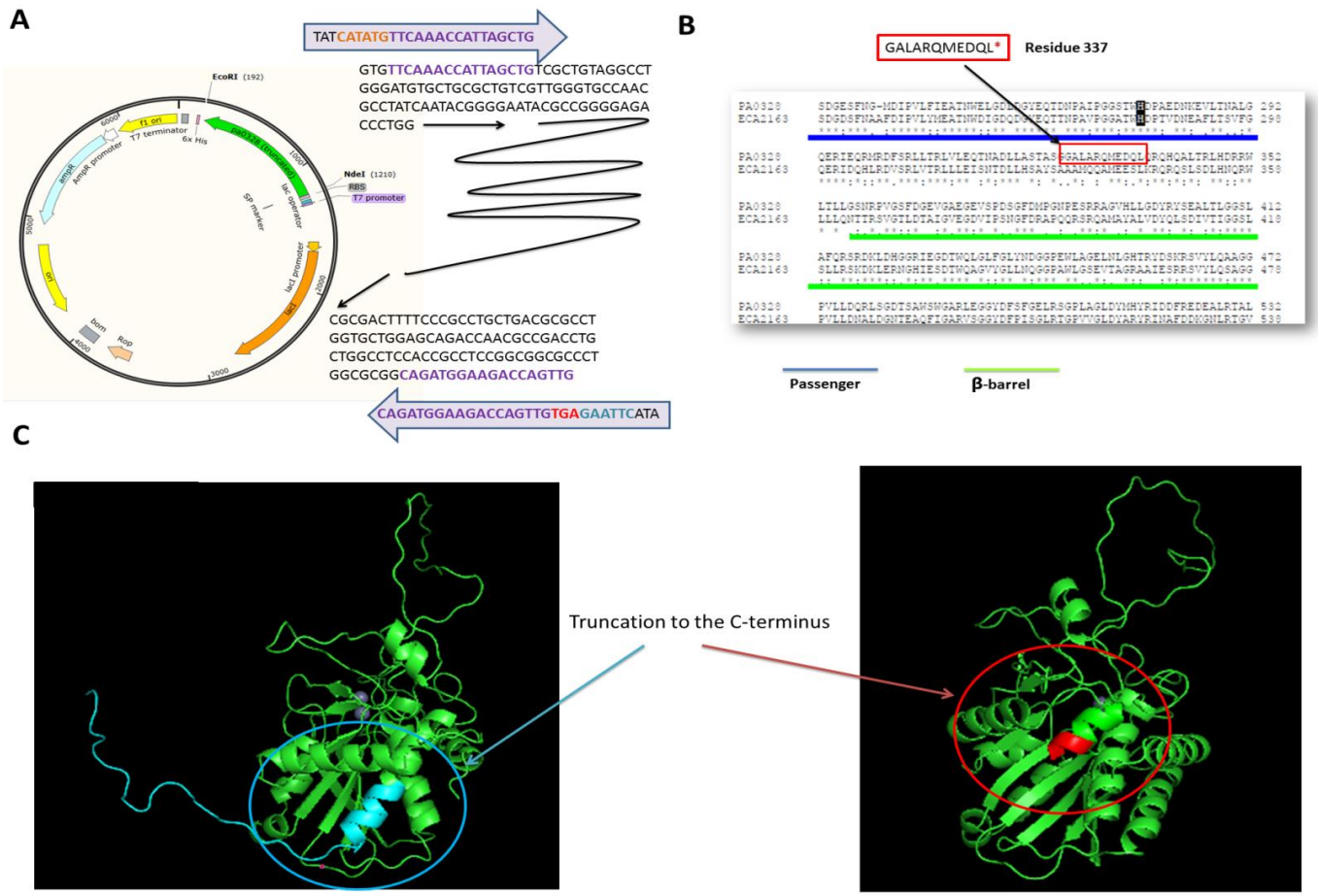


Figure 5.2.1: Truncation of AaaA to facilitate protein purification. A) Cloning details of AaaAt1. The *pET21a (+)* plasmid (generated using Snapgene viewer) is shown on the left with the green arrow representing *aaaA.* Purple arrows indicate primers, the reverse primer shown 3'-5' for better illustration purposes. Purple font indicates homologous binding nucleotides, orange font indicates an NdeI recognition site, cyan font indicates an EcoRI recognition site, and red font indicates an introduced stop codon. The black arrows and squiggly line represent the nucleotides of the *aaaA* ORF between cloning sites. B) Site of truncation in protein sequence (sequence picture adapted from Darch 2013). The final L in the red box is the last residue included in this truncation of *aaaA*, the red asterisk represents the introduced stop codon. C) Predicted truncation changes to the protein structure (pictures generated in Pymol) before and after residue removal. Cyan highlights the residues which were removed and red shows the last residues that were included in the truncation (i.e. just before the cut site) for clarity of comparison.

AaaAt1 was produced by growing the *E. coli* BL21 (DE3) *pET21a::aaaAt1* cells at 37°C until exponential phase was reached (OD_{600} 0.4-0.6) with subsequent induction using 1 mM IPTG for 1.5 hours at 37°C. The induced cells were harvested and normalised to an OD_{600} of 1.0 before washing and resuspending in PBS. For a whole cell protein sample, the media was aspirated and cell pellet suspended in 200 µl 1x SDS loading buffer. Of this, 7 µl was loaded onto an SDS-PAGE gel for visualisation (Figure 5.2.2). The same protocol was followed for immunoblotting analysis with the addition of protein transferral to a nitrocellulose membrane and incubation of this membrane with AaaA specific polyclonal antisera followed by detection using α-rabbit-HRP (Chapter 2; Luckett *et al* 2012). The primary antibody was diluted 2x more (1:2000 rather than 1:1000) than in previously conducted assays (Luckett *et al* 2012) as this concentration was sufficient for the conditions used in these experiments. Unless stated otherwise, this concentration was used in all the following immunoblotting assays in this chapter. Instead of the 7 µl per well used for the SDS-PAGE analysis, 5 µl were loaded for the immunoblotting due to the greater sensitivity of this technique. Following standardisation of the bacterial sample to OD_{600} 1.0, 3 dilutions were made with fresh media so that 3 separate cell densities could be tested (OD_{600} 0.5, 0.2 and 0.1) by immunoblot. This enabled an assessment of the assay sensitivity for the different variants of AaaA: truncated and full-length.

High levels of AaaAt1 were observed by immunoblotting at a slightly higher than expected (Table 5.2.2) molecular weight of approximately 50 kDa. To determine whether protease activity was retained by AaaAt1, the L-arginine-p-nitroanilide activity assay was employed.

	Nucleotides	Residues	Predicted size (kDa)	Size by blotting	Predicted charge pH7	Kyte-Doolittle hydrophobicity value	Isoelectric point (pI) predicted
AaaAt1	1-1011 (1011)	1-337 (337)	36.05	50 kDa	-16.4	-0.256 (GRAVY score) min (-2.711) and max(2.367)	4.70
AaaAt2	67-1047 (980)	22-349 (327)	35.48	50 kDa	-15.9	-0.421 (GRAVY score) min (-2.767) and max (1.800)	4.81
AaaAt3	1-1047 (1047)	1-349 (349)	37.53	50 kDa	-14.9	-0.307 (GRAVY score) min (-2.767) and max (2.367)	4.86

Table 5.2.2: Basic properties of the truncated versions of AaaA protein. ProteinCalculator (http://protcalc.sourceforge.net) was used to predict size, charge and isoelectric point). Min and max hydrophobicity Kyte-Doolittle values predicted using the ExPEASy online tool (https://web.expasy.org/cgi-bin/protscale/protscale.pl?1)window set at 9. The GRAVY value is calculated by adding the hydropathy value for each residue and dividing by the length of the sequence (Kyte and Doolittle 1982).

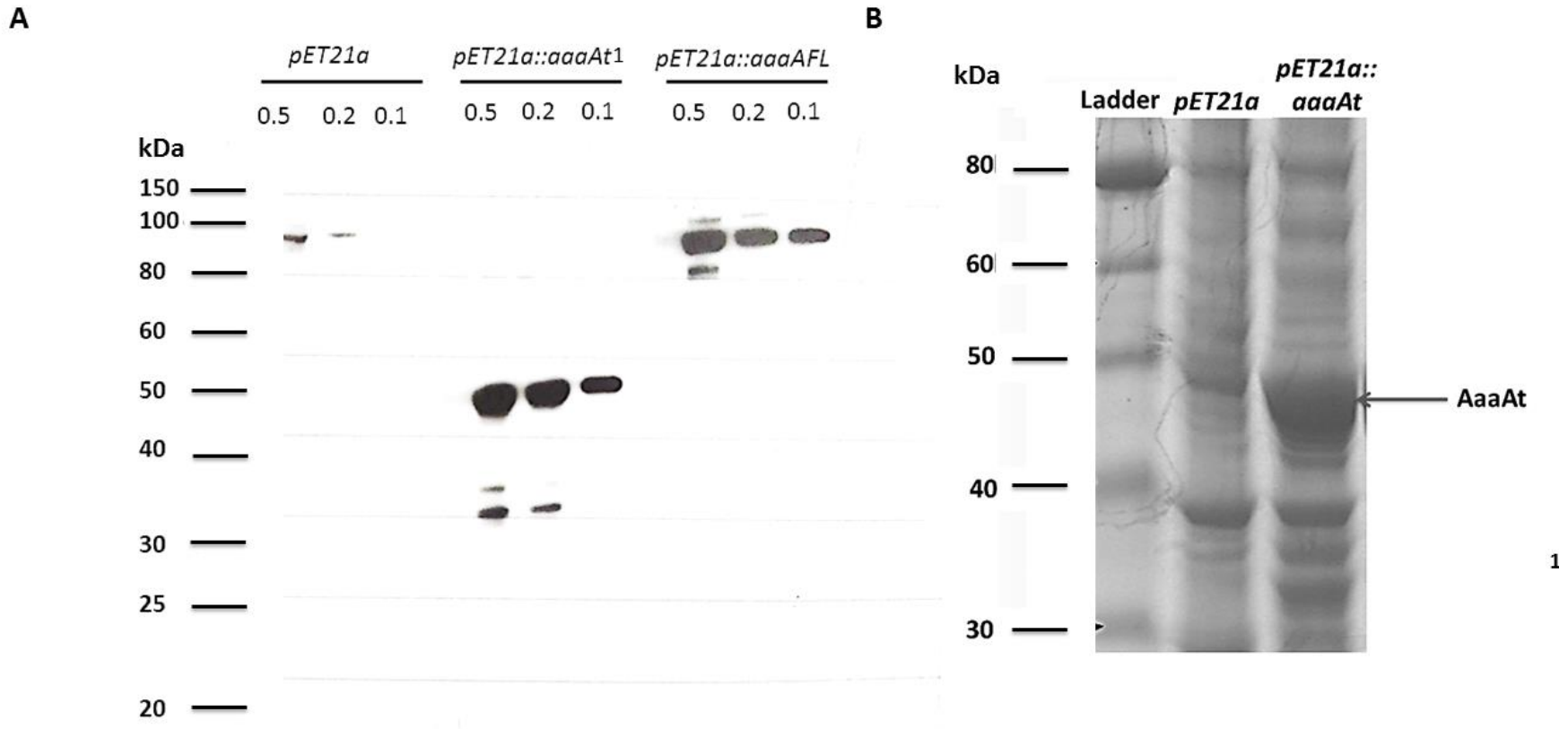


Figure 5.2.2: AaaAt1 is overproduced at the slightly higher than expected size of 50 kDa. Left (A): Immunoblotting showing the detection of AaaAt1 and AaaAFL from a whole cell (WC) culture (*E. coli* BL21 *pET21a; E. coli* BL21 *pET21a::aaaAt1*; *E. coli* BL21 *pET21::aaaAFL*). From the standardised OD $_{600}$ 1.0 sample, 3 dilutions were tested (OD $_{600}$ 0.5, 0.2 and 0.1). Specific polyclonal antisera (α-rabbit-AaaA) was used at a concentration of 1:2000 and the secondary antibody (α-rabbit-HRP) was used at a concentration of 1:2000. The size of AaaAt1 was just under the size predicted by the sequence (50kDa). Right (B): SDS-PAGE gel showing the overexpression of AaaAt1 from the *pET21a* vector.

5.2.1.2 AaaAt1 was active

The L-arginine P-nitroanilide activity assay (Chapters 2 & 4) was used to determine whether a detectable proportion of AaaA had remained intact, folded correctly, and retained its function after production in *E. coli* BL21 (DE3).

The BL21 cells containing *pET21a::aaaAt1* were grown at 37°C overnight in LB broth and diluted 1:10 in fresh media the following day. Once exponential phase was reached (OD_{600} 0.4-0.6), AaaAt1 production was induced using 1 mM IPTG at 37°C for 1.5 hours.

The truncated form of AaaA showed less activity than the full length version (Figure 5.2.3). It was hypothesised that the reduction in activity was due to the formation of inclusion bodies. It is also being expressed in the periplasm rather than the cell surface and so less exposure to the substrate could be occurring. This influenced the purification strategy choice which is shown in the following section.

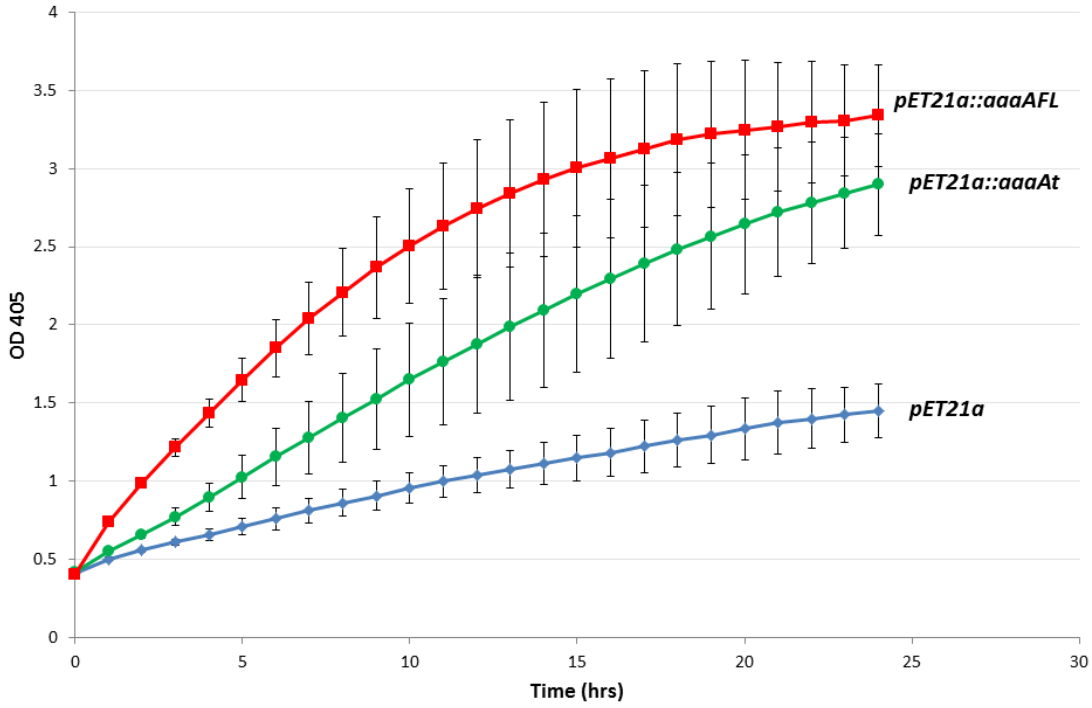


Figure 5.2.3*: AaaAt1 produced from E. coli* BL21 *pET21a::aaaAt1* was less active than full length (FL) AaaA. Bacteria producing AaaAFL (*E. coli* BL21 (DE3) *pET21a::aaaAFL*), AaaAt1 (*E. coli* BL21 (DE3) *pET21a::aaaAt1*), or containing the empty plasmid vector (*E. coli* BL21 (DE3) *pET21a*) were grown to exponential phase, induced for 1.5 hours with 1 mM IPTG and incubated with the L-arginine-p-nitroanilide substrate. The resultant change in OD_{405} is plotted over time of incubation at 37°C and represents the activity of AaaA. During this time the bacteria are not able to grow or divide. Blue diamonds= *pET21a* vector, red squares = *pET21a* ::*aaaAFL*, green circles = *pET21a* ::*aaaAt1*. Error bars show the standard deviation between two separate experiments (X6 technical, X2 biological) replicates.

5.2.1.3 Although truncated AaaA is insoluble, it can be semi-purified and solubilised in an active form

The reduced activity of AaaAt1 prompted an investigation of its accessibility to the p-nitroanilide substrate and tendency to form insoluble inclusion bodies when not translocated to the bacterial cell surface due to the absence of the β-barrel. To this end, a culture of *E. coli* BL21 *pET21a::aaaAt1* was grown until exponential phase, lysed by sonication and separated into pellet and supernatant fractions. AaaAt1 was found exclusively in the pellet fraction, indicating it was insoluble and likely forming inclusion bodies that presumably reflects a sub-optimal conformation that would correspond with the observed reduction of activity (Figure 5.2.4). Taking advantage of this, the insolubility of AaaAt1 was used as the basis for a purification process which involved sequential washing of the pellet fraction to remove the other proteins native to *E. coli*. The first attempts at this method were unsuccessful due to the insufficient lysis of large culture volumes by sonication and therefore an alternative lysis method was used. Lysis by French Press proved to be successful and following this, 3 washes in PBS were sufficient

to remove the majority of other proteins detectable by Coomassie staining SDS-PAGE (Figure 5.2.4). A protease inhibitor (0.1 mM PMSF) was added to the lysate directly after French Pressing to reduce protein degradation.

To solubilise the semi-purified protein, aliquots (1 ml), were incubated for 2 hours with a range of substances at room temperature and 4°C. These included the detergent Tween (20%), the ion chelator EDTA (0.5%), NaCl (1 M), and the chaotropic agents NaDeoxycholate (10%) and urea (8 M). Of these, only the 8 M urea was able to solubilise AaaAt1 (Figure 5.2.4, for optimisation data see dissertation: Ms Rupa Rai 2014), the yield being slightly greater when the incubation was at 4°C. Lower concentrations of urea were not found to be as effective (1-6 M). To reduce degradation of AaaAt1 during the process of washing and resolubilisation, a higher concentration of PMSF (1 mM) was found to be effective.

To restore the secondary structure and catalytic capability of the solubilised AaaAt1, dialysis with Tris 10 mM pH 7.4 at 4°C was undertaken for 24 hours. This was effective in removing the urea and restoring activity (Figure 5.2.4). Storage of AaaAt1 + 8 M urea proved to be a good method for maintaining protein stability. When needed, this preparation was dialysed.

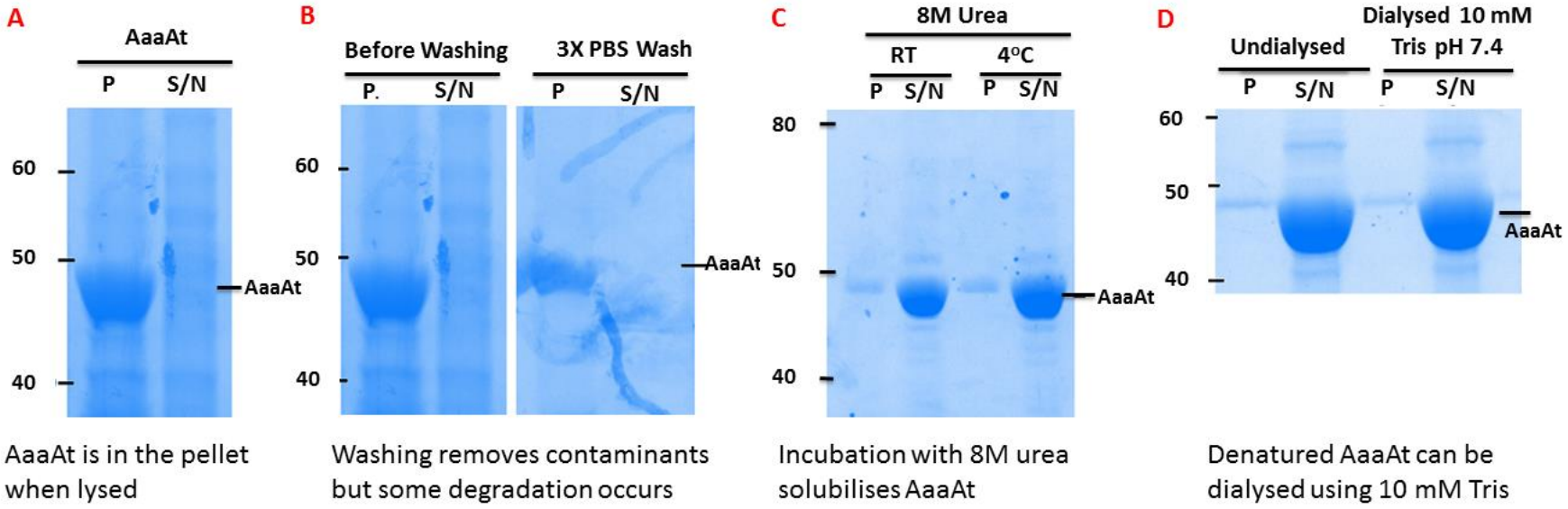


Figure 5.2.4: Process of AaaAt1 purification. A culture volume of 50 µl of *E. coli* BL21 (DE3) *pET21a::aaaAt1* was grown to exponential, washed 3x in PBS and lysed using the French Pressure Cell. P= pellet, S =S/N, 7 µl of sample was loaded per well. A= Lysis by French Press shows AaaAt1 to be in the pellet fraction. B=Washing with PBS is sufficient for removing the majority of other proteins but a higher 1 mM rather than 0.1 mM concentration of PMSF is required to slow degradation. C= 8 M urea is able to solubilise AaaAt1 and the yield is slightly higher at 4°C possibly due to less degradation. D= Dialysis with 10 mM Tris does not affect the yield of protein and solubility is retained.

5.2.1.4 Semi-pure AaaAt1 is active and can be inhibited by ion chelators

Further to achieving solubilisation of AaaAt1, the activity was tested to determine if the protein was folding correctly and to see whether the level of activity was suitable for cell-free inhibitor assays. Two ion chelators were chosen as representative non-specific inhibitors due to the predicted incorporation of two zinc ions in the catalytic pocket.

Dialysed protein was mixed with L-arginine P-nitroanilide in a 1:1 ratio. For consistency, the same batch of protein is shown in the figure presented here. Directly prior to the combination of substrate and protein, the inhibitor was added to the protein sample at the concentration of 0.1 mM, 0.5 mM and 1 mM. The assay continued for 24 hours at 37°C.

As Figure 5.2.5 shows, dialysed AaaAt1 was highly active and could be inhibited by the ion chelators EDTA and phenanthroline. Phenanthroline is a strong zinc chelator, but its action is not exclusive to this metal ion, additionally chelating iron and other divalent metals (2+). To determine if zinc is indeed the ion required by AaaA for activity, a further experimental step of selectively adding zinc back to the media would be required (Cooper *et al* 2009). This was promising for the use of AaaAt1 to test the bank of specific inhibitors available (Roche). The effective inhibition by the ion chelators supports the reliance AaaA has on incorporated zinc ions for catalytic function.

The dialysed protein showed more activity than the equivalent amount of unextracted AaaAt1, although the activity of the *E. coli* BL21 *pET21a::aaaAt1* was a bit lower than in the previous assay (Figure 5.2.3). The reason for this discrepancy is unknown but would be consistent with slight differences in the cell state during induction or an increase in waiting time as the protein sample was prepared.

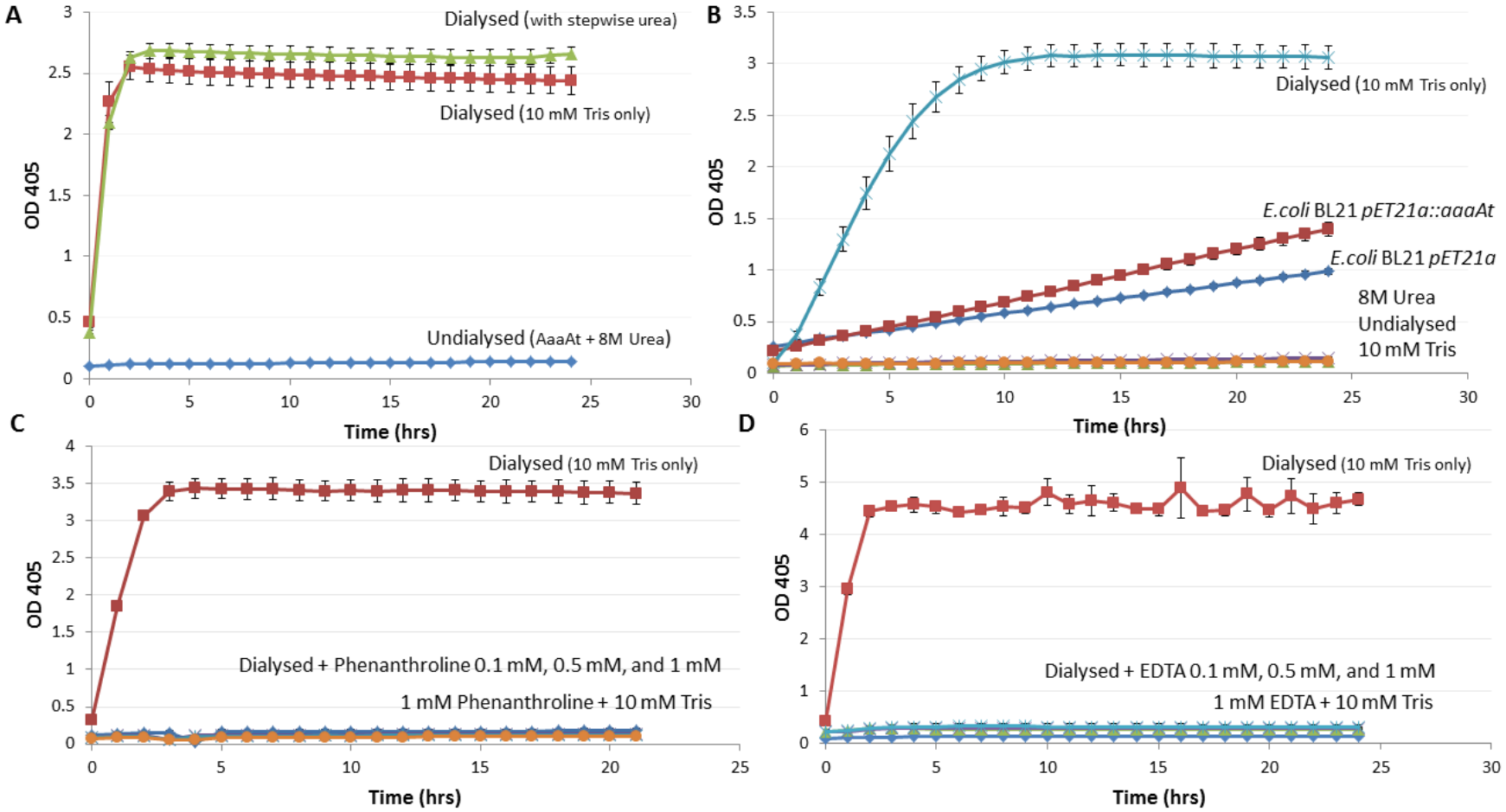


Figure 5.2.5: Dialysed AaaAt1 is active and sensitive to inhibition by ion chelators. Each sample was incubated with L-arginine-p-nitroanilide and the resultant change in OD_{405} is plotted over time of incubation at 37°C, representing the activity of AaaA. The same batch of purified AaaAt1 was used in these assays. A) Dialysed AaaAt1 protein conducted by either by a gradual urea reduction in the buffer or by using a Tris 10 mM only buffer are compared with the undialysed control. B) Dialysed AaaAt1 protein is compared to cell-attached AaaAt1 (*E. coli* BL21 (DE3) *pET21a::aaaAt1*), empty vector (*E. coli* BL21 (DE3) *pET21a*), undialysed soluble AaaAt1 and buffer only controls. C) Dialysed AaaAt1 is compared with dialysed AaaAt1 that was incubated with 0.1, 0.5, or 1 mM phenanthroline. D) Dialysed AaaAt1 is compared with dialysed AaaAt1 that was incubated with 0.1, 0.5, or 1 mM EDTA. Error bars represent the standard deviation over 3 repeats using the same batch of protein.

5.2.1.5 Refolded AaaAt1 is not compatible with further purification by gel filtration that is required for crystallisation

It was hoped that the solubilised AaaAt1 would be suitable for crystallisation and structural analysis including inhibitor docking. Gel filtration chromatography was performed by Dr Simon Caulton to further purify the solution of AaaAt1 and to confirm its size. Unfortunately, AaaAt1 was eluted into the void volume (Figure 5.2.6). This was likely due to it aggregating when the solution was concentrated for the procedure. There was also a peak corresponding to the fraction associated with a less than 10 kDa protein size which could indicate degradation of AaaAt1 or sample impurities. To attempt to circumvent this problem, a dialysis buffer of 50 mM Tris pH 7.5, 500 mM NaCl and 10 % glycerol was used in the hope that this would improve the solubility of the protein at higher concentrations (data not shown). This was unsuccessful and it was concluded that AaaAt1 was too hydrophobic to withstand the concentration process necessary for further purification and crystallisation. This prompted the design of a second form of truncated AaaA, AaaAt2.

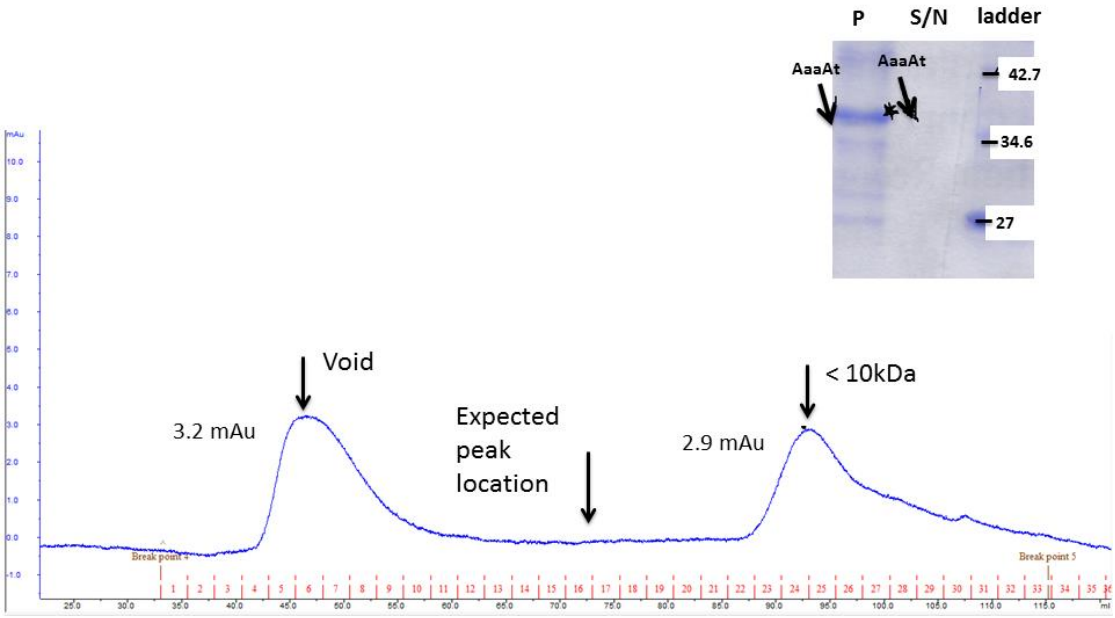


Figure 5.2.6: Gel filtration chromatography shows AaaAt1 to be aggregating (data kindly provided by Dr Simon Caulton). Peaks are observed at the locations associated with the void and <10 kDa fractions. No peak is observed at the expected location. The SDS-PAGE at the top right-hand corner shows that AaaAt1 shows a band of the correct size for AaaAt1 in the precipitate (P) but not the supernatant (S/N).

5.2.1.6 Word of thanks

The work with the first version of AaaAt1 was achieved with the help of MSc student Ms Rupa Rai. For more details on the optimisation processes please see her dissertation (Rai 2014).

5.2.2 Production of a second truncated version of AaaA (AaaAt2) to improve solubility and ease of purification

Due to the issues with solubility experienced with AaaAt1, a second version was designed with the help of Dr Simon Caulton and was named AaaAt2. AaaAt2 differed from its predecessor by the exclusion of the signal peptide sequence. This would localise the translated protein sequence to the cytoplasm rather than the periplasm. The removal of the signal peptide would also ensure that when the cells were lysed, the folding would not be impeded by retention of the signal peptide sequence. Furthermore, the C-terminus of AaaAt2 was extended to prevent the exposure of hydrophobic residues (shown in Figure 5.2.7) in the hope that this would also increase the solubility, and also had a His-tag incorporated. The β-barrel was omitted from this construct to avoid OM insertion that might limit production levels and complicate purification strategies.

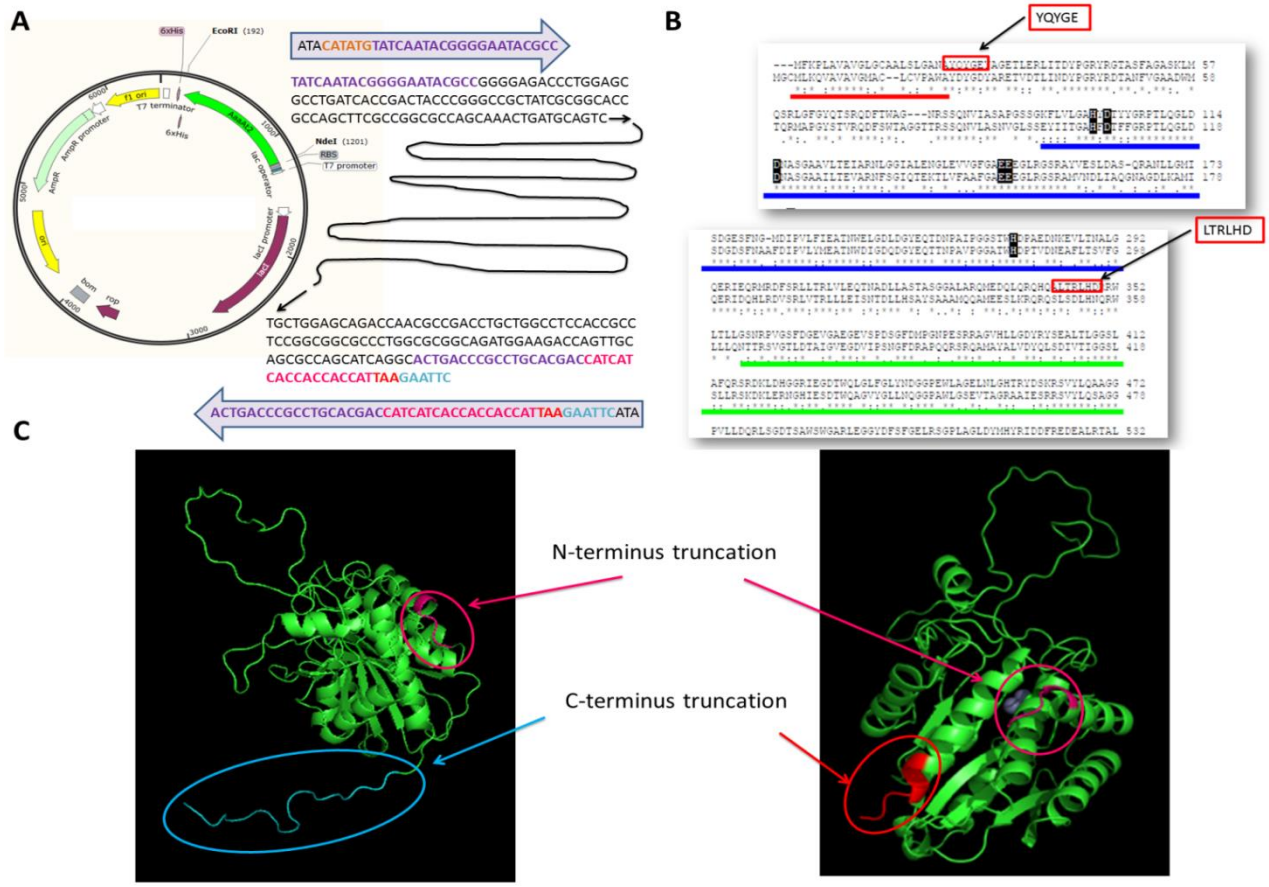


Figure 5.2.7: Truncation of AaaA to facilitate protein purification, version 2. A) Cloning details of AaaAt2. *The pET21a (+)* plasmid (generated using Snapgene viewer) is shown on the left with the green arrow representing *aaaA.* Purple arrows indicate primers, the reverse primer shown 3'-5' for better illustration purposes. Purple font indicates homologous binding nucleotides, orange font indicates an NdeI recognition site, cyan font indicates an EcoRI recognition site, pink font indicates the His-tag residues and red font indicates an introduced stop codon. The black arrows and squiggly line represent the nucleotides of the *aaaA* ORF between cloning sites. B) Site of truncation in protein sequence (sequence picture adapted from Darch 2013). The first Y in the top red box is the first residue and the final D in the bottom red box is the last residue included in this truncation of *aaaA*. The introduced His-tag and subsequent stop codon is not shown. C) Showing how the truncation changes the protein structure (pictures generated in Pymol) before and after residue removal. Cyan highlights the residues which were removed; red shows the last residues that were included in the truncation (i.e. just before the cut site) for clarity of comparison and pink shows the first N-terminus residues that were included in the truncation. The angles are adjusted to help bring to focus the slightly different shapes of the protein in the before and after truncation states.

5.2.2.1 Engineering AaaAt2, a cytoplasmic derivative of AaaA with an extended passenger domain and C-terminal His-tag

Figure 5.2.8 shows the cloning strategy used to create *pET21a::aaaAt2*. The primers 5'-ATACATATGTATCAATACGGGGAATACGCC-3' and 5'-TATGAATTCTTAATGGTGGTGGTGATGATGGTCGTGCAGGCGGGTCAGT-3', containing the NdeI and EcoR1 restriction sites respectively, were used to amplify *aaaAt2* from extracted genomic template DNA. The resulting PCR product was inserted into a T-tailed vector, pGemT-easy. This additional step ensured that completed digestion was identifiable for the ends of the insert. Digestion with the appropriate enzymes was conducted on both *pET21a::aaaAFL* and *pGemT-easy::aaaAt2.* Specific digestion conditions were optimised to ensure the digestion by NdeI was sufficient (1 hour 37°C NdeI only, followed by 2 hours with the addition of EcoRI and more NdeI). The linearized vector was ligated with the cut fragment of *aaaAt2* and transformed into DH5α cells. Following transformation, the cells were grown at 30°C rather than 37°C due to the killing of viable cells at a higher temperature. The harvested clones were screened by restriction digest and the sequence analysed before the *pET21a::aaaAt2* construct was transferred to the *E. coli* BL21 (DE3) expression host.

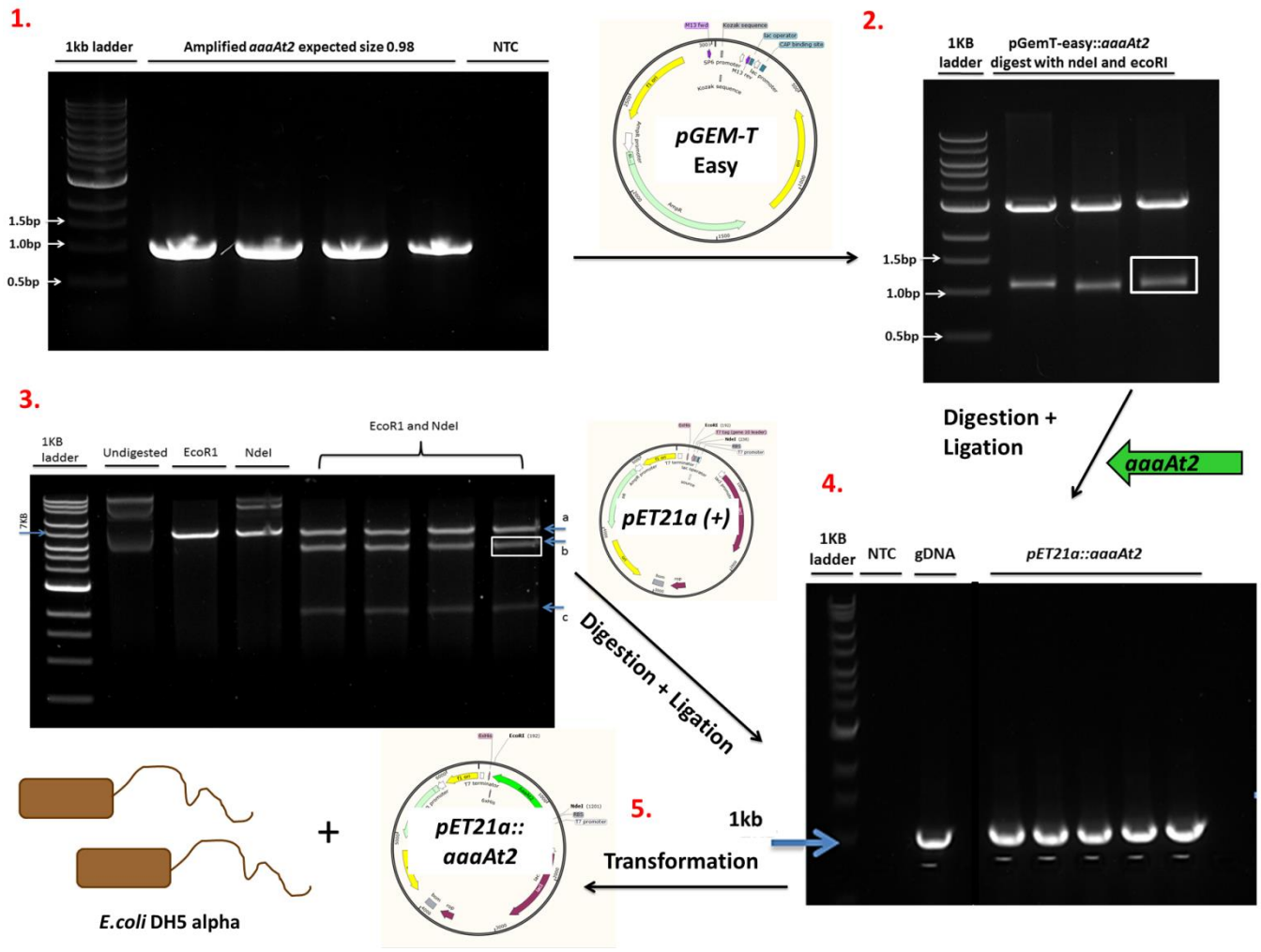


Figure 5.2.8: Cloning *aaaAt2*. (1) The portion of sequence desired for this truncation was amplified by PCR (gel 1), purified, poly adenylated and ligated into pGEM-T Easy, a T-tailed vector. (2) The ligated vector and insert were transformed into DH5 alpha, colonies screened by restriction digestion and sequenced. The selected clone was digested and the insert extracted from the gel for ligation with digested *pET21a (+)* (gels 3 and 4). Due to some digestion issues with the vector and NdeI, *pET21a (+)* with the full length AaaA insert was used instead of the empty vector (3) to ensure the digestion had been successful. (5) After ligation, the plasmid was transformed into DH5alpha cells (growth at 30°C), the colonies screened by PCR and confirmed by sequence analysis (gel 4).

5.2.2.2 AaaAt2 is active, insoluble and requires particular conditions for suitable expression

The growth of *E. coli* BL21 (DE3) expressing *aaaAt2* was impaired at 37°C with induction using 1 mM IPTG for 1.5 hours. Consequentially the yield of active protein was comparable to the uninduced control. The conditions were thus modified to increase the amount of protein produced (Figure 5.2.11). The cells were grown at 37°C until late exponential. They were subsequently induced with 0.3 mM IPTG and placed in a 22°C incubator overnight. The cells were then harvested. To assess the solubility of AaaAt2, a whole cell preparation was compared with a lysed (sonicated) culture which was separated into pellet and soluble fractions by centrifugation. The fractions were viewed on a SDS-PAGE gel and by immunoblotting with α-AaaA and α-His antibodies (Figure 5.2.9).

From this analysis it could be seen that AaaAt2 was insoluble and not compatible with strong induction in *E. coli* BL21 cells. It also appeared to degrade at a faster rate than AaaAt1. To observe the enzyme activity of AaaAt2, an activity assay was performed with whole, unlysed cells (data not shown). No activity was detected and the activity assay was modified to include a cell lysis step subsequent to normalisation and prior to mixing with the substrate (Figure 5.2.10). Activity was observed in the lysed cells. The localisation of AaaAt2 to the cytoplasm rather than the periplasm likely causes the inactivity observed in unlysed cells.

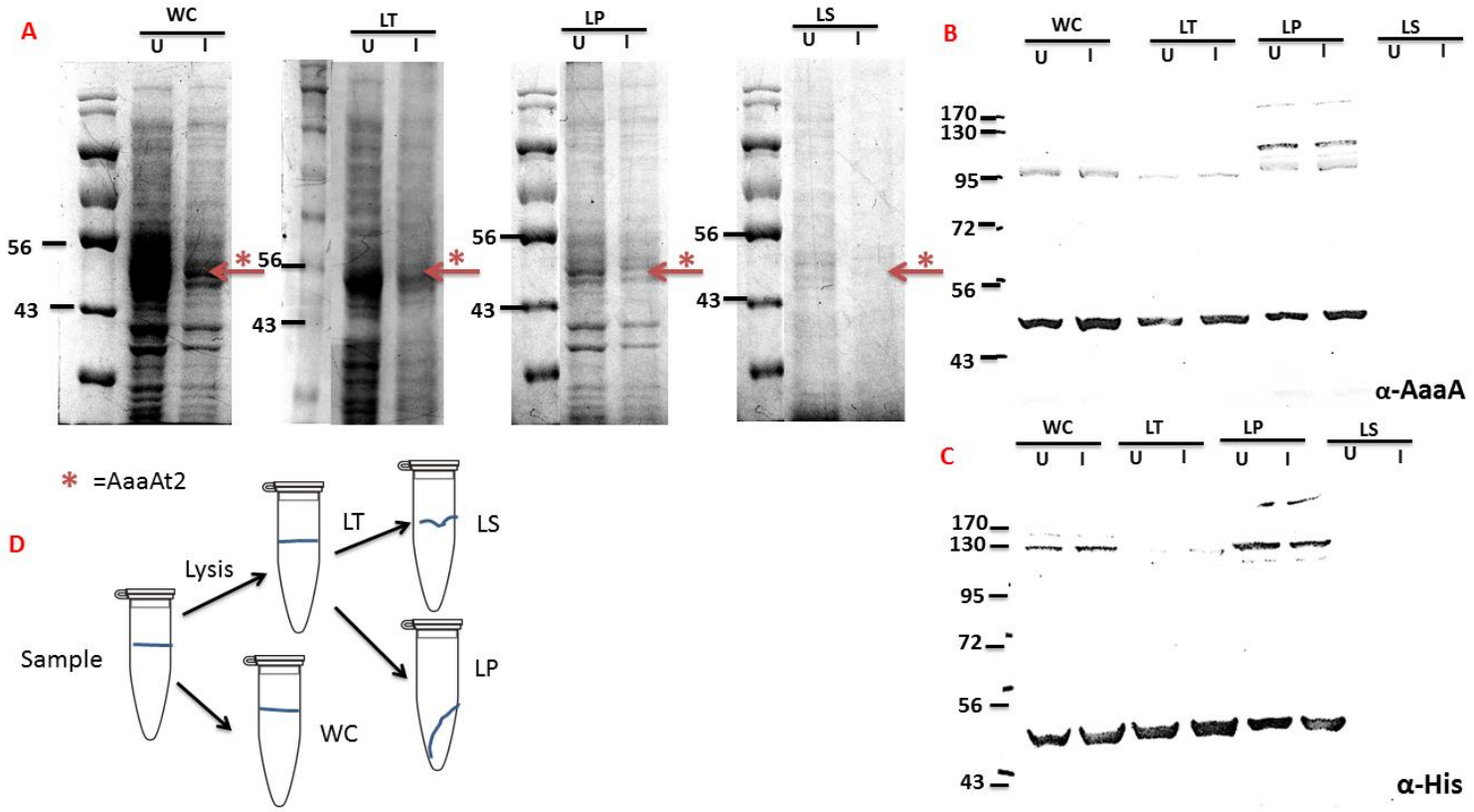


Figure 5.2.9: AaaAt2 is insoluble and overproduction kills the producing cells. A and D) SDS-PAGE gels showing the relative quantities of AaaAt2 in each cell fraction. A culture of *E. coli* BL21 *pET21a::aaaAt2* was grown until late exponential in LB medium and induced with 0.3 mM IPTG overnight at 22°C (the non-induced was incubated at 22°C but the IPTG was not added). The culture was normalised to OD $_{600}$ 1.0 and divided into 1 ml aliquots. The WC condition involved washing the cells in PBS and suspending the pellet in SDS loading buffer before boiling and adding to the gel. The LT condition was washed as the WC condition but resuspended in lysis buffer which was a mix of DNase, RNase, PMSF and lysozyme buffered by Tris 10 mM pH 7.4 (materials and methods). The cells were sonicated for 2 minutes at 15 amps. The lysed cells were TCA precipitated, suspended in SDS-PAGE buffer, boiled and loaded onto the gel. To produce the LP and lysed supernatant LS fractions the lysed cells were separated into pellet and supernatant fractions by spinning. The supernatant was TCA precipitated and then both conditions were suspended in SDS loading buffer, boiled and added to the SDS-PAGE gel. Ten microliters were added to the gel. AaaAt2 was detected at roughly 50 kDa in the pellet samples. There appeared to be a loss of protein the more the samples were processed which suggests degradation. There is a thinner band corresponding to the size of AaaAt2 protein in the induced samples than the uninduced samples. No band of AaaAt2 size was detected in the soluble fraction. B) Immunoblotting with α-*aaaA* antibody. No band corresponding to the expected size of AaaAt2 was present in the soluble fraction. C) Immunoblotting with α-his antibody. No band corresponding to the expected size of AaaAt2 was present in the soluble fraction. Fischer's EZ-Run™ Prestained Rec Protein ladder (10-170kDa) was used as the marker. WC= whole cell; LT= lysed total; LP = lysed pellet; LS= lysed supernatant; NI= non induced; I = induced.

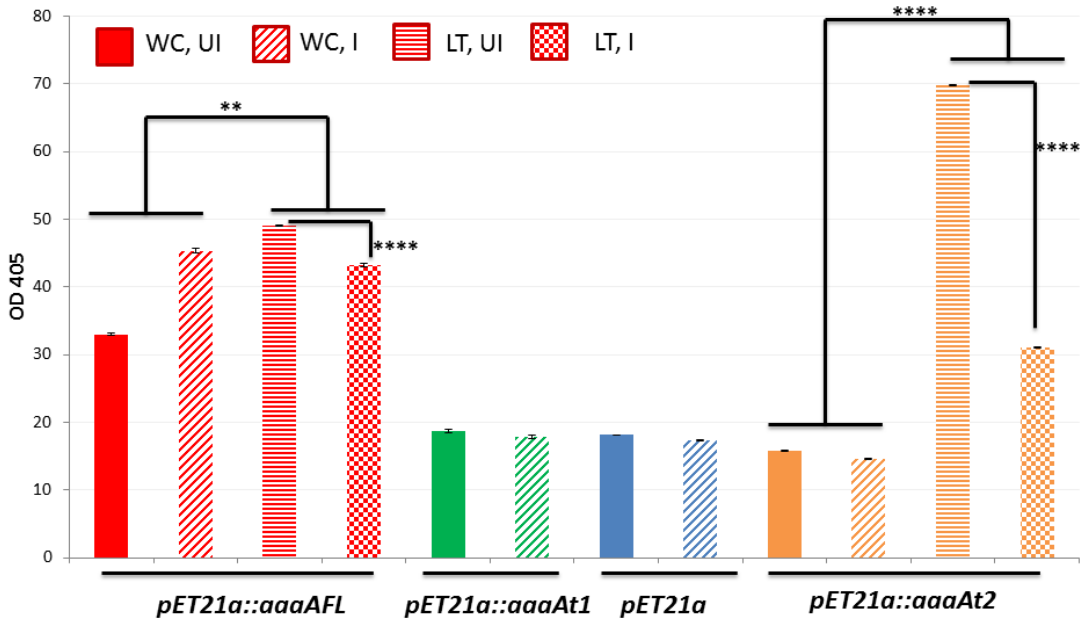


Figure 5.2.10: Lysis is necessary for activity of AaaAt2. *E. coli* BL21 with *pET21a*, *pET21a::aaaAFL*, *pET21a::aaaAt1* or *pET21a::aaaAt2,* was grown until exponential, induced with 1 mM IPTG added to the induced condition cultures and then incubated for 1.5 hours at 37°C before washing and resuspension in MMP, normalisation and lysis by sonication for the lysed conditions. The cells were then incubated with the AaaA substrate L-arginine-p-nitroanilide. The resultant change in OD_{405} was plotted over time of incubation at 37°C for 24 hours and the AUC calculated from these values. This represents the activity of AaaA over 24 hours. During this time, the bacteria are not able to grow or divide. Solid bars show the uninduced cells and striped bars the induced cells. Horizontal stripes show the lysed non induced cells and checked bars show the lysed induced cells. The experiment was repeated 3 X with 3 technical repeats per experiment, the error bars show the standard deviation between repeats. A t-test was performed between the indicated pairs. The symbol **** indicates a P value of <0.0001 and the symbol ** indicates a P value of <0.01.

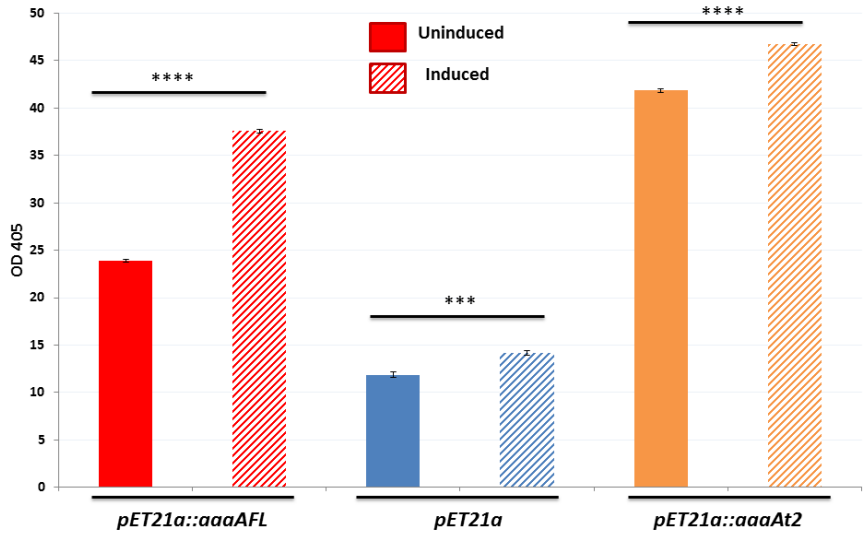


Figure 5.2.11: Induction is better at 22°C for AaaAt2. *E. coli* BL21 with *pET21a*, *pET21a::aaaAFL* or *pET21a::aaaAt2,* was grown until exponential, 0.3 mM IPTG added to the induced condition cultures and then grown overnight at 22°C before washing and resuspension in MMP, normalisation and lysis by sonication. The cells were then incubated with the AaaA substrate L-arginine-p-nitroanilide. The resultant change in OD_{405} was plotted over time of incubation at 37°C for 24 hours and the AUC calculated from these values. This represents the activity of AaaA over 24 hours. During this time, the bacteria are not able to grow or divide. Solid bars show the uninduced cells and striped bars the induced cells. The experiment was repeated 3 X with 3 technical repeats per experiment, the error bars show the standard deviation between repeats. Comparison by t-test was performed. The symbol **** indicates a P value of <0.0001 and the symbol *** indicates a P value of <0.001.

5.2.3 Engineering AaaAt3

The third strategy to generate truncated AaaA aimed to avoid the intracellular toxicity experienced with AaaAt2 by retaining the signal peptide and locating the protein to the periplasm. The extended C-terminus featured in the design of AaaAt2 was included to improve the probability that soluble protein could be produced, as was the His-tag. Figure 5.2.12 shows the design of AaaAt3.

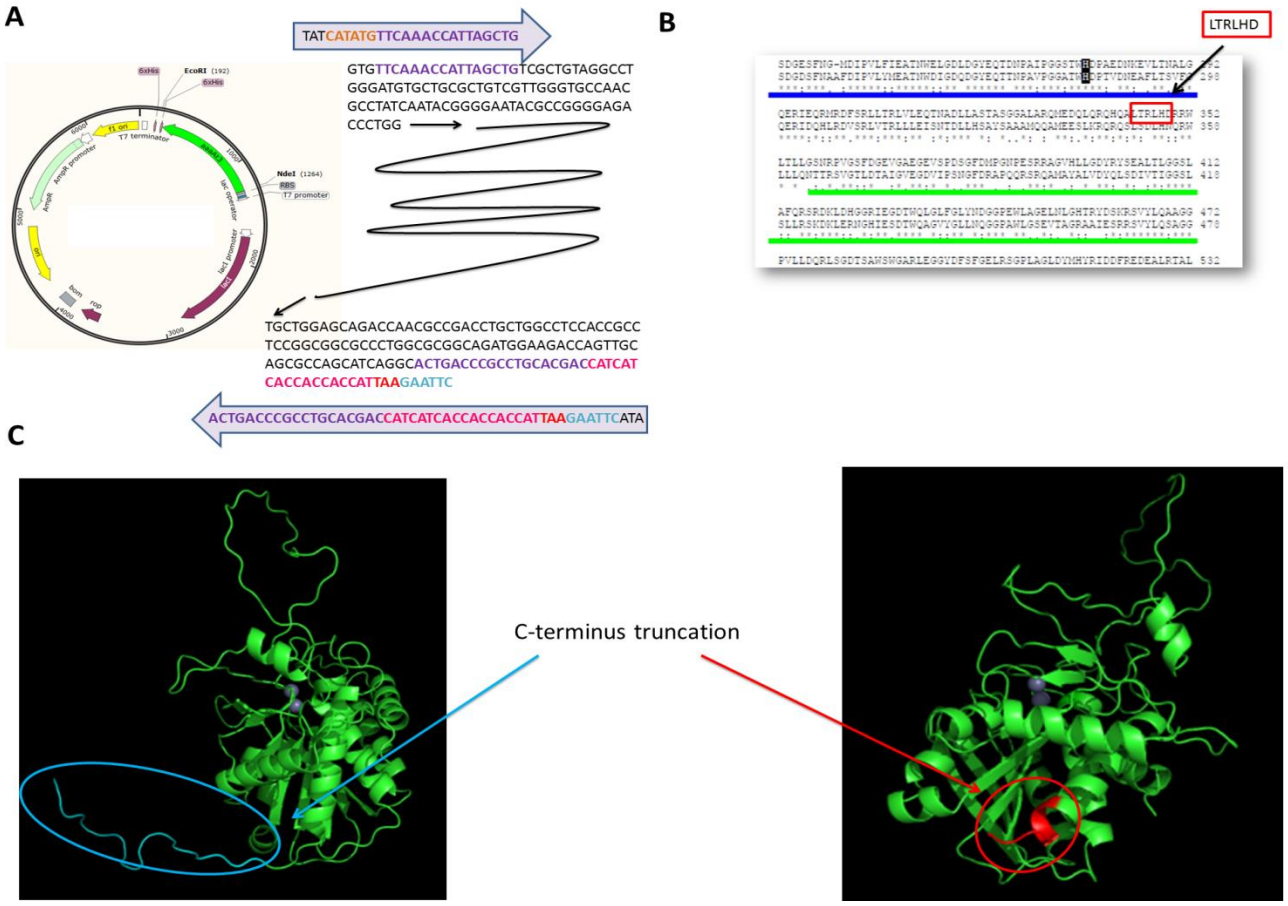


Figure 5.2.12: AaaAt3 engineering. A) Cloning details of AaaAt3. The *pET21a (+)* plasmid (generated using Snapgene viewer) is shown on the left with the green arrow representing *aaaA.* Purple arrows indicate primers, the reverse primer shown 3'-5' for better illustration purposes. Purple font indicates homologous binding nucleotides, orange font indicates an NdeI recognition site, cyan font indicates an EcoRI recognition site, pink font indicates the His-tag residues and red font indicates an introduced stop codon. The black arrows and squiggly line represent the nucleotides of the *aaaA* ORF between cloning sites. B) Site of truncation in protein sequence (sequence picture adapted from Darch 2013). The final D in the red box is the last residue included in this truncation of *aaaA*. The introduced His-tag and subsequent stop codon is not shown. C) Showing how the truncation changes the protein structure (pictures generated in Pymol) before and after residue removal. Cyan highlights the residues which were removed and red shows the last residues that were included in the truncation for clarity of comparison.

5.2.3.1 Designing and cloning the third version of AaaAt

The cloning strategy used for *pET21a::aaaAt3* is shown in Figure 5.2.13. The primers 5'-TATCATATGTTCAAACCATTAGCTGTCGCTG-3' and 5'-TATGAATTCTTAATGGTGGTGGTGATGATGGTCGTGCAGGCGGGTCAGT-3', containing the restriction sites NdeI and EcoRI respectively, were used to amplify *aaaAt3* from extracted genomic template DNA. The resulting PCR product was inserted into pGemT-easy. Digestion with the appropriate enzymes was conducted on both *pET21a::aaaAtFL* and *pGemT-easy::aaaAt3*. The linearized vector was ligated with the cut fragment *of aaaAt3* and transformed into DH5alpha cells. Following transformation, the cells were grown at 37°C and the harvested clones were screened by restriction digest and verified by sequence analysis before the *pET21a::aaaAt3* construct was transferred to the *E. coli BL21* (DE3) expression host.

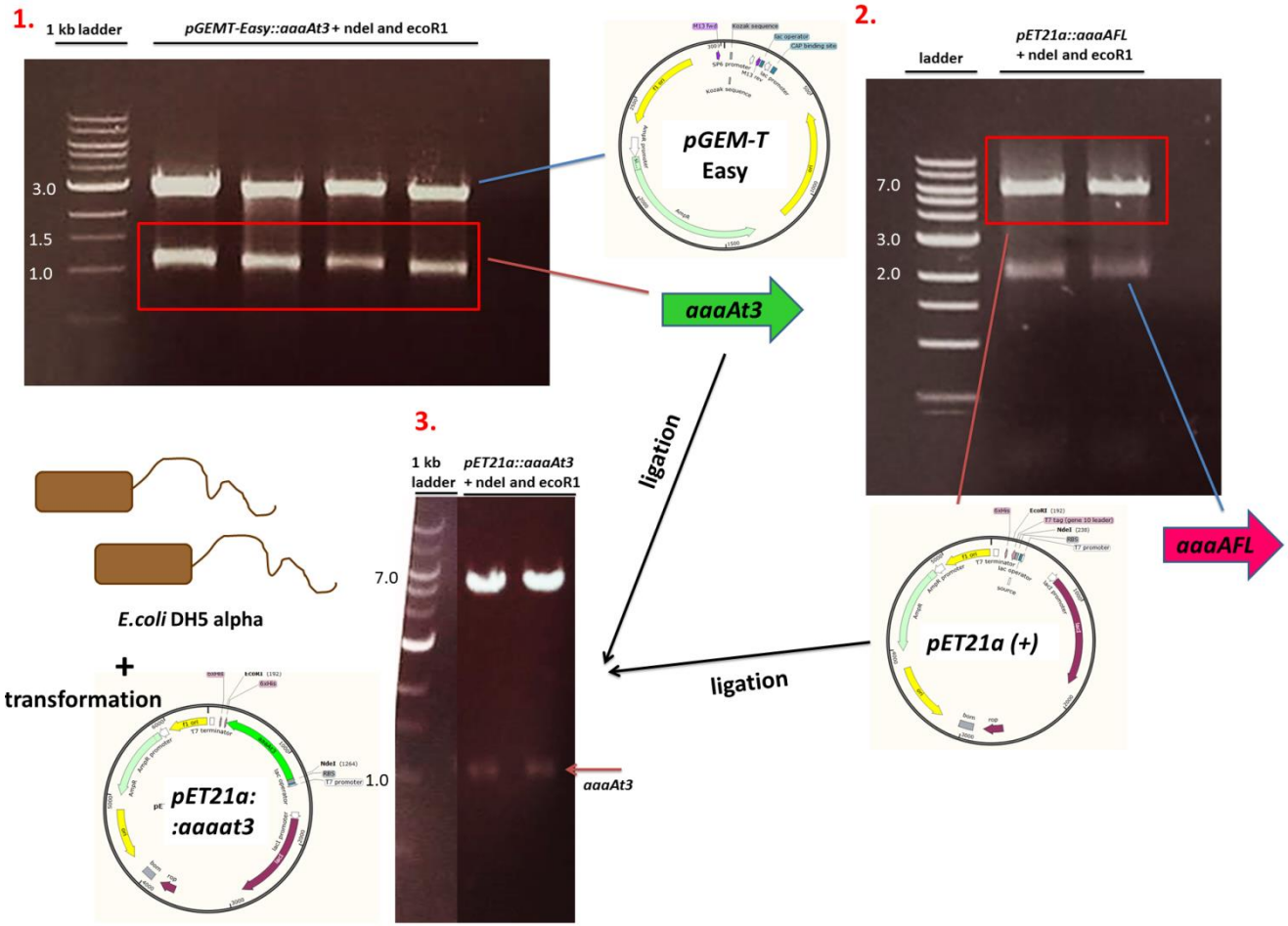


Figure 5.2.13: Cloning process of AaaAt3. (1) The portion of sequence desired for this truncation was amplified by PCR, purified, poly adenylated and ligated into pGEM-T Easy, a T-tailed vector. The ligated vector and insert were transformed into DH5α, colonies screened by restriction digestion and sequenced. The selected clone was digested (gel 1) and the insert extracted from the gel for ligation with digested *pET21a (+)* (gel 2). (2) Due to some digestion issues with the vector and NdeI, *pET21a (+)* with the full length AaaA insert was used instead of the empty vector to ensure the digestion had been successful. (3) After ligation, the plasmid was transformed into DH5alpha cells (growth at 30°C) the colonies screened by PCR, and sequence analysis performed (gel 3). Red lines show the part of the digested vector which was taken forward and blue lines show discarded DNA.

5.2.3.2 A proportion of AaaAt3 is soluble

The conditions used for the expression of *aaaAt2* were found to produce the best yield of AaaAt3 to date. The *E. coli* BL21 (DE3) cells did not show the growth impairment observed with AaaAt2, and notably more protein was produced with the addition of IPTG than the uninduced controls. The harvesting of the cells after induction and further steps including lysis in some samples was carried out in the same manner as for AaaAt2.

SDS-PAGE analysis to detect the relative amounts of protein produced and the solubility of AaaAt3, showed that no AaaAt3 was detected in the soluble fraction (Figure 5.2.14, A). However, further analysis by immunoblotting using α-AaaA and α-His antibodies revealed a small amount of soluble AaaAt3 (Figure 5.2.14, B and C).

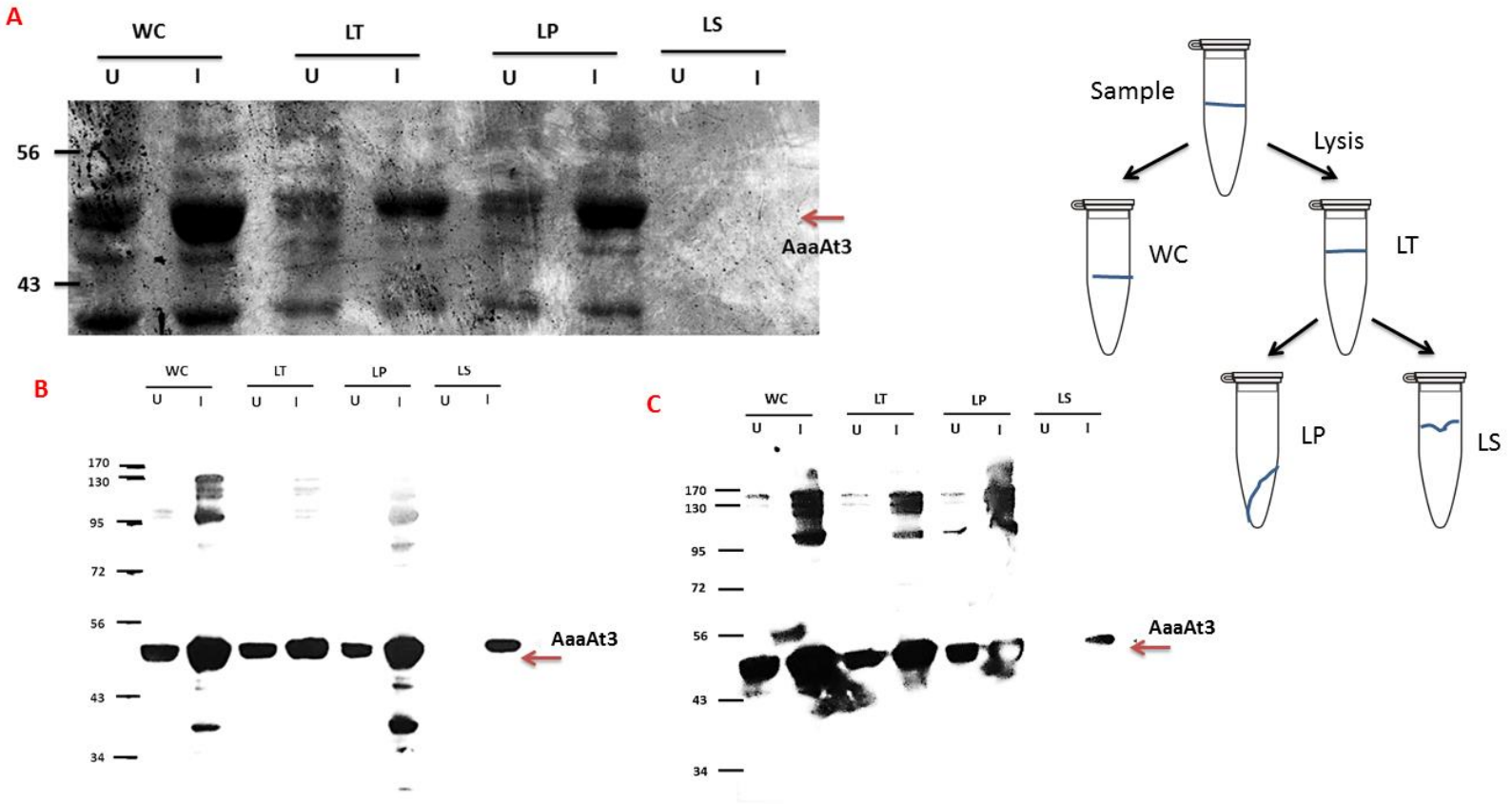


Figure 5.2.14: A small amount of AaaAt3 is soluble. A) SDS-PAGE gel showing the relative quantities of AaaAt3 in each cell fraction. A culture of *E. coli BL21 pET21a::aaaAt3* was grown until late exponential in LB medium and induced with 0.3 mM IPTG overnight at 22°C. The culture was normalised to OD_{600} 1.0 and divided into 1 ml aliquots. The WC condition involved washing the cells in PBS and suspending the pellet in SDS loading buffer before boiling and adding to the gel. The LT condition was washed as the WC condition but resuspended in lysis buffer which was a mix of DNase, RNase, PMSF and lysozyme buffered by Tris 10 mM pH 7.4 (materials and methods). The cells were sonicated for 2 minutes at 15 amps. The lysed cells were TCA precipitated, suspended in SDS-PAGE buffer, boiled and loaded onto the gel. To produce the LP and lysed supernatant LS fractions the lysed cells were separated into pellet and supernatant fractions by spinning. The supernatant was TCA precipitated and then both conditions were suspended in SDS loading buffer, boiled and added to the SDS-PAGE gel. Ten microliters were added to the gel. Bands corresponding to the expected size of AaaAt3 were detected at roughly 50 kDa in only the pellet fractions. B) Immunoblotting with α-AaaA antibody (1: 1000). Some bands corresponding to the expected size of AaaAt3 (induced) were present in the soluble fraction. C) Immunoblotting with α-his antibody. Some bands corresponding to the expected size of AaaAt3 were also present in the soluble fraction. The ladder used was Fischer's EZ-Run™ Prestained Rec Protein ladder (10-170 kDa). WC= whole cell; LT= lysed total; LP = lysed pellet; LS= lysed supernatant; NI= non induced; I = induced.

5.2.3.3 AaaAt3 is active

To see whether AaaAt3 was active and to optimise the induction temperature, cultures of *E. coli* BL21 (DE3) *pET21a* and *E. coli* BL21 *pET21a::aaaAt3* were grown in LB and induced with 1.0 mM or 0.3 mM IPTG, either at 37°C for 1.5 hours or 22°C overnight respectively. Unlysed cells did not show sufficient activity (data not shown but represented in Figure 5.2.16). Following lysis, the cells were combined with L-arginine-p-nitroanilide and the activity assay undertaken as normal.

AaaAt3 was active and appeared to respond better to the higher temperature of induction than AaaAt2, showing more similarity to AaaAt1 (Figure 5.2.15). The *E. coli* producing AaaAt3 were much healthier than those expressing AaaAt2, which could have accounted for this. The proportion of AaaAt3 this activity coming from insoluble or soluble protein cannot be determined from this experiment.

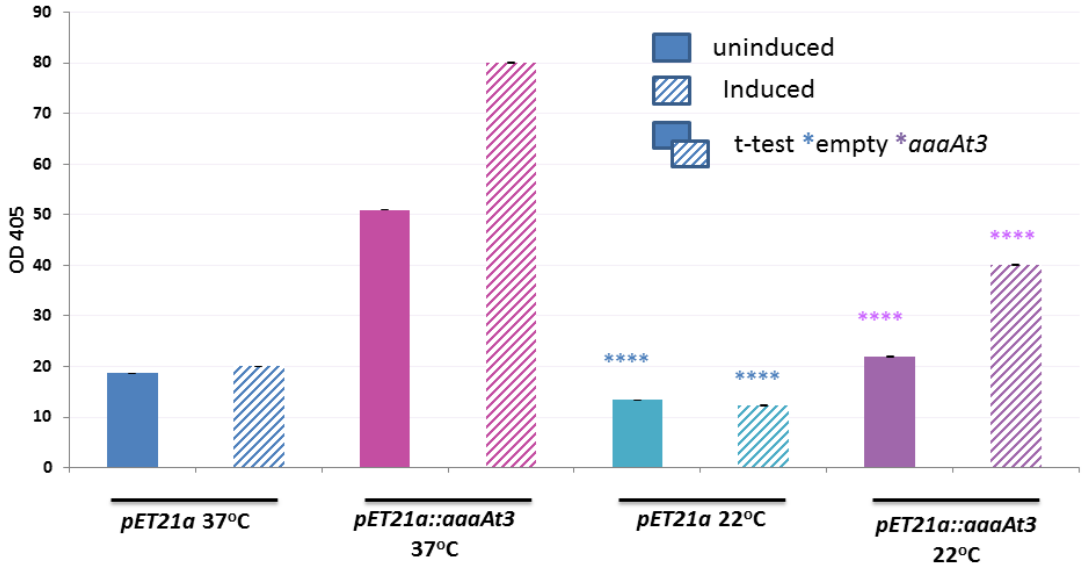


Figure 5.2.15: Induction at 37°C yields more AaaAt3 activity than at 22°C with 0.3 mM IPTG. *E. coli* BL21 *pET21a* and *E. coli* BL21 *pET21a::aaaAt3* were grown in LB until exponential and then induced at either temperature, the 22°C condition taking place overnight and the 37°C condition occurring for 1.5 hours. Lysis by sonication occurred prior to the combination of the L-arginine-p-nitroanilide substrate and cells. The resultant change in OD_{405} was plotted over time of incubation at 37°C for 24 hours and the AUC calculated from these values. This represents the activity of AaaA over 24 hours. During this time, the bacteria are not able to grow or divide. The experiment was performed 2 X for each temperature, 6 X technical replicates (the 37°C samples and 22°C samples were not run together on the same plate). The bars show the AUC of a 24 hour experiment. Solid bars show uninduced controls and striped bars induced samples. The error bars show standard deviation from the mean. Comparison by t-test was performed between the 37°C and 22°C conditions. The symbol **** indicates a P value of <0.0001.

Although more activity was detected following growth at 37°C, to limit inclusion body formation, induction at 22°C overnight was used in the following experiments, and combined with cell lysis before assaying for AaaAt3 activity. The activity of insoluble and soluble AaaAt3 produced from *E. coli* BL21 (DE3) cells

was compared. *E. coli* BL21 (DE3) *pET21a::aaaAt3* was grown in LB at 37°C until exponential phase was reached. Following induction with 0.3 mM IPTG overnight at 22°C, the cultures were washed 3 X in MMP. The resuspended cultures were normalised to OD $_{600}$ 1.0 and lysed using sonication, the lysis pellet and the lysis soluble fractions were harvested by centrifugation, and AaaAt3 activity assessed using the L-arginine-p-nitroanilide assay.

AaaAt3 activity was detected in the soluble lysate (Figure 5.2.16). The unlysed whole cells and the pellet fraction from lysed cells showed little activity, indicating that cell lysis is necessary to observe activity of AaaAt3 and that the insoluble portion of AaaAt3 was perhaps misfolded or the active sites masked by the formation of inclusion bodies. This experiment can now be scaled up by using larger culture volumes or pooling together separate cultures and lysed by French press.

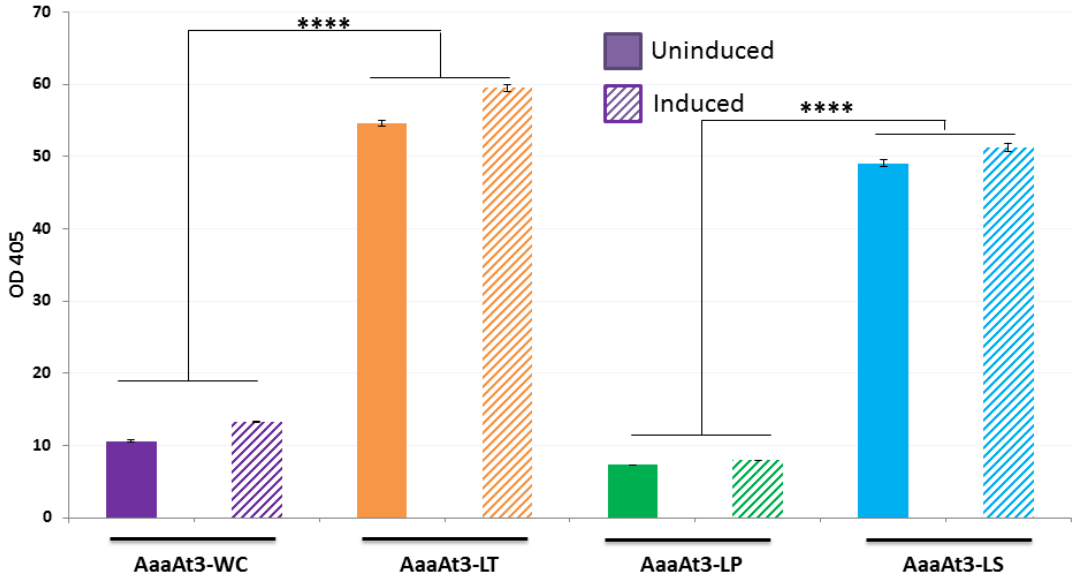


Figure 5.2.16: The soluble fraction of AaaAt3 is active. WC = whole cell, LT= lysed total, LP=lysed pellet, LS=lysed supernatant. *E. coli* BL21 *pET21a::aaaAt3* was grown in LB at 37°C until exponential phase was reached. Following induction with 0.3 mM IPTG overnight at 22°C, WC cells were washed in MMP before mixing with the substrate L-arginine p-nitroanilide as in previous activity assays, while the lysed samples were washed in MMP before sonication and then mixed with L-arginine-p-nitroanilide. The resultant change in OD_{405} was plotted over time of incubation at 37°C for 24 hours and the AUC calculated from these values. This represents the activity of AaaA over 24 hours. During this time, the bacteria are not able to grow or divide. The bars show the AUC of a 24 hour experiment. Solid bars indicate uninduced samples and striped bars induced samples. The experiment was performed 3 x with 3 technical replicates in each experiment. Error bars show the standard deviation. Comparison by t-test was performed. The symbol **** indicates a P value of <0.0001.

5.3 Discussion

The aim of this chapter was to produce recombinant AaaA for the purpose of cell-free functional analysis, inhibitor screening, crystallisation and discovery of the protein structure. Due to the attachment of AaaA to the OM, the difficulties associated with membrane protein purification were circumvented by truncating AaaA so that it lacked the β-barrel domain. Unfortunately, relocation of AaaA to the periplasm or cytoplasm caused insolubility, presumabley due to inclusion body formation. It is possible that the impact of inclusion body formation on cell physiology may have been exacerbated by the exopeptidase activity of AaaA which would presumably degrade intracellular proteins.

The insoluble nature of AaaAt1 could be taken advantage of for purification purposes. Other cellular proteins were less dense and could be separated from AaaAt1 aggregates by centrifugation. This process was combined with subsequent chemical solubilisation to produce semi-pure and soluble protein. Unfortunately this approach was limited by the sensitivity of AaaAt1 stability to protein concentration and therefore not an ideal strategy to take forward. Removal of the signal peptide (AaaAt2) did not increase solubility either, and the cytoplasmic location exacerbated host cell toxicity. Extending the final alpha helix (α-linker) in the passenger domain to mask a hydrophobic region exposed in AaaAt1 was attempted, as this was hypothesised to increase solubility (AaaAt2 and AaaAt3). The desired effect was observed with the periplasmic version (AaaAt3), but this was at the expense of the yield.

Activity was maintained in all the recombinant proteins (AaaAt1, AaaAt2 and AaaAt3), suggesting that the tertiary structure was not affected by the removal of the β-barrel. The solubility of AaaAt3 makes it the most promising to take forward for further purification steps and crystallisation, following optimisation to increase the production levels.

5.3.1 Inclusion body formation: what are they, how do they form and how can they be dealt with

One challenge of AaaAt1 production evident from the work undertaken so far is a tendency to become insoluble, which is suspected to originate from the formation of inclusion bodies. Inclusion bodies are tightly packed clusters of protein that is normally non-native, often hydrophobic to some degree, and expressed from a highly active promoter (García-Fruitós 2010). If the protein being produced contains disulphide bonds, inclusion bodies are expected (Singh and Panda 2005). The protein is normally partially folded, retaining some native-like secondary

structure but due to the incompleteness of the folding, is inactive (Goeddel *et al* 1979). Inclusion bodies can be found in either the cytoplasm or periplasm, are typically between 0.5-1 μm in diameter, and are dense, hydrated, porous structures (Taylor *et al* 1986). They are highly homogenous, containing one type of polypeptide and very little contaminants (Rhinas and Bailey 1992).

The formation of inclusion bodies (Figure 5.3.1) has been attributed to the accumulation of partially folded protein intermediates interacting with each other through hydrophobic or ionic interactions (Betts and King 1999). Inclusion body formation is associated with a high level of expression and consequent accumulation of denatured protein (Singh and Panda 2005). Additionally, in their native organism, proteins susceptible to aggregation are assisted by molecular chaperones which help with the folding process (Mamipour *et al* 2017). Different chaperones, or chaperones which are unable to cope with the increased production of protein from an overexpression system, could be a contributing factor in inclusion body formation (Sorenson and Mortensen 2005).

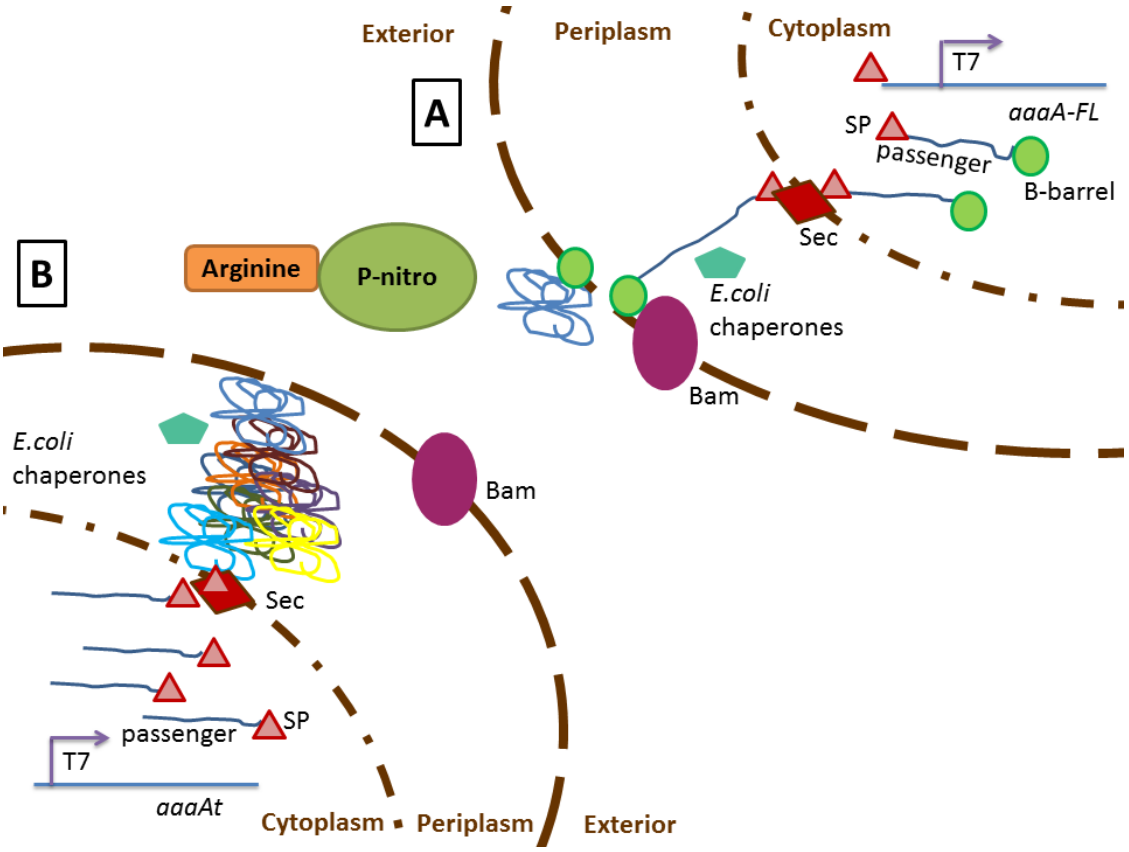


Figure 5.3.1: How inclusion bodies of AaaAt1 could form in *E. coli* BL21. Inclusion bodies are dense clusters of denatured protein which consists of mostly one type of polypepeptide. They can be found in the cytoplasm or periplasm, are typically 0.5-1.3 μm in diameter and are usually the product of a highly expressed foreign protein and/or the expression of hydrophobic proteins (Singh and Panda 2005). Panel A (top right) = normal autotransporter expression. Panel B (bottom left) = inclusion body formation.

The strategies deployed when inclusion bodies are encountered are broadly divided into whether to work with them or against them (Sorenson and Mortensen 2005, Figure 5.3.2). As in the case of AaaAt1, their advantages can be exploited to isolate them from other cellular components, solubilise artificially and refold. This potentially can be very effective: the density of inclusion bodies being greater than that of the other cellular components making separation by centrifugation a viable option, the resistance to degradation and proteolytic attack helpful in retaining high quality protein, and the homogenous nature of the aggregates facilitating in purification (Upadhyay *et al* 2012). Additionally the large yields of protein generated by allowing the formation of inclusion bodies can compensate for the loss of protein through the resolubilisation and refolding process (Hoffman *et al* 2017). However, such processes can be inefficient and expensive, especially when needing high quantities of protein (Sorenson and Mortensen 2005). Another problem, which was experienced with AaaAt1, is the aggregation of protein occurring during refolding (Vallejo and Rinas 2004). This occurs because some folding intermediates have exposed hydrophobic regions

which when in close proximity to other hydrophobic regions on neighbouring proteins, can interact causing aggregation (Singh and Panda 2005). The higher the concentration, the higher probability that this post-solubilisation aggregation will occur. This can be overcome by using an alternative to a strong chaotrophic agent (e.g. 8 M urea) for solubilisation. Such strong chaotrophic agents induce a random coil structure where the hydrophobic regions are exposed; using a buffer, pH, solubilising agent and low concentration denaturant specialised to the protein of interest can avoid disrupting the structure to the level induced by a strong chaotropic agent (Singh and Panda 2005; Vallejo and Rinas 2004). However, this takes a considerable amount of optimisation and can still be unsuccessful. With AaaAt1 a urea concentration gradient was attempted to reduce the strength of denaturing effect. This was also tried with the combination of an ion chelator, EDTA. High levels of solubility were only generated with the highest concentration of urea used and EDTA had little to no effect. Different solubilising agents were also tried with little success. It was therefore decided that a structural change to the protein itself would be a more effective strategy.

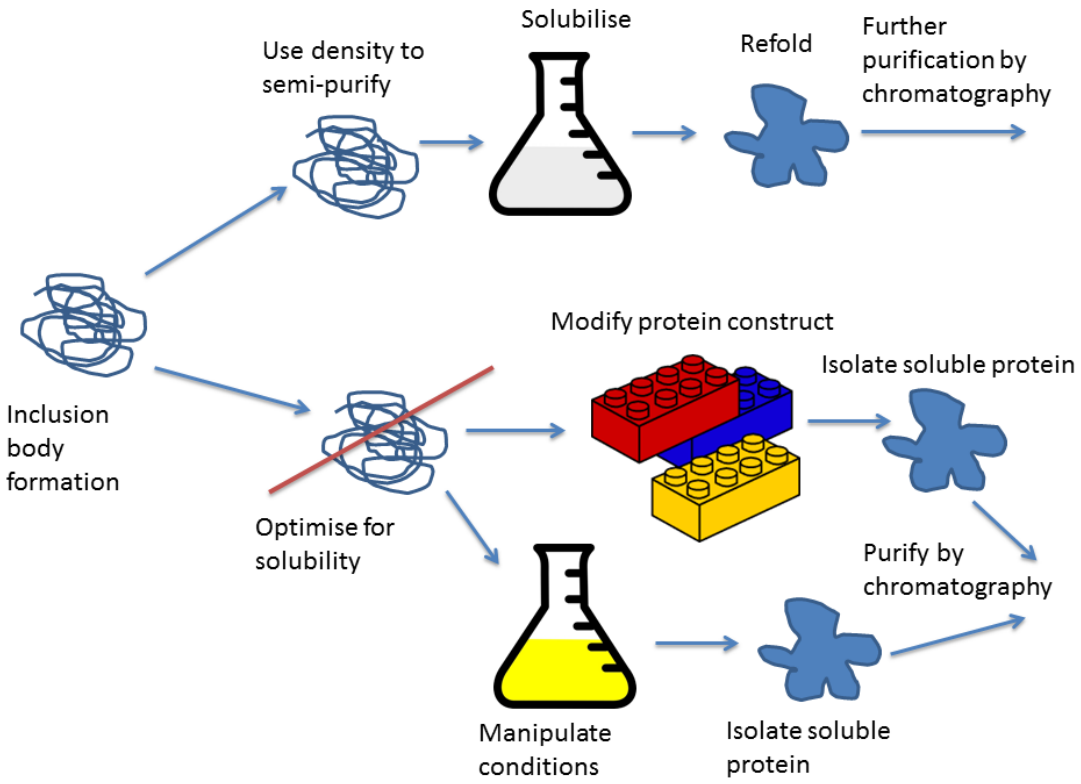


Figure 5.3.2: How to deal with inclusion bodies summary. Inclusion bodies can either be solubilised and refolded or avoided by manipulation of growth conditions or protein construct. Based on figure in Sorenson and Mortensen (2005).

The other option is to try to increase the solubility of the protein. This can be achieved through manipulation of the experimental conditions or by modifying the protein construct. Manipulating the experimental conditions largely aims to reduce the metabolic burden the cells are under, in addition to preventing a large build-up of denatured protein (Sorenson and Mortensen 2005). This can be through temperature modulation, media selection, selection of an appropriate expression system, choice of *E. coli* host, co-expression with chaperones or known expression partners and optimisation of available salts or ions (Yang *et al* 2003; Rosano and Ceccarelli 2014; Mamipour *et al* 2017; Sivashanmugam *et al* 2009).

A reduction in temperature was used to slight improvement in the expression of AaaAt2. A higher temperature favours aggregation, in part because hydrophobic interactions are highly dependent on this (Kiefhaber *et al* 1991). Additionally, the inhibition of heat shock proteases at lower temperatures could limit degradation and misfolding through the post-degradation exposure of hydrophobic sites (Chesshyre and Hipkiss 1989). At lower temperatures, gene expression is slowed, giving the cell more time to process the peptides and reducing the concentration

of peptides occupying the same location. This should benefit protein folding (Vasina and Baneyx 1996). This benefit can also be created through lowering the strength of induction by the promoter which the protein is under control of (Sorenson and Mortensen 2005). This was attempted by inducing with lower IPTG concentrations with AaaAt2 and AaaAt3 and had a mild beneficial effect (Figure 5.2.11 and Figure 5.2.15). The disadvantage of incubating at a lower temperature during protein induction, was that cell growth was slower thereby affecting the yield. Since the low levels of AaaAt2 were not accompanied by a substantial increase in the amount of soluble protein, a better strategy might be to couple the reduction in temperature with a promoter system which was more suited to operate at these conditions. One such system is the *cspA* promoter system which has been used for the expression of membrane proteins (Vasina and Baneyx 1996). Furthermore, an *E. coli* strain such as C41 (DE3) or C43 (DE3), adapted from *E. coli* BL21 (DE3) (Miroux and Walker 1996; Dumon-Seignovert *et al* 2004) might be more suited for the overproduction of AaaAt1 and AaaAt3. Alternatively a cell type like artic express could allow the temperature to be reduced further (Ferrer *et al* 2004). Another small change could be used is terrific broth (TB) rather than LB as it is richer and is buffered by phosphate which in some cases improves solubility (Letterer and Schagat 2006). Two zinc ions are predicted to form part of the active site in AaaA (Luckett *et al* 2012); it would be interesting to see if adding a source of zinc ions had any effect.

In this work AaaA was modified to remove the hydrophobic β-barrel, further modified to remove the signal peptide and re-modified to respect the positioning of hydrophobic residues (Figure 5.3.3). It is not known whether purifying AaaA with the β-barrel attached would ultimately result in a greater yield of soluble, active protein. This could have been a further avenue to take had not AaaAt3 been a viable option to pursue. The pitfalls with purifying membrane proteins (Smith 2017) however made this a last resort. The removal of the signal peptide increased the toxicity AaaA had to its *E. coli* host. It was also degraded more readily, perhaps due to its location in the cytoplasm. The toxicity could be overcome by transferral into a more tightly controlled promoter system (Marschall *et al* 2017), but because the signal peptide seems to be more than a help than hindrance, the inclusion of it seemed prudent. Another option would be to replace the signal peptide with a solubility tag such as maltose binding protein (MBP) or a smaller alternative such as translation initiation factor (IFL2) (Sorensen *et al* 2003; Fox *et al* 2003). This would necessitate a cleavage step and may not be any more effective than the signal peptide. Changes to the C-terminus to versions AaaAt2 and AaaAt3 included the addition of a His-tag. Although its primary

purpose was to facilitate easy purification, it could have also helped by blocking the terminal residues of AaaA from protease degradation. It is not clear from the data whether this effect occurred.

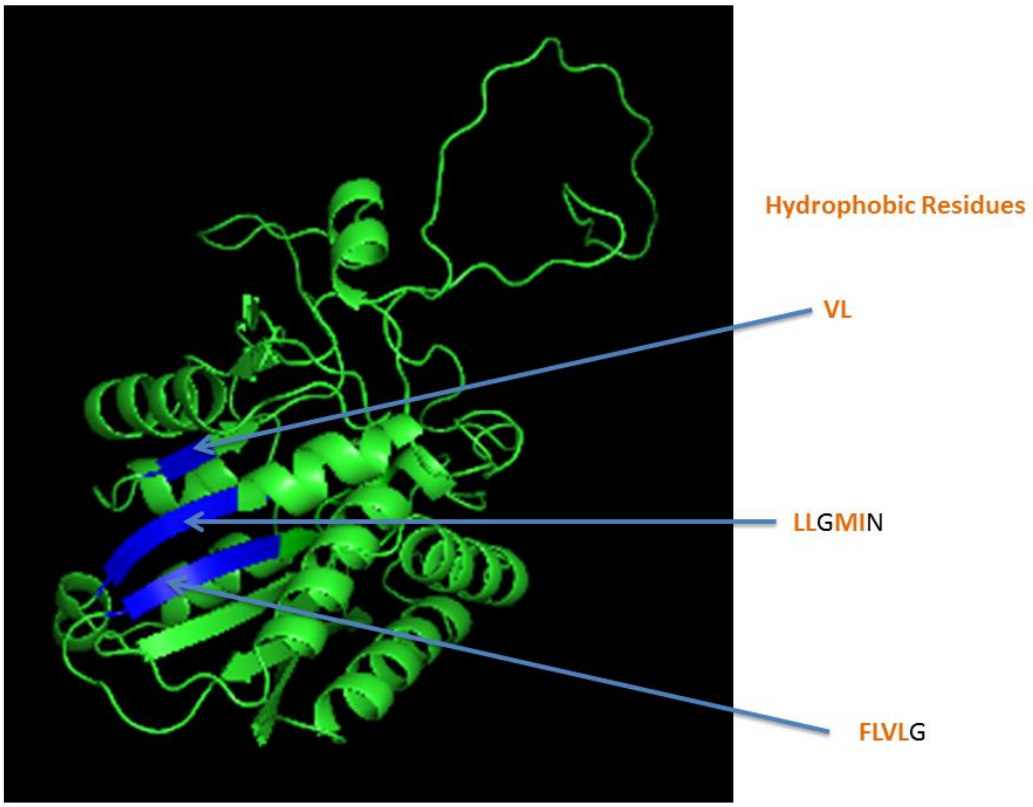


Figure 5.3.3: The first truncation left hydrophobic residues exposed which could have compromised protein solubility. Residues in orange have high hydrophobicity indexes. Figure was constructed using Pymol software.

Another modification option is the site-directed mutagenesis of residues which could be lowering the solubility or increasing the aggregation of the protein (Dale *et al* 1994). This would not be a favourable option in this case as the purpose of generating purified protein was partly for determination of the crystal structure. Since the aminopeptidase activity of AaaA could reduce the yields of soluble AaaAt through their degradation of host proteins, it would be interesting to mirror the strategies described here with the available inactive site-directed mutants generated by Paredes (2014). However this would have the disadvantage that the activity assay would not be able to be used to check the success of refolding.

An avenue which would be interesting to explore is co-expression with *PA0329*, the neighbouring ORF. Using the String database, *PA0329* was found to be co-expressed with *aaaA.* This was investigated and explained in Chapter 3. The function of this ORF is unknown and there is an outside chance that it could be involved in aiding AaaA expression in *P. aeruginosa.*

5.3.2 Taking AaaAt3 further

The next steps in optimising AaaAt3 production include increasing the amount of protein produced, ideally while maintaining or improving the soluble portion. Increasing the culture volume and then concentration before and after lysis by French Press was attempted, but the resulting lysate was highly viscous. More rigorous DNase treatment, both with enzymes and through mechanical disruption (passing lysate through a needle) was trialled with some improvement and could be taken further. However, another option is to grow smaller cultures, lyse these individually and pool them. This could result in less DNase produced due to a lower cell density (Newton *et al* 2016; Balasundaram *et al* 2009; Boynton *et al* 1999).

Alongside the upscaling optimisation process, a method of purification which would circumvent the problems associated with denaturation by a chaotrophic agent but provide an easy way to simultaneously solubilise and purify AaaAt3 is use of ammonium sulphate to salt out the proteins from solution (Duong-Ly and Gabelli 2014; Wingfield 2001). It was hoped that by using a gradient, contaminating proteins could be salted out at lower ammonium sulphate concentrations and AaaAt3 could be salted out at a higher concentration. Dialysis could then be used to reintroduce AaaAt3 into solution. As ammonium sulphate does not denature proteins (Duong-Ly and Gabelli 2014; Wingfield 2001), the problems associated with folding intermediates interacting through their transiently exposed hydrophobic regions would be avoided. The improvement in structure AaaAt3 has in comparison to AaaAt1 would also hopefully improve its long term solubility and ability to exist in soluble form when the solution was more concentrated. Because a His-tag also was placed onto the C-terminus of AaaAt3, further purification could be achieved through affinity chromatography (Urh *et al* 2009). Figure 5.3.4 illustrates the salting-out method.

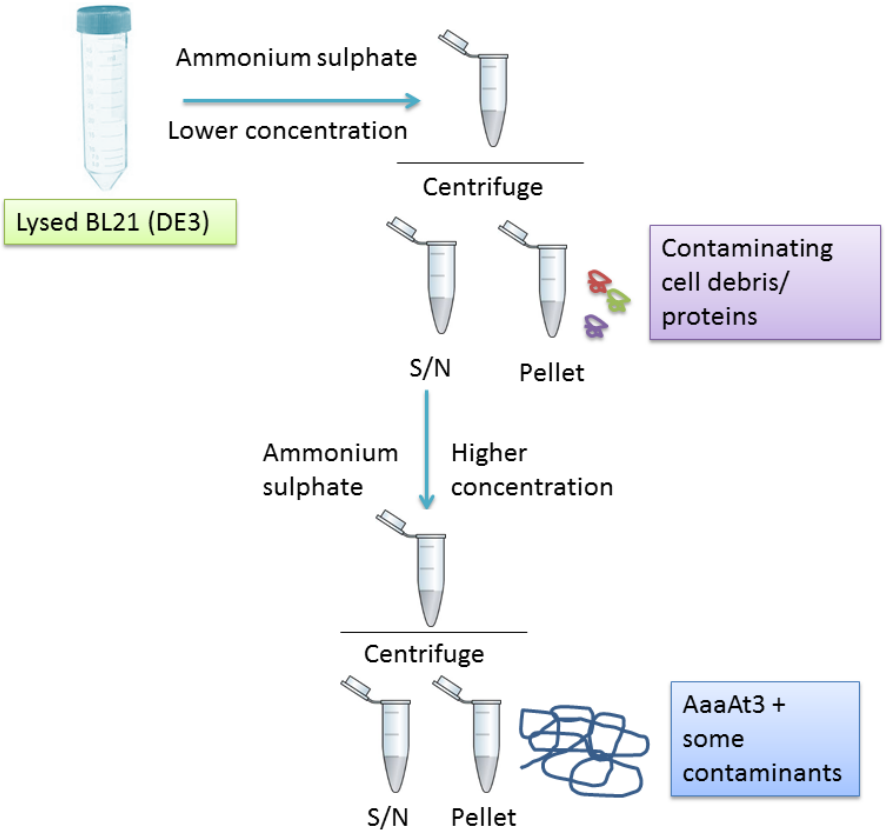


Figure 5.3.4: Solubilisation and Purification of AaaAt3 by use of the 'salting-out' method. Ammonium sulphate can be used to decrease the charged water molecule availability for the dissolved proteins which results in their precipitation. Unlike chaotrophic agents, the secondary structure of the precipitated proteins is normally unaffected. Depending on the amount of Ammonium sulphate added, different proteins will precipitate. This principle can be used to remove contaminating proteins with one concentration of salt and precipitate the target protein with another concentration. Diagram is based on the information from Duong-Ly and Gabelli 2014; Wingfield 2001.

5.3.3 Conclusion

The journey towards the purification of AaaA has not been simple and unfortunately the goals of crystallisation and inhibitor testing have not been reached. The last version of truncated AaaA, AaaAt3, is however promising and it is hoped that it will be a more suitable candidate for purification. Preliminary steps following the path outlined in the previous subsection have been encouraging (data not shown) and hopefully the final barriers can be overcome.

6 Chapter 6: impact of AaaA on biofilm formation and virulence

6.1 Introduction

6.1.1 Background

The highly prevalent *P. aeruginosa* CF airway infections are carefully managed by health professionals through aggressive antibiotic therapy (Smith *et al* 2017). This is largely successful in controlling acute episodes of disease, known as exacerbations, but is often unable to clear the bacteria completely (Bryan *et al* 1972; Kobayashi *et al* 1972; Lyczak *et al* 2002). This leaves a low-symptomatic, persistent community of bacteria which can cause future exacerbations and over time lead to poor patient outcomes such as irreversible lung damage (Konstan *et al* 1995). The mechanism for antibiotic resistance employed by these persisting cells is in large part through their growth as a biofilm (Costerton *et al* 1999; Lewis 2001; Khoury *et al* 1992). Thus, understanding how *P. aeruginosa* biofilm growth is sustained in the CF airway environment could reveal new ways of treating chronic infection with the goal of eradication.

Growth as a biofilm requires substantial inter-cell coordination and structuring in order for it to function optimally (Costerton *et al* 1999; O'Toole *et al* 2000; Stoodley *et al* 2002; Klausen *et al* 2003; Flemming and Wingender 2010; Ryder *et al* 2007; Ghafoor *et al* 2011; Whitchurch *et al* 2002). The high density of cells increases the competition for essential nutrients and oxygen by slowing the rate of diffusion and creating chemical gradients (Stewart 2003). This results in a differentiation of cell states within the biofilm, with alternative metabolic pathways operating in the cells which have less access to oxygen and preferred nutrient sources (Werner *et al* 2004; Sternberg *et al* 1999; Xu *et al* 1998). As well as the consumption of oxygen by competing bacterial cells, (deBeer *et al* 1994; Stewart 2003) availability is reduced further by the surrounding environment in the CF airway. Located deep within the mucus layer, close to the airway epithelia (Worlitzsch *et al* 2002; Boucher 2004) and in the vicinity of recruited neutrophil cells (Jensen *et al* 2010); oxygen is a rapidly consumed commodity (Worlitzsch *et al* 2002).

P. aeruginosa is a flexible organism and possesses a number of metabolic pathways for growth in low oxygen environments (Arai 2011). In fact, some studies have found that *P. aeruginosa* prefers a microaerobic mode of growth (Mouncy *et al* 1998; Preisig *et al* 1996; Otten *et al* 2001; Alvarez-Ortega and

Harwood 2007; Sabra *et al* 2002; Yoon *et al* 2002). The known metabolic systems operating under hypoxic conditions include: high affinity oxidases (for example Cbb_3-2) which help utilise available oxygen as efficiently as possible (Lazazzera *et al* 1996; Ye *et al* 1995); nitrogen which can act as an alternative electron acceptor to oxygen (Palmer *et al* 2007); arginine that can be fermented through the ADI pathway to generate ATP independently from the cell redox state (Vander Wauven *et al* 1984; Lu *et al* 2001; Maghnouj *et al* 1998); pyruvate that can promote survival without oxygen (Eschbach *et al* 2004) and phenazines which can shuttle electrons externally to readdress the redox balance of the cell (Glasser *et al* 2014; Dietrich *et al* 2003). These are likely to work in concert, making *P. aeruginosa* very capable of survival in such conditions.

Studies have found arginine metabolism to be an important aspect of *P. aeruginosa* biofilm growth. Musken *et al* (2010) showed that impairment in arginine metabolism genes correlated with poor biofilm growth. Furthermore, Bernier *et al* (2011) found that exogenous arginine added to *P. aeruginosa* promoted biofilm formation while repressing swarming through upregulation of c-di-GMP. It has also been observed that exogenous arginine added to biofilms can increase antibiotic efficacy through increased metabolism of persistor cells (Borriello *et al* 2006) showing that arginine can support cell growth in less accessible regions of the biofilm. Arginine is thought to support biofilm growth mainly through the ADI pathway which is not only beneficial from the point of view of oxygen independent ATP production, it has also been found to modulate pH through the production of ammonia (Lindgren *et al* 2014; Xiong *et al* 2014). As discussed previously, the CF airway environment is thought to be acidic and this product of the ADI pathway could protect against pH mediated cell damage (Ballard *et al* 1999; Poulsen *et al* 1994; Poulsen and Machen 1996; Pezzulo *et al* 2012). That metabolism of arginine in biofilms could promote chronic survival of *P. aeruginosa* in the CF airway is supported by the work of Hoboth *et al* (2009) which observed an increased expression of ADI pathway genes in the *P. aeruginosa* isolated over a period of 3-5 years in CF patients.

During an infection, arginine is not always readily available. Arginine was found to be depleted at *P. aeruginosa* infection sites in burn wound patients with *P. aeruginosa* seeking further arginine by chemotaxis (Everett *et al* 2017). An absence of arginine or inability to process it through the ADI pathway has been found to be detrimental to bacteria. An example of this is the attenuated bacterial virulence in a mouse model which was observed in *S. typhimurium* lacking a component of the ADI pathway (Choi *et al* 2012). Past work and the previous

chapters in this thesis support the idea that AaaA assists the ADI pathway by providing arginine upon demand. Without AaaA, the virulence of *P. aeruginosa* in a murine chronic wound model was found to be attenuated (Luckett *et al* 2012). The release of arginine from peptides by AaaA was therefore hypothesised to be an important part of the metabolic balancing act exerted by *P. aeruginosa* under conditions of limited oxygen. This would place AaaA as an integral part in the success of *P. aeruginosa* survival in a biofilm and persistence in the CF lung.

6.1.2 Aims

This chapter explores whether AaaA affects *P. aeruginosa* biofilm formation and how it might do this. The central questions are:

- Is AaaA needed by *P. aeruginosa* to grow in biofilm communities?
- How does it interact with other cellular machinery in this environment?

Additionally, some tools are developed to aid further analyses of AaaA and different biofilm models are compared.

6.2 Results

6.2.1 Biofilms grown in 10% LB media using 8 well chamber slides show no difference between PAO1 and PAO1 *ΔaaaA* strains

It was hypothesised that removal of AaaA would attenuate the biofilm formation capability of *P. aeruginosa*. To test this, an *in vitro* biofilm growth model using an 8 well microchamber slide was used. Overnight cultures of PAO1, PAO1 *ΔaaaA*, PAO1 *ΔaaaA* miniCTX*::aaaA* tagged with T7-GFP were grown for 18 hours in LB. The cultures were washed twice, resuspended in 10% LB (LB: PBS) and normalised to an OD_{600} of 0.05. Five hundred microliters of normalised culture were added to each well of a microchamber slide and the slide incubated at 37°C for 48 hours statically. The media was removed gently using a Gilson pipette and the biofilms imaged using confocal microscopy. Figure 6.2.1 shows that there was no difference in biofilm formation between the strains when grown in this manner.

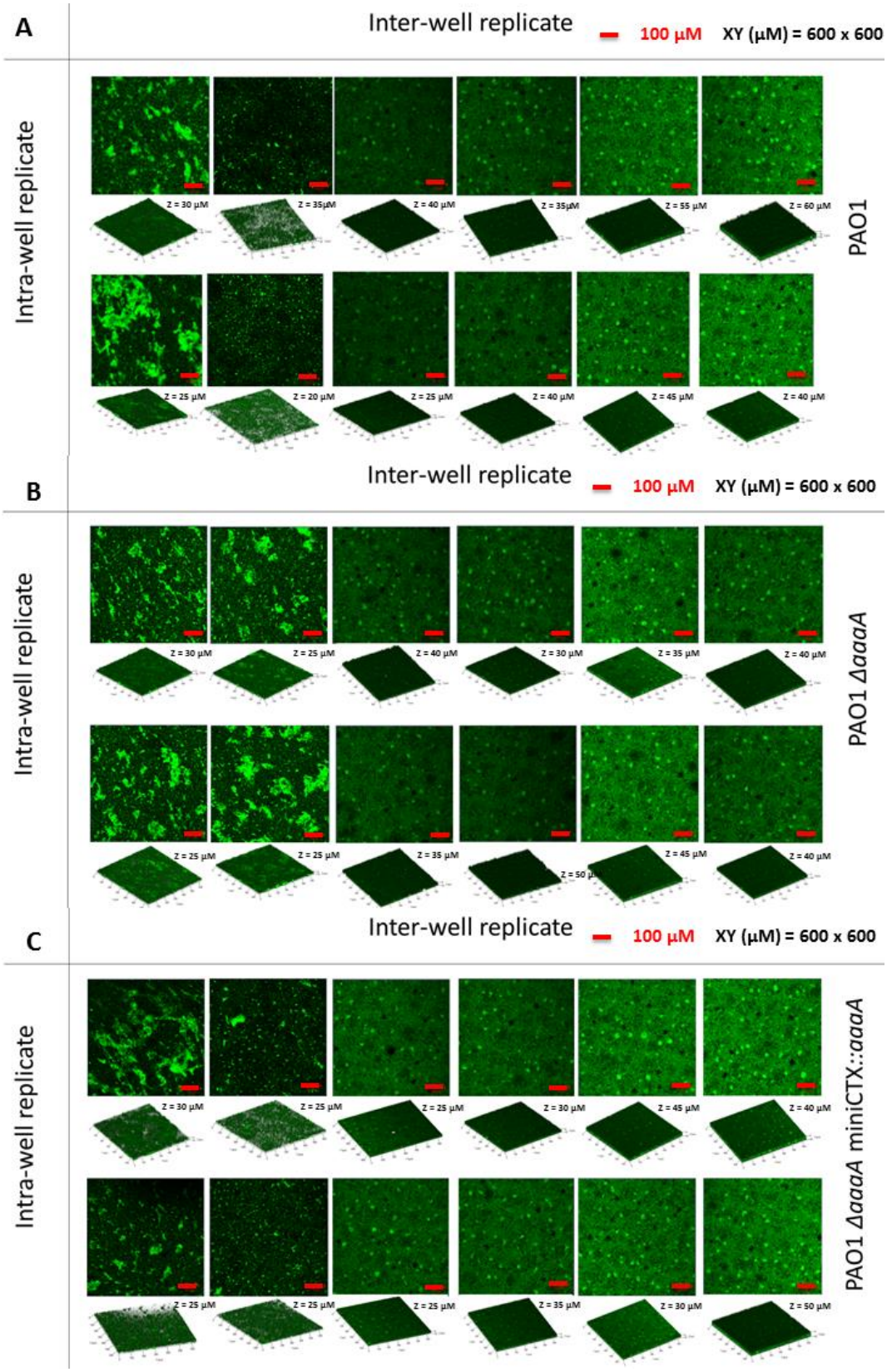


Figure 6.2.1: No difference in biofilm formation was found between PAO1, PAO1 *ΔaaaA* and PAO1 *ΔaaaA* miniCTX*::aaaA* strains grown in aerated, LB using the microchamber system. The biofilms were grown statically at 37°C for 48 hours. A= PAO1, B= *ΔaaaA,* C= PAO1 *ΔaaaA* miniCTX*::aaaA*. Six biological replicates are shown (left to right) and 2 technical replicates from each of these (top and bottom). All strains were tagged with T7-gfp and imaging was achieved using confocal microscopy. A magnification of 10x was used and z-stacks taken.

6.2.2 Nitrogen limited media optimisation and comparison to artificial sputum media

LB is a complex, rich media that is not easily manipulated for specific phenotype requirements. This can make it difficult to determine which nutritional components are responsible for observed changes in gene expression or biofilm structure. Therefore an alternative medium is required. Artificial sputum media (ASM) is time consuming and costly to prepare. It also contains multiple sources of nitrate (Palmer *et al* 2007). The creation of a simpler medium which can be tailored to the needs of individual experiments was attempted. Minimal media P (MMP) is a defined media which has been used previously (Luckett *et al* 2012) to measure metabolite dependency of *P. aeruginosa*. It contains Na_2HPO_4, KH_2PO_4, $MgSO_4$ and $FeSO_4$. Succinate is an organic acid which feeds directly into the TCA cycle and therefore could be used as a carbon source for *P. aeruginosa* growth (Collier *et al* 1996). Added to this base of sugar and salts, other substrates and environmental changes could be assessed for their effect.

6.2.2.1 Comparison of nitrate sources: KNO_3, arginine and tripeptide (arg-gly-asp) influence growth and PaaaA activation differently in PAO1 and PAO1 ΔaaaA

Prior to the data shown below, a gradient of concentrations (0 mM, 1 mM, 10 mM, 20 mM) of each nitrate source was tested (data not included) and 10 mM identified as allowing sufficient growth which was not improved sufficiently by increasing the concentration further. Succinate was included at a concentration of 20 mM in all conditions.

Figure 6.2.2 shows that the addition of arginine facilitates growth when the sole nitrate source. The activation of the *aaaA* and *kan* promoters (*PaaaA* and *Pkan*) is significantly higher in the arginine containing media. As noted previously (Chapter 3), the activation of the *aaaA* promoter was significantly higher in the PAO1 *ΔaaaA* miniCTX-*lux*::*PaaaA* strain than in PAO1 miniCTX-*lux*::*PaaaA*. In contrast, no significant difference is seen between the PAO1 *ΔaaaA* miniCTX-*lux*::*Pkan* and PAO1 miniCTX-*lux*::*Pkan* strains.

Addition of the tripeptide arg-gly-asp which serves as a substrate for AaaA also supported growth of PAO1 (Figure 6.2.3), especially when AaaA was present. Again, P*aaaA* activation was higher in the PAO1 *ΔaaaA* strain background. This difference is not seen between the PAO1 *ΔaaaA* miniCTX-*lux*::*Pkan* and PAO1 miniCTX-*lux*::*Pkan* strains.

Figure 6.2.4 shows that the addition of KNO_3 supports growth of PAO1 and PAO1 *ΔaaaA* but to a lesser extent than arginine or tripeptide. This may be because arginine and tripeptide are also carbon sources and contain more than one nitrogen atom per total molecule. Additionally, amino acids are among the preferred carbon sources for *P. aeruginosa* (Collier *et al* 1996) which could enhance growth. *PaaaA* activation is low with an absence of the exponential phase peak present in the arginine and tripeptide containing media. There is a late peak in *PaaaA* activation which could correspond to exhaustion of KNO_3 availability. This late peak in promoter activation is shared by the *Pkan* controls and could be a consequence of weaker growth.

Figure 6.2.5 brings together the data presented so far to compare the activation of P*aaaA* or P*kan* in KNO_3, arginine, and tripeptide supplemented media. Both tripeptide and arginine media support greater promoter activation which is mostly statistically significant. Because both *kan* and *aaaA* promoters have the same trend, it could be due to the better growth of *P. aeruginosa* with these supplements.

There is a significant difference in *PaaaA* activation between PAO1 grown in arginine or tripeptide which is not shared by the *Pkan* promoter. Ten millimolar of arginine stimulates *PaaaA* to a greater extent than the equivalent concentration of tripeptide. This would suggest that the substrate of AaaA, peptide chains with terminal arginine molecules, is not a stimulus of *PaaaA*. The stimulation appears instead to come from the product, arginine. This supports the hypothesis discussed in the Chapter 3, where arginine and AaaA exist in a positive feedback loop mediated by ArgR.

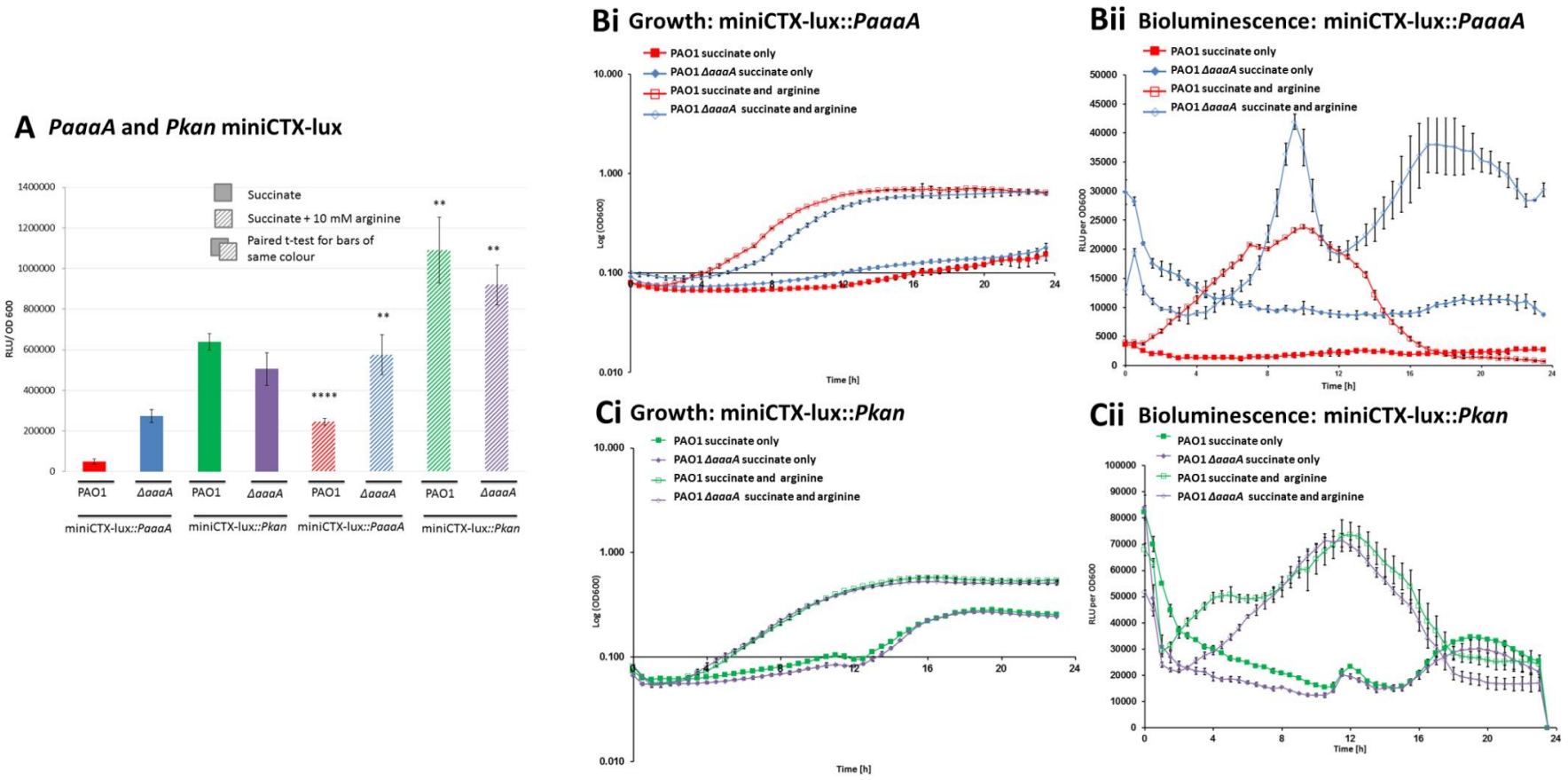


Figure 6.2.2: Growth of *P. aeruginosa* is supported by arginine and succinate.PAO1 miniCTX-*lux*::*PaaaA* (red), PAO1 *ΔaaaA* miniCTX-*lux*::*PaaaA* (blue), PAO1 miniCTX-*lux*::*Pkan* (green) and PAO1 *ΔaaaA* miniCTX-*lux*::*Pkan* (purple) were grown in MMP containing 20 mM succinate alone (solid filled) or with additional 10 mM arginine (open filled). The growth was recorded as OD_{600} over time and the bioluminescence measured as RLU/ OD_{600} which is proportional to promoter activation. A: AUC of RLU/ OD_{600} in each media. B: Growth (i) and *PaaaA* activation (ii) of PAO1 and PAO1 *ΔaaaA* strains in each media. C: Growth (i) and *Pkan* activation (ii) of PAO1 and PAO1 *ΔaaaA* strains in each media. Error bars show the standard deviation from 3 biological replicates. A t-test was performed between the succinate only and succinate + arginine media and the level of significance is represented by ns (non-significant) or by * ($P<0.05$).

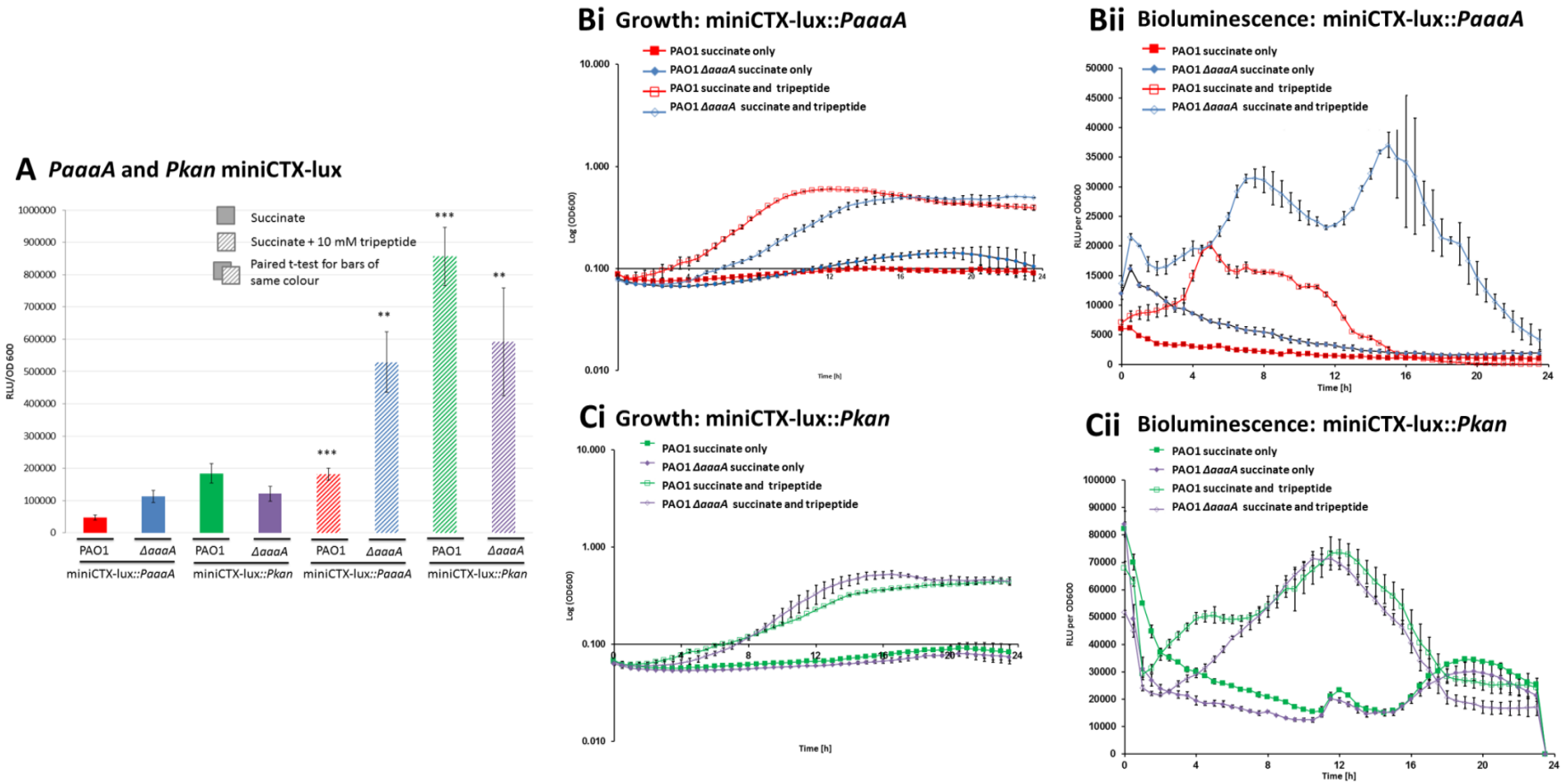


Figure 6.2.3: Growth of *P. aeruginosa* is supported by tripeptide and succinate. PAO1 miniCTX-*lux*::*PaaaA* (red), PAO1 *ΔaaaA* miniCTX-*lux*::*PaaaA* (blue), PAO1 miniCTX-*lux*::*Pkan* (green) and PAO1 *ΔaaaA* miniCTX-*lux*::*Pkan* (purple) were grown in MMP containing 20 mM succinate alone (solid filled) or with additional 10 mM tripeptide (open filled). The growth was recorded as OD_{600} over time and the bioluminescence measured as RLU/ OD_{600} which is proportional to promoter activation. A: AUC of RLU/ OD_{600} in each media. B: Growth (i) and *PaaaA* activation (ii) of PAO1 and PAO1 *ΔaaaA* strains in each media. C: Growth (i) and *Pkan* activation (ii) of PAO1 and PAO1 *ΔaaaA* strains in each media. Error bars show the standard deviation from 3 biological replicates. A t-test was performed between the succinate only and succinate + tripeptide media and the level of significance is represented by ns (non-significant) or by * ($P<0.05$).

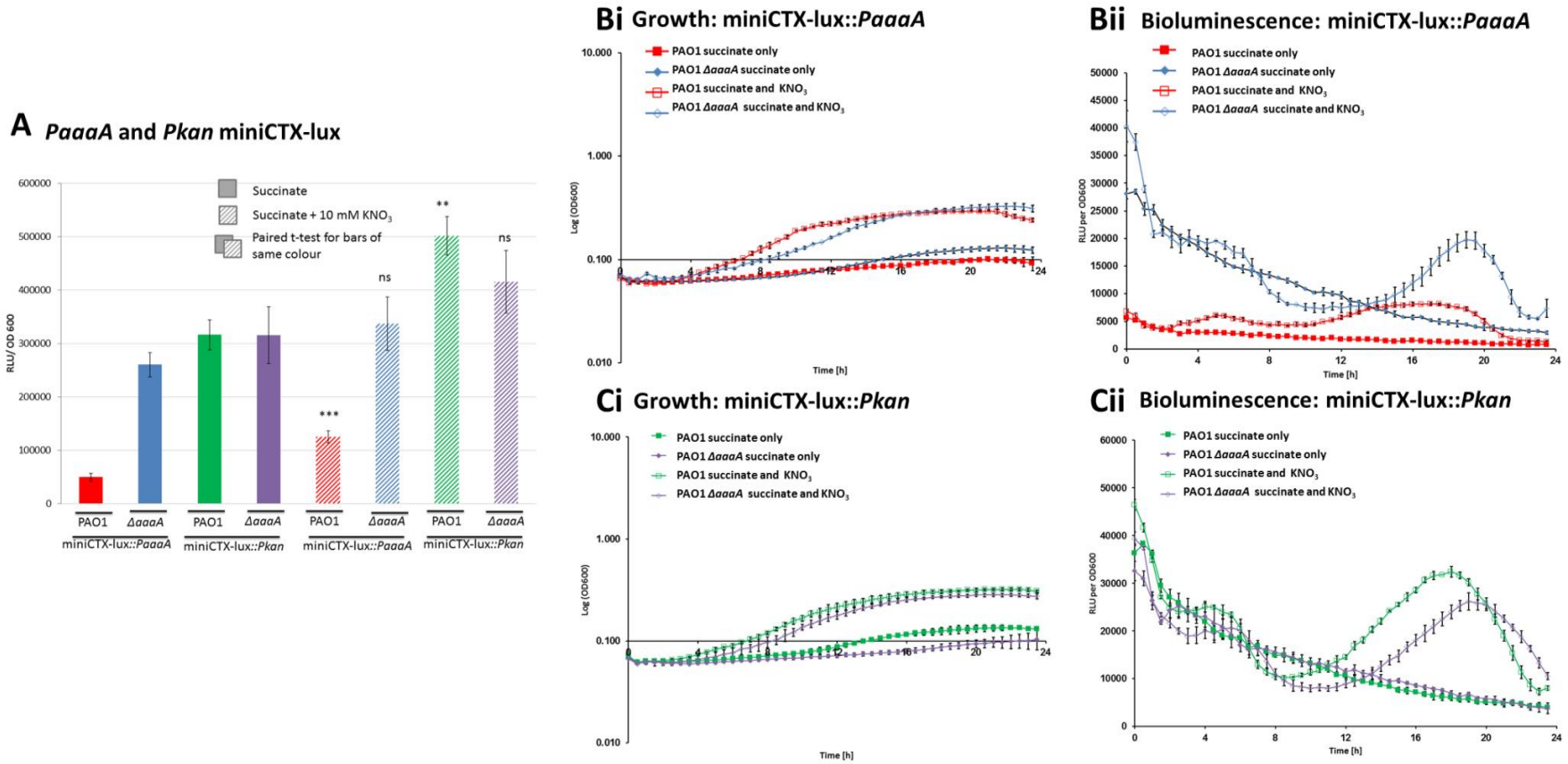


Figure 6.2.4: Growth of *P. aeruginosa* is supported by KNO_3 and succinate. PAO1 miniCTX-*lux*::*PaaaA* (red), PAO1 *ΔaaaA* miniCTX-*lux*::*PaaaA* (blue), PAO1 miniCTX-*lux*::*Pkan* (green) and PAO1 *ΔaaaA* miniCTX-*lux*::*Pkan* (purple) were grown in MMP containing 20 mM succinate alone (solid filled) or with additional 10 mM KNO_3 (open filled). The growth was recorded as OD_{600} over time and the bioluminescence measured as RLU/ OD_{600} which is proportional to promoter activation. A: AUC of RLU/ OD_{600} in each media. B: Growth (i) and *PaaaA* activation (ii) of PAO1 and PAO1 *ΔaaaA* strains in each media. C: Growth (i) and *Pkan* activation (ii) of PAO1 and PAO1 *ΔaaaA* strains in each media. Error bars show the standard deviation from 3 biological replicates. A t-test was performed between the succinate only and succinate + KNO_3 media and the level of significance is represented by ns (non-significant) or by * ($P<0.05$).

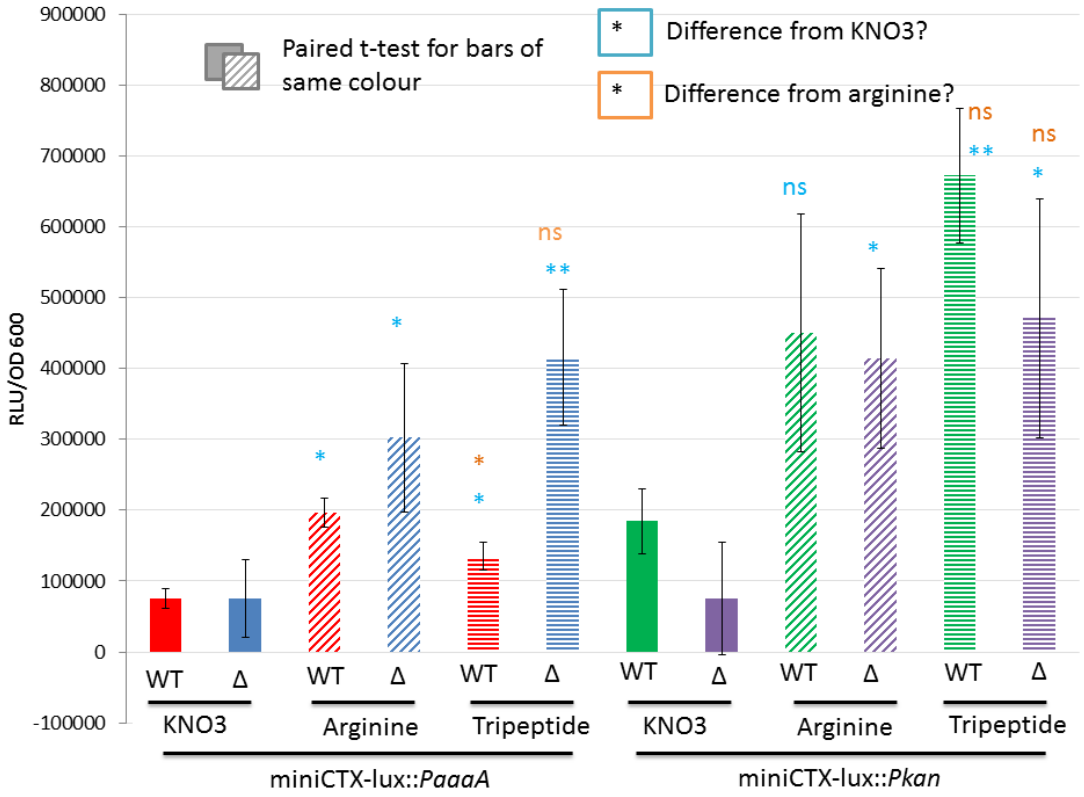


Figure 6.2.5: Comparison between MMP + 20 mM succinate media supplemented with KNO_3, arginine or tripeptide shows that arginine and tripeptide activate both *PaaaA* and *Pkan* more than KNO_3, while arginine significantly increases *PaaaA* compared to tripeptide. PAO1 miniCTX-*lux*::*PaaaA* (red), PAO1 *ΔaaaA* miniCTX-*lux*::*PaaaA* (blue), PAO1 miniCTX-*lux*::*Pkan* (green) and PAO1 *ΔaaaA* miniCTX-*lux*::*Pkan* (purple) were grown in MMP containing 20 mM succinate alone (solid bars) or with a supplement (striped bars). The growth was recorded as OD_{600} over time and the bioluminescence measured as RLU/ OD_{600} which is proportional to promoter activation. Each supplementation was tested in a separate experiment and standardisation was achieved by subtracting the mean RLU/ OD_{600} AUC (3 bio reps) of the supplemented media from the mean RLU/ OD 600 AUC succinate only control. The error bars represent the SQRT (supplemented SD^2+succinate only^2). SD = standard deviation. The labels ns and * indicate the significance of variation determined by a t-test. A t-test between a KNO_3 and another supplement is indicated in light blue, while a comparison between arginine and another supplement is indicated in orange.

6.2.2.2 Development of an amino acid cocktail to support growth of PAO1 and PAO1 ΔaaaA

There were two aspects from these results which warranted further investigation. The first was to determine if the enhancement in *PaaaA* activation was specific to arginine, or if it was shared by other amino acids with particular characteristics. The second was to examine the effect of nitrate on promoter activation independently of its influence on growth.

To do this, a media which supports the growth of both strains equally without affecting *PaaaA* activation was required. It also needs to be defined for consistency between repetitions. The MMP+ succinate media base was built upon to include NaCl, $CaCl_2$ (appendix A) and a cocktail of amino acids (10 mM of each

amino acid, see materials and methods). To avoid the potentially negative influence of nitrate on *PaaaA*, KNO_3 or NH_4Cl were excluded. Additionally, it was not known whether nitrogen atoms from amino acid R-groups would stimulate or inhibit *PaaaA* activation. Therefore, amino acids with R-group nitrogen atoms were also excluded from the media.

Growth in all strains was supported by this media composition. Interestingly there remains a difference in the promoter activation of P*aaaA* in WT and mutant strains (Figure 6.2.6). As this media does not contain complex peptides, is limited in nitrogen availability and does not contain arginine, the *aaaA* promoter in the PAO1 *ΔaaaA* strain must be being stimulated by a mechanism independent of these.

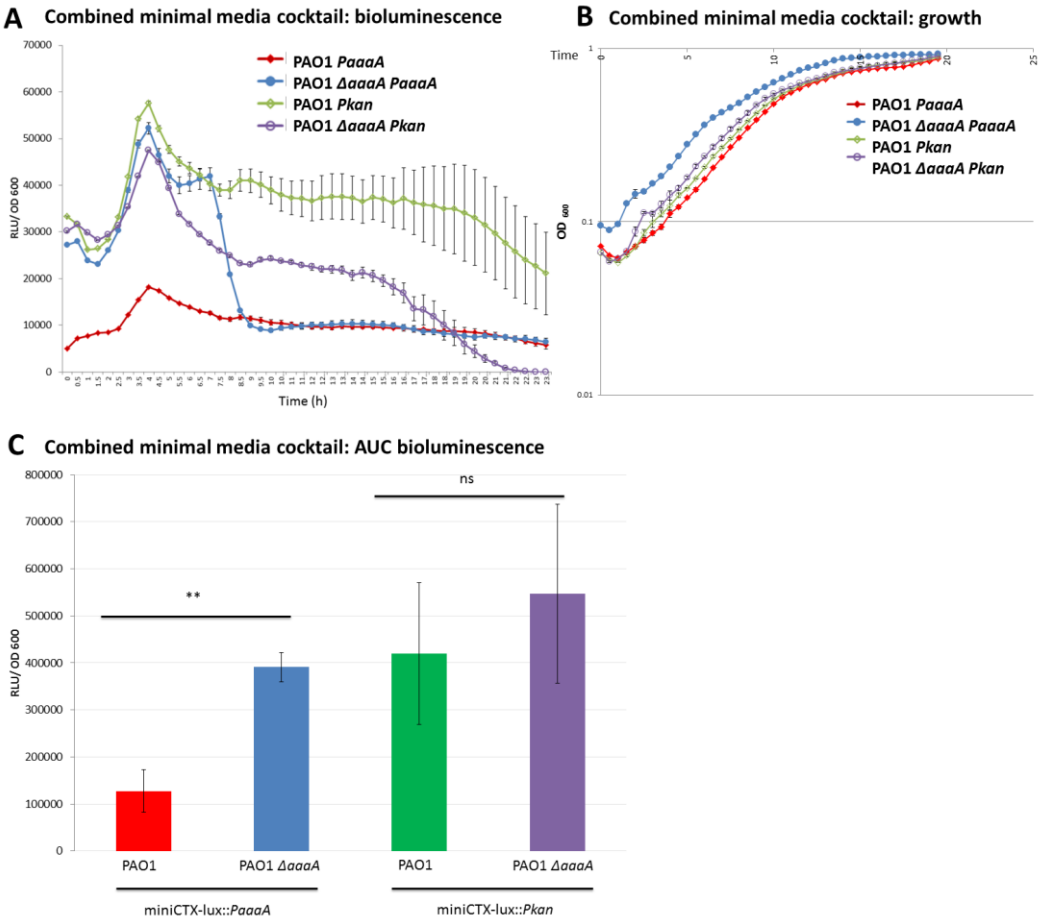


Figure 6.2.6: Minimal media cocktail containing non-nitrogen containing R-group amino acids supports growth, while *PaaaA* remains more activated in PAO1 than PAO1 *ΔaaaA*. PAO1 miniCTX-*lux*::*PaaaA* (red), PAO1 *ΔaaaA* miniCTX-*lux*::*PaaaA* (blue), PAO1 miniCTX-*lux*::*Pkan* (green) and PAO1 *ΔaaaA* miniCTX-*lux*::*Pkan* (purple) were grown in MMP containing 20 mM succinate, 10 mM $CaCl_2$, 10 mM NaCl and 10 mM of each non-nitrogen containing R-group amino acid. The growth was recorded as OD_{600} over time and the bioluminescence measured as RLU/ OD_{600} which is proportional to promoter activation. Error bars represent the standard deviation from 3 biological replicates. A t-test was performed between the RLU/OD_{600} AUC of PAO1 and PAO1 *ΔaaaA* strains, ns = not significant and * =significant. Panel A: comparison of the bioluminescence produced by each strain in the minimal media cocktail. Panel B: growth of each strain in the minimal media cocktail over 24 hours. C: the AUC of bioluminescence produced by each strain in the minimal media cocktail.

6.2.2.3 Investigation of PaaaA activation using the minimal media cocktail reveals PaaaA responds to the addition of amino acids other than arginine

Once a suitable media composition was achieved (here named 'minimal media cocktail') the effect of individual amino acids (both with and without nitrogen containing R-groups) and exogenous nitrate on *PaaaA* activation was tested. Figure 6.2.7 and Figure 6.2.8 show the results from this experiment. These findings are complex and to help clarify the description below, Table 6.2.1 summarises the results.

Addition of KNO_3 to the media cocktail (Figure 6.2.7, A) resulted in a significant reduction of P*aaaA* activation in the PAO1 *ΔaaaA* strain, but no difference in

P*aaaA* activation in the PAO1 WT background. There was no significant difference in the expression from the kanamycin promoter. Conversely, addition of arginine (Figure 6.2.7, B) significantly increased *PaaaA* activation in PAO1 and PAO1 *ΔaaaA*. However, *Pkan* activation was also significantly increased in the WT background when arginine was added which could mean arginine does not specifically activate *PaaaA* in the PAO1 WT. Histidine and glutamine (Figure 6.2.7 C and D), which have N containing R-groups, also showed a similar pattern to arginine with significantly greater *PaaaA* activation in the PAO1 *ΔaaaA* mutant when these amino acids were added. Both *Pkan* and *PaaaA* activation increased in PAO1 with addition of the amino acids and therefore a specific effect on *PaaaA* activation in the WT strain cannot be concluded. Asparagine addition (Figure 6.2.8, A) significantly increased *PaaaA* activation in PAO1 but not PAO1 *ΔaaaA* where there was no difference. *Pkan* activation was not significantly different when asparagine was added. Addition of glycine (Figure 6.2.8, B) caused a significant reduction in *PaaaA* activation in the PAO1 *ΔaaaA* strain but not the PAO1 strain. The activation of *Pkan* was not significantly different in either condition. Addition of serine (Figure 6.2.8, C) increased P*aaaA* and P*kan* mediated expression in the PAO1 background. There was no significant effect on the activation of either promoter in PAO1 *ΔaaaA*. Methionine (Figure 6.2.8, D) presence significantly increased *PaaaA* and *Pkan* in PAO1 and significantly decreased P*aaaA* activation, but not *Pkan* activation, in the PAO1 *ΔaaaA* background.

Amino acid or KNO_3	**Activation of *PaaaA***		**Activation of *Pkan***	
	PAO1	**PAO1 *ΔaaaA***	**PAO1**	**PAO1 *ΔaaaA***
KNO_3	NS	**Down**	NS	NS
Arginine*	Up	**Up**	Up	NS
Histidine*	Up	**Up**	Up	NS
Glutamine*	Up	**Up**	Up	NS
Asparagine	**Up**	NS	NS	NS
Glycine	**Up**	**Down**	NS	NS
Serine	Up	NS	Up	NS
Methionine	Up	**Down**	Up	NS

Table 6.2.1: Summary of amino acid addition effect on the activation of *PaaaA* or *Pkan*. Up = an increase in bioluminescence corresponding to promoter activation; Down = a decrease in bioluminescence corresponding to promoter activation; NS =no significant difference in bioluminescence corresponding to promoter activation. Where *PaaaA* activation is affected and the equivalent *Pkan* control is not affected, the text is highlighted in red. Amino acids with a nitrogen containing R-group are indicated with an asterisk.

The effects of amino acid addition on *Pkan* activation in the PAO1 strain is a concern which should be highlighted. Why this has occurred is not yet known. The two hypotheses are: (i) the kanamycin promoter is responding to the same change in internal cell environment from the amino acid addition as *PaaaA* and (ii) the bioluminescence genes (*luxDABC*) are affected. For example, the bioluminescence genes were affected by a reduction in oxygen (Chapter 4). The repetition of this experiment with higher concentrations of added amino acid and with a different technique (e.g. qRT-PCR) will be needed to validate these results.

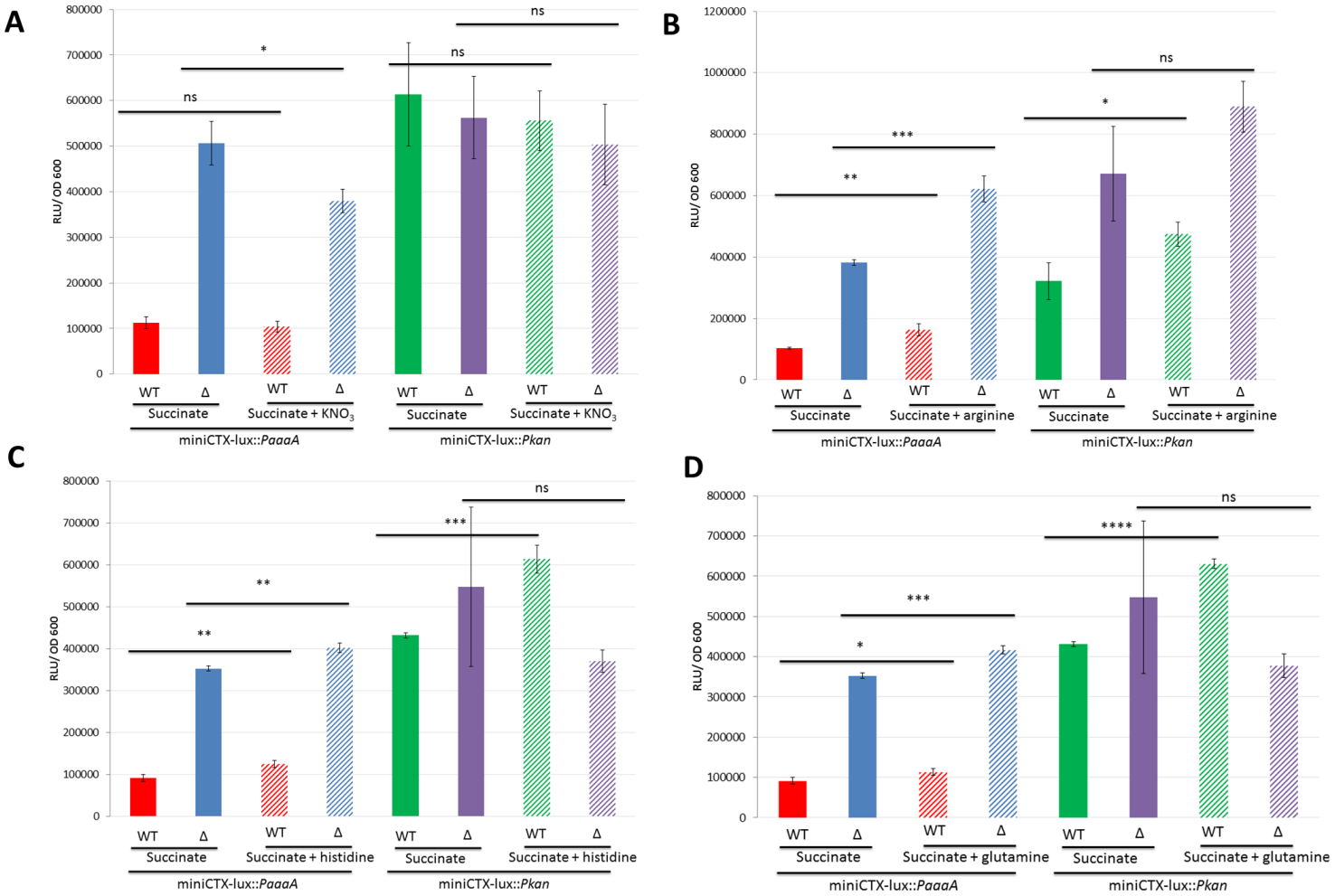


Figure 6.2.7: Addition of different amino acids and KNO_3 to the minimal media cocktail influence *PaaaA* activation (part 1). PAO1 miniCTX-*lux*::*PaaaA* (red), PAO1 *ΔaaaA* miniCTX-*lux*::*PaaaA* (blue), PAO1 miniCTX-*lux*::*Pkan* (green) and PAO1 *ΔaaaA* miniCTX-*lux*::*Pkan* (purple) were grown in the minimal media cocktail (solid bars) or in the minimal media cocktail (striped bars) with the addition of 10 mM KNO_3 (A), arginine (R-group N) (B), histidine (R-group N) (C) or glutamine (R-group N) (D). The growth was recorded as OD_{600} over time and the bioluminescence measured as RLU/ OD_{600} which is proportional to promoter activation. Error bars represent the standard deviation from 3 biological replicates. A t-test was performed between the same strain grown in minimal media cocktail and minimal media cocktail + KNO_3 or amino acid: ns = not significant and * =significant.

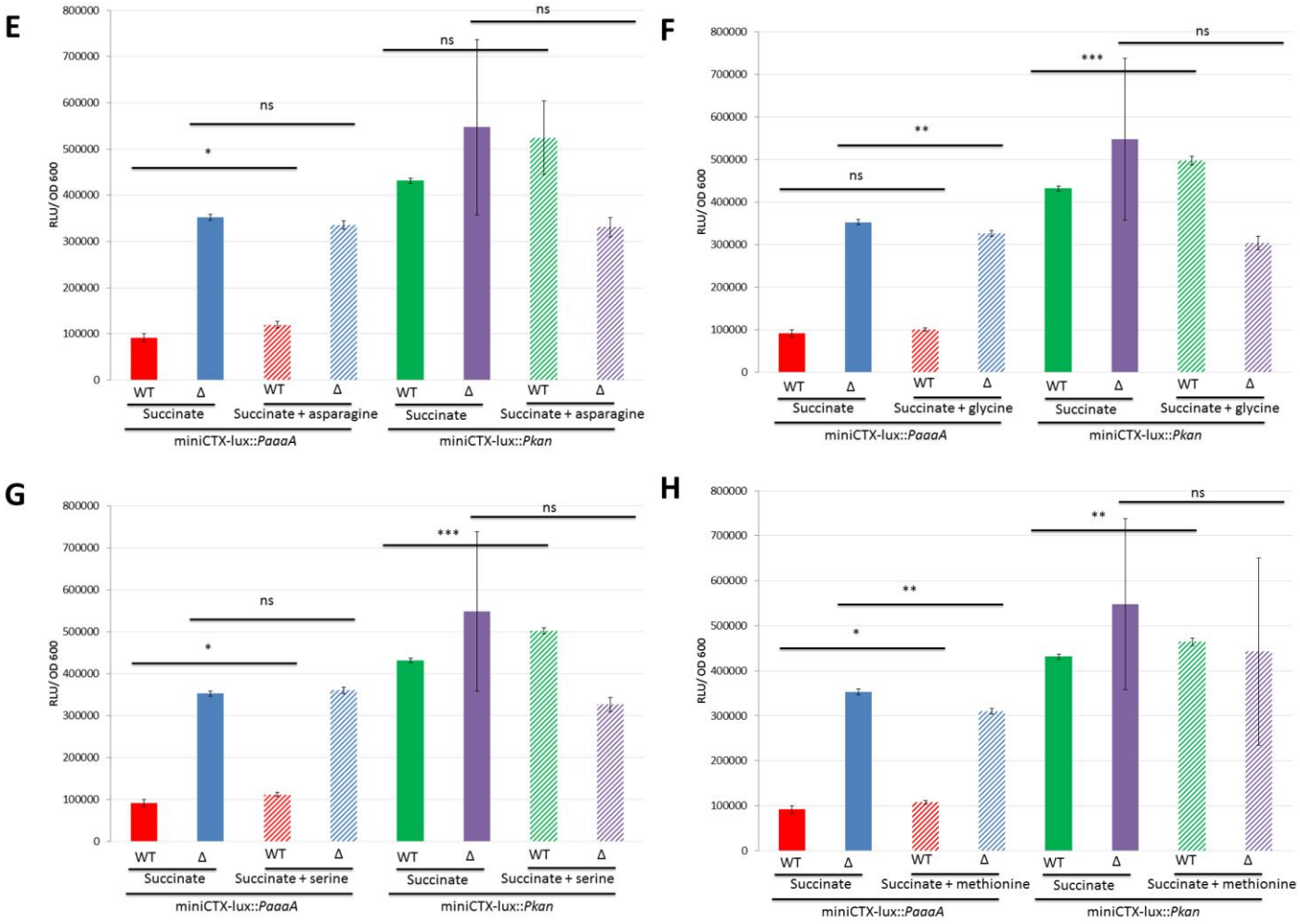


Figure 6.2.8: Addition of different amino acids and KNO_3 to the minimal media cocktail influence *PaaaA* activation (part 2). PAO1 miniCTX-*lux*::*PaaaA* (red), PAO1 *ΔaaaA* miniCTX-*lux*::*PaaaA* (blue), PAO1 miniCTX-*lux*::*Pkan* (green) and PAO1 *ΔaaaA* miniCTX-*lux*::*Pkan* (purple) were grown in the minimal media cocktail (solid bars) or in the minimal media cocktail (striped bars) with the addition of asparagine (A), glycine (B), serine (C) or methionine (D). The growth was recorded as OD_{600} over time and the bioluminescence measured as RLU/ OD_{600} which is proportional to promoter activation. Error bars represent the standard deviation from 3 biological replicates. A t-test was performed between the same strain grown in minimal media cocktail and minimal media cocktail + amino acid: ns = not significant and * =significant.

6.2.2.4 Word of thanks

The minimal media development work was assisted by MSc student Nabid Bhuiyan (2015) and BMedSci student Aone Sethibe (2016). For more detail regarding the development process of the cocktail solution please refer to their dissertations.

6.2.3 Biofilms using the minimal media cocktail in 8 well chamber slides do not differ between PAO1 and PAO1 *ΔaaaA* strains

That there was no difference between PAO1 and PAO1 *ΔaaaA* strains when grown aerobically in a rich media such as LB is not altogether surprising. LB contains a high amount of nitrate and arginine sources which is likely to reduce the requirement for AaaA. To control for this, the repetition of this experiment with the nitrate limited minimal media cocktail previously described was explored. The experimental procedure for growing and imaging biofilms using the microchamber model was followed as previously described with the exception that the minimal media cocktail replaced LB as the growth medium.

Figure 6.2.9 shows the biofilms produced when the minimal media cocktail was used instead of 10% LB in the microchamber system. In general the biofilms were thicker but still were unable to withstand washing. There was no noticeable difference between PAO1 and PAO1 *ΔaaaA* strains but the PAO1 *ΔaaaA* miniCTX*::aaaA* strain produced biofilm which was thinner than the other two strains when washed.

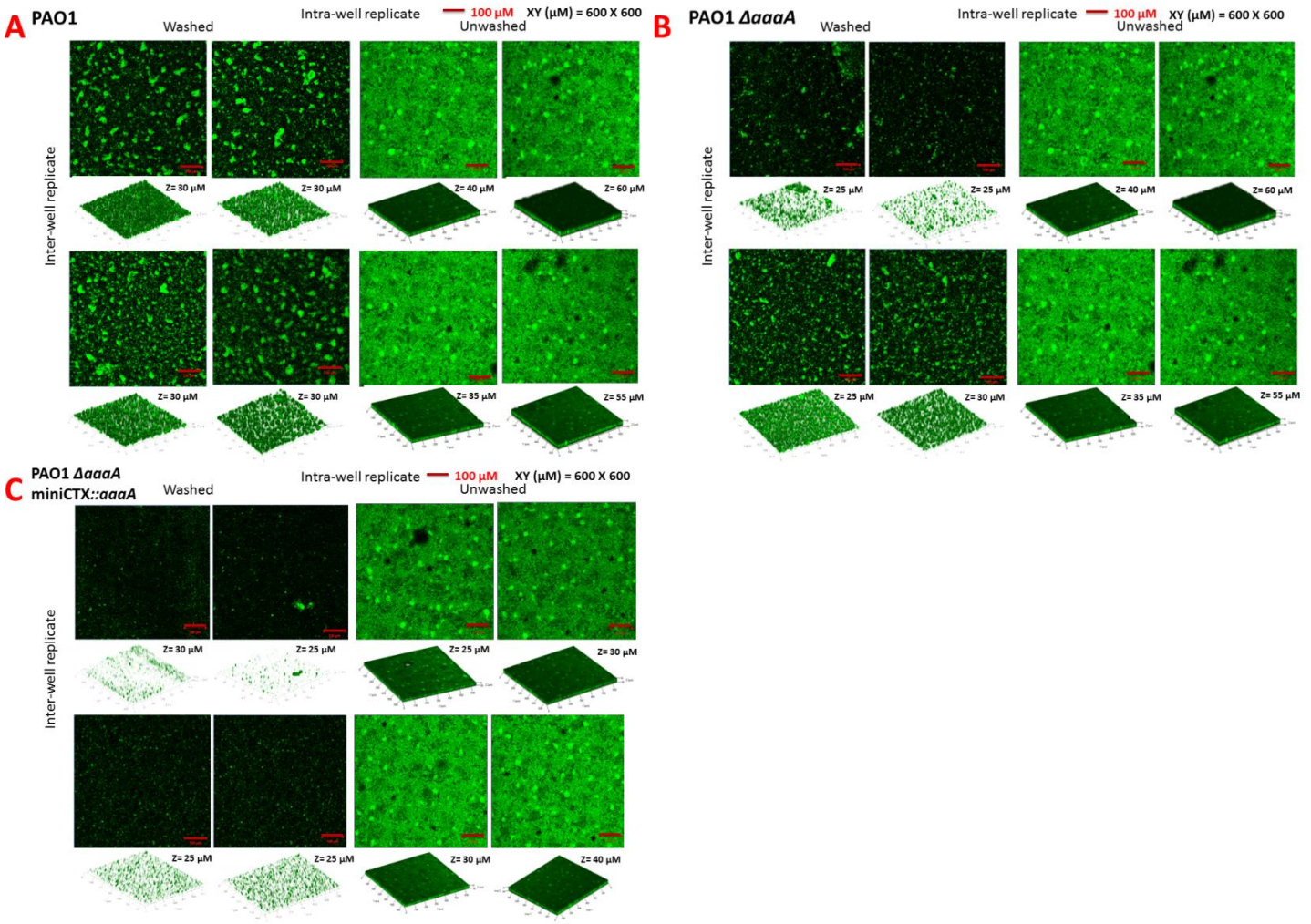
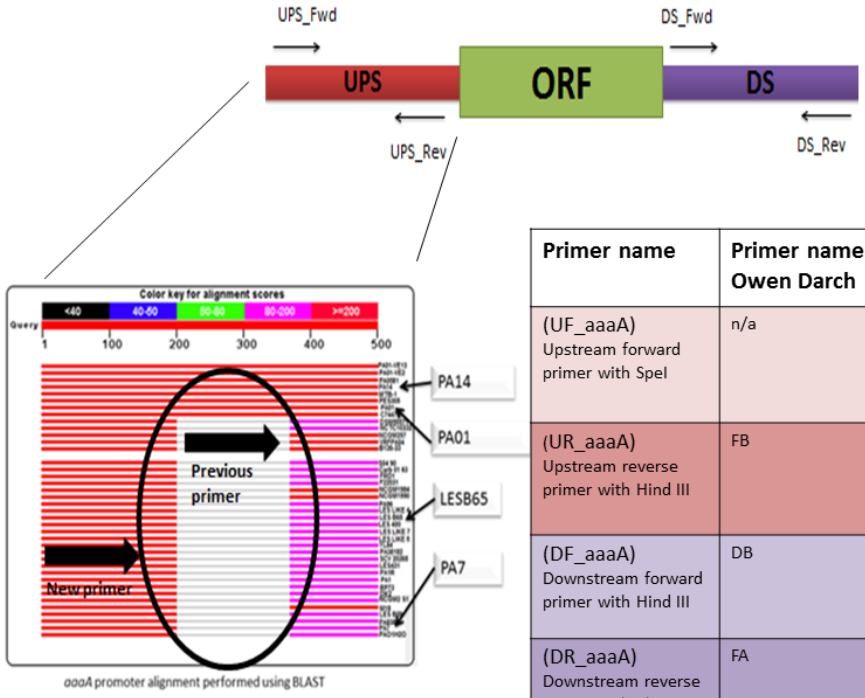


Figure 6.2.9: No difference in biofilm formation was found between PAO1 and PAO1 *ΔaaaA* strains grown in aerated, minimal media cocktail using the microchamber system, but PAO1 *ΔaaaA* miniCTX*::aaaA* produced less biofilm. The biofilms were grown statically at 37°C for 48 hours using the minimal media cocktail previously described. A= PAO1, B= *ΔaaaA,* C= PAO1 *ΔaaaA* miniCTX*::aaaA*. Two biological replicates are shown (top and bottom) and 2 technical replicates from each of these (left to right). All strains were tagged with T7-gfp and imaging was achieved using confocal microscopy. A magnification of 10x was used and z-stacks taken.

6.2.4 A LESB65 *ΔaaaA* strain was constructed which showed an activity phenotype similar to PAO1 *ΔaaaA*

In addition to creating laboratory conditions which are closer to an *in vivo* situation, experiments can be made more biologically relevant by the use of a *P. aeruginosa* strain endemic to CF patient airways. The Liverpool epidemic strain (LES) presents such an alternative. A collaboration project with Liverpool University and Roche biosciences aimed to investigate the link between AaaA and biofilm viability in both *in vitro* and *in vivo* (murine model) conditions. The *in vivo* work was carried out by Dr Elaine Waters and Prof Aras Kadioglu at the University of Liverpool and is mentioned later in this chapter.

The creation of a LESB65 *ΔaaaA* strain was a collaborative effort with the design and testing done here and the cloning work kindly achieved by Dr Elaine Waters. The LESB65 WT strain was provided by Dr Elaine Waters and Prof Aras Kadioglu. Thanks are also due to the kind help of Dr Diana Palenzuela who assisted with the design and initial cloning process. The previous construction of PAO1 *ΔaaaA* was achieved by Dr Owen Darch (thesis, 2013) by the amplification of upstream and downstream sequences, their insertion into a suicide vector pDM4 and cross-over event in PAO1. A similar strategy was used for the mutagenesis of LESB65 with the principle amendment that a new forward primer for the upstream section was designed to account for the deletion region in LESB65. This is shown in Figure 6.2.10.



Primer name	Primer name Owen Darch	Sequence 5-3'
(UF_aaaA) Upstream forward primer with SpeI	n/a	tatactagtATCTGAAGAAAGCGAAAGAC
(UR_aaaA) Upstream reverse primer with Hind III	FB	CTACAGCGACAGCTAATGGTTTGAACACggatcca
(DF_aaaA) Downstream forward primer with Hind III	DB	ataaagcttCTGGCAGTTCTGAGCG
(DR_aaaA) Downstream reverse primer with Xho1	FA	tatctcgagAGGCCATCGAGTACATCA

Figure 6.2.10: Strategy for the deletion of *aaaA* in LESB65. Sequences upstream and downstream of the aaaA ORF were selected for amplification by Dr Owen Darch (thesis, 2013). The forward primer fell within the upstream deletion region of LESB65 and therefore a new primer was designed to anneal further upstream.

Upon receiving the PAO1 *ΔaaaA* strain it was sequenced and the activity tested in LB media against PAO1 and PAO1 *ΔaaaA* strains (Figure 6.2.11). The activity of the LESB65 *ΔaaaA* strain was significantly different from the LESB65 WT.

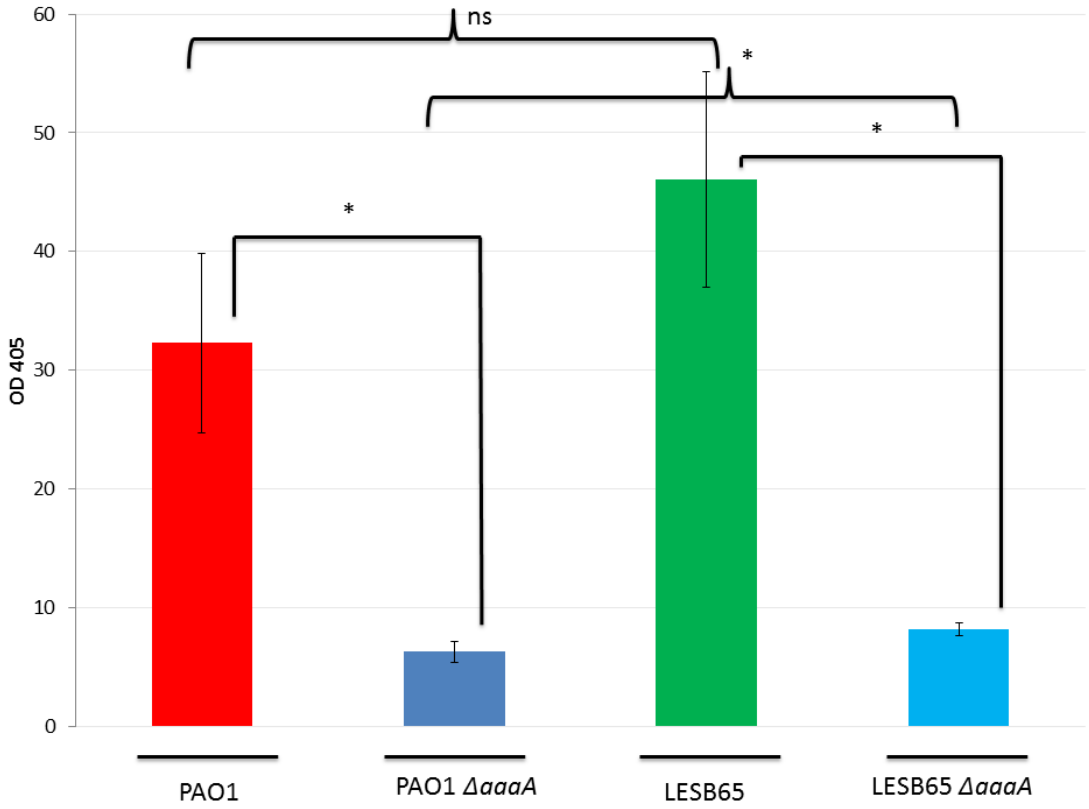


Figure 6.2.11: Activity of AaaA in LESB65 and LESB65 ΔaaaA strains grown in LB media is significantly different. PAO1, PAO1 *ΔaaaA,* LESB65 and LESB65 *ΔaaaA* were grown in LB until exponential phase. The cultures were washed 3x in MMP and standardised to OD_{600} 0.5. The cells were then incubated with the AaaA substrate L-arginine-p-nitroanilide for 24 hours at 37°C. The OD_{405} is representative of the p-nitroaniline dye cleavage from original molecule. Each bar shows the AUC of the OD_{405}.of the average of 3 biological replicates over 3 experiments. Error bars show the standard deviation between these. A t-test (with Welch's correction) was used between WT and *ΔaaaA* strains and between PAO1 and LESB65 strains, ns refers to non-significant and * refers to a significant result ($P < 0.05$).

As subsequent biofilm experiments would use ASM as a growth medium, the activity of PAO1, PAO1 *ΔaaaA*, LESB65 and LESB65 *ΔaaaA* was tested and compared to the activity of these strains in LB. There was no significant difference (Figure 6.2.12).

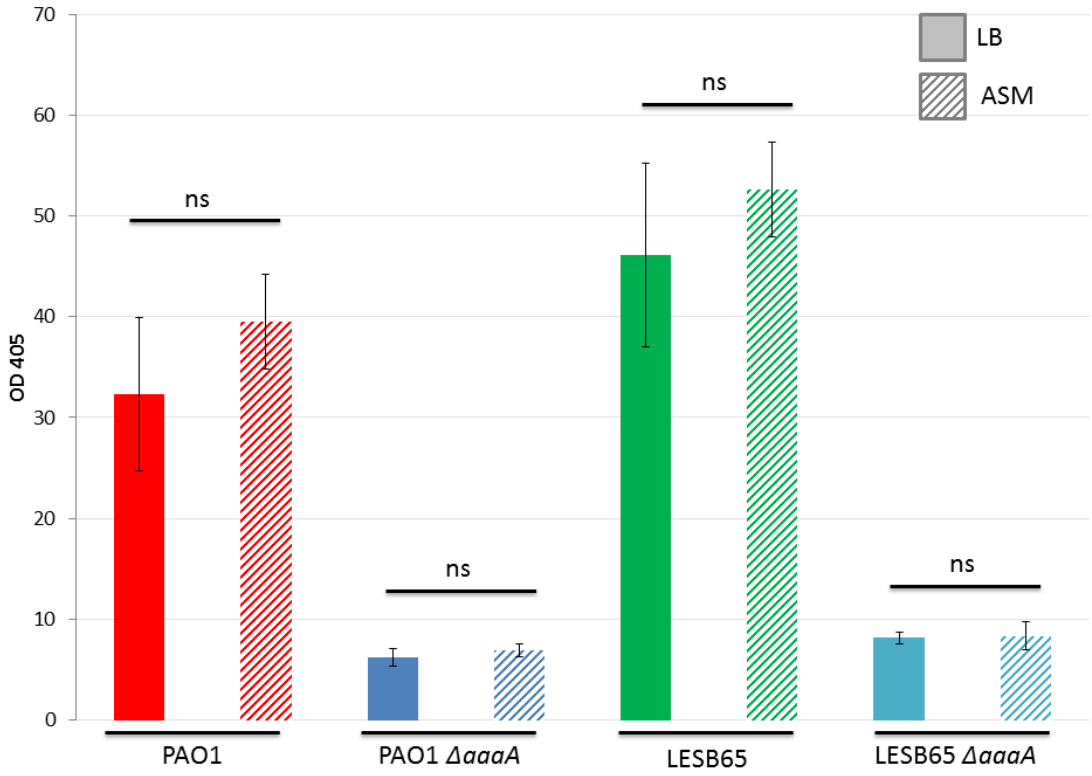


Figure 6.2.12: The activity of AaaA in LESB65 and PAO1 backgrounds did not differ significantly between ASM and LB. PAO1, PAO1 *ΔaaaA,* LESB65 and LESB65 *ΔaaaA* were grown in LB or ASM until exponential phase. The cultures were washed 3x in MMP and standardised to OD_{600} 0.5. The cells were then incubated with the AaaA substrate L-arginine-p-nitroanilide for 24 hours at 37°C. The OD_{405} is representative of the p-nitroaniline dye cleavage from original molecule. Each bar shows the AUC of the OD_{405}.of the average of 3 biological replicates over 3 experiments. Error bars show the standard deviation between these. A series of t-tests were used between equivalent strains in the different conditions: ns refers to non-significant and * refers to a significant result ($P < 0.05$). Note that the LB activity experiments were conducted on separate days to the ASM activity experiments.

6.2.5 PAO1 and PAO1 *ΔaaaA* do not differ when grown in aerobic ASM in a Bioflux system

To investigate whether there was a difference in the biofilm structure of PAO1 and PAO1 *ΔaaaA* when grown in a different model, the two strains were grown in the Bioflux system (previously described) starting from a cell density of OD_{600} 0.05 and continuing for 15 hours. The media used was ASM and the dyes were added to the inlet with the media at the concentrations of 1:4 µl/ml Syto9:PI. Confocal microscopy was conducted directly after the 15 hours was completed. Figure 6.2.13, Figure 6.2.14, and Figure 6.2.15 show the biofilms produced using this method.

Deletion of *aaaA* appeared not to have an effect on the biofilm forming capacity of PAO1. The two strains produced biofilms which were a similar consistency (clumpy), included a similar amount of red fluorescence (dead cells), and spanned a similar length of the tube. It was hypothesised that this could be due

to the experimental conditions, compensating systems such as pyruvate-phenazine, and the lab adjusted acute status of PAO1 (Chapter 4).

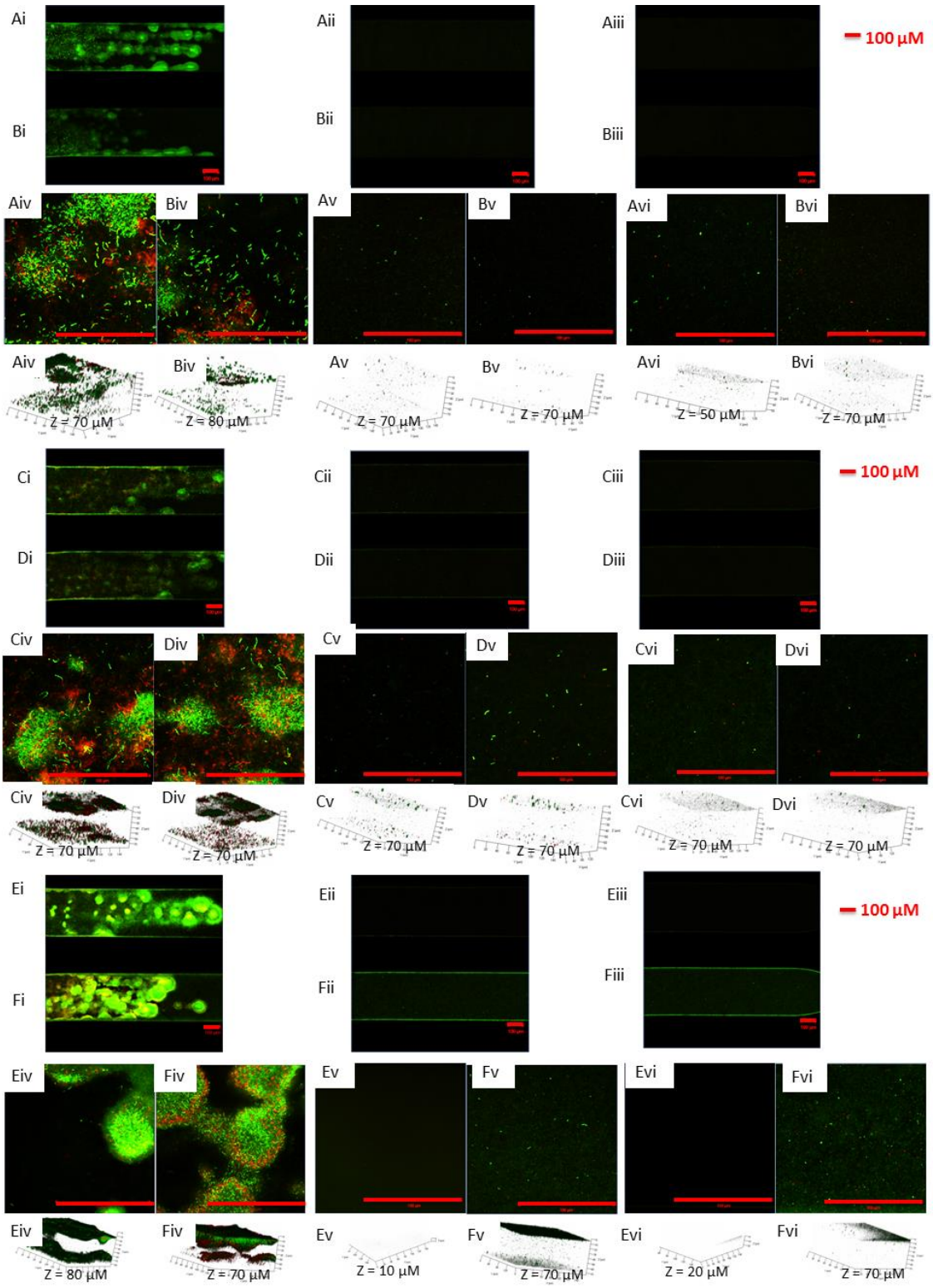


Figure 6.2.13: PAO1 forms a clumpy biofilm which is not affected by the deletion of *aaaA* in a Bioflux system. Biofilms were grown in ASM at 37°C over 15 hours aerobically. Confocal microscopy was taken at end point. Syto9 and PI were added to media in the inlet. Each letter refers to a separate flow cell containing a bacterial strain: A, C, E = PAO1 *ΔaaaA*; B, D, F = PAO1. Each pair (e.g A &B) were tested on the same day. Roman numerals refer to picture replicate number within the same flow cell. A picture was taken at the left side of the channel at 5x magnification (i), centre 5x (ii), right 5x (iii), a z stack at 20x left (iv), z stack at 20x centre (v), z stack at 20x right (vi).

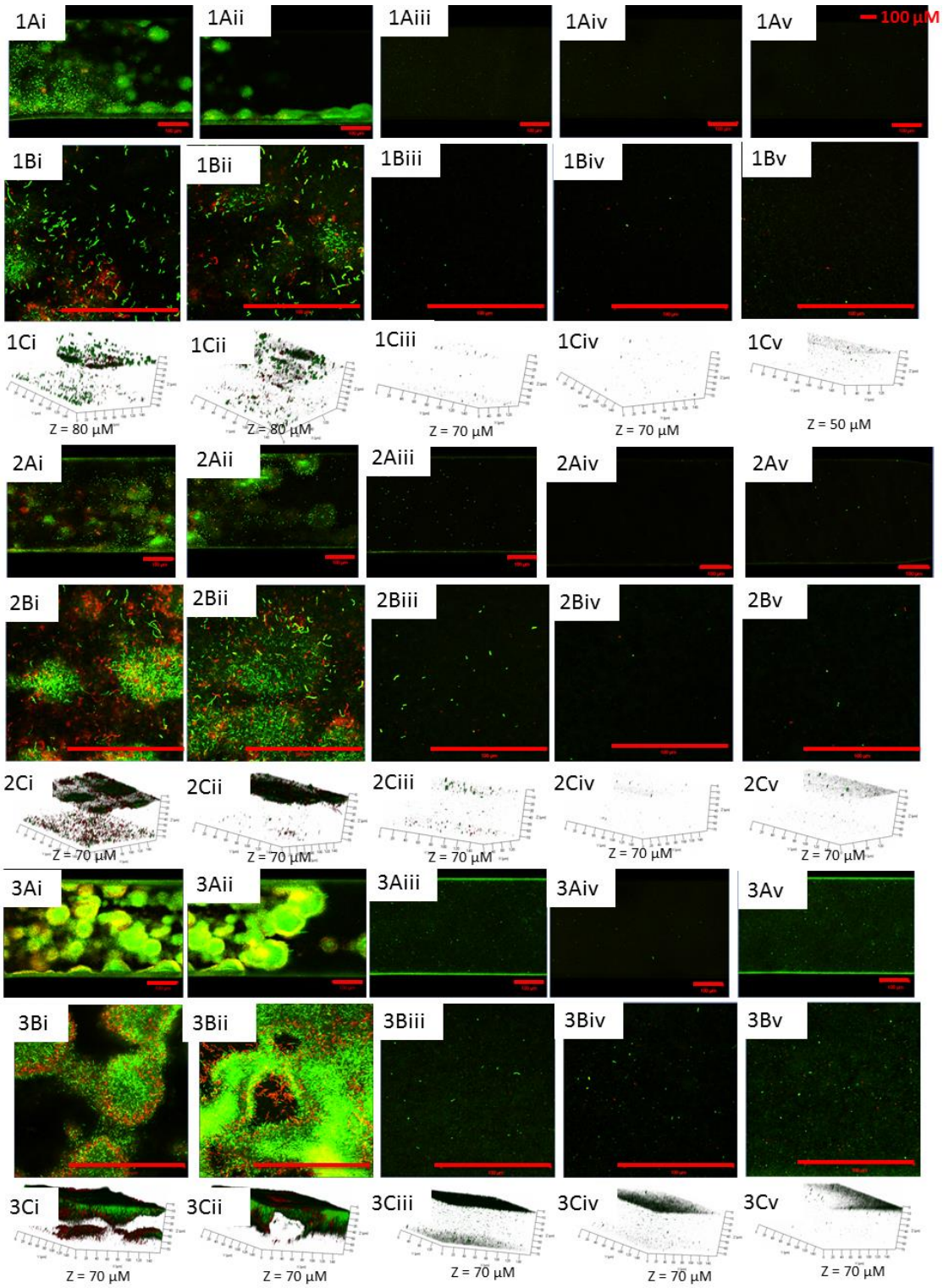


Figure 6.2.14: Showing all images taken across the Bioflux channel for the PAO1 biofilms. Biofilms were grown in ASM at 37°C over 15 hours aerobically. Confocal microscopy was taken at end point. Syto9 and PI were added to media in the inlet. Showing the 3 replications with 5 pictures spanning from left (inlet) to right (outlet) of the flow cell. Number refers to biological repeat; letter refers to the magnification A= 10x, B=40x and C=40x z stack; roman numerals refer to distance along the channel i=most left and v=most right.

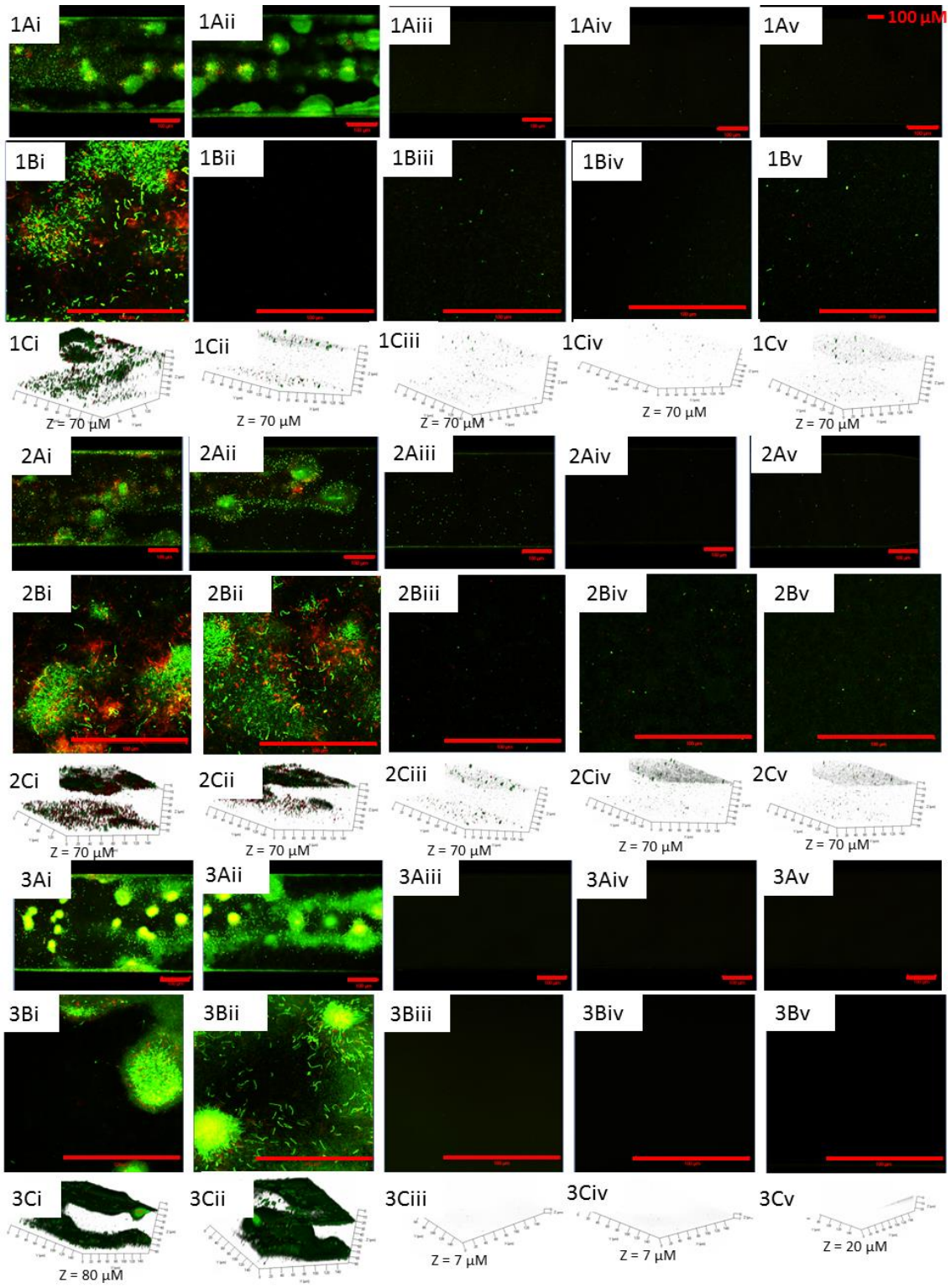


Figure 6.2.15: Showing all images taken across the Bioflux channel for the PAO1 *ΔaaaA* biofilms. Biofilms were grown in ASM at 37°C over 15 hours aerobically. Confocal microscopy was taken at end point. Syto9 and PI were added to media in the inlet. Showing the 3 replications with 5 pictures spanning from left (inlet) to right (outlet) of the flow cell. Number refers to biological repeat; letter refers to the magnification A= 10x, B=40x and C=40x z stack; roman numerals refer to distance along the channel i=most left and v=most right.

6.2.6 LESB65 biofilms differ structurally from PAO1 and the LESB65 *ΔaaaA* biofilms are thinner than the WT

Once the LESB65 *ΔaaaA* strain was available, the biofilm forming capacity of WT and mutant LESB65 strains were tested using the Bioflux system. The experiment was conducted in an identical manner to the PAO1 Bioflux experiment with the exception that only 3 pictures per channel (left, middle and right) at each magnification were taken due to time constraints and a magnification of 20x substituting the 40x due to issues with the objectives at the time of these experiments. However it was thought that this did not greatly affect the interpretation of the images.

The LESB65 biofilm structure was different from that of PAO1 and is unsurprisingly closer to the biofilms produced by the CF isolates shown in Chapter 4 (Figure 6.2.16). There are less distinct microcolonies, more small clusters throughout a wider area. This could be due to the chronic nature of LESB65 and the biofilms could be slower to form. Alternatively, this type of biofilm structure could be the result of a *lasB* mutation, flagella loss or lack of type IV pili (Kamath *et al* 1998; Klausen *et al* 2003; Costerton *et al* 1999; O'Toole *et al* 2000; Stoodley *et al* 2002). There are less red fluorescent units (dead cells), perhaps due to a greater spacing of smaller clusters rather than big tight clumps which would theoretically increase the oxygen and nutrient gradient between the surface and inner cells.

There was a marked difference between the LESB65 WT and LESB65 *ΔaaaA* strains. This contrasts with the PAO1 and PAO1 *ΔaaaA* biofilms which were similar to each other. This could indicate the *aaaA* has more of a role in chronic conditions and other genetic modifications in the LESB65 strain for the CF lung environment cause this strain to be more dependent on AaaA.

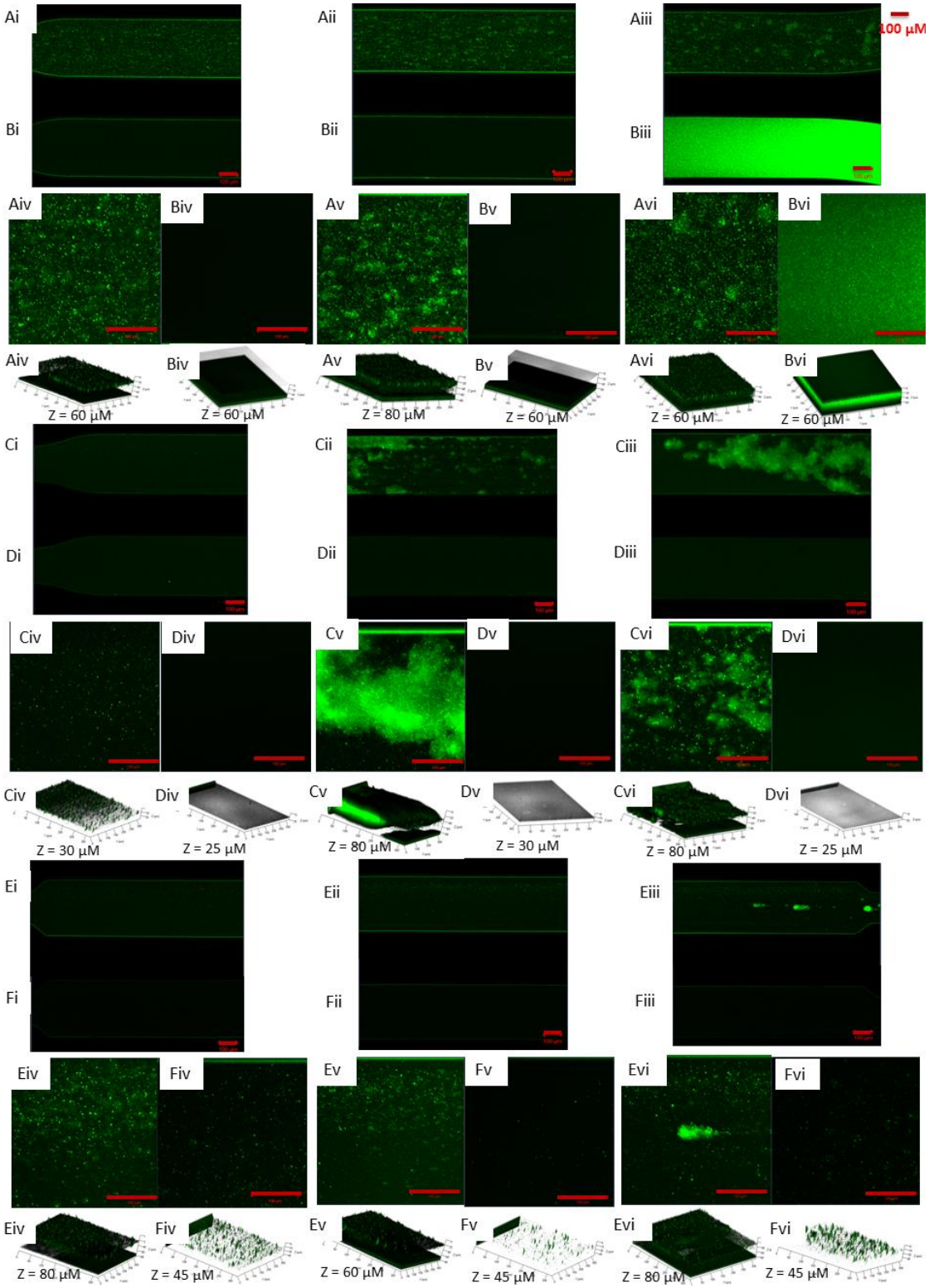


Figure 6.2.16: LESB65 forms biofilm that is reduced in thickness upon deletion of *aaaA* in a Bioflux system. Biofilms were grown in ASM at 37°C over 15 hours aerobically. Confocal microscopy was taken at end point. Syto9 and PI were added to media in the inlet. Each letter refers to a separate flow cell containing a bacterial strain: A, C, E = LESB65 WT; B, D, F = LESB65 *ΔaaaA.* Each pair (e.g A &B) were tested on the same day. Roman numerals refer to picture replicate number within the same flow cell. A picture was taken at the left side of the channel at 5x magnification (i), centre 5x (ii), right 5x (iii), a z stack at 20x left (iv), z stack at 20x centre (v), z stack at 20x right (vi).

6.2.7 Investigation of arginine and tripeptide on PAO1 biofilms using the Bioflux model showed biofilm production in the *ΔaaaA* mutant was impaired when arginine was absent

To investigate if arginine availability affected the reliance of *P. aeruginosa* on AaaA to form biofilm, the ASM was modified to contain no arginine, twice the amount of arginine, 10 mM tripeptide and 10 mM tripeptide with no arginine. The concentration of tripeptide was chosen because the minimal media experiments demonstrated that PAO1 was able to grow using this amount and the high expense of the compound made its use limiting. The strains were grown in the appropriate media overnight, normalised to OD_{600} 0.05 in fresh media of the same category and the corresponding media added to the inlet well during the Bioflux set up.

In ASM without modifications (Figure 6.2.17) PAO1 and PAO1 *ΔaaaA* produced similar biofilms. There were no striking differences in the structure and spread. Addition of twice the usual amount of arginine to the ASM resulted in both strains producing a biofilm showing more dispersal around the edges of the clusters (Figure 6.2.18). There was not a repeatable difference between the biofilms produced by WT and mutant strains. The addition of tripeptide 10 mM to ASM (Figure 6.2.19) did also not result in a difference in biofilm production between the strains. Whether the biofilm differed from that of the normal ASM is difficult to say as the two repeats were different from one another. ASM without arginine however (Figure 6.2.20), created a disadvantage for the PAO1 *ΔaaaA* strain which produced less biofilm than the PAO1 WT. This could also be the case for ASM without arginine + tripeptide (Figure 6.2.21) but in one repeat the biofilms appeared mostly dead (largely red fluorescence) and therefore more repeats with a higher concentration of tripeptide (the equivalent concentration to the starting concentration of arginine in ASM) would need to be generated to determine this.

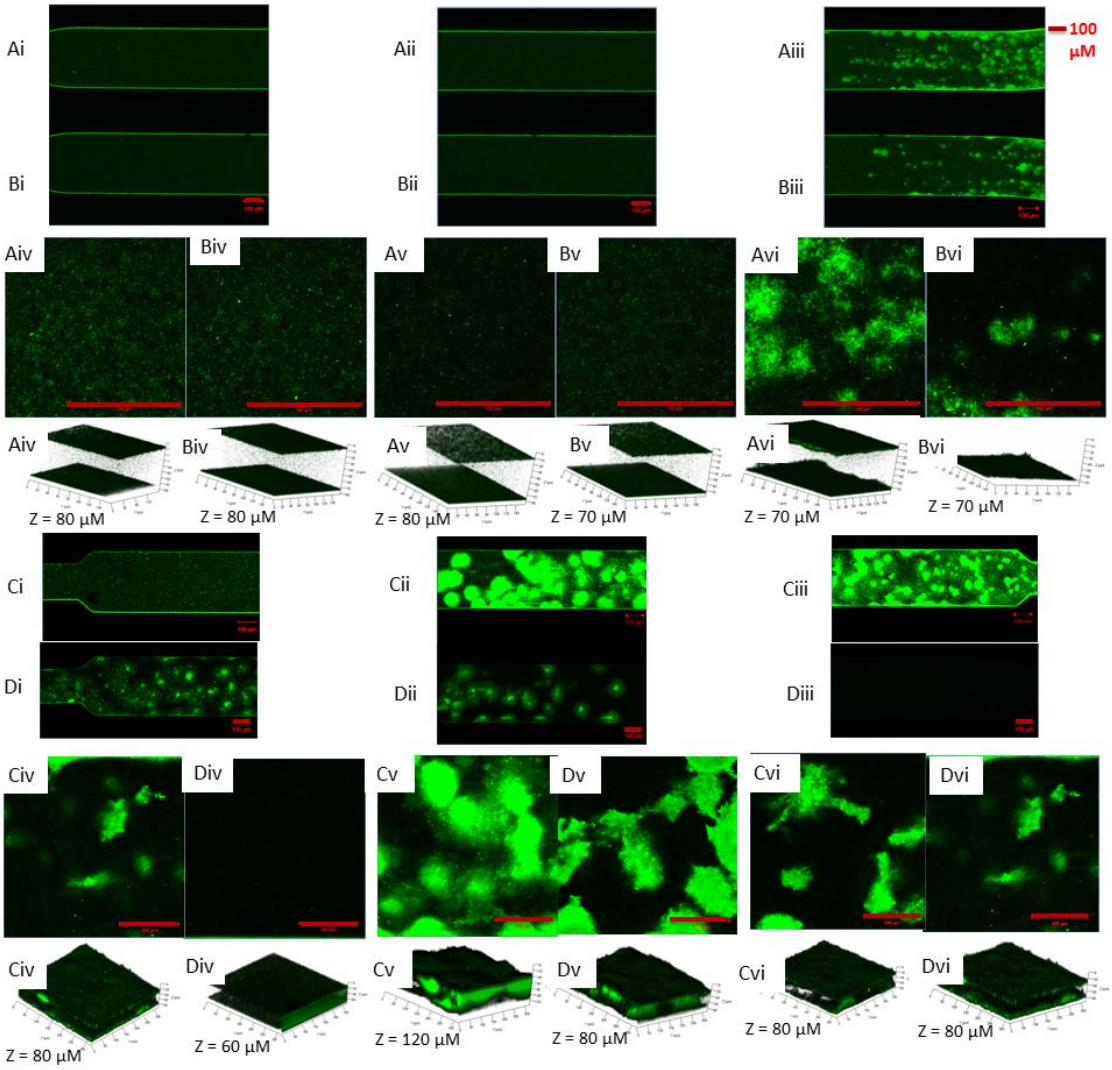


Figure 6.2.17: PAO1 and PAO1 *ΔaaaA* in normal ASM produce biofilms similar to each other when grown in the Bioflux system for 15 hours, 37°C aerobically. Confocal microscopy was taken at end point. Syto9 and PI were added to media in the inlet. Each letter refers to a separate flow cell containing a bacterial strain: A &C = PAO1; B & D = PAO1 *ΔaaaA.* Roman numerals refer to picture replicate number within the same flow cell. A picture was taken at the left side of the channel at 5x magnification (i), centre 5x (ii), right 5x (iii), a z stack at 20x left (iv), z stack at 20x centre (v), z stack at 20x right (vi).

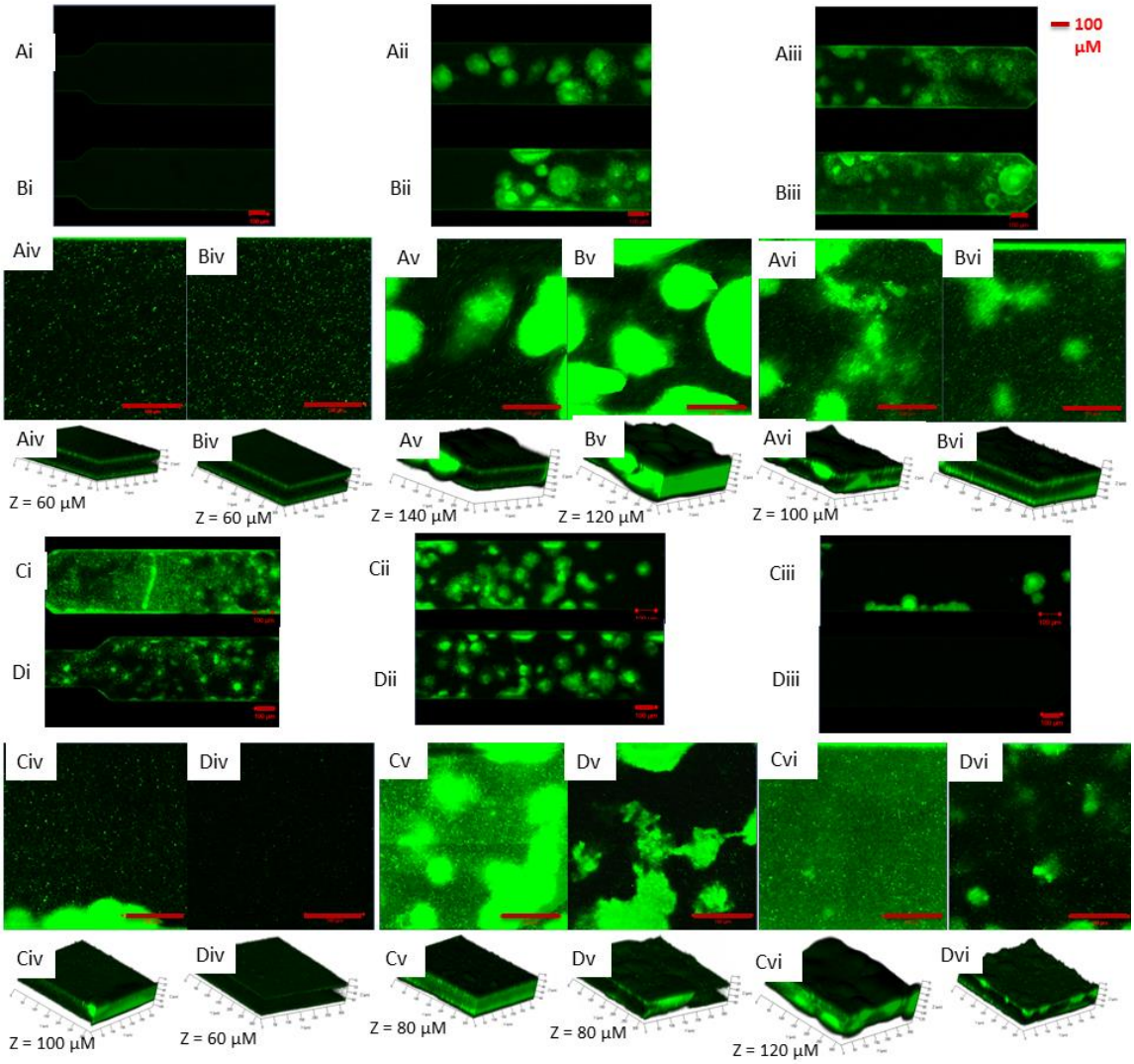


Figure 6.2.18: PAO1 and PAO1 *ΔaaaA* in ASM 2x arginine produced biofilms showing greater dispersal from the clusters and did not show a repeatable difference between the strains when grown in the Bioflux system for 15 hours, 37°C aerobically. Confocal microscopy was taken at end point. Syto9 and PI were added to media in the inlet. Each letter refers to a separate flow cell containing a bacterial strain: A &C = PAO1; B & D = PAO1 *ΔaaaA.* Roman numerals refer to picture replicate number within the same flow cell. A picture was taken at the left side of the channel at 5x magnification (i), centre 5x (ii), right 5x (iii), a z stack at 20x left (iv), z stack at 20x centre (v), z stack at 20x right (vi).

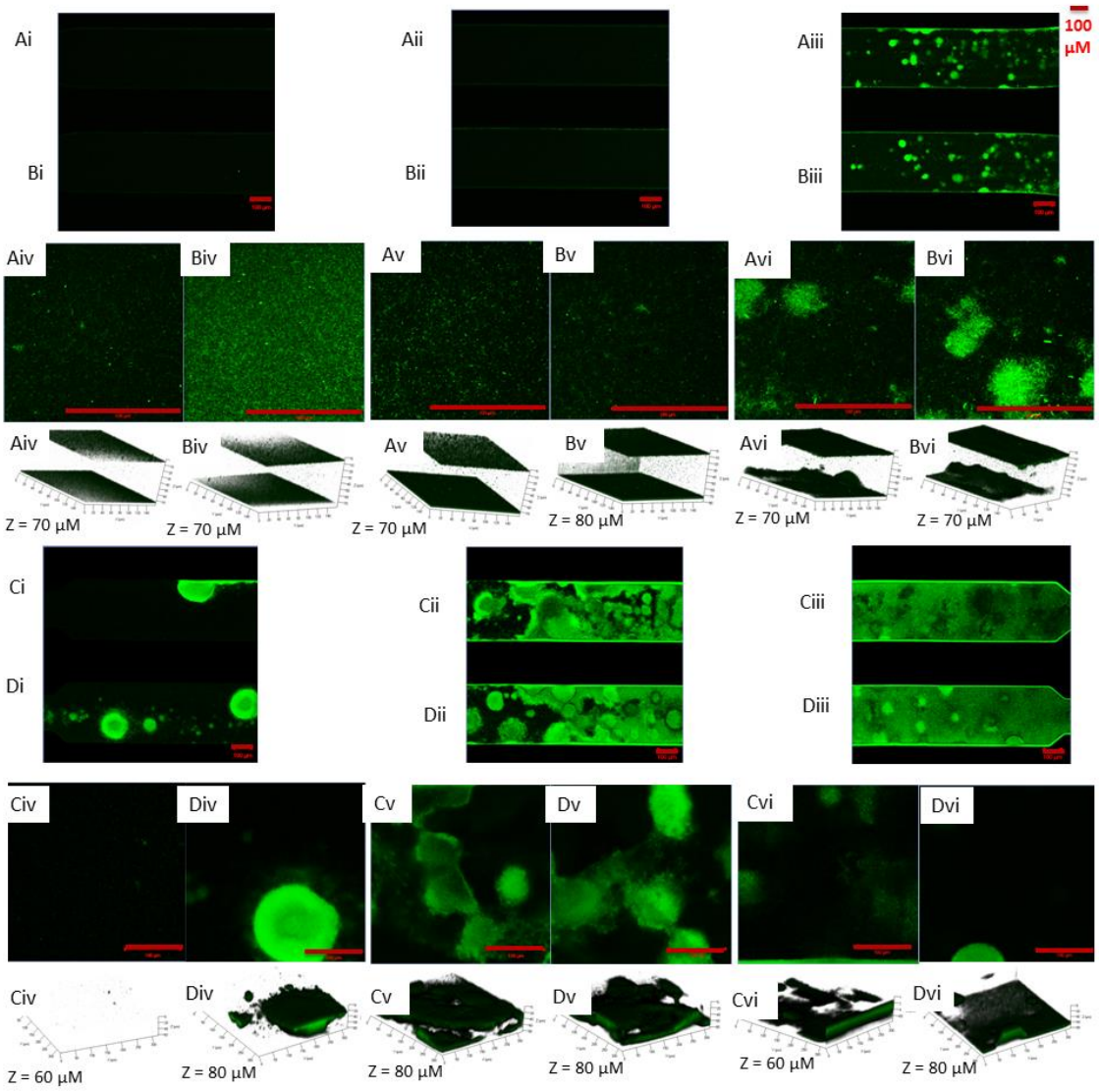


Figure 6.2.19: PAO1 and PAO1 *ΔaaaA* in ASM + 10 mM tripeptide produced biofilms which were similar in both strains when grown in the Bioflux system for 15 hours, 37°C aerobically. Confocal microscopy was taken at end point. Syto9 and PI were added to media in the inlet. Each letter refers to a separate flow cell containing a bacterial strain: A &C = PAO1; B & D = PAO1 *ΔaaaA.* Roman numerals refer to picture replicate number within the same flow cell. A picture was taken at the left side of the channel at 5x magnification (i), centre 5x (ii), right 5x (iii), a z stack at 20x left (iv), z stack at 20x centre (v), z stack at 20x right (vi).

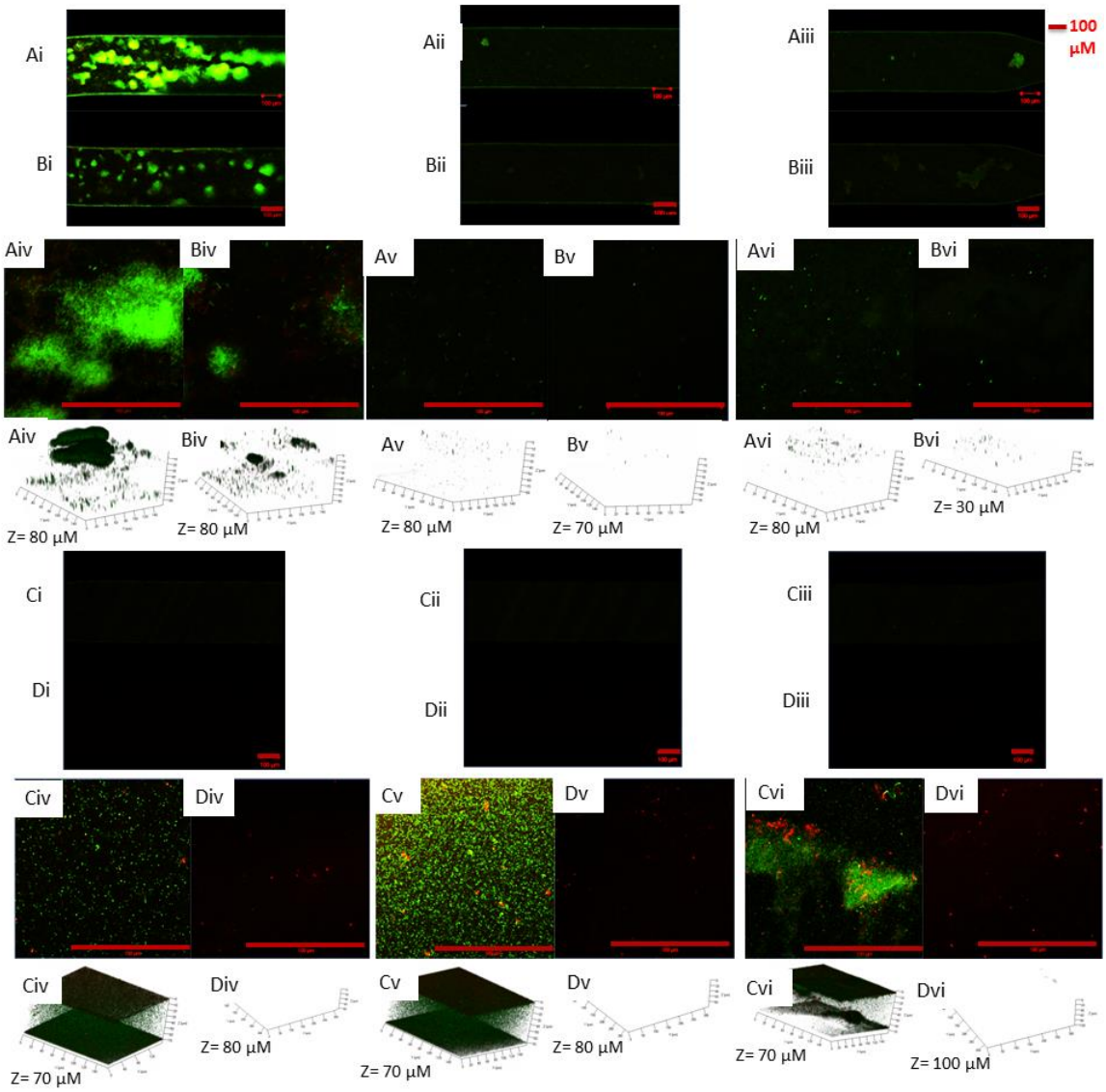


Figure 6.2.20: PAO1 and PAO1 *ΔaaaA* in ASM without arginine created a difference in biofilm formation between the WT and mutant strains when grown in the Bioflux system for 15 hours, 37°C aerobically. Confocal microscopy was taken at end point. Syto9 and PI were added to media in the inlet. Each letter refers to a separate flow cell containing a bacterial strain: A &C = PAO1; B & D = PAO1 *ΔaaaA.* Roman numerals refer to picture replicate number within the same flow cell. A picture was taken at the left side of the channel at 5x magnification (i), centre 5x (ii), right 5x (iii), a z stack at 20x left (iv), z stack at 20x centre (v), z stack at 20x right (vi).

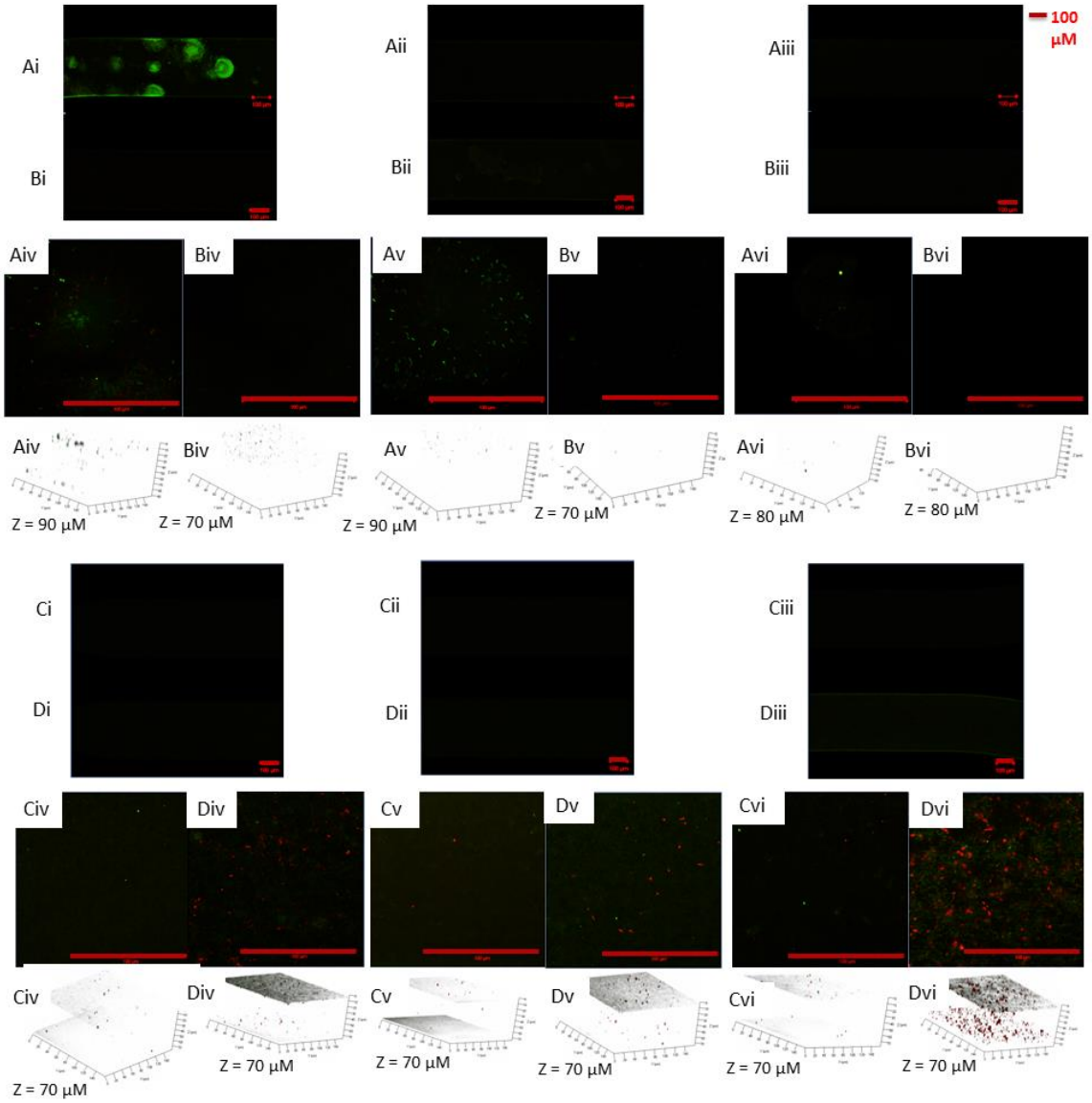


Figure 6.2.21: PAO1 and PAO1 *ΔaaaA* in ASM without arginine + tripeptide may have created a difference in biofilm formation between the WT and mutant strains when grown in the Bioflux system for 15 hours, 37°C aerobically, but as the biofilms are not healthy in the second repeat this would need to be determined by further investigation. Confocal microscopy was taken at end point. Syto9 and PI were added to media in the inlet. Each letter refers to a separate flow cell containing a bacterial strain: A &C = PAO1; B & D = PAO1 *ΔaaaA.* Roman numerals refer to picture replicate number within the same flow cell. A picture was taken at the left side of the channel at 5x magnification (i), centre 5x (ii), right 5x (iii), a z stack at 20x left (iv), z stack at 20x centre (v), z stack at 20x right (vi).

6.2.8 PAO1 and PAO1 *ΔaaaA* biofilms do not differ when grown in either aerobic or microaerobic conditions in ASM using the microchamber model

The previous biofilm experiments had been conducted in aerobic conditions and as it was hypothesised that *aaaA* would have the greatest influence under low oxygen concentrations, biofilm growth in microaerobic conditions was investigated. Microaerobic conditions in particular were chosen to be as close as possible to the CF airway oxygen concentrations. This could not be achieved using

the Bioflux system available and therefore an alternative system was used to generate biofilms: the 8 well chamber slide system used previously. Overnight cultures of PAO1 and PAO1 *ΔaaaA* tagged with T7-gfp were grown for 18 hours in ASM 37°C 200 rpm and then normalised to an OD_{600} of 0.05 in fresh ASM. To each well 500 µl of normalised culture was added. The chamber slide was then placed in a 37°C incubator (static) and left to grow for 48 hours. A 24 and 48 hour comparison previously showed that this amount of time was required for more robust biofilms to be formed (data not shown). For the microaerobic conditions the overnight cultures were placed in a jar containing a microaerobic sachet and treated in the same manner as the aerobic counterparts. Following normalisation, the chamber slides were sealed inside a pouch containing a microaerobic sachet and treated in the same way as the aerobic chamber slides.

Prior to imaging the biofilms were incubated for 30 minutes at room temperature, in aerobic conditions shielded from light with PI for the dead cell staining. This also allowed the GFP protein fluorescence to develop in the microaerobic chamber biofilms. The media was gently removed from the top of the biofilms leaving a meniscus of liquid covering the thicker bottom layer. Previous trials with chambers where the media was not removed showed poorer images and full media removal disrupted the biofilm. Washing was also tried but this also caused a disruption of the biofilm which was decided to be more of a problem than the potential for some planktonic cells to remain in the well (data not shown). Six images were taken per chamber well (random positioning) to ensure that variation within the well was represented faithfully.

The first observation from this experiment was that the microaerobic biofilms showed slightly more coverage than the aerobically grown biofilms in both PAO1 and PAO1 *ΔaaaA* (Figure 6.2.22, Figure 6.2.23, Figure 6.2.24, and Figure 6.2.25). Following this it was observed that the PAO1 and PAO1 *ΔaaaA* did not differ substantially from one another. This suggests that low oxygen tension is not enough for the cells to require the action of AaaA. ASM contains arginine and nitrate sources (previously described and also shown in the materials and methods). This may be enough for the biofilms to cope without the activity of AaaA. Further experiments using the minimal media cocktail and comparison of LESB65 and LESB65 *ΔaaaA* would be helpful in investigating which conditions cause AaaA to have a pivotal role.

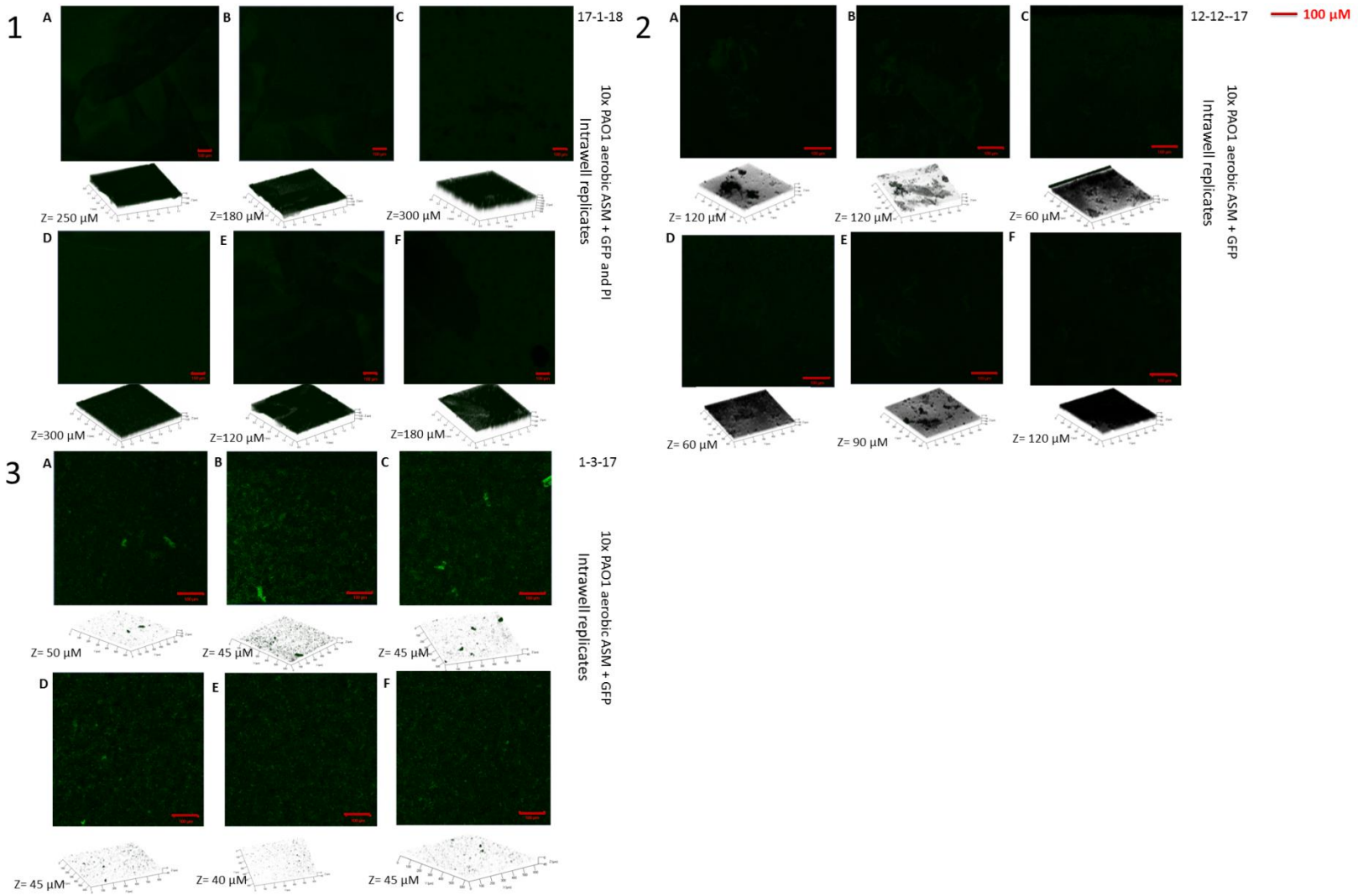


Figure 6.2.22: : PAO1 T7-gfp biofilms grown in aerobic ASM in 8 well chamber slides for 48 hours show a flat, thin patchy biofilm. Images were taken using confocal microscopy, the green colour showing GFP fluorescence and the red colour showing PI stained cells. Each number shows a separate biological isolate and each letter shows a randomly selected area within the well (intrawell replicate). Images and z stacks were taken at 10x magnification.

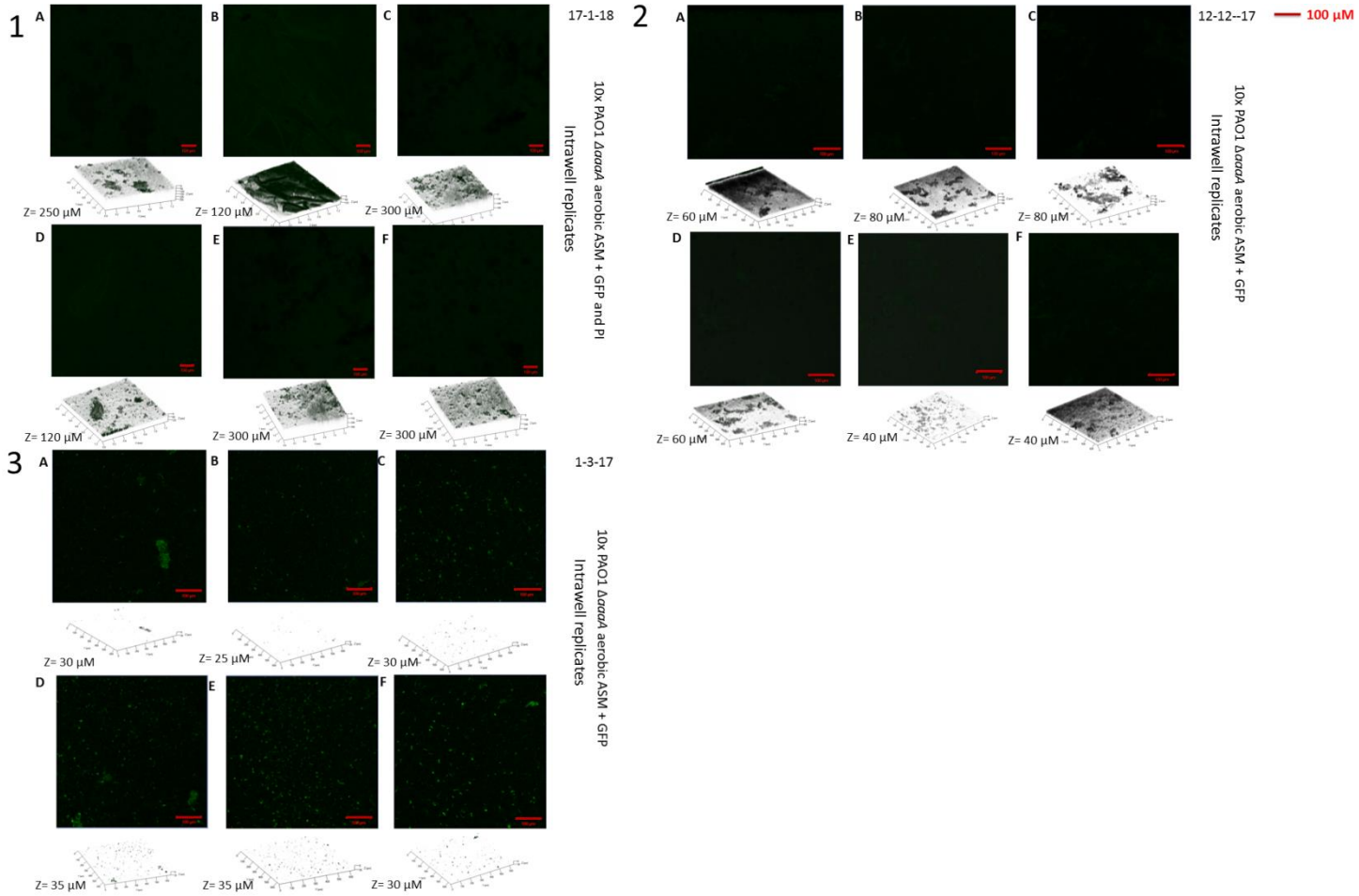


Figure 6.2.23: PAO1 *ΔaaaA* T7-gfp biofilms grown in aerobic ASM in 8 well chamber slides for 48 hours show a flat, thin patchy biofilm. Images were taken using confocal microscopy, the green colour showing gfp fluorescence and the red colour showing PI stained cells. Each number shows a separate biological isolate and each letter shows a randomly selected area within the well (intrawell replicate). Images and z stacks were taken at 10x magnification.

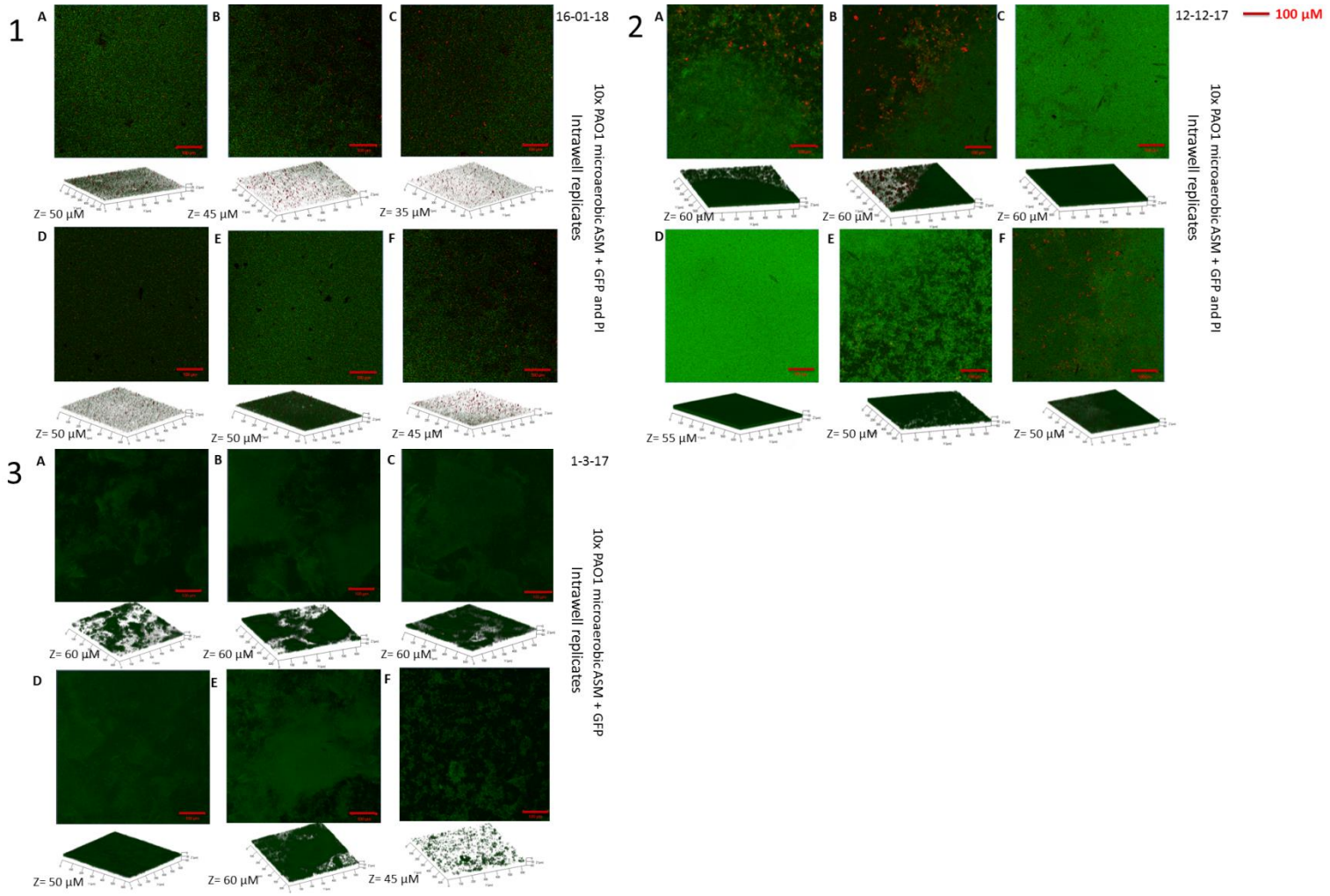


Figure 6.2.24: PAO1 T7-gfp biofilms grown in microaerobic ASM in 8 well chamber slides for 48 hours show a flat, thin patchy biofilm. Images were taken using confocal microscopy, the green colour showing GFP fluorescence and the red colour showing PI stained cells. Each number shows a separate biological isolate and each letter shows a randomly selected area within the well (intrawell replicate). Images and z stacks were taken at 10x magnification.

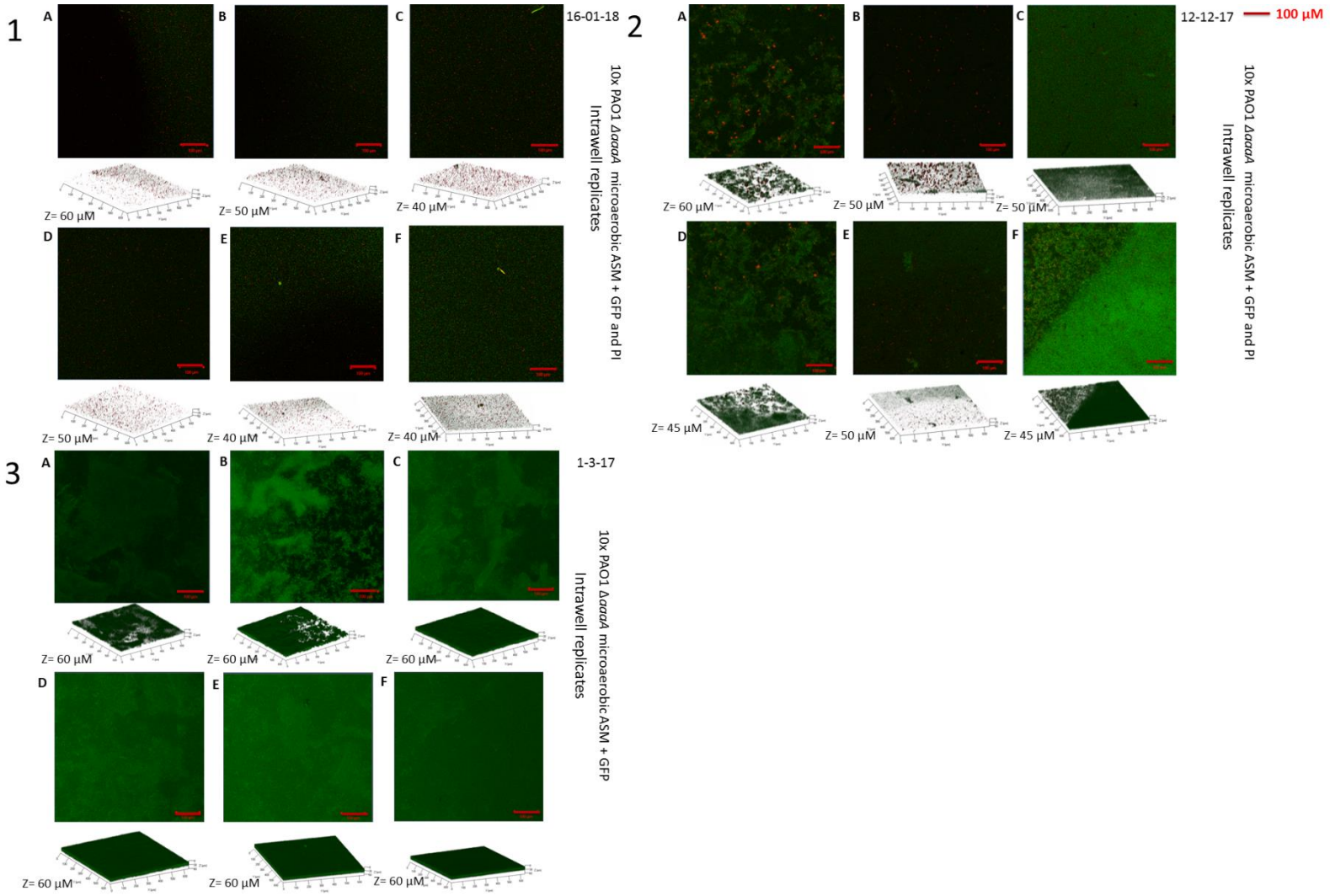


Figure 6.2.25: PAO1 *ΔaaaA* T7-gfp biofilms grown in microaerobic ASM in 8 well chamber slides for 48 hours show a flat, thin patchy biofilm. Images were taken using confocal microscopy , the green colour showing gfp fluorescence and the red colour showing PI stained cells. Each number shows a separate biological isolate and each letter shows a randomly selected area within the well (intrawell replicate). Images and z stacks were taken at 10x magnification.

6.2.9 Making an IPTG independent complemented PA01 *ΔaaaA* strain

Prior to this work the PAO1 *ΔaaaA* strain had been complemented by a copy of the *aaaA* ORF inserted under a *Ptac* promoter in the pME6032 plasmid. This had the two caveats that that the copy number of *aaaA* would be greater in the complemented strain than the WT and induction by IPTG would be required. A previous study found that IPTG can have a dispersive effect on biofilms (Johansson *et al* 2008). An alternative to this complementation strategy was also available in the form of the *aaaA* ORF under the control of its own promoter inserted into the chromosome using the vector miniCTX-1 which has been previously described in this thesis. This has the advantage of a chromosomal location and as close to natural expression as can be achieved when a gene is placed in a non-native location (Hoang *et al* 2000). However, this does not allow the controlled comparison of activated (induced) and non-activated (non-induced) gene conditions within the same strain. Additionally, an inducible strain can be activated at different points in an experiment which would allow observation of the effect *aaaA* has in an already mature biofilm. For this purpose an inducible *aaaA* strain was designed that placed *aaaA* under the control of an arabinose inducible promoter *araBAD* (Newman and Fuqua 1999; Khlebnikov *et al* 2000) at the neutral *attB* site targeted by the miniCTX-1 vector.

6.2.10 Cloning

Figure 6.2.26 depicts the cloning strategy of the new inducible *aaaA* strain. A copy of the *aaaA* ORF under the control of *araBAD* existed (*pla33::araC::aaaA*) for use in an *E. coli* based localisation study by Dr Mahmoud Ashawesh (thesis, 2017) and was kindly donated by Dr Mahmoud Ashawesh for this work. The *araBAD* promoter, *araC* gene and *aaaA* ORF were removed from the *pla33::araC::aaaA* plasmid by restriction digestion. The enzymes used were NsiI (prior to *araC*) and EcoRI (post *aaaA*). The cut fragment was ligated with miniCTX-1 cut with PstI and EcoRI. This resulted in a desulting site at the NsiI-PstI ligated ends. Further checking of the clones was achieved with using a NotI site slightly upstream from this. The ligated vector was transformed into *E. coli* S17-λpir, checked by restriction digest and sequencing, and then conjugated into PAO1 and PAO1 *ΔaaaA*. These strains were subsequently labelled PAO1 miniCTX*::araC::aaaA* and PAO1 *ΔaaaA* miniCTX*::araC::aaaA*. The cloning strategy was generously assisted by Professor Stephan Heeb.

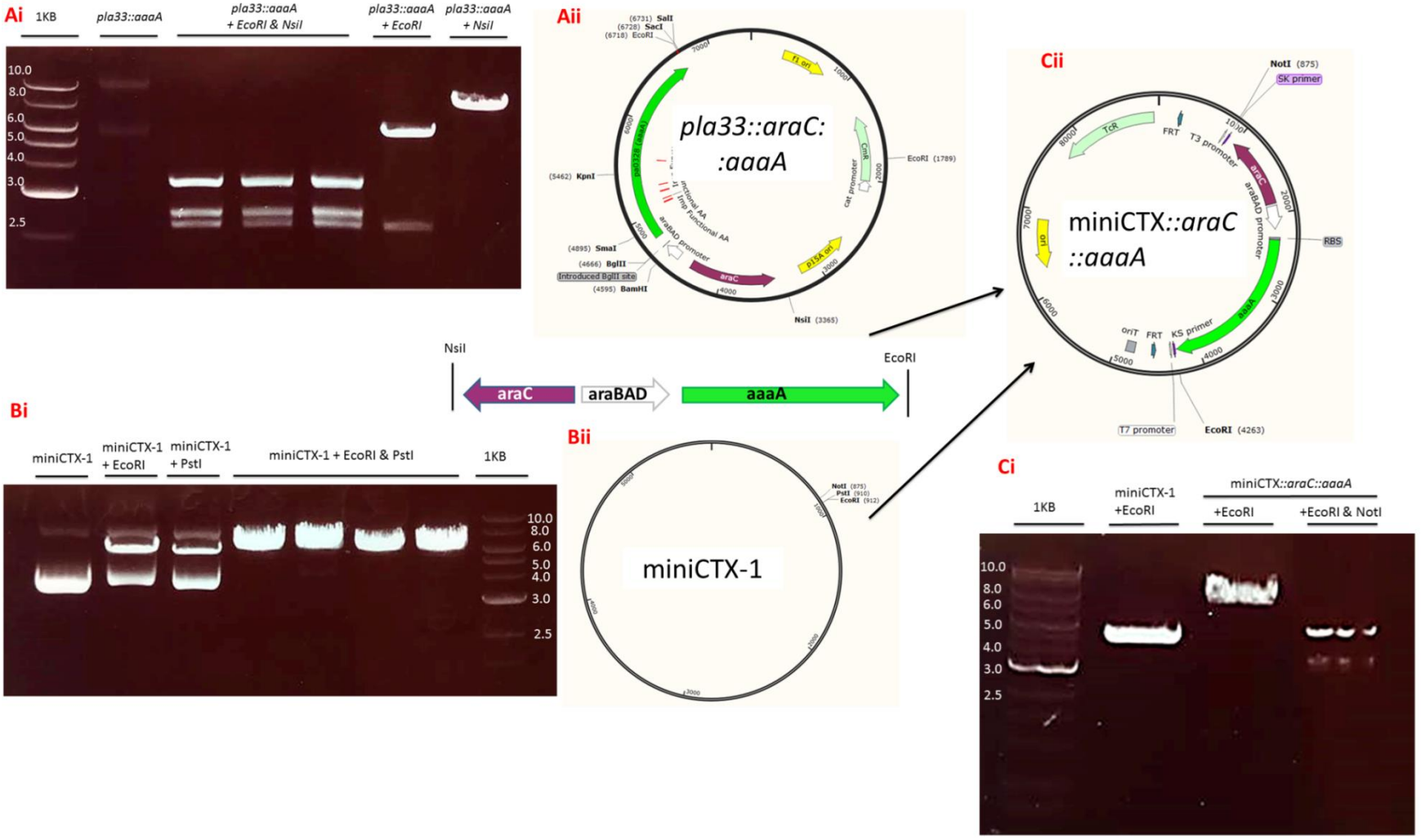


Figure 6.2.26: Construction of *miniCTX::araC::aaaA*. The plasmid *pla33::araC::aaaA* was digested with NsiI and EcoRI (A). Three bands can be seen on the gel, which are the result of a second EcoRI site (Ai). The top band was taken, purified, and ligated with cut miniCTX-1 (B). The ligation of the NsiI and PstI cut sites resulted in a desulting site and therefore NotI was used to liberate the ligated insert from the plasmid backbone following successful transformation (C).

6.2.10.1 Testing of the miniCTX::araC::aaaA clones for AaaA activity

Following the insertion of the *miniCTX::araC::aaaA* construct into the *P. aeruginosa* strains, the strains were tested for AaaA activity. This testing included 3 separate conjugant clones of WT and mutant background over the course of 3 experiments. The activity assay proceeded as previously described in LB medium. The inducible strains were incubated for 2 hours with 0.02% of arabinose. The activity assay proceeded for 24 hours and the AUC of this is represented in Figure 6.2.27 below.

As Figure 6.2.27 shows, the induced and non-induced conditions were not statistically different. This indicated that the concentration of arabinose or length of induction required optimisation.

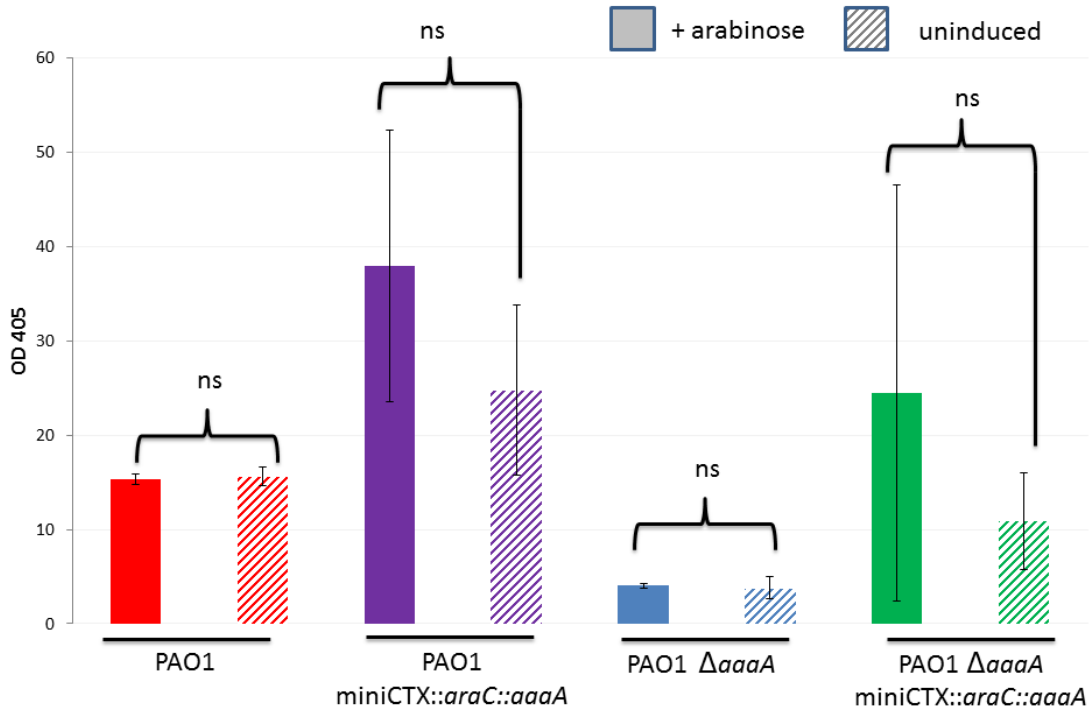


Figure 6.2.27: Activity of AaaA in PAO1 and PAO1 *ΔaaaA* conjugated with miniCTX::*araC::aaaA* in LB is not significantly different when the inducer is present. PAO1, PAO1 miniCTX::*araC::aaaA*, PAO1 *ΔaaaA* and PAO1 *ΔaaaA* miniCTX::*araC::aaaA* were grown in LB until exponential phase. One strain representative was induced with 0.02% arabinose for 2 hours and the other was incubated for 2 hours without the inducer. The cultures were then washed 3x in MMP and standardised to OD_{600} 0.5, before incubation with the AaaA substrate L-arginine-p-nitroanilide for 24 hours at 37°C. The OD_{405} is representative of the p-nitroaniline dye cleavage from original molecule. Each bar shows the AUC of the OD_{405}.of the average of 3 biological replicates over 3 experiments. Solid bars indicate non-induced and striped bars indicate induced strains. The labels ns and * indicate the significance of variation determined by t- test.

6.2.10.2 Selection of arabinose concentration to use and leakage testing

For the inducible strain to be useful for biofilm investigation experiments there needed to be a difference between induced and non-induced conditions. The induced strain should also show WT or greater levels of AaaA activity. Therefore an arabinose induction gradient was tested and is shown in Figure 6.2.28. Both PAO1 *ΔaaaA* miniCTX*::araC::aaaA* strains induced with 0.02% or 0.2% were significantly different from the PAO1 *ΔaaaA* strain. The 0.02% condition showed that the induced PAO1 *ΔaaaA* miniCTX*::araC::aaaA* strain was not significantly different from the WT activity, while the 0.2% condition showed that induced PAO1 *ΔaaaA* miniCTX*::araC::aaaA* had increased AaaA activity. These two concentrations of arabinose would therefore be suitable in further experiments which compared the inducible strain with the PAO1 and PAO1 *ΔaaaA* strains. When the comparison would be between induced and uninduced strains the higher concentration of arabinose should be used (Figure 6.2.28, Figure 6.2.27).

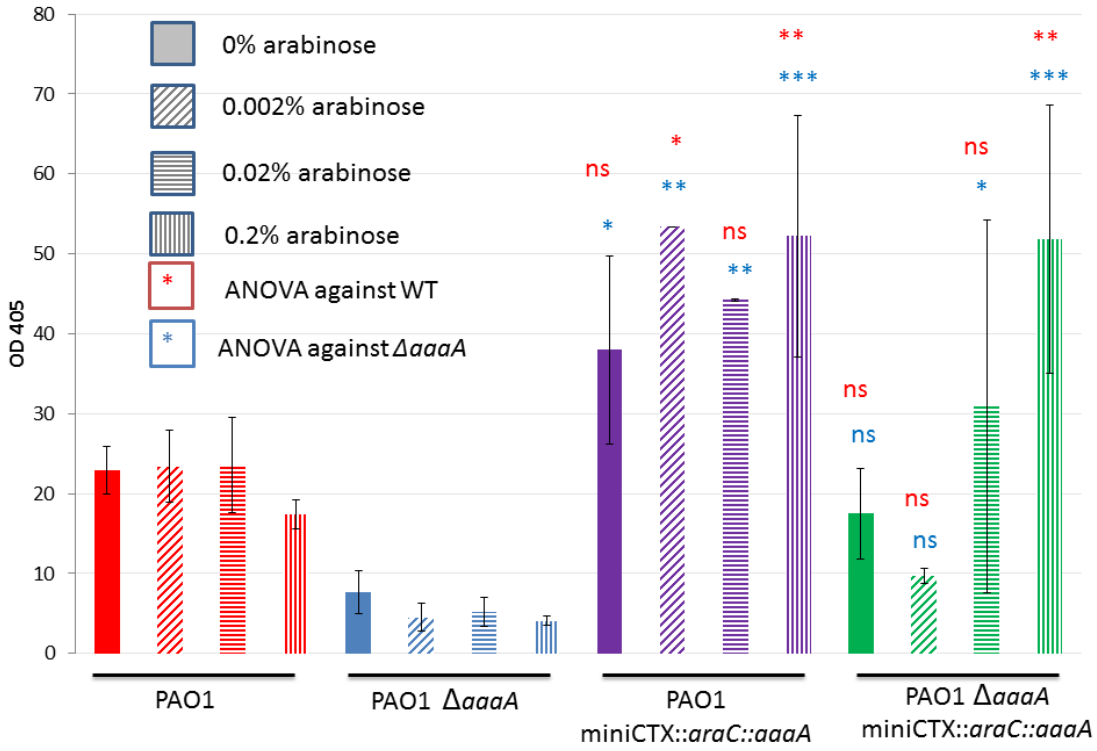


Figure 6.2.28: Comparison of arabinose concentrations to test induction efficacy of the miniCTX::*araC::aaaA* construct in PAO1 and PAO1 *ΔaaaA* backgrounds shows that 0.2% arabinose is best for differentiation between induced and uninduced strains. PAO1, PAO1 *ΔaaaA,* PAO1 miniCTX::*araC::aaaA* and PAO1 *ΔaaaA* miniCTX::*araC::aaaA* were grown in LB until exponential phase. They were then induced with 0.002% (diagonal stripes), 0.02% (horizontal stripes) or 0.2% arabinose (vertical stripes) for 2 hours and with the non-induced (0% arabinose, solid bars) were incubated for 2 hours. The cultures were then washed 3x in MMP and standardised to OD_{600} 0.5, before incubation with the AaaA substrate L-arginine-p-nitroanilide for 24 hours at 37°C. The OD_{405} is representative of the p-nitroaniline dye cleavage from original molecule. Each bar shows the AUC of the OD_{405}.of the average of 3 biological replicates over 3 experiments. A one-way ANOVA was used in each arabinose concentration category to test the variance from the WT and *ΔaaaA* strains. The labels ns and * indicate the significance of variation determined by this test. Red represents difference from the WT and blue difference from the mutant strain.

6.2.10.3 Testing of sugars on arabinose inducible plasmid shows a slight increase in the activity of PAO1 ΔaaaA miniCTX::araC::aaaA when glucose is present

To be sure that the presence of different sugars in the media subsequently used would not affect the arabinose inducible plasmid, an activity assay comparing two sugars likely to be used in following experiments was conducted. Glucose which represses *araBAD* when in *E. coli* (data not shown; Guzman *et al* 1995) and is a component of ASM (Palmer *et al* 2007), was compared with succinate, which feeds directly into the TCA cycle and is a component of the media optimised here as an alternative to ASM. As previously mentioned, (Costerton *et al* 1999; O'Toole *et al* 2000; Stoodley *et* al 2002; Klausen *et al* 2003; Shrout *et al* 2006) studies found that succinate and glucose formed different biofilm structures and the behaviour of AaaA in the background of both sugars could be interesting to investigate in the future.

Three biological replicates of each strain were grown overnight in ASM minus glucose (see materials and methods for full recipe) and refreshed the following morning (post 18 hours) as normal by adding 1 ml of culture to 9 ml of fresh media. In this case 1 ml of each replicate was added to a tube of fresh media containing either glucose or succinate 20 mM. Half of each of these tubes were induced with 0.2 % arabinose when cultures reached an OD_{600} of 0.4-0.6. This amount is above the normal concentration of glucose in ASM which is 3 mM. Interestingly, the only significant difference between the conditions was between the induced PAO1 *ΔaaaA* miniCTX*::araC::aaaA* strain in glucose or succinate supplemented media but the difference was in the opposite direction than was expected (Figure 6.2.29). More activity was observed when glucose was the sugar additive. This indicates that glucose is not having a repressive effect on the *araBAD* promoter in the PAO1 *ΔaaaA* background. Why glucose appears to increase the activity of the inducible strain is still not known but is taken account of in further experiments.

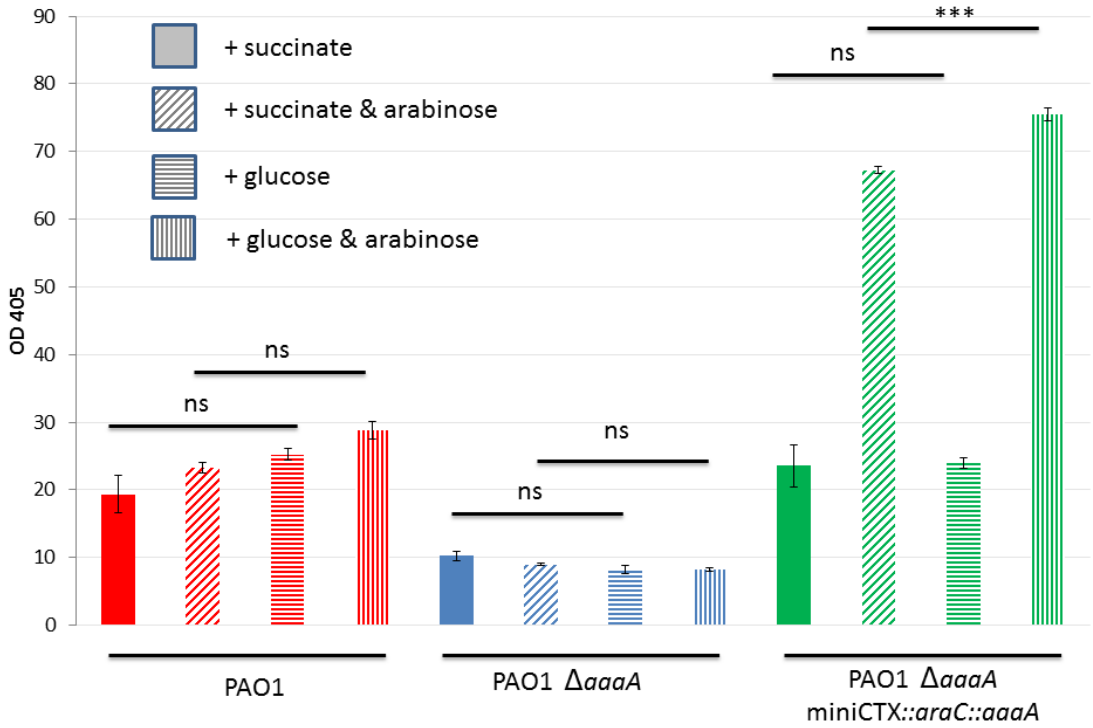


Figure 6.2.29: Comparison of AaaA activity in succinate and glucose supplemented ASM shows there is increased activity in glucose media in the PAO1 *ΔaaaA* miniCTX::*araC::aaaA* strain. PAO1, PAO1 *ΔaaaA* and PAO1 *ΔaaaA* miniCTX::*araC::aaaA* were grown in LB with 20 mM succinate or glucose until exponential phase. Arabinose 0.2% was added to the induced counterparts and the cultures incubated for 2 hours. They were washed 3x in MMP and standardised to OD_{600} 0.5, before incubation with the AaaA substrate L-arginine-p-nitroanilide for 24 hours at 37°C. The OD_{405} is representative of the p-nitroaniline dye cleavage from original molecule. Each bar shows the AUC of the OD_{405} of the average of 3 biological replicates (in one experiment). Error bars show the standard deviation between these. Solid bars = succinate non-induced; diagonal stripes = succinate induced; horizontal stripes = glucose non-induced; vertical stripes = glucose induced. T-tests were used to compare activity between the sugars in non-induced and induced conditions. The labels ns and * indicate the significance of variation determined by this test.

6.2.11 Comparison of the inducible strains show all to have activity greater than PAO1 *ΔaaaA* in LB

To aid in further experiments, a comparison of the AaaA activity in all the *aaaA* complemented strains was conducted. Each strain was grown in LB and induced as appropriate with either 0.2% (13.3 mM) arabinose or 1 mM of IPTG. Figure 6.2.30 shows the result of this comparison. All inducible strains show significantly different AaaA activity from the PAO1 *ΔaaaA* strain. Both *pME6032::aaaA* and miniCTX::*araC::aaaA* complemented strains show this difference even when uninduced, indicating that their promoters are leaky to some extent. This will need to be taken account of where applicable.

The investigation was extended to compare AaaA activity between the *aaaA* complemented strains in ASM (Palmer *et al* 2007). This is shown in Figure 6.2.31. The media appears to influence AaaA activity resulting in a lessening induction effect by IPTG, perhaps due to the lactose component of ASM. Arabinose induction appears to be more useful in this media as there is a greater difference

between induced and non-induced conditions so that when induced, this strain is significantly different from the PAO1 *ΔaaaA* strain. Not to be ignored is the smaller difference between WT and mutant strains and therefore use of the arabinose induced strain may exaggerate any differences found between these when applied in ASM media.

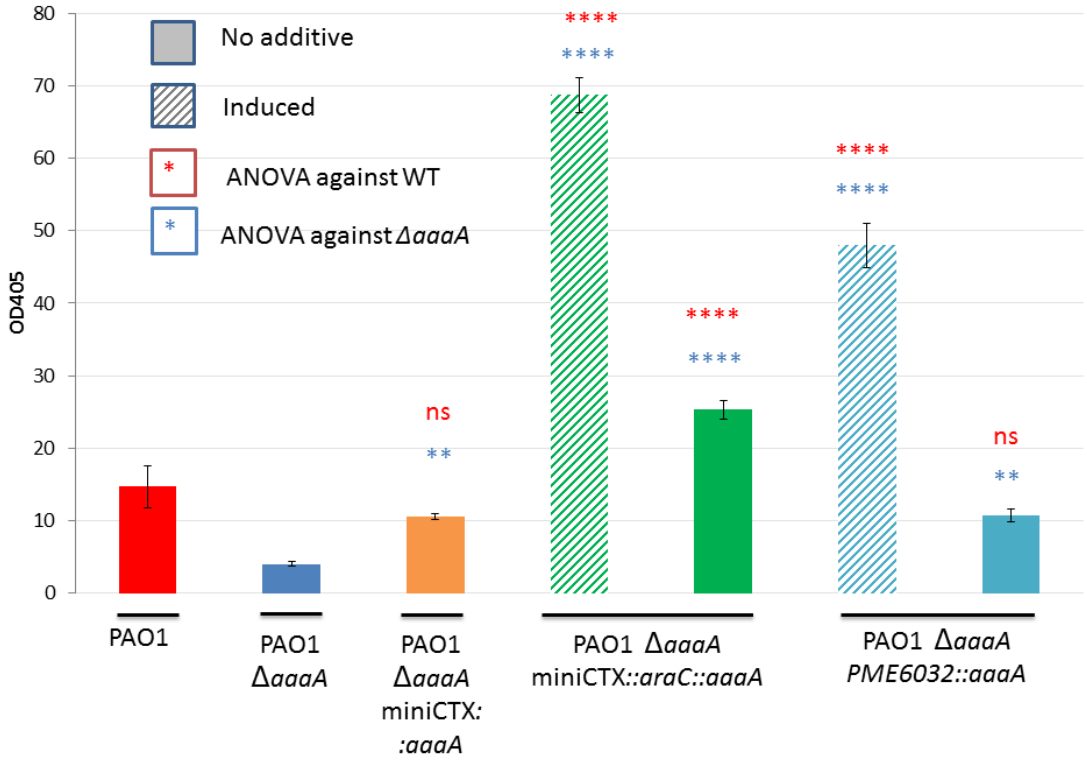


Figure 6.2.30: Comparison of AaaA activity in different complementation strains in LB shows all inducible strains are significantly more active than the PAO1 *ΔaaaA* strain. PAO1, PAO1 *ΔaaaA*, PAO1 *ΔaaaA* miniCTX::*aaaA*, PAO1 *ΔaaaA* miniCTX::*araC::aaaA* and PAO1 *ΔaaaA* *pME6032::aaaA* were grown in LB until exponential phase. The inducible strains were induced with 0.2% arabinose or 1 mM IPTG and the cultures incubated for 2 hours. They were washed 3x in MMP and standardised to OD_{600} 0.5, before incubation with the AaaA substrate L-arginine-p-nitroanilide for 24 hours at 37°C. The OD_{405} is representative of the p-nitroaniline dye cleavage from original molecule. Each bar shows the AUC of the OD_{405} of the average of 3 biological replicates (in one experiment) and error bars show the standard deviation between these. Solid bars indicate uninduced and striped bars indicate induced cultures. A one way ANOVA was used to compare each strain to either the WT or *ΔaaaA* strain. The labels ns and * indicate the significance of variation determined by this test. Red shows an ANOVA using the WT as a reference and blue shows an ANOVA using the mutant as a reference.

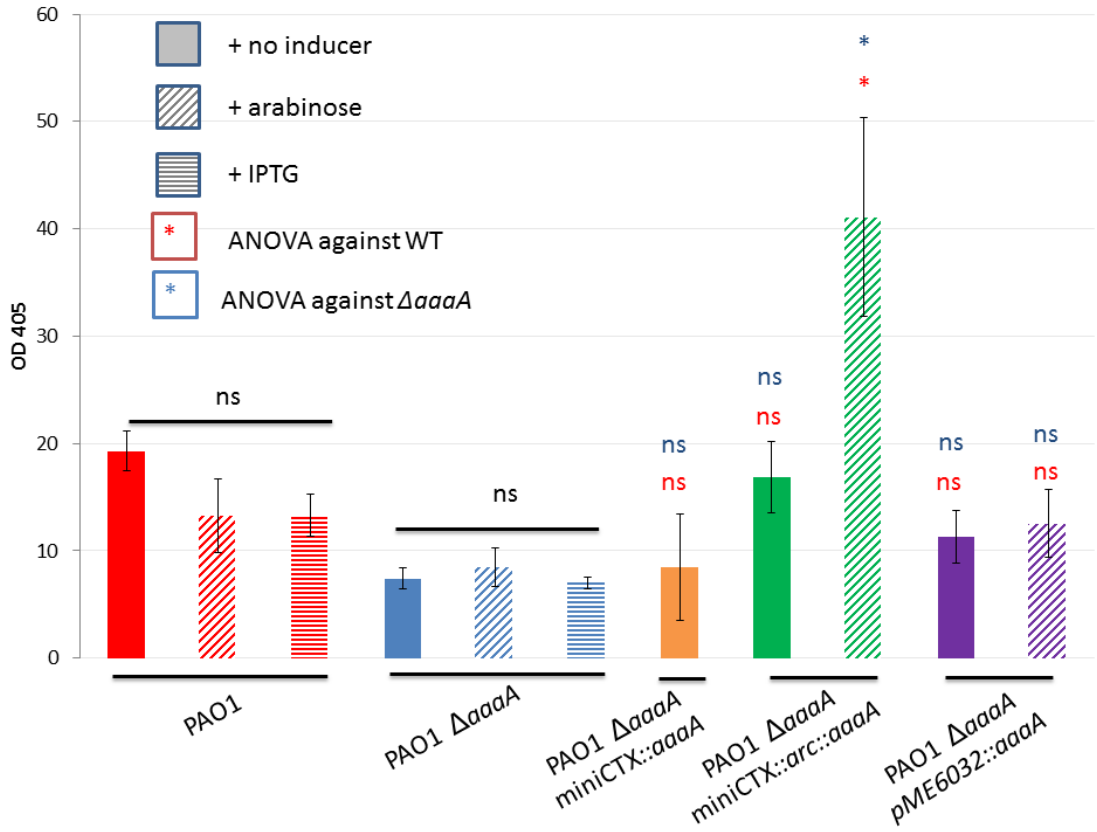


Figure 6.2.31: Comparison of AaaA activity in different complementation strains in ASM shows IPTG induction to be less effective in differentiating induced and uninduced strains. PAO1, PAO1 *ΔaaaA*, PAO1 *ΔaaaA* miniCTX::*aaaA*, PAO1 *ΔaaaA* miniCTX::*araC::aaaA* and PAO1 *ΔaaaA pME6032::aaaA* were grown in ASM until exponential phase. The inducible strains were induced with 0.2% arabinose or 1 mM IPTG and the cultures incubated for 2 hours. They were washed 3x in MMP and standardised to OD_{600} 0.5, before incubation with the AaaA substrate L-arginine-p-nitroanilide for 24 hours at 37°C. The OD_{405} is representative of the p-nitroaniline dye cleavage from original molecule. Each bar shows the AUC of the OD_{405} of the average of 3 biological replicates over 3 experiments and error bars show the standard deviation between these. Solid bars show uninduced strains, diagonal striped bars show arabinose induced strains and horizontal striped bars show IPTG induced strains. A one way ANOVA was used to compare each strain to either the WT or *ΔaaaA* strain. The labels ns and * indicate the significance of variation determined by this test. Red shows an ANOVA using the WT as a reference and blue shows an ANOVA using the mutant as a reference.

6.2.12 A complementation disparity could be due to alternatively reading ORFs

After constructing the PAO1 *ΔaaaA* miniCTX*::araC::aaaA* complemented strain, the biofilm forming capability of this strain was compared with PAO1 and PAO1 *ΔaaaA* strains, using the Bioflux system. The inclusion of this complemented strain for different biofilm assays was anticipated, with a comparison of induced and non-induced states. Figure 6.2.32 shows a representative sample of the biofilms produced by the PAO1 *ΔaaaA* miniCTX*::araC::aaaA* complemented strain, with and without arabinose induction. This strain produces much less biofilm than both the PAO1 and PAO1 *ΔaaaA* strains. The addition of arabinose itself does not reduce biofilm production in PAO1 and PAO1 *ΔaaaA* strains. The PAO1 *ΔaaaA pME6032::aaaA* complemented strain was also tested for comparison with and

without IPTG, which showed the biofilm to be thicker in the uninduced state (Figure 6.2.32 (4), representative image). This suggests the possibility of this effect being *aaaA* related or that the translocation of the *aaaA* gene or other genetic elements within the *aaaA* gene may have an inhibitory effect on biofilm formation. This is investigated *in silico* in the following section.

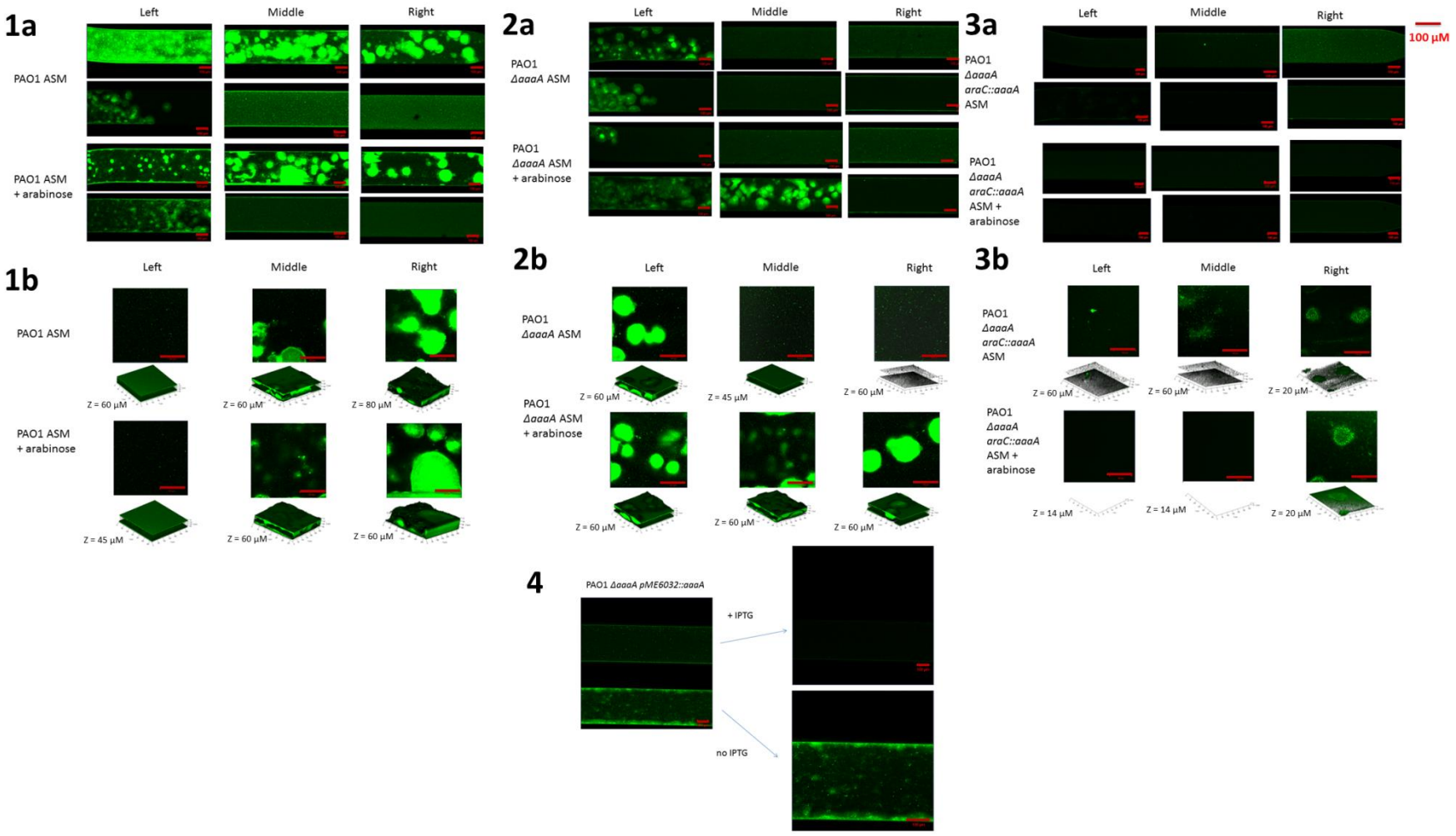
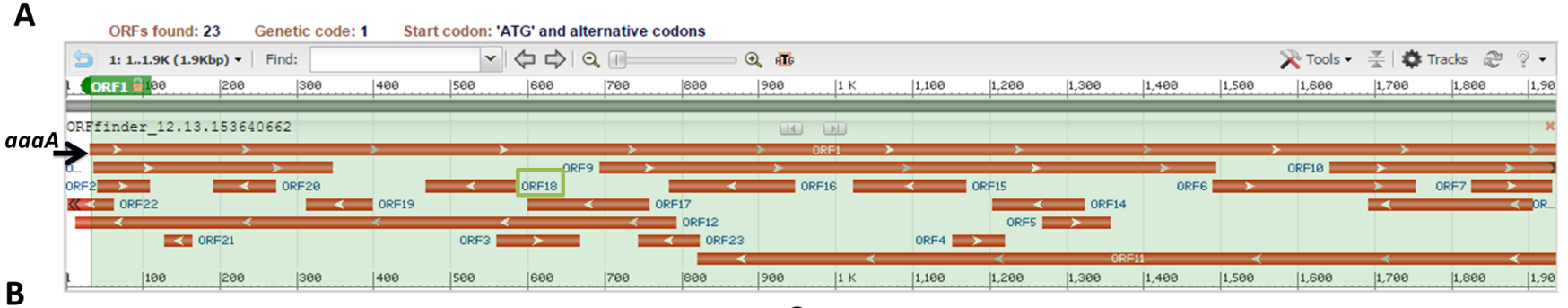


Figure 6.2.32: Regardless of arabinose induction PAO1 *ΔaaaA* miniCTX*::araC::aaaA* forms less biofilm than both PAO1 and PAO1 *ΔaaaA* strains. Biofilms were grown using the Bioflux system for 15 hours, 37°C aerobically in ASM media. Confocal microscopy was taken at end point. Syto9 and PI were added to media in the inlet. Numbers refer to the strain 1= PAO1, 2= PAO1 *ΔaaaA*, 3=PAO1 *ΔaaaA* miniCTX*::araC::aaaA,* 4= PAO1 *ΔaaaA pME6032::aaaA* . Part (a) shows the images taken at 5x magnification (2 biological repeats are shown) while part (b) shows the images taken at 20x magnification (1 representative image is shown for clarity).

6.2.12.1 Investigation of alternative ORFs within aaaA

The complementation of *aaaA* was successful regarding the restoration of AaaA activity. However, the biofilms produced by the inducible strains are weaker than both the PAO1 WT and *ΔaaaA* strains. To find out whether these effects of complementation may be due to the deletion of internal ORFs within the *aaaA* gene, alternatively reading ORFs were searched for within *aaaA* using the NCBI ORF finder. Twenty three possible ORFs were found using this tool, in parallel and anti-parallel orientations to *aaaA*. Further investigation for -10 and -35 sites by the program Softberry Bprom (threshold set at 0.20) found only 1 set of -10 and -35 promoter markers at position 679 (1265 from antiparallel start) (-10) and 700 (1244 from antiparallel start) (-35). The possible promoter start was identified at position 664 (1280 from antiparallel start). The most likely ORF to be controlled by this would be ORF 18, which BLAST analysis found to be a hypothetical protein. No oligonucleotides from known transcription factor binding sites were identified to associate with this putative promoter by Softberry Bprom. From this analysis it is has been revealed that there may be alternatively coding ORFs which could be displaced by removal and transferral of genetic material from the *aaaA* gene to a new site. A clear resolution to the problem was not found however and therefore the complemented strains were used with caution or omitted from further biofilm analysis until an answer to this phenomenon is found. This is summarised in Figure 6.2.33.

A



B

ORF number	Direction to *aaaA*	Length (nucleotide)	Protein matches	More detail on matches
1	parallel	1914	AaaA	
2	parallel	16		
3	parallel	108		
4	parallel	69		
5	parallel	90		
6	parallel	264		
7	parallel	105		
8	parallel	312		
9	parallel	801		
10	parallel	303		
11	antiparallel	1119	none	
12	antiparallel	780	none	
13	antiparallel	213	transposase/ hypothetical protein	*Streptomyces hygroscopicus* (47%), *bodo saltans* (50%),most similar to *Strptomyces turbidiscabies* car8 STRUTUCAR8_00165 (89%)
14	antiparallel	120	DNA polymerase III subunit delta	100% identity *P. aeruginosa syringae* pv actinidae
15	antiparallel	147	none	
16	antiparallel	165	none	
17	antiparallel	159	hypothetical protein	75% identity hypothetical protein JCM19314 360 *Nonlabens ulvanivorans*
18	antiparallel	117	hypothetical protein	80% *Peptostreptococcus anaerobius* 50% *Crysochromulinia*
19	antiparallel	87	uncharacterised/hypothetical protein	90% *Eucyptus grandis*, 75% *Provotella copri*
20	antiparallel	81	arc-like DNA binding domain protein/hypothetical protein	58% *Burkholderia cepacia*, 90% *nocardiopsis prasina*
21	antiparallel	36	none	
22	antiparallel	60	none	
23	antiparallel	81	none	

C



Figure 6.2.33: Investigation of alternative ORFs within *aaaA*. A: putative ORFs found using the NCBI ORF finder tool. B: table of BLAST results for each putative ORF. Each ORF number corresponds to the ORF number in figure A. C: showing the putative -10 and -35 sites in the alternative direction to *aaaA* found using Softberry. Underlined, green = -10; underlined, purple = -35; yellow highlighted =promoter start. Olive green sequence = ORF 18 which is most likely to be controlled by the putative promoter, if genuine.

6.2.13 Floating ASM tube biofilms show a difference between PAO1 and PAO1 *ΔaaaA* strains

The floating biofilm assay has already been mentioned in Chapter 4. Here the aim was to observe whether AaaA affected the clumping phenotype seen in some cultures of *P. aeruginosa* grown in this manner. The method was adjusted in this chapter in that a 1 µl loop of glycerol stored culture was added directly to the media. Other than this, the method was identical to the one previously described.

There was a difference in clumping between the PAO1 and PAO1 *ΔaaaA* strains when grown in ASM (Figure 6.2.34). This did not occur in LB or 1:1 ASM and LB combined media. The PAO1 *ΔaaaA* miniCTX::*aaaA* complimented strain did not rescue the clumping phenotype. The PAO1 miniCTX::*araC*::*aaaA* and PAO1 *ΔaaaA* miniCTX::*araC*::*aaaA* strains showed a slight increase in clumping with the addition of arabinose which became more apparent after a longer growth period (Figure 6.2.35). The PAO1 *ΔaaaA pME6032::aaaA* strain also showed an increase in clumping with the addition of IPTG but this was phenotypically different to the PAO1 WT (Figure 6.2.36).

The assay was repeated with the LESB65 strain and the clumping phenotype was not observed (Figure 6.2.37).

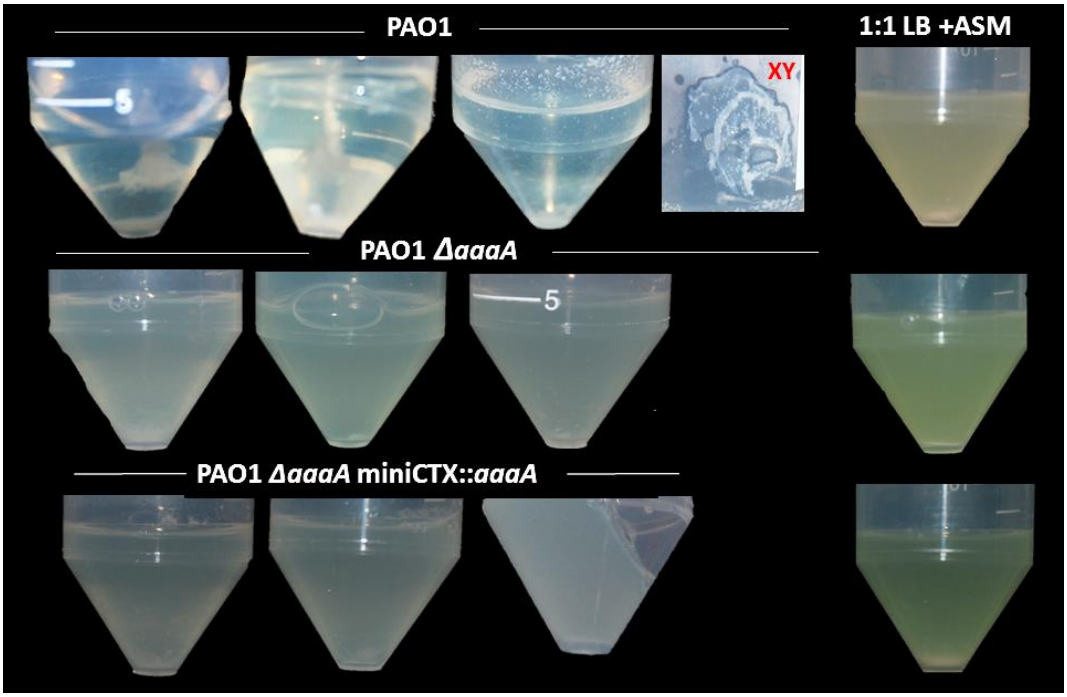


Figure 6.2.34: Clumping is observed in PAO1 but not PAO1 *ΔaaaA* in ASM. Tubes of ASM (Palmer *et al* 2007) were inoculated with a 1 µl loop of glycerol culture and shook for 18 hours at 37°C 200 rpm. For the LB comparisons the same procedure was followed by the ASM was mixed 1:1 with LB. Photography was achieved with a digital camera (Nikon). XY shows a zoomed in view of the WT clump.

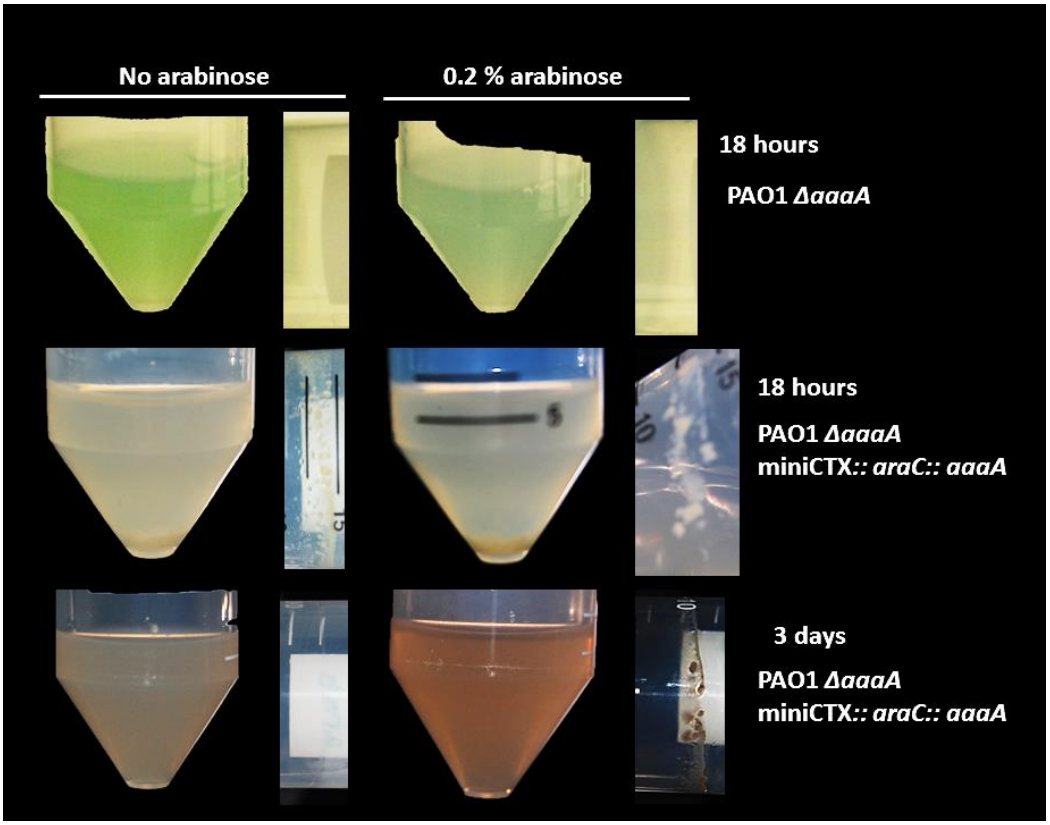


Figure 6.2.35: Clumping is observed in the PAO1 *ΔaaaA* miniCTX::*araC::aaaA* strains grown in ASM. Tubes of ASM (Palmer *et al* 2007) were inoculated with a 1 µl loop of glycerol culture and shook for 18 hours or 3 days at 37°C 200 rpm. Photography was achieved with a digital camera (Nikon).

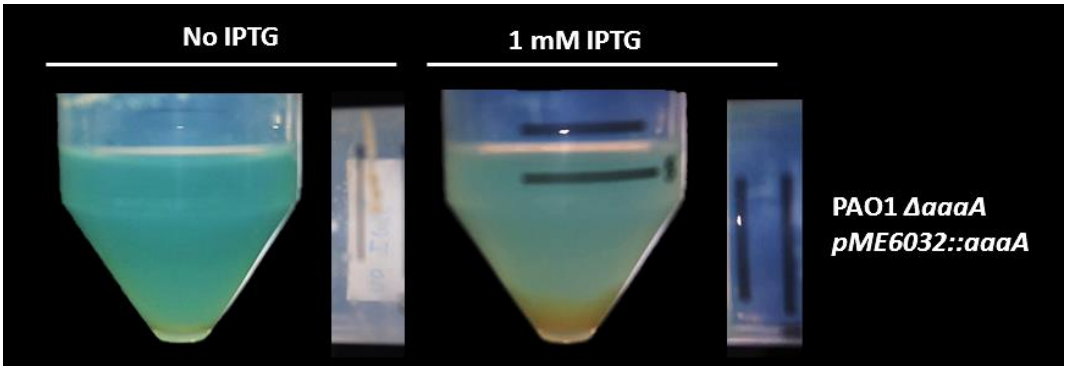


Figure 6.2.36: Clumping is observed in the PAO1 *ΔaaaA pME6032::aaaA* strain grown in ASM. Tubes of ASM (Palmer *et al* 2007) were inoculated with a 1 µl loop of glycerol culture and shook for 18 hours at 37°C 200 rpm. Photography was achieved with a digital camera (Nikon).

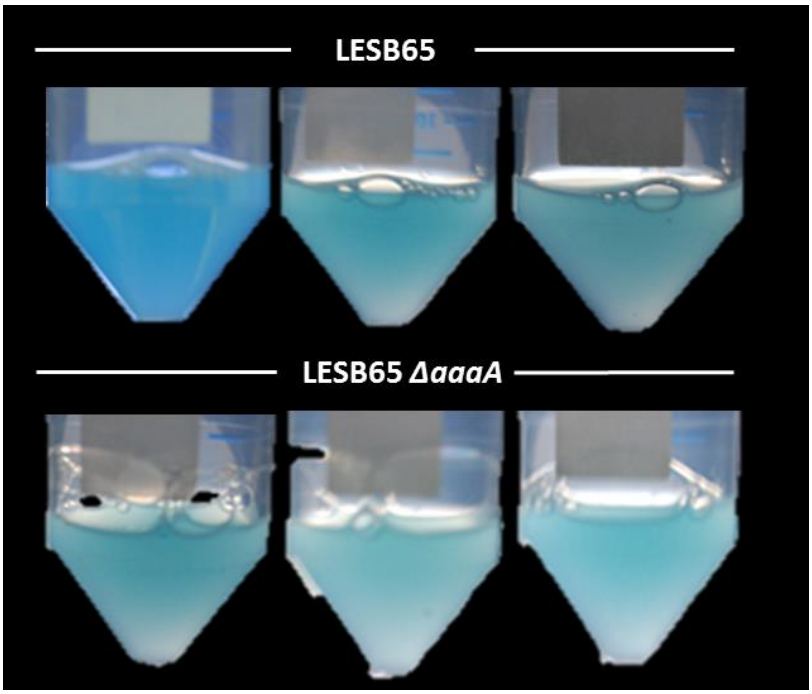


Figure 6.2.37: Clumping is not observed in LESB65 or LESB65 *ΔaaaA* in ASM. Tubes of ASM (Palmer *et al* 2007) were inoculated with a 1 µl loop of glycerol culture and shook for 18 hours at 37°C 200 rpm. Photography was achieved with a digital camera (Nikon).

6.2.13.1 Word of thanks

Work with the floating biofilm cultures was achieved with the kind help of MSc Student Maria Michail. For more information on the optimisation and different conditions trialled using this assay please refer to her dissertation (Michail 2016).

6.2.14 AaaA could compensate for phenazine mediated redox dependent systems in low oxygen areas of biofilm

In Chapter 4 the Congo red colony biofilm plate assay was used to assess differences between different *P. aeruginosa* CF isolates. In this assay no difference was seen between the PAO1 and PAO1 *ΔaaaA* strains. Dietrich *et al* (2013) found that arginine processed through the ADI pathway was not reliant on

a favourable redox cell state. This would suggest that the ADI pathway could rescue the cell when there was a malfunction in the phenazine mediated electron shuttling system. To test this, the biofilm growth of 4 *P. aeruginosa* strains on Congo red, coomassie plates was compared. PA14, PA14 *ΔaaaA*, PA14 *Δphz*, PA14 *Δphz ΔaaaA* strains were kindly supplied by Dr Lars Dietrich and colleagues. The assay was conducted in the same manner as was described in Chapter 4 with the exception that a microaerobic growth condition was included. For this, overnight cultures were grown in sealed jars containing a microaerobic campy pouch and the early stationary phase culture spotted onto Congo red coomassie blue plates which were placed into a microaerobic pouch and sachet system.

Days 1-2 of growth (Figure 6.2.38) show little difference between the strains in the aerobic or microaerobic condition. The microaerobic colony biofilms are smooth and pale while the aerobic biofilms become more textured on day 2. There is some differentiation in the colony biofilms on days 3-4 (Figure 6.2.39). In general there is deepening in colour, the aerobic biofilms turning red and the microaerobic colonies turning a pale yellow. The colonies of PA14 *Δphz*, PA14 *Δphz ΔaaaA* strains look qualitatively bigger. Interestingly, in the aerobic condition the start of wrinkling can be observed in the PA14 *Δphz ΔaaaA* strain.

The most pronounced differences between the biofilms produced by the different strains was seen on days 5-6 (Figure 6.2.40). In the microaerobic condition the PA14 *Δphz* and PA14 *Δphz ΔaaaA* look a deeper colour with the PA14 *Δphz ΔaaaA* strain looking the most red. More striking are the aerobically grown colony biofilms on day 6 which show a pronounced wrinkling in the PA14 *Δphz ΔaaaA* which is different to the other strains. A zoomed in view is shown in Figure 6.2.41.

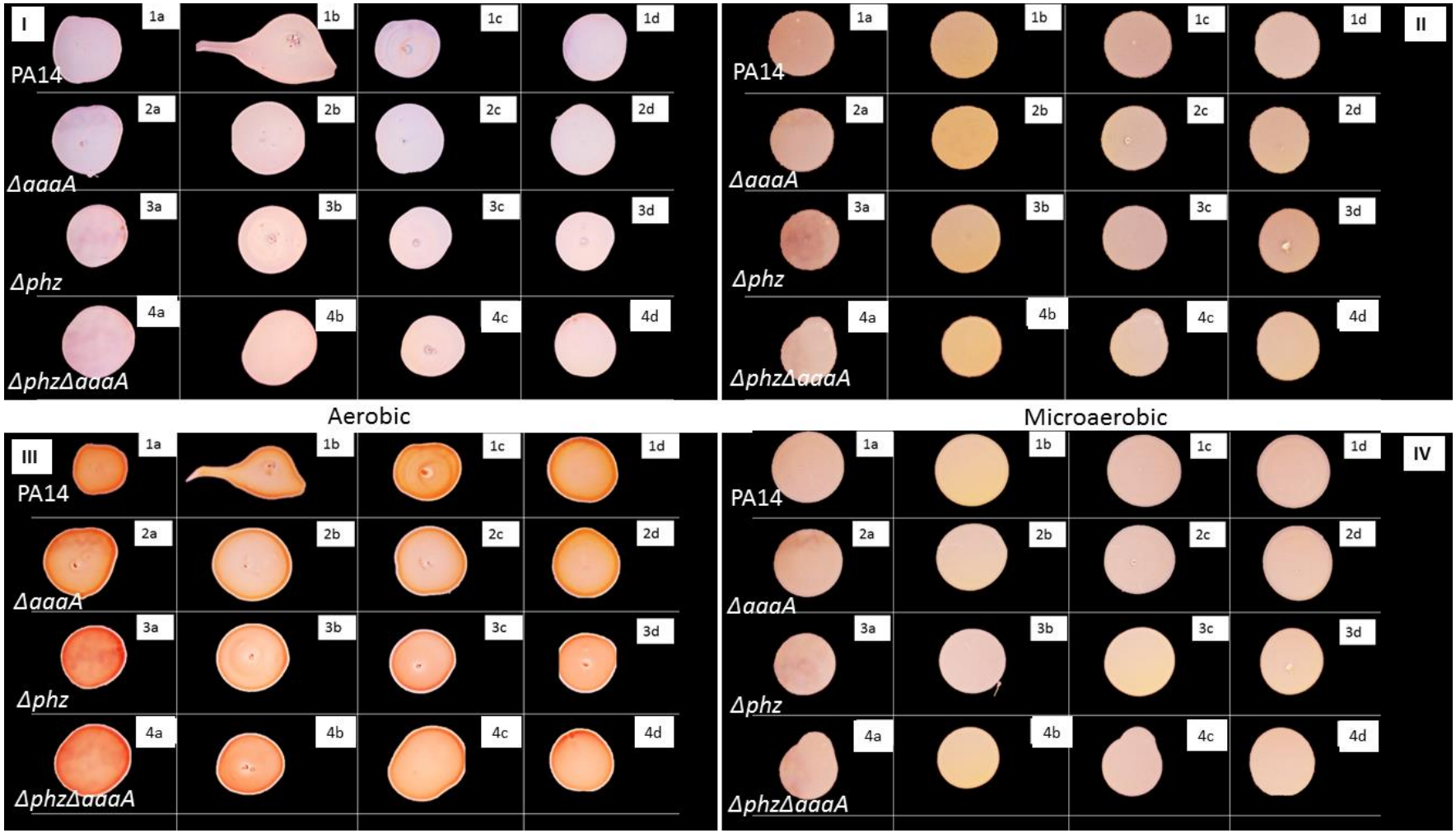


Figure 6.2.38: *aaaA* and *phz* could work in parallel to support *P. aeruginosa* growth in biofilms. Showing the first 2 days of colony biofilm growth on Congo red, coomassie blue plates. Numbers refer to the strain 1= PA14; 2= PA14 *ΔaaaA*; 3= PA14 *Δphz*; 4= PA14 *ΔphzΔaaaA*. Letters (a-d) refer to the number of biological repeats which were generated from a drop of overnight culture grown from a single colony. The left panel shows aerobic conditions and the right panel shows microaerobic conditions (sachet and pouch system). Both were grown at room temperature.

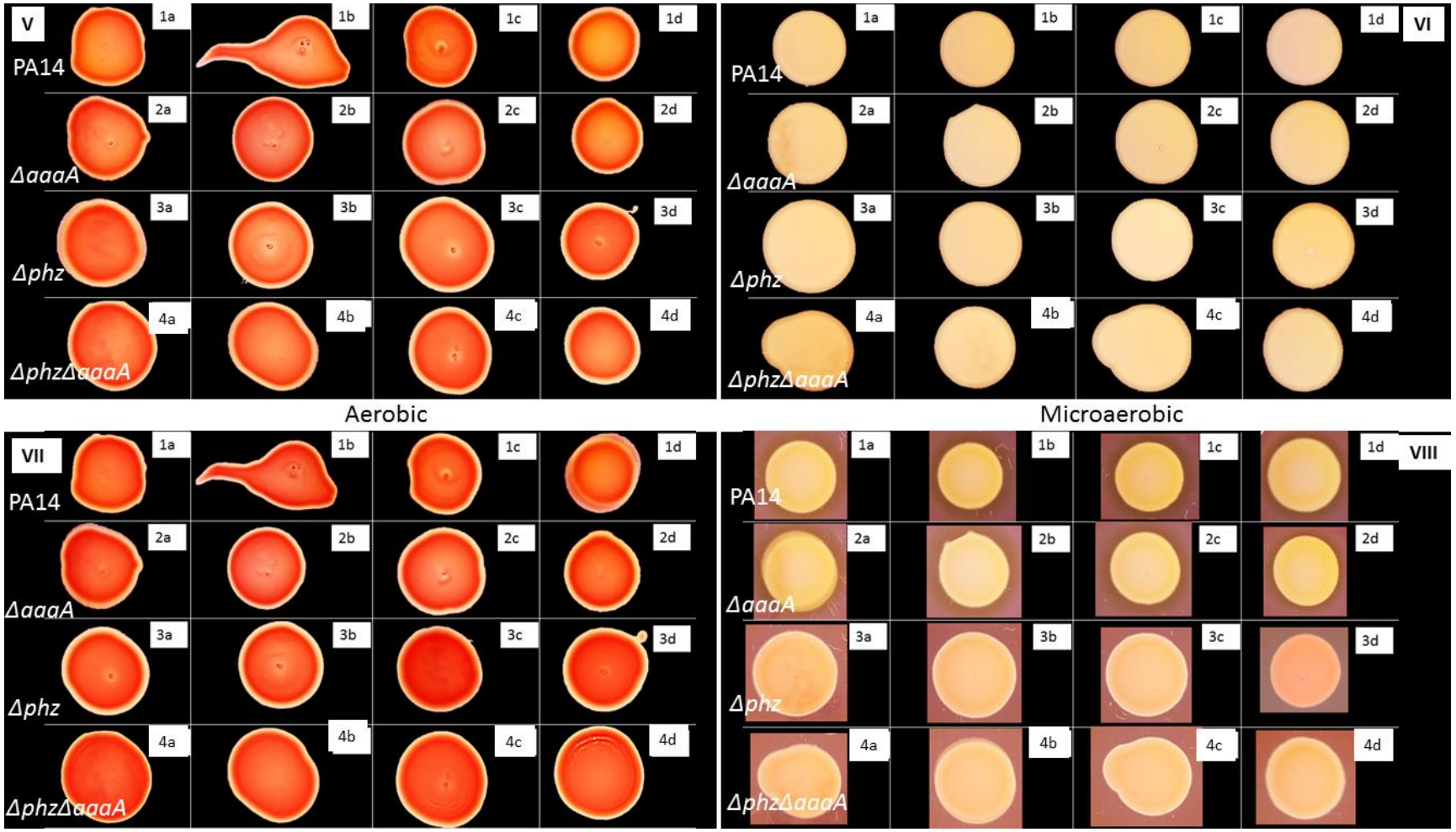


Figure 6.2.39: *aaaA* and *phz* could work in parallel to support *P. aeruginosa* growth in biofilms. Showing days 3-4 biofilm growth on Congo red, coomassie blue plates. Numbers refer to the strain 1= PA14; 2= PA14 *ΔaaaA*; 3= PA14 *Δphz*; 4= PA14 *ΔphzΔaaaA*. Letters (a-d) refer to the number of biological repeats which were generated from a drop of overnight culture grown from a single colony. The left panel shows aerobic conditions and the right panel shows microaerobic conditions (sachet and pouch system). Both were grown at room temperature.

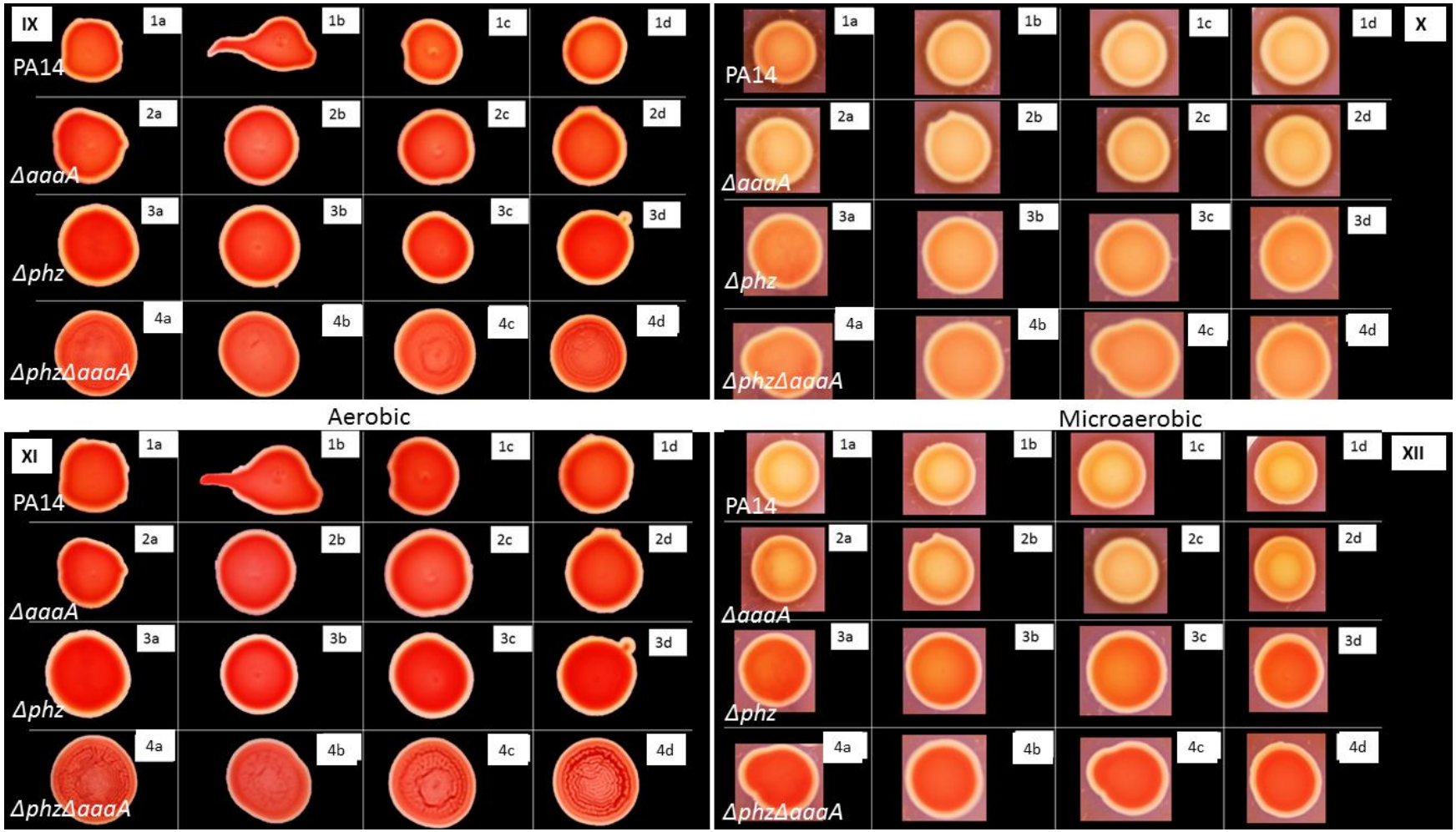


Figure 6.2.40: *aaaA* and *phz* could work in parallel to support *P. aeruginosa* growth in biofilms. Showing days 5-6 of colony biofilm growth on Congo red, coomassie blue plates. Numbers refer to the strain 1= PA14; 2= PA14 *ΔaaaA*; 3= PA14 *Δphz*; 4= PA14 *ΔphzΔaaaA*. Letters (a-d) refer to the number of biological repeats which were generated from a drop of overnight culture grown from a single colony. The left panel shows aerobic conditions and the right panel shows microaerobic conditions (sachet and pouch system). Both were grown at room temperature.

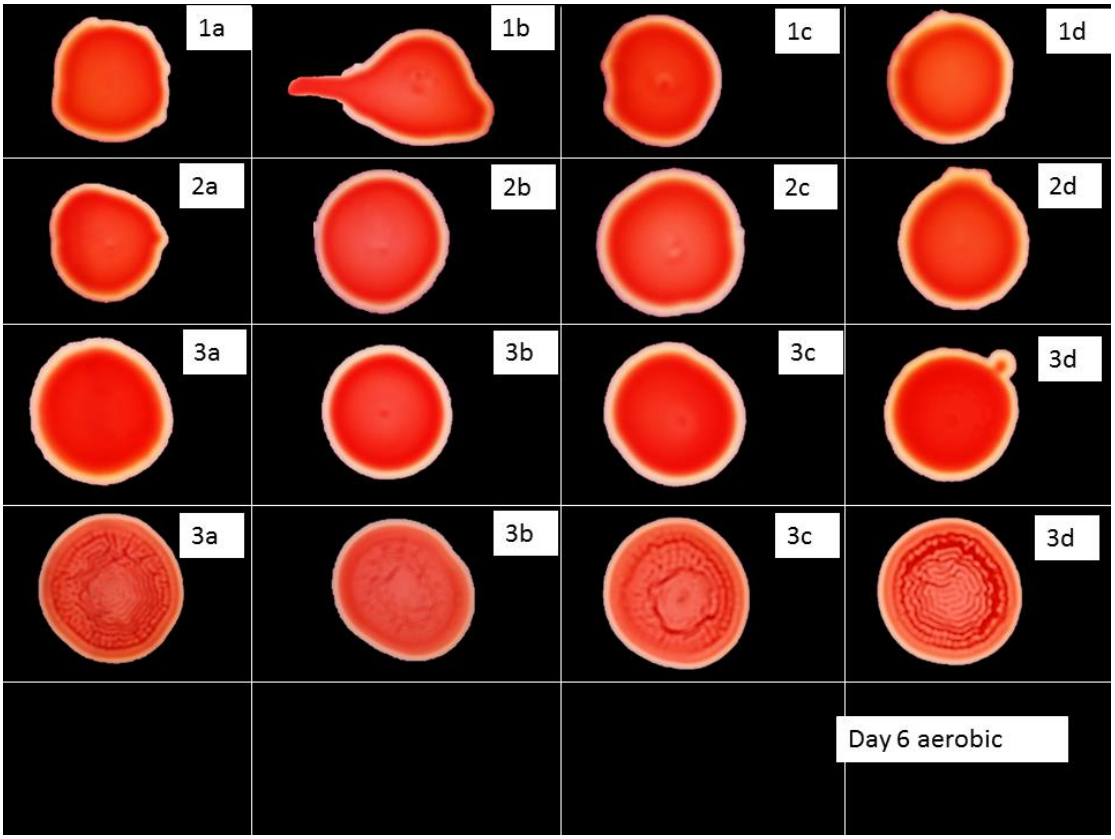


Figure 6.2.41: PA14 *ΔphzΔaaaA* shows a wrinkly phenotype that is indicative of increased oxygen reliance. Showing day 6 of colony biofilm growth on Congo red, coomassie blue plates at room temperature, aerobic conditions. Numbers refer to the strain 1= PA14; 2= PA14 *ΔaaaA*; 3= PA14 *Δphz*; 4= PA14 *ΔphzΔaaaA*. Letters (a-d) refer to the number of biological repeats which were generated from a drop of overnight culture grown from a single colony.

6.2.15 The PAO1 *ΔaaaA* CFU count is higher than PAO1 from biofilms grown in an *ex vivo* pig lung model

Several studies have produced data illustrating the importance of studying organisms in conditions as close as possible to the native environment (Cornforth *et al* 2018; Gonzalez *et al* 2018; Son *et al* 2007; Dotsch *et al* 2012; Palmer *et al* 2007). It was hypothesised that AaaA would give *P. aeruginosa* a survival advantage in specific conditions and that these should exist in the CF lung. The biofilm models previously described attempted to narrow the disparity between laboratory and patient by using ASM. The structural environment is however very different. In this section a further step towards *in vivo* imitation was taken by using the *ex vivo* pig lung model (EVPL) developed by Dr Freya Harrison (Harrison and Diggle 2016). In addition to scientific advantages this model presents an ethical alternative to the use of laboratory animals. A local butcher (JT Beedham & Sons) supplied lungs which were collected on the day of delivery and dissected in the manner described in Chapter 2 to produce approximately 0.5-1 cm^2 bronchiole sections. These were placed into the wells of a 24 well plate supplemented with 0.5 ml ASM lacking glucose and containing 50 µg/ ml

ampicillin to help protect against any resident microbes in the lung tissue (Figure 6.2.42). A hypodermic needle was used to pierce the tissue with a colony from a LB agar plate or with no colony in the case of the mock infected control. The plate was incubated for 24 hours and homogenised with a beadbeater for the CFU count and 24 or 72 hours with subsequent preservation in formalin for the histology sections. The histology department in the QMC performed the sectioning and staining with Hematoxylin and eosin stain (H&E) of the tissue.

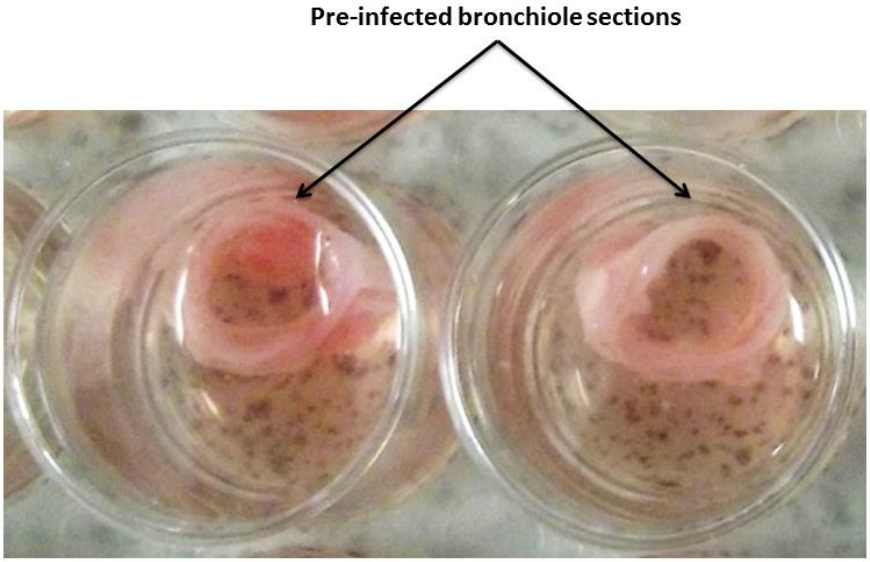


Figure 6.2.42: Bronchiole sections used as a scaffold for biofilm growth. Extracted from pig lung tissue and suspended in ASM (Palmer *et al* 2007). Showing 2 wells of a 24 well plate.

The CFU counts were consistent across different lungs on different days. This is perhaps an advantage of using bronchiole tissue in comparison to alveolar tissue. There was a small difference between PAO1 and PAO1 *ΔaaaA* strains with the PAO1 *ΔaaaA* strains showing a slightly higher CFU count. Figure 6.2.43 illustrates this.

Figure 6.2.44 shows representative sections from infected and uninfected bronchiole tissue incubated for 24 (A, B, C, D) or 72 (E, F, G, H) hours at 37°C. There does not appear to be a difference between PAO1, PAO1 *ΔaaaA* and PAO1 *ΔaaaA* miniCTX::*aaaA* strains in biofilm thickness or invasion into the tissue during 24 hours. Evidence of surviving biofilms was not seen in the bronchiole tissue sections following 72 hours of bacterial incubation. There is evidence of tissue damage which here was identified by missing cell nuclei and an absence of tissue folding at the edge of the sample (breakdown of structure) which remains evident in the control sample. Variation in the damage caused between the different bacterial strains was not observed.

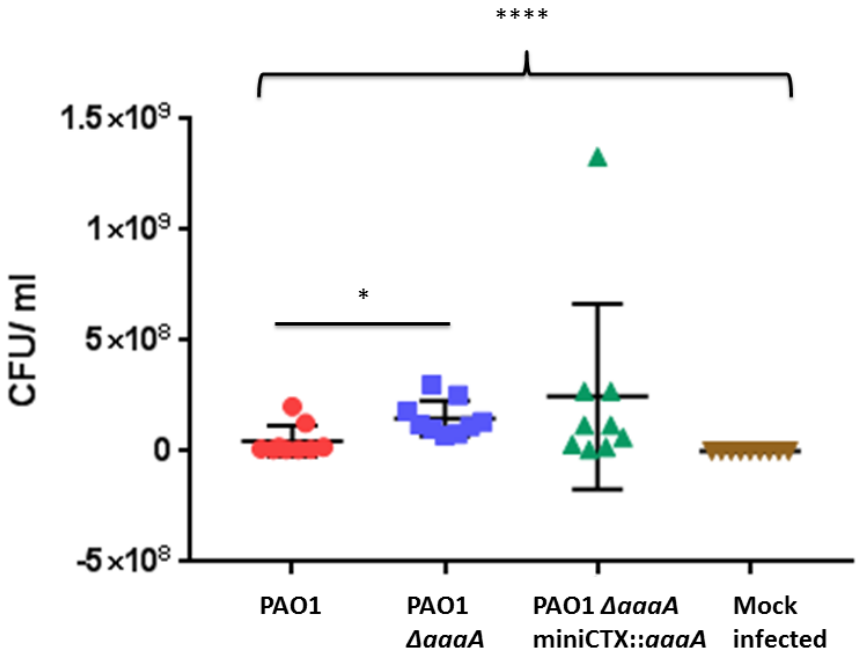


Figure 6.2.43: CFU count from homogenised EVPL bronchiole tissue after 24 hours of growth shows increased growth of PAO1 *ΔaaaA* compared to PAO1. Bronchiole sections of 0.5-1 cm^2 were liberated from *ex vivo* pig lungs, washed in tissue culture media and ASM, and suspended on a bed of agarose in ASM. Infection was achieved by inserting a hypodermic needle with a single bacterial colony (or no colony for the control) taken from an agar plate into the tissue. The bronchiole sections were then incubated for 37°C for 24 hours, homogenised in a bead beater and a dilution series plated. Each data point shows 1 biological replicate (a separate colony grown on one piece of bronchiole). Three biological replicates were tested in 3 experiments (i.e. 3 biological replicates per separate lung). Error bars show the standard deviation between these. A Kruskal-Wallis test was used to compare all the categories and a Mann-Whitney test used to compare PAO1 and PAO1 *ΔaaaA* strains and is represented by * to indicate a P value less than 0.05.

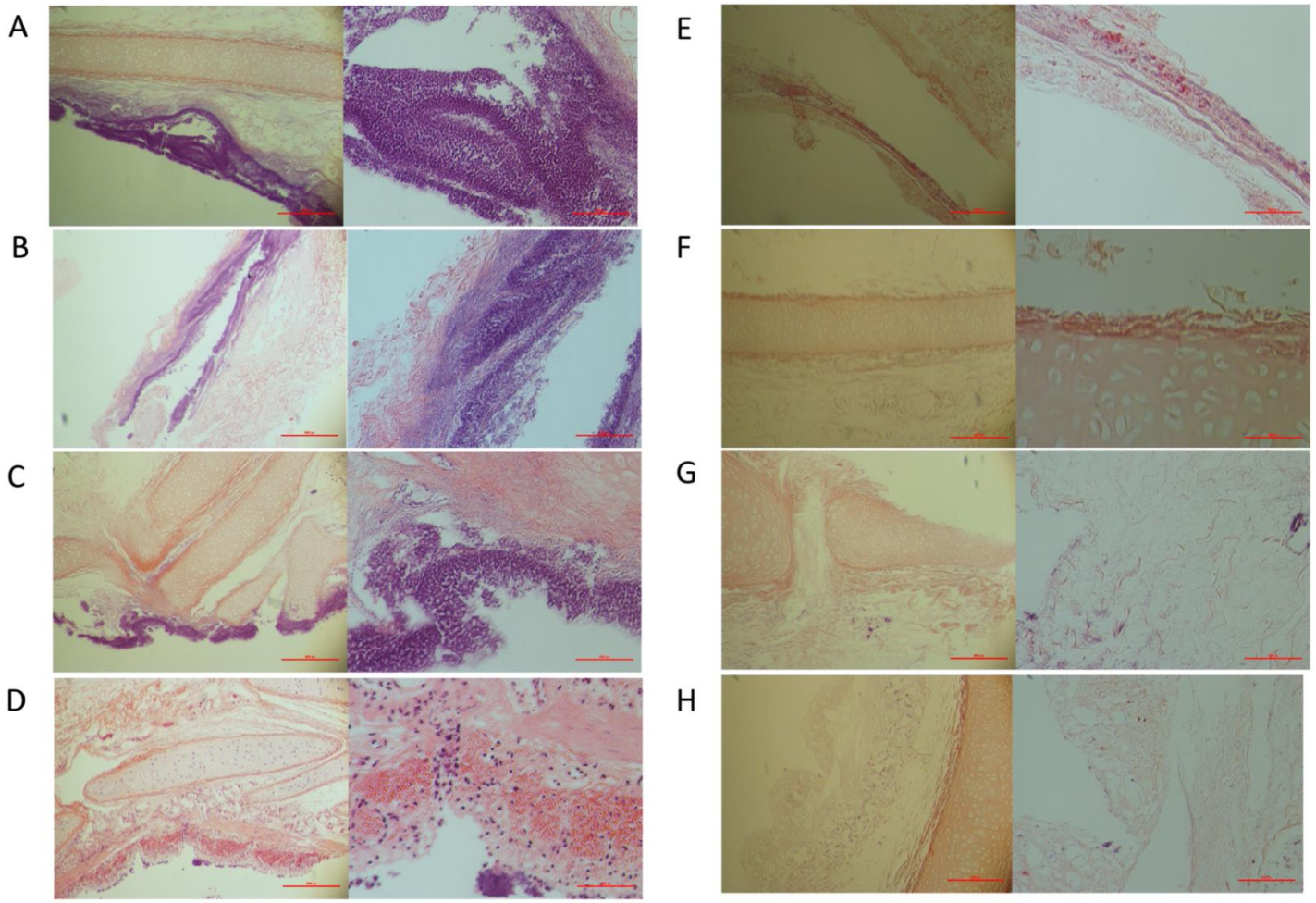


Figure 6.2.44: *Ex vivo* pig lung bronchiole tissue sections infected with PAO1, PAO1 *ΔaaaA* or PAO1 *ΔaaaA* miniCTX::*aaaA* strains show a similar amount of bacterial invasion and tissue damage, which is not apparent in the mock-infected control. Bronchiole sections of 0.5-1 cm^2 were liberated from *ex vivo* pig lungs, washed in tissue culture media and ASM, and suspended on a bed of agarose in ASM. Infection was achieved by inserting a hypodermic needle with a single bacterial colony (or no colony for the control) taken from an agar plate into the tissue. The bronchiole sections were then incubated for 37°C for 24 (A-D) or 72 (E-H) hours before suspension in formalin, sectioned, and stained with H&E. A, E = PAO1; B,F =PAO1 *ΔaaaA*; C, G = PAO1 miniCTX::*aaaA*; D, H = mock infected control. The left image is 10x and the right image 40x magnification.

6.2.16 A chronic murine infection model with PAO1 and PAO1 *ΔaaaA* showed mixed findings (Liverpool data)

The above biofilm growth methods have taken place *in vitro* or *ex vivo* and have therefore been removed from the host immune response. One of the possible advantages AaaA could give *P. aeruginosa* in the CF lung is to disrupt the balance of arginine around the infection site and interfere with iNOS and arginase host defence mechanisms (Grasemann *et al* 2006; Grasemann *et al* 2005). To investigate this aspect of the environment, PAO1 and PAO1 *ΔaaaA* strains were introduced to a chronic infection mouse model by our Roche grant (coordinated and directed by Maria Bobadilla and Andreas Tschumi) collaborators at Liverpool University, Dr Elaine Waters and Prof Aras Kadioglu.

To observe whether differences in viable cell count existed between PAO1 WT and PAO1 *ΔaaaA* strains, Balb/c mice were given an intranasal dose of $8x10^6$ exponential phase *P. aeruginosa* that was taken directly from a plate and suspended in PBS. Previous tests showed that this growth method and CFU quantity produced the best colonisation levels and accurate CFU count (data not shown). The lungs and nasopharynx were collected at selected time points and homogenised for determination of the CFUs and immune marker concentrations.

The CFUs of the 2 strains over 5 days were compared (Figure 6.2.45). No significant difference was found between WT and mutant strains in the CFU counts but PAO1 *ΔaaaA* appeared to be cleared quicker from the lung than PAO1. Additionally, lungs of the mice infected with the PAO1 WT had spots that were not visible in the mice infected with PAO1 *ΔaaaA*. This correlated with a higher pain score shown by the mice infected with PAO1 *ΔaaaA*, than PAO1 (Figure 6.2.46). The scoring for this was followed according to Morton (1985). Dr Elaine Waters and Prof Aras Kadioglu hypothesised that this could be due to the PAO1 *ΔaaaA* strain forming an acute rather than chronic infection. To test this hypothesis, 4 pro-inflammatory markers (IL-10, GM-CSF, KC and TNF-alpha) were monitored during this time period and no significant difference was found between the PAO1 and PAO1 *ΔaaaA* strains for any of these (Figure 6.2.47). The generation of the LESB65 *ΔaaaA* strain will allow a more chronic infection to be sustained and therefore a greater difference between the WT and *ΔaaaA* mutant strains may be revealed.

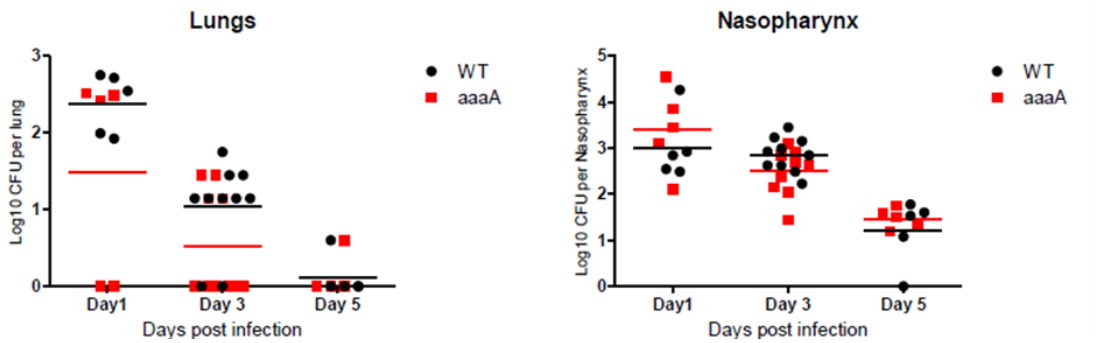


Figure 6.2.45: No significant difference in CFU count was found between PAO1 and PAO1 *ΔaaaA* strains in a 5 day mouse model. The left hand figure shows the CFUs from the lungs and the right hand the CFUs from the nasopharynx. Each data point shows a biological repeat, black = PAO1 and red= PAO1 *ΔaaaA.* Data was produced and presented by Dr Elaine Waters and Aras Kadioglu of Liverpool University.

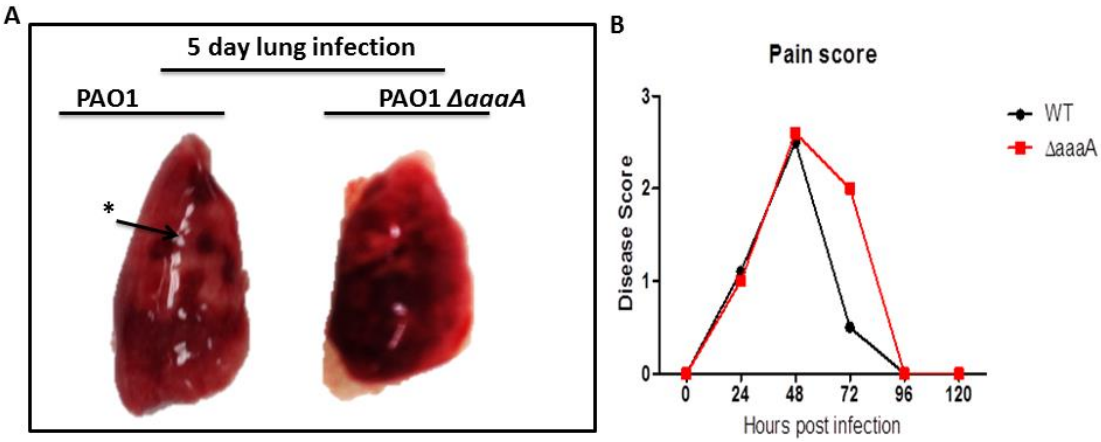


Figure 6.2.46: AaaA may be involved in facilitating chronic infection. A = lung tissue photos post infection reveals that black spots are particular to the PAO1 WT. The asterisk highlights a black spot. B = showing the mean pain score in mice infected with PAO1 (black) or PAO1 *ΔaaaA* (red).

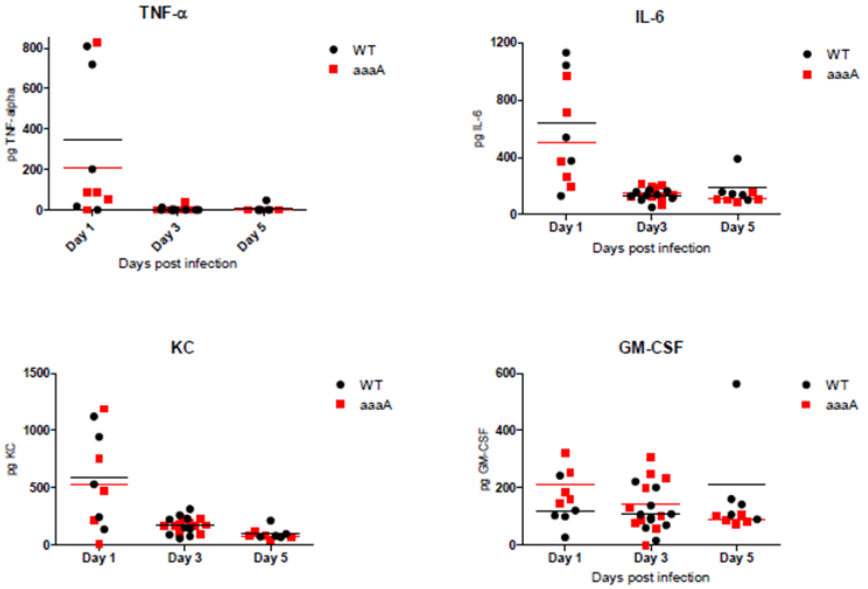


Figure 6.2.47: No significant difference between PAO1 and PAO1 *ΔaaaA* strains was found in the four pro-inflammatory indicators tested. Top left = tumour necrosis factor alpha (TNF-α); top right = interleukin 6 (IL6); bottom left = Murine KC, IL-8 homolog (Hol *et al* 2010) (CXCL1) (KC); bottom right = granulocyte-macrophage colony-stimulating factor (GM-CSF). Each data point shows a biological repeat, black = PAO1 and red= PAO1 *ΔaaaA.* Data was produced and presented by Dr Elaine Waters and Aras Kadioglu of Liverpool University.

6.3 Discussion

This chapter aimed to investigate if AaaA influenced the ability of *P. aeruginosa* to form biofilms. In addition to comparing PAO1 and PAO1 *ΔaaaA* strains in different biofilm models, the effect of different environmental conditions and strain backgrounds was explored. A subtle link between AaaA and biofilm formation has been found but this is dependent on the strain, the viability of other compensating pathways and the environmental conditions representing a more chronic system.

A secondary aim was the creation of tools to facilitate further investigation of AaaA. A minimal media cocktail was developed to allow consistent growth between WT and *ΔaaaA* strains without inclusion of exogenous nitrate or arginine. Additionally, a chromosomally located arabinose inducible complemented strain, PAO1 *ΔaaaA* miniCTX*::araC::aaaA,* was constructed for the validation of comparisons between PAO1 and PAO1 *ΔaaaA* strains . The biofilm formation of PAO1 *ΔaaaA* miniCTX*::araC::aaaA* was tested in parallel with the IPTG inducible PAO1 *ΔaaaA pME6032::aaaA* strain which revealed some unexpected results.

It is hoped that the models, methods, and findings in this Chapter can be utilized in subsequent investigations to further understand the role AaaA has in chronic biofilm-forming infections.

6.3.1 Biofilm assays: what they have revealed about AaaA

6.3.1.1 In vitro methods

Superior to the glass-slide method (data not shown), the microchamber slide system was used to investigate if PAO1 *ΔaaaA* showed an impairment in biofilm formation. Inter-experimental variation was increased upon washing of the pre-imaged biofilms and for this reason most of the media covering the biofilm was removed but the biofilm not washed. Comparison of PAO1 and PAO1 *ΔaaaA* biofilm growth using this method with LB media showed there was no impairment of biofilm formation in the mutant strain. The biofilm produced by the PAO1 *ΔaaaA* miniCTX*::aaaA* complemented strain was also consistent with the other strains. Repeating this assay with the minimal media cocktail also did not reveal differences in the biofilm formed by PAO1 and PAO1 *ΔaaaA* strains. It did however show that the minimal media cocktail was suitable for biofilm growth and could be adapted in future assays with the addition of different amino acids, polypeptides and external conditions.

To simulate the conditions found in the CF airway more closely, ASM was also used to grow PAO1 and PAO1 *ΔaaaA* biofilms in the microchamber model. To investigate the contribution of environmental oxygen concentrations similar to the CF lung (microaerobic) (Worlitzsch *et al* 2002; Hassett *et al* 2009; Rogers *et al* 2004; Worlitzsch *et al* 2009; Tunney *et al* 2008) on the biofilms produced, half the biofilms were grown in microaerobic conditions. Between PAO1 and PAO1 *ΔaaaA* strains there was no difference in either aerobically or microaerobically grown biofilms. This suggests that a deficit of oxygen alone is not enough to make AaaA an essential component for biofilm formation in this model. The biofilms were slightly thicker in microaerobic conditions and healthy (i.e. not many dead cells) for each strain. There is some evidence to suggest that *P. aeruginosa* prefers microaerobic conditions (Alvarez-Ortega and Harwood 2007; Sabra *et al* 2002; Yoon *et al* 2002). Alternatively, the slower growth seen in the microaerobic conditions of this study could be advantageous for biofilm growth. As a further step, extension of incubation time beyond 48 hours could be trialled.

Rather than the adherence of *P. aeruginosa* biofilm to a glass surface, the aggregation and suspension of cells in a liquid may be more similar to *in vivo* generated microbial communities (Worlitzsch *et al* 2002; Kirchner *et al* 2012; Sriramulu *et al* 2005; Wright *et al* 2013). The floating biofilm assay was used to test whether there was a difference in the PAO1 and PAO1 *ΔaaaA* strains tendency to self-aggregate. The ASM was of the same formula all assays in this thesis used in that it was the Palmer *et al* (2007) version and it did not contain mucin or eDNA. Therefore it did not have a high viscosity. Nevertheless, the PAO1 and PAO1 *ΔaaaA* strains differed in their tendency to aggregate. The PAO1 strain formed a cohesive ball of cells while the PAO1 *ΔaaaA* resembled more planktonic growth with some smaller more numerous clumps. The difference seen between the two strains using this model but not the microchamber model is intriguing and highlights the effect experimental conditions have on research outcomes. The causative agent for this difference has not yet been elucidated by this study and could be because the expression of different genes are necessary when binding to a glass surface such as type IV pili (Whitchurch *et al* 1991; Merz *et al* 2000). It has been observed in this work that PAO1 forms a clumpy style of biofilm in ASM which is characteristic of clonal growth in microcolonies which get progressively larger rather than spreading out. This is typical of type IV pili independent biofilm growth and may be influenced by the glucose in the ASM (Klausen *et al* 2003; O'Toole *et al* 2000) This type of growth would likely create a steeper oxygen and nutrient gradient than in a flatter biofilm which might present more challenges for the PAO1 *ΔaaaA* strain.

Another alternative to the microchamber model is the Bioflux system. This is more dynamic with an influx of fresh nutrients and efflux of products and planktonic bacteria. It perhaps better represents the more changeable nature of environmental conditions *in vivo* with areas of greater and lesser flow (Button and Button 2013). Another advantage of this system is that it is closed, limiting disturbance of the biofilm. With ASM as a growth media the biofilm growth of PAO1 and PAO1 *ΔaaaA* strains were compared. The Bioflux-generated biofilms of PAO1 and PAO1 *ΔaaaA* differed structurally from the microchamber biofilms, exhibiting a clustered structure. The PAO1 *ΔaaaA* strain produced biofilm equitable to the PAO1 WT. This, like the microchamber biofilms, was hypothesised to be because the environmental conditions were permissive of AaaA independent growth. The role of arginine and tripeptide availability was then examined by the comparison of ASM (normal arginine concentration of 0.306 M), ASM with no arginine, ASM with 2x (0.612 M) arginine, ASM with 0.01 M tripeptide and ASM with no arginine and 0.01 M tripeptide. Of these conditions, the biofilms grown in ASM without arginine differed between PAO1 WT and *ΔaaaA* strains. It was difficult to determine whether this effect would also be the case for the tripeptide + no arginine ASM grown biofilms as neither strain grew well in this condition. More replicates would be needed to confirm this. ASM itself does not contain complex peptides for AaaA to release arginine from but a source of these peptides may be from dead cells (Allocati *et al* 2015; Webb *et al* 2003). Repeating this experiment with the minimal media cocktail would also be interesting, once fully optimised in the manner described in the media subsection below.

Working with collaborators in Roche and Liverpool University, a LESB65 *ΔaaaA* strain was created. Biofilms formed by LESB65 could then be compared with the PAO1 strains. Surprisingly, a difference in biofilm formation between LESB65 and LESB65 *ΔaaaA* strains was found using the Bioflux system. The structure of the biofilms produced by the LESB65 strains was also different from the PAO1 strains. The difference seen in the LESB65 strains could be due to their more chronic phenotype (Carter *et al* 2010; Jeukens *et al* 2014) and highlights the importance of working with clinically relevant strains where possible. Intriguingly, the LESB65 WT did not show the clumping phenotype in the floating biofilm model. This highlights the probability that different mechanisms are involved in the biofilm development of each model. Although there was not time to replicate the other biofilm assays with LESB65 *ΔaaaA*, this would be recommended for further investigation of AaaA. Additionally informative could be an investigation of the LESB65 genome sequence to identify mutations in genes which could interact with AaaA, such as the regulatory elements discussed in Chapter 3.

Previously, the Congo red colony biofilm assay had identified no observable difference between PAO1 and PAO1 *ΔaaaA* colony biofilms when grown aerobically at 22°C (Chapter 4). The investigation was extended in this chapter to compare aerobic and microaerobic conditions in different strain backgrounds: PA14, PA14 *ΔaaaA,* PA14 *Δphz* and PA14 *ΔphzΔaaaA* (Kindly donated by Dr Lars Dietrich). A suspected association between AaaA and the phenazine system was discussed in Chapter 4. Arginine processed through the ADI pathway was found to be independent of the redox state of the cell (Glasser *et al* 2014) and could hypothetically compensate for an ineffective phenazine mediated electron shuttling system in oxygen deficient conditions. For this reason a PA14 *ΔphzΔaaaA* strain where both phenazine operons *phzA1-G1* and *phzA2-G2* were deleted in addition to *aaaA*. After 6 days of aerobic growth PA14 *ΔphzΔaaaA* formed wrinkles, which was not observed in the other strains. The wrinkle phenotype is thought to result from a cellular inability to exist in hypoxic regions of a biofilm (Dietrich *et al* 2013). The wrinkles decrease the distance to the surface to compensate. The biofilms grown in microaerobic conditions did not show wrinkling but because growth was much slower, the biofilms were likely less mature and a difference may be observed upon continuation of the experiment or its repetition at a higher temperature. These results demonstrate a link between phenazine mediated metabolic pathways operating under low oxygen conditions and the ADI-AaaA arginine fermentation system. Further investigation using the Bioflux and microchamber systems could reveal if differences in biofilm structure exist at a microscopic level.

6.3.1.2 Ex vivo and in vivo biofilm methods

This thesis has demonstrated the impact of experimental conditions on research outcomes. To increase the similarity of experimental conditions with the CF airway infection environment, biofilm generation by PAO1 and PAO1 *ΔaaaA* strains was investigated in an *ex vivo* pig lung (EVPL) model developed by Dr Freya Harrison and in a 5 day *in vivo* murine model, performed by Dr Elaine Waters and Prof Aras Kadioglu at the University of Liverpool.

The EVPL model increases the biological similarity to a CF lung infection by providing the spatial structure that is absent from typical *in vitro* methods. The nutrient aspect combines ASM (minus glucose) with the lung tissue. It does not however include the immune component of *in vivo* systems. Other microbiota are absent and the oxygenation is different. It is however a more ethical and high throughput system than using animal models and can be viewed as a bridge between *in vitro* and *in vivo* systems. A recommendation would be to test

promising *in vitro* findings using this method before moving to an *in vivo* system to ensure that the use of animal models would be reduced. In this work the bronchiole tissue was selected to represent a mid-stage infection. In the future this could be compared with alveolar tissue to represent a more end-stage infection. PAO1 and PAO1 *ΔaaaA* colonisation was compared after 24 hours of growth in this model. The PAO1 *ΔaaaA* strain showed slightly more growth than PAO1. There was high reproducibility between replicates including when different lungs were used. The infected bronchiole tissue was also sectioned and stained to observe infection progression. The invasion of the biofilm into the tissue was similar in both strains and resulted in a similar amount of tissue damage. Future work should include the LESB65 strains, the PA14 *ΔphzΔaaaA* strain, microaerobic and aerobic growth comparisons and viewing the biofilm structure with confocal microscopy. Additionally different time points could be compared.

For the closest representation of a typical *P. aeruginosa* CF airway infection, a murine model was employed (Waters, E and Kadioglu, A, unpublished data). PAO1 and PAO1 *ΔaaaA* strains showed a similar CFU count during the 5 day infection. The pro inflammatory immune markers were also affected similarly upon infection with either strain. It was noted however that PAO1 *ΔaaaA* was cleared quicker, produced a higher pain score and affected the lung tissue differently than the WT (absence of black spots on the tissue). Together these findings indicated that AaaA may be allowing *P. aeruginosa* to form a chronic infection opposed to an acute, more virulent invasion (Bayes *et al* 2016). To investigate this further, the LESB65 and LESB65 *ΔaaaA* strains would perhaps yield more informative results due to their acclimatisation to chronic lung disease, permitting a longer infection time to be studied. Additionally, the difference found between the biofilm formation in LESB65 and LESB65 *ΔaaaA* in the Bioflux could be predictive for their differing success in an *in vivo* environment.

6.3.2 Development of minimal media for AaaA assays and the effect of amino acids on *aaaA* expression

In Chapter 4 there was ambiguity in some of the AaaA activity and expression assays due to the complex, undefined media used, LB. A more defined media which limited the available nitrogen and arginine sources but which allowed similar growth in each strain was desirable for clearer comparison results. This is particularly relevant for biofilm comparisons where there are a lot of variables. The optimisation process for such a media began with the salt-buffer base and the principle carbon source. MMP, which had been used in previous activity assays in this work, was chosen as the buffer. The cells are stable in MMP but do not

grow. The principle carbon source chosen was succinate which is an organic acid preferred by *P. aeruginosa* over glucose in the carbon catabolite repression hierarchy (Collier *et al* 1996; Rojo 2010; Moreno *et al* 2010). This formula allowed a very slow level of growth which barely increased from the starting number of cells. Addition of arginine allowed a similar growth in both PAO1 and PAO1 *ΔaaaA* strains, as did KNO_3 and NH_4Cl (for NH_4Cl see appendix A). Addition of tripeptide supported the growth of PAO1 to a greater extent than the PAO1 *ΔaaaA* strain as expected from previous work (Luckett *et al* 2012). The expression of *aaaA* was also tested in these different growth additives and found to be lower in the KNO_3 condition than the arginine and tripeptide sources. This correlated with the hypothesis that expression would be lower when higher nitrate was present and expression would be higher when an arginine source was present (Chapter 3). However, as the kanamycin control promoter also showed reduced activation in the KNO_3 condition this effect may not be specific to *aaaA*.

For the media to be utilized as a base for the comparison of *aaaA* expression, activity and biofilm growth, it was desired that the growth of PAO1 and PAO1 *ΔaaaA* strains be equal without the potentially dampening effect of nitrate on *aaaA* expression or stimulatory effect of arginine. To achieve this, an amino acid cocktail containing amino acids lacking R-group nitrogen atoms was composed. This formulation allowed equal growth of the two strains.

An amino acid screen was then conducted to observe whether the expression of *aaaA* was affected by particular amino acids or exogenous nitrate. KNO_3 significantly reduced PaaaA activation in the *ΔaaaA* mutant but not the WT. Why KNO_3 appears to affect *PaaaA* differently in the 2 strains could be a consequence of a stronger inhibition on *PaaaA* in the WT strain (Chapter 3) making other inhibitory influences less noticeable. To investigate this further, a range of KNO_3 concentrations could be tested. Additionally, qRT-PCR could be used to test the effect of KNO_3 addition under microaerobic conditions or in a NarXL mutant. In contrast to the addition of KNO_3, addition of arginine significantly increased the expression of *aaaA* in PAO1 and PAO1 *ΔaaaA* strains. Although there was additionally a significant change in the kanamycin control strain in the PAO1 strain, this was not seen in the PAO1 *ΔaaaA* strain. The activating effect of arginine on *aaaA* was previously identified (Paredes 2014) and these results correlate. For further validation, a range of arginine concentrations could be tested and the qRT-PCR assay used to overcome the issues with the kanamycin promoter.

The addition of histidine and glutamine produced an effect on *aaaA* expression which was similar to arginine in the PAO1 *ΔaaaA* strain. This is intriguing because these amino acids have nitrogen containing R groups. Perhaps there is a missing piece of the regulatory puzzle where exopeptidases in *P. aeruginosa* are upregulated when nitrogen rich amino acids are present in the absence of nitrate abundance. The STRING database (Chapter 3) found amino acid permeases and oligopeptide transporter proteins were potentially associated with *aaaA* and could form part of this feedback mechanism. It would be interesting to explore this link further. Histidine and arginine are also both basic amino acids and may share transportation routes into the cell. One of these is through the OprD (D2) outer membrane transporter which transports basic amino acids (Trias and Nikaido 1990; Li *et al* 2013). Additionally the gene *PA5153* is shown by the *Pseudomonas* genome database to encode a periplasmic ABC transporter which transports lysine, arginine, ornithine, histidine, and octopine. There could be some positive feedback from these transportation systems. Glutamine could also be associated with arginine through nitrate availability and RpoN. One of the putative regulators of *aaaA* was found to be glnG (NtrC) in Chapter 3. NtrC activates pathways that can provide alternative sources of nitrogen in nitrogen limited conditions (Janssen *et al* 1982). The increase in *aaaA* expression in response to glutamine supports the prediction that glutamine through NtrC is involved in the control of *aaaA*. This illustrated in Figure 6.3.1.

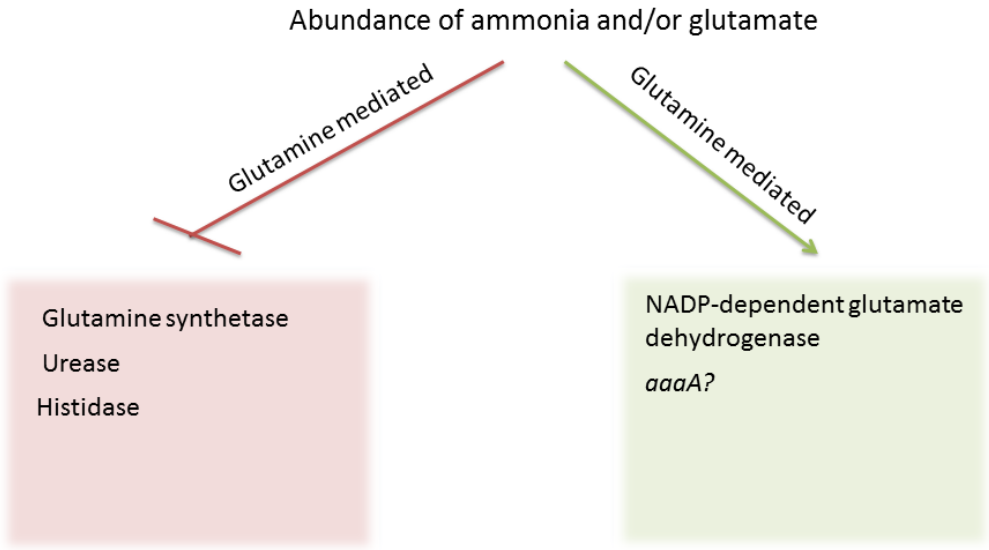


Figure 6.3.1: Association between nitrogen availability, glutamine, histidine and *aaaA*.
Based on Janssen *et al* (1982).

Addition of serine increased both P*aaaA* and P*kan* activation and is therefore not thought to be *aaaA* specific. Glycine, which does not have a nitrogen containing

R-group, caused an *aaaA* specific decrease in expression in the PAO1 *ΔaaaA* strain but not the PAO1 WT. The assimilation of glycine and pyocyanin biosynthesis both depend on the *PA2449* gene (Lundgren *et al* 2013). The link between *aaaA* and phenazines has been explored in this thesis and perhaps glycine is a part of this association in some way. The addition of asparagine resulted in an increase of *PaaaA* activation in the WT strain. It is unexpected that asparagine would positively affect *PaaaA* because a product of asparagine metabolism is ammonium (NH_4+), both an exogenous source of nitrate and pH increasing molecule (Figure 6.3.2, PseudoCyc database). Further investigation is needed to understand how this connection could be mediated. Like asparagine, methionine increased P*aaaA* activation in the PAO1 WT, but as *Pkan* activation was also affected this may not be *aaaA* specific. Methionine addition also decreased P*aaaA* activation in the PAO1 *ΔaaaA* strain which did not occur in the *Pkan* control. Further investigation is needed to confirm this effect and the mechanism behind it.

Taken as a whole, a preliminary hypothesis from these data is that the amino acids with R-group nitrogen atoms stimulate *aaaA* expression and amino acids without R-group nitrogen atoms either do not affect *aaaA* or downregulate it. Because of the negative regulatory influences on *PaaaA* when the gene is present, these effects are masked in the PAO1 WT. It remains to be seen how true this hypothesis is and would be an exciting aspect of *aaaA* regulation to explore.

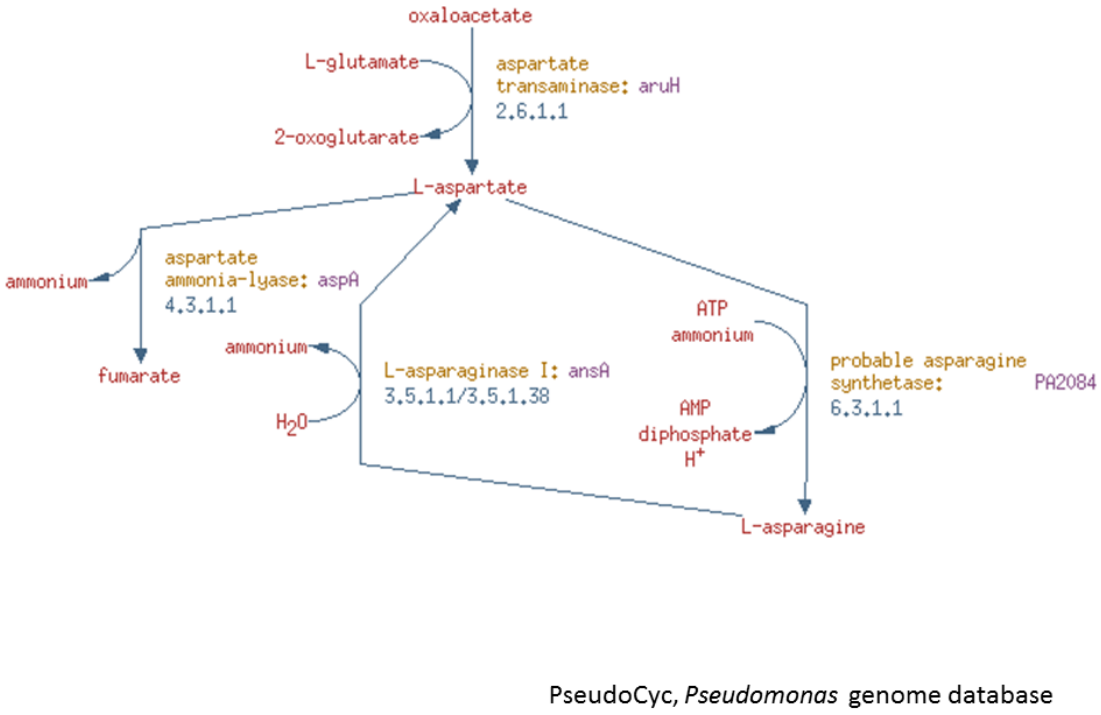


Figure 6.3.2: Ammonium and ammonia are produced in the asparagine metabolic pathway. Image taken from the PseudoCyc database.

The minimal media cocktail was then trialled for use in biofilm assays. As the microchamber assay shows, both strains produced healthy biofilms in this media. It was hoped that media would also be used for the Bioflux assays; however there was a short shelf life of the combined media which started to precipitate within 24 hours. Until this issue could be resolved use of the media was suspended and the assays conducted using ASM which also had the advantage of being relevant to CF. However, the repetition of some of the experiments in Chapter 4 and the investigation of arginine and tripeptide availability in the Bioflux assay could be informative because this media contains neither arginine, KNO_3 or NH_4Cl. The media should be re-optimised by reducing the concentrations of the most insoluble amino acids (for example isoleucine) and subsequently testing PAO1 and PAO1 *ΔaaaA* to ensure that the growth was sufficient and equal to each other with this revision.

6.3.3 The complementation phenomenon

The complementation of PAO1 *ΔaaaA* with an arabinose inducible, chromosomally situated, copy of the *aaaA* ORF was achieved and an inducer concentration found to be optimal at 0.2 % for distinguishing non induced and induced cell phenotypes. The AaaA activity of PAO1 *ΔaaaA* miniCTX::*araC::aaaA* was compared with miniCTX*::aaaA* and *pME6032::aaaA*: complemented strains used in previous work (Luckett *et al* 2012). All complemented strains exhibited the

expected levels of AaaA activity. When used as a control in the comparison of PAO1 and PAO1 *ΔaaaA* biofilm formation in the Bioflux however, it was found that both induced and uninduced versions of miniCTX*::araC::aaaA* resulted in reduced biofilm formation compared to the WT or *ΔaaaA* strains. Moreover, testing of the *pME6032::aaaA* strain revealed that the addition of the inducer IPTG reduced biofilm formation. Previous studies found that IPTG can disperse biofilms (Johansson *et al* 2008), which is in part why the arabinose inducible complementation was constructed. However as both strains showed this unexpected result of less biofilm, and arabinose itself did not disperse the PAO1 and PAO1 *ΔaaaA* generated biofilms the inducer did not appear to be at fault. One hypothesis was that the induction of *aaaA* threw its expression out of balance with the cell's requirements, having a detrimental rather than beneficial effect. The regulation of *aaaA* appears to be complex, dependent on several environmental triggers, and still largely not understood (Chapter 3). Expression of *aaaA* from the inducible strains would be timed differently during cell growth and more enzyme activity than the WT would be occurring. As has been observed in Chapters 3 & 5, the expression of native *aaaA* is generally low. Perhaps there is a very good reason *aaaA* is expressed at this low level. Although the more obvious effect of an overproduction of AaaA is more available arginine which has been shown to disperse biofilms in the right circumstances (Everett *et al* 2017), increases in arginine concentration did not appear to increase biofilm dispersal in the Bioflux system. Another possibility is the overburdening of the cell transportation machinery and consequent fitness cost to the cell. This was noted in Chapter 5 and may apply to the overproduction of full-length as well as truncated AaaA. Comparative growth curves could be produced to find out if this fitness cost exists and at which stage of growth. To be sure it is not a strain specific effect, the complementation plasmids could also be tested in the LESB65 background.

A second hypothesis is that other ORFs encoded within *aaaA* were disturbed when they were placed in a different location. This was investigated by searching for internal ORFs, analysis of these by BLAST to detect any matches of interest, and exploration for alternatively coding putative promoters that could activate any of these ORFs. The only ORF found to have an associated putative promoter sequence was ORF 18 which the BLAST search identified as a hypothetical protein of unknown function. No identified transcription factors were predicted to bind to this putative promoter. Although there remains a small possibility that OFR 18 or one of the other identified ORFs with a promoter that has been missed by the tools used here, has a role in biofilm production, it would be a surprising finding.

One suggestion for further investigation is a qRT-PCR experiment which could be employed with 1 set of primers designed to bind within ORF 18 and another set to bind to a location outside of ORF 18 but within *aaaA*. The comparison of ORF 18 specific product expression could be compared to the alternatively binding primers and any differences identified.

6.3.4 Conclusion

This chapter has indicated that AaaA has a subtle role in biofilm formation. It appears to be part of a balanced cell response to different environmental conditions which include but are not limited to: oxygen availability, arginine availability, nitrate availability and potentially other amino acid availability. It also seems to be influenced by other cellular processes including those particular to chronically infecting strains such as LESB65 and the phenazine mediated redox balancing pathways including pyruvate fermentation. As such it is an integral part of the *P. aeruginosa* machinery necessary to sustain growth in the crowded conditions typical of a biofilm. How important AaaA is to biofilm formation varies in response to these different variables and further understanding of the metabolic and regulatory links with each of these will be essential to unravelling the place AaaA has in the *P. aeruginosa* biofilm.

7 Chapter 7: Final Conclusion and Future Directions

7.1 Introduction

To shed light on the involvement of AaaA in persistent CF lung infections, the current study has explored how the requirement of this autotransporter is influenced by the environment, particular *P. aeruginosa* backgrounds, and mode of growth. The association between AaaA and the CF airway environment was examined using a two pronged approach: unravelling the regulatory network to expose triggers for AaaA recruitment, and observation of its response to environmental factors using a dedicated activity assay, transcriptional reporter system and qRT-PCR. This was further extended to study the manifestation of AaaA in CF isolates. In addition to this, tools have been developed to produce AaaA for structural analysis and inhibitor screening. The demonstrated contribution of AaaA to biofilm establishment emphasizes the importance of inhibitor design which is further supported by its link to chronic infection in the murine model.

Together, this work has revealed that in addition to playing a role in skin wound infections (Luckett *et al* 2012), AaaA is a component of the multifactorial virulence network *P. aeruginosa* utilizes in the CF airway. AaaA appears to have a metabolic function within hypoxic environments and could be targeted by novel therapies with the aim of eradicating this stubborn pathogen.

7.2 Discussion

7.2.1 The AaaA functional domain is highly conserved between *P. aeruginosa* CF isolates and the population can be divided into two types of *aaaA* upstream region

All the CF isolates analysed harboured an intact *aaaA* open reading frame (ORF) with conserved active site residues. Of the residue substitutions identified in AaaA, only a subset were shared between different isolates. Whether these changes affected the stability or catalytic function of AaaA remains to be seen, and could be tested in cell-free protein activity assays by incorporating AaaA purified according to the protocol described in Chapter 5. Alternatively, site-directed mutagenesis could be employed to assess the effect of each substitution in the native PAO1 background using the established whole cell AaaA activity assay. By extending such an approach to incorporate AaaA variants in known virulent strains e.g. LESB65 and wound isolates, a full picture of AaaA activity relative to infection could be constructed.

Despite the similarities in the ORFs, AaaA activity varied between the CF isolates and from PAO1. Although the changes observed in the non-catalytic residues of AaaA could be the cause of this variation, the hypothesis that regulation and specific strain background strongly influenced *aaaA* expression was tested. Sequencing of *aaaA* promoter regions identified similarity between those of the CF isolates (with the exception of CF 393 and potentially CF 030) and LESB65. In addition to scattered SNPs, a 160 bp deletion (relative to PAO1) which included the putative binding sites for NarL and ArgR was identified in LESB65 and the majority of the CF isolates. The deletion was shared by a large percentage of *P. aeruginosa* strains in the NCBI genome database, and engineering this deletion into PAO1 would enable the effects it has on AaaA activity, timing of *aaaA* expression in different conditions and differences in biofilm production to be specifically investigated. A preliminary biofilm investigation was conducted with the CF isolates. The biofilms formed from isolates with a LES-like promoter differed structurally from PAO1. Conversely CF 393, which has a PAO1-like promoter, formed a biofilm more structurally similar to PAO1. Compared to LESB type strains, PAO1 biofilms had a more heterogeneous, clustered profile with large microcolonies. This difference in phenotype was also observed in previous studies (O'May *et al* 2007 and Fricks-Limax *et al* 2011), and has been attributed to the slower growth and biofilm formation in *in vitro* assays. Notably, the biofilm forming capacity of LESB65 *ΔaaaA* was reduced from LESB65 WT levels, a difference not evident for PAO1 and its derived *ΔaaaA* mutant. A study by O'May *et al* (2007) comparing the biofilms of CF isolates with PAO1, suggests that PAO1 *in vitro* biofilms are more robust, and therefore could be more susceptible to collapse when *aaaA* was absent. This is contested in part by the findings of Cullen *et al* (2015), where the slower growing biofilm phenotype was less susceptible to detachment. Alternatively, changes in the QS regulation, phenazine system (Cullen *et al* 2015) and yet to be revealed metabolic changes in LESB65, could necessitate increased reliance on *aaaA* activity. The differences in the *aaaA* UPS region could have occurred in line with one or more of these changes. Together these data suggest that the promoter differences between PAO1 and the chronic CF isolates tested may be part of *P. aeruginosa's* evolution from an acute to a chronically infecting strain and in this background AaaA is more important. It will be important to see if this prediction is correct with further study.

To take the promoter investigation further, expression of *aaaA* by the CF isolates was compared to the PAO1 strains. Difficulty introducing the miniCTX-*lux*::*PaaaA* construct into the clinical isolates limited this analysis. However, it was possible to conclude that there was variation in *aaaA* expression between the CF isolates

and PAO1 which did not correlate with differences in the ORF or promoter. The qRT-PCR assay developed in Chapter 3 could now be applied to investigate this further; however due to time constraints it was not possible to incorporate this into the current study.

7.2.2 Phenotypic traits associated with a more virulent cell state were reduced or absent in CF isolates, and no difference was observed between PAO1 and PAO1 *ΔaaaA* strains

To determine if particular variations of AaaA correlated with certain virulence-associated phenotypic traits of *P. aeruginosa*, a range of assays were performed. Elastase production, swarming, swimming, twitching motility, pyocyanin and growth profiles were compared. The majority of isolates were deficient in the phenotypes associated with acute virulence including elastase, motility and fast growth in planktonic aerobic conditions. This correlates with the findings of Cullen *et al* (2015), which found CF isolates to be less virulent, have longer lag phases in planktonic growth, and show reduced motility than other *P. aeruginosa* strains. CF 030, which likely had a promoter profile more similar to PAO1, was the exception in growth and flagella mediated motility, while CF 892 produced more pyocyanin than the PAO1 strains. Interestingly, CF 393 (PAO1-like promoter) clumped in the ASM floating biofilm model like PAO1 and formed a biofilm in the Bioflux which was more structurally similar to PAO1. In reverse of this, LESB65 did not clump in the ASM floating model and formed a biofilm structurally similar to those exhibited by the other CF isolates tested in the Bioflux (Chapter 6). Different environmental preferences for biofilm formation have been exhibited in CF isolates to PAO1, including oxygen concentration and the difference in the models could reflect this (Fricks-Limax *et al* 2011; Davies and Bilton 2009; Yoon *et al* 2002). Together, this data supports the hypothesis that the deletion in the promoter region of *aaaA* correlates with strains which have a more chronic profile, but requires further investigation.

7.2.3 The expression and activity of AaaA in CF relevant conditions was most affected by oxygen and arginine presence

AaaA activity was tested in a number of conditions chosen to represent environmental components of the CF airway which could influence AaaA. Additionally, the expression of *aaaA* was tested using the transcriptional reporter miniCTX-*lux*::*PaaaA* and by qRT-PCR analysis. NaCl concentration, nitrate availability, pH, ASM, and oxygen concentration were tested. The only condition which had an outstanding effect on AaaA activity was oxygen availability. Intriguingly, oxygen-limited biofilms of PAO1 and PAO1 *ΔaaaA* strains did not

differ, indicating that other pathways could be compensating for the absence of AaaA in this environment. The effect of oxygen on the expression of *aaaA* could not be tested using the transcriptional reporter because of the requirement of oxygen for luminescence. In the qRT-PCR assay a possible effect of oxygen on the expression of *aaaA* was observed but this was not significant and the generally low expression of *aaaA* made it difficult to draw firm conclusions. The assay could be modified simply by adding a greater concentration of cDNA to the reaction or by harvesting RNA from a greater number of cells. Once a higher concentration of cells is used for the qRT-PCR assay, the findings of PAO1 can be compared with LESB65. Following this, *aaaA* expression in the regulator mutant strain backgrounds can be tested which would help determine the effect different putative regulators have on *aaaA* expression in oxygen limited conditions.

The fact that nitrate did not reduce the activity was unexpected and potentially due to the experimental set up. The cultures were grown aerobically in a rich media and were in a planktonic state. A preliminary screen using a media developed in this thesis for the testing of AaaA with minimal interference from nitrate and arginine sources showed that 10 mM nitrate reduced *aaaA* expression. This should be repeated with higher concentrations of nitrate, inclusion of AaaA activity measurements, and using biofilms as the latter is more reflective of the real infection environment in CF (Hoiby *et al* 2010; Bjarnsholt *et al* 2010; Costerton *et al* 1981; Yoon *et al* 2002; Moreau-Marquis 2008). Adjusting ASM to remove the KNO_3, NH_4Cl and arginine might also provide tighter control over the nitrate levels. The presence and absence of arginine was also tested in the minimal media cocktail and found to increase *aaaA* expression, which would be predicted to increase AaaA activity. An activity test in this media would establish if this was the case.

Higher NaCl concentrations have been found to increase surface adhesion and reduce motility in *P. aeruginosa* (Cowell *et al* 1997; Soutourina *et al* 2001). As these phenotypes are linked to biofilm development (Dunne 2002; Garrett *et al* 2008) which is hypothesised to be influenced by *aaaA*, the relationship between NaCl and *aaaA* was examined. Although the expression of *aaaA* in PAO1 *ΔaaaA* was higher when more NaCl was available in LB media, AaaA activity was not significantly affected consistently. If a trend exists, it appears a lower NaCl concentration correlates with increased AaaA activity. When AaaA activity was measured in CF isolates grown in different NaCl concentrations however, a low NaCl correlated with a reduced activity.

It was hypothesised that AaaA could support *P. aeruginosa in vivo* by helping to balance an acidic environment (Ballard *et al* 1999; Poulsen *et al* 1994; Poulsen and Machen 1996) with the basic product of the ADI pathway, ammonia (Lindgren *et al* 2014; Xiong *et al* 2014) and possibly arginine itself (Boriello *et al* 2006; Lebeaux *et al* 2014). Within the pH range tested, *aaaA* expression and AaaA activity was highest at pH 6.8 in the PAO1 background. This is thought to be the typical pH of a CF airway (Palmer *et al* 2007) and AaaA may be helpful for pH balancing in these conditions. Both the higher and lower pHs of 7.2 and 6.2 resulted in a lower expression of *aaaA,* which suggests that if AaaA does help to balance the pH of the environment encountered by *P. aeruginosa*, it is only effective within a fairly narrow range.

Taken together these results suggest that *aaaA* may or may not be affected by NaCl concentration, is upregulated at a slightly lowered pH and when more arginine is available. More AaaA activity appears to be stimulated by a pH of 6.8 and low oxygen concentration. These conditions match those typical of the CF airway (discussed in Chapter 4).

7.2.4 Regulation of *aaaA* is complex and analysis of its promoter reveals the potential for a highly intricate multilayer regulation

Chapter 3 explored the *aaaA* regulatory network. This was mainly through *in silico* analysis which was compared with previous *aaaA* expression data using the miniCTX-*lux*::*PaaaA* transcriptional reporter (Paredes 2014).

A number of putative regulator binding sites were found in the promoter region of *aaaA* for ArgR, ArcA, NarL, RhlR and RpoN which correlated with the data from Paredes (2014). This supports the hypotheses that these regulators are involved in the control of *aaaA* and that the expression of this gene is highly sensitive to changes in a wide range of environmental conditions. Therefore, changes in the availability of arginine (ArgR), nitrate (NarL), oxygen (ArcA), as well as alterations in cell density (RhlR) would have an impact on the expression of *aaaA*. To determine if the putative sites are true and these regulators are binding directly to the *aaaA* promoter, alterations in these by site-directed mutagenesis will need to be performed. Additionally, further putative regulator binding sites were found which correlated with the environmental conditions expected to influence AaaA. These were FleQ and NtrC. NtrC and FleQ are 2 of 3 putative regulators of *aaaA* which could interact with RpoN to control transcription. NtrC responds to low environmental nitrate concentrations and can activate its target genes by using the ATPase function to convert RpoN into an open confirmation

(Janssen *et al* 1982; UniProtKB - P0AFB8 (NTRC_ECOLI)). FleQ, responding to c-di-GMP, can also activate gene transcription through RpoN in a similar way to NtrC. It may also act independently from RpoN to distort the DNA structure to prevent the binding of repressors (Baraquet *et al* 2012). In the case of *aaaA*, these repressors could be the H-NS like DNA bending proteins MvaU and MvaT. An area of low GC and high curvature which is predictive of a site recognised by MvaU/T (Winardhi *et al* 2014; Castang *et al* 2008; Worrell thesis, 2005; Falconi *et al* 1993), was found to be overlapping the putative RpoN binding site. The interactions of these regulators could explain how RpoN specifically activates the *aaaA* promoter in certain conditions, and also helps explain why relatively low expression of *aaaA* was observed during this study.

The hypothesis of RpoN mediated transcription of *aaaA* is a complex one and requires further unravelling. Correlating with the transcriptional reporter data of Paredes (2014), a putative RpoN site was found upstream of the *aaaA* ORF. To analyse this further, the transcriptional reporter was used in this study to test *aaaA* expression in PAO1, PAO1 *ΔrpoN*, and PAO1 *ΔrpoN att Tn7:rpoN* strains. No significant increase in *aaaA* expression was observed between WT and *ΔrpoN* strains, in contrast to Paredes (2014), where *aaaA* expression was increased in PA14 *ΔrpoN* from the PA14 WT. In both Paredes (2014) and Chapter 3, LB was used as the growth medium and the problems with using LB to accurately determine *aaaA* expression have already been discussed. Additionally, to support the auxotrophic nature of *ΔrpoN* for glutamine, the media was supplemented with 0.4% glutamine. In Chapter 3, all strains were grown in LB with the supplementation of glutamine whereas in Paredes (2014) it appeared that only the *ΔrpoN* mutant was grown in the supplemented media. Addition of glutamine could distort the results because it could promote NtrC which could release the repressive effect of RpoN on *aaaA* (Chapter 6, minimal media section). A preliminary test comparing PAO1 with and without glutamine however, found no significant difference in *aaaA* expression when glutamine was added to LB. Not only limited to glutamine, mutation of RpoN would affect multiple systems, including the denitrification pathway (Totten *et al* 1990) which could have a cumulative effect on *aaaA* but individually be difficult to identify in LB. For example, glutamine had a stimulatory effect on *aaaA* expression in the minimal media. The change in strain background could also complicate this if the two strains had differences in their regulatory mechanisms or metabolism (Kukavica-Ibrulj *et al* 2008). Without establishing whether RpoN is indeed directly binding to the promoter region of *aaaA* using approaches such as site-directed mutagenesis of the binding site, the relationship between *aaaA* and RpoN remains elusive.

The use of the *lux*-based transcriptional reporter to investigate *aaaA* expression is limited to aerobic conditions. As upregulation of *aaaA* was hypothesised to be principally in lower oxygen environments, another strategy was needed. For this aim a qRT-PCR assay for *aaaA* was developed and pilot-tested in microaerobic conditions with ASM and LB media. Although the detection of significant differences were prevented by the generally low expression of *aaaA*, the assay can now be easily adjusted by using a higher cell density to compensate for this low expression. In addition to the comparison of *aaaA* expression in high and low oxygen concentrations, the expression of *aaaA* can be compared in different regulator mutant backgrounds grown in these different oxygen concentrations. This could help further understand the link between regulation and environment.

7.2.5 A recombinant version of AaaA is suitable for further purification and crystallisation

With a view to investigate the potential of AaaA as a therapeutic target, an attempt to further understand the structure-function of this protein was performed by designing a strategy which could potentially enable its purification and subsequent crystallisation. Three different recombinant versions of AaaA were engineered and assessed for yield, stability, solubility and purification potential. All were truncated to remove the beta-barrel attaching the passenger domain to the OM. All modified copies of *aaaA* were placed under a T7 promoter of the *pET21a (+)* system which is inducible by IPTG. The first version was designed and cloned by Paredes (2014) and was truncated at residue 337. This version was able to be produced at fairly high levels of the recombinant protein, but formed inclusion bodies which prompted an isolation method using centrifugation to semi-purify, denaturation to solubilise and dialysis to resolubilise. The resolubilised protein was suitable for cell free activity assays, but was not able to be sufficiently concentrated for crystallisation purposes. The second version of truncated AaaA was then designed with the aim of increasing the solubility. To do this, the signal peptide was removed in case this hindered protein folding. Additionally, the C-terminus was extended to protect hydrophobic residues that were potentially exposed in the first construct (AaaAt1). AaaAt2 reduced the viability of the producing bacteria, which had to be grown at low temperatures while inducing expression of *aaaAt2* at low levels. The resulting protein was not soluble and showed a high rate of degradation. It therefore follows that the presence of the signal peptide is required for AaaA purification, and that localisation to the cytoplasm could result in toxicity. With this information, the final version of truncated AaaA was designed and expressed (AaaAt3). The AaaAt3 version included the signal peptide and also the extended

C-terminus of AaaAt2. It was also less harmful to the host bacteria than the AaaAt2, and enabled the detection of soluble protein, which is encouraging for further purification. Ammonium sulphate precipitation (salting out) could be used as a gentle purification strategy in future work since it has been successfully employed previously (e.g. Duong-Ly and Gabelli 2014; Wingfield 2001).

7.2.6 Abnormally high expression of *aaaA* may be problematic for cell viability, and weaken *P. aeruginosa's* ability to form biofilm

It was noticed during the purification of different recombinant versions of AaaA that cells producing a high quantity of $AaaAt_{1\text{-}3}$ had attenuated growth and more protein was inactive due to increased inclusion body formation. Natively produced, full length AaaA is undetectable by immunoblotting and qRT-PCR analysis showed that *aaaA* expression is low in comparison to *16S* and *PA0329*. This implies that the expression is tightly controlled which correlates with the identification of numerous transcription factors putatively controlling *aaaA* expression. It also suggests that AaaA activity is beneficial in limited amounts and how limited this is depends on the environment. The overexpression of *aaaA* from an artificial promoter therefore may hinder rather than help *P. aeruginosa.* This may explain the lack of biofilm produced from *aaaA* overexpressing strains. This will be useful to consider in further investigations: more AaaA is not necessarily better for the individual cell. In part, this is contradicted by a study undertaken by Toyofuku *et al* (2012), which identified AaaA as a protein of high abundance in biofilm cultures, along with ADI pathway genes. However, it may be that in concert with other changes in gene expression and protein production, AaaA is required in higher amounts. Moreover, the timing of expression would likely be very different in an *in vivo* setting: no sudden increases in protein production upon artificial induction for example. Greater understanding of the regulation will now be helpful in determining why this phenomenon exists.

7.2.7 The dependence of *P. aeruginosa* on AaaA for biofilm formation applies to particular conditions and strain backgrounds

In Chapter 6, biofilm growth by PAO1 and PAO1 *ΔaaaA* strains were compared in a number of different models. In the microchamber, Bioflux and Congo-red models, using LB or ASM, there was no difference between the two strains. This differed from when ASM floating biofilm clumps were analysed since PAO1 formed sizable clumps not evident with the PAO1 *ΔaaaA* mutant (Chapter 6). This supports the hypothesis that *P. aeruginosa* uses multiple systems to sustain growth in a biofilm and when these other systems are fully operational, the cells can survive without AaaA. Both media would have supported these compensating

systems (Palmer *et al* 2007) and likely provided sufficient arginine for the ADI pathway to operate over the time tested. The inability of PAO1 *ΔaaaA* to form floating clumps in ASM model could be due to the size of the clump, which was bigger than in the other models and therefore more cells would be buried in the centre, and thus at a distance from the surface of the biofilm in contact with nutrients and oxygen. Moreover, the ASM floating model does not rely on the action of Type IV pili (Davies *et al* 2017). However, as both PAO1 and PAO1 *ΔaaaA* were found to twitch equally well in Chapter 3, and the non-clumping LES has been reported to have lost this motility (Kukavica-Ibrulj ; Cullen et al 2015), the anomaly is perhaps more likely to be due to reduced surface area:volume ratio of the biofilm than Type IV pili production. Comparison of PAO1 and PAO1 *ΔaaaA* strains in the EVPL model resulted in a higher colony count of the mutant strain than the WT. Again, ASM was used as the growth media which may have provided sufficient nutrient sources for the 24 hours of biofilm growth. The repetition of this experiment at different time points and testing in microaerobic conditions would be of interest for further work. Additionally, the PAO1 strains were found to exhibit a more acute phenotypic profile, testing positive for elastase, motility appendages, and faster growth in aerobic conditions. It may be that only after several generations in a biofilm growth state these strains would be more adapted to long-term chronic infection. The work of Dr Alex Day (thesis, 2017), showed a divergence of phenotypes produced from a PAO1 strain passaged for multiple generations in a *C. elegans* model.

Rather than a generational study which would be interesting but time consuming, further experiments should now use the LESB65 and LESB65 *ΔaaaA* strains for CF associated work. The comparison of LESB65 and PAO1 strains over several days in the EVPL model could support the acute/chronic adaption hypothesis if LESB65 was better at surviving for longer. Additionally, the localisation of the biofilm produced by the two strain types may be different which could influence the results. After 72 hours, detectable biofilm was no longer detectable by H & E staining on the bronchiole sections and it is probable that the strains migrated to other areas of the well. A study by Kukavica-Ibrulj *et al* (2008), using a rat model, placed beads with attached LESB58 or PAO1 into the bronchus and found that PAO1 migrated to the alveolar tissue but LESB58 remained in the bronchus. This illustrates the more aggressive nature of PAO1 and more persistent nature of LES. The findings from the LESB65 and LESB65 *ΔaaaA* Bioflux comparison support the importance of strain background on experimental outcomes, and it will be exciting to see whether the difference in biofilm formation between the two strains is repeatable in other assays. The only other assay tested with the

LESB65 and LESB65 *ΔaaaA* strains in this work is the floating ASM assay. Surprisingly, neither strain showed the clumping phenotype exhibited by PAO1. Why the two assays showed different results and these were the reverse of each other in PAO1 and LESB65 strains is curious and highlights the importance of using a range of biofilm models.

The ASM used in the assays described above contained the amounts of arginine and nitrate sources quoted in Palmer *et al* (2007). These were conjectured to be the amounts typical of CF sputum. The lung however is heterogeneous, and includes a number of micro-environments (Button and Button 2013). The amount of some of the amino acids and nutrient sources could differ in the deeper pockets of mucus plugs and areas which may be poorly sampled by sputum expirations (Roncetti *et al* 2018; Mamessier *et al* 2006). To test the importance of AaaA when *P. aeruginosa* biofilms were faced with lower or higher arginine concentrations, ASM with no arginine, twice the amount of arginine normally in ASM (0.612 M), 10 mM tripeptide and 10 mM tripeptide instead of arginine, was tested as a biofilm growth medium in the Bioflux system. A deficit of arginine was found to produce a difference between PAO1 and PAO1 *ΔaaaA* biofilms. This would support the hypothesis that AaaA becomes more important for biofilm growth when arginine is limited. The next experiment to try is the combination of no arginine and low oxygen. This could be achieved in the microchambers with adjusted ASM or minimal media cocktail.

That the growth of *P. aeruginosa* in a biofilm is supported by several overlapping pathways is supported by the comparison of PA14, PA14 *ΔaaaA,* PA14 *Δphz* and PA14 *ΔaaaA Δphz* strains using the Congo-red colony biofilm model. The wrinkling observed when the combined mutant was grown suggests that the AaaA-ADI and phenazine systems can compensate for each other. This is useful for the bacterium, but more difficult from an inhibitory drug design viewpoint. It also makes studying the effect of AaaA on biofilm growth more difficult because there could be pathway compensation in some conditions and not others, affecting the results. Now that this has been identified, some of the assays could be repeated with this strain included to control for this effect (Figure 7.2.1). Additionally, it would be interesting to assess the LESB65 strains for phenazine gene expression and pyocyanin production. Cullen *et al* (2015) and colleagues found that the data gathered from a panel of CF isolates suggested a trade-off between pyocyanin and biofilm production which was skewed towards the later phenotype the longer the isolates had been resident in the CF lung.

In Luckett *et al* (2012) the long term survival of PAO1 *ΔaaaA* was attenuated in a mouse chronic wound model. This correlates with the results generated using the murine lung infection model. Although the growth between PAO1 and PAO1 *ΔaaaA* strains was similar, the PAO1 *ΔaaaA* strain was cleared quicker and effected more symptoms more typical of an acute infection than the PAO1 WT. This suggests that AaaA is implicated in a chronic mode of growth and cells without this protein may find it more difficult to form a chronic infection. A repetition in the future with the LESB65 strains would be interesting to see if this continues over a longer infection period.

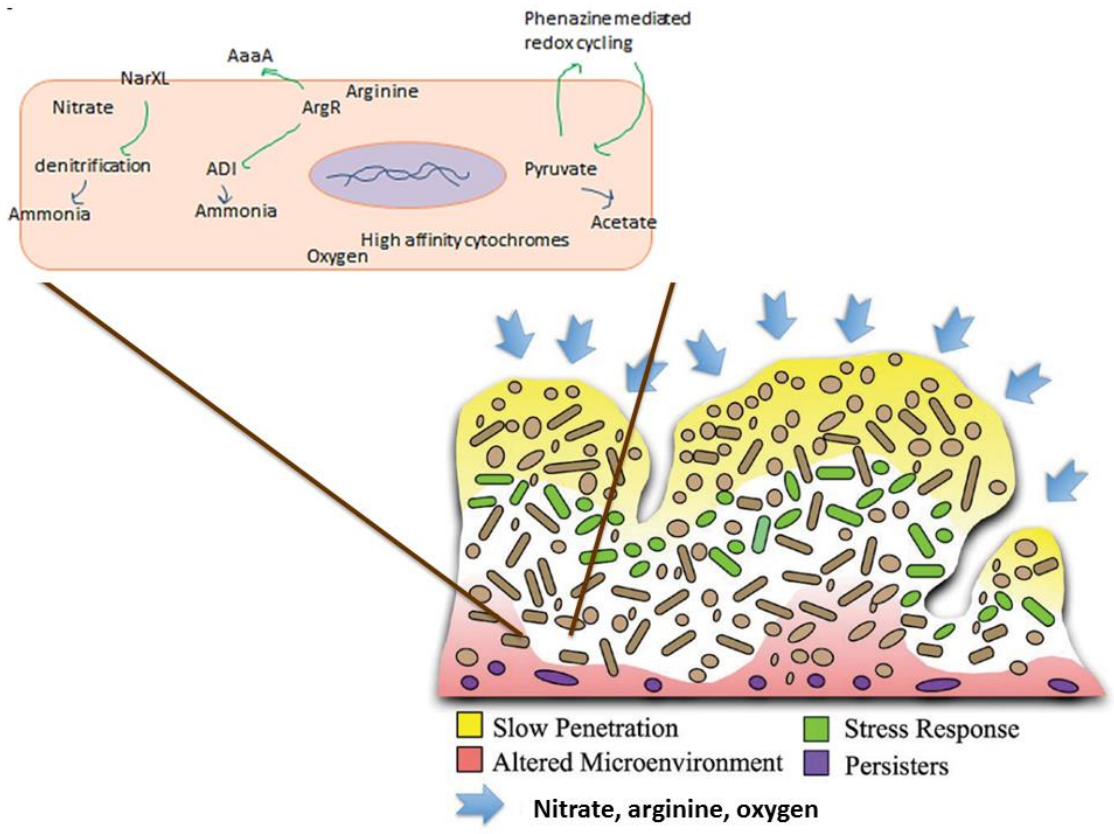


Figure 7.2.1: Simple model for how AaaA could support the metabolism of *P. aeruginosa* in a biofilm. Figure adapted from Toyofuku *et al* (2012). Cells within a biofilm are exposed to different microenvironments and *P. aeruginosa* adjusts its metabolism for those specific conditions. In the deeper areas of the biofilm, particularly within the centres of microcolonies, substance penetration is reduced. To thrive in these conditions, different metabolic systems work in concert to maintain sufficient ATP. High affinity cytochromes, denitrification, phenazine mediated redox cycling and the AaaA-ADI arginine fermentation likely work in concert, orchestrated by an intricate regulatory system. The waste products from these metabolic pathways can also help balance an acidic environment.

7.3 Summary

This study has furthered our understanding of the role AaaA plays in the biology of *P. aeruginosa*. It has also revealed a number of areas to pursue in greater detail for more insight into how this protein interacts with other systems in *P. aeruginosa* to mediate its success in *in vivo* infection.

The retention of AaaA activity in CF isolates supports its importance in helping *P. aeruginosa* thrive in the CF airway environment. Investigation of specific CF relevant conditions revealed that oxygen availability is likely the greatest factor leading to an increase in AaaA activity. AaaA may also help *P. aeruginosa* cope with particular pH and NaCl levels as well as responding to biofilm specific conditions. Environmental conditions such as arginine, nitrate, glutamine, cell density and biofilm growth could influence AaaA via the identified putative regulator binding sites in the promoter of *aaaA.* These, if genuine, reveal that AaaA is required in low nitrate, low oxygen, and mid to high cell densities, while arginine induces a positive feedback loop. Although the role of RpoN remains elusive, the amalgamation of reporter and *in silico* data supports a model involving RpoN, NtrC, FleQ and MvaU/T which can be further tested through site-directed mutagenesis and qRT-PCR. The AaaA mediated ADI pathway catalysis of arginine dovetails with the phenazine redox cycling system and together with nitrate and high affinity cytochromes allows *P. aeruginosa* to flourish in microaerobic conditions. AaaA is likely more important to *P. aeruginosa* strains more adapted to chronic conditions which supports the hypothesis that it aids *P. aeruginosa* survival in long term infections. Although the purification of AaaA has required a considerable amount of fine-tuning, a construction is now available to be taken forward through the later stages of purification and it is hoped that elucidation of the crystal structure is not far away. This will enable the selection of inhibitors by *in silico* docking and the testing of these using cell-free activity assays.

7.4 The End

Appendices

1.1 Appendix A: minimal media cocktail validation

To test if the type of nitrate source affected the promoter activation of *PaaaA* or *Pkan* in PAO1 and PAO1 *ΔaaaA*, the addition of 20 mM KNO_3 and NH_4Cl to the MMP + succinate base was compared. Figure 1.1.1 shows there was no significant difference between the nitrate sources except in PAO1 *ΔaaaA* miniCTX-*lux::Pkan*, with higher activation occurring in the NH_4Cl media.

To further enhance growth and biofilm forming capacity in the MMP + succinate media, the inclusion of NaCl and $CaCl_2$ in the final media composition was explored. MMP already includes a source of magnesium ($MgSO_4$). The addition of $CaCl_2$ at concentrations as low as 1.0 mM was found to produce thicker *P. aeruginosa* biofilms in part due to increased alginate production. A 3 to 5 fold production increase in pycocyanin was also linked to the addition of $CaCl_2$ which also supports growth at low oxygen concentrations (Sarkisova *et al* 2005). The concentration of NaCl can affect gene transcription (Chapter 4). Additionally, NaCl was found to affect the adhesion of *P. aeruginosa* to surfaces, increasing with greater concentrations of NaCl present (Cowell *et al* 1998). NaCl presence also increases the production of biosurfactants such as rhamnolipids (Ikhwani *et al* 2017; Rodrigues *et al* 2017). To ensure that NaCl or $CaCl_2$ did not affect the *aaaA* promoter, 10 mM of each salt was added the MMP, succinate, nitrate media which PAO1 and PAO1 *ΔaaaA* with *PaaaA* or *Pkan* lux fusions were grown in. There were no significant differences in promoter activation between NaCl and $CaCl_2$ containing media in either *PaaaA* or *Pkan* at the concentrations tested. This is shown in Figure 1.1.2.

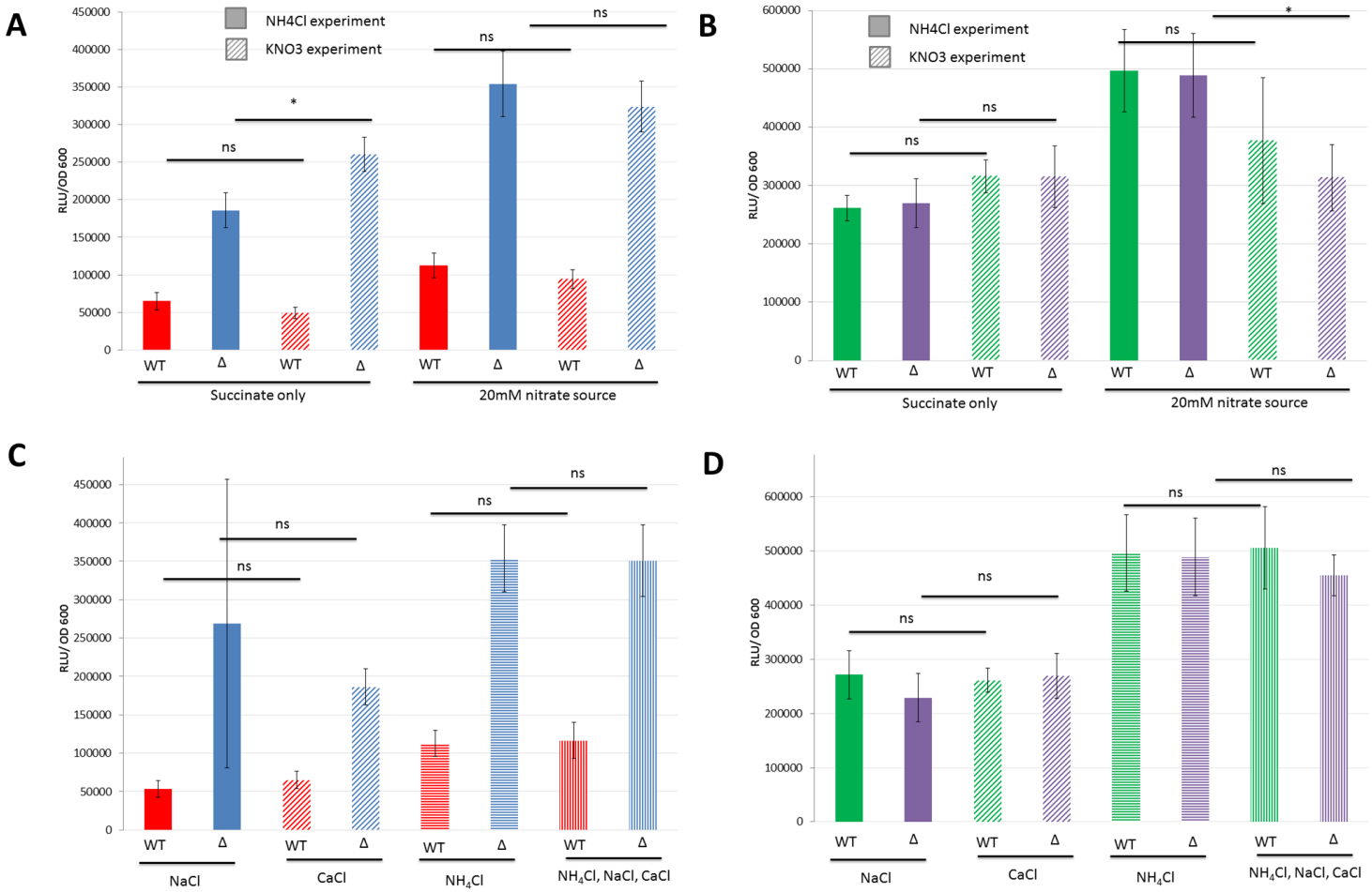


Figure 1.1.1: Comparison between KNO_3 and NH_3Cl nitrate sources with the investigation of the effect of different salts on growth & expression. PAO1 miniCTX-*lux*::*PaaaA* (red), PAO1 *ΔaaaA* miniCTX-*lux*::P*aaaA* (blue), PAO1 miniCTX-*lux*::P*kan* (green) and PAO1 *ΔaaaA* miniCTX-*lux*::P*kan* (purple) were grown in MMP + 20 mM succinate with 20 mM KNO_3, 20 mM NH_4Cl, 10 mM NaCl, 10 mM $CaCl_2$ or 20 mM NH_4Cl, 10 mM NaCl, 10 mM $CaCl_2$. The growth was recorded as OD_{600} over time and the bioluminescence measured as RLU/ OD_{600} which is proportional to promoter activation. A) Comparison between 20 mM KNO_3 and NH_4Cl with miniCTX-*lux*::P*aaaA*. B) Comparison between 20 mM KNO_3 and NH_4Cl with miniCTX-*lux*::Pkan. C) Effect of 10 mM CaCl and NaCl, on *aaaA* expression with miniCTX-*lux*::P*aaaA*. D) Effect of 10 mM CaCl and NaCl, on *aaaA* expression with miniCTX-*lux*::P*kan.* Bars represent the average of three biological replicates and the error bars show the standard deviation between these. Conditions are compared using t-tests with the labels ns and * indicating the significance of variation determined by this test.

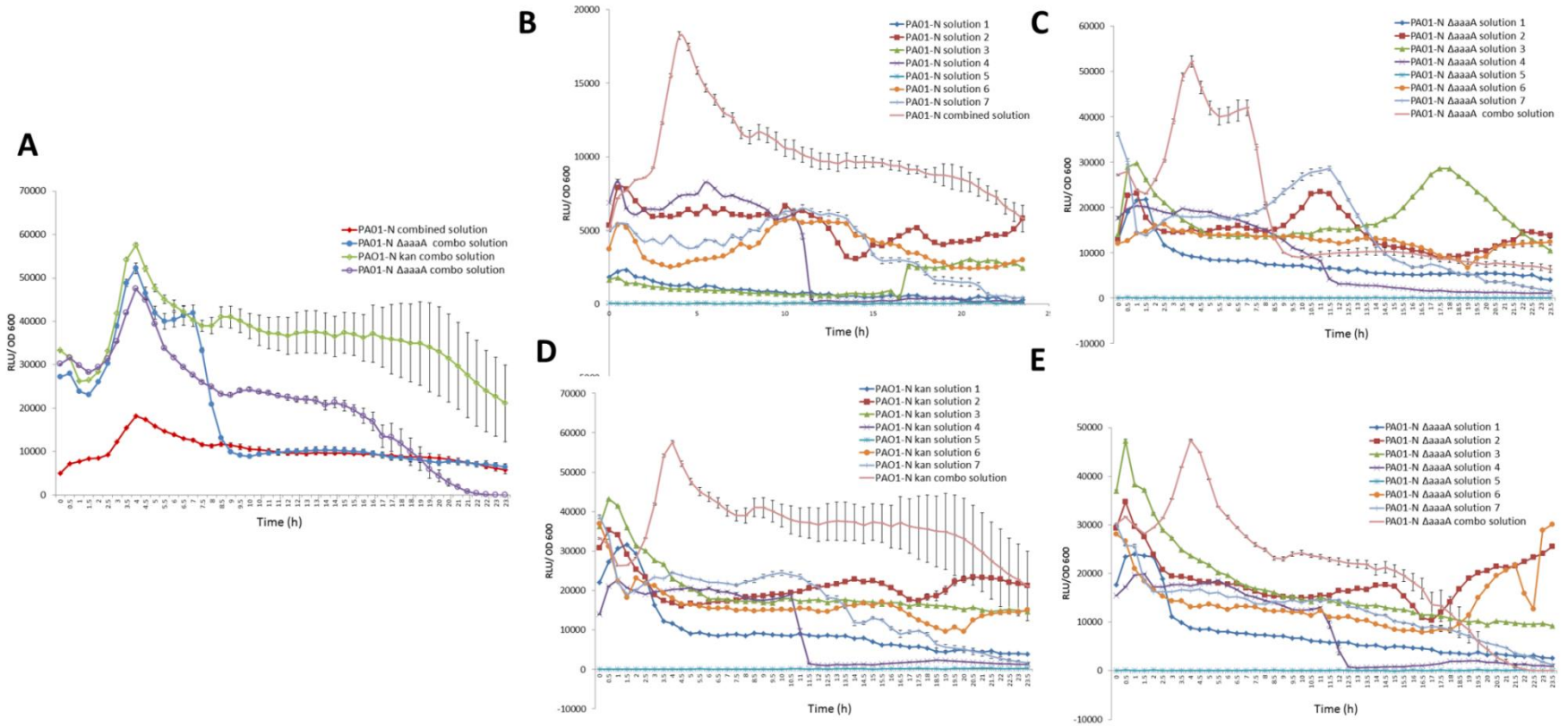


Figure 1.1.2: Showing the activation of the P*aaaA* and Pkan promoters in PAO1 and PAO1 *ΔaaaA* strains in the optimised combined solution named minimal media cocktail. The minimal media cocktail is made as 7 separate solutions which are combined before use. Alignment of the typical 4 hour peak is present in the combined media (all lines panel A, pink lines panels B-E). Panel A shows PAO1 miniCTX-*lux*::P*aaaA* (red), PAO1 *ΔaaaA* miniCTX-*lux*::P*aaaA* (blue), PAO1 miniCTX-*lux*::P*kan* (green) and PAO1 *ΔaaaA* miniCTX-*lux*::P*kan* (purple) bioluminescence when grown and tested in the combined minimal media cocktail. Panel B shows PAO1 miniCTX-*lux*::P*aaaA* when grown and tested in solution 1-7 and the combined solution. Panel C shows PAO1 *ΔaaaA* miniCTX-*lux*::P*aaaA* when grown and tested in solution 1-7 and the combined solution. Panel D shows PAO1 miniCTX-*lux*::Pkan when grown and tested in solution 1-7 and the combined solution. Panel E shows PAO1 *ΔaaaA* miniCTX-*lux*::P*kan* when grown and tested in solution 1-7 and the combined solution. Error bars show the standard deviation between 3 biological replicates

References

Abby, S. S., Cury, J., Guglielmini, J., Neron, B., Touchon, M. & Rocha, E. P. 2016. Identification of protein secretion systems in bacterial genomes. *Sci Rep,* 6, 23080.

Abdel-Mawgoud, A. M., Lepine, F. & Deziel, E. 2010. Rhamnolipids: diversity of structures, microbial origins and roles. *Appl Microbiol Biotechnol,* 86, 1323-36.

Achermann, Y., Goldstein, E. J., Coenye, T. & Shirtliff, M. E. 2014. *Propionibacterium acnes*: from commensal to opportunistic biofilm-associated implant pathogen. *Clin Microbiol Rev,* 27**,** 419-40.

Acosta, N., Heirali, A., Somayaji, R., Surette, M. G., Workentine, M. L., Sibley, C. D., Rabin, H. R. & Parkins, M. D. 2018. Sputum microbiota is predictive of long-term clinical outcomes in young adults with cystic fibrosis. *Thorax,* 73**,** 1016-1025.

Albert, M. L., Pearce, S. F. A., Francisco, L. M., Sauter, B., Roy, P., Silverstein, R. L. & Bhardwaj, N. 1998. Immature dendritic cells phagocytose apoptotic cells via alphavbeta5 and CD36, and cross-present antigens to cytotoxic T lymphocytes. *J Exp Med. ,* 188, 1359-68.

Alexeeva, S., Hellingwerf, K. J. & De Mattos, M. J. T. 2003. Requirement of ArcA for Redox Regulation in *Escherichia coli* under Microaerobic but Not Anaerobic or Aerobic Conditions. *JOURNAL OF BACTERIOLOGY,,* 185, p. 204–209

Allesen-Holm, M., Barken, K. B., Yang, L., Klausen, M., Webb, J. S., Kjelleberg, S., Molin, S., Givskov, M. & Tolker-Nielsen, T. 2006. A characterization of DNA release in *Pseudomonas aeruginosa* cultures and biofilms *Mol Microbiol,* 59, 1114-28.

Allocati, N., Masulli, M., Di Ilio, C. & De Laurenzi, V. 2015. Die for the community: an overview of programmed cell death in bacteria. *Cell Death Dis,* 6, e1609.

Alvarez-Ortega, C. & Harwood, C. S. 2007. Responses of *Pseudomonas aeruginosa* to low oxygen indicate that growth in the cystic fibrosis lung is by aerobic respiration. *molecular microbiology,* 65, 153–165.

Anderson, G. G., Moreau-Marquis, S., Stanton, B. A. & O'toole, G. A. 2008. *In vitro* analysis of tobramycin-treated *Pseudomonas aeruginosa* biofilms on cystic fibrosis-derived airway epithelial cells. *Infect Immun,* 76, 1423-33.

Anderson, M. P., Gregory, R. J., Thompson, S., Souza, D. W., Paul, S., Mulligan, R. C., Smith, A. E. & Welsh, M. J. 1991. Demonstration that CFTR is a chloride channel by alteration of its anion selectivity. *Science,* 253, 202-205.

Anderson, R. M., Zimprich, C. A. & Rust, L. 1999. A Second Operator Is Involved in *Pseudomonas aeruginosa* Elastase (lasB) Activation. *JOURNAL OF BACTERIOLOGY,* 181, p. 6264–6270

Arai, H. 2011. Regulation and function of versatile aerobic and anaerobic respiratory metabolism in Pseudomonas aeruginosa. *Frontiers in microbiology,* 2, 1-13.

Arai, H., Igarashi, Y. & Kodama, T. 1994. Structure and ANR-dependent transcription of the nir genes for denitrification from Pseudomonas aeruginosa. *Biosci Biotechnol Biochem,* 58, 1286-91.

Arai, H., Igarashi, Y. & Kodama, T. 1995. Expression of the nir and nor genes for denitrification of *Pseudomonas aeruginosa* requires a novel CRP/FNR-related transcriptional regulator, DNR, in addition to ANR. *FEBS Federation of European Biochemical Societies,* 371, 73-76.

Arai, H., Kawakami, T., Osamura, T., Hirai, T., Sakai, Y. & Ishii, M. 2014. Enzymatic characterization and *in-vivo* function of five terminal oxidases in Pseudomonas aeruginosa. *J Bacteriol*, 1-30.

Arai, H., Kodama, T. & Igarashi, Y. 1997. Cascade regulation of the two CRP/FNR-related transcriptional regulators (ANR and DNR) and the denitrification enzymes in Pseudomonas aeruginosa. *Molecular Microbiology,* 25, 1141–1148.

Arai, H., Kodama, T. & Igarashi, Y. 1998. The role of the nirQOP genes in energy conservation during anaerobic growth of Pseudomonas aeruginosa. *Biosci Biotechnol Biochem.,* 62, 1995-9.

Arai, H., Mizutani, M. & Igarashi, Y. 2003. Transcriptional regulation of the nos genes for nitrous oxide reductase in Pseudomonas aeruginosa. *Microbiology,* 149, 29-36.

Arai, H., Y, I. & Kodama, T. 1991. Nitrite activates the transcription of the *Pseudomonas aeruginosa* nitrite reductase and cytochrome c-551 operon under anaerobic conditions. *FEBS Federation of European Biochemical Societies,* 288, 227-228

Armstrong, D. S., Grimwood, K., Carlin, J. B., Carzino, R., Olinsky, A. & Phelan, P. D. 1996. Bronchoalveolar lavage or oropharyngeal cultures to identify lower respiratory pathogens in infants with cystic fibrosis. *Pediatric Pulmonology* 21**,** 267-275

Ashish, A., Paterson, S., Mowat, E., Fothergill, J. L., Walshaw, M. J. & Winstanley, C. 2013. Extensive diversification is a common feature of *Pseudomonas aeruginosa* populations during respiratory infections in cystic fibrosis. *J Cyst Fibros,* 12, 790-3.

Atkinson, R. M., Lipuma, J. J., Rosenbluth, D. B. & Dunne, W. M. 2006. Chronic Colonization with Pandoraea apista in Cystic Fibrosis Patients Determined by Repetitive-Element-Sequence PCR. *Journal of Clinical Microbiology,* 44**,** 833-836.

Azghani, A. O. 1996. *Pseudomonas aeruginosa* and epithelial permeability: role of virulence factors elastase and exotoxin A. *American Journal of Respiratory Cell and Molecular Biology,* 15, 132-40.

Backman, K., Chen, Y.-M. & Magasanik, B. 1981. Physical and genetic characterization of the glnA--glnG region of the *Escherichia coli* chromosome. *Proc. Nati. Acad. Sci. USA Genetics* 78, pp. 3743-3747,.

Bagge, N., Schuster, M., Hentzer, M., Ciofu, O., Givskov, M., Greenberg, E. P. & Hoiby, N. 2004. *Pseudomonas aeruginosa* Biofilms Exposed to Imipenem Exhibit Changes in Global Gene Expression and -Lactamase and Alginate Production. *Antimicrobial Agents and Chemotherapy,* 48, 1175-1187.

Balasubramanian, D., Kumari, H. & Mathee, K. 2015. *Pseudomonas aeruginosa* AmpR: an acute-chronic switch regulator. *Pathog Dis,* 73, 1-14.

Balasundaram, B., Nesbeth, D., Ward, J. M., Keshavarz-Moore, E. & Bracewell, D. G. 2009. Step change in the efficiency of centrifugation through cell engineering: co-expression of Staphylococcal nuclease to reduce the viscosity of the bioprocess feedstock. *Biotechnol Bioeng,* 104, 134-42.

Ballard, S. T., Trout, L., Bebo, Z., Sorscher, E. J. & Crews, A. 1999. CFTR involvement in chloride, bicarbonate, and liquid secretion by airway submucosal glands. *American Journal of Physiology - Lung Cellular and Molecular Physiology,* 277, L694-L699.

Banin, E., Vasil, M. L. & Greenberg, E. P. 2005. Iron and *Pseudomonas aeruginosa* biofilm formation. *Proc Natl Acad Sci U S A,* 102, 11076-81.

Baraquet, C., Murakami, K., Parsek, M. R. & Harwood, C. S. 2012. The FleQ protein from *Pseudomonas aeruginosa* functions as both a repressor and an activator to control gene expression from the pel operon promoter in response to c-di-GMP. *Nucleic Acids Res,* 40, 7207-18.

Barker, A. P., Vasil, A. I., Filloux, A., Ball, G., Wilderman, P. J. & Vasil, M. L. 2004. A novel extracellular phospholipase C of *Pseudomonas aeruginosa* is required for phospholipid chemotaxis. *Molecular Microbiology* 53, 1089–1098

Barnard, T. J., Dautin, N., Lukacik, P., Bernstein, H. D. & Buchanan, S. K. 2007. Autotransporter structure reveals intra-barrel cleavage followed by conformational changes. *Nat Struct Mol Biol,* 14, 1214-20.

Barrios, H., Valderrama, B. & Morett, E. 1999. Compilation and analysis of sigma(54)-dependent promoter sequences. *Nucleic Acids Res. ,* 27, 4305-13.

Barth, A. L. & Plttt, L. 1996. The high amino-acid content of sputum from cystic fibrosis patients promotes growth of auxotrophic Pseudomonas aeruginosa.pdf. *J. Med. Microbiol. ,* 45, 110-119.

Baur , H., Luethi, E., Stalon, V., Mercenier, A. & Haas, D. 1989. Sequence analysis and expression of the arginine-deiminase and carbamate-kinase genes of Pseudomonas aeruginosa. *Eur J Biochem,* 179, 53 - 60.

Bayer, A. S., Eftekhar, F., Tu, J., Nast, C. C. & Speert, D. P. 1990,. Oxygen-dependent up-regulation of mucoid exopolysaccharide (alginate) production in Pseudomonas aeruginosa. *INFECTION AND IMMUNITY,* 58, p. 1344-1349

Bayes, H. K., Ritchie, N., Irvine, S. & Evans, T. J. 2016. A murine model of early *Pseudomonas aeruginosa* lung disease with transition to chronic infection. *Sci Rep,* 6, 35838.

Baynham, P. J., Ramsey, D. M., Gvozdyev, B. V., Cordonnier, E. M. & Wozniak, D. J. 2006. The *Pseudomonas aeruginosa* ribbon-helix-helix DNA-binding protein AlgZ (AmrZ) controls twitching motility and biogenesis of type IV pili. *J Bacteriol,* 188, 132-40.

Becher, A., Benchmarks, H. & Schweizer, P. 2000. Integration-Proficient *Pseudomonas aeruginosa* Vectors for Isolation of Single-Copy Chromosomal lacZand luxGene Fusions. *BioTechniques,* 29, 948-952.

Ben-Meir, D., Spungin, A., Ashkenazi, R. & Blumberg, S. 1993. Specificity of Streptomyces griseus aminopeptidase and modulation of activity by divalent metal ion binding and substitution. *Eur. J. Biochem. ,* 212, 107-112

Benach, J., Swaminathan, S. S., Tamayo, R., Handelman, S. K., Folta-Stogniew, E., Ramos, J. E., Forouhar, F., Neely, H., Seetharaman, J., Camilli, A. & Hunt, J. F. 2007. The structural basis of cyclic diguanylate signal transduction by PilZ domains. *The EMBO Journal,* 26, 5153–5166.

Benkert, B., Quack, N., Schreiber, K., Jaensch, L., Jahn, D. & Schobert, M. 2008. Nitrate-responsive NarX-NarL represses arginine-mediated induction of the *Pseudomonas aeruginosa* arginine fermentation arcDABC operon. *Microbiology,* 154, 3053-60.

Benz, I. & Schmidt, M. A. 2011. Structures and functions of autotransporter proteins in microbial pathogens. *Int J Med Microbiol,* 301, 461-8.

Berghmans, T., Sculier, J. P. & Klastersky, J. 2003. A prospective study of infections in lung cancer patients admitted to the hospital. *Chest,* 124, 114-20.

Berks, B. C., Ferguson, S. J., Moir, J. W. B. & Richardson, D. J. 1995. Enzymes and associated electron transport systems that catalyse the respiratory reduction of nitrogen oxides and oxyanions. *Biochimica et Biophysics Acta* 1232, 97-173.

Bernier, S. P., Ha, D. G., Khan, W., Merritt, J. H. & O'toole, G. A. 2011. Modulation of *Pseudomonas aeruginosa* surface-associated group behaviors by individual amino acids through c-di-GMP signaling. *Res Microbiol,* 162, 680-8.

Bernstein, H. D. 2015. Looks can be deceiving: recent insights into the mechanism of protein secretion by the autotransporter pathway. *Mol Microbiol,* 97, 205-15.

Berry, A., Devault, J. D. & Chakrabarty, A. M. 1989. High osmolarity is a signal for enhanced algD transcription in mucoid and nonmucoid *Pseudomonas aeruginosa* strains. *JOURNAL OF BACTERIOLOGY,,* 171, p. 2312-2317.

Bertoni, G., Fujita, N., Ishihama, A. & De Lorenzo, V. 1998. Active recruitment of sigma54-RNA polymerase to the Pu promoter of Pseudomonas putida- role of IHF and alphaCTD. *The EMBO Journal,* 17, pp.5120–5128.

Betts, S. & King, J. 1999. There's a right way and a wrong way- *in vivo* and *in vitro* folding, misfolding and subunit assembly of the P22 tailspike. *Structure* 7.

Birrer, P., Mcelvaney, N. G., Rüdeberg, A., Sommer, C. W., Liechti-Gallati, S., Kraemer, R., Hubbard, R. & Crystal, R. G. 1994. Protease-antiprotease imbalance in the lungs of children with cystic fibrosis. *Am J Respir Crit Care Med. ,* 150, 207-13.

Bjarnsholt, T., Jensen, P. O., Fiandaca, M. J., Pedersen, J., Hansen, C. R., Andersen, C. B., Pressler, T., Givskov, M. & Hoiby, N. 2009. Pseudomonas aeruginosa biofilms in the respiratory tract of cystic fibrosis patients. *Pediatr Pulmonol,* 44, 547-58.

Bodelon, G., Marin, E. & Fernandez, L. A. 2009. Role of periplasmic chaperones and BamA (YaeT/Omp85) in folding and secretion of intimin from enteropathogenic *Escherichia coli* strains. *J Bacteriol,* 191, 5169-79.

Boles, B. R., Thoendel, M. & Singh, P. K. 2004. Self-generated diversity produces ''insurance effects'' in biofilm communities. *PNAS,* 101, 16630–16635.

Boles, B. R., Thoendel, M. & Singh, P. K. 2005. Rhamnolipids mediate detachment of *Pseudomonas aeruginosa* from biofilms. *Mol Microbiol,* 57, 1210-23.

Bonfield , T. L., Panuska , J. R., Konstan , M. W., Hilliard , K. A., Hilliard , J. B., Ghnaim , H. & Berger, M. 1995. Inflammatory cytokines in cystic fibrosis lungs. *American Journal of Respiratory and critical care medicine,* 152.

Borlee, B. R., Goldman, A. D., Murakami, K., Samudrala, R., Wozniak, D. J. & Parsek, M. R. 2010. *Pseudomonas aeruginosa* uses a cyclic-di-GMP-regulated adhesin to reinforce the biofilm extracellular matrix. *Mol Microbiol,* 75, 827-42.

Borriello, G., Richards, L., Ehrlich, G. D. & Stewart, P. S. 2006. Arginine or nitrate enhances antibiotic susceptibility of *Pseudomonas aeruginosa* in biofilms. *Antimicrob Agents Chemother,* 50, 382-4.

Boucher, J. C. 2002. An overview of the pathogenesis of cystic fibrosis lung disease. *Advanced Drug Delivery Reviews,* 54, 1359–1371.

Boucher, J. C., Yu, H., Mudd, M. H. & Deretic, V. 1997. Mucoid *Pseudomonas aeruginosa* in cystic fibrosis- characterization of muc mutations in clinical isolates and analysis of clearance in a mouse model of respiratory infection. *INFECTION AND IMMUNITY,* 65, p. 3838–3846.

Boucher, R. C. 2004. New concepts of the pathogenesis of cystic fibrosis lung disease. *European Respiratory Journal,* 23, 146-158.

Boucher, H. W. & Corey, G. R. 2008. Epidemiology of methicillin-resistant *Staphylococcus aureus. Clin Infect Dis,* 46 Suppl 5**,** S344-9.

Boynton, Z. L., Koon, J. J., Brennan, E. M., Clouart, J. D., Horowitz, D. M., Gerngross, T. U. & Huisman, G. W. 1999. Reduction of Cell Lysate Viscosity during Processing of Poly(3-Hydroxyalkanoates) by Chromosomal Integration of the Staphylococcal Nuclease Gene in Pseudomonas putida. *APPLIED AND ENVIRONMENTAL MICROBIOLOGY,* 65, p. 1524–1529.

Br0ndsted, L. & Atlung, T. 1994. Anaerobic regulation of the hydrogenase 1 (hya) operon of *Escherichia coli*. *JOURNAL OF BACTERIOLOGY,,* 176, p. 5423-5428

Bragonzi, A., Worlitzsch, D., Pier, G. B., Timpert, P., Ulrich, M., Hentzer, M., Andersen, J. B., Givskov, M., Conese, M. & Döring, G. 2005. Nonmucoid *Pseudomonas aeruginosa* Expresses Alginate in the Lungs of Patients with Cystic Fibrosis and in a Mouse Model. *J Infect Dis.,* 192, 410–419.

Brandel, J., Humbert, N., Elhabiri, M., Schalk, I. J., Mislin, G. L. & Albrecht-Gary, A. M. 2012. Pyochelin, a siderophore of Pseudomonas aeruginosa: physicochemical characterization of the iron(III), copper(II) and zinc(II) complexes. *Dalton Trans,* 41, 2820-34.

Brandon, L. D., Goehring, N., Janakiraman, A., Yan, A. W., Wu, T., Beckwith, J. & Goldberg, M. B. 2003. IcsA, a polarly localized autotransporter with an atypical signal peptide, uses the Sec apparatus for secretion, although the Sec apparatus is circumferentially distributed. *Molecular Microbiology,* 50, 45-60.

Braud, A., Hannauer, M., Mislin, G. L. & Schalk, I. J. 2009. The *Pseudomonas aeruginosa* pyochelin-iron uptake pathway and its metal specificity. *J Bacteriol,* 191, 3517-25.

Briel, M., Greger, R. & Kunzelmann, K. 1998. Cl− transport by cystic fibrosis transmembrane conductance regulator (CFTR) contributes to the inhibition of epithelial Na+ channels (ENaCs) in Xenopus oocytes co-expressing CFTR and ENaC. *Journal of Phsiology,* 508, 825—836.

Brint, J. M. & Ohman, D. E. 1995. Synthesis of multiple exoproducts in *Pseudomonas aeruginosa* is under the control of RhlR-RhlI, another set of regulators in strain PAO1 with homology to the autoinducer-responsive LuxR-LuxI family. *JOURNAL OF BACTERIOLOGY, ,* 177, p. 7155–7163

Britigan, B. E., Railsback, M. A. & Cox, C. D. 1999. The *Pseudomonas aeruginosa* Secretory Product Pyocyanin Inactivates α1 Protease Inhibitor- Implications for the Pathogenesis of Cystic Fibrosis Lung Disease. *INFECTION AND IMMUNITY,* 67, 1207–1212.

Britigan, B. E., Rasmussen, G. T. & Cox, C. D. 1997. Augmentation of Oxidant Injury to Human Pulmonary Epithelial Cells by the *Pseudomonas aeruginosa* Siderophore Pyochelin. *INFECTION AND IMMUNITY,* Vol. 65, p. 1071–1076.

Brooke, J. S. 2012. *Stenotrophomonas maltophilia*: an emerging global opportunistic pathogen. *Clin Microbiol Rev,* 25**,** 2-41.

Brooun, A., Liu, S. & Lewis, K. 2000. A Dose-Response Study of Antibiotic Resistance in *Pseudomonas aeruginosa* Biofilms. *ANTIMICROBIAL AGENTS AND CHEMOTHERAPY,* 44, p. 640–646.

Brown, M. R., Allison, D. G. & Gilbert, P. 1988. Resistance of bacterial biofilms to antibiotics- a growth-rate related effect. *Journal of Antimicrobial Chemotherapy* 22, 777-78.

Brown, P. S., Pope, C. E., Marsh, R. L., Qin, X., Mcnamara, S., Gibson, R., Burns, J. L., Deutsch, G. & Hoffman, L. R. 2014. Directly sampling the lung of a young child with cystic fibrosis reveals diverse microbiota. *Ann Am Thorac Soc,* 11**,** 1049-55.

Bryan, L. E., Van Den Elzen, H. M. & Tseng, J. T. 1972. Transferable Drug Resistance in Pseudomonas aeruginosa. *ANTIMICROBIAL AGENTS AND CHEMOTHERAPY,* 1, 22-29.

Buck, M., Gallegos, M.-T., Studholme, D. J., Guo, Y. & Gralla, J. D. 2000. The Bacterial Enhancer-Dependent s54 (sN) Transcription Factor. *JOURNAL OF BACTERIOLOGY,* 182, p. 4129–4136.

Burgess, R. R., Travers, A. A., Dunn, J. J. & Bautz, E. K. F. 1969. Factor Stimulating Transcription by RNA Polymerase. *Nature* 221, 43-46.

Burns, J. L., Gibson, R. L., Mcnamara, S., Yim, D., Emerson, J., Rosenfeld , M., Hiatt, P., Mccoy, K., Castile, R., Smith, A. L. & Ramsey, B. W. 2001;. Longitudinal Assessment of *Pseudomonas aeruginosa* in Young Children with Cystic Fibrosis. *The Journal of Infectious Diseases* 183, 444–52

Bush, M. & Dixon, R. 2012. The role of bacterial enhancer binding proteins as specialized activators of sigma54-dependent transcription. *Microbiol Mol Biol Rev,* 76, 497-529.

Bustin, S. A., Benes, V., Garson, J. A., Hellemans, J., Huggett, J., Kubista, M., Mueller, R., Nolan, T., Pfaffl, M. W., Shipley, G. L., Vandesompele, J. & Wittwer, C. T. 2009. The MIQE guidelines: minimum information for publication of quantitative real-time PCR experiments. *Clin Chem,* 55, 611-22.

Button, B. M. & Button, B. 2013. Structure and function of the mucus clearance system of the lung. *Cold Spring Harb Perspect Med,* 3.

Byrd, M. S., Sadovskaya, I., Vinogradov, E., Lu, H., Sprinkle, A. B., Richardson, S. H., Ma, L., Ralston, B., Parsek, M. R., Anderson, E. M., Lam, J. S. & Wozniak, D. J. 2009. Genetic and biochemical analyses of the *Pseudomonas aeruginosa* Psl exopolysaccharide reveal overlapping roles for polysaccharide synthesis enzymes in Psl and LPS production. *Mol Microbiol,* 73, 622-38.

Bzymek, K. P., Moulin, A., Swierczek, S. I., Ringe, D., Petsko, G. A., Bennett, B. & Holz, R. C. 2005. Kinetic, Spectroscopic, and X-ray Crystallographic Characterization of the Functional E151H Aminopeptidase from Aeromonas proteolytica. *Biochemistry* 44, 12030-12040.

Caldwell, C. C., Chen, Y., Goetzmann, H. S., Hao, Y., Borchers, M. T., Hassett, D. J., Young, L. R., Mavrodi, D., Thomashow, L. & Lau, G. W. 2009. *Pseudomonas aeruginosa* exotoxin pyocyanin causes cystic fibrosis airway pathogenesis. *Am J Pathol,* 175, 2473-88.

Campbell, E. A., Muzzin, O., Chlenov, M., Sun, J. L., Olson, C. A., Weinman, O., Trester-Zedlitz, M. L. & Darst, S. A. 2002. Structure of the Bacterial RNA Polymerase Promoter Specificity σ Subunit. *Molecular Cell,* 9, 527-539.

Cant, N., Pollock, N. & Ford, R. C. 2014. CFTR structure and cystic fibrosis. *Int J Biochem Cell Biol,* 52, 15-25.

Cao, H., Krishnan, G., Goumnerov, B., Tsongalis, J., Tompkins, R. & Rahme, L. G. 2001. A quorum sensing-associated virulence gene of *Pseudomonas aeruginosa* encodes a LysR-like transcription regulator with a unique self-regulatory mechanism. *Proc Natl Acad Sci U S A,* 98, 14613-8.

Carlsson, M., Shukla, S., Petersson, A. C., Segelmark, M. & Hellmark, T. 2011. *Pseudomonas aeruginosa* in cystic fibrosis: pyocyanin negative strains are associated with BPI-ANCA and progressive lung disease. *J Cyst Fibros,* 10, 265-71.

Carter, M. E., Fothergill, J. L., Walshaw, M. J., Rajakumar, K., Kadioglu, A. & Winstanley, C. 2010. A subtype of a *Pseudomonas aeruginosa* cystic fibrosis epidemic strain exhibits enhanced virulence in a murine model of acute respiratory infection. *J Infect Dis,* 202, 935-42.

Cascales, E. & Christie, P. J. 2003. The versatile bacterial type IV secretion systems. *Nat Rev Microbiol,* 1, 137-49.

Casasanta, M. A., Yoo, C. C., Smith, H. B., Duncan, A. J., Cochrane, K., Varano, A. C., Allen-Vercoe, E. & Slade, D. J. 2017. A chemical and biological toolbox for Type Vd secretion: Characterization of the phospholipase A1 autotransporter FplA from *Fusobacterium nucleatum. J Biol Chem,* 292, 20240-20254.

Castang, S., Mcmanus, H. R., Turner, K. H. & Dove, S. L. 2008. H-NS family members function coordinately in an opportunistic pathogen. *Proc Natl Acad Sci U S A,* 105, 18947-52.

Cathcart, G. R., Quinn, D., Greer, B., Harriott, P., Lynas, J. F., Gilmore, B. F. & Walker, B. 2011. Novel inhibitors of the *Pseudomonas aeruginosa* virulence factor LasB: a potential therapeutic approach for the attenuation of virulence mechanisms in pseudomonal infection. *Antimicrob Agents Chemother,* 55, 2670-8.

Celik, N., Webb, C. T., Leyton, D. L., Holt, K. E., Heinz, E., Gorrell, R., Kwok, T., Naderer, T., Strugnell, R. A., Speed, T. P., Teasdale, R. D., Likic, V. A. & Lithgow, T. 2012. A bioinformatic strategy for the detection, classification and analysis of bacterial autotransporters. *PLoS One,* 7, e43245.

Cheema, M. S., Rassing, J. E. & Marriott, C. 1986. THE DIFFUSION CHARACTERISTICS OF ANTIBIOTICS IN MUCUS GLYCOPROTEIN GELS. *Pharmacy and Pharmacology,* 38, 53P.

Chen, X. & Stewart, P. 1996. Chlorine Penetration into Artificial Biofilm Is Limited by a Reaction−Diffusion Interaction. *Environ. Sci. Technol,* 30, 2078-2083.

Cheng, S. H., Gregory, R. J., Marshall, J., Paul, S., Souza, D. W., White, G. A., D'riordan, C. F. & Smith, A. E. 1990. Defective intracellular transport and processing of CFTR is the molecular basis of most cystic fibrosis. *Cell,* 63, 627-634, .

Chesshyre , J. A. & Hipkiss, A. R. 1989. Low temperatures stabilize interferon α-2 against proteolysis in Methylophilus methylotrophus and *Escherichia coli*. *Appl Microbiol Biotechnol* 31, 158-162

Chevalier, N., Moser, M., Koch, H. G., Schimz, K. L., Willery, E., Locht, C., Jacob-Dubuisson, F. & Müller, M. 2004. Membrane targeting of a bacterial virulence factor harbouring an extended signal peptide. *J Mol Microbiol Biotechnol.,* 8, 7-18.

Chevrier, B., D'orchymont, H., Schalk, C., Tarnus, C. & D, M. 1996. The structure of the Aeromonas proteolytica aminopeptidase complexed with a hydroxamate inhibitor. Involvement in catalysis of Glu151 and two zinc ions of the co-catalytic unit. *Eur. J. Biochem. 237, 393-398* 237, 393-398.

Chevrierl, B., Schalk, C., D'orchymont , H., Rondeau, J., Moras, D. & Tarnus, C. 1994 Crystal structure of Aeromonas proteolytica aminopeptidase- a prototypical member of the co-catalytic zinc enzyme family. *Structure,* 2, 283-291.

Chi, E., Mehl, T., Nunn, D. & Lory, S. 1991. Interaction of *Pseudomonas aeruginosa* with A549 pneumocyte cells. *INFECTION AND IMMUNITY,* 53, p. 822-828

Choi, Y., Choi, J., Groisman, E. A., Kang, D. H., Shin, D. & Ryu, S. 2012. Expression of STM4467-encoded arginine deiminase controlled by the STM4463 regulator contributes to Salmonella enterica serovar Typhimurium virulence. *Infect Immun,* 80, 4291-7.

Chua, S. L., Hultqvist, L. D., Yuan, M., Rybtke, M., Nielsen, T. E., Givskov, M., Tolker-Nielsen, T. & Yang, L. 2015. *In vitro* and *in vivo* generation and characterization of *Pseudomonas aeruginosa* biofilm-dispersed cells via c-di-GMP manipulation. *Nat Protoc,* 10, 1165-80.

Ciofu, O., Lee, B., Johannesson, M., Hermansen, N. O., Meyer, P., Hoiby, N. & Scandinavian Cystic Fibrosis Study, C. 2008. Investigation of the algT operon sequence in mucoid and non-mucoid *Pseudomonas aeruginosa* isolates from 115 Scandinavian patients with cystic fibrosis and in 88 *in vitro* non-mucoid revertants. *Microbiology,* 154, 103-13.

Ciofu, O., Mandsberg, L. F., Bjarnsholt, T., Wassermann, T. & Høiby, N. 2010. Genetic adaptation of *Pseudomonas aeruginosa* during chronic lung infection of patients with cystic fibrosis: strong and weak mutators with heterogeneous genetic backgrounds emerge in mucA and/or lasR mutants. *Microbiology,* 156, 1108-19.

Clark, S. T., Diaz Caballero, J., Cheang, M., Coburn, B., Wang, P. W., Donaldson, S. L., Zhang, Y., Liu, M., Keshavjee, S., Yau, Y. C., Waters, V. J., Elizabeth Tullis, D., Guttman, D. S. & Hwang, D. M. 2015. Phenotypic diversity within a *Pseudomonas aeruginosa* population infecting an adult with cystic fibrosis. *Sci Rep,* 5, 10932.

Coenye, T., Vandamme, P., Govan, J. R. & Lipuma, J. J. 2001. Taxonomy and identification of the Burkholderia cepacia complex. *J Clin Microbiol,* 39**,** 3427-36

Coenye, T. & Nelis, H. J. 2010. *In vitro* and *in vivo* model systems to study microbial biofilm formation. *J Microbiol Methods,* 83, 89-105.

Cole, N., Bao, S., Thakur, A., Willcox, M. & Husband, A. J. 2000. KC production in the cornea in response to *Pseudomonas aeruginosa* challenge. *Immunology and Cell Biology* 78, 1-4.

Collier, D. N., Hager , P. W. & Phibbs, P. V. 1996. Catabolite repression control in the Pseudomonads *Res Microbiol. ,* 147, 551-61.

Comolli, J. C. & Donohue, T. J. 2004. Differences in two *Pseudomonas aeruginosa* cbb3 cytochrome oxidases. *Molecular Microbiology,* 51, 1193–1203.

Conibear, T. C. R., Willcox, M. D. P., Flanagan, J. L. & Zhu, H. 2012. Characterization of protease IV expression in *Pseudomonas aeruginosa* clinical isolates. *Journal of Medical Microbiology* 61, 180–190.

Cooper, E. M., Cutcliffe, C., Kristiansen, T. Z., Pandey, A., Pickart1, C. M. & Cohen, R. E. 2009. K63-specific deubiquitination by two JAMM/MPN+ complexes- BRISC-associated Brcc36 and proteasomal Poh1. *The EMBO Journal,* 28**,** 621–631.

Cornforth, D. M., Dees, J. L., Ibberson, C. B., Huse, H. K., Mathiesen, I. H., Kirketerp-Møller, K., Wolcott, R. D., Rumbaugh, K. P., Bjarnsholt, T. & Whiteley, M. 2018. Pseudomonas aeruginosatranscriptome during human infection. *Proceedings of the National Academy of Sciences,* 115, E5125-E5134.

Costa, T. R., Felisberto-Rodrigues, C., Meir, A., Prevost, M. S., Redzej, A., Trokter, M. & Waksman, G. 2015. Secretion systems in Gram-negative bacteria: structural and mechanistic insights. *Nat Rev Microbiol,* 13, 343-59.

Costello, A., Herbert, G., Fabunmi, L., Schaffer, K., Kavanagh, K. A., Caraher, E. M., Callaghan, M. & Mcclean, S. 2011. Virulence of an emerging respiratory pathogen,

genus Pandoraea, in vivo and its interactions with lung epithelial cells. *J Med Microbiol,* 60**,** 289-99.

Costerton, J. W. 1995. Overview of microbial biofilms. *Journal of Industrial Microbiology* 15, pp 137–140.

Costerton, J. W., Cheng, K.-J., Geesey, G. G., Ladd, T. I., Nickel, J. C., Dasgupta, M. & Marrie, T. J. 1987. BACTERIAL BIOFILMS IN NATURE AND DISEASE. *Ann. Rev. Microbiol.,* 41, 435~4.

Costerton, J. W., Stewart, P. S. & Greenberg, E. P. 1999 Bacterial Biofilms: A Common Cause of Persistent Infections. *SCIENCE,* 284, 1318-1322.

Cowell, B. A., Willcox, M. D. P. & Schneider, R. P. 1998. A relatively small change in sodium chloride concentration has a strong effect on adhesion of occular bacteria to contact lenses. *Journal of Applied Microbiology* 84, 950–958

Craig, N. L. & Nash, H. A. 1984. *E. coli* integration host factor binds to specific sites in DNA. *Cell, Vol.,* 39, 707-716.

Cullen, L., Weiser, R., Olszak, T., Maldonado, R. F., Moreira, A. S., Slachmuylders, L., Brackman, G., Paunova-Krasteva, T. S., Zarnowiec, P., Czerwonka, G., Reilly, J., Drevinek, P., Kaca, W., Melter, O., De Soyza, A., Perry, A., Winstanley, C., Stoitsova, S. R., Lavigne, R., Mahenthiralingam, E., Sa-Correia, I., Coenye, T., Drulis-Kawa, Z., Augustyniak, D., Valvano, M. A. & Mcclean, S. 2015. Phenotypic characterization of an international *Pseudomonas aeruginosa* reference panel: strains of cystic fibrosis (CF) origin show less in vivo virulence than non-CF strains. *Microbiology,* 161, 1961-77.

Cunin, R., Glansdorff, N., Pierard, A. & Stalon, V. 1986. Biosynthesis and Metabolism of Arginine in Bacteria. *MICROBIOLOGICAL REVIEWS,,* 50, 314-352

Da Mata Madeira, P. V., Zouhir, S., Basso, P., Neves, D., Laubier, A., Salacha, R., Bleves, S., Faudry, E., Contreras-Martel, C. & Dessen, A. 2016. Structural Basis of Lipid Targeting and Destruction by the Type V Secretion System of Pseudomonas aeruginosa. *J Mol Biol,* 428, 1790-803.

Dale , G. E., Broger , C., Langen, H., D'arcy, A. & Stüber, D. 1994. Improving protein solubility through rationally designed amino acid replacements: solubilization of the trimethoprim-resistant type S1 dihydrofolate reductase. *Protein Eng. ,* 7, 933-9.

Dalton, T., Dowd, S. E., Wolcott, R. D., Sun, Y., Watters, C., Griswold, J. A. & Rumbaugh, K. P. 2011. An *In vivo* Polymicrobial Biofilm Wound Infection Model to Study Interspecies Interactions. *Plos one,* 6, e27317.

Darch, S. E., Mcnally, A., Harrison, F., Corander, J., Barr, H. L., Paszkiewicz, K., Holden, S., Fogarty, A., Crusz, S. A. & Diggle, S. P. 2015. Recombination is a key driver of genomic and phenotypic diversity in a *Pseudomonas aeruginosa* population during cystic fibrosis infection. *Sci Rep,* 5, 7649.

Darling, K. E., Dewar, A. & Evans, T. J. 2004. Role of the cystic fibrosis transmembrane conductance regulator in internalization of *Pseudomonas aeruginosa* by polarized respiratory epithelial cells. *Cell Microbiol,* 6, 521-33.

Darveau, R. P. & Hancock, R. E. W. 1983. Procedure for Isolation of Bacterial Lipopolysaccharides from Both Smooth and Rough *Pseudomonas aeruginosa* and *Salmonella typhimurium* strains. *JOURNAL OF BACTERIOLOGY,*155, 831-838.

Darwin, A. J., Tyson, K. L., Busby, S. J. & Stewart, V. 1997. Differential regulation by the homologous response regulators NarL and NarP of *Escherichia coli* K-12 depends on DNA binding site arrangement. *Molecular Microbiology* 25, 583–595

Dasgupta, N., Wolfgang, M. C., Goodman, A. L., Arora, S. K., Jyot, J., Lory, S. & Ramphal, R. 2003. A four-tiered transcriptional regulatory circuit controls flagellar biogenesis in Pseudomonas aeruginosa. *Molecular Microbiology,* 50, 809-824.

Dautin, N. 2010. Serine protease autotransporters of *enterobacteriaceae* (SPATEs): biogenesis and function. *Toxins (Basel),* 2, 1179-206.

Dautin, N. & Bernstein, H. D. 2007. Protein secretion in gram-negative bacteria via the autotransporter pathway. *Annu Rev Microbiol,* 61, 89-112.

Davies, D. G., Chakrabarty, A. M. & Geesey, G. G. 1993. Exopolysaccharide production in biofilms- substratum activation of alginate gene expression by *Pseudomonas aeruginosa*. *APPLIED AND ENVIRONMENTAL MICROBIOLOGY,* 59, p. 1181-1186

Davies, D. G. & Geesey, G. G. 1995. Regulation of the alginate biosynthesis gene algC in *Pseudomonas aeruginosa* during biofilm development in continuous culture. *APPLIED AND ENVIRONMENTAL MICROBIOLOGY,* 61, p. 860–867.

Davies, D. G., Parsek, M. R., Pearson, J. P., Iglewski, B. H., Costerton, J. W. & Greenberg, E. P. 1998. The involvement of cell-to-cell signals in the development of a bacterial biofilm. *Science,* 280, 295-8.

Davies, E. V., James, C. E., Brockhurst, M. A. & Winstanley, C. 2017. Evolutionary diversification of *Pseudomonas aeruginosa* in an artificial sputum model. *BMC Microbiol,* 17, 3.

Davies, J. C. & Bilton, D. 2009. Bugs, biofilms, and resistance in cystic fibrosis. *RESPIRATORY CARE,* 54, 628-640.

De Baets, F., Schelstraete, P., Van Daele, S., Haerynck, F. & Vaneechoutte, M. 2007. Achromobacter xylosoxidans in cystic fibrosis: prevalence and clinical relevance. *J Cyst Fibros,* 6**,** 75-8.

De Beer, D., Stoodley, P. & Lewandowski, Z. 1994a. Liquid flow in heterogeneous biofilms. *Biotechnol Bioeng,* 44, 636-41.

De Beer, D., Stoodley, P., Roe, F. & Lewandowski, Z. 1994b. Effects of biofilm structures on oxygen distribution and mass transport. *Biotechnology and Bioengineering,,* 43, Pp. 1131-1138.

De Bentzmann, S., Roger, P. & Puchelle, E. 1996. *Pseudomonas aeruginosa* adherence to remodelling respiratory epithelium. *European Respiratory Journal,* 9, 2145-2150.

De Dios Caballero, J., Vida, R., Cobo, M., Maiz, L., Suarez, L., Galeano, J., Baquero, F., Canton, R. & Del Campo, R. 2017. Individual Patterns of Complexity in Cystic Fibrosis Lung Microbiota, Including Predator Bacteria, over a 1-Year Period. *MBio,* 8.

De Vargas, L. M., Kim, S. & Landy, A. 1989. DNA Looping Generated by DNA Bending Protein IHF and the Two Domains of Lambda Integrase. *Science,* 244, 1457–1461.

Deneuville, E., Perrot-Minot, C., Pennaforte, F., Roussey, M., Zahm, J.-M., Clavel, C., Puchelle, E. & De Bentzmann, S. 1997. Revisited physicochemical and transport properties of respiratory mucus in genotyped cystic fibrosis patients. *Am J Respir Crit Care Med,* 156, 166-72.

Denning, G. M., Anderson, M. P., Amara, J. F., Marshall, J., Smith, A. E. & Welsh, M. J. 1992. Processing of mutant cystic fibrosis transmembrane conductance regulator is temperature-sensitive. *Nature,* 358, 761-4.

Denning, G. M., Iyer, S. S., Reszka, K. J., O'malley, Y., Rasmussen, G. T. & Britigan, B. E. 2003. Phenazine-1-carboxylic acid, a secondary metabolite of Pseudomonas aeruginosa, alters expression of immunomodulatory proteins by human airway epithelial cells. *American Journal of Physiology - Lung Cellular and Molecular Physiology,* 285, L584-L592.

Denning, G. M., Railsback, M. A., Rasmussen, G. T., Cox, C. D. & Britigan, B. E. 1998a. *Pseudomonas* pyocyanine alters calcium signaling in human airway epithelial cells. *Am J Physiol.,* 274, L893-900.

Denning, G. M., Wollenweber, L. A., Railsback, M. A., Cox, C. D., Stoll, L. L. & Britigan, B., E 1998b. *Pseudomonas* pyocyanin increases interleukin-8 expression by human airway epithelial cells. *INFECTION AND IMMUNITY,* 66, p. 5777–5784.

Deretic, V., Schurr, M. J., Boucher, J. C. & Martin, D. W. 1994. Conversion of *Pseudomonas aeruginosa* to Mucoidy in CF- Environmental stress and regulation of bacterial virulence by alternative sigma factors. *JOURNAL OF BACTERIOLOGY,,* 176, p. 2773-2780

Desvaux, M., Scott-Tucker, A., Turner, S. M., Cooper, L. M., Huber, D., Nataro, J. P. & Henderson, I. R. 2007. A conserved extended signal peptide region directs posttranslational protein translocation via a novel mechanism. *Microbiology,* 153, 59-70.

Devault, J. D., Kimbara, K. & Chakrabarty, A. M. 1990. Pulmonary dehydration and infection in cystic fibrosis- evidence that ethanol activates alginate gene expression and induction of mucoidy in *Pseudomonas aeruginosa*. *Mol Microbiol. ,* 4, 737-45.

Devries, C. A. & Ohman, D. E. 1994. Mucoid-to-nonmucoid conversion in alginate-producing *Pseudomonas aeruginosa* often results from spontaneous mutations in algT, encoding a putative alternate sigma factor, and shows evidence for autoregul. *JOURNAL OF BACTERIOLOGY,,* 176, p. 6677-6687.

Deziel, E., Comeau, Y. & Villemur, R. 2001. Initiation of biofilm formation by *Pseudomonas aeruginosa* 57RP correlates with emergence of hyperpiliated and highly adherent phenotypic variants deficient in swimming, swarming, and twitching motilities. *J Bacteriol,* 183, 1195-204.

Deziel, E., Lepine, F., Milot, S., He, J., Mindrinos, M. N., Tompkins, R. G. & Rahme, L. G. 2004. Analysis of *Pseudomonas aeruginosa* 4-hydroxy-2-alkylquinolines (HAQs)

reveals a role for 4-hydroxy-2-heptylquinoline in cell-to-cell communication. *Proc Natl Acad Sci U S A,* 101, 1339-44.
Di Leva, F., Domi, T., Fedrizzi, L., Lim, D. & Carafoli, E. 2008. The plasma membrane Ca2+ ATPase of animal cells: structure, function and regulation. *Arch Biochem Biophys,* 476, 65-74.
Dietrich, L. E. P., Okegbe, C., Price-Whelan, A., Sakhtah, H., Hunter, R. C. & Newmana, D. K. 2013. Bacterial Community Morphogenesis is Intimately Linked to the Intracellular Redox State. *JOURNAL OF BACTERIOLOGY,,* 195, p. 1371–1380.
Dietrich, L. E. P., Teal, T. K., Price-Whelan, A. & Newman, D. K. 2008. Redox-active antibiotics control gene expression and community behavior in divergent bacteria. *Science,* 321, 1203–1206.
Diggle, S. P., Winzer, K., Chhabra, S. R., Worrall, K. E., Cámara, M. & Williams, P. 2003. The *Pseudomonas aeruginosa* Quinolone Signal Molecule Overcomes the Cell Density-Dependency of the Quorum Sensing Hierarchy, Regulates Rhl-Dependent Genes at the Onset of Stationary Phase and Can Be Produced in the Absence of LasR. *Molecular Microbiology,* 50, 29–43.
Dimango, E., Zar, H. J., Bryan, R. & Prince, A. 1995. Diverse *Pseudomonas aeruginosa* Gene Products Stimulate Respiratory Epithelial Cells to Produce Interleukin-8. *The American Society for Clinical Investigation,,* 96 2204-2210.
Doè Ring, G., Conway, S. P., Heijerman, H. G. M., Hodson, M. E., Hùiby, N., Smyth, A. & Touw, D. J. 2000. Antibiotic therapy against *Pseudomonas aeruginosa* in cystic fibrosis- a European consensus. *Eur Respir J* 16, 749±767
Domínguez-Cuevas, P. & Marqués, S. Compiling Sigma-70-Dependent Promoters. *Ramos JL. (eds) Virulence and Gene Regulation. Springer, Boston, MA*, pp 319-343.
Donlan, R. M. 2002. Biofilms- microbial life on surfaces. *Emerging Infectious Diseases,* 8, 881-890.
Döring, G. & Høiby, N. 1983. Longitudinal study of immune response to *Pseudomonas aeruginosa* antigens in cystic fibrosis. *Infect Immun.,* 42, 197–201.
Drenkard, E. 2003. Antimicrobial resistance of *Pseudomonas aeruginosa* biofilms. *Microbes and Infection* 5, 1213–1219.
Dunne, W. M. 2002. Bacterial Adhesion: Seen Any Good Biofilms Lately? *Clinical Microbiology Reviews,* 15, 155-166.
Dumon-Seignovert, L., Cariot, G. & Vuillard, L. 2004. The toxicity of recombinant proteins in *Escherichia coli*: a comparison of overexpression in BL21(DE3), C41(DE3), and C43(DE3). *Protein Expr Purif,* 37, 203-6.
Duong-Ly, K. C. & Gabelli, S. B. 2014. Salting out of proteins using ammonium sulfate precipitation. *Methods Enzymol,* 541, 85-94.
Dutta, P. R., Cappello, R., Navarro-Garcia, F. & Nataro, J. P. 2002. Functional Comparison of Serine Protease Autotransporters of *Enterobacteriaceae*. *Infection and Immunity,* 70, 7105-7113.
Dwyer, M., Shan, Q., D'ortona, S., Maurer, R., Mitchell, R., Olesen, H., Thiel, S., Huebner, J. & Gadjeva, M. 2014. Cystic fibrosis sputum DNA has NETosis characteristics and neutrophil extracellular trap release is regulated by macrophage migration-inhibitory factor. *J Innate Immun,* 6, 765-79.
Elborn, S. & Vallieres, E. 2014. Cystic fibrosis gene mutations: evaluation and assessment of disease severity. *Advances in Genomics and Genetics*, 161.
Engel, L. S., Hobden, J. A., Moreau, J. M., Callegan, M. C., Hill, J. M. & O'callaghan, R. J. 1997. Pseudomonas deficient in protease IV has significantly reduced corneal virulence. *Invest Ophthalmol Vis Sci. ,* 38, 1535-42.
Ernst, L., Mercenier, A. & Haas, D. 1986. The arcABC operon required for fermentative growth of *Pseudomonas aeruginosa* on arginine: Tn5-751-assisted cloning and localization of structural genes. *Journal of General Microbiology,* 132, 2667-2675.
Ernst, R. K., Yi, E. C., Guo, L., Lim, K. B., Burns, J. L., Hackett, M. & Miller, S. I. 1999. Specific Lipopolysaccharide Found in Cystic Fibrosis Airway Pseudomonas aeruginosa. *Science,* 286, 1561-1565.
Ertesvig, H. & Valla, S. 1998. Biosynthesis and applications of alginates. *Polymer Degradation and Stability,* 59, 85-91
Eschbach, M., Schreiber, K., Trunk, K., Buer, J., Jahn, D. & Schobert, M. 2004. Long-term anaerobic survival of the opportunistic pathogen *Pseudomonas aeruginosa* via pyruvate fermentation. *Journal of bacteriology,* 186, p. 4596–4604.
Etherington, C., Naseer, R., Conway, S. P., Whitaker, P., Denton, M. & Peckham, D. G. 2014. The role of respiratory viruses in adult patients with cystic fibrosis receiving intravenous antibiotics for a pulmonary exacerbation. *J Cyst Fibros.,* 13, 49-55. .

Evans, M. L. & Chapman, M. R. 2014. Curli biogenesis: order out of disorder. *Biochim Biophys Acta,* 1843, 1551-8.
Everett, J., Turner, K., Cai, Q., Gordon, V., Whiteley, M. & Rumbaugh, K. 2017. Arginine Is a Critical Substrate for the Pathogenesis of *Pseudomonas aeruginosa* in Burn Wound Infections. *MBio,* 8.
Falagas, M. E. & Siakavellas, E. 1999. *Bacteroides, Prevotella*, and *Porphyromonas* species- a review of antibiotic resistance and therapeutic options. *International Journal of Antimicrobial Agents* 15**,** 1-9.
Falconi, M., Gualtieri, M. T., Teana, A. L., Losso, M. A. & Pon, C. L. 1998. Proteins from the prokaryotic nucleoid-primary and quaternary structure of the 15-kD *Escherichia coli* DNA binding protein H-NS. *Molecular Microbiology* 2, 323-329
Fan, E., Chauhan, N., Udatha, D. B., Leo, J. C. & Linke, D. 2016. Type V Secretion Systems in Bacteria. *Microbiol Spectr,* 4.
Favorov, A. V., Gelfand, M. S., Gerasimova, A. V., Ravcheev, D. A., Mironov, A. A. & Makeev, V. J. 2005. A Gibbs sampler for identification of symmetrically structured, spaced DNA motifs with improved estimation of the signal length. *Bioinformatics,* 21, 2240-5.
Feldman, M., Bryan, R., Rajan, S., Scheffler, L., Brunnert, S., Tang, H. & Prince, A. 1998a. Role of flagella in pathogenesis of *Pseudomonas aeruginosa* pulmonary infection. *INFECTION AND IMMUNITY,* 66, 43–51.
Ferrer, M., Chernikova, T. N., Timmis, K. N. & Golyshin, P. N. 2004. Expression of a temperature-sensitive esterase in a novel chaperone-based *Escherichia coli* strain. *Appl Environ Microbiol,* 70, 4499-504.
Filkins, L. M. & O'toole, G. A. 2015. Cystic Fibrosis Lung Infections: Polymicrobial, Complex, and Hard to Treat. *PLoS Pathog,* 11, e1005258.
Filloux, A. 2011. Protein Secretion Systems in Pseudomonas aeruginosa: An Essay on Diversity, Evolution, and Function. *Front Microbiol,* 2, 155.
Finkel, S. E. & Kolter, R. 2001. DNA as a nutrient: novel role for bacterial competence gene homologs. *J Bacteriol,* 183, 6288-93.
Firoved, A. M., Boucher, J. C. & Deretic, V. 2002. Global Genomic Analysis of AlgU (E)-Dependent Promoters (Sigmulon) in *Pseudomonas aeruginosa* and Implications for Inflammatory Processes in Cystic Fibrosis. *Journal of Bacteriology,* 184, 1057-1064.
Flanagan , D. A., Gregory, L. G., Carter , J. P., Karakas-Sen , A., Richardson, D. J. & Spiro, S. 1999. Detection of genes for periplasmic nitrate reductase in nitrate respiring bacteria and in community DNA. *FEMS Microbiology Letters* 177, 263-270.
Flemming, H. C. & Wingender, J. 2010. The biofilm matrix. *Nat Rev Microbiol,* 8, 623-33.
Fothergill, J. L., Mowat, E., Ledson, M. J., Walshaw, M. J. & Winstanley, C. 2010. Fluctuations in phenotypes and genotypes within populations of *Pseudomonas aeruginosa* in the cystic fibrosis lung during pulmonary exacerbations. *J Med Microbiol. ,* 59, 472-81.
Fothergill, J. L., Neill, D. R., Loman, N., Winstanley, C. & Kadioglu, A. 2014. *Pseudomonas aeruginosa* adaptation in the nasopharyngeal reservoir leads to migration and persistence in the lungs. *Nat Commun,* 5**,** 4780.
Fox, J. D., Routzahn, K. M., Bucher, M. H. & Waugh, D. S. 2003. Maltodextrin-binding proteins from diverse bacteria and archaea are potent solubility enhancers. *FEBS Letters,* 537, 53-57.
Frank, D. W. 1997. The exoenzyme S regulon of Pseudomonas aeruginosa. *Mol Microbiol. ,* 26, 621-9.
Frank, S., Kampfer, H., Wetzler, C. & Pfeilschifter, J. 2002. Nitric oxide drives skin repair: novel functions of an established mediator. *Kidney Int,* 61, 882-8.
Franklin, M. J., Nivens, D. E., Weadge, J. T. & Howell, P. L. 2011. Biosynthesis of the *Pseudomonas aeruginosa* Extracellular Polysaccharides, Alginate, Pel, and Psl. *Front Microbiol,* 2, 167.
Fraylick, J. E., Rucks, E. A., Greene, D. M., Vincent, T. S. & Olson, J. C. 2002. Eukaryotic cell determination of ExoS ADP-ribosyltransferase substrate specificity. *Biochem Biophys Res Commun,* 291, 91-100.
Freeman, D. J., Falkiner, F. R. & Keane, C. T. 1989. New method for detecting slime production by coagulase negative staphylococci. *J Clin Pathol,* 42, 872-874.
Freschi , L., Jeukens , J., Kukavica-Ibrulj, I., Boyle, B., Dupont, M.-J., Laroche, J., Larose , S., Maaroufi, H., Fothergill, J. L., Moore, M., Winsor, G., Aaron, S. D., Barbeau, J., Bell, S. C., Burns, J. L., Camara, M., Cantin , A., Charette, S. J., Dewar, K., Déziel, É., Grimwood, K., Hancock, R. E. W., Harrison , J. J., Heeb, S., Jelsbak, L., Jia , B.,

Kenna, D. T., Kidd, T. J., Klockgether, J., Lam, J. S., Lamont, I. L., Lewenza, S., Loman, N., Malouin , F., Manos, J., Mcarthur, A. G., Mckeown, J., Milot , J., Naghra, H., Nguyen, D., Pereira , S. K., Perron, G. G., Pirnay , J.-P., Rainey, P. B., Rousseau, S., Santos, P. M., Stephenson, A., Taylor, V., Turton, J. F., Waglechner, N., Williams , P., Thrane, S. W., Wright , G. D., Brinkman, F. S. L., Tucker , N. P., Tümmler, B., Winstanley, C. & Levesque, R. C. 2015. Clinical Utililization of genomics data produced by the international *Pseudomonas aeruginosa* consortium. *Frontiers in microbiology,* 6, 1-8.

Freundlich, M., Ramani, N., Mathew, E., Sirko, A. & Tsuf, P. 1992. The role of integration host factor in gene expression in *Escherichia coli*. *Molecular Microbiology* 6, 2557-2563

Fricks-Lima, J., Hendrickson, C. M., Allgaier, M., Zhuo, H., Wiener-Kronish, J. P., Lynch, S. V. & Yang, K. 2011. Differences in biofilm formation and antimicrobial resistance of *Pseudomonas aeruginosa* isolated from airways of mechanically ventilated patients and cystic fibrosis patients. *Int J Antimicrob Agents,* 37, 309-15.

Friedman 1988. Integration Host Factor- A protein for all reasons. *Cell, Vol. ,* 55, 545-554,.

Friedman, L. & Kolter, R. 2003. Genes involved in matrix formation in *Pseudomonas aeruginosa* PA14 biofilms. *Molecular Microbiology,* 51, 675-690.

Frimmersdorf, E., Horatzek, S., Pelnikevich, A., Wiehlmann, L. & Schomburg, D. 2010. How *Pseudomonas aeruginosa* adapts to various environments: a metabolomic approach. *Environmental Microbiology,* 12, 1734-1747.

Frithz-Lindsten, E., Du, Y., Rosqvist, R. & Forsberg, A. 1997. Intracellular targeting of exoenzyme S of *Pseudomonas aeruginosa* via type III-dependent translocation induces phagocytosis resistance, cytotoxicity and disruption of actin microfilaments. *Molecular Microbiology,* 25, 1125-39.

Fronzes, R., Christie, P. J. & Waksman, G. 2009. Schematic overview of the major protein secretion systems in Gram-negative bacteria. *Nature Reviews Microbiology* 7, 703-714.

Fujita, M., Tanaka, K., Takahashi, H. & Amemura, A. 1994a. Transcription of the principal sigma-factor genes, rpoD and rpoS, in *Pseudomonas aeruginosa* is controlled according to the growth phase. *mol Microbiol,* 13, 1071-7.

Fujiwara, T., Fukumori , Y. & Yamanaka, T. 1992. A Novel Terminal Oxidase, Cytochrome Baa3 Purified From Aerobically Grown Pseudomonas Aeruginosa: It Shows a Clear Difference Between Resting State and Pulsed State. *Journal of Biochemistry,* 112, 290-298.

Fuller, C. M. & Benos, D. J. 1992. CFTR! *Am J Physiol.,* 263, C267-86.

Fundoiano-Hershcovitz, Y., Rabinovitch, L., Langut, Y., Reiland, V., Shoham, G. & Shoham, Y. 2004. Identification of the catalytic residues in the double-zinc aminopeptidase from Streptomyces griseus. *FEBS Lett,* 571, 192-6.

Fuqua, C., Parsek, M. R. & Greenberg, E. P. 2001. Regulation of gene expression by cell-to-cell communication- acyl-homoserine lactone quorum sensing. *Annu. Rev. Genet.,* 35, 439–68.

Furiga, A., Lajoie, B., El Hage, S., Baziard, G. & Roques, C. 2015. Impairment of *Pseudomonas aeruginosa* Biofilm Resistance to Antibiotics by Combining the Drugs with a New Quorum-Sensing Inhibitor. *Antimicrob Agents Chemother,* 60, 1676-86.

Gacesa , P. 1998. Bacterial alginate biosynthesis--recent progress and future prospects. *Microbiology,* 144, 1133-43.

Gadsby, D. C., Vergani, P. & Csanady, L. 2006. The ABC protein turned chloride channel whose failure causes cystic fibrosis. *Nature,* 440, 477-83.

Galan-Vasquez, E., Luna, B. & Martinez-Antonio, A. 2011. The Regulatory Network of Pseudomonas aeruginosa. *Microb Inform Exp,* 1, 3.

Gallagher, L. A., Mcknight, S. L., Kuznetsova, M. S., Pesci, E. C. & Manoil, C. 2002. Functions Required for Extracellular Quinolone Signaling by Pseudomonas aeruginosa. *Journal of Bacteriology,* 184, 6472-6480.

Gambello, M. J. & Iglewski, B. H. 1991. Cloning and characterization of the *Pseudomonas aeruginosa* lasR gene, a transcriptional activator of elastase expression. *JOURNAL OF BACTERIOLOGY,,* 173, p. 3000-3009

Gambello, M. J., Kaye, S. & Iglewski, B. H. 1993. LasR of *Pseudomonas aeruginosa* is a transcriptional activator of the alkaline protease gene (apr) and an enhancer of exotoxin A expression. *INFECTION AND IMMUNITY,* 61, p. 1180-1184

Garcia-Fruitos, E. 2010. Inclusion bodies: a new concept. *Microb Cell Fact,* 9, 80.

Garcia-Medina, R., Dunne, W. M., Singh, P. K. & Brody, S. L. 2005. *Pseudomonas aeruginosa* acquires biofilm-like properties within airway epithelial cells. *INFECTION AND IMMUNITY,* 73, p. 8298–8305.

Gardan, R., Rapoport, G. & Débarbouillé, M. 1997. Role of the transcriptional activator RocR in the arginine-degradation pathway of Bacillus subtilis. *Mol Microbiol,* 24, 825-37.

Garrett, E. S., Perlegas, D. & Wozniak, D. J. 1999. Negative Control of Flagellum Synthesis in *Pseudomonas aeruginosa* Is Modulated by the Alternative Sigma Factor AlgT (AlgU). *JOURNAL OF BACTERIOLOGY,* 181, p. 7401–7404.

Garrett, T. R., Bhakoo, M. & Zhang, Z. 2008. Bacterial adhesion and biofilms on surfaces. *Progress in Natural Science,* 18, 1049-1056.

Gaston, B., Ratjen, F., Vaughan, J. W., Malhotra, N. R., Canady, R. G., Snyder, A. H., Hunt, J. F., Gaertig, S. & Goldberg, J. B. 2002. Nitrogen Redox Balance in the Cystic Fibrosis Airway *Am J Respir Crit Care Med* 165, 387-390.

Gavira, M., Roldán, M. D., Castillo, F. & Moreno-Vivián, C. 2002. Regulation of nap gene expression and periplasmic nitrate reductase activity in the phototrophic bacterium *Rhodobacter sphaeroides* DSM158. *Journal of Bacteriology,* 184, p. 1693–1702.

Ghafoor, A., Hay, I. D. & Rehm, B. H. 2011. Role of exopolysaccharides in *Pseudomonas aeruginosa* biofilm formation and architecture. *Appl Environ Microbiol,* 77, 5238-46.

Ghebremedhin, B. 2014. Human adenovirus: Viral pathogen with increasing importance. *Eur J Microbiol Immunol (Bp),* 4**,** 26-33.

Gibson, R. L., Burns, J. L. & Ramsey, B. W. 2003. Pathophysiology and management of pulmonary infections in cystic fibrosis. *Am J Respir Crit Care Med,* 168, 918-51.

Gilboa, R., Greenblatt, H., Perach, M., Spungin-Bialik, A., Lessel, U., Wohlfahrt, G., Schomburg, D., Blumberg, S. & Shoham, G. 2000. Interactions of Streptomyces griseus aminopeptidase with a methionine product analogue: a structural study at 1.53 A resolution. *Acta Crystallogr D Biol Crystallogr.,* 56, 551-8.

Gilboa, R., Spungin-Bialik, A., Wohlfahrt, G., Schomburg, D., Blumberg, S. & Shoham, G. 2001. Interactions of *Streptomyces griseus aminopeptidase* with amino acid reaction products and their implications toward a catalytic mechanism. *Proteins,* 44, 490-504.

Gilligan, P. H. 2014. Infections in patients with cystic fibrosis: diagnostic microbiology update. *Clin Lab Med. ,* 34, 197-217.

Gilpin, D. F., Nixon, K. A., Bull, M., Mcgrath, S. J., Sherrard, L., Rolain, J. M., Mahenthiralingam, E., Elborn, J. S. & Tunney, M. M. 2017. Evidence of persistence of Prevotella spp. in the cystic fibrosis lung. *J Med Microbiol*.

Glasser, N. R., Kern, S. E. & Newman, D. K. 2014. Phenazine redox cycling enhances anaerobic survival in *Pseudomonas aeruginosa* by facilitating generation of ATP and a proton-motive force. *Mol Microbiol.,* 92, 399–412.

Gloag, E. S., Turnbull, L., Huang, A., Vallotton, P., Wang, H., Nolan, L. M., Mililli, L., Hunt, C., Lu, J., Osvath, S. R., Monahan, L. G., Cavaliere, R., Charles, I. G., Wand, M. P., Gee, M. L., Prabhakar, R. & Whitchurch, C. B. 2013. Self-organization of bacterial biofilms is facilitated by extracellular DNA. *Proc Natl Acad Sci U S A,* 110, 11541-6.

Goeddel, D. V., Kleid, D. G., Bolivar, F., Heyneker, H. L., Yansura, D. G., Crea, R., Hirose , T., Kraszewski, A., Itakura, K. & Riggs, A. D. 1979. Expression in *Escherichia coli* of chemically synthesized genes for human insulin. *Proc. Nati. Acad. Sci. USA,* 76, pp. 106-110.

Goehring, U.-M., Schmidt, G., Pederson, K. J., Aktories, K. & Barbieri, J. T. 1999. The N-terminal domain of *Pseudomonas aeruginosa* exoenzyme S is a GTPase-activating protein for Rho GTPases. *THE JOURNAL OF BIOLOGICAL CHEMISTRY,* 274, 36369–36372.

Goldberg, J. B. 2010. Why is *Pseudomonas aeruginosa* a pathogen? *F1000 Biol Rep,* 2.

Goldman, M. J., Anderson, G. M., Stolzenberg, E. D., Kari, U. P., Zasloff, M. & Wilson, J. M. 1997. Human beta-defensin-1 is a salt-sensitive antibiotic in lung that is inactivated in cystic fibrosis. *Cell. ,* 88, 553-60.

Gomila, M., Peña, A., Mulet, M., Lalucat, J. & García-Valdés, E. 2015. Phylogenomics and systematics in *Pseudomonas*. *frontiers in microbiology,* 6, 1-13.

Gonzalez, M. R., Ducret, V., Leoni, S., Fleuchot, B., Jafari, P., Raffoul, W., Applegate, L. A., Que, Y. A. & Perron, K. 2018. Transcriptome Analysis of *Pseudomonas aeruginosa* Cultured in Human Burn Wound Exudates. *Front Cell Infect Microbiol,* 8, 39.

Goodman, A. L., Kulasekara, B., Rietsch, A., Boyd, D., Smith, R. S. & Lory, S. 2004. A signaling network reciprocally regulates genes associated with acute infection and chronic persistence in Pseudomonas aeruginosa. *Dev Cell,* 7, 745-54.

Goodman, A. L., Merighi, M., Hyodo, M., Ventre, I., Filloux, A. & Lory, S. 2009. Direct interaction between sensor kinase proteins mediates acute and chronic disease phenotypes in a bacterial pathogen. *Genes Dev,* 23, 249-59.

Goodsell, D. S. & Dickerson, R. E. 1994. bending and curvature calculations in B-DNA. *Nucleic Acids Res. ,* 22, 5497–5503.

Görke, B. & Stülke, J. 2008. Carbon catabolite repression in bacteria: many ways to make the most out of nutrients. *Nature Reviews,* 6, 613-624.

Govan, J. R. & Harris, G. S. 1986. *Pseudomonas aeruginosa* and cystic fibrosis: unusual bacterial adaptation and pathogenesis. *Microbiol sci,* 3, 302-8.

Govan, J. R. W. & Nelson, J. W. 1992. Microbiology of lung infection in cystic fibrosis. *British Medical Bulletin* 48**,** pp9I2-93O.

Govan, J. R. W. & Deretic, V. 1996. Microbial pathogenesis in cystic fibrosis- mucoid *Pseudomonas aeruginosa* and *Burkholderia cepacia*. *MICROBIOLOGICAL REVIEWS,* 60, p. 539–574.

Govantes, F., Orjalo, A. V. & Gunsalus, R. P. 2000. Interplay between three global regulatory proteins mediates oxygen regulation of the *Escherichia coli* cytochrome d oxidase (cydAB) operon. *Molecular Microbiology,* 38, 1061±1073.

Grasemann, H., Ioannidis, I., Tomkiewicz, R. P., De Groot, H., Rubin, B. K. & Ratjen, F. 1998. Nitric oxide metabolites in cystic fibrosis lung disease. *Arch Dis Child* 78, 49–53.

Grasemann, H., Kurtz, F. & Ratjen, F. 2006a. Inhaled L-arginine improves exhaled nitric oxide and pulmonary function in patients with cystic fibrosis. *Am J Respir Crit Care Med,* 174, 208-12.

Grasemann, H., Schwiertz, R., Grasemann, C., Vester, U., Racke, K. & Ratjen, F. 2006b. Decreased systemic bioavailability of L-arginine in patients with cystic fibrosis. *Respir Res,* 7, 87.

Grasemann, H., Schwiertz, R., Matthiesen, S., Racke, K. & Ratjen, F. 2005. Increased arginase activity in cystic fibrosis airways. *Am J Respir Crit Care Med,* 172, 1523-8.

Green, H. D., Bright-Thomas, R., Kenna, D. T., Turton, J. F., Woodford, N. & Jones, A. M. 2017. Ralstonia infection in cystic fibrosis. *Epidemiol Infect,* 145**,** 2864-2872.

Greenblatt, H. M., Almog, O., Maras, B., Spungin-Bialik, A., Barra, D., Blumberg, S. & Shoham, G. 1997. Streptomyces griseus aminopeptidase-X-ray crystallographic structure at 1.75 A resolution. *J. Mol. Biol. ,* 265, 620–636

Gregory, R. J., Cheng, S. H., Rich, D. P., Marshall, J., Paul, S., Hehir, K., Ostedgaard, L., Klinger, K. W., Welsh, M. J. & Smith, A. E. 1990. Expression and characterization of the cystic fibrosis transmembrane conductance regulator. *Nature,* 347, 382-6.

Griffiths, C., Drews, S. J. & Marchant, D. J. 2017. Respiratory Syncytial Virus: Infection, Detection, and New Options for Prevention and Treatment. *Clin Microbiol Rev,* 30**,** 277-319.

Gruber, T. M. & Gross, C. A. 2003. Multiple sigma subunits and the partitioning of bacterial transcription space. *Annu Rev Microbiol,* 57, 441-66.

Gunsalus, R. P. & Park, S.-J. 1994. Aerobic-anaerobic gene regulation in *Escherichia coli*: control by the ArcAB and Fnr regulons. *Research in Microbiology,* 145, 437-450.

Guzman, L.-M., Belin, D., Carson, M. J. & Beckwith, J. 1995. Tight Regulation, Modulation, and High-Level Expression by vectors containing the arabinose PBAD promoter. *JOURNAL OF BACTERIOLOGY, ,* 177, p. 4121–4130.

Ha¨Rtig, E., Schiek, U., Vollack, K.-U. & Zumft, W. G. 1999. Nitrate and Nitrite Control of Respiratory Nitrate Reduction in Denitrifying Pseudomonas stutzeri by a Two-Component Regulatory System Homologous to NarXL of*Escherichia coli*. *Journal of Bacteriology,* 181, p. 3658–3665.

Haas, D., Matsumoto, H., Moretti, P., Stalon, V. & Mercenier, A. 1984. Arginine degradation in *Pseudomonas aeruginosa* mutants blocked in two arginine catabolic pathways. *Mol Gen Genet. ,* 193, 437-44.

Hall-Stoodley, L., Costerton, J. W. & Stoodley, P. 2004. Bacterial biofilms: from the Natural environment to infectious diseases. *Nature Reviews Microbiology* 2, 95-108.

Hammond, J. H., Dolben, E. F., Smith, T. J., Bhuju, S. & Hogan, D. A. 2015. Links between Anr and Quorum Sensing in *Pseudomonas aeruginosa* Biofilms. *Journal of bacteriology,* 197, 2810-2820.

Hancock, R. E. W., Mutharia, L. M., Chan, L., Darveau, R. P., Speert, D. P. & Pier, G. B. 1983. *Pseudomonas aeruginosa* isolates from patients with cystic fibrosis- a class

of serum-sensitive, nontypable strains deficient in lipopolysaccharide O side chains. *INFECTION AND IMMUNITY,,* 42,, 170-177.
Harrison, F. & Diggle, S. P. 2016. An *ex vivo* lung model to study bronchioles infected with *Pseudomonas aeruginosa* biofilms. *Microbiology,* 162, 1755-1760.
Hasegawa, N., Arai, H. & Igarashi, Y. 1998. Activation of a consensus FNR-dependent promoter by DNR of *Pseudomonas aeruginosa* in response to nitrate. *FEBS Federation of European Biochemical Societies,* 166, 213-217.
Hasherry, D.-G., Kuchma, L. & O'toole, G. A. 2014. Plate-Based Assay for Swimming Motility in Pseudomonas aeruginosa. *Pseudomonas Methods and Protocols, Methods in Molecular Biology (Methods and Protocols),* 1149, pp 59-65.
Hassett, D. J., Sutton, M. D., Schurr, M. J., Herr, A. B., Caldwell, C. C. & Matu, J. O. 2009. *Pseudomonas aeruginosa* hypoxic or anaerobic biofilm infections within cystic fibrosis airways. *Trends Microbiol,* 17, 130-8.
Haussler, S., Ziegler, I., Lottel, A., Von Gotz, F., Rohde, M., Wehmhohner, D., Saravanamuthu, S., Tummler, B. & Steinmetz, I. 2003. Highly adherent small-colony variants of *Pseudomonas aeruginosa* in cystic fibrosis lung infection. *J Med Microbiol,* 52, 295-301.
Havasi, V., Hurst, C. O., Briles, T. C., Yang, F., Bains, D. G., Hassett, D. J. & Sorscher, E. 2008. Inhibitory effects of hypertonic saline on *P. aeruginosa* motility. *J Cyst Fibros,* 7, 267-9.
Head, N. E. & Yu, H. 2003. Cross-Sectional Analysis of Clinical and Environmental Isolates of Pseudomonas aeruginosa: Biofilm Formation, Virulence, and Genome Diversity. *Infection and Immunity,* 72, 133-144.
Heck, L. W., Morihara, K. & Abrahamson, D. R. 1986. Degradation of soluble laminin and depletion of tissue-associated basement membrane laminin by *Pseudomonas aeruginosa* elastase and alkaline protease. *Infect Immun.,* 54, 149-53.
Heinz, E., Stubenrauch, C. J., Grinter, R., Croft, N. P., Purcell, A. W., Strugnell, R. A., Dougan, G. & Lithgow, T. 2016. Conserved Features in the Structure, Mechanism, and Biogenesis of the Inverse Autotransporter Protein Family. *Genome Biol Evol,* 8, 1690-705.
Henderson, I. R., Cappello, R. & Nataro, J. P. 2000. Autotransporter proteins, evolution and redefining protein secretion. *TRENDS IN MICROBIOLOGY,* 8, p529–532.
Henderson, I. R. & Nataro, J. P. 2001. Virulence functions of autotransporter proteins. *Infect Immun,* 69, 1231-43.
Henderson, I. R., Navarro-Garcia, F., Desvaux, M., Fernandez, R. C. & Ala'aldeen, D. 2004. Type V protein secretion pathway: the autotransporter story. *Microbiol Mol Biol Rev,* 68, 692-744.
Hengge, R. 2009. Principles of c-di-GMP signalling in bacteria. *Nat Rev Microbiol,* 7, 263-73.
Henrickson, K. J. 2003. Parainfluenza Viruses. *Clinical Microbiology Reviews,* 16**,** 242-264.
Hernandez-Garcia, C. M. & Finer, J. J. 2014. Identification and validation of promoters and cis-acting regulatory elements. *Plant Sci,* 217-218, 109-19.
Hershcovitz, Y. F., Gilboa, R., Reiland, V., Shoham, G. & Shoham, Y. 2007. Catalytic mechanism of SGAP, a double-zinc aminopeptidase from Streptomyces griseus. *FEBS J,* 274, 3864-76.
Hervas, A. B., Canosa, I. & Santero, E. 2008. Transcriptome analysis of Pseudomonas putida in response to nitrogen availability. *J Bacteriol,* 190, 416-20.
Heurlier, K., Denervaud, V., Pessi, G., Reimmann, C. & Haas, D. 2003. Negative Control of Quorum Sensing by RpoN (54) in *Pseudomonas aeruginosa* PAO1. *Journal of Bacteriology,* 185, 2227-2235.
Hibbing, M. E., Fuqua, C., Parsek, M. R. & Peterson, S. B. 2010. Bacterial competition: surviving and thriving in the microbial jungle. *Nat Rev Microbiol,* 8, 15-25.
Hickman, J. W. & Harwood, C. S. 2008. Identification of FleQ from *Pseudomonas aeruginosa* as a c-di-GMP-responsive transcription factor. *Mol Microbiol,* 69, 376-89.
Hirschman, J., Wong, P.-K., Se1, K., Keener, J. & Kustu, S. 1985. Products of nitrogen regulatory genes ntrA and ntrC of enteric bacteria activate glnA transcription *in vitro*- evidence that the ntrA product is a sigma factor. *Proc. Natl. Acad. Sci. USA,* 82, pp. 7525-7529,.
Hoang, T. T., Kutchma, A. J., Becher, A. & Schweizer, H. P. 2000. Integration-proficient plasmids for *Pseudomonas aeruginosa*: site-specific integration and use for engineering of reporter and expression strains. *Plasmid,* 43, 59-72.

Hoboth, C., Hoffmann, R., Eichner, A., Henke, C., Schmoldt, S., Imhof, A., Heesemann, J. & Hogardt, M. 2009. Dynamics of adaptive microevolution of hypermutable *Pseudomonas aeruginosa* during chronic pulmonary infection in patients with cystic fibrosis. *J Infect Dis,* 200, 118-30.

Hoffman, L. R., Richardson, A. R., Houston, L. S., Kulasekara, H. D., Martens-Habbena, W., Klausen, M., Burns, J. L., Stahl, D. A., Hassett, D. J., Fang, F. C. & Miller, S. I. 2010. Nutrient availability as a mechanism for selection of antibiotic tolerant *Pseudomonas aeruginosa* within the CF airway. *PLoS Pathog,* 6, e1000712.

Hoffmann, D., Ebrahimi, M., Gerlach, D., Salzig, D. & Czermak, P. 2017. Reassessment of inclusion body-based production as a versatile opportunity for difficult-to-express recombinant proteins. *Crit Rev Biotechnol*, 1-16.

Høiby, N., Ciofu, O. & Bjarnsholt, T. 2010 Pseudomonas aeruginosa biofilms in cystic fibrosis. *Future Microbiol.,* 5, 1663-74.

Hol, J., Wilhelmsen, L. & Haraldsen, G. 2010. The murine IL-8 homologues KC, MIP-2, and LIX are found in endothelial cytoplasmic granules but not in Weibel-Palade bodies. *J Leukoc Biol,* 87, 501-8.

Hong, Y. Q. & Ghebrehiwet, B. 1992. Effect of *Pseudomonas aeruginosa* elastase and alkaline protease on serum complement and isolated components C1q and C3. *Clin Immunol Immunopathol.,* 62, 133-8.

Horino, T., Matsumoto, T., Ishikawa, H., Kimura, S., Uramatsu, M., Tanabe, M., Tateda, K., Miyazaki, S., Aramaki, Y., Iwakura, Y., Yoshida, M., Onodera, S. & Yamaguchi, K. 2009. Interleukin-1 deficiency in combination with macrophage depletion increases susceptibility to *Pseudomonas aeruginosa* bacteremia. *Microbiol Immunol,* 53, 502-11.

Hornef, M. W., Roggenkamp, A., Geiger, A. M., Hogardt, M., Jacobi, C. A. & Heesemann, J. 2000. Triggering the ExoS regulon of *Pseudomonas aeruginosa*: A GFP-reporter analysis of exoenzyme (Exo) S, ExoT and ExoU synthesis. *Microb Pathog,* 29, 329-43.

Horvat, R. T. & Parmely, M. J. 1988. *Pseudomonas aeruginosa* alkaline protease degrades human gamma interferon and inhibits its bioactivity. *Infect Immun. ,* 56, 2925-32.

Houben, E. N., Korotkov, K. V. & Bitter, W. 2014. Take five - Type VII secretion systems of Mycobacteria. *Biochim Biophys Acta,* 1843, 1707-16.

Hrv, R., Devaki, R. & Kandi, V. 2016. Evaluation of Different Phenotypic Techniques for the Detection of Slime Produced by Bacteria Isolated from Clinical Specimens. *Cureus,* 8, e505.

Hug, M. J., Tamada, T. & Bridges, R. J. 2003. CFTR and Bicarbonate Secretion to Epithelial Cells. *Physiology,* 18, 38-42.

Hunt, T. P. & Magasanik, B. 1985. Transcription of glnA by purified *Escherichia coli* components- core RNA polymerase and the products of glnF, glnG, and glnL. *Proc. Nati. Acad. Sci. USA,* 82, pp. 8453-8457.

Hurley, M. N. 2018. *Staphylococcus aureus* in cystic fibrosis: problem bug or an innocent bystander? *Breathe,* 14**,** 87–90.

Hypolite, T., Grant-Kels, J. M. & Chirch, L. M. 2015. Nontuberculous mycobacterial infections: a potential complication of cosmetic procedures. *Int J Womens Dermatol,* 1**,** 51-54.

Ieva, R. & Bernstein, H. D. 2009. Interaction of an autotransporter passenger domain with BamA during its translocation across the bacterial outer membrane. *Proc Natl Acad Sci U S A,* 106, 19120-5.

Ieva, R., Tian, P., Peterson, J. H. & Bernstein, H. D. 2011. Sequential and spatially restricted interactions of assembly factors with an autotransporter beta domain. *Proc Natl Acad Sci U S A,* 108, E383-91.

Iglewski, B. H., Sadoff, J., Bjorn, M. J. & Maxwell, E. S. 1978. *Pseudomonas aeruginosa* exoenzyme S- an adenosine diphosphate ribosyltransferase distinct from toxin A. *Proc Natl Acad Sci U S A.,* 75, 3211-5.

Ikhwani, A. Z. N., Nurlaila, H. S., Ferdinand, F. D. K., Fachria, R., Hasan, A. E. Z., Yani, M., Setyawati, I. & Suryani 2017. Preliminary study : optimization of pH and salinity for biosurfactant production from *Pseudomonas aeruginosa* in diesel fuel and crude oil medium. *IOP Conf. Series: Earth and Environmental Science* 58, 012056

Imaizumi, T., Tran, H. G., Swartz, T. E., Briggs, W. R. & Kay, S. A. 2003. FKF1 is essential for photoperiodic-specific light signalling in *Arabidopsis*. *Nature,* 426, 302-6.

Ishihama, A. 2010. Prokaryotic genome regulation: multifactor promoters, multitarget regulators and hierarchic networks. *FEMS Microbiol Rev,* 34, 628-45.

Ishimoto, K. S. & Lory, S. 1989. Formation of pilin in *Pseudomonas aeruginosa* requires the alternative sigma factor (RpoN) of RNA polymerase. *Proc. Natd. Acad. Sci. USA,* 86, pp. 1954-1957.

Ishino, Y., Shinagawa, H., Makino, K., Amemura, M. & Nakata, A. 1987. Nucleotide sequence of the iap gene, responsible for alkaline phosphatase isozyme conversion in *Escherichia coli*, and identification of the gene product. *JOURNAL OF BACTERIOLOGY,,* 169, p. 5429-5433

Itoh, S., Honda, H., Tomita, F. & Suzuki, T. 1971. Rhamnolipids produced by *Pseudomonas aeruginosa* grown on n-paraffin (Mixture of C12, C13, and C14 fractions). *J Antibiot,* 24, 855-859.

Itoh, Y. 1997. Cloning and Characterization of the aru Genes Encoding Enzymes of the Catabolic Arginine Succinyltransferase Pathway in Pseudomonas aeruginosa. *Journal of Bacteriology* 179, p. 7280–7290.

Iuchi, S. & Lin, E. C. C. 1992. Mutational analysis of signal transduction by ArcB, a membrane sensor protein responsible for anaerobic repression of operons involved in the central aerobic pathways in *Escherichia coli*. *JOURNAL OF BACTERIOLOGY, ,* 174, p. 3972-3980.

Jacob-Dubuisson, F., Fernandez, R. & Coutte, L. 2004. Protein secretion through autotransporter and two-partner pathways. *Biochim Biophys Acta,* 1694, 235-57.

James, G. A., Swogger, E., Wolcott, R., Pulcini, E., Secor, P., Sestrich, J., Costerton, J. W. & Stewart, P. S. 2008. Biofilms in chronic wounds. *Wound Repair Regen,* 16**,** 37-44.

Jann, A., Matsumoto, H. & Haas, D. 1988. The Fourth Arginine Catabolic Pathway of *Pseudomonas aeruginosa*. *Journal of General Microbiology,* 134, 1043-1053.

Janssen, D. B., Habets, W. J. A., Marugg, J. T. & Van Der Drift, C. 1982. Nitrogen Control in *P. aeruginosa*- mutants affected in the synthesis of glutamine synthetase, urease and NADP-Dependent Glutamate Dehydrogenase. *JOURNAL OF BACTERIOLOGY, ,* 151, p. 22-28

Jefferson, K. K. 2004. What drives bacteria to produce a biofilm? *FEMS Microbiol Lett,* 236, 163-73.

Jeffries, J. L., Jia, J., Choi, W., Choe, S., Miao, J., Xu, Y., Powell, R., Lin, J., Kuang, Z., Gaskins, H. R. & Lau, G. W. 2016. *Pseudomonas aeruginosa* pyocyanin modulates mucin glycosylation with sialyl-Lewis(x) to increase binding to airway epithelial cells. *Mucosal Immunol,* 9, 1039-1050.

Jenal, U. & Malone, J. 2006. Mechanisms of cyclic-di-GMP signaling in bacteria. *Annu Rev Genet,* 40, 385-407.

Jensen, P. O., Givskov, M., Bjarnsholt, T. & Moser, C. 2010. The immune system vs. *Pseudomonas aeruginosa* biofilms. *FEMS Immunol Med Microbiol,* 59, 292-305.

Jeukens, J., Boyle, B., Kukavica-Ibrulj, I., Ouellet, M. M., Aaron, S. D., Charette, S. J., Fothergill, J. L., Tucker, N. P., Winstanley, C. & Levesque, R. C. 2014. Comparative genomics of isolates of a *Pseudomonas aeruginosa* epidemic strain associated with chronic lung infections of cystic fibrosis patients. *PLoS One,* 9, e87611.

Jimenez, P. N., Koch, G., Thompson, J. A., Xavier, K. B., Cool, R. H. & Quax, W. J. 2012. The multiple signaling systems regulating virulence in *Pseudomonas aeruginosa*. *Microbiol Mol Biol Rev,* 76, 46-65.

Johansson, E. M., Crusz, S. A., Kolomiets, E., Buts, L., Kadam, R. U., Cacciarini, M., Bartels, K. M., Diggle, S. P., Camara, M., Williams, P., Loris, R., Nativi, C., Rosenau, F., Jaeger, K. E., Darbre, T. & Reymond, J. L. 2008. Inhibition and dispersion of *Pseudomonas aeruginosa* biofilms by glycopeptide dendrimers targeting the fucose-specific lectin LecB. *Chem Biol,* 15, 1249-57.

Johnson, T. A., Qiu, J., Plaut, A. G. & Holyoak, T. 2009. Active-site gating regulates substrate selectivity in a chymotrypsin-like serine protease the structure of haemophilus influenzae immunoglobulin A1 protease. *J Mol Biol,* 389, 559-74.

Jones, A. M. 2011. Anaerobic bacteria in cystic fibrosis: pathogens or harmless commensals? *Thorax,* 66, 558-9.

Jones, C. J., Newsom, D., Kelly, B., Irie, Y., Jennings, L. K., Xu, B., Limoli, D. H., Harrison, J. J., Parsek, M. R., White, P. & Wozniak, D. J. 2014. ChIP-Seq and RNA-Seq reveal an AmrZ-mediated mechanism for cyclic di-GMP synthesis and biofilm development by Pseudomonas aeruginosa. *PLoS Pathog,* 10, e1003984.

Jones, C. J., Ryder, C. R., Mann, E. E. & Wozniaka, D. J. 2013. AmrZ modulates *Pseudomonas aeruginosa* biofilm architecture by directly repressing transcription of the psl operon. *Journal of Bacteriology* 195, p. 1637–1644.

Jones, D. H. A., Franklin, C. H. & Thomas, C. M. 1994. Molecular analysis of the operon which encodes the RNA polymerase sigma factor sigma54 of E.coli. *Microbiology,* 140, 1035-1043.

Jones, K. L., Hegab, A. H., Hillman, B. C., Simpson, K. L., Jinkins, P. A., Grisham, M. B., Owens, M. W., Sato, E. & Robbins, R. A. 2000. levation of nitrotyrosine and nitrate concentrations in cystic fibrosis sputum. *Pediatric Pulmonology,* 30, 79-85.

Jorth, P., Staudinger, Benjamin j., Wu, X., Hisert, K. B., Hayden, H., Garudathri, J., Harding, Christopher l., Radey, Matthew c., Rezayat, A., Bautista, G., Berrington, William r., Goddard, Amanda f., Zheng, C., Angermeyer, A., Brittnacher, Mitchell j., Kitzman, J., Shendure, J., Fligner, Corinne l., Mittler, J., Aitken, Moira l., Manoil, C., Bruce, James e., Yahr, Timothy l. & Singh, Pradeep k. 2015. Regional Isolation Drives Bacterial Diversification within Cystic Fibrosis Lungs. *Cell Host & Microbe,* 18, 307-319.

Jüngst, A, & Zumft, W. G. 1992. Interdependence of respiratory NO reduction and nitrite reduction revealed by mutagenesis of nirQ, a novel gene in the denitrification gene cluster of Pseudomonas stutzeri. *FEBS Federation of European Biochemical Societies,* 314, 308-14.

Junker, M., Besingi, R. N. & Clark, P. L. 2009. Vectorial transport and folding of an autotransporter virulence protein during outer membrane secretion. *Mol Microbiol,* 71, 1323-32.

Jyot, J., Dasgupta, N. & Ramphal, R. 2002. FleQ, the Major Flagellar Gene Regulator in Pseudomonas aeruginosa, Binds to Enhancer Sites Located Either Upstream or Atypically Downstream of the RpoN Binding Site. *Journal of Bacteriology,* 184, 5251-5260.

Kamath, J. M., Britigan, B. E., Cox, C. D. & Shasby, D. M. 1995,. Pyocyanin from *Pseudomonas aeruginosa* inhibits prostacyclin release from endothelial cells. *INFECTION AND IMMUNITY,* 63, 4921–4923.

Kamath, S., Kapatral, V. & Chakrabarty, A. M. 1998. Cellular function of elastase in Pseudomonas aeruginosa- role in the cleavage of nucleoside diphosphate kinase and in alginate synthesis. *Molecular Microbiology,* 30, 933–941.

Kang'ethe, W. & H.D, B. 2013. Charge-dependent secretion of an intrinsically disordered protein via the autotransporter pathway. *PNAS,* 110, E4246–E4255.

Kaplan, E., Shwachman, H., Perlmutter, A. D., Rule, A., Khaw, K.-T. & Holsclaw, D. S. 1968. Reproductive Failure in Males with Cystic Fibrosis. *N Engl J Med,* 279, 65-69.

Kawakami, T., Kuroki, M., Ishii, M., Igarashi, Y. & Arai, H. 2010. Differential expression of multiple terminal oxidases for aerobic respiration in *Pseudomonas aeruginosa*. *Environmental Microbiology,* 12, 1399–1412.

Kay, W. W. & Gronlund, A. F. 1969. Influence of carbon or nitrogen starvation on amino acid transport in *Pseudomonas aeruginosa*. *JOURNAL OF BACTERIOLOGY, ,* 100, p. 276-282.

Kenna, D. T., Doherty, C. J., Foweraker, J., Macaskill, L., Barcus, V. A. & Govan, J. R. 2007. Hypermutability in environmental *Pseudomonas aeruginosa* and in populations causing pulmonary infection in individuals with cystic fibrosis. *Microbiology,* 153, 1852-9.

Kerem, B.-S., Zielenski, J., Markiewicz, D., Bozon, D., Gazit, E., Yahav, J., Kennedy, D., Riordan, J. R., Collins, F. S., Rommens, J. M. & Tsui, L.-C. 1990. Identification of mutations in regions corresponding to the two putative nucleotide (ATP)-binding folds of the cystic fibrosis gene. *Proc. Nati. Acad. Sci. USA,* 87, 8447-8451.

Kerem, B., Rommens, J. M., Buchanan, J. A., Markiewicz, D., Cox, T. K., Chakravarti, A., Buchwald , M. & Tsui, L. C. 1989. Identification of the cystic fibrosis gene: genetic analysis. *Science,* 245, 1073-80.

Kerem, E., Conway, S., Elborn, S., Heijerman, H. & Consensus, C. 2005. Standards of care for patients with cystic fibrosis: a European consensus. *J Cyst Fibros,* 4, 7-26.

Kessler, E., Safrin, M., Gustin, J. K. & Ohmani, D. E. 1998. Elastase and the LasA Protease of *Pseudomonas aeruginosa* are Secreted with Their Propeptides. *THE JOURNAL OF BIOLOGICAL CHEMISTRY,* 273, pp. 30225–30231.

Khalid, S., Bond, P. J., Deol, S. S. & Sansom, M. S. 2006. Modeling and simulations of a bacterial outer membrane protein: OprF from Pseudomonas aeruginosa. *Proteins,* 63, 6-15.

Khan, T. Z., Wagener, J. S., Bost, T., Martinez, J., Accurso, F. J. & Riches, D. W. 1995. Early pulmonary inflammation in infants with cystic fibrosis. *Am J Respir Crit Care Med. ,* 151, 1075-82.

Khan, S., Mian, H. S., Sandercock, L. E., Chirgadze, N. Y. & Pai, E. F. 2011. Crystal structure of the passenger domain of the Escherichia coli autotransporter EspP. *J Mol Biol,* 413, 985-1000.

Khlebnikov, A., Risa, Ø., Skaug, T., Carrier, T. A. & Keasling, J. D. 2000. Regulatable Arabinose-Inducible Gene Expression System with Consistent Control in All Cells of a Culture. *JOURNAL OF BACTERIOLOGY,* 182, p. 7029–7034.

Khoury, A. E., Lam, K., Ellis, B. & Costerton, J. W. 1992. Prevention and control of bacterial infections associated with medical devices. *ASAIO J. ,* 38, M174-8.

Khrapunov, S., Brenowitz, M., Rice, P. A. & Catalano, C. E. 2006. Binding then bending: a mechanism for wrapping DNA. *Proc Natl Acad Sci U S A,* 103, 19217-8.

Kida, Y., Higashimoto, Y., Inoue, H., Shimizu, T. & Kuwano, K. 2008. A novel secreted protease from *Pseudomonas aeruginosa* activates NF-kappaB through protease-activated receptors. *Cell Microbiol,* 10, 1491-504.

Kida, Y., Taira, J., Yamamoto, T., Higashimoto, Y. & Kuwano, K. 2013. EprS, an autotransporter protein of *Pseudomonas aeruginosa*, possessing serine protease activity induces inflammatory responses through protease-activated receptors. *Cell Microbiol,* 15, 1168-81.

Kiefhaber, T., Rudolph, R., Kohler, H.-H. & Buchner, J. 1991. Protein Aggregation *in vitro* and *in vivo*: A Quantitative Model of the Kinetic Competition between Folding and Aggregation. *Bio/Technology volume,* 9, 825–829.

King, P. 2012. *Haemophilus influenzae* and the lung (*Haemophilus* and the lung). *Clinical and Translational Medicine* 1**,** 1-9.

Kirchner, S., Fothergill, J. L., Wright, E. A., James, C. E., Mowat, E. & Winstanley, C. 2012. Use of Artificial Sputum Medium to Test Antibiotic Efficacy Against *Pseudomonas aeruginosa* in Conditions More Relevant to the Cystic Fibrosis Lung. *Journal of Visualized Experiments,* 64, 1-7.

Kirketerp-Møller, K., Zulkowski, K. & James, G. 2011. Chronic Wound Colonization, Infection, and Biofilms. 11-24.

Klare, W., Das, T., Ibugo, A., Buckle, E., Manefield, M. & Manos, J. 2016. Glutathione-Disrupted Biofilms of Clinical *Pseudomonas aeruginosa* Strains Exhibit an Enhanced Antibiotic Effect and a Novel Biofilm Transcriptome. *Antimicrob Agents Chemother,* 60, 4539-51.

Klausen, M., Heydorn, A., Ragas, P., Lambertsen, L., Aaes-Jørgensen, A., Molin, S. & Tolker-Nielsen, T. 2003. Biofilm formation by *Pseudomonas aeruginosa* wild type, flagella and type IV pili mutants. *Molecular Microbiology,* 48, 1511-1524.

Klauser, T., Pohiner, J. & Meyer, T. F. 1992. Selective extracellular release of cholera toxin B subunit by *Escherichia coli*- dissection of Neisseria Iga beta-mediated outer membrane transport. *The EMBO Journal* 11, pp.2327 - 2335.

Knowles, M. R. & Drumm, M. 2012. The influence of genetics on cystic fibrosis phenotypes. *Cold Spring Harb Perspect Med,* 2, a009548.

Ko¨ Hler, T., Curty, L. K., Barja, F., Van Delden, C. & Peche`Re, J.-C. 2000. Swarming of *Pseudomonas aeruginosa* Is Dependent on Cell-to-Cell Signaling and Requires Flagella and Pili. *JOURNAL OF BACTERIOLOGY,,* 182, p. 5990–5996.

Kobayashi, F., Yamaguchi, M. & Mitsuhashi, S. 1972. Drug Resistance to Aminoglycosidic Antibiotics in *Pseudomonas aeruginosa* and Its Lability. *Japan. J. Microbiol. ,* 16, 425-431,.

Koch, A.-K., Brömme, S., Wollschläger, B., Horneff, G. & Keyszer, G. 2008. Musculoskeletal Manifestations and Rheumatic Symptoms in Patients with Cystic Fibrosis (CF) —No Observations of CF-specific Arthropathy. *The Journal of Rheumatology,* 35, 1882-1891.

Koch, A. K., Kappeli, O., Fiechter, A. & Reiser, J. 1991. Hydrocarbon assimilation and biosurfactant production in *Pseudomonas aeruginosa* mutants. *JOURNAL OF BACTERIOLOGY,* 173, p. 4212-4219

Kohler, T., Curty, L. K., Barja, F., Van Delden, C. & Pechere, J. C. 2000. Swarming of *Pseudomonas aeruginosa* Is Dependent on Cell-to-Cell Signaling and Requires Flagella and Pili. *Journal of Bacteriology,* 182, 5990-5996.

Kolderman, E., Bettampadi, D., Samarian, D., Dowd, S. E., Foxman, B., Jakubovics, N. S. & Rickard, A. H. 2015. L-arginine destabilizes oral multi-species biofilm communities developed in human saliva. *PLoS One,* 10, e0121835.

Kolpen, M., Ku, M., Bjarnsholt, T., Moser, C., Rønne Hansen, C., Liengaard, L., Kharazmi, A., Pressler, T., Høiby, N. & Jensen, Ø. P. 2014. Nitrous Oxide Production in Sputum from Cystic Fibrosis Patients with Chronic *Pseudomonas aeruginosa* Lung Infection. *plos one,* 9, e84353, 1-9.

Kon, Y., Tsukada, H., Hasegawa, T., Igarashi, K., Wada, K., Suzuki, E., Arakawa, M. & Gejyo, F. 1999. The role of *Pseudomonas aeruginosa* elastase as a potent inflammatory factor in a rat air pouch inflammation model. *FEMS Immunology and Medical Microbiology* 25, 313^321.

Kononen, E. & Wade, W. G. 2015. *Actinomyces* and related organisms in human infections. *Clin Microbiol Rev,* 28**,** 419-42.

Konstan, M. W., Byard, P. J., Hoppel, C. L. & Davis, P. B. 1995. Effect of High-Dose Ibuprofen in Patients with Cystic Fibrosis. *THE NEW ENGLAND JOURNAL OF MEDICINE,* 332, 848-854.

Konstan, M. W., Hilliard, K. A., Norvell, T. M. & Berger, M. 1994. Bronchoalveolar lavage findings in cystic fibrosis patients with stable, clinically mild lung disease suggest ongoing infection and inflammation. *Am J Respir Crit Care Med. ,* 150, 448-54.

Kuang, Z., Hao, Y., Walling, B. E., Jeffries, J. L., Ohman, D. E. & Lau, G. W. 2011. *Pseudomonas aeruginosa* Elastase Provides an Escape from Phagocytosis by Degrading the Pulmonary Surfactant Protein-A. *Plos one,* 6, 1-14.

Kukavica-Ibrulj, I., Bragonzi, A., Paroni, M., Winstanley, C., Sanschagrin, F., O'toole, G. A. & Levesque, R. C. 2008. In vivo growth of Pseudomonas aeruginosa strains PAO1 and PA14 and the hypervirulent strain LESB58 in a rat model of chronic lung infection. *J Bacteriol,* 190, 2804-13.

Kung, V. L., Ozer, E. A. & Hauser, A. R. 2010. The Accessory Genome of Pseudomonas aeruginosa. *MICROBIOLOGY AND MOLECULAR BIOLOGY REVIEWS,* Vol. 74, p. 621–641.

Kyte, J. & Doolittle, R. F. 1982. A simple method for displaying the hydropathic character of a protein. *J Mol Biol. ,* 157**,** 105-32.

Laarman, A. J., Bardoel, B. W., Ruyken, M., Fernie, J., Milder, F. J., Van Strijp, J. A. & Rooijakkers, S. H. 2012. *Pseudomonas aeruginosa* alkaline protease blocks complement activation via the classical and lectin pathways. *J Immunol,* 188, 386-93.

Lam, J. S., Chan, R., Lam, K. & Costerton, J. W. 1980. Production of mucoid microcolonies by *Pseudomonas aeruginosa* within infected lungs in cystic fibrosis. *INFECTION AND IMMUNITY,,* 28, p. 546-556.

Lamont, I. L., Konings, A. F. & Reid, D. W. 2009. Iron acquisition by *Pseudomonas aeruginosa* in the lungs of patients with cystic fibrosis. *Biometals,* 22, 53-60.

Landry, R. M., An, D., Hupp, J. T., Singh, P. K. & Parsek, M. R. 2006. Mucin-*Pseudomonas aeruginosa* interactions promote biofilm formation and antibiotic resistance. *Mol Microbiol,* 59, 142-51.

Lanotte, P., Watt, S., Mereghetti, L., Dartiguelongue, N., Rastegar-Lari, A., Goudeau, A. & Quentin, R. 2004. Genetic features of *Pseudomonas aeruginosa* isolates from cystic fibrosis patients compared with those of isolates from other origins. *J Med Microbiol,* 53, 73-81.

Latge, J.-P. 1999. Aspergillus fumigatus and Aspergillosis. *CLINICAL MICROBIOLOGY REVIEWS,* 12**,** p. 310–350.

Latifi, A., Foglino, M., Tanaka, K., Williams, P. & Lazdunski, A. 1996. A hierarchical quorum-sensing cascade in *Pseudomonas aeruginosa* links the transcriptional activators LasR and RhIR (VsmR) to expression of the stationary-phase sigma factor RpoS. *Molecular Microbiology,* 21, 1137-1 146.

Lavrrar, J. L. & Mcintosh, M. A. 2003. Architecture of a Fur Binding Site: a Comparative Analysis. *Journal of Bacteriology,* 185, 2194-2202.

Lau, G. W., Hassett, D. J., Ran, H. & Kong, F. 2004. The role of pyocyanin in *Pseudomonas aeruginosa* infection. *Trends Mol Med,* 10, 599-606.

Lazazzera, B. A., Beinert, H., Khoroshilova, N., Kennedyi, M. C. & Kiley, P. J. 1996. DNA Binding and Dimerization of the Fe–S-containing FNR Protein from *Escherichia coli* Are Regulated by Oxygen. *Journal of biological chemistry,* 271, pp. 2762–2768.

Lebeaux, D., Chauhan, A., Letoffe, S., Fischer, F., De Reuse, H., Beloin, C. & Ghigo, J. M. 2014. pH-mediated potentiation of aminoglycosides kills bacterial persisters and eradicates *in vivo* biofilms. *J Infect Dis,* 210, 1357-66.

Lebeaux, D., Chauhan, A., Rendueles, O. & Beloin, C. 2013. From *in vitro* to *in vivo* Models of Bacterial Biofilm-Related Infections. *Pathogens,* 2, 288-356.

Lee, J., Wu, J., Deng, Y., Wang, J., Wang, C., Wang, J., Chang, C., Dong, Y., Williams, P. & Zhang, L.-H. 2013. A cell-cell communication signal integrates quorum sensing and stress response. *Nature Chemical Biology,* 9, 339-343.

Lee, J. & Zhang, L. 2015. The hierarchy quorum sensing network in Pseudomonas aeruginosa. *Protein Cell,* 6, 26-41.

Lee, V. T., Matewish, J. M., Kessler, J. L., Hyodo, M., Hayakawa, Y. & Lory, S. 2007. A cyclic-di-GMP receptor required for bacterial exopolysaccharide production. *Mol Microbiol,* 65, 1474-84.

Lee, M.-R., Sheng, W.-H., Hung, C.-C., Yu, C.-J., Lee, L.-N. & Hsueh, P.-R. 2015. *Mycobacterium abscessus* Complex Infections in Humans. *Emerging Infectious Diseases* 21**,** 1638-1646.

Leighton, T. L., Buensuceso, R. N., Howell, P. L. & Burrows, L. L. 2015. Biogenesis of *Pseudomonas aeruginosa* type IV pili and regulation of their function. *Environ Microbiol,* 17, 4148-63.

Leisinger, H., Haas, D. & Hegarty, M. P. 1972. Indospicine as an arginine antagonist in *Escherichia coli* and *Pseudomonas aeruginosa*. *Biochimica et Biophysica Acta (BBA) - Nucleic Acids and Protein Synthesis,* 262, 214-219.

Leo, J. C., Grin, I. & Linke, D. 2012. Type V secretion: mechanism(s) of autotransport through the bacterial outer membrane. *Philos Trans R Soc Lond B Biol Sci,* 367, 1088-101.

Letterer, L. & Schagat, T. [Internet] 2007. Cited 2018-05-09. Protein Expression in Less Time: A Short Induction Protocol for KRX. *Available from: http://www.promega.co.uk/resources/pubhub/enotes/protein-expression-in-less-time/*.

Levanon, S. S., San, K. Y. & Bennett, G. N. 2005. Effect of oxygen on the *Escherichia coli* ArcA and FNR regulation systems and metabolic responses. *Biotechnol Bioeng,* 89, 556-64.

Lewis, K. 2001. Riddle of biofilm resistance. *Antimicrob Agents Chemother,* 45, 999-1007.

Leyton, D. L., Johnson, M. D., Thapa, R., Huysmans, G. H., Dunstan, R. A., Celik, N., Shen, H. H., Loo, D., Belousoff, M. J., Purcell, A. W., Henderson, I. R., Beddoe, T., Rossjohn, J., Martin, L. L., Strugnell, R. A. & Lithgow, T. 2014. A mortise-tenon joint in the transmembrane domain modulates autotransporter assembly into bacterial outer membranes. *Nat Commun,* 5, 4239.

Leyton, D. L., Rossiter, A. E. & Henderson, I. R. 2012. From self sufficiency to dependence: mechanisms and factors important for autotransporter biogenesis. *Nat Rev Microbiol,* 10, 213-25.

Li, C., Wally, H., Miller, S. J. & Lu, C. D. 2009. The multifaceted proteins MvaT and MvaU, members of the H-NS family, control arginine metabolism, pyocyanin synthesis, and prophage activation in *Pseudomonas aeruginosa* PAO1. *J Bacteriol,* 191, 6211-8.

Li, F., Svarovsky, M. J., Karlsson, A. J., Wagner, J. P., Marchillo, K., Oshel, P., Andes, D. & Palecek, S. P. 2007. Eap1p, an adhesin that mediates Candida albicans biofilm formation *in vitro* and *in vivo*. *Eukaryot Cell,* 6, 931-9.

Li, H., Luo, Y. F., Williams, B. J., Blackwell, T. S. & Xie, C. M. 2012. Structure and function of OprD protein in *Pseudomonas aeruginosa*: from antibiotic resistance to novel therapies. *Int J Med Microbiol,* 302, 63-8.

Lia, C. & Lua, C.-D. 2009. Arginine racemization by coupled catabolic and anabolic dehydrogenases. *PNAS,* 106, 906–911.

Lindgren, J. K., Thomas, V. C., Olson, M. E., Chaudhari, S. S., Nuxoll, A. S., Schaeffer, C. R., Lindgren, K. E., Jones, J., Zimmerman, M. C., Dunman, P. M., Bayles, K. W. & Feya, P. D. 2014. Arginine Deiminase in *Staphylococcus epidermidis* Functions To Augment Biofilm Maturation through pH Homeostasis. *Journal of Bacteriology* 196, p. 2277–2289.

Line, L., Alhede, M., Kolpen, M., Kuhl, M., Ciofu, O., Bjarnsholt, T., Moser, C., Toyofuku, M., Nomura, N., Hoiby, N. & Jensen, P. O. 2014. Physiological levels of nitrate support anoxic growth by denitrification of *Pseudomonas aeruginosa* at growth rates reported in cystic fibrosis lungs and sputum. *Front Microbiol,* 5, 554.

Linke, D., Riess, T., Autenrieth, I. B., Lupas, A. & Kempf, V. A. 2006. Trimeric autotransporter adhesins: variable structure, common function. *Trends Microbiol,* 14, 264-70.

Linker, A. & Jones, R. S. 1996. A new polysaccharide resembling alginic acid isolated from pseudomonads. *J Biol Chem,* 241, 3845-51.

Linnane, S. J., Keatings, V. M., Costello, C. M., Moynihan, J. B., O'connor, C. M., Fitzgerald, M. X. & Mcloughlin, P. 1998. Total Sputum Nitrate plus Nitrite Is Raised during Acute Pulmonary Infection in Cystic Fibrosis. *AMERICAN JOURNAL OF RESPIRATORY AND CRITICAL CARE MEDICINE,* 158, 207-2012.

Lipford, G. B., Heeg, K. & Wagner, H. 1998. Bacterial DNA as immune cell activator. *Trends Microbiol. ,* 6, 496-500.

Lipuma, J. J. 2010. The changing microbial epidemiology in cystic fibrosis. *Clin Microbiol Rev,* 23**,** 299-323.
Lipuma, J. J. 2014. Expanding our understanding of respiratory microbiota in cystic fibrosis. *Ann Am Thorac Soc,* 11**,** 1084-5.
Liu, G., Tang, C. M. & Exley, R. M. 2015. Non-pathogenic *Neisseria*: members of an abundant, multi-habitat, diverse genus. *Microbiology,* 161**,** 1297-1312.
Lobell, R. & Schleif, R. 1991. AraC-DNA looping: orientation and distance-dependent loop breaking by the cyclic AMP receptor protein. *Journal of Molecular Biology,* 218, 45 - 54.
Lopes, S. P., Azevedo, N. F. & Pereira, M. O. 2014. Emergent bacteria in cystic fibrosis: *in vitro* biofilm formation and resilience under variable oxygen conditions. *Biomed Res Int,* 2014, 678301.
Lu, C.-D. & Abdelal, A. T. 2001. The gdhB gene of *Pseudomonas aeruginosa* encodes an arginine-inducible NAD(+)-dependent glutamate dehydrogenase which is subject to allosteric regulation. *JOURNAL OF BACTERIOLOGY,* 183, p. 490–499.
Lu, C.-D., Yang, Z. & Li, W. 2004. Transcriptome Analysis of the ArgR Regulon in *Pseudomonas aeruginosa*. *J Bacteriol,* 186, 3855–3861.
Lu, C. D., Winteler, H., Abdelal, A. & Haas, D. 1999. The ArgR Regulatory Protein, a Helper to the Anaerobic Regulator ANR during Transcriptional Activation of the arcD Promoter in Pseudomonas aeruginosa. *JOURNAL OF BACTERIOLOGY,* 181, p. 2459–2464
Lu, X., Roe, F., Jesaitis, A. & Lewandowski, Z. 1998. Resistance of biofilms to the catalase inhibitor 3-amino-1,2, 4-triazole. *Biotechnol Bioeng. ,* 59, 156-62.
Luckett, J. C., Darch, O., Watters, C., Abuoun, M., Wright, V., Paredes-Osses, E., Ward, J., Goto, H., Heeb, S., Pommier, S., Rumbaugh, K. P., Camara, M. & Hardie, K. R. 2012. A novel virulence strategy for *Pseudomonas aeruginosa* mediated by an autotransporter with arginine-specific aminopeptidase activity. *PLoS Pathog,* 8, e1002854.
Lundgren, B. R., Thornton, W., Dornan, M. H., Villegas-Peñaranda, L. R., Boddy, C. N. & Nomuraa, C. T. 2013. Gene PA2449 Is Essential for Glycine Metabolism and Pyocyanin Biosynthesis in *Pseudomonas aeruginosa* PAO1. *Journal of Bacteriology* 195, p. 2087–2100.
Luzar, M. A. & Montie, T. C. 1985. Avirulence and altered physiological properties of cystic fibrosis strains of Pseudomonas aeruginosa. *INFECTION AND IMMUNITY,* 50, p. 572-576.
Luzar, M. A., Thomassen, M. J. & Montie, T. C. 1985. Flagella and motility alterations in *Pseudomonas aeruginosa* strains from patients with cystic fibrosis- relationship to patient clinical condition. *INFECTION AND IMMUNITY,* 50, 577-582.
Lyczak, J. B., Cannon, C. L. & Pier, G. B. 2002. Lung Infections Associated with Cystic Fibrosis. *CLINICAL MICROBIOLOGY REVIEWS,* 15, p. 194–222.
Ma, J., Campbell, A. & Karlin, S. 2002. Correlations between Shine-Dalgarno Sequences and Gene Features Such as Predicted Expression Levels and Operon Structures. *Journal of Bacteriology,* 184, 5733-5745.
Ma, L., Conover, M., Lu, H., Parsek, M. R., Bayles, K. & Wozniak, D. J. 2009. Assembly and Development of the *Pseudomonas aeruginosa* Biofilm Matrix. *PLoS Pathogens,* 5, 1-11.
Ma, L., Wang, J., Wang, S., Anderson, E. M., Lam, J. S., Parsek, M. R. & Wozniak, D. J. 2012. Synthesis of multiple *Pseudomonas aeruginosa* biofilm matrix exopolysaccharides is post-transcriptionally regulated. *Environ Microbiol,* 14, 1995-2005.
Ma, Q., Zhai, Y., Schneider, J. C., Ramseier, T. M. & Saier, M. H. 2003. Protein secretion systems of *Pseudomonas aeruginosa* and P. fluorescens. *Biochimica et Biophysica Acta (BBA) - Biomembranes,* 1611, 223-233.
Maghnouj, A., Franco, T., Cabral, D. S., Stalon, V. & Vander Wauven, C. 1998. The arcABDC Gene Cluster, Encoding the Arginine Deiminase Pathway of Bacillus licheniformis, and Its Activation by the Arginine Repressor ArgR. *JOURNAL OF BACTERIOLOGY,,* 180, p. 6468–6475
Mah, T.-F., Pitts, B., Pellock, B., Walker, G. C., Stewart, P. S. & O'toole, G. A. 2003. A genetic basis for *Pseudomonas aeruginosa* biofilm antibiotic resistance. *NATURE* 426, 306-310.
Mah, T.-F. C. & O'toole, G. A. 2001. Mechanisms of biofilm resistance to antimicrobial agents. *TRENDS in Microbiology* 9, 34-39.

Mahenthiralingam, E., Campbell, M. E. & Speert, D. P. 1994. Nonmotility and phagocytic resistance of *Pseudomonas aeruginosa* isolates from chronically colonized patients with cystic fibrosis. *INFECTION AND IMMUNITY,,* 62, , p. 596-605

Mamessier, E., Milhe, F., Badier, M., Thomas, P., Magnan, A. & Reynaud-Gaubert, M. 2006. Comparison of Induced Sputum and Bronchoalveolar Lavage in Lung Transplant Recipients. *The journal of heart and lung transplantation,* 25,, Pages 523-532

Mamipour, M., Yousefi, M. & Hasanzadeh, M. 2017. An overview on molecular chaperones enhancing solubility of expressed recombinant proteins with correct folding. *Int J Biol Macromol,* 102, 367-375.

Mann, E. E. & Wozniak, D. J. 2012. Pseudomonas biofilm matrix composition and niche biology. *FEMS Microbiol Rev,* 36, 893-916.

Marrie, T. J., Nelligan, J. & Costerton, J. W. 1982. A scanning and transmission electron microscopic study of an infected endocardial pacemaker lead. *Circulation,* 66, 1339-41.

Marschall, L., Sagmeister, P. & Herwig, C. 2017. Tunable recombinant protein expression in *E. coli*: promoter systems and genetic constraints. *Appl Microbiol Biotechnol,* 101, 501-512.

Martin, D. W., Schurr, M. J., Yu, H. & Deretic, V. 1994. Analysis of promoters controlled by the putative sigma factor AlgU regulating conversion to mucoidy in Pseudomonas aeruginosa- relationship to sigma E and stress response. *JOURNAL OF BACTERIOLOGY,,* 176, , p. 6688-6696

Martínez-Granero, F., Redondo-Nieto, M., Vesga, P., Martín, M. & Rivilla, R. 2014. AmrZ is a global transcriptional regulator implicated in iron uptake and environmental adaption in *P. fluorescens*F113. *BMC Genomics* 15, 1471-2164.

Masduki, A., Nakamura, J., Ohga, T., Umezaki, R., Kato, J. & Ohtake, H. 1995. Isolation and characterization of chemotaxis mutants and genes of *Pseudomonas aeruginosa*. *JOURNAL OF BACTERIOLOGY,* 177, p. 948–952

Mashburn, L. M., Jett, A. M., Akins, D. R. & Whiteley, M. 2005. *Staphylococcus aureus* serves as an iron source for *Pseudomonas aeruginosa* during *in vivo* coculture. *J Bacteriol,* 187, 554-66.

Mashima, I. & Nakazawa, F. 2015. The interaction between S*treptococcus spp.* and *Veillonella tobetsuensis* in the early stages of oral biofilm formation. *J Bacteriol*.

Mathee, K., Ciofu, O., Sternberg, C., Lindum, P. W., Campbell, J. I. A., Jensen, P., Johnsen, A. H., Givskov, M., Ohman, D. E., Molin, S., Høiby, N. & Kharazmi, A. 1999. Mucoid conversion of *Pseudomonas aeruginosa* by hydrogen peroxide-a mechanism for virulence activation in the cystic fibrosis lung. *Microbiology,* 145,, 1349–1357.

Matsui, H., Grubb, B. R., Tarran, R., Randell, S. H., Gatzy, J. T., Davis, C. W. & Boucher, R. C. 1998. Evidence for periciliary liquid layer depletion, not abnormal ion composition, in the pathogenesis of cystic fibrosis airways disease. *Cell,* 95, 1005–1015,.

Matsui, H., Wagner, V. E., Hill, D. B., Schwab, U. E., Rogers, T. D., Button, B., Taylor, R. M., 2nd, Superfine, R., Rubinstein, M., Iglewski, B. H. & Boucher, R. C. 2006. A physical linkage between cystic fibrosis airway surface dehydration and *Pseudomonas aeruginosa* biofilms. *Proc Natl Acad Sci U S A,* 103, 18131-6.

Matsukawa, M. & Greenberg, E. P. 2004. Putative exopolysaccharide synthesis genes influence *Pseudomonas aeruginosa* biofilm development. *J Bacteriol,* 186, 4449-56.

Matsushita K, Shinagawa E, Adachi O & M., A. 1982. o-Type cytochrome oxidase in the membrane of aerobically grown Pseudomonas aeruginosa. *Federation of European Biochemical Societies* 139, 255-258.

Mavrodi, D. V., Bonsall, R. F., Delaney, S. M., Soule, M. J., Phillips, G. & Thomashow, L. S. 2001. Functional analysis of genes for biosynthesis of pyocyanin and phenazine-1-carboxamide from *Pseudomonas aeruginosa* PAO1. *J Bacteriol,* 183, 6454-65.

May, T. B., Shinabarger, D., Maharaj, R., Kato, J., Chu, L., Devault, J. D., Roychoudhury, S., Zielinski, N. A., Berry, A., Rothmel, R. K., Misra, T. K. & Chakrabarty, A. M. 1991a. Alginate Synthesis by *Pseudomonas aeruginosa*- a Key Pathogenic Factor in Chronic Pulmonary Infections of Cystic Fibrosis Patients. *CLINICAL MICROBIOLOGY REVIEWS, A,* 4, 191-206

Mcclure, C. D. & Schiller, N. L. 1992. Effects of *Pseudomonas aeruginosa* rhamnolipids on human monocyte-derived macrophages. *J Leukoc Biol. ,* 51, 97-102.

Mcclure, C. D. & Schiller, N. L. 1996. Inhibition of macrophage phagocytosis by *Pseudomonas aeruginosa* rhamnolipids *in vitro* and *in vivo*. *Curr Microbiol. ,* 33, 109-17.

Mcdonnell, M. J., Jary, H. R., Perry, A., Macfarlane, J. G., Hester, K. L., Small, T., Molyneux, C., Perry, J. D., Walton, K. E. & De Soyza, A. 2015. Non cystic fibrosis bronchiectasis: A longitudinal retrospective observational cohort study of Pseudomonas persistence and resistance. *Respir Med,* 109, 716-26.

Mcguffie, E. M., Frank, D. W., Vincent, T. S. & Olson, J. C. 1998. Modification of Ras in Eukaryotic Cells by *Pseudomonas aeruginosa* Exoenzyme S. *INFECTION AND IMMUNITY,* 66, 2607–2613.

Mcknight, S. L., Iglewski, B. H. & Pesci, E. C. 2000. The Pseudomonas quinolone signal regulates rhl quorum sensing in Pseudomonas aeruginosa. *JOURNAL OF BACTERIOLOGY,,* 182, 2702–2708.

Meng, G., Spahich, N., Kenjale, R., Waksman, G. & St Geme, J. W., 3rd 2011. Crystal structure of the Haemophilus influenzae Hap adhesin reveals an intercellular oligomerization mechanism for bacterial aggregation. *EMBO J,* 30, 3864-74.

Mercenier, A., Simon, J.-P., Haas, D. & Stalonl, V. 1980a. Catabolism of L-Arginine by *Pseudomonas aeruginosa Journal of General Microbiology,* 116, 381-389.

Mercenier, A., Simon, J. P., Vander Wauven, C., Haas, D. & Stalon, V. 1980b. Regulation of enzyme synthesis in the arginine deiminase pathway of *Pseudomonas aeruginosa*. *J Bacteriol,* 144, 159-63.

Mering, C. 2003. STRING: a database of predicted functional associations between proteins. *Nucleic Acids Research,* 31, 258-261.

Merrick, M. J. 1993. In a class of its own--the RNA polymerase sigma factor sigma 54 (sigma N). *Molecular Microbiology,* 10, 903-909.

Merz, A. J., So, M. & Sheetz, M. P. 2000. Pilus retraction powers bacterial twitching motility. *Nature,* 407, 98-102.

Meyer, J.-M., Neely, A., Stintzi, A., Georges, C. & Holder, I. A. 1996,. Pyoverdin Is Essential for Virulence of Pseudomonas aeruginosa. *INFECTION AND IMMUNITY,,* 64, 518–523.

Meyers, D. J., Palmer, K. C., Bale, L. A., Kernacki, K., Preston, M., Brown, T. & Berk, R. S. 1992. *In vivo* and *in vitro* toxicity of phospholipase C from Pseudomonas aeruginosa. *Toxicon. 1992* 30, 161-9.

Michalska, M. & Wolf, P. 2015. Pseudomonas Exotoxin A: optimized by evolution for effective killing. *Front Microbiol,* 6, 963.

Mickle, J. E. & Cutting, G. R. 2000. GENOTYPE-PHENOTYPE RELATIONSHIPS IN CYSTIC FIBROSIS. *MEDICAL CLINICS OF NORTH AMERICA* 84, 597-607.

Mika, F. & Hengge, R. 2005. A two-component phosphotransfer network involving ArcB, ArcA, and RssB coordinates synthesis and proteolysis of σS (RpoS) in *E. coli*. *GENES & DEVELOPMENT* 19, 2770–2781.

Mikkelsen, H., Sivaneson, M. & Filloux, A. 2011. Key two-component regulatory systems that control biofilm formation in *Pseudomonas aeruginosa*. *Environ Microbiol,* 13, 1666-81.

Miller, M. B. & Bassler, B. L. 2001. Miller and Bassler 2001. *Annu Rev Microbiol. ,* 55, 165-99.

Miroux, B. & Walker, J. E. 1996. Over-production of proteins in *Escherichia coli*- mutant hosts that allow synthesis of some membrane proteins and globular proteins at high levels. *J. Mol. Biol. ,* 260, 289–298

Monsó, E., Ruiz, J., Rosell, A., Manterola, J., Fiz, J., Morera, J. & Ausina, V. 1995. Bacterial infection in chronic obstructive pulmonary disease. A study of stable and exacerbated outpatients using the protected specimen brush. *Am J Respir Crit Care Med,* 152, pp1316-1320.

Moore, L. V. H. & Moore, W. E. C. 1994. F *Oribaculum catoniae* gen. nov., sp. nov.; *Catonella morbi* gen. nov., sp. nov.; *Hallella seregens* gen. nov., sp. nov.; *Johnsonella ignava* gen. nov., sp. nov.; and *Dialister pneumosintes* gen. nov., comb. nov., nom. rev., Anaerobic Gram-Negative Bacilli from the Human Gingival *INTERNATIONAL JOURNAL OFSYSTEMATIC BACTERIOLOGY,,* 44**,** p. 187-192.

Moreau-Marquis, S., O'toole, G. A. & Stanton, B. A. 2009. Tobramycin and FDA-approved iron chelators eliminate *Pseudomonas aeruginosa* biofilms on cystic fibrosis cells. *Am J Respir Cell Mol Biol,* 41, 305-13.

Moreau-Marquis, S., Stanton, B. A. & O'toole, G. A. 2008. *Pseudomonas aeruginosa* biofilm formation in the cystic fibrosis airway. *Pulm Pharmacol Ther,* 21, 595-9.

Moreno, R., Fonseca, P. & Rojo, F. 2010. The Crc Global Regulator Inhibits the Pseudomonas putida pWW0 Toluene/Xylene Assimilation Pathway by Repressing the Translation of Regulatory and Structural Genes*. *THE JOURNAL OF BIOLOGICAL CHEMISTRY* VOL. 285,, pp. 24412–24419,.

Morihara, K. 1964. PRODUCTION OF ELASTASE AND PROTEINASE BY PSEUDOMONAS AERUGINOSA. *J Bacteriol,* 88, 745-57.
Morihara, K., Tsuzuki, H. & Oda, K. 1979. Protease and elastase of *Pseudomonas aeruginosa*: inactivation of human plasma α1-proteinase inhibitor. *Infect Immun,* 24, 188-193.
Mornon, J.-P., Lehn, P. & Callebaut, I. 2009. Molecular models of the open and closed states of the whole human CFTR protein. *Cellular and Molecular Life Sciences,* 66, 3469–3486.
Morrison, T.B., Weis, J. J. & Wittwer, C. T. 1998. Quantification of low-copy transcripts by continuous SYBR Green I monitoring during amplification. *Biotechniques.,* 24, 954-8 960, 962.
Morton 1985. Pain and Laboratory Animals. *Nature,* 315, 106.
Mouncey, N. J. & Kaplan, S. 1998. Oxygen regulation of the ccoN gene encoding a component of the cbb3 oxidase in *Rhodobacter sphaeroide*s 2.4.1T: involvement of the FnrL protein. *Journal of bacteriology,* 180, p. 2228–2231.
Mowat, E., Paterson, S., Fothergill, J. L., Wright, E. A., Ledson, M. J., Walshaw, M. J., Brockhurst, M. A. & Winstanley, C. 2011. Pseudomonas aeruginosaPopulation Diversity and Turnover in Cystic Fibrosis Chronic Infections. *American Journal of Respiratory and Critical Care Medicine,* 183, 1674-1679.
Muhammadi & Ahmed*, N. 2007. Genetics of Bacterial Alginate- Alginate Genes Distribution, Organization and Biosynthesis in Bacteria. *Current Genomics,* 8, 191-202
Mulcahy, H., Charron-Mazenod, L. & Lewenza, S. 2008. Extracellular DNA chelates cations and induces antibiotic resistance in *Pseudomonas aeruginosa* biofilms. *PLoS Pathog,* 4, e1000213.
Mulcahy, H., Charron-Mazenod, L. & Lewenza, S. 2010. *Pseudomonas aeruginosa* produces an extracellular deoxyribonuclease that is required for utilization of DNA as a nutrient source. *Environ Microbiol,* 12, 1621-9.
Mulcahy, L. R., Isabella, V. M. & Lewis, K. 2014. *Pseudomonas aeruginosa* biofilms in disease. *Microb Ecol,* 68, 1-12.
Munch, R., Hiller, K., Grote, A., Scheer, M., Klein, J., Schobert, M. & Jahn, D. 2005. Virtual Footprint and PRODORIC: an integrative framework for regulon prediction in prokaryotes. *Bioinformatics,* 21**,** 4187-9.
Murakami, K. S., Masuda, S. & Darst, S. A. 2002. Structural basis of transcription initiation: RNA polymerase holoenzyme at 4 A resolution. *Science.,* 296, 1280-4.
Musken, M., Di Fiore, S., Dotsch, A., Fischer, R. & Haussler, S. 2009. Genetic determinants of *Pseudomonas aeruginosa* biofilm establishment. *Microbiology,* 156, 431-441.
Nagano, Y., Elborn, J. S., Millar, B. C., Walker, J. M., Goldsmith, C. E., Rendall, J. & Moore, J. E. 2010. Comparison of techniques to examine the diversity of fungi in adult patients with cystic fibrosis. *Med Mycol,* 48**,** 166-76 e1.
Nair, N., Biswas, R., Gotz, F. & Biswas, L. 2014. Impact of *Staphylococcus aureus* on pathogenesis in polymicrobial infections. *Infect Immun,* 82**,** 2162-9.
Nakada, Y. & Y., I. 2003. Identification of the putrescine biosynthetic genes in *Pseudomonas aeruginosa* and characterization of agmatine deiminase and N-carbamoylputrescine amidohydrolase of the arginine decarboxylase pathway. *Microbiology,* 149, 707–714.
Nanne, S. 2015. Arginine: New study exposes additional oral health benefits. *Dentistry iQ (News article)*.
Nash, K. L., Collier, J. D., French, J., Mckeon, D., Gimson, A. E., Jamieson, N. V., Wallwork, J., Bilton, D. & Alexander, G. J. 2008. Cystic fibrosis liver disease: to transplant or not to transplant? *Am J Transplant,* 8, 162-9.
Nealson, K. H. & Hastings, J. W. 1979. Bacterial bioluminescence- its control and ecological significance. *MICROBIOLoGIcAL REVIEWS,,* 43, p. 496-518
Newman , J. R. & Fuqua, C. 1999. Broad-host-range expression vectors that carry the l-arabinose-inducible *Escherichia coli* araBAD promoter and the araC regulator. *Gene* 277, 197–203
Newton, J. M., Schofield, D., Vlahopoulou, J. & Zhou, Y. 2016. Detecting cell lysis using viscosity monitoring in *E. coli* fermentation to prevent product loss. *Biotechnol Prog,* 32, 1069-76.
Ng, F. M. & Dawes, E. A. 1967 Regulation of enzymes of glucose metabolism by citrate in Pseudomonas aeruginosa. *Biochem J,* 104, 48–48P.
Ng, W. L. & Bassler, B. L. 2009. Bacterial quorum-sensing network architectures. *Annu Rev Genet,* 43, 197-222.

Nickel, J. C., Ruseska, I., Wright, J. B. & Costerton, J. W. 1985. Tobramycin resistance of *Pseudomonas aeruginosa* cells growing as a biofilm on urinary catheter material. *ANTIMICROBIAL AGENTS AND CHEMOTHERAPY,* 27, p. 619-624

Nicolay, T., Devleeschouwer, K., Vanderleyden, J. & Spaepen, S. 2012. Characterization of Esterase A, a Pseudomonas stutzeri A15 Autotransporter. *Appl Environ Microbiol,* 78, 2533-42.

Nicotra, M. B., Rivera, M., Dale, A. M., Shepherd, R. & Carter, R. 1995. Clinical, pathophysiologic, and microbiologic characterization of bronchiectasis in an aging cohort. *Chest,* 108, 955-61.

Nobile, C. J. & Johnson, A. D. 2015. *Candida albicans* Biofilms and Human Disease. *Annu Rev Microbiol,* 69**,** 71-92.

O'malley, Y. Q., Reszka, K. J., Spitz, D. R., Denning, G. M. & Britigan, B. E. 2004. *Pseudomonas aeruginosa* pyocyanin directly oxidizes glutathione and decreases its levels in airway epithelial cells. *Am J Physiol Lung Cell Mol Physiol,* 287, L94–L103.

O'toole, G., Kaplan, H. B. & Kolter, R. 2000. Biofilm Formation as Microbial Development. *Annu. Rev. Microbiol,* 54, 49-79.

O'toole, G. A. & Kolter, R. 1998. Flagellar and twitching motility are necessary for *Pseudomonas aeruginosa* biofilm development. *Molecular Microbiology,* 30, 295–304.

O'toole, G. A. 2018. Cystic Fibrosis Airway Microbiome: Overturning the Old, Opening the Way for the New. *J Bacteriol,* 200.

Oberhettinger, P., Leo, J. C., Linke, D., Autenrieth, I. B. & Schutz, M. S. 2015. The inverse autotransporter intimin exports its passenger domain via a hairpin intermediate. *J Biol Chem,* 290, 1837-49.

Okabe, S., Satoh, H. & Watanabe, Y. 1999. In Situ Analysis of Nitrifying Biofilms as Determined by In Situ Hybridization and the Use of Microelectrodes. *APPLIED AND ENVIRONMENTAL MICROBIOLOGY,* 65, p. 3182–3191.

Oliver, A., Cantón, R., Campo, P., Baquero, F. & Blázquez, J. 2000. High Frequency of Hypermutable *Pseudomonas aeruginosa* in Cystic Fibrosis Lung Infection. *Science,* 288, pp. 1251-1253.

O'may, C. Y., Reid, D. W. & Kirov, S. M. 2006. Anaerobic culture conditions favor biofilm-like phenotypes in Pseudomonas aeruginosa isolates from patients with cystic fibrosis. *FEMS Immunol Med Microbiol,* 48, 373-80.

Omotajo, D., Tate, T., Cho, H. & Choudhary, M. 2015. Distribution and diversity of ribosome binding sites in prokaryotic genomes. *BMC Genomics,* 16, 604.

Oomen, C. J., Van Ulsen, P., Van Gelder, P., Feijen, M., Tommassen, J. & Gros, P. 2004. Structure of the translocator domain of a bacterial autotransporter. *The EMBO Journal* 23, 1257–1266.

Otten, M. F., Stork, D. M., Reijnders, W. N., Westerhoff, H. V. & Van Spanning, R. J. 2001. Regulation of expression of terminal oxidases in Paracoccus denitrificans. *Eur. J. Biochem.,* 268, 2486±2497

Otto, B. R., Sijbrandi, R., Luirink, J., Oudega, B., Heddle, J. G., Mizutani, K., Park, S. Y. & Tame, J. R. 2005. Crystal structure of hemoglobin protease, a heme binding autotransporter protein from pathogenic Escherichia coli. *J Biol Chem,* 280, 17339-45.

Palmer, K. L., Aye, L. M. & Whiteley, M. 2007a. Nutritional cues control *Pseudomonas aeruginosa* multicellular behavior in cystic fibrosis sputum. *J Bacteriol,* 189, 8079-87.

Palmer, K. L., Brown, S. A. & Whiteley, M. 2007b. Membrane-Bound Nitrate Reductase Is Required for Anaerobic Growth in Cystic Fibrosis Sputum. *American Society for Microbiology,* 189, p. 4449–4455.

Pamp, S. J. & Tolker-Nielsen, T. 2007. Multiple roles of biosurfactants in structural biofilm development by Pseudomonas aeruginosa. *J Bacteriol,* 189, 2531-9.

Papenfort, K. & Bassler, B. L. 2016. Quorum sensing signal-response systems in Gram-negative bacteria. *Nat Rev Microbiol,* 14, 576-88.

Papi, A., Bellettato, C. M., Braccioni, F., Romagnoli, M., Casolari, P., Caramori, G., Fabbri, L. M. & Johnston, S. L. 2006. Infections and Airway Inflammation in Chronic

Obstructive Pulmonary Disease Severe Exacerbations. *Am J Respir Crit Care Med,* 176, pp 1114–1121.

Parizad, E., Parizad, E., Pakzad, I. & Valizadeh, A. 2016. A Review of Secretion Systems in Pathogenic and Non-Pathogenic Bacteria. *Biosciences, Biotechnology Research Asia,* 13, 135-145.

Park, D. M., Akhtar, M. S., Ansari, A. Z., Landick, R. & Kiley, P. J. 2013. The bacterial response regulator ArcA uses a diverse binding site architecture to regulate carbon oxidation globally. *PLoS Genet,* 9, e1003839.

Park, S.-M., Lu, C.-D. & Abdelal, A. T. 1997. Purification and characterization of an arginine regulatory protein, ArgR, from *Pseudomonas aeruginosa* and its interactions with the control regions for the car, argF, and aru operons. *JOURNAL OF BACTERIOLOGY,* 179, p. 5309–5317.

Parks, Q. M., Young, R. L., Poch, K. R., Malcolm, K. C., Vasil, M. L. & Nick, J. A. 2009. Neutrophil enhancement of *Pseudomonas aeruginosa* biofilm development: human F-actin and DNA as targets for therapy. *J Med Microbiol,* 58, 492-502.

Parks, T., Barrett, L. & Jones, N. 2015. Invasive *streptococcal* disease: a review for clinicians. *Br Med Bull,* 115**,** 77-89.

Patriquin, G. M., Banin, E., Gilmour, C., Tuchman, R., Greenberg, E. P. & Poole, K. 2008. Influence of quorum sensing and iron on twitching motility and biofilm formation in *Pseudomonas aeruginosa*. *J Bacteriol,* 190, 662-71.

Pavlova, O., Peterson, J. H., Ieva, R. & Bernstein, H. D. 2013. Mechanistic link between β barrel assembly and the initiation of autotransporter secretion. *PNAS,* 110, E938–E947

Pearson, J. P., Feldman, M., Iglewski, B. H. & Prince, A. 2000. *Pseudomonas aeruginosa* cell-to-cell signaling is required for virulence in a model of acute pulmonary infection. *INFECTION AND IMMUNITY,* 68, p. 4331–4334.

Pearson, J. P., Gray, K. M., Passador, L., Tucker, K. D., Eberhard, A., Iglewski, B. H. & Greenberg, E. P. 1994. Structure of the autoinducer required for expression of *Pseudomonas aeruginosa* virulence genes. (1). *Proc. Natl. Acad. Sci. USA,* 91, pp. 197-201.

Pearson, J. P., Pesci, E. C. & Iglewski, B. H. 1997. Roles of *Pseudomonas aeruginosa* las and rhl Quorum-Sensing Systems in Control of Elastase and Rhamnolipid Biosynthesis Genes. *JOURNAL OF BACTERIOLOGY,* 179, p. 5756–5767

Pedersen, S. S., Kharazmi, A., Espersen, F. & H0iby, N. 1990. *Pseudomonas aeruginosa* alginate in cystic fibrosis sputum and the inflammatory response. *INFECTION AND IMMUNITY, O,* 58, p. 3363-3368

Perrenoud, A. & Sauer, U. 2005. Impact of global transcriptional regulation by ArcA, ArcB, Cra, Crp, Cya, Fnr, and Mlc on glucose catabolism in *Escherichia coli*. *J Bacteriol,* 187, 3171-9.

Pesci, E. C., Milbank, J. B. J., Pearson, J. P., Mcknight, S., Kende, A. S., Greenberg, E. P. & Iglewski, B. H. 1999. Quinolone signaling in the cell-to-cell communication system of *Pseudomonas aeruginosa*. *Proc. Natl. Acad. Sci. USA,* 96, pp. 11229–11234.

Pessi, G. & Haas, D. 2000. Transcriptional Control of the Hydrogen Cyanide Biosynthetic Genes hcnABC by the Anaerobic Regulator ANR and the Quorum-Sensing Regulators LasR and RhlR inPseudomonas aeruginosa. *JOURNAL OF BACTERIOLOGY,* 182, p. 6940–6949

Pessi, G., Williams, F., Hindle, Z., Heurlier, K., Holden, M. T., Camara, M., Haas, D. & Williams, P. 2001. The global posttranscriptional regulator RsmA modulates production of virulence determinants and N-acylhomoserine lactones in Pseudomonas aeruginosa. *J Bacteriol,* 183, 6676-83.

Peterson, J. H., Szabady, R. L. & Bernstein, H. D. 2006. An unusual signal peptide extension inhibits the binding of bacterial presecretory proteins to the signal recognition particle, trigger factor, and the SecYEG complex. *J Biol Chem,* 281, 9038-48.

Peterson, J. H., Tian, P., Ieva, R., Dautin, N. & Bernstein, H. D. 2010. Secretion of a bacterial virulence factor is driven by the folding of a C-terminal segment. *Proc Natl Acad Sci U S A,* 107, 17739-44.

Petersen, T. N., Brunak, S., Von Heijne, G. & Nielsen, H. 2011. SignalP 4.0: discriminating signal peptides from transmembrane regions. *Nat Methods,* 8**,** 785-6.

Pezzulo, A. A., Tang, X. X., Hoegger, M. J., Abou Alaiwa, M. H., Ramachandran, S., Moninger, T. O., Karp, P. H., Wohlford-Lenane, C. L., Haagsman, H. P., Van Eijk, M., Banfi, B., Horswill, A. R., Stoltz, D. A., Mccray, P. B., Jr., Welsh, M. J. & Zabner, J. 2012. Reduced airway surface pH impairs bacterial killing in the porcine cystic fibrosis lung. *Nature,* 487, 109-13.

Pfaffl 2004. Quantification strategies in real-time PCR. *A-Z of quantitative PCR (Editor: S.A. Bustin)* Chapter 3:Quantification strategies in real-time PCR, 87 - 112

Pier, G. B. 2007. *Pseudomonas aeruginosa* lipopolysaccharide: a major virulence factor, initiator of inflammation and target for effective immunity. *Int J Med Microbiol,* 297, 277–295.
Pier, G. B., Grout, M. & Zaidi, T. S. 1997. Cystic fibrosis transmembrane conductance regulator is an epithelial cell receptor for clearance of *Pseudomonas aeruginosa* from the lung. *Proc. Natl. Acad. Sci. USA,* 94 pp. 12088–12093, .
Pier, G. B., Grout, M., Zaidi, T. S., Olsen, J. C., Johnson, L. G., Yankaskas, J. R. & Goldberg, J. B. 1996. Role of mutant CFTR in hypersusceptibility of cystic fibrosis patients to lung infections. *Science,* 271, 64–67.
Potvin, E., Sanschagrin, F. & Levesque, R. C. 2008. Sigma factors in Pseudomonas aeruginosa. *FEMS Microbiol Rev,* 32, 38-55.
Poulsen, J. H., Fischer, H., Illek, B. & Machen, T. E. 1994. Bicarbonate conductance and pH regulatory capability of cystic fibrosis transmembrane conductance regulator. *Proc. Nati. Acad. Sci. USA,* 91, 5340-5344,.
Poulsen, J. H. & Machen, T. E. 1996. HCO3-dependent pHi regulation in tracheal epithelial cells. *Eur J Physiol* 432, 546–554.
Preisig, O., Anthamatten, D. & Hennecke, H. 1993. Genes for a microaerobically induced oxidase complex in Bradyrhizobium japonicum are essential for a nitrogen-fixing endosymbiosis. *Proc. Natl. Acad. Sci. USA,* 90, 3309-3313.
Preisig, O., Zufferey, R., Ny-Meyer, L. T., Appleby, C. A. & Hennecke, H. 1996. A high-affinity cbb3-type cytochrome oxidase terminates the symbiosis-specific respiratory chain of Bradyrhizobium japonicum. *Journal of bacteriology,* 178, p. 1532–1538.
Price-Whelan, A., Dietrich, L. E. & Newman, D. K. 2007. Pyocyanin alters redox homeostasis and carbon flux through central metabolic pathways in *Pseudomonas aeruginosa* PA14. *J Bacteriol,* 189, 6372-81.
Quinn, R. A., Lim, Y. W., Maughan, H., Conrad, D., Rohwer, F. & Whiteson, K. L. 2014. Biogeochemical forces shape the composition and physiology of polymicrobial communities in the cystic fibrosis lung. *MBio,* 5, e00956-13.
Rabin, R. S. & Stewart, V. 1993. Dual response regulators (NarL and NarP) interact with dual sensors (NarX and NarQ) to control nitrate- and nitrite-regulated gene expression in *Escherichia coli* K-12. *Journal of Bacteriology,* 175, p. 3259-3268.
Rahme, L. G., Stevens, E. J., Wolfort, S. F., Shao, J., Tompkins, R. G. & Ausubelt, F. M. 1995. Common Virulence Factors for Bacterial Pathogenicity in Plants and Animals. *Science,* VOL. 268.
Ramirez-Estrada, S., Borgatta, B. & Rello, J. 2016. *Pseudomonas aeruginosa* ventilator-associated pneumonia management. *Infect Drug Resist,* 9**,** 7-18.
Ran, H., Hassett, D. J. & Lau, G. W. 2003. Human targets of *Pseudomonas aeruginosa* pyocyanin. *Proc Natl Acad Sci U S A,* 100, 14315-20.
Rappas, M., Bose, D. & Zhang, X. 2007. Bacterial enhancer-binding proteins: unlocking sigma54-dependent gene transcription. *Curr Opin Struct Biol,* 17, 110-6.
Rasamiravaka, T., Labtani, Q., Duez, P. & El Jaziri, M. 2015. The formation of biofilms by P*seudomonas aeruginosa:* a review of the natural and synthetic compounds interfering with control mechanisms. *Biomed Res Int,* 2015, 759348.
Rawlings, N. D., Barrett, A. J. & Bateman, A. 2010. MEROPS: the peptidase database. *Nucleic Acids Res,* 38, D227-233.
Ray, V. A., Morris, A. R. & Visick, K. L. 2012. A semi-quantitative approach to assess biofilm formation using wrinkled colony development. *J Vis Exp*, e4035.
Raymond, C. K., Sims, E. H., Kas, A., Spencer, D. H., Kutyavin, T. V., Ivey, R. G., Zhou, Y., Kaul, R., Clendenning, J. B. & Olson, M. V. 2002. Genetic Variation at the O-Antigen Biosynthetic Locus in *Pseudomonas aeruginosa. Journal of Bacteriology,* 184, 3614-3622.
Read, R. C., Roberts, P., Munro, N., Rutman, A., Hastie, A., Shryock, T., Hall, R., Mcdonald-Gibson, W., Lund, V. & Taylor, G. 1985. Effect of *Pseudomonas aeruginosa* rhamnolipids on mucociliary transport and ciliary beating. *Journal of applied physiology,* 72, 2271-7.
Records, A. R. 2011. The Type VI Secretion System: A Multipurpose Delivery System with a Phage-Like Machinery *MPMI* 24, pp. 751–757
Registry, C. F. F. P. 2016. Annual Data Report 2015. *Bethesda, Maryland*, 29-32.
Rella, M., Mercenier, A. & Haas, D. 1985. Transposon insertion mutagenesis of *Pseudomonas aeruginosa* with a Tn5 derivative: application to physical mapping of the arc gene cluster *Gene,* 33, 293–303.

Rinas, U. & Bailey, J. E. 1992. Protein compositional analysis of inclusion bodies produced in recombinant *Escherichia coli*. *Appl Microbiol Biotechnol* 37, 609-614

Riordan, J. R., Rommens, J. M., Kerem, B., Alon, N., Rozmahel, R., Grzelczak, Z., Zielenski, J., Lok, S., Plavsic, N. & Chou, J. L. 1989. Identification of the cystic fibrosis gene: cloning and characterization of complementary DNA. *Science,* 245, 1066-73.

Ririe, K. M., Rasmussen, R. P. & Wittwer, C. T. 1997. Product differentiation by analysis of DNA melting curves during the polymerase chain reaction. *ANALYTICAL BIOCHEMISTRY* 245, 154–160.

Robbins, R. A. & Grisham, M. B. 1997. Nitric oxide. *Int J Biochem Cell Biol,* 29, 857-860.

Roberts, A. E., Kragh, K. N., Bjarnsholt, T. & Diggle, S. P. 2015. The Limitations of *In vitro* Experimentation in Understanding Biofilms and Chronic Infection. *J Mol Biol,* 427, 3646-61.

Rocha, C. L., Coburn, J., Rucks, E. A. & Olson, J. C. 2003. Characterization of *Pseudomonas aeruginosa* Exoenzyme S as a Bifunctional Enzyme in J774A.1 Macrophages. *Infection and Immunity,* 71, 5296-5305.

Rodrigue, A., Quentin, Y., Lazdunski, A., Méjean, V. & Foglino, M. 2000. Two-component systems in Pseudomonas aeruginosa: why so many? *TRENDS IN MICROBIOLOGY,* 8, 498-504.

Rodrigues, A. I., Gudiña, E. J., Teixeira, J. A. & Rodrigues, L. R. 2017. Sodium chloride effect on the aggregation behaviour of rhamnolipids and their antifungal activity. *Scientific Reports,* 7.

Rogers, G. B., Carroll, M. P., Serisier, D. J., Hockey, P. M., Jones, G. & Bruce, K. D. 2004. characterization of bacterial community diversity in cystic fibrosis lung infections by use of 16s ribosomal DNA terminal restriction fragment length polymorphism profiling. *J Clin Microbiol,* 42, 5176-83.

Rogers, G. B., Hart, C. A., Mason, J. R., Hughes, M., Walshaw, M. J. & Bruce, K. D. 2003. Bacterial Diversity in Cases of Lung Infection in Cystic Fibrosis Patients: 16S Ribosomal DNA (rDNA) Length Heterogeneity PCR and 16S rDNA Terminal Restriction Fragment Length Polymorphism Profiling. *Journal of Clinical Microbiology,* 41, 3548-3558.

Rojo, F. 2010. Carbon catabolite repression inPseudomonas :optimizing metabolic versatilityand interactionswith the environment. *FEMS* 34, 658–684.

Romling, U., Gomelsky, M. & Galperin, M. Y. 2005. C-di-GMP: the dawning of a novel bacterial signalling system. *Mol Microbiol,* 57, 629-39.

Ronchetti, K., Tame, J.-D., Paisey, C., Thia, L. P., Doull, I., Howe, R., Mahenthiralingam, E. & Forton, J. T. 2018. The CF-Sputum Induction Trial (CF-SpIT) to assess lower airway bacterial sampling in young children with cystic fibrosis: a prospective internally controlled interventional trial. *The Lancet Respiratory Medicine,* 6, 461-471.

Rosano, G. L. & Ceccarelli, E. A. 2014. Recombinant protein expression in *Escherichia coli*: advances and challenges. *Front Microbiol,* 5, 172.

Rosenthali, R. S. & Rodwell, V. W. 1998. Purification and characterization of the heteromeric transcriptional activator MvaT of the *Pseudomonas mevalonii* mvaAB operon. *Protein Science* 7, 178-1 84.

Rovery, C., Etienne, A., Foucault, C., Berger, P. & Brouqui, P. 2005. *Veillonella montpellierensis* Endocarditis. *Emerging Infectious Diseases* 11**,** 1112-1114.

Ruiz-Perez, F. & Nataro, J. P. 2014. Bacterial serine proteases secreted by the autotransporter pathway: classification, specificity, and role in virulence. *Cell Mol Life Sci,* 71, 745-70.

Rumbaugh, K. P., Diggle, S. P., Watters, C. M., Ross-Gillespie, A., Griffin, A. S. & West, S. A. 2009. Quorum sensing and the social evolution of bacterial virulence. *Curr Biol,* 19, 341-5.

Rumbaugh, K. P., Griswold, J. A., Iglewski, B. H. & Hamood, A. N. 1999. Contribution of quorum sensing to the virulence of *Pseudomonas aeruginosa* in burn wound infections. *INFECTION AND IMMUNITY,* 67, p. 5854–5862

Rust, L., Pesci, E. C. & Iglewski, B. H. 1996. Analysis of the *Pseudomonas aeruginosa* elastase (lasB) regulatory region. *JOURNAL OF BACTERIOLOGY,,* 178, p. 1134–1140.

Ryan, R. P., Fouhy, Y., Lucey, J. F. & Dow, J. M. 2006. Cyclic di-GMP signaling in bacteria: recent advances and new puzzles. *J Bacteriol,* 188, 8327-34.

Ryder, C., Byrd, M. & Wozniak, D. J. 2007. Role of polysaccharides in *Pseudomonas aeruginosa* biofilm development. *Curr Opin Microbiol,* 10, 644–648.

Sabra, W., Kim, E.-J. & Zeng, A.-P. 2002. Physiological responses of *Pseudomonas aeruginosa* PAO1 to oxidative stress in controlled microaerobic and aerobic cultures. *Microbiology,* 148, 3195–3202.

Sadikot, R. T., Zeng, H., Azim, A. C., Joo, M., Dey, S. K., Breyer, R. M., Peebles, R. S., Blackwell, T. S. & Christman, J. W. 2007. Bacterial clearance of*Pseudomonas aeruginosa* is enhanced by the inhibition of COX-2. *European Journal of Immunology,* 37, 1001-1009.

Salacha, R., Kovacic, F., Brochier-Armanet, C., Wilhelm, S., Tommassen, J., Filloux, A., Voulhoux, R. & Bleves, S. 2010. The *Pseudomonas aeruginosa* patatin-like protein PlpD is the archetype of a novel Type V secretion system. *Environ Microbiol,* 12, 1498-512.

Salmon, K. A., Hung, S. P., Steffen, N. R., Krupp, R., Baldi, P., Hatfield, G. W. & Gunsalus, R. P. 2005. Global gene expression profiling in *Escherichia coli* K12: effects of oxygen availability and ArcA. *J Biol Chem,* 280, 15084-96.

Sana, T. G., Soscia, C., Tonglet, C. M., Garvis, S. & Bleves, S. 2013. Divergent control of two type VI secretion systems by RpoN in Pseudomonas aeruginosa. *PLoS One,* 8, e76030.

Sanger, N. A. 1961. Purification and Specificity of Pancreatic Elastase *Biochem.J.,* 78, 156-163.

Sarkisova, S., Patrauchan, M. A., Berglund, D., Nivens, D. E. & Franklin, M. J. 2005. Calcium induced virulence factors associated with the extracellular matrix of mucoid *Pseudomonas aeruginosa* biofilms. *J Bacteriol,* 187, 4327-37.

Sato, H., Frank, D. W., Hillard, C., Feix, J. B., Pankhaniya, R. R., Moriyama, K., Finck-Barbançon, V., Buchaklian, A., Lei, M., Long, R. M., Wiener-Kronish, J. & Sawa, T. 2003. The mechanism of action of the *Pseudomonas aeruginosa*-encoded type III cytotoxin, ExoU. *The EMBO Journa,* 22, 2959±2969,.

Sauri, A., Soprova, Z., Wickstrom, D., De Gier, J. W., Van Der Schors, R. C., Smit, A. B., Jong, W. S. & Luirink, J. 2009. The Bam (Omp85) complex is involved in secretion of the autotransporter haemoglobin protease. *Microbiology,* 155, 3982-91.

Sauri, A., Ten Hagen-Jongman, C. M., Van Ulsen, P. & Luirink, J. 2012. Estimating the size of the active translocation pore of an autotransporter. *J Mol Biol,* 416, 335-45.

Sawers, G. & Suppmann, B. 1992. Anaerobic induction of pyruvate formate-lyase gene expression is mediated by the ArcA and FNR proteins. *JOURNAL OF BACTERIOLOGY, ,* 174, p. 3474-3478.

Schaber, J. A., Triffo, W. J., Suh, S. J., Oliver, J. W., Hastert, M. C., Griswold, J. A., Auer, M., Hamood, A. N. & Rumbaugh, K. P. 2007. *Pseudomonas aeruginosa* forms biofilms in acute infection independent of cell-to-cell signaling. *Infect Immun,* 75, 3715-21.

Schaefer, J., Engl, C., Zhang, N., Lawton, E. & Buck, M. 2015. Genome wide interactions of wild-type and activator bypass forms of sigma54. *Nucleic Acids Res,* 43, 7280-91.

Schalk, I. J. & Guillon, L. 2013. Pyoverdine biosynthesis and secretion in *Pseudomonas aeruginosa*: implications for metal homeostasis. *Environ Microbiol,* 15, 1661-73.

Schauder, S., Shokat, K., Surette, M. G. & Bassler, B. L. 2001. The LuxS family of bacterial autoinducers- biosynthesis of a novel quorum-sensing signal molecule. *Molecular Microbiology* 41, 463–476.

Schiffer, T. & Weitzberg, E. 2008. The nitrate–nitrite–nitric oxide pathway in physiology and therapeutics. *Nature reviews,* 7, 156-167.

Schiøtz, P. O., Sørensen, H. & Høiby, M. 1979. Activated complement in the sputum from patients with cystic fibrosis. *Acta Pathol Microbiol Scand C. ,* 87C, 1-5.

Schlegel, S., Hjelm, A., Baumgarten, T., Vikstrom, D. & De Gier, J. W. 2014. Bacterial-based membrane protein production. *Biochim Biophys Acta,* 1843, 1739-49.

Schmidtchen, A., Frick, I. M., Andersson, E., Tapper, H. & Björck, L. 2002 Proteinases of common pathogenic bacteria degrade and inactivate the antibacterial peptide LL-37. *Mol Microbiol.,* 46, 157-68.

Schobert, M. & Jahn, D. 2010. Anaerobic physiology of *Pseudomonas aeruginosa* in the cystic fibrosis lung. *Int J Med Microbiol,* 300, 549-56.

Schreiber, K., Krieger, R., Benkert, B., Eschbach, M., Arai, H., Schobert, M. & Jahn, D. 2007. The Anaerobic Regulatory Network Required for *Pseudomonas aeruginosa* Nitrate Respiration. *Journal of Bacteriology,* 189, p. 4310–4314.

Schultz, D. R. & Miller, K. D. 1974, . Elastase of Pseudomonas aeruginosa: inactivation of complement components and complement-derived chemotactic and phagocytic factors. *INFECTION AND IMMUNITY,* 10, p. 128-135.

Schulz, S., Eckweiler, D., Bielecka, A., Nicolai, T., Franke, R., Dotsch, A., Hornischer, K., Bruchmann, S., Duvel, J. & Haussler, S. 2015. Elucidation of sigma factor-associated networks in *Pseudomonas aeruginosa* reveals a modular architecture with limited and function-specific crosstalk. *PLoS Pathog,* 11, e1004744.

Schurr, M. J., Martin, D. W., Mudd, M. H. & Deretic, V. 1994. Gene cluster controlling conversion to alginate-overproducing phenotype in Pseudomonas aeruginosa-functional analysis in a heterologous host and role in the instability of mucoidy. *JOURNAL OF BACTERIOLOGY,,* 176, p. 3375-3382.

Schuster, M., Hawkins, A. C., Harwood, C. S. & Greenberg, E. P. 2004a. The *Pseudomonas aeruginosa* RpoS regulon and its relationship to quorum sensing. *Mol Microbiol,* 51, 973-85.

Schuster, M., Urbanowski, M. L. & Greenberg, E. P. 2004b. Promoter specificity in *Pseudomonas aeruginosa* quorum sensing revealed by DNA binding of purified LasR. *Proc Natl Acad Sci U S A,* 101, 15833-9.

Selkrig, J., Mosbahi, K., Webb, C. T., Belousoff, M. J., Perry, A. J., Wells, T. J., Morris, F., Leyton, D. L., Totsika, M., Phan, M. D., Celik, N., Kelly, M., Oates, C., Hartland, E. L., Robins-Browne, R. M., Ramarathinam, S. H., Purcell, A. W., Schembri, M. A., Strugnell, R. A., Henderson, I. R., Walker, D. & Lithgow, T. 2012. Discovery of an archetypal protein transport system in bacterial outer membranes. *Nat Struct Mol Biol,* 19, 506-10, S1.

Serino, L., Reimmann, C., Visca, P., Beyeler, M., Della Chiesa, V. & Haas, D. 1997. Biosynthesis of pyochelin and dihydroaeruginoic acid requires the iron-regulated pchDCBA operon in Pseudomonas aeruginosa. *JOURNAL OF BACTERIOLOGY,,* 179, 248–257.

Sheppard, D. N. & Welsh, M. J. 1999. Structure and function of the CFTR chloride channel. *PHYSIOLOGICAL REVIEWS,* 79, S24-S43.

Shiau, S.-P., Chen, P. & Reitzer, L. J. 1993. Effects of Insertions and Deletions in ginG (ntrC) of e.coli on nitrogen regulator I-dependent DNA Binding and Transcriptional Activation. *JOURNAL OF BACTERIOLOGY,* 175, p. 190-199

Shigematsu, T., Fukushima, J., Oyama, M., Tsuda, M., Kawamoto, S. & Okuda, K. 2001. Iron-Mediated regulation of alkaline proteinase production in Pseudomonas aeruginosa. *Microbiol Immunol.,* 45, 579-90.

Shoesmith, J. H. & Sherris, J. C. 1960. Studies on the mechanism of arginine-activated motility in a Pseudomonas strain. *J Gen Microbiol,* 22.

Shrout, J. D., Chopp, D. L., Just, C. L., Hentzer, M., Givskov, M. & Parsek, M. R. 2006. The impact of quorum sensing and swarming motility on *Pseudomonas aeruginosa* biofilm formation is nutritionally conditional. *Mol Microbiol,* 62, 1264-77.

Sijbrandi, R., Urbanus, M. L., Ten Hagen-Jongman, C. M., Bernstein, H. D., Oudega, B., Otto, B. R. & Luirink, J. 2003. Signal recognition particle (SRP)-mediated targeting and Sec-dependent translocation of an extracellular *Escherichia coli* protein. *J Biol Chem,* 278, 4654-9.

Silvestrini, M. C., Falcinelli, S., Ciabatti, I., Cutruzzolà, F. & Brunori, M. 1994. *Pseudomonas aeruginosa* nitrite reductase (or cytochrome oxidase): an overview. *Biochimie.,* 76, 641-54.

Silvestrini, M. C., Galeotti, C. L., Gervais, M., Schininà, E., Barra, D., Bossa, F. & Brunori, M. 1989. Nitrite reductase from *Pseudomonas aeruginosa*: sequence of the gene and the protein. *FEBS Federation of European Biochemical Societies,* 254, 33-8.

Sinaasappel , M., Stern , M., Littlewood , J., Wolfe , S., Steinkamp , G., Heijerman , H. G. M., Robberecht , E. & Doring, G. 2002. Nutrition in patients with cystic fibrosis- a European Consensus. *Journal of Cystic Fibrosis* 1, 51-75.

Singh, R., Ray, P., Das, A. & Sharma, M. 2009. Role of persisters and small-colony variants in antibiotic resistance of planktonic and biofilm-associated Staphylococcus aureus: an *in vitro* study. *J Med Microbiol,* 58, 1067-73.

Singh, S., Singh, S. K., Chowdhury, I. & Singh, R. 2017. Understanding the Mechanism of Bacterial Biofilms Resistance to Antimicrobial Agents. *Open Microbiol J,* 11, 53-62.

Singh, S. M. & Panda, A. K. 2005. Solubilization and refolding of bacterial inclusion body proteins. *J Biosci Bioeng,* 99, 303-10.

Sivaneson, M., Mikkelsen, H., Ventre, I., Bordi, C. & Filloux, A. 2011. Two-component regulatory systems in Pseudomonas aeruginosa: an intricate network mediating fimbrial and efflux pump gene expression. *Mol Microbiol,* 79, 1353-66.

Sivashanmugam, A., Murray, V., Cui, C., Zhang, Y., Wang, J. & Li, Q. 2009. Practical protocols for production of very high yields of recombinant proteins using *Escherichia coli*. *Protein Sci,* 18, 936-48.

Skillman, K. M., Barnard, T. J., Peterson, J. H., Ghirlando, R. & Bernstein, H. D. 2005. Efficient secretion of a folded protein domain by a monomeric bacterial autotransporter. *Mol Microbiol,* 58, 945-58.

Skolnik, K., Kirkpatrick, G. & Quon, B. S. 2016. Nontuberculous Mycobacteria in Cystic Fibrosis. *Curr Treat Options Infect Dis,* 8**,** 259-274.

Smith, E. E., Buckley, D. G., Wu, Z., Saenphimmachak, C., Hoffman, L. R., D'argenio, D. A., Miller, S. I., Ramsey, B. W., Speert, D. P., Moskowitz, S. M., Burns, J. L., Kaul, R. & Olson, M. V. 2006. Genetic adaptation by *Pseudomonas aeruginosa* to the airways of cystic fibrosis patients. *Proc Natl Acad Sci U S A,* 103, 8487-92.

Smith, J. J., Travis, S. M., Greenberg, E. P. & Welsh, M. J. 1996. Cystic Fibrosis Airway Epithelia Fail to Kill Bacteria Because of Abnormal Airway Surface Fluid. *Cell,* 85, 229–236.

Smith, S. M. 2017. Strategies for the Purification of Membrane Proteins. *Methods Mol Biol,* 1485, 389-400.

Smith, W. D., Bardin, E., Cameron, L., Edmondson, C. L., Farrant, K. V., Martin, I., Murphy, R. A., Soren, O., Turnbull, A. R., Wierre-Gore, N., Alton, E. W., Bundy, J. G., Bush, A., Connett, G. J., Faust, S. N., Filloux, A., Freemont, P. S., Jones, A. L., Takats, Z., Webb, J. S., Williams, H. D. & Davies, J. C. 2017. Current and future therapies for *Pseudomonas aeruginosa* infection in patients with cystic fibrosis. *FEMS Microbiol Lett,* 364.

Smith, D. J., Badrick, A. C., Zakrzewski, M., Krause, L., Bell, S. C., Anderson, G. J. & Reid, D. W. 2014. Pyrosequencing reveals transient cystic fibrosis lung microbiome changes with intravenous antibiotics. *Eur Respir J,* 44**,** 922-30.

Smyth, A. R., Bell, S. C., Bojcin, S., Bryon, M., Duff, A., Flume, P., Kashirskaya, N., Munck, A., Ratjen, F., Schwarzenberg, S. J., Sermet-Gaudelus, I., Southern, K. W., Taccetti, G., Ullrich, G., Wolfe, S. & European Cystic Fibrosis, S. 2014. European Cystic Fibrosis Society Standards of Care: Best Practice guidelines. *J Cyst Fibros,* 13 Suppl 1, S23-42.

Smyth, R. L. 2005. Diagnosis and management of cystic fibrosis. *Archives of Disease in Childhood - Education and Practice,* 90, ep1-ep6.

Solano, C., García, B., Valle, J., Berasain, C., Ghigo, J.-M., Gamazo, C. & Lasa, I. 2002. Genetic analysis of Salmonella enteritidis biofilm formation- critical role of cellulose. *Molecular Microbiology,* 43, 793–808.

Son, M. S., Matthews, W. J., Jr., Kang, Y., Nguyen, D. T. & Hoang, T. T. 2007. *In vivo* evidence of *Pseudomonas aeruginosa* nutrient acquisition and pathogenesis in the lungs of cystic fibrosis patients. *Infect Immun,* 75, 5313-24.

Sonderholm, M., Bjarnsholt, T., Alhede, M., Kolpen, M., Jensen, P. O., Kuhl, M. & Kragh, K. N. 2017. The Consequences of Being in an Infectious Biofilm: Microenvironmental Conditions Governing Antibiotic Tolerance. *Int J Mol Sci,* 18.

Sorensen, H. P. & Mortensen, K. K. 2005. Soluble expression of recombinant proteins in the cytoplasm of *Escherichia coli*. *Microb Cell Fact,* 4, 1.

Sorensen, H. P., Sperling-Petersen, H. U. & Mortensen, K. K. 2003. A favorable solubility partner for the recombinant expression of streptavidin. *Protein Expr Purif,* 32, 252-9.

Sorensen, R. U. & Klinger, J. D. 1987. Biological effects of *Pseudomonas aeruginosa* phenazine pigments. *Antibiot Chemother* 39, 113-24.

Sousa, A. M. & Pereira, M. O. 2014. *Pseudomonas aeruginosa* Diversification during Infection Development in Cystic Fibrosis Lungs-A Review. *Pathogens,* 3, 680-703.

Soutourina, O. A., Semenova, E. A., Parfenova, V. V., Danchin, A. & Bertin, P. 2001. Control of Bacterial Motility by Environmental Factors in Polarly Flagellated and Peritrichous Bacteria Isolated from Lake Baikal. *Applied and Environmental Microbiology,* 67, 3852-3859.

Speert, D. P., Farmer, S. W., Campbell, M. E., Musser, J. M., Selander, R. K. & Kuo, S. 1990. Conversion of *Pseudomonas aeruginosa* to the Phenotype characteristic of strains from patients with Cystic Fibrosis. *JOURNAL OF CLINICAL MICROBIOLOGY,* 28, p. 188-194.

Spoering, A. L. & Lewis, K. 2001. Biofilms and planktonic cells of *Pseudomonas aeruginosa* have similar resistance to killing by antimicrobials. *J Bacteriol,* 183, 6746-51.

Sriramulu, D. D., Lunsdorf, H., Lam, J. S. & Romling, U. 2005. Microcolony formation: a novel biofilm model of *Pseudomonas aeruginosa* for the cystic fibrosis lung. *J Med Microbiol,* 54, 667-76.

Stalon, V., Ramos, F., Piérard, A. & Wiame, J. M. 1967. The occurrence of a catabolic and an anabolic ornithine carbamoyltransferase in Pseudomonas. *Biochim Biophys Acta.,* 139, 91-7.

Stamper , C. C., Bienvenue , D. L., Bennett , B., Ringe , D., Petsko , G. A. & Holz, R. C. 2004. Spectroscopic and X-ray crystallographic characterization of bestatin bound to the aminopeptidase from Aeromonas (Vibrio) proteolytica. *Biochemistry,* 43.

Stebbins, C.E. & Galán, J. E. 2003. Priming virulence factors for delivery into the host. *Nature Reviews Molecular Cell Biology* 4, 738-744.

Sternberg, C., Christensen, B. B., Johansen, T., Nielsen, A. T., Andersen, J. B., Givskov, M. & Molin, S. 1999. Distribution of Bacterial Growth Activity in Flow-Chamber Biofilms. *APPLIED AND ENVIRONMENTAL MICROBIOLOGY,* 65, p. 4108–4117.

Stewart, L., Ford, A., Sangal, V., Jeukens, J., Boyle, B., Kukavica-Ibrulj, I., Caim, S., Crossman, L., Hoskisson, P. A., Levesque, R. & Tucker, N. P. 2014. Draft genomes of 12 host-adapted and environmental isolates of *Pseudomonas aeruginosa* and their positions in the core genome phylogeny. *Pathogens and Disease,* 71, 20-25.

Stewart, P. S. 2003. Diffusion in Biofilms. *Journal of Bacteriology,* 185, 1485-1491.

Stewart, P. S. & Franklin, M. J. 2008. Physiological heterogeneity in biofilms. *Nat Rev Microbiol,* 6, 199-210.

Stewart, P. S., Grab, L. & Diemer, J. A. 1998. Analysis of biocide transport limitation in an artificial biofilm system. *Applied microbiology,* 85, 495–500.

Stewart, V. & Bledsoe, P. J. 2003. Synthetic lac Operator Substitutions for Studying the Nitrate- and Nitrite-Responsive NarX-NarL and NarQ-NarP Two-Component Regulatory Systems of *Escherichia coli* K-12. *Journal of bacteriology,* 185, p. 2104–2111.

Stewart, V. & Bledsoe, P. J. 2005. Fnr-, NarP- and NarL-dependent regulation of transcription initiation from the Haemophilus influenzae Rd napF (periplasmic nitrate reductase) promoter in *Escherichia coli* K-12. *J Bacteriol,* 187, 6928-35.

Stoodley, P., Sauer, K., Davies, D. G. & Costerton, J. W. 2002. Biofilms as complex differentiated communities. *Annu Rev Microbiol. ,* 56, 187-209.

Stover, C. K., Pham, X. Q., Erwin, A. L., Mizoguchi, S. D., Warrener, P., Hickey, M. J., Brinkman, F. S. L., Hufnagle, W. O., Kowalik, D. J., Lagrou, M., Garber, R. L., Goltry, L., Tolentino, E., Westbrock-Wadman, S., Yuan, Y., Brody, L. L., Coulter, S. N., Folger, K. R., Kas, A., Larbig, K., Lim, R., Smith, K., Spencer, D., Wong, G. K.-S., Wu, Z., Paulsenk, I. T., Reizer, J., Saier, M. H., Hancock, R. E. W., Lory, S. & Olson, M. V. 2000. Complete genome sequence of *Pseudomonas aeruginosa* PA01, an opportunistic pathogen. *nature,* 406, 959-962.

Strom, M. S. & Lory, S. 1986. Cloning and expression of the pilin gene of *Pseudomonas aeruginosa* PAK in *Escherichia coli*. *JOURNAL OF BACTERIOLOGY,,* 165, p. 367-372.

Sun, F., Qu, F., Ling, Y., Mao, P., Xia, P., Chen, H. & Zhou, D. 2013. Biofilm-associated infections: antibiotic resistance and novel therapeutic strategies. *Future Microbiol.,* 8, 877-86.

Swanson, B. L., Colmer, J. A. & Hamood, A. N. 1999. The *Pseudomonas aeruginosa* Exotoxin A Regulatory Gene, ptxS- Evidence for Negative Autoregulation. *JOURNAL OF BACTERIOLOGY,,* 181, 4890–4895.

Swenson, C. E. & Sadikot, R. T. 2015. Achromobacter respiratory infections. *Ann Am Thorac Soc,* 12**,** 252-8.

Szabady, R. L., Peterson, J. H., Skillman, K. M. & Bernstein, H. D. 2005. An unusual signal peptide facilitates late steps in the biogenesis of a bacterial autotransporter. *Proc Natl Acad Sci U S A,* 102, 221-6.

Szczesny, P. & Lupas, A. 2008. Domain annotation of trimeric autotransporter adhesins--daTAA. *Bioinformatics,* 24, 1251-6.

Szklarczyk, D., Morris, J. H., Cook, H., Kuhn, M., Wyder, S., Simonovic, M., Santos, A., Doncheva, N. T., Roth, A., Bork, P., Jensen, L. J. & Von Mering, C. 2017. The STRING database in 2017: quality-controlled protein-protein association networks, made broadly accessible. *Nucleic Acids Res,* 45**,** D362-D368.

Tajima, N., Kawai, F., Park, S. Y. & Tame, J. R. 2010. A novel intein-like autoproteolytic mechanism in autotransporter proteins. *J Mol Biol,* 402, 645-56.

Tang, A., Caballero, A. R., Marquart, M. E. & O'callaghan, R. J. 2013. *Pseudomonas aeruginosa* small protease (PASP), a keratitis virulence factor. *Invest Ophthalmol Vis Sci.,* 54, 2821-8.

Tarran, R., Grubb, B. R., Parsons, D., Picher, M., Hirsh, A. J., Davis, C. W. & Boucher, R. C. 2001. The CF salt controversy- *in vivo* observations and therapeutic approaches. *Molecular Cell,* 8, 149–158.

Tart, A. H., Blanks, M. J. & Wozniak, D. J. 2006. The AlgT-dependent transcriptional regulator AmrZ (AlgZ) inhibits flagellum biosynthesis in mucoid, nonmotile *Pseudomonas aeruginosa* cystic fibrosis isolates. *J Bacteriol,* 188, 6483-9.

Tate, S., Macgregor, G., Davis, M., Innes, J. A. & Greening, A. P. 2002. Airways in cystic fibrosis are acidified- detection by exhaled breath condensate. *Thorax,* 57, 926–929.

Taylor, G., Hoare, M., Gray, D. R. & Marston, F. a. O. 1986. Size and Density of Protein Inclusion Bodies. *Nature biotechnology,* 4, , pages 553–557.

Taubenberger, J. K. & Morens, D. M. 2008. The Pathology of Influenza Virus Infections *Annu Rev Pathol. ,* 3**,** 499–522.

Terada, L. S., Johansen, K. A., Nowbar, S., Vasil, A. I. & Vasil, M. L. 1999. *Pseudomonas aeruginosa* Hemolytic Phospholipase C Suppresses Neutrophil Respiratory Burst Activity. *INFECTION AND IMMUNITY,* 67, p. 2371–2376.

Terry, J. M., Pina, S. E. & Mattingly, S. J. 1991. Environmental conditions which influence mucoid conversion *Pseudomonas aeruginosa* PAO1. *INFECTION AND IMMUNITY,,* 59, p. 471-477.

Thanassi, D. G., Stathopoulos, C., Karkal, A. & Li, H. 2005. Protein secretion in the absence of ATP: the autotransporter, two-partner secretion and chaperone/usher pathways of gram-negative bacteria (review). *Mol Membr Biol. ,* 22, 63-72.

Thauer, R. K., Jungermann, K. & Decker, K. 1977. Energy conservation in chemotrophic anaerobic bacteria. *BACTERIOLOGICAL REVIzWs,* 41, p. 100-180.

Thayikkannu, A. B., Kindo, A. J. & Veeraraghavan, M. 2015. Malassezia—Can it be Ignored? *Indian J Dermatol. ,* 60**,** 332-339.

Thi Dao, K.-H., Hamer, K. E., Clark, C. L. & Harshman, L. G. 1999, . PYOVERDINE PRODUCTION BY PSUEDOMONAS AERUGINOSA EXPOSED TO METALS OR AN OXIDATIVE STRESS AGENT. *Ecological Applications,,* 9, pp. 441-448.

Thomas, S. R., Ray, A., Hodson, M. E. & Pitt, T. L. 2000. Increased sputum amino acid concentrations and auxotrophy of *Pseudomonas aeruginosa* in severe cystic fibrosis lung disease. *Thorax,* 55, 795–797.

Tian, P. & Bernstein, H. D. 2010. Molecular basis for the structural stability of an enclosed beta-barrel loop. *J Mol Biol,* 402, 475-89.

Toder, D. S., Qambelto, M. J. & Iglewski, B. H. 1991. *Pseudomonas aeruginosa* LasA- a second elastase under the transcriptional control of lasR. *Moiecuiar Microbiology* 5, 2003-2010.

Tokuda, H. 2009. Biogenesis of outer membranes in Gram-negative bacteria. *Biosci Biotechnol Biochem,* 73, 465-73.

Totten, P. A., Lara, J. C. & Lory, S. 1990. The rpoN Gene Product of *Pseudomonas aeruginosa* Is Required for expression of diverse genes, including the flagellin gene. *JOURNAL OF BACTERIOLOGY, ,* 172, p. 389-396

Totten, P. A. & Lory, S. 1990. Characterization of the type a flagellin gene from *Pseudomonas aeruginosa* PAK. *JOURNAL OF BACTERIOLOGY,,* 172, p. 7188-7199

Toyofuku, M., Roschitzki, B., Riedel, K. & Eberl, L. 2012. Identification of proteins associated with the *Pseudomonas aeruginosa* biofilm extracellular matrix. *J Proteome Res,* 11, 4906-15.

Travis, S. M., Conway, B.-a. D., Zabner, J., Smith, J. J., Anderson, N. N., Singh, P. K., Greenberg, E. P. & Welsh, M. J. 1999. Activity of abundant antimicrobials of the human airway. *Am J Respir Cell Mol Biol. ,* 20, 872-9.

Travis, S. M., Singh, P. K. & Welsh, M. J. 2001. Antimicrobial peptides and proteins in the innate defense of the airway surface. *Curr Opin Immunol.,* 13, 89–95.

Tremblay, J., Richardson, A. P., Lépine, F. & Déziel, E. 2007. Self-produced extracellular stimuli modulate the *Pseudomonas aeruginosa* swarming motility behaviour. *Environ Microbiol,* 9, 2622-30.

Trias, J. & Nikaidog, H. 1990. Protein D2 Channel of the *Pseudomonas aeruginosa* Outer Membrane. *THE JOURNAL OF BIOLOGICAL CHEMI~TAY,* 265, , pp. 15680-15684, .

Trunk, K., Benkert, B., Quäck, N., Münch, R., Scheer, M., Garbe, J., Jänsch, L., Trost, M., Wehland, J., Buer, J., Jahn, M., Schobert, M. & Jahn, D. 201. Anaerobic adaptation in Pseudomonas aeruginosa: definition of the Anr and Dnr regulons. *Environ Microbiol,* 12, 1719-33.

Tsai, J. C., Yen, M. R., Castillo, R., Leyton, D. L., Henderson, I. R. & Saier, M. H., Jr. 2010. The bacterial intimins and invasins: a large and novel family of secreted proteins. *PLoS One,* 5, e14403.

Tsuji, A., Kaneko, Y., Takahashi, K., Ogawa, M. & Goto, S. 1982. The Effects of Temperature and pH on the growth of eight enteric and nine glucose non-fermenting species of the gram-ve rods. *microbiol Immunol,* 26, 15-24.

Tunney, M. M., Field, T. R., Moriarty, T. F., Patrick, S., Doering, G., Muhlebach, M. S., Wolfgang, M. C., Boucher, R., Gilpin, D. F., Mcdowell, A. & Elborn, J. S. 2008. Detection of anaerobic bacteria in high numbers in sputum from patients with cystic fibrosis. *Am J Respir Crit Care Med,* 177, 995-1001.

Turner, K. H., Everett, J., Trivedi, U., Rumbaugh, K. P. & Whiteley, M. 2014. Requirements for *Pseudomonas aeruginosa* acute burn and chronic surgical wound infection. *PLoS Genet,* 10**,** e1004518.

Twining, S. S., Kirschner, S. E., Mahnke, L. A. & Frank, D. W. 1993 Effect of *Pseudomonas aeruginosa* elastase, alkaline protease, and exotoxin A on corneal proteinases and proteins. *Invest Ophthalmol Vis Sci.,* 34, 2699-712.

Upadhyay, A. K., Murmu, A., Singh, A. & Panda, A. K. 2012. Kinetics of inclusion body formation and its correlation with the characteristics of protein aggregates in *Escherichia coli*. *PLoS One,* 7, e33951.

Urh, M., Simpson, D. & Zhao, K. 2009. Chapter 26 Affinity Chromatography. *Methods in Enzymology,,* 463, 417-438.

Usher, L. R., Lawson, R. A., Geary, I., Taylor, C. J., Bingle, C. D., Taylor, G. W. & Whyte, M. K. B. 2002. Induction of Neutrophil Apoptosis by the *Pseudomonas aeruginosa* Exotoxin Pyocyanin: A Potential Mechanism of Persistent Infection. *The Journal of Immunology,* 168, 1861-1868.

Valentini, M., Garcı´a-Maurin˜O, S. M., Pe´Rez-Martı´Nez, I., Santero, E., Canosa, I. & Lapouge, K. 2014, . Hierarchical management of carbon sources isregulated similarly by the CbrA/B systems in *Pseudomonas aeruginosa* and Pseudomonas putida. *Microbiology,* 160, , 2243–2252.

Vallejo, L. F. & Rinas, U. 2004. Strategies for the recovery of active proteins through refolding of bacterial inclusion body proteins. *Microb Cell Fact,* 3, 11.

Van Alst, N. E., Picardo, K. F., Iglewski, B. H. & Haidaris, C. G. 2007. Nitrate Sensing and Metabolism Modulate Motility, Biofilm Formation, and Virulence in Pseudomonas aeruginosa▽. *Infection and Immunity,* 75, p. 3780–3790.

Van Alst, N. E., Sherrill, L. A., Iglewski, B. H. & Haidaris, C. G. 2009. Compensatory periplasmic nitrate reductase activity supports anaerobic growth of *Pseudomonas aeruginosa* PAO1 in the absence of membrane nitrate reductase. *Can J Microbiol,* 55, 1133–1144.

Van Den Berg, B. 2010. Crystal Structure of a Full-Length Autotransporter. *Journal of Molecular Biology,* 396, 627-633.

Van Der Gast, C. J., Walker, A. W., Stressmann, F. A., Rogers, G. B., Scott, P., Daniels, T. W., Carroll, M. P., Parkhill, J. & Bruce, K. D. 2011. Partitioning core and satellite taxa from within cystic fibrosis lung bacterial communities. *ISME J,* 5, 780-91.

Van Der Plas, M. J. A., Bhongir, R. K. V., Kjellstro¨, S., Siller, H., Kasetty, G., Mo¨Rgelin, M. & Schmidtchen, A. 2016. *Pseudomonas aeruginosa* elastase cleaves a C-terminal peptide from human thrombin that inhibits host inflammatory responses. *nature communications*, 1-13.

Van Ulsen, P., Rahman, S., Jong, W. S., Daleke-Schermerhorn, M. H. & Luirink, J. 2014. Type V secretion: from biogenesis to biotechnology. *Biochim Biophys Acta,* 1843, 1592-611.

Vance, R. E., Rietsch, A. & Mekalanos, J. J. 2005. Role of the type III secreted exoenzymes S, T, and Y in systemic spread of *Pseudomonas aeruginosa* PAO1 *in vivo*. *Infect Immun,* 73, 1706-13.

Vander Wauven, C., Pijrard, A., Kley-Raymann, M. & Haas, D. 1984. *Pseudomonas aeruginosa* mutants affected in anaerobic growth on arginine- evidence for a four-gene cluster encoding the arginine deiminase pathway. *JOURNAL OF BACTERIOLOGY,,* 160, p. 928-934.

Vasina, J. A. & Baneyx, F. 1996. Recombinant protein expression at low temperatures under the transcriptional control of the major *Escherichia coli* cold shock promoter cspA. *APPLIED AND ENVIRONMENTAL MICROBIOLOGY, ,* 62, p. 1444–1447.

Veiga, E., De Lorenzo, V. & Fernandez, L. A. 2004. Structural tolerance of bacterial autotransporters for folded passenger protein domains. *Mol Microbiol,* 52, 1069-80.

Ventre, I., Goodman, A. L., Vallet-Gely, I., Vasseur, P., Soscia, C., Molin, S., Bleves, S., Lazdunski, A., Lory, S. & Filloux, A. 2006. Multiple sensors control reciprocal expression of *Pseudomonas aeruginosa* regulatory RNA and virulence genes. *Proc Natl Acad Sci U S A,* 103, 171-6.

Verhoogt, H. J. C., Smit, H., Abee, T., Gamper, M., Driessen, A. J. M., Haas, D. & Konings, W. N. 1992. arcD, the first gene of the arc operon for anaerobic arginine catabolism in Pseudomonas aeruginosa, encodes an arginine-ornithine exchanger. *JOURNAL OF BACTERIOLOGY,* 174, p. 1568-1573.

Vincent, M. S., Canestrari, M. J., Leone, P., Stathopulos, J., Ize, B., Zoued, A., Cambillau, C., Kellenberger, C., Roussel, A. & Cascales, E. 2017. Characterization of the Porphyromonas gingivalis Type IX Secretion Trans-envelope PorKLMNP Core Complex. *J Biol Chem,* 292, 3252-3261.

Vital-Lopez, F. G., Reifman, J. & Wallqvist, A. 2015. Biofilm Formation Mechanisms of *Pseudomonas aeruginosa* Predicted via Genome-Scale Kinetic Models of Bacterial Metabolism. *PLoS Comput Biol,* 11, e1004452.

Vlahovicek, K. & Pongor, S. K. 2003. DNA analysis servers: plot.it., bend.it, model.it and IS. *Nucleic Acids Res.,* 31, 3686-7.

Voulhoux, R., Filloux, A. & Schalk, I. J. 2006. Pyoverdine-mediated iron uptake in Pseudomonas aeruginosa: the Tat system is required for PvdN but not for FpvA transport. *J Bacteriol,* 188, 3317-23.

Wang, J., Lory, S., Ramphal, R. & Jin, S. 1996. Isolation and characterization of *Pseudomonas aeruginosa* genes inducible by respiratory mucus derived from cystic fibrosis patients. *Mol Microbiol* 22, 1005–1012.

Wang, Y. & Rodwell, V. W. 1991. The cis-acting regulatory element of the mvaAB operon of Pseudomonas mevalonii. *JOURNAL OF BACTERIOLOGY, ,* Vol. 173, , p. 3803-3806.

Waters, C. M. & Bassler, B. L. 2005. Quorum sensing- cell-to-cell communication in bacteria. *Annu Rev Cell Dev Biol. ,* 21, 319-46.

Waters, V., Yau, Y., Prasad, S., Lu, A., Atenafu, E., Crandall, I., Tom, S., Tullis, E. & Ratjen, F. 2011. *Stenotrophomonas maltophilia* in cystic fibrosis: serologic response and effect on lung disease. *Am J Respir Crit Care Med,* 183**,** 635-40.

Waters, E. M., Neill, D. R., Kaman, B., Sahota, J. S., Clokie, M. R. J., Winstanley, C. & Kadioglu, A. 2017. Phage therapy is highly effective against chronic lung infections with *Pseudomonas aeruginosa*. *Thorax,* 72**,** 666-667.

Watnick, P. & Kolter, R. 2000. Biofilm, City of Microbes. *JOURNAL OF BACTERIOLOGY,* 182, p. 2675–2679.

Watters, C., Deleon, K., Trivedi, U., Griswold, J. A., Lyte, M., Hampel, K. J., Wargo, M. J. & Rumbaugh, K. P. 2013. *Pseudomonas aeruginosa* biofilms perturb wound resolution and antibiotic tolerance in diabetic mice. *Med Microbiol Immunol,* 202, 131-41.

Webb, J. S., Lau, M. & Kjelleberg, S. 2004. Bacteriophage and phenotypic variation in *Pseudomonas aeruginosa* biofilm development. *J Bacteriol,* 186, 8066-73.

Webb, J. S., Thompson, L. S., James, S., Charlton, T., Tolker-Nielsen, T., Koch, B., Givskov, M. & Kjelleberg, S. 2003. Cell Death in *Pseudomonas aeruginosa* Biofilm Development. *Journal of Bacteriology,* 185, 4585-4592.

Wei, Q. & Ma, L. Z. 2013. Biofilm matrix and its regulation in Pseudomonas aeruginosa. *Int J Mol Sci,* 14, 20983-1005.

Welsh, M. J. & Smith, A. E. 1993. Molecular mechanisms of CFTR chloride channel dysfunction in cystic fibrosis. *Cell,* 73, 1251-1254, .

Werner, E., Roe, F., Bugnicourt, A., Franklin, M. J., Heydorn, A., Molin, S., Pitts, B. & Stewart, P. S. 2004. Stratified growth in *Pseudomonas aeruginosa* biofilms. *Appl Environ Microbiol,* 70, 6188-96.

Whitchurch, C. B., Hobbs, M., Livingstona, S. P., Krishnapillaib, V. & Mattick, J. S. 1991. Characterisation of a *Pseudomonas aeruginosa* twitching motility gene and evidence for a specialised protein export system widespread in eubacteria. *Gene,* 101, 33-44.

Whitchurch, C. B., Tolker-Nielsen, T., Ragas, P. C. & Mattick, J. S. 2002. Extracellular DNA Required for Bacterial Biofilm Formation. *Science,* 295, 1487.

Whiteley, M., Bangera, M. G., Bumgarner, R. E., Parsek, M. R., Teitzel, G. M., Lory, S. & Greenberg, E. P. 2001. Gene expression in *Pseudomonas aeruginosa* biofilms. *Nature,* 413, 860-4.

Whiteley, M. & Greenberg, E. P. 2001. Promoter specificity elements in *Pseudomonas aeruginosa* quorum-sensing-controlled genes. *J Bacteriol,* 183, 5529-34.

Whiteley, M., Lee, K. M. & Greenberg, E. P. 1999. Identification of genes controlled by quorum sensing in *Pseudomonas aeruginosa*. *PNAS* 96, 13904–13909

Wilderman, P. J., Vasil, A. I., Johnson, Z., Wilson, M. J., Cunliffe, H. E., Lamont, I. L. & Vasil, M. L. 2001. Characterization of an endoprotease (PrpL) encoded by a PvdS-regulated gene in Pseudomonas aeruginosa. *Infect Immun,* 69, p. 5385–5394.

Wilhelm, S., Rosenau, F., Kolmar, H. & Jaeger, K. E. 2011. Autotransporters with GDSL passenger domains: molecular physiology and biotechnological applications. *Chembiochem,* 12, 1476-85.

Wilhelm, S., Tommassen, J.,& Jaeger, K.-E. 1999. A Novel Lipolytic Enzyme Located in the Outer Membrane of *Pseudomonas aeruginosa*. *JOURNAL OF BACTERIOLOGY,,* 181, p. 6977–6986.

Willger, S. D., Grim, S. L., Dolben, E. L., Shipunova, A., Hampton, T. H., Morrison, H. G., Filkins, L. M., O'Toole, G. A., Moulton, L. A., Ashare, A., Sogin, M. L. & Hogan, D. A. 2014. Characterization and quantification of the fungal microbiome in serial samples from individuals with cystic fibrosis. *Microbiome,* 2, 1-15.

Williams, D., Paterson, S., Brockhurst, M. A. & Winstanley, C. 2016. Refined analyses suggest that recombination is a minor source of genomic diversity in *Pseudomonas aeruginosa* chronic cystic fibrosis infections. *Microbial Genomics,* 2, 1-8.

Wills, P. J., Hall, R. L., Chan, W.-M. & Cole, P. J. 1997. Sodium chloride increases the ciliary transportability of cystic fibrosis and bronchiectasis sputum on the mucus-depleted bovine trachea. *J Clin Invest. ,* 99, 9-13.

Wilson, R., Pitt, T., Taylor, G., Watson, D., Macdermot, J., Sykes, D., Roberts, D. & Cole, P. 1987. Pyocyanin and 1-hydroxyphenazine produced by *Pseudomonas aeruginosa* inhibit the beating of human respiratory cilia *in vitro*. *J Clin Invest.,* 79, 221-9.

Wilson, R., Sykes, D. A., Watson, D., Rutman, A., Taylor, L. G. W. & Cole, P. J. 1988,. Measurement of *Pseudomonas aeruginosa* phenazine pigments in sputum and assessment of their contribution to sputum sol toxicity for respiratory epithelium. *INFECTION AND IMMUNITY,,* 56, 2515-2517

Winardhi, R. S., Castang, S., Dove, S. L. & Yan, J. 2014. Single-Molecule Study on Histone-Like Nucleoid Structuring Protein (H-NS) Paralogue in Pseudomonas aeruginosa: MvaU Bears DNA Organization Mode Similarities to MvaT. *Plos one,* Volume 9 e112246.

Wingfield, P. 2001. Protein precipitation using ammonium sulfate. *Curr Protoc Protein Sci,* Appendix 3, Appendix 3F.

Winson, M. K., Swift, S., Fish, L., Throup, J. P., Jörgensen , F., Chhabra , S. R., Bycroft , B. W., Williams , P. & Stewart, G. S. a. B. 1998. Construction and analysis of luxCDABE-based plasmid sensors for investigating N-acyl homoserine lactone-mediated quorum sensing. *FEMS Microbiology Letters* 163, 185-192

Winsor, G. L., Griffiths, E. J., Lo, R., Dhillon, B. K., Shay, J. A. & Brinkman, F. S. 2016. Enhanced annotations and features for comparing thousands of Pseudomonas genomes in the Pseudomonas genome database. *Nucleic Acids Res,* 44, D646-53.

Winstanley, C., O'brien, S. & Brockhurst, M. A. 2016. *Pseudomonas aeruginosa* Evolutionary Adaptation and Diversification in Cystic Fibrosis Chronic Lung Infections. *Trends Microbiol,* 24, 327-37.

Wong, D., Nielsen, T. B., Bonomo, R. A., Pantapalangkoor, P., Luna, B. & Spellberg, B. 2017. Clinical and Pathophysiological Overview of Acinetobacter Infections: a Century of Challenges. *Clin Microbiol Rev,* 30**,** 409-447.

Workentine, M. L., Sibley, C. D., Glezerson, B., Purighalla, S., Norgaard-Gron, J. C., Parkins, M. D., Rabin, H. R. & Surette, M. G. 2013. Phenotypic heterogeneity of *Pseudomonas aeruginosa* populations in a cystic fibrosis patient. *PLoS One,* 8, e60225.

Worlitzsch, D., Rintelen, C., Bohm, K., Wollschlager, B., Merkel, N., Borneff-Lipp, M. & Doring, G. 2009. Antibiotic-resistant obligate anaerobes during exacerbations of cystic fibrosis patients. *Clin Microbiol Infect,* 15, 454-60.

Worlitzsch, D., Tarran, R., Ulrich, M., Schwab, U., Cekici, A., Meyer, K. C., Birrer, P., Bellon, G., Berger, J., Weiss, T., Botzenhart, K., Yankaskas, J. R., Randell, S., Boucher, R. C. & Döring, G. 2002. Effects of reduced mucus oxygen concentration in airway Pseudomonas infections of cystic fibrosis patients. *The Journal of Clinical Investigation,* 109, 317-325.

Wretlind, B. & Pavlovskis, O. R. 1983. *Pseudomonas aeruginosa* elastase and its role in pseudomonas infections. *Rev Infect Dis.,* 5, 998-1004.

Wright, E. A., Fothergill, J. L., Paterson, S., Brockhurst, M. A. & Winstanley, C. 2013. sub-inhibitory concentrations of some antibiotics can drive diversification of *P. aeruginosa* populations in asm. *BMC Microbiology,* 13, 1-12.

Xie, F., Xiao, P., Chen, D., Xu, L. & Zhang, B. 2012. miRDeepFinder: a miRNA analysis tool for deep sequencing of plant small RNAs. *Plant molecular biology,* 80, 75-84.

Xu, B., Soukup, R. J., Jones, C. J., Fishel, R. & Wozniak, D. J. 2016. *Pseudomonas aeruginosa* AmrZ Binds to Four Sites in the algD Promoter, Inducing DNA-AmrZ Complex Formation and Transcriptional Activation. *J Bacteriol,* 198, 2673-81.

Xu, K. D., Stewart, P. S., Xia, F., Huang, C.-T. & Mcfeters1, G. A. 1998. Spatial physiological heterogeneity in *Pseudomonas aeruginosa* biofilm is determined by oxygen availability. *APPLIED AND ENVIRONMENTAL MICROBIOLOGY,* 64, p. 4035–4039

Yahr, T. L., Hovey, A. K., Kulich, S. M. & Frank, D. W. 1995. Transcriptional analysis of the *Pseudomonas aeruginosa* exoenzyme S structural gene. *JOURNAL OF BACTERIOLOGY,,* 177, 1169–1178.

Yahr, T. L., Vallis, A. J., Hancock, M. K., Barbieri, J. T. & Frank, D. W. 1998. ExoY, an adenylate cyclase secreted by the *Pseudomonas aeruginosa* type III system. *Proc. Natl. Acad. Sci. USA,* 95, 13899–13904,.

Yanagihara, K., Tomono, K., Kuroki, M., Kaneko, Y., Sawai, T., Ohno, H., Miyazaki, Y., Higashiyama, Y., Maesaki, S., Kadota, J.-I. & Kohno, S. 2000. Intrapulmonary concentrations of inflammatory cytokines in a mouse model of chronic respiratory infection caused by *Pseudomonas aeruginosa. Clin Exp Immunol* 122, 67-71.

Yang, L., Haagensen, J. A., Jelsbak, L., Johansen, H. K., Sternberg, C., Hoiby, N. & Molin, S. 2008. In situ growth rates and biofilm development of *Pseudomonas aeruginosa* populations in chronic lung infections. *J Bacteriol,* 190, 2767-76.

Yang, L., Hu, Y., Liu, Y., Zhang, J., Ulstrup, J. & Molin, S. 2011a. Distinct roles of extracellular polymeric substances in *Pseudomonas aeruginosa* biofilm development. *Environ Microbiol,* 13, 1705-17.

Yang, L., Jelsbak, L., Marvig, R. L., Damkiaer, S., Workman, C. T., Rau, M. H., Hansen, S. K., Folkesson, A., Johansen, H. K., Ciofu, O., Hoiby, N., Sommer, M. O. & Molin, S. 2011b. Evolutionary dynamics of bacteria in a human host environment. *Proc Natl Acad Sci U S A,* 108, 7481-6.

Yang, Q., Xu, J., Li, M., Lei, X. & An, L. 2003. High-level expression of a soluble snake venom enzyme, gloshedobin, in *E. coli* in the presence of metal ions. *Biotechnology Letters* 25, 607–610,.

Yang, Z. & Lu, C. D. 2007. Functional Genomics Enables Identification of Genes of the Arginine Transaminase Pathway in *Pseudomonas aeruginosa*. *JOURNAL OF BACTERIOLOGY,* 189, p. 3945–3953.

Yap, M.-N. F. & Bernstein, H. D. 2013. Mutations in the *Escherichia coli* Ribosomal Protein L22 Selectively Suppress the Expression of a Secreted Bacterial Virulence Factor. *Journal of Bacteriology* 195, p. 2991–2999.

Ye, R. W., Haas, D., Ka, J. O., Krishnapillai, V., Zimmermann, A., Baird, C. & Tiedje, J. M. 1995. Anaerobic activation of the entire denitrification pathway in *Pseudomonas aeruginosa* requires Anr, an analog of Fnr. *J Bacteriol,* 177, 3606-9.

Yoon, S. S., Hilliard, G. M., Parvatiyar, K., Allen, H. L., Gardner, P. R., Hennigan, R. F., Ochsner, U. A., Kamani, M. C., Dekievit, T. R., Schwab, U., Iglewski, B. H., Mason, R. P., Hancock, R. E. W., Noah, T. L., Rowe, J. J., Mcdermott, T. R., Wozniak, D. J., Parsek, M. R., Boucher, R. C., Departments of Molecular Genetics, Biochemistry and Microbiology, 2cell Biology & Hassett, D. J. 2002. *Pseudomonas aeruginosa* anaerobic respiration in biofilms- relationships to cystic fibrosis pathogenesis. *Developmental Cell,* 3, 593–603.

Yu, H., Schurr, M. J. & Deretic, V. 1995. Microbial pathogenesis in cystic fibrosis- mucoid *Pseudomonas aeruginosa* and Burkholderia cepacia. *JOURNAL OF BACTERIOLOGY,,* 177, , p. 3259–3268.

Yuan, X., Johnson, M. D., Zhang, J., Lo, A. W., Schembri, M. A., Wijeyewickrema, L. C., Pike, R. N., Huysmans, G. H. M., Henderson, I. R. & Leyton, D. L. 2018. Molecular basis for the folding of beta-helical autotransporter passenger domains. *Nat Commun,* 9, 1395.

Zabner, J., Smith, J. J., Karp, P. H., Widdicombe, J. H. & Welsh, M. J. 1998. Loss of CFTR chloride channels alters salt absorption by cystic fibrosis airway epithelia *in vitro*. *Molecular Cell,* 2, 397–403.

Zafar, M. A., Carabetta, V. J., Mandel, M. J. & Silhavy, T. J. 2014. Transcriptional occlusion caused by overlapping promoters. *Proc Natl Acad Sci U S A,* 111, 1557-61.

Zhai, Y., Zhang, K., Huo, Y., Zhu, Y., Zhou, Q., Lu, J., Black, I., Pang, X., Roszak, A. W., Zhang, X., Isaacs, N. W. & Sun, F. 2011. Autotransporter passenger domain secretion requires a hydrophobic cavity at the extracellular entrance of the beta-domain pore. *Biochem J,* 435, 577-87.
Zielenski, J. 2000. Genotype and phenotype in cystic fibrosis. *Respiration,* 67, 117-33
Zlosnik, J. E., Zhou, G., Brant, R., Henry, D. A., Hird, T. J., Mahenthiralingam, E., Chilvers, M. A., Wilcox, P. & Speert, D. P. 2015. Burkholderia species infections in patients with cystic fibrosis in British Columbia, Canada. 30 years' experience. *Ann Am Thorac Soc,* 12**,** 70-8.

Thesis references

Ashawesh, M.2016. Investigation of the spiral secretion pattern of the serine protease autotransporter, EspC using innovative fluorescent labelling approaches. Unpublished doctoral dissertation. University of Nottingham, Nottingham, UK.
Bhuiyan, N.2015. Optimization Luciferases Assay using of Minimal Media P and creation of rpoN and argR vectors which may be involved in regulation of AaaA in *Pseudomonas aeruginosa*. Unpublished masters dissertation. University of Nottingham, Nottingham, UK.
Darch, O.M.2013. A study on the function of the *Pseudomonas aeruginosa* autotransporter PA0328. Unpublished doctoral dissertation. University of Nottingham, Nottingham, UK.
Day, A. 2016. The Evolution of Virulence in the Opportunistic Pathogen *Pseudomonas aeruginosa*. Unpublished doctoral dissertation. University of Nottingham, Nottingham, UK.
Michail, M.2016. To experimentally determine the environmental influences acting on *P. aeruginosa* virulence factor expression in biofilms and understand the catalytic mechanism of the surface tethered aminopeptidase AaaA.Unpublished masters dissertation. University of Nottingham, Nottingham, UK.
Mohammad, M.2015**.** Bioinformatics approach to predict AaaA activity and its expression level in various strains of *P. aeruginosa*. Unpublished masters dissertation. University of Nottingham, Nottingham, UK.
Palenzuela, D.2016. Linking fatty acid derivatives with signalling and cross-talk in Pseudomonas aeruginosa. Unpublished doctoral dissertation. University of Nottingham, Nottingham, UK.
Paredes, P.O.2014. A novel virulence strategy for Pseudomonas aeruginosa mediated by an autotransporter with arginine specific aminopeptidase activity. Unpublished doctoral dissertation. University of Nottingham, Nottingham, UK.
Rai, R. 2014. Purification of AaaA lacking its Beta barrel transporter domain for structural analysis and demonstration that AaaA is active in clinical isolates of *Pseudomonas aeruginosa* and could thus be a virulence factor. Unpublished masters dissertation. University of Nottingham,Nottingham, UK.
Sethibe, A. 2016. How does the surface-associated arginine specific aminopeptidase autotransporter of *Pseudomonas aeruginosa* (AaaA) contribute to chronic infection? Unpublished masters dissertation. University of Nottingham, Nottingham, UK.